PLANT GLUTATHIONE TRANSFERASES: DIVERSE, MULTI-TASKING ENZYMES WITH YET-TO-BE DISCOVERED FUNCTIONS

EDITED BY: Jolán Csiszár, Arnaud Hecker, Nikolaos E. Labrou, Dean E. Riechers and Peter Schröder

PUBLISHED IN: Frontiers in Plant Science

frontiers Research Topics

ISSN 1664-8714
ISBN 978-2-88963-240-4
DOI 10.3389/978-2-88963-240-4

About Frontiers

Frontiers is more than just an open-access publisher of scholarly articles: it is a pioneering approach to the world of academia, radically improving the way scholarly research is managed. The grand vision of Frontiers is a world where all people have an equal opportunity to seek, share and generate knowledge. Frontiers provides immediate and permanent online open access to all its publications, but this alone is not enough to realize our grand goals.

Frontiers Journal Series

The Frontiers Journal Series is a multi-tier and interdisciplinary set of open-access, online journals, promising a paradigm shift from the current review, selection and dissemination processes in academic publishing. All Frontiers journals are driven by researchers for researchers; therefore, they constitute a service to the scholarly community. At the same time, the Frontiers Journal Series operates on a revolutionary invention, the tiered publishing system, initially addressing specific communities of scholars, and gradually climbing up to broader public understanding, thus serving the interests of the lay society, too.

Dedication to Quality

Each Frontiers article is a landmark of the highest quality, thanks to genuinely collaborative interactions between authors and review editors, who include some of the world's best academicians. Research must be certified by peers before entering a stream of knowledge that may eventually reach the public - and shape society; therefore, Frontiers only applies the most rigorous and unbiased reviews.
Frontiers revolutionizes research publishing by freely delivering the most outstanding research, evaluated with no bias from both the academic and social point of view. By applying the most advanced information technologies, Frontiers is catapulting scholarly publishing into a new generation.

What are Frontiers Research Topics?

Frontiers Research Topics are very popular trademarks of the Frontiers Journals Series: they are collections of at least ten articles, all centered on a particular subject. With their unique mix of varied contributions from Original Research to Review Articles, Frontiers Research Topics unify the most influential researchers, the latest key findings and historical advances in a hot research area! Find out more on how to host your own Frontiers Research Topic or contribute to one as an author by contacting the Frontiers Editorial Office: researchtopics@frontiersin.org

PLANT GLUTATHIONE TRANSFERASES: DIVERSE, MULTI-TASKING ENZYMES WITH YET-TO-BE DISCOVERED FUNCTIONS

Topic Editors:
Jolán Csiszár, Department of Plant Biology, University of Szeged, Hungary
Arnaud Hecker, Université de Lorraine, France
Nikolaos E. Labrou, Agricultural University of Athens, Greece
Dean E. Riechers, University of Illinois at Urbana-Champaign, United States
Peter Schröder, Helmholtz Center Munich, Germany

Citation: Csiszár, J., Hecker, A., Labrou, N. E., Riechers, D. E., Schröder, P., eds. (2019). Plant Glutathione Transferases: Diverse, Multi-Tasking Enzymes with Yet-to-Be Discovered Functions. Lausanne: Frontiers Media SA.
doi: 10.3389/978-2-88963-240-4

Table of Contents

frontiers in Plant Science

EDITORIAL
published: 18 October 2019
doi: 10.3389/fpls.2019.01304

Editorial: Plant Glutathione Transferases: Diverse, Multi-Tasking Enzymes With Yet-to-Be Discovered Functions

*Jolán Csiszár[1], Arnaud Hecker[2], Nikolaos E. Labrou[3], Peter Schröder[4] and Dean E. Riechers[5]**

[1] Department of Plant Biology, Faculty of Science and Informatics, University of Szeged, Szeged, Hungary, [2] Interactions Arbres-Microorganismes, Institut National de la Recherche Agronomique, Université de Lorraine, Nancy, France, [3] Laboratory of Enzyme Technology, Department of Biotechnology, School of Applied Biology and Biotechnology, Agricultural University of Athens, Athens, Greece, [4] Research Unit for Comparative Microbiome Analyses, Department of Environmental Sciences, Helmholtz Zentrum München, German Research Center for Environmental Health (GmbH), Neuherberg, Germany, [5] Department of Crop Sciences, University of Illinois at Urbana-Champaign, Urbana, IL, United States

OPEN ACCESS

Edited by:
Vasileios Fotopoulos,
University of Technology,
Cyprus

Reviewed by:
Kocsy Gábor,
Agricultural Research (MTA),
Hungary
Amna Mhamdi,
Ghent University,
Belgium

***Correspondence:**
Dean E. Riechers
riechers@illinois.edu

Specialty section:
This article was submitted to Plant Physiology, a section of the journal Frontiers in Plant Science

Received: 20 August 2019
Accepted: 18 September 2019
Published: 18 October 2019

Citation:
Csiszár J, Hecker A, Labrou NE, Schröder P and Riechers DE (2019) Editorial: Plant Glutathione Transferases: Diverse, Multi-Tasking Enzymes With Yet-to-Be Discovered Functions. Front. Plant Sci. 10:1304. doi: 10.3389/fpls.2019.01304

Keywords: glutathione transferases, catalysis, detoxification, glutathionylation, ligand binding, redox state, gene regulation, secondary metabolism

Editorial on the Research Topic

Plant Glutathione Transferases: Diverse, Multi-Tasking Enzymes With Yet-To-Be Discovered Functions

Plant genomes contain dozens of *GSTs* (Chi et al., 2011) encoding subunits that can form homodimers or heterodimers, leading to enormous diversity within GST protein families (Labrou et al., 2015). From its inception, plant GST research has successfully focused on investigating catalytic reactions with xenobiotic substrates (Cummins et al., 2011). By contrast, relatively few plant GST studies have successfully identified natural roles for this versatile multifunctional enzyme class, and despite few exceptions (Mueller et al., 2000; Bjarnholt et al., 2018), major breakthroughs have eluded researchers investigating their endogenous substrates and functions. With recent progress in molecular-genetics, physiology, and biochemistry, coupled with greatly increased sensitivity of mass spectrometry, it is timely to revisit potential candidates for natural GST substrates regarding catalysis, ligand binding, and transport roles, as well as summarize recent reports on xenobiotic detoxification and gene regulation mechanisms.

Cellular membrane lipids may become oxidized in plants growing under stress as well as during normal metabolic activity (Wasternack and Feussner, 2018). The resulting "oxylipins" show great variability depending on the carbon affected. Reactive carbonyls formed necessitate plant defense mechanisms. Mano et al. describe how aliphatic acrolein-type molecules and hydroxynonenals are detoxified by tau-class GSTs (GSTU). This metabolic activity applies to approximately 30% of GSTUs tested in *Arabidopsis*, distinguishing them as remarkable natural GST substrates. Regarding xenobiotic metabolism, Tzafestas et al. studied detoxification of trinitrotoluene (TNT) by *Arabidopsis* GSTs. The authors focused on the unusual finding that, between two GSTUs with 79% sequence identity, only one catalyzes substitution of a nitro group with reduced glutathione (GSH). The authors concluded this reaction and subsequent degradation may render the aromatic moiety more susceptible to cleavage, thus stimulating removal of TNT from the environment.

Regarding gene regulation, Baek et al. investigated expression of *GSTs* and other genes involved in detoxification and signaling in sorghum shoots to comprehensively understand tissue-specific expression following safener treatment (Riechers and Green, 2017). Interestingly, transcriptome analysis revealed

strong induction of genes encoding several detoxification enzymes, including cytochrome P450s, GSTs, and glucosyl-transferases, and several upregulated GSTs were similar to enzymes involved with recycling the cyanogenic glycoside dhurrin. Additionally, a genome-wide association study identified two phi-class *GSTs* (*SbGSTF1/F2*) strongly associated with tolerance to the herbicide *S*-metolachlor. This information establishes a new framework for further studies on detoxification and signaling mechanisms for crop protection. Gallé et al. reviewed literature regarding effects of light quality, intensity, duration, and circadian rhythms on plant *GST*s. Patterns and regulation of *GST* expression were discussed in the context of diurnal variations in cellular GSH and reactive oxygen species levels. Importantly, light-regulated expression of GST enzymes possessing detoxification activities could affect whole-plant tolerance levels to abiotic or biotic stresses.

Numerous studies have shown that GSTs are involved in biotic stress responses. Gullner et al. proposed a model describing diverse roles of plant GSTs in interactions of plant hosts with pathogenic microbes considering four scenarios: (i) symptomless resistance, (ii) hypersensitive response-associated resistance, (iii) limiting susceptibility to systemic pathogen spread and plant cell/tissue death, and (iv) promoting susceptibility to biotrophic fungi and viruses. The authors' concluded the most important function of GSTs in influencing plant-pathogen interactions is likely suppression of oxidative stress in infected host tissues. Upon pathogen recognition, secondary compounds (e.g., glucosinolates and indole-type phytoalexins) are induced in Brassicaceae species. Czerniawski and Bednarek summarized current knowledge on GST involvement in sulfur-containing secondary metabolites. Only AtGSTF6 and AtGSTU13 were required for their biosynthesis, but the roles of several other GSTs were suggested. One main conclusion is that specificities of these GSTs may result from their varying expression patterns and cellular/subcellular localizations.

GSTs may also have novel uses for biotechnology applications toward plant improvement (Perperopoulou et al., 2018). Chronopulou et al. employed a strategy to produce synthetic GSTUs by generating a cDNA library of GSTUs from abiotic stress-treated common bean (*Phaseolus vulgaris*) and soybean (*Glycine max*) using degenerate GST-specific primers and reverse transcription-PCR. This library was then diversified by directed evolution *via* a procedure called "DNA shuffling". Using this method, the authors demonstrated the power of forced evolution for generation of variants (synthetic enzymes) with enhanced enzymatic properties that could be valuable in biotechnology. Stavridou et al. used transplastomic (i.e., plants whose transgene has been inserted into the chloroplast genome) tobacco lines as an alternative approach to nuclear transgene expression. Analysis of such lines expressing either of two different GSTs—an *Arabidopsis* theta-class GST normally expressed in the peroxisomes and a chimera engineered from two maize GSTUs—showed an increase in salt, osmotic, and oxidative stress tolerance. This information is of great importance for better understanding the role of GSTs in abiotic stress responses and development of stress-tolerant plants *via* plastome engineering. Dixon and Edwards utilized a protein-ligand fishing strategy to identify natural ligands for AtGSTU19 and AtGSTF2 expressed as *Strep*-tagged fusion proteins *in planta*. Following transient and stable expression in *Nicotiana* and *Arabidopsis*, respectively, the GSTs were recovered using *Strep*-Tactin affinity chromatography and bound ligands characterized by LC-MS. AtGSTF2 predominantly bound phenolic derivatives, whereas AtGSTU19 captured mainly glutathionylated oxylipin conjugates. Such ligand fishing has great potential for providing new insights into protein function *in planta* as well as identifying novel classes of natural product-derived enzyme inhibitors.

Sylvestre-Gonon et al. reviewed the serinyl-GST (Ser-GST) protein family, which have a conserved serine in their N-terminal active site. Ser-GSTs catalyze GSH conjugation reactions and display high peroxidase activity, both of which are important for stress tolerance and herbicide detoxification. Furthermore, Ser-GSTs participate in binding and transport of small heterocyclic ligands (e.g., flavonoids such as anthocyanins and polyphenols) through noncatalytic or "ligandin" properties. The authors discussed the known enzymatic and structural properties of Ser-GSTs and described their biochemical and physiological functions.

The current Frontiers research topic sheds new light on myriad functions of plant GSTs and provides an up-to-date, comprehensive understanding of the GST protein family by defining roles of great importance to endogenous plant metabolism, xenobiotic detoxification mechanisms, and tolerance to abiotic and biotic stresses. Several important questions remained unresolved and significant challenges need to be addressed in the future, however, to allow even deeper mechanistic insights into GST functions *in planta*. Critical knowledge gaps include identifying distinct structural and biochemical features of each subclass within the plant GST protein superfamily, molecules transformed and/or transported by GSTs *via* ligandin properties, molecular-genetic mechanisms and cellular factors that regulate precise cell- and tissue-specific expression of plant *GST* genes before and after stress, and exploring new proteins and the plant defense signaling pathways with which they interact. By highlighting the most recent discoveries in this exciting field of biology, we hope to stimulate further research into unravelling the complex roles of GSTs in plant physiology and crop improvement.

AUTHOR CONTRIBUTIONS

All authors listed made a substantial, direct, and intellectual contribution to the work and approved it for publication.

ACKNOWLEDGMENTS

The research of JC was supported by the Hungarian National Research, Development and Innovation Office (Grant Number NKFI-6 K 125265). The Interactions Arbres-Microorganismes (IAM) laboratory of AH is supported by a grant overseen by the French National Research Agency (ANR) as part of the "Investissements d'Avenir" program (ANR-11-LABX-0002-01, Lab of Excellence ARBRE). NL acknowledges the financial support from Bayer CropScience AG through the "Grants4Targets-Novel targets for crop protection" program. DR acknowledges the support by the Agriculture and Food Research Initiative (Competitive Grant No. 2015-67013-22818) of the USDA-National Institute of Food and Agriculture and expresses

his gratitude to Dr. Anatoli V. Lygin and Dr. Rong Ma for their expert assistance with technique development and optimization.

REFERENCES

Bjarnholt, N., Neilson, E. H., Crocoll, C., Jørgensen, K., Motawia, M. S., Olsen, C. E., et al. (2018). Glutathione transferases catalyze recycling of auto-toxic cyanogenic glucosides in sorghum. *Plant J.* 94, 1109–1125. doi: 10.1111/tpj.13923

Chi, Y., Cheng, Y., Vanitha, J., Kumar, N., Ramamoorthy, R., Ramachandran, S., et al. (2011). Expansion mechanisms and functional divergence of the glutathione *S*-transferase family in sorghum and other higher plants. *DNA Res.* 18, 1–16. doi: 10.1093/dnares/dsq031

Cummins, I., Dixon, D. P., Freitag-Pohl, S., Skipsey, M., and Edwards, R. (2011). Multiple roles for plant glutathione transferases in xenobiotic detoxification. *Drug Metab. Rev.* 43, 266–280. doi: 10.3109/03602532.2011.552910

Labrou, N. E., Papageorgiou, A. C., Pavil, O., and Flemetakis, E. (2015). Plant GSTome: structure and functional role in xenome network and plant stress response. *Curr. Opin. Biotechnol.* 32, 186–194. doi: 10.1016/j.copbio.2014.12.024

Perperopoulou, F., Pouliou, F., and Labrou, N. E. (2018). Recent advances in protein engineering and biotechnological applications of glutathione transferases. *Crit. Rev. Biotechnol.* 38, 511–528. doi: 10.1080/07388551.2017.1375890

Mueller, L. A., Goodman, C. D., Silady, R. A., and Walbot, V. (2000). AN9, a petunia glutathione *S*-transferase required for anthocyanin sequestration, is a flavonoid-binding protein. *Plant Physiol.* 123, 1561–1570. doi: 10.1104/pp.123.4.1561

Riechers, D. E., and Green, J. M. (2017). "Crop selectivity and herbicide safeners: Historical perspectives and development, safener-regulated gene expression, signaling, and new research directions," in *Biology, Physiology and Molecular Biology of Weeds*. Ed. M. Jugulam (Boca Raton, FL: CRC Press, Taylor & Francis Group), 123–143. doi: 10.1201/9781315121031-7

Wasternack, C., and Feussner, I. (2018). The oxylipin pathways: biochemistry and function. *Annu. Rev. Plant Biol.* 69, 363–386. doi: 10.1146/annurev-arplant-042817-040440

Conflict of Interest: The authors declare that the research was conducted in the absence of any commercial or financial relationships that could be construed as a potential conflict of interest.

frontiers in Plant Science

MINI REVIEW
published: 13 November 2018
doi: 10.3389/fpls.2018.01639

Glutathione *S*-Transferases in the Biosynthesis of Sulfur-Containing Secondary Metabolites in Brassicaceae Plants

*Paweł Czerniawski and Paweł Bednarek**

Institute of Bioorganic Chemistry, Polish Academy of Sciences, Poznań, Poland

Plants in the Brassicaceae family have evolved the capacity to produce numerous unique and structurally diverse sulfur-containing secondary metabolites, including constitutively present thio-glucosides, also known as glucosinolates, and indole-type phytoalexins, which are induced upon pathogen recognition. Studies on the glucosinolate and phytoalexin biosynthetic pathways in the model plant *Arabidopsis thaliana* have shown that glutathione donates the sulfur atoms that are present in these compounds, and this further suggests that specialized glutathione *S*-transferases (GSTs) are involved in the biosynthesis of glucosinolates and sulfur-containing phytoalexins. In addition, experimental evidence has shown that GSTs also participate in glucosinolate catabolism. Several candidate GSTs have been suggested based on co-expression analysis, however, the function of only a few of these enzymes have been validated by enzymatic assays or with phenotypes of respective mutant plants. Thus, it remains to be determined whether biosynthesis of sulfur-containing metabolites in Brassicaceae plants requires specific or nonspecific GSTs.

Keywords: glutathione, glutathione *S*-transferase (GST), glucosinolate, sulfur-containing phytoalexin, Brassicaceae

OPEN ACCESS

Edited by:
Jolán Csiszár,
University of Szeged, Hungary

Reviewed by:
Jim Tokuhisa,
Virginia Tech, United States
Gabor Gullner,
Plant Protection Institute (MTA), Hungary

***Correspondence:**
Paweł Bednarek
bednarek@ibch.poznan.pl

Specialty section:
This article was submitted to Plant Metabolism and Chemodiversity, a section of the journal Frontiers in Plant Science

Received: *31 July 2018*
Accepted: *22 October 2018*
Published: *13 November 2018*

Citation:
Czerniawski P and Bednarek P (2018) Glutathione S-Transferases in the Biosynthesis of Sulfur-Containing Secondary Metabolites in Brassicaceae Plants. Front. Plant Sci. 9:1639. doi: 10.3389/fpls.2018.01639

INTRODUCTION

Glutathione *S*-transferases (GSTs) constitute a family of multifunctional enzymes that catalyze the nucleophilic attack of the sulfur atom of the tripeptide glutathione (GSH) on electrophilic centers of low-molecular weight compounds (Dixon and Edwards, 2010; Labrou et al., 2015). GSTs were identified as stress response proteins that accumulated in response to biotic and abiotic stimuli. Many studies on plant GSTs have focused on their role in xenobiotic detoxification. In addition, some GSTs have been implicated in plant secondary metabolism, particularly in the formation of natural products containing carbon-sulfur bonds, including the sulfur-containing phytochemicals characteristic of Brassicaceae species (Dixon et al., 2010; Sonderby et al., 2010; Pedras et al., 2011; Bednarek, 2012; Dunbar et al., 2017).

CONJUGATION OF GSH IS REQUIRED FOR THE BIOSYNTHESIS OF GLUCOSINOLATES

Glucosinolates are sulfur-containing secondary metabolites produced by plants of the Brassicales order, and their core structure contains a β-D-thioglucose moiety connected to a sulfonated aldoxime and a variable side chain derived from amino acids, such as tryptophan, tyrosine, and methionine (Halkier and Gershenzon, 2006). The first two steps of glucosinolate biosynthesis are catalyzed by specific isoforms of CYP79 and CYP83 cytochrome P450 monooxygenases, which convert precursor amino acids to aldoximes and then to *aci*-nitro compounds. It has been postulated that these intermediates can react with an alkylthiol to form conjugates that can be converted to glucosinolates by the sequential activities of C-*S* lyase (SUR1), glucosyltransferases (UGTs), and sulfotransferases (SOTs) (**Figure 1**; Sonderby et al., 2010). Decreased glucosinolate accumulation in the *phytoalexin deficient 2* (*pad2*) mutant, which has a reduced GSH biosynthesis rate, suggested that GSH is the alkylthiol that conjugates with the products of CYP83 activity (Parisy et al., 2007; Schlaeppi et al., 2008). In line with this hypothesis, upon engineering benzyl glucosinolate biosynthesis in *Nicotiana benthamiana*, it was found that expression of CYP79A2 and CYP83B1 led to an accumulation of *S*-(phenylacetohydroximoyl)-GSH, the predicted GSH conjugate (Geu-Flores et al., 2009). Introduction of SUR1, UGT74B1, and SOT18 into the engineered *N. benthamiana* line led to low level production of benzyl glucosinolate, but did not significantly reduce the *S*-(phenylacetohydroximoyl)-GSH level suggesting that this intermediate is not a substrate of SUR1. This was confirmed by additional expression of γ-glutamyl peptidase 1 (GGP1) or GGP3, enzymes cleaves γ-Glu from GSH conjugates, which resulted in depletion of the *S*-(phenylacetohydroximoyl)-GSH intermediate along with a significant increase in the rate of benzyl glucosinolate production in transgenic *N. benthamiana* (Geu-Flores et al., 2009, 2011). In addition, glucosinolate levels decreased and levels of the corresponding GSH-containing intermediates increased in an Arabidopsis *ggp1 ggp3* double mutant (Geu-Flores et al., 2011).

Collectively, these findings confirmed that GSH-conjugates are glucosinolate biosynthetic intermediates and raised the question of whether conjugation of GSH with products of CYP83 activity requires specific enzymatic activity. Candidate GSTs involved in this process have been proposed based on their co-expression with glucosinolate biosynthesis enzymes and on an analysis of metabolic and gene expression profiles of quantitative trait loci (Hirai et al., 2005; Wentzell et al., 2007; Hirai, 2009). It has been suggested that GSTF11 and GSTU20 are involved in aliphatic glucosinolate (AG) biosynthesis and that GSTF9 and GSTF10 contribute to indolic glucosinolate (IG) formation (**Figures 1**,**2A**). In addition, transcriptome analyses of Arabidopsis *myb28* knock-out and *MYB28*-overexpressing cell cultures showed that *GSTF11* and *GSTU20* expression is regulated by the MYB28 transcription factor, which controls the AG biosynthetic pathway (Hirai et al., 2007).

However, despite these correlations, no GST function in glucosinolate biosynthesis has yet been validated experimentally. For instance, successful engineering of benzyl glucosinolate or glucoraphanin (an AG) biosynthesis in *N. benthamiana* did not require any Arabidopsis GSTs (Geu-Flores et al., 2009; Mikkelsen et al., 2010). Moreover, introduction of GSTF11 increased the efficiency of glucoraphanin production by only 20% (Mikkelsen et al., 2010). Similarly, expression of Arabidopsis IG biosynthetic genes in yeast (*Saccharomyces cerevisiae*) showed that GSTF9 and GSTF10 are dispensable for conjugation of the product of CYP83B1 activity with GSH in this microorganism. Additional introduction of GSTF9 in the engineered yeast strain boosted the level of glucosinolate by only 25% (Mikkelsen et al., 2012). These results suggest that GSH conjugation in glucosinolate biosynthesis can occur spontaneously without GST activity or that tested GSTs are not specific for glucosinolate biosynthesis and can be replaced by GSTs from other organisms. However, overexpression of Arabidopsis enzymes in *N. benthamiana* or in yeast obscures their native temporal and spatial accumulation patterns. Opposite, fluorophore-tagged glucosinolate biosynthetic enzymes, including CYP83 monooxygenases that produce putative GST substrates, localized to specific tissues and cell types when expressed under their native promoters in Arabidopsis (Nintemann et al., 2018). Thus, it is likely that GSTs involved in glucosinolate biosynthesis are not specific with regards to their substrate preference or catalytic properties, but can be specific with regards to their localization, which can be not observed in glucosinolate-engineered strains.

In addition to the missing functional validation, experiments have suggested that the GSTs that have been proposed to contribute to glucosinolate biosynthesis may have alternative *in planta* functions. For instance, in a yeast two-hybrid screen, GSTU20 interacted with Far-Red Insensitive 219, a jasmonate-conjugating enzyme linked to phytochrome signaling, and a partial loss of GSTU20 function resulted in hyposensitivity to continuous far-red light. Moreover, under the same condition *GSTU20* was differentially expressed in *suppressor of phytochrome A-105 1* and *constitutive photomorphogenic 1* mutant plants (Chen et al., 2007). To explain these phenotypes, it has been hypothesized that GSTU20 can bind, stabilize, or transport jasmonic acid or its derivatives within the cell.

Another yeast two-hybrid screen indicated that GSTF10 interacts with Brassinosteroid Insensitive 1 (BAK1), a leucine-rich repeat receptor-like kinase involved in brassinosteroid signaling and plant defense (Ryu et al., 2009). RNA interference (RNAi)-mediated down-regulation of *GSTF10* and *GSTF9* expression led to a more compact rosette shape, which is similar to the phenotype of weak *bak1* mutant alleles. However, plants that underexpressed (via RNAi) or overexpressed *GSTF10* showed wild type (WT)-like growth in the presence of brassinolide (a brassinosteroid) or brassinazole (an inhibitor of brassinosteroid biosynthesis), thus GSTF10 is probably not involved in brassinosteroid signaling. In addition to the compact rosette phenotype, *GSTF10/9* RNAi plants had

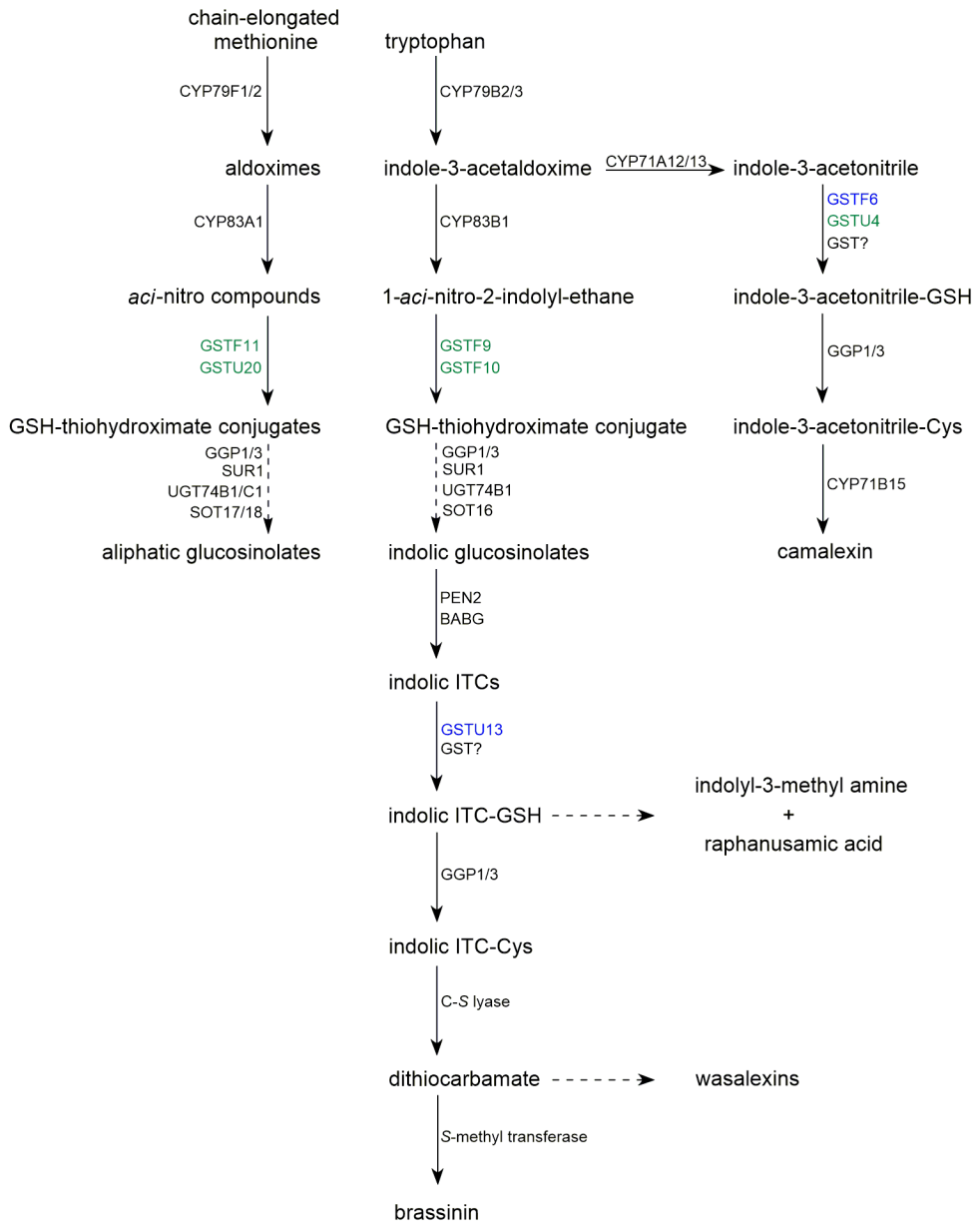

FIGURE 1 | Biosynthetic pathways of glucosinolates and selected sulfur-containing phytoalexins occurring in Brassicaceae. Dashed arrows represent multistage processes. GSTs with function confirmed with mutant phenotype are indicated in blue. GSTs with contribution proposed based on co-expression analysis are indicated in green.

higher anthocyanin levels and a lower tolerance for NaCl or *N*-acetylcysteine, a pharmacological reagent that scavenges free radicals (Ryu et al., 2009). Similar to the RNAi line, a *gstf9* mutant had a lower tolerance for NaCl and was defective in redox homeostasis (Horváth et al., 2015). It has also been shown that GSTF9 is induced in response to the gravity persistent signal (GPS), and *gstf9* mutants displayed defective GPS responses in inflorescence stems, as well as in root skewing, waving, and curvature (Schenck et al., 2013). Collectively, these findings suggest that GSTF9 and GSTF10 contribute to redox homeostasis and responses to environmental stimuli, but it is unclear whether these putative functions depend on glucosinolate biosynthesis.

GSTS ARE IMPORTANT FOR GLUCOSINOLATE METABOLISM

Specific β-thioglucosidases, known as myrosinases, and glucosinolates constitute a binary defense system against generalist insects and pathogens (Hopkins et al., 2009; Pastorczyk and Bednarek, 2016). Upon tissue damage or in response to

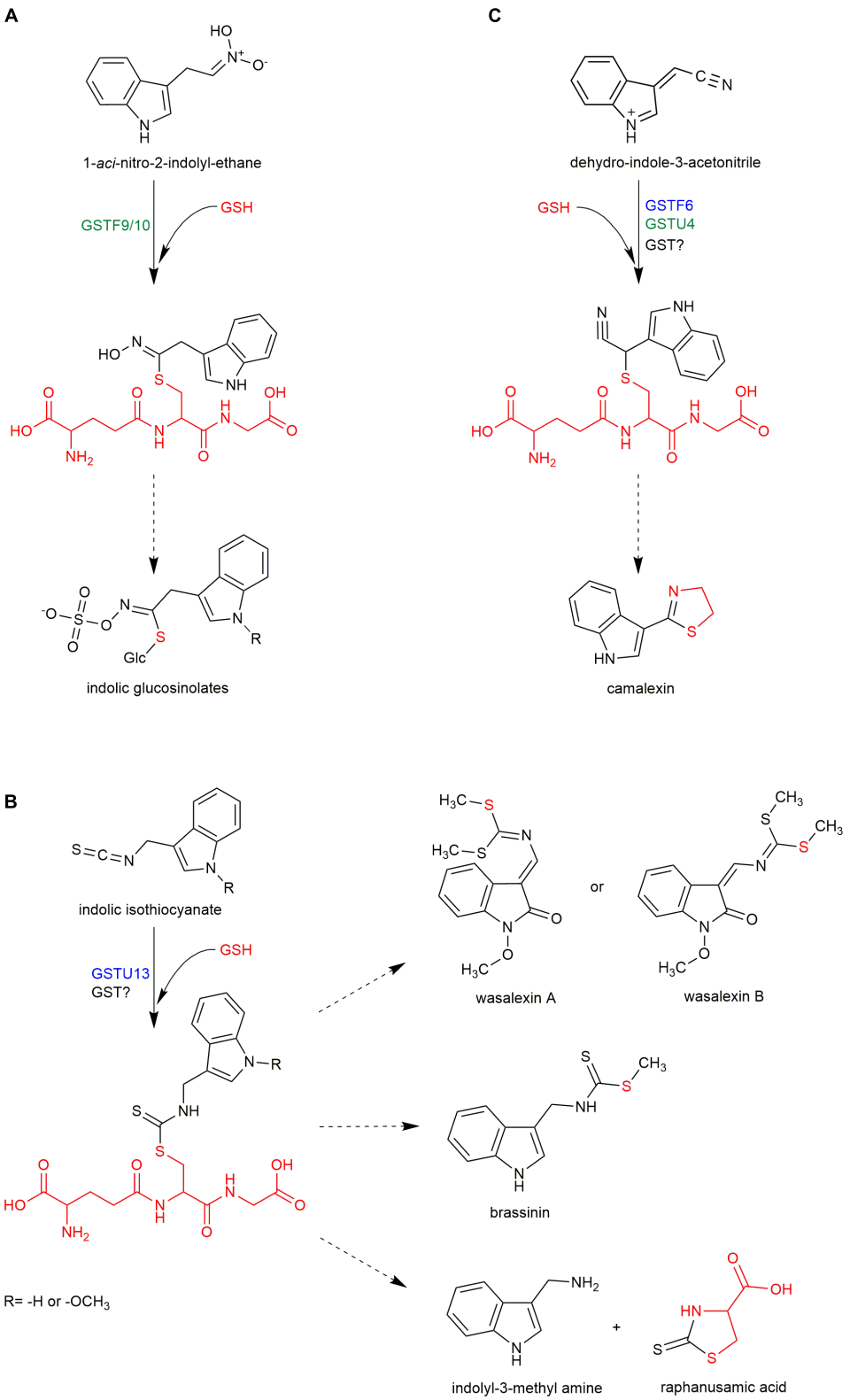

FIGURE 2 | Proposed involvement of GSTs in biosynthesis of indolic glucosinolates **(A)**, camalexin **(C)**, and other sulfur-containing phytoalexins **(B)**. Dashed arrows represent multistage processes. Red color indicates glutathione and its fragments in structures of respective sulfur-containing metabolites. GSTs with function confirmed with mutant phenotype are indicated in blue. GSTs with contribution proposed based on co-expression analysis are indicated in green.

environmental stimuli, glucosinolates can be hydrolyzed by myrosinases leading to the formation of unstable aglycones. Based on their side chain structure and the presence of specifier proteins, these aglycones can rearrange into different end products, including highly chemically reactive and biologically active isothiocyanates (ITCs), which can be harmful for the host plant (Wittstock et al., 2016). It has been shown that exogenous ITC application has negative effects on Arabidopsis growth (Hara et al., 2010; Urbancsok et al., 2017). Notably, Arabidopsis GSH-deficient mutants have been shown to be more susceptible to ITCs than WT plants suggesting that deactivation of ITCs *in planta* requires their conjugation with GSH (Urbancsok et al., 2018). As indicted by experimental evidence this reaction is spontaneous, but its efficiency can be significantly enhanced with GST-mediated catalysis, and leads to the formation of dithiocarbamate-type ITC-GSH adducts (Zhang et al., 1995). Enzymatic studies demonstrated that many Arabidopsis GSTs process benzyl-ITC, which is a model ITC used in *in vitro* enzyme assays (Wagner et al., 2002; Dixon et al., 2009). Moreover, in Arabidopsis, it has been shown that some GST genes are induced in response to external ITC application (Hara et al., 2010; Øverby et al., 2015). Overall, these results indicate that GSTs function in the detoxification of glucosinolate-derived ITCs in Brassicales plants.

In addition to its role in ITC detoxification, conjugation with GSH can lead to the formation of novel products with important roles in plant fitness. During the immune response in Arabidopsis, Penetration 2 myrosinase (PEN2) metabolizes IGs to several end products, including indol-3-yl methyl amine (I3A), raphanusamic acid (RA), and 4-*O*-β-glucosyl-indol-3-ylformamide (4OGlcI3F) (**Figure 1**; Bednarek et al., 2009; Lu et al., 2015). The reduced accumulation of these metabolites in GSH-deficient *pad2* plants indicates that their formation is GSH dependent (Bednarek et al., 2009; Piślewska-Bednarek et al., 2018). In addition, the structures of I3A and RA suggest that they are derived from a dithiocarbamate-type adduct formed from indol-3-ylmethyl-ITC (I3-ITC), a product of indol-3-ylmethyl glucosinolate (I3G) hydrolysis (**Figure 2B**). However, in contrast to aliphatic- or benzyl-ITCs, indolic ITCs are highly unstable, and their spontaneous conjugation with GSH is preceded by a release of a thiocyanate ion leading to products different from dithiocarbamates (Kim et al., 2008; Agerbirk et al., 2009). Thus, the formation of I3A and RA most likely requires a GST that can efficiently conjugate GSH with the labile I3-ITC formed by PEN2 myrosinase, and gene co-expression analysis pointed to GSTU13 as a candidate for this function (Piślewska-Bednarek et al., 2018). This selection was additionally supported by *in vitro* enzymatic assays, which indicated that among 35 tested Arabidopsis GSTs GSTU13 together with GSTU4 and GSTU6 had not only the highest activity against benzyl-ITC, but also the highest specificity toward this compound as compared with the other tested substrates (Wagner et al., 2002; Dixon et al., 2009). The reduced accumulation of I3A, RA, and 4OGlcI3F observed in *gstu13* mutant plants confirms that GSTU13 is involved in biosynthesis of these compounds. Moreover, an analysis of the susceptibility of *pen2* and *gstu13* single and double mutants to selected fungal pathogens suggested that PEN2 and GSTU13 are part of the same immune pathway (Piślewska-Bednarek et al., 2018). Because PEN2, which localizes to the mitochondrial membranes, is actively delivered with a subpopulation of mitochondria to pathogen contact sites (Fuchs et al., 2016), in addition to its substrate specificity, spatial and temporal localization may also be critical for GSTU13 function.

GSTS CONTRIBUTE TO PHYTOALEXIN BIOSYNTHESIS

Apart from glucosinolates, Brassicaceae plants produce another group of sulfur-containing metabolites known as Brassicaceae phytoalexins. In general, phytoalexins are highly diverse, low molecular weight antimicrobial compounds that are produced in plants in response to infection. Phytoalexins produced by Brassicaceae plants are usually composed of an indole core and a side chain with one or two sulfur atoms (Pedras et al., 2011). Interestingly, it has been shown that biosynthesis of some indolic phytoalexins, including brassinin, is tightly linked with IG biosynthesis and metabolism (**Figure 1**). Brassinin is a phytoalexin produced by *Brassica* species that consists of an indole ring conjugated with an *S*-methylated dithiocarbamate group (**Figure 2B**). Upon application of benzyl-ITC to the roots of turnip plants (*Brassica campestris* ssp. *rapa*), a benzyl-type structural analog of brassinin was formed indicating that brassinin and related metabolites can be produced from IGs via corresponding ITCs (Monde et al., 1994). Similarly, upon application of labeled I3G to the leaves of salt cress (*Thellungiella salsuginea*), the label was incorporated into wasalexins, which are structurally related to brassinin (**Figure 2B**; Pedras et al., 2010). These results confirmed that IGs may serve as precursors to some Brassicaceae phytoalexins and raised the question of whether myrosinases are involved in the biosynthesis of these compounds. Transcriptome analysis of *Brassica rapa* combined with a comparative genomic approach to eliminate genes with direct orthologs in Arabidopsis, which does not produce brassinin, led to the identification of two Brassinin-Associated β-Glucosidases (BABGs), putative myrosinases that may hydrolyze IGs during biosynthesis of this phytoalexin (Klein and Sattely, 2017). Engineered expression of the IG pathway enzymes, the identified BABGs, and a dithiocarbamate *S*-methyltransferase, which catalyzes the last step in brassinin biosynthesis, in *N. bethamiana* resulted in accumulation of brassinin in transfected leaves confirming biosynthetic link between this compound and IGs. This link combined with the presence of the dithiocarbamate group in brassinin molecule suggests that biosynthesis of this phytoalexin involves the same I3-ITC-GSH adduct proposed as an intermediate in the PEN2 pathway (**Figure 2B**; Bednarek et al., 2009). This in turn raised the question of whether GSTs are involved in the conjugation of I3-ITC with GSH during brassinin biosynthesis. Brassinin was produced efficiently in transfected *N. bethamiana* leaves suggesting that the conjugation step can be catalyzed by *Br*GSTF9, which was included in the engineered IG pathway, or by nonspecific GSTs from *N. benthamiana* (Klein and Sattely, 2017). However, a relatively high level of indole-3-carbinol, an

I3-ITC degradation product, also accumulated in the engineered *N. benthamiana* suggesting that *Br*GSTF9 or non-specific GSTs are insufficient to conjugate unstable I3-ITC with GSH efficiently, thus a specific GST may be involved in brassinin biosynthesis. Unfortunately, transcriptome analysis did not identify a unique *B. rapa* GST that was induced upon pathogen inoculation (Klein and Sattely, 2017).

The only identified sulfur-containing phytoalexin in Arabidopsis is camalexin, and production of this compound is dependent on sulfate nutritional status (Kruse et al., 2012). Reduced accumulation of camalexin in *pad2* mutant plants suggested that GSH is the precursor to the thiazole ring present in its structure (**Figure 2C**; Parisy et al., 2007). Camalexin shares the first biosynthetic step, conversion of tryptophan to indole-3-acetaldoxime by CYP79B2/3 enzymes, with IGs. In the next step, indole-3-acetaldoxime is converted by CYP71A12 and CYP71A13 to indole-3-acetonitrile (IAN), and then a conjugate of GSH and IAN (GS-IAN) is formed as indicated by enhanced accumulation of GS-IAN in a double mutant line depleted of GGP1 and GGP3, which cleave γ-Glu from this intermediate (**Figure 1**; Geu-Flores et al., 2011; Klein et al., 2013; Müller et al., 2015). However, despite the identification of GGPs as enzymes processing GS-IAN the nature of the substrate that reacts with GSH to form this conjugate remains obscure. Geu-Flores et al. (2011) suggested that an unknown enzyme activates IAN before conjugation with GSH. *In vitro* assays showed that CYP71A12/13 monooxygenases can play this role by further oxidizing IAN to α-hydroxy-IAN and to dehydro-IAN, which can react spontaneously with GSH (**Figure 2C**; Klein et al., 2013). Although the mechanism of *in planta* IAN activation remains unclear, it is likely that GSTs are involved in the subsequent biosynthetic step and respective enzymes have been searched for. It is known that camalexin biosynthesis is activated by the mitogen-activated protein kinase (MAPK) cascade, which includes MAPKK9 (Xu et al., 2008). Proteome analysis of constitutively active $MAPKK9^{DD}$ transgenic plants showed that GSTF2, GSTF6, and GSTF7 accumulate to high levels during camalexin production (Su et al., 2011). To validate the putative function of these transferases, transgenic lines overexpressing GSTF2, GSTF6, or GSTF7 individually in the $MAPKK9^{DD}$ background were generated, and a significant increase in camalexin production was observed in the GSTF6/$MAPKK9^{DD}$ line indicating that GSTF6 contributes to camalexin biosynthesis. In addition, *gstf6* knock-out seedlings showed a slight but significant reduction in camalexin production suggesting that GSTF6 along with additional GSTs participate in biosynthesis of this phytoalexin (Su et al., 2011). A candidate GST involved in camalexin biosynthesis is GSTU4, which is co-expressed tightly with CYP71A13 and PAD3 (Piślewska-Bednarek et al., 2018), however, the function of this enzyme has not yet been evaluated experimentally. In contrast to the conclusions of Su et al. (2011), additional expression of *GSTF6*, in engineered *N. benthamiana* line expressing *CYP79B2*, *CYP71A13*, *GGP1*, and *PAD3* did not affect camalexin accumulation indicating that enzymatic catalysis is not required for GSH conjugation during biosynthesis of this phytoalexin or that *N. benthamiana* GSTs can replace GSTF6 (Møldrup et al., 2013). However, similar to the glucosinolate pathway, it is possible that GSTF6 specificity in camalexin biosynthesis results from its spatial and temporal expression pattern rather than from substrate specificity.

Despite the reported defect in camalexin accumulation in *gstf6* plants, experimental data suggests that GSTF6 plays alternative roles in anthocyanin biosynthesis and drought tolerance. Because *GSTF6* transcript levels were highly elevated in transgenic plants overexpressing *Production of Anthocyanin Pigment 1* (*PAP1*/*MYB75*), *GSTF6* expression appears to be regulated by the PAP1 transcription factor that controls anthocyanin biosynthesis (Tohge et al., 2005). In addition, *GSTF6*, also known as *Early Responsive to Dehydration 11*, was identified as a gene that is induced strongly in response to dehydration (Kiyosue et al., 1993), a condition that may induce anthocyanin biosynthesis (Nakabayashi et al., 2014). These findings suggest that GSTF6 may act redundantly with GSTF12, also known as Transparent Testa 19, which has been postulated to facilitate transport of anthocyanins and proanthocyanidins from the cytosol into the vacuole (Kitamura et al., 2004). However, in contrast to *gstf12*, *gstf6* mutant plants did not display any defects in anthocyanin accumulation (Wangwattana et al., 2008).

CONCLUSION

Recent experimental evidence indicated that GSH-conjugates are intermediates in the biosynthesis of sulfur-containing secondary metabolites in Brassicaceae plants, thus there has been a search for the GSTs responsible for the formation of these intermediates. Several candidate GSTs have been identified based on co-expression with enzymes involved in the corresponding biosynthetic pathways. From those, so far only GSTF6 and GSTU13 have been shown to be required for the formation of the corresponding end products. Metabolic engineering of the Brassicaceae biosynthetic pathways in other organisms suggests that GSTs from Brassicaceae plants, with the possible exception of those involved in the conjugation of unstable indolic ITCs, are generalists rather than specific in their catalytic properties and substrate specificity. However, distinct spatial and temporal distributions of enzymes linked with IG biosynthesis and metabolism suggest that the specificities of GSTs involved in biosynthesis of sulfur-containing phytochemicals may result from their expression patterns and from their cellular and subcellular localizations. Therefore investigation of GSTs involved in the production of sulfur-containing phytochemicals from Brassicaceae should also address these aspects in a greater detail.

AUTHOR CONTRIBUTIONS

PC drafted the manuscript. PB supervised the writing, revised the manuscript, and prepared its final version.

FUNDING

This work was supported by a National Science Center SONATA BIS grant UMO-2012/07/E/NZ2/04098.

REFERENCES

Agerbirk, N., De Vos, M., Kim, J. H., and Jander, G. (2009). Indole glucosinolate breakdown and its biological effects. *Phytochem. Rev.* 8:101. doi: 10.1007/s11101-008-9098-0

Bednarek, P. (2012). Sulfur-containing secondary metabolites from Arabidopsis thaliana and other Brassicaceae with function in plant immunity. *Chembiochem* 13, 1846–1859. doi: 10.1002/cbic.201200086

Bednarek, P., Pislewska-Bednarek, M., Svatos, A., Schneider, B., Doubsky, J., Mansurova, M., et al. (2009). A glucosinolate metabolism pathway in living plant cells mediates broad-spectrum antifungal defense. *Science* 323, 101–106. doi: 10.1126/science.1163732

Chen, I.-C., Huang, I.-C., Liu, M.-J., Wang, Z.-G., Chung, S.-S., and Hsieh, H.-L. (2007). Glutathione *S*-transferase interacting with far-red insensitive 219 is involved in phytochrome A-mediated signaling in Arabidopsis. *Plant Physiol.* 143, 1189–1202. doi: 10.1104/pp.106.094185

Dixon, D. P., and Edwards, R. (2010). Glutathione transferases. *Arabidopsis Book* 8:e0131. doi: 10.1199/tab.0131

Dixon, D. P., Hawkins, T., Hussey, P. J., and Edwards, R. (2009). Enzyme activities and subcellular localization of members of the Arabidopsis glutathione transferase superfamily. *J. Exp. Bot.* 60, 1207–1218. doi: 10.1093/jxb/ern365

Dixon, D. P., Skipsey, M., and Edwards, R. (2010). Roles for glutathione transferases in plant secondary metabolism. *Phytochemistry* 71, 338–350. doi: 10.1016/j.phytochem.2009.12.012

Dunbar, K. L., Scharf, D. H., Litomska, A., and Hertweck, C. (2017). Enzymatic carbon–sulfur bond formation in natural product biosynthesis. *Chem. Rev.* 117, 5521–5577. doi: 10.1021/acs.chemrev.6b00697

Fuchs, R., Kopischke, M., Klapprodt, C., Hause, G., Meyer, A. J., Schwarzländer, M., et al. (2016). Immobilized subpopulations of leaf epidermal mitochondria mediate PENETRATION2-dependent pathogen entry control in Arabidopsis. *Plant Cell* 28, 130–145. doi: 10.1105/tpc.15.00887

Geu-Flores, F., Møldrup, M. E., Böttcher, C., Olsen, C. E., Scheel, D., and Halkier, B. A. (2011). Cytosolic γ-glutamyl peptidases process glutathione conjugates in the biosynthesis of glucosinolates and camalexin in Arabidopsis. *Plant Cell* 23, 2456–2469. doi: 10.1105/tpc.111.083998

Geu-Flores, F., Nielsen, M. T., Nafisi, M., Moldrup, M. E., Olsen, C. E., Motawia, M. S., et al. (2009). Glucosinolate engineering identifies gamma-glutamyl peptidase. *Nat. Chem. Biol.* 5, 575–577. doi: 10.1038/nchembio.185

Halkier, B. A., and Gershenzon, J. (2006). Biology and biochemistry of glucosinolates. *Annu. Rev. Plant Biol.* 57, 303–333. doi: 10.1146/annurev.arplant.57.032905.105228

Hara, M., Yatsuzuka, Y., Tabata, K., and Kuboi, T. (2010). Exogenously applied isothiocyanates enhance glutathione *S*-transferase expression in Arabidopsis but act as herbicides at higher concentrations. *J. Plant Physiol.* 167, 643–649. doi: 10.1016/j.jplph.2009.11.006

Hirai, M. Y. (2009). A robust omics-based approach for the identification of glucosinolate biosynthetic genes. *Phytochem. Rev.* 8, 15–23. doi: 10.1007/s11101-008-9114-4

Hirai, M. Y., Klein, M., Fujikawa, Y., Yano, M., Goodenowe, D. B., Yamazaki, Y., et al. (2005). Elucidation of gene-to-gene and metabolite-to-gene networks in arabidopsis by integration of metabolomics and transcriptomics. *J. Biol. Chem.* 280, 25590–25595. doi: 10.1074/jbc.M502332200

Hirai, M. Y., Sugiyama, K., Sawada, Y., Tohge, T., Obayashi, T., Suzuki, A., et al. (2007). Omics-based identification of Arabidopsis Myb transcription factors regulating aliphatic glucosinolate biosynthesis. *Proc. Natl. Acad. Sci. U.S.A.* 104, 6478–6483. doi: 10.1073/pnas.0611629104

Hopkins, R. J., van Dam, N. M., and van Loon, J. J. A. (2009). Role of glucosinolates in insect-plant relationships and multitrophic interactions. *Annu. Rev. Entomol.* 54, 57–83. doi: 10.1146/annurev.ento.54.110807.090623

Horváth, E., Bela, K., Papdi, C., Gallé, Á., Szabados, L., Tari, I., et al. (2015). The role of Arabidopsis glutathione transferase F9 gene under oxidative stress in seedlings. *Acta Biol. Hung.* 66, 406–418. doi: 10.1556/018.66.2015.4.5

Kim, J. H., Lee, B. W., Schroeder, F. C., and Jander, G. (2008). Identification of indole glucosinolate breakdown products with antifeedant effects on *Myzus persicae* (green peach aphid). *Plant J.* 54, 1015–1026. doi: 10.1111/j.1365-313X.2008.03476.x

Kitamura, S., Shikazono, N., and Tanaka, A. (2004). TRANSPARENT TESTA 19 is involved in the accumulation of both anthocyanins and proanthocyanidins in Arabidopsis. *Plant J.* 37, 104–114. doi: 10.1046/j.1365-313X.2003.01943.x

Kiyosue, T., Yamaguchi-Shinozaki, K., and Shinozaki, K. (1993). Characterization of two cDNAs (ERD11 and ERD13) for dehydration-inducible genes that encode putative glutathione *S*-transferases in *Arabidopsis thaliana* L. *FEBS Lett.* 335, 189–192. doi: 10.1016/0014-5793(93)80727-C

Klein, A. P., Anarat-Cappillino, G., and Sattely, E. S. (2013). Minimum set of cytochromes P450 for reconstituting the biosynthesis of camalexin, a major Arabidopsis antibiotic. *Angew. Chem. Int. Edit.* 52, 13625–13628. doi: 10.1002/anie.201307454

Klein, A. P., and Sattely, E. S. (2017). Biosynthesis of cabbage phytoalexins from indole glucosinolate. *Proc. Natl. Acad. Sci. U.S.A.* 114, 1910–1915. doi: 10.1073/pnas.1615625114

Kruse, C., Haas, F. H., Jost, R., Reiser, B., Reichelt, M., Wirtz, M., et al. (2012). Improved sulfur nutrition provides the basis for enhanced production of sulfur-containing defense compounds in Arabidopsis thaliana upon inoculation with *Alternaria brassicicola*. *J. Plant Physiol.* 169, 740–743. doi: 10.1016/j.jplph.2011.12.017

Labrou, N. E., Papageorgiou, A. C., Pavli, O., and Flemetakis, E. (2015). Plant GSTome: structure and functional role in xenome network and plant stress response. *Curr. Opin. Biotechnol.* 32, 186–194. doi: 10.1016/j.copbio.2014.12.024

Lu, X., Dittgen, J., Pislewska-Bednarek, M., Molina, A., Schneider, B., Svatos, A., et al. (2015). Mutant allele-specific uncoupling of PENETRATION3 functions reveals engagement of the ATP-binding cassette transporter in distinct tryptophan metabolic pathways. *Plant Physiol.* 168, 814–827. doi: 10.1104/pp.15.00182

Mikkelsen, M. D., Buron, L. D., Salomonsen, B., Olsen, C. E., Hansen, B. G., Mortensen, U. H., et al. (2012). Microbial production of indolylglucosinolate through engineering of a multi-gene pathway in a versatile yeast expression platform. *Metab. Eng.* 14, 104–111. doi: 10.1016/j.ymben.2012.01.006

Mikkelsen, M. D., Olsen, C. E., and Halkier, B. A. (2010). Production of the cancer-preventive glucoraphanin in Tobacco. *Mol. Plant* 3, 751–759. doi: 10.1093/mp/ssq020

Møldrup, M. E., Salomonsen, B., Geu-Flores, F., Olsen, C. E., and Halkier, B. A. (2013). De novo genetic engineering of the camalexin biosynthetic pathway. *J. Biotechnol.* 167, 296–301. doi: 10.1016/j.jbiotec.2013.06.013

Monde, K., Takasugi, M., and Ohnishi, T. (1994). Biosynthesis of cruciferous phytoalexins. *J. Am. Chem. Soc.* 116, 6650–6657. doi: 10.1021/ja00094a021

Müller, T. M., Böttcher, C., Morbitzer, R., Götz, C. C., Lehmann, J., Lahaye, T., et al. (2015). Transcription activator-like effector nuclease-mediated generation and metabolic analysis of camalexin-deficient cyp71a12 cyp71a13 double knockout lines. *Plant Physiol.* 168, 849–858. doi: 10.1104/pp.15.00481

Nakabayashi, R., Yonekura-Sakakibara, K., Urano, K., Suzuki, M., Yamada, Y., Nishizawa, T., et al. (2014). Enhancement of oxidative and drought tolerance in Arabidopsis by overaccumulation of antioxidant flavonoids. *Plant J.* 77, 367–379. doi: 10.1111/tpj.12388

Nintemann, S. J., Hunziker, P., Andersen, T. G., Schulz, A., Burow, M., and Halkier, B. A. (2018). Localization of the glucosinolate biosynthetic enzymes reveals distinct spatial patterns for the biosynthesis of indole and aliphatic glucosinolates. *Physiol. Plant.* 163, 138–154. doi: 10.1111/ppl.12672

Øverby, A., Stokland, R. A., Åsberg, S. E., Sporsheim, B., and Bones, A. M. (2015). Allyl isothiocyanate depletes glutathione and upregulates expression of glutathione *S*-transferases in *Arabidopsis thaliana*. *Front. Plant Sci.* 6:277. doi: 10.3389/fpls.2015.00277

Parisy, V., Poinssot, B., Owsianowski, L., Buchala, A., Glazebrook, J., and Mauch, F. (2007). Identification of PAD2 as a γ-glutamylcysteine synthetase highlights the importance of glutathione in disease resistance of Arabidopsis. *Plant J.* 49, 159–172. doi: 10.1111/j.1365-313X.2006.02938.x

Pastorczyk, M., and Bednarek, P. (2016). "The function of glucosinolates and related metabolites in plant innate immunity," in *Glucosinolates*, ed. S. Kopriva (London: Academic Press Ltd-Elsevier Science Ltd.), 171–198. doi: 10.1016/bs.abr.2016.06.007

Pedras, M. S. C., Yaya, E. E., and Glawischnig, E. (2011). The phytoalexins from cultivated and wild crucifers: chemistry and biology. *Nat. Prod. Rep.* 28, 1381–1405. doi: 10.1039/C1NP00020A

Pedras, M. S. C., Yaya, E. E., and Hossain, S. (2010). Unveiling the phytoalexin biosynthetic puzzle in salt cress: unprecedented incorporation of glucobrassicin into wasalexins A and B. *Org. Biomol. Chem.* 8, 5150–5158. doi: 10.1039/c0ob00265h

Piślewska-Bednarek, M., Nakano, R. T., Hiruma, K., Pastorczyk, M., Sanchez-Vallet, A., Singkaravanit-Ogawa, S., et al. (2018). Glutathione transferase U13 functions in pathogen-triggered glucosinolate metabolism. *Plant Physiol.* 176, 538–551. doi: 10.1104/pp.17.01455

Ryu, H. Y., Kim, S. Y., Park, H. M., You, J. Y., Kim, B. H., Lee, J. S., et al. (2009). Modulations of AtGSTF10 expression induce stress tolerance and BAK1-mediated cell death. *Biochem. Biophys. Res. Commun.* 379, 417–422. doi: 10.1016/j.bbrc.2008.11.156

Schenck, C. A., Nadella, V., Clay, S. L., Lindner, J., Abrams, Z., and Wyatt, S. E. (2013). A proteomics approach identifies novel proteins involved in gravitropic signal transduction. *Am. J. Bot.* 100, 194–202. doi: 10.3732/ajb.1200339

Schlaeppi, K., Bodenhausen, N., Buchala, A., Mauch, F., and Reymond, P. (2008). The glutathione-deficient mutant pad2-1 accumulates lower amounts of glucosinolates and is more susceptible to the insect herbivore *Spodoptera littoralis*. *Plant J.* 55, 774–786. doi: 10.1111/j.1365-313X.2008.03545.x

Sonderby, I. E., Geu-Flores, F., and Halkier, B. A. (2010). Biosynthesis of glucosinolates - gene discovery and beyond. *Trends Plant Sci.* 15, 283–290. doi: 10.1016/j.tplants.2010.02.005

Su, T., Xu, J., Li, Y., Lei, L., Zhao, L., Yang, H., et al. (2011). Glutathione-indole-3-acetonitrile is required for camalexin biosynthesis in *Arabidopsis thaliana*. *Plant Cell* 23, 364–380. doi: 10.1105/tpc.110.079145

Tohge, T., Nishiyama, Y., Hirai Masami, Y., Yano, M., Nakajima, J.-I., Awazuhara, M., et al. (2005). Functional genomics by integrated analysis of metabolome and transcriptome of Arabidopsis plants over-expressing an MYB transcription factor. *Plant J.* 42, 218–235. doi: 10.1111/j.1365-313X.2005.02371.x

Urbancsok, J., Bones, A., and Kissen, R. (2017). Glucosinolate-derived isothiocyanates inhibit Arabidopsis growth and the potency depends on their side chain structure. *Int. J. Mol. Sci.* 18:2372. doi: 10.3390/ijms18112372

Urbancsok, J., Bones, A. M., and Kissen, R. (2018). Arabidopsis mutants impaired in glutathione biosynthesis exhibit higher sensitivity towards the glucosinolate hydrolysis product allyl-isothiocyanate. *Sci. Rep.* 8:9809. doi: 10.1038/s41598-018-28099-1

Wagner, U., Edwards, R., Dixon, D. P., and Mauch, F. (2002). Probing the diversity of the Arabidopsis glutathione *S*-transferase gene family. *Plant Mol. Biol.* 49, 515–532. doi: 10.1023/a:1015557300450

Wangwattana, B., Koyama, Y., Nishiyama, Y., Kitayama, M., Yamazaki, M., and Saito, K. (2008). Characterization of PAP1-upregulated glutathione *S*-transferase genes in *Arabidopsis thaliana*. *Plant Biotechnol.* 25, 191–196. doi: 10.5511/plantbiotechnology.25.191

Wentzell, A. M., Rowe, H. C., Hansen, B. G., Ticconi, C., Halkier, B. A., and Kliebenstein, D. J. (2007). Linking metabolic QTLs with network and cis-eQTLs controlling biosynthetic pathways. *PLoS Genet.* 3:e162. doi: 10.1371/journal.pgen.0030162

Wittstock, U., Kurzbach, E., Herfurth, A. M., and Stauber, E. J. (2016). "Glucosinolate breakdown," in *Glucosinolates*, ed. S. Kopriva (London: Academic Press Ltd-Elsevier Science Ltd.), 125–169. doi: 10.1016/bs.abr.2016.06.006

Xu, J., Li, Y., Wang, Y., Liu, H., Lei, L., Yang, H., et al. (2008). Activation of MAPK Kinase 9 induces ethylene and camalexin biosynthesis and enhances sensitivity to salt stress in Arabidopsis. *J. Biol. Chem.* 283, 26996–27006. doi: 10.1074/jbc.M801392200

Zhang, Y. S., Kolm, R. H., Mannervik, B., and Talalay, P. (1995). Reversible conjugation of isothiocyanates with glutathione catalyzed by human glutathione transferases. *Biochem. Biophys. Res. Commun.* 206, 748–755. doi: 10.1006/bbrc.1995.1106

Conflict of Interest Statement: The authors declare that the research was conducted in the absence of any commercial or financial relationships that could be construed as a potential conflict of interest.

frontiers in Plant Science

ORIGINAL RESEARCH
published: 15 November 2018
doi: 10.3389/fpls.2018.01659

Protein-Ligand Fishing *in planta* for Biologically Active Natural Products Using Glutathione Transferases

David P. Dixon[1†] *and Robert Edwards*[2*]

[1] *Biophysical Sciences Institute, Durham University, Durham, United Kingdom,* [2] *Agriculture, School of Natural and Environmental Sciences, Newcastle University, Newcastle upon Tyne, United Kingdom*

Screening for natural products which bind to proteins *in planta* has been used to identify ligands of the plant-specific glutathione transferase (GST) tau (U) and phi (F) classes, that are present in large gene families in crops and weeds, but have largely undefined functions. When expressed as recombinant proteins in *Escherichia coli* these proteins have been found to tightly bind a diverse range of natural product ligands, with fatty acid-and porphyrinogen-derivatives associated with GSTUs and a range of heterocyclic compounds with GSTFs. With an interest in detecting the natural binding partners of these proteins *in planta*, we have expressed the two best characterized GSTs from *Arabidopsis thaliana* (*At*), *At*GSTF2 and *At*GSTU19, as *Strep*-tagged fusion proteins *in planta.* Following transient and stable expression in Nicotiana and Arabidopsis, respectively, the GSTs were recovered using Strep-Tactin affinity chromatography and the bound ligands desorbed and characterized by LC-MS. *At*GSTF2 predominantly bound phenolic derivatives including *S*-glutathionylated lignanamides and methylated variants of the flavonols kaempferol and quercetin. *At*GSTU19 captured glutathionylated conjugates of oxylipins, indoles, and lignanamides. Whereas the flavonols and oxylipins appeared to be authentic *in vivo* ligands, the glutathione conjugates of the lignanamides and indoles were artifacts formed during extraction. When tested for their binding characteristics, the previously undescribed indole conjugates were found to be particularly potent inhibitors of *At*GSTU19. Such ligand fishing has the potential to both give new insight into protein function *in planta* as well as identifying novel classes of natural product inhibitors of enzymes of biotechnological interest such as GSTs.

Keywords: glutathione conjugates, oxylipins, indole derivatives, lignanamides, flavonoids

OPEN ACCESS

Edited by:
Nikolaos E. Labrou, Agricultural University of Athens, Greece

Reviewed by:
Nerino Allocati, Università degli Studi G. d'Annunzio Chieti e Pescara, Italy
Elif Öztetik, Eskisehir Technical University, Turkey

***Correspondence:**
Robert Edwards
robert.edwards@ncl.ac.uk

†Present address:
David P. Dixon, GlaxoSmithKline, Stevenage, United Kingdom

Specialty section:
This article was submitted to Plant Physiology, a section of the journal Frontiers in Plant Science

Received: *08 June 2018*
Accepted: *25 October 2018*
Published: *15 November 2018*

Citation:
Dixon DP and Edwards R (2018) Protein-Ligand Fishing in planta for Biologically Active Natural Products Using Glutathione Transferases. Front. Plant Sci. 9:1659. doi: 10.3389/fpls.2018.01659

INTRODUCTION

The Arabidopsis genome encodes 55 members of the soluble glutathione transferase (GSTs; EC 2.5.1.18) superfamily, notably members of the plant specific phi (F), tau (U), lambda (L) and dehydroascorbate reductase (DHAR) classes, as well as theta (T), zeta (Z) enzymes (Dixon and Edwards, 2010). The majority of these genes are expressed *in planta* as the respective proteins and show both a complex regulation and sub-cellular localization (Dixon et al., 2009; Jiang et al., 2013; Labrou et al., 2015). As enzymes, plant GSTs can use glutathione (GSH) as either a cofactor,

or co-substrate. Activities described to date include the reduction of dehydroascorbate (DHAR), the isomerization of tyrosine degradation products (GSTZ), the reduction of oxidized phenolics (GSTLs) and organic hydroperoxides (GSTF, GSTU, and GSTT) as well as glutathionylating electrophilic natural products and xenobiotics (GSTF and GSTU), including herbicides (Dixon and Edwards, 2010). However, despite displaying this range of enzyme activities *in vitro*, we know relatively little of the function of these proteins *in planta* (Labrou et al., 2015). Using *Arabidopsis thaliana* (*At*) as a model, it has been recognized for some time that the large families of *At*GSTUs and *At*GSTFs (Dixon and Edwards, 2010), are subject to complex regulation in response to infection, abiotic stress, and development (Marrs, 1996; Moons, 2005; Jiang et al., 2013). In some cases, reverse-genetic approaches have confirmed roles for specific GSTs. For example, *At*GSTF12 is involved in the regulation of anthocyanin accumulation (Kitamura et al., 2004), while *At*GSTU20 modulates responses to light reception (Chen et al., 2007) and *At*GSTU17 plays a regulatory role in seedling development (Jiang et al., 2013).

In the case of *At*GSTF12, biochemical function can be linked to the observed phenotype of the knock-out, as inferred through metabolic profiling of the flavonoids present in the respective transparent testa 19 (TT19) mutants (Kitamura et al., 2004; Sun et al., 2012). The *tt19* mutants, which are defective in functional *At*GSTF12 expression, were deficient in anthocyanin and anthocyanidin pigments, while showing elevated levels of flavonol intermediates as compared with wild type plants. Subsequently, *At*GSTF12 was shown to bind the anthocyanins cyanidin and cyanidin-3-*O*-glycoside, but was unable to conjugate them with GSH (Sun et al., 2012). From this it was concluded that *At*GSTF12 is an anthocyanin transporter protein, or ligandin, able to transport these pigments for deposition in the vacuole, through its concerted action with TT12, a tonoplast-localized flavonoid/H+-antiporter (Kitamura et al., 2010). As such, *At*GSTF12 has orthologous functions to other GSTF genes involved in flavonoid accumulation namely, *AN9* in petunia (Mueller et al., 2000), *Fl3* in carnation (Larsen et al., 2003), and *VvGST4* in grapevine (Gomez et al., 2011).

The observation that *At*GSTF12 has a non-enzymic ligand transport, or ligandin function has prompted us to look for binding associations for these proteins in plants, using 'ligand fishing' to identify associations with natural products. In its simplest format, individual GSTs are expressed in microbial, or plant hosts, and then subjected to metabolic profiling to identify intermediates that accumulate due to binding interactions with the 'ligandin.' Using this methodology with tau class proteins expressed in *Escherichia coli*, we identified that maize (*Zea mays*) *Zm*GSTU1 and *Zm*GSTU2 interacted with porphyrinogen intermediates and caused the hyperaccumulation of colored porphyrins (Dixon et al., 2008). In contrast, when 25 *At*GSTUs were expressed in *E. coli*, they each caused the aberrant accumulation of acylated glutathione thioesters, showing a surprising degree of enzyme-specific ligand selectivity in terms of chain length, oxygenation and desaturation (Dixon and Edwards, 2009). As a refinement to this ligand interaction screening, the GSTs were modified with an N-teminal *Strep*-binding motif, that allowed for the selective recovery of protein-ligand complexes using this tag (**Figure 1**). The *Strep*-motif was found to be particularly useful in the efficient recovery of fusion proteins, having been developed from a peptide library as the optimal tag-partner of the modified streptavidin termed *Strep*-Tactin (Wisser et al., 2011). Using Strep-tagged *At*GSTUs and *At*GSTFs, we have recovered a variety of ligands from bacteria and plant extracts. These can be broadly divided into a chemically diverse group of natural products that bind as their glutathionylated derivatives (fatty acids, oxylipins, chlorogenic acid), or as a more discreet group of unconjugated natural products derived from indoles, phenols or heterocycles (Dixon et al., 2008; Dixon and Edwards, 2009; Dixon et al., 2011). In the majority of cases, the biological significance of these binding interactions is questionable, as either the ligands available to the tagged GSTs were present in heterologous microbial or plant hosts, or in *in vitro* plant extracts.

In the current study, we now report on a directed and systematic search for natural products that selectively bind to the two best characterized and abundant GSTs in Arabidopsis, namely *At*GSTU19 and *At*GSTF2, when these proteins are expressed in living plants. The strategy adopted has used the *Strep*-tagged GSTs as protein 'hooks,' which when either expressed *in planta* transiently (*Nicotiana benthamiana*), or stably (Arabidopsis) bind endogenous ligands in the host which can then be recovered following affinity capture of the fusion

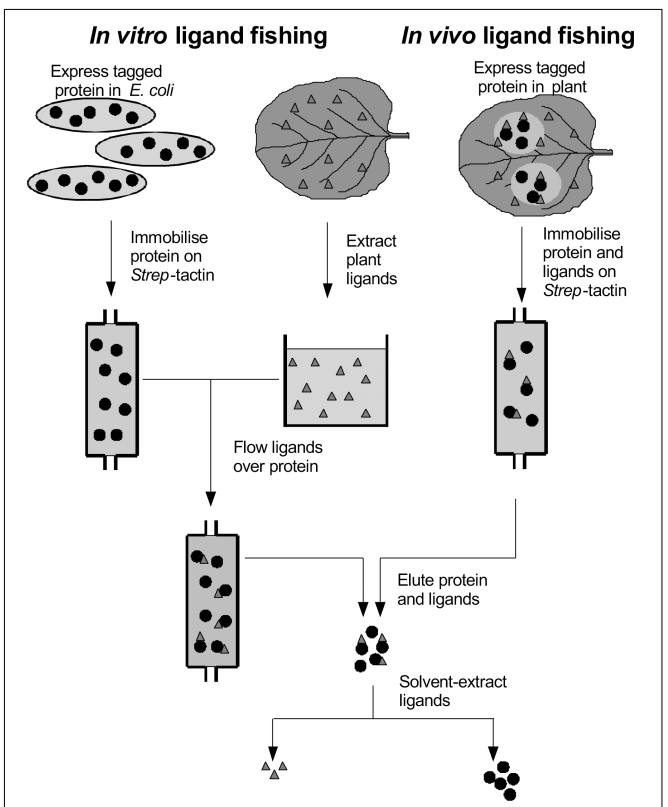

FIGURE 1 | Ligand fishing with Strep-tagged glutathione transferases.

protein (**Figure 1**). Any compounds recovered have then been characterized in detail by high resolution mass spectrometry (MS) and by reference to prepared standards.

MATERIALS AND METHODS

Preparation of Reference Ligands

Kaempferol and kaempferol-3,4′-dimethyl were obtained from Apin (Abingdon, United Kingdom). Other flavonols were extracted from the surface of *N. benthamiana* by dipping 200 g of intact leaves in 500 ml methanol. The extract was concentrated, clarified by centrifugation and hexane added to 20% v/v. After centrifugation, the aqueous phase was applied onto an Accubond II C18 SPE column (1000 mg; Agilent Technologies United Kingdom Ltd., Stockport, United Kingdom). After washing with methanol:water (1:1), flavonols were recovered in methanol (5 ml) and individually purified by preparative reversed phase HPLC as described (Dixon et al., 2012), but using a 5–100% gradient of acetonitrile. Flavonols were quantified by UV absorbance, assuming $\varepsilon_{351\ nm} = 14\ mM^{-1}$.

To generate 3-methylindolyl glutathionyl disulfide (ISSG), *bis*-(3-indolemethyl) disulfide (ISSI) was synthesized as described (Himel et al., 1962) and reduced to 3-thiomethylindole (ISH) by mixing 125 μl of 165 mM ISSI in dimethyl sulphoxide (DMSO) with 125 μl of 200 mM tris-(2-carboxyethyl)phosphine (TCEP) in DMSO and 125 μl of 1.0 M Tris-Cl pH 7.5. After 30 min at 22°C, 750 μl of 0.1M GSH pH 7.0 was added together with 375 μl DMSO and 40 μl of 30% H_2O_2, and the reaction incubated for 16 h at 22°C. ISSG was purified from the reaction mixture by preparative reversed phase HPLC, and quantified by UV absorbance, assuming $\varepsilon_{280\ nm} = 5\ mM^{-1}$. N-*trans*-feruloyltyramine was prepared as described (Villegas and Brodelius, 1990). Mixed lignanamides were formed by reacting 40 mM feruloyltyramine in methanol at 20°C for 1 h with one volume of 2.5% w/v aqueous solution of $FeCl_3$ (Sakakibara et al., 1992). Products were extracted with ethyl acetate, partitioned against water and the organic phase dried and re-dissolved in methanol. Lignanamide-GSH conjugates were synthesized by incubating 160 μM feruloyltyramine (or mixed lignanamides) for 30 min at 20°C with 0.1 μM horseradish peroxidase, 1 mM GSH and 200 μM H_2O_2 in 50 mM Tris-Cl pH 7.5.

Enzyme and Ligand Binding Assays

Isothermal titration calorimetry (ITC) experiments were performed at 25°C in HBS buffer and analyzed using a VP-ITC instrument with Origin 7.0 software (GE Healthcare, Amersham, United Kingdom). Where ligands were added in solvents, an equivalent volume of ethanol was used as control. With the flavonols, 0.1% w/v Tween 20 was used to increase ligand solubility. In addition to titrating ligand into protein, control titrations of ligand into buffer and buffer into protein were performed. For studies with *At*GSTF2, the respective Strep-tagged protein was purified from *E. coli* grown in minimal medium to minimize contamination with pre-bound ligands and used in ITC assuming 1:1 binding to ligand, as previously determined (Dixon et al., 2011).

Plant Studies

Untransformed Arabidopsis root cultures were grown as described (DeRidder et al., 2002), without illumination. GST coding sequences were sub-cloned into BIN-STRP3 to allow constitutive and transient expression of N-terminally *Strep*-tagged enzymes in Arabidopsis and Nicotiana, respectively (Dixon et al., 2009). Stable transformants of arabidopsis (ecotype Columbia) were generated by floral dipping (Clough and Bent, 1998). Control plants were generated by transforming with the empty vector pCAMBIA3300[1]. Transformants were selected by spraying soil-grown seedlings with 0.02% w/v glufosinate ammonium, and lines expressing high levels of recombinant protein chosen by western blotting using alkaline phosphatase-linked *Strep*-Tactin as probe. Herbicide-resistant T2 and T3 plants were used for pull-down experiments. GSTs were purified from frozen plant tissue using 4 v/w 100 mM Tris-Cl pH 7.5 containing 150 mM NaCl, 1 mM EDTA, 50 μg/ml avidin, 10 $\mu g.ml^{-1}$ bovine pancreatic DNase I, 10 $\mu g.ml^{-1}$ bovine pancreatic RNase A and 5% w/v insoluble polyvinylpolypyrrolidone. For *N. benthamiana* extractions, 10 mM sodium ascorbate was also included. After filtration through miracloth (Calbiochem) and clarification by centrifugation (15,000 *g*, 20 min, 4°C), the *Strep*-GSTs were affinity purified as described (Dixon and Edwards, 2009). Purified proteins were concentrated to approx. 100 μl by ultrafiltration through a 10 kDa-cutoff membrane (2 ml Vivaspin; Sartorius Stedim United Kingdom Ltd., Epsom, United Kingdom). Ligands from bacterial, plant and *in vitro* pull-downs were analyzed by HPLC-MS as described (Dixon and Edwards, 2009).

RESULTS

Fishing for Ligands of Plant GSTs *in planta*: Transient Expression in *N. benthamiana*

*At*GSTF2 and *At*GSTU19 were individually transformed into the leaves of *N. benthamiana* through *Agrobacterium* infection using vacuum infiltration. In addition, *At*GSTU7, a tau class enzyme showing similar binding activities to *At*GSTU19 (Dixon and Edwards, 2009), was used in early studies for comparative purposes. After 3 days, the infiltrated leaves (50 g) were harvested and the *Strep*-tagged proteins purified from crude extracts using *Strep*-Tactin affinity chromatography. Both *Strep*-tagged GSTs were strongly expressed in *N. benthamiana* and were recovered in good yields as the pure proteins (**Figure 2**). Having immobilized the GSTs on the *Strep*-Tactin columns, the washed proteins were selectively desorbed using desthiobiotin and then solvent-extracted with methanol. The bound ligands were then analyzed by HPLC-MS (**Figure 3**), with the chemical characteristics of each metabolite identified summarized in **Table 1**. For reference, the

[1]www.cambia.org

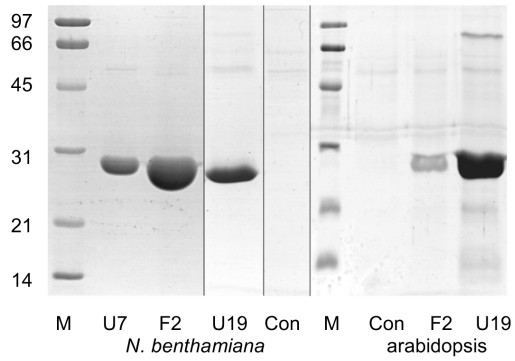

FIGURE 2 | Composite image showing Coomassie Brilliant Blue-stained SDS-PAGE analysis of GST purified by *Strep*-tactin affinity chromatography after expression in *Nicotiana benthamiana* and arabidopsis. Lane M, molecular weight markers (sizes as indicated, in kDa); U7, *At*GSTU7; F2, *At*GSTF2; U19, *At*GSTU19; Con, infiltration control.

ligands recovered when the Strp-tagged proteins were expressed in *E. coli* is shown (**Figure 1**). In each case, the deduced identities of the ligands are summarized in **Figure 4**, with each ligand assigned a unique number (**1–19**).

When over-expressed in *E. coli* grown on minimal media as described previously (Dixon et al., 2008), the recovered Strep-tagged GSTU proteins were found to exclusively retain glutathionylated porphyrins (**Figure 3A**). While *At*GSTU7 preferentially retained the protoporphyrin conjugate (**2**), *At*GSTU19 showed a marked preference for the harderoporphyrin (**1**) derivative. These metabolites were not retained by *At*GSTF2, neither were they identified in any of the subsequent plant expression studies. When expressed in Nicotiana, *At*GSTU19 was found to bind multiple metabolites (**Figure 3B**), which on the basis of their mass spectra (Dixon and Edwards, 2009), could be identified as glutathionylated conjugates of chlorogenic acid (**3**, **4**) and oxylipins (**8**, **10**). The other tau protein, *At*GSTU7 was not found to bind any unique ligands and was not analyzed further. *At*GSTF2 bound similar oxylipin conjugates, as well as retaining metabolites which based on their UV absorbance spectra, were aromatic in nature (compounds **5** to **13**; **Figure 3B**). The more polar ligands (compounds **5**, **6,** and **7**)**,** had the characteristic UV spectra of phenolics. In each case, tandem MS analysis showed neutral losses of fragments of 75 Da, 129 Da, and 307 Da, along with an *m/z* 308 ion, characteristic of glutathione conjugates (**Supplementary Figure S1**). Compound **7** was the most abundant of these ligands, with its properties consistent with it being a glutathione conjugate of the condensation product of two *trans-N*-feruloyltyramine molecules, such as grossamide (Yoshihara et al., 1981), or cannabisin D (Sakakibara et al., 1992). Previously undescribed in the literature, such a conjugate would be most likely formed from the 1,4-Michael addition of GSH to the α, β-unsaturated amide (**Figure 4**). By analogy, **5** was most likely a glutathionylated derivative of grossamide K (**Table 1** and **Figure 4**), which consists of feruloyltyramine condensed with coniferyl alcohol (Seca et al., 2001). Compound **6** appeared to be a

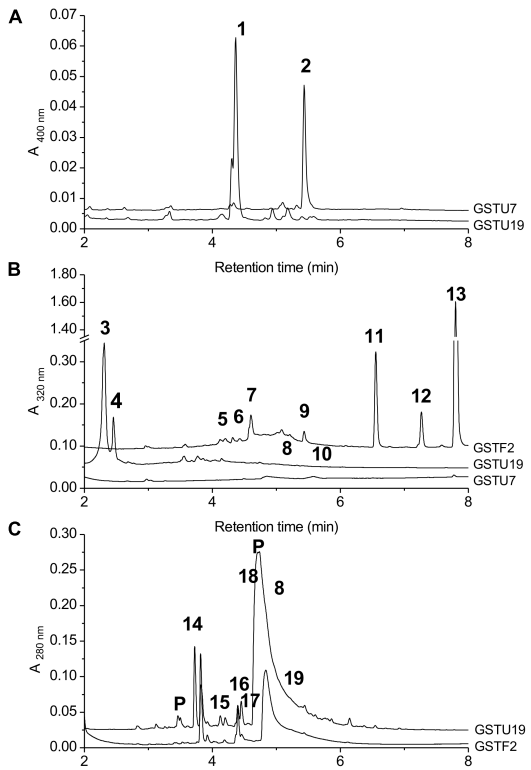

FIGURE 3 | HPLC-MS of GST ligands described in the text. **(A)** Extracts from bacteria expressing GSTU19 (black line) or GSTU7 (gray line), showing accumulation of porphyrin metabolites **1** and **2**. No major peaks at 400 nm were observed in comparable extracts from control bacteria. **(B)** Bound ligands recovered from purified *Strep*-tagged GSTU7, GSTU19 and GSTF2 transiently expressed in *N. benthamiana*, showing additional ligands **5**–**13** bound to GSTF2 and ligands **3**, **4**, **8,** and **10** bound to GSTU19. **(C)** Bound ligands from purified GSTF2 (gray line) and GSTU19 (black line) following stable expression in arabidopsis showing additional ligands **8** and **14**–**19** bound to GSTU19. Peaks labeled "P" were GSTs or proteolysis-derived oligopeptide fragments.

glutathionylated derivative of the condensate of feruloyltyramine with hydroxyconiferyl alcohol (**Table 1** and **Figure 4**). By way of confirmation of these structural assignments, orthologues of **7** were synthesized by the oxidative glutathionylation of feruloyltyramine. The resulting products were shown to have near identical chromatographic characteristics and MS spectra to **7**, consistent with them being structural isomers of the *At*GSTF2 ligand (**Supplementary Figure S2**). To investigate the origins of the conjugated ligand, *At*GSTU19 was incubated with feruloyltyramine and GSH. *At*GSTU19 was unable to catalyze the formation of the conjugate indicating that the ligands had been generated by an alternative mechanism.

The UV spectra of the more hydrophobic compounds **9**, **11**, **12,** and **13** were consistent with them being related to flavonoids. To characterize these compounds in greater detail, whole *N. benthamiana* leaves were extracted using two protocols to extract total and surface associated hydrophobic metabolites, respectively. Using total methanolic extracts of homogenized *N. benthamiana* leaves, compounds **11**, **12,** and

TABLE 1 | Properties of GST ligands identified by HPLC-MS.

Peak	λ_{max} (nm)	*m/z*	Likely identity
1	394	916.374	harderoporphyrin-SG
2	399	870.356	protoporphyrin-SG
3	252, 323	660.163	chlorogenic acid-SG
4	252, 314	660.165	isomer of chlorogenic acid-SG
5	277	799.276	grossamide K-SG
6	284	815.270	hydroxy-grossamide K-SG
7	283, 307 (sh)	932.326	grossamide-SG, cannabisin D-SG
8	–	600.283	10-*S*-glutathionyl-12-oxo-phytodienoic acid
9	265, 344	477.127	kaempferol-3,7′-dimethylether-4′-*O*-glucoside
10	–	600.284	oxylipin-SG
11	267, 348	315.080	kaempferol-3,7′-dimethylether
12	253, 268 (sh), 353	359.105	quercetin-3,7,3′,4′-tetramethylether
13	267, 346	329.103	kaempferol-3,7,4′-trimethylether
14	279	469.121	ISSG
15	272, 374	501.094	ISSSG
16	272, 375	533.068	ISSSSG
17	–	602.312	oxylipin-SG
18	Not resolved	565.037	ISSSSSG
19	Not resolved	597.001	ISSSSSSG

*Compounds **1** and **2** bound AtGSTU19 and AtGSTU7, respectively in Escherichia coli, compounds **3**, **4**, **8**, and **10** bound AtGSTU19 in Nicotiana benthamiana (Dixon and Edwards, 2009), compounds **5**–**13** bound GSTF2 in N. benthamiana and compounds **8** and **14**–**19** bound AtGSTU19 in arabidopsis. Sh, shoulder; SG, S-glutathione; IS, 3-thiomethylindole. Compound structures are illustrated in **Figure 2** and CID mass and UV spectra are as published (Dixon and Edwards, 2009), or are shown in **Supplementary Figure S1**.*

13 could all be identified as minor components (**Figure 3**). In contrast, **11**, **12,** and **13** were major metabolites when leaves were surface-washed with solvent, suggesting these metabolites selectively accumulated on the leaf surface. To confirm their identity, surface washes from multiple leaves were combined and the phenolics present concentrated and characterized (**Table 1**). All the compounds were identified as polymethylated flavonols, namely kaempferol-3,7-dimethylether (**11**), quercetin-3,7,3′,4′-tetramethylether (**12**), and kaempferol-3,7,4′-trimethylether (**13**). The minor polar compound **9** was tentatively identified as the 4′-*O*-glucoside of **11** (**Figure 4**).

Expression of GSTs *in planta* should be the best way to promote interactions between GSTs and physiologically relevant ligands. However, the inevitable tissue disruption on extraction into aqueous buffer has the potential to generate artifacts arising from the interaction between a GST and a ligand usually found in a different compartment, or the generation of ligands formed through chemical- or enzyme-mediated oxidation during extraction. To examine the effects of oxidation during processing, *in vitro* ligand fishing experiments were performed where metabolites were initially extracted in solvent and then passed over the immobilized GST, thereby reducing the potential for spontaneous, or enzyme-catalyzed oxidative reactions. In the case of the *At*GSTF2 ligands, while the flavonols and oxylipin conjugates observed in plant expression studies were consistently recovered, the flavonolignans were not identified, suggesting these were artifacts of the extraction protocol and not true metabolites.

Identification of Ligands of GSTs Stably Expressed in Arabidopsis

Arabidopsis was stably transformed with constructs allowing the constitutive expression of *Strep*-tagged *At*GSTF2 and *At*GSTU19. The foliage of 12 week old plants was then harvested and the *Strep*-tagged GSTs isolated. Compared to the studies *in N. benthamiana*, *At*GSTF2 was only weakly expressed in Arabidopsis (**Figure 2**), with the associated poor recoveries of protein resulting in a failure to identify associated ligands. In contrast, *Strep*-tagged *At*GSTU19 was obtained in reasonable yield and found to co-purify with five UV-absorbing peaks that were not present in the controls (**Figure 3C**). These compounds (**14**, **15**, **16**, **18**, and **19**), were a series of related metabolites that eluted as a series of peaks, each differing in *m/z* value by +31.97 when analyzed by MS. Taking into account the increasing contribution of the M+2 isotopic ion, it was clear that the chemical composition of these compounds differed solely in the number of sulfur atoms present. UV spectral and MS-MS analysis suggested the presence of an indole moiety, while fragmentation with neutral losses of 75 Da and 129 Da were characteristic of glutathionylated conjugates (**Supplementary Figure S1**). The simplest compound in the series (**14**, **Table 1**), was identified as 3-methylindolyl glutathionyl disulfide (ISSG; **Figure 4**), with its identity confirmed after synthesizing a reference standard (**Supplementary Figure S3**). By analogy, the later-eluting compounds were the respective tri- (**15**), tetra- (**16**), penta- (**18**), and hexa-sulfide (**19**) analogs (ISS_nG; **Table 1** and **Figure 4**). The presence of disulfide bonds was confirmed by reducing the mixture of ligands (compounds **14**–**19**) with 40 mM DTT for 3 h at 4°C. This treatment released a single indole compound, identified as 3-thiomethylindole. To determine whether or not these indole conjugates were formed in the course of extraction, solvent extracts from Arabidopsis foliage were incubated with recombinant *At*GSTU19. ISSG together with low levels of ISSSG were identified, while the higher polysulfides were absent. In their place, 3-glutathionyl-*S*-methylindole (ISG; MH^+ = *m/z* 437.15) was observed. This result suggested that the higher molecular weight disulfides were probably formed as a result of oxidative reactions during processing. Further non-UV absorbing ligands of *At*GSTU19 were identified as the glutathione conjugate of 12-oxo-phytodienoic acid (OPDA) **8**, and a related metabolite **17** with an elemental composition of GSH + $C_{18}H_{30}O_3$. After subtraction of the glutathionyl-moiety, compound **17** was most likely a conjugate of the oxylipin keto-octadecadienoic acid. In the case of these conjugates, it was likely that their binding was a consequence of the catalytic activity of the ligandin, with *At*GSTU19 previously shown to catalyze the glutathionylation of OPDA (Dixon and Edwards, 2009).

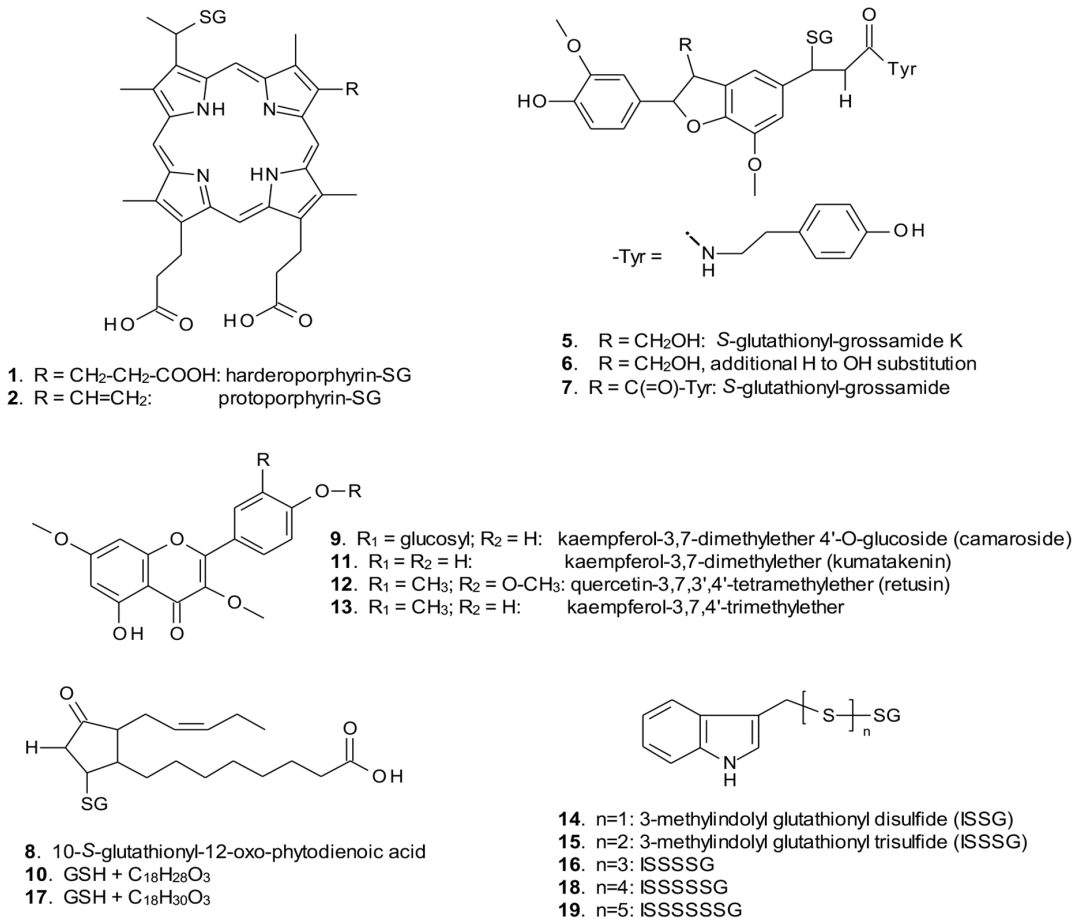

FIGURE 4 | Structures of GST ligands isolated from bacteria and plants in current and earlier studies. SG, *S*-glutathionyl. For ligands **2**, **5**–**7**, **9**, **11**, **12**, and **13**, multiple possible structural isomers exist, and one example is shown.

Binding and Inhibition of GSTs by *in vivo* Ligands

To investigate the binding characteristics of the ligands to the GSTs, isothermal titration calorimetry (ITC) was used to determine binding affinity and stoichiometry. With *At*GSTF2 the commercially available compounds kaempferol and kaempferol-3,7′-dimethylether were used, along with the methylated flavonols purified from the surface of the tobacco leaves (**Table 2** and **Supplementary Figure S4**). Kaempferol was a relatively poor ligand (K_d = 12 μM), with tighter binding determined with kaempferol-3,7′-dimethylether (**11**; K_d = 0.22 μM) and kaempferol-3,7,4′-trimethylether (**13**; K_d < 1 μM). The flavonols bound with a stoichiometry close to 0.5:1, suggesting a single high-affinity binding site per *At*GSTF2 dimer. When *At*GSTU19 was tested with ISSG, tight and stoichiometric binding was determined (**Table 2** and **Supplementary Figure S5**). *At*GSTU19 enzyme activity, as determined by the GSH conjugation of 1-chloro-2,4-dinitrobenzene, was inhibited by ISSG in a competitive manner with respect to GSH, confirming that ISSG binding occurred at the enzyme active site.

DISCUSSION

Identifying compounds that selectively bind to the active and regulatory sites of proteins is a well established method in defining the substrates and catalytic intermediates of enzymes, and ligands for receptors (Shinohara and Matsubayashi, 2007). In addition, assaying for potent binding activity is a powerful

TABLE 2 | ITC-derived thermodynamic parameters for titration of the compounds listed into GSTF2 in the presence of 1 mM glutathione.

	Parameter		
Interaction (+cofactors)	**N**	**K_a (μM^{-1})**	**ΔH (kcal/mol)**
GSTF2 + kaempferol (+GSH)	0.60 ± 0.05	0.08 ± 0.01	−12.6 ± 1.4
GSTF2 + **13** (+ GSH)	0.54 ± 0.01	4.50 ± 0.29	−18.4 ± 0.2
GSTU19 + ISSG	0.98 ± 0.01	8.54 ± 0.76	−10.6 ± 0.1
GSTU19 + *S*-hexylglutathione	0.84 ± 0.01	3.22 ± 0.19	−11.8 ± 0.1

In each case, parameters were obtained from fits to a one set of sites binding model, with errors representing standard error in the fitted model. Certain experiments contained GSH (1 mM).

route to discover small molecules that disrupt protein function through direct inhibition, or allosteric effects. Such inhibitors can then be used in applications in biomedicine and crop protection, with plant GSTs being an attractive target for selective chemical intervention given their multiple roles in stress tolerance of biotechnological interest (Nianiou-Obeidat et al., 2017). Classically, natural product ligands are discovered by fractionating crude biological extracts, screening preparations for biological activities against protein or cellular targets and then purifying and characterizing the compounds of interest (Weller, 2012). While such approaches have good provenance, the associated methods are time consuming and require the compounds to be isolated as being stable and present in quantities amenable for compositional and structural determination. As such, there is a real need to develop methods which accelerate the discovery of novel ligands, including intermediates which may be relatively unstable, and/or in low abundance as leads for new chemical intervention tools.

Using *Strep*-tagged GSTs as a test-bed, the current studies have demonstrated that previously undescribed ligands can be isolated from gram quantities of tissue following transient, or stable, expression in plants. The retained ligands could then be identified in yields allowing them to be identified by high resolution MS. Such 'ligand-fishing,' is a potentially powerful technology to both identify natural product high affinity binding partners of proteins as well as shedding light on their potential endogenous functions *in vivo*. The power of the approach was that it allowed for the recovery of protein-specific ligands that in several cases were unstable and therefore unlikely to be identified using conventional screening of total plant extracts. For both *At*GSTF2 and *At*GSTU19, the efficiency of ligand discovery was dependent on the level of protein expression *in planta*, the specificity and strength of recognition and the availability of low molecular weight binding partners in the host cell. The ligands identified could be functionally divided into those which were formed as artifacts of extraction, natural products recognized as reaction product orthologues and biologically active metabolites that were not linked to any known enzyme activity related to the GSTs.

With respect to artifacts, a comparison of the ligands bound when *At*GSTF2 was recovered from being expressed transiently in *Nicotiana* with those retained by the enzyme when solvent extracts from the identical plant tissue were passed over the immobilized protein, strongly suggested that the glutathionylated lignanamides (**5, 6, 7**) were artifacts formed during extraction. While the lignanamides cannabisin, grossamide and grossamide K have been described previously in plants (Yoshihara et al., 1981; Sakakibara et al., 1992; Seca et al., 2001), this is the first report of the corresponding glutathione conjugates being determined. The conjugates appear to be generated when feruloyltyramines are mixed with GSH in the presence of a radical-generating enzyme such as horseradish peroxidase acting on hydrogen peroxide. A similar mechanism has been described for ascorbate peroxidases catalyzing the glutathionylation of phenylpropanoids (Dean and Devarenne, 1997). Intriguingly, *At*GSTU19 did not bind to these ligands even though it did bind to a glutathionylated conjugate of the phenylpropanoid derivative chlorogenic acid (**3**). This may suggest that either the two GSTs have fundamentally different binding affinities for the liganamide conjugates, or that during extraction, *At*GSTF2 was transiently in closer proximity to the generation of these artifacts than *At*GSTU19. The functional significance of the binding to these ligands is unknown, though there is one report of feruloyltyramine weakly inhibiting GSTUs from poppy (Yu and Facchini, 2000). In the case of *At*GSTU19, evidence was obtained that at least some of the higher order polysulfides of glutathionylated 3-methylindole (**14**) isolated following expression in Arabidopsis were also formed as extraction artifacts. These derivatives have not been described previously and are presumably derived from indole-3-carbinol, a known degradation product of antifungal glucosinolates. The indole-3-carbinol is then proposed to interconvert to a reactive 3-methyleneindolenine intermediate that can react spontaneously with GSH to form a thiolated product (Staub et al., 2002). Our current work suggests that this reaction occurs in Arabidopsis and that the glutathione conjugate is enzymically processed to 3-thiomethylindole by a C-S lyase. The 3-thiomethylindole then forms a mixed disulfide with GSH to give **14**, with higher order di- tri- and tetra-sulfides forming through radical-enhanced disproportionation during the course of extraction. Thus, while the presence of 3-thiomethylindole would be likely to be a true product resulting from processing an endogenously formed glutathionylated detoxification product, the observed polysulfides would be most likely maintained at very low levels *in planta*, or only produced under conditions of oxidative stress.

The next group of ligands to be identified were glutathionylated natural products that represented examples of intermediates of GST-mediated metabolism *in planta*. Of these the glutathione conjugates of fatty acid oxylipin derivatives (**8, 10, 17**), detected bound to *At*GSTF2 in *N. benthamiana* and *At*GSTU19 in Arabidopsis were good examples. There has been significant interest in the *S*-glutathionylation of 12-oxo-phytodienoic acid (OPDA) and related compounds, with the conjugates accumulating in plants fed with oxylipins or infected with bacterial pathogens (Davoine et al., 2005, 2006). The lack of observed conjugate binding to *At*GSTF2 in arabidopsis and to *At*GSTU19 in *N. benthamiana* was most likely due to assay sensitivity and the relative levels of expression of the two *Strep*-tagged proteins in these plant hosts. Another key difference may be that while *At*GSTU19 could catalyze the formation of the oxylipin-glutathione conjugate, *At*GSTF2 could only capture the conjugate following its formation elsewhere. It is of interest that *At*GSTU19 catalyzes the formation of the OPDA conjugate, an activity previously reported for *At*GSTF8 in arabidopsis (Mueller et al., 2008). To date the physiological consequence of these conjugation reactions in plants are unknown, though similar derivatives of the chemically related leukotrienes are known to control the biological activity of chemically related prostraglandins in mammals (Wang and Ballatori, 1998).

Finally there were those ligands representing compounds that had no functional link to the catalytic activities of GSTs, but point to important endogenous functions in the binding and transport of secondary metabolites. The ligand fishing

studies with *At*GSTF2 in *N. benthamiana* identified a series of polyphenolic metabolites, identified as methylated derivatives of kaempferol and quercetin. In their unmethylated forms these flavonols had previously been shown to bind weakly to *At*GSTF2 (Smith et al., 2003), along with synthetic aromatics such as naphthalene acetic acid and 1-*N*-naphthylphthalamic acid (Zettl et al., 1994; Smith et al., 2003). The significance of flavonoid binding by plant GSTs has been most clearly demonstrated in genetic studies with the tau class AN9 GST from petunia and the phi GSTs Bz2 in maize and TT19 (=*At*GSTF12) in arabidopsis (Marrs et al., 1995; Mueller et al., 2000; Kitamura et al., 2004). Unlike *At*GSTF12, *At*GSTF2 is not essential to anthocyanin pigment biosynthesis in arabidopsis (Dixon et al., 2005). However, *At*GSTF2 has been linked to flavonoid metabolism *in planta*, showing reduced levels of expression in *tt4* flavonoid-deficient mutants and a relocation to the cytosol rather than the plasma membrane (Smith et al., 2003). Recent structural biology studies have revealed a specific binding pocket for flavonoids in *At*GSTF2 remote from the active site at the dimer interface of the protein (Ahmad et al., 2017). The current binding studies confirm that AtGSTF2 dimers bind a single molecule of kaempferol, or related methylated derivatives (**Table 2**), further pointing to a very specific interaction of this protein with flavonoids. In *N. benthamiana*, *At*GSTF2 selectively bound the hydrophobic flavonoids associated with the leaf surface, consistent with an association of the protein with membranes and extracellular deposition of hydrophobic natural products. In arabidopsis, no flavonoids were associated with *At*GSTF2, but both crude and surface-extracted metabolites in arabidopsis lacked the hydrophobic flavonoids seen in *N. benthamiana*.

Collectively, the current ligand fishing studies have identified a group of GST binding partners not previously identified in experiments conducted in recombinant bacteria. Our results demonstrate that the different GST classes exhibit a degree of ligand specificity. Predictably, ligands such as flavonoids derived from species-specific secondary metabolism clearly differed in the ligand fishing experiments in bacteria and plants. In the case of the more conserved primary metabolism the GSTUs were found to bind glutathionylated fatty acid derivatives in both plants and *E. coli*. In contrast the flavin and porphyrin metabolites that are core primary metabolites in the different hosts were only determined in the experiments in *E. coli*. *At*GSTU19 was only one of two Arabidopsis GSTs that selectively bound the glutathione conjugates of the heme precursors harderoporphyrin (ogen) (**1**) and protoporphyrin (ogen) (**2**) when expressed in *E. coli*, but failed to retain these ligands when present in either plant hosts. Based on previous studies with porphyrin binding maize GSTUs, this failure to bind these metabolites *in planta* is most likely because GSTU19 is predominantly expressed in the cytosol whereas these metabolites are synthesized in the chloroplast (Dixon et al., 2008).

Our studies shed further light on the ability of plant GSTs to bind, and in some cases glutathione-conjugate natural and synthetic ligands, which may well influence the availability, and biological activity of such ligands. While the ligands identified here are diverse, they represent many chemistries commonly encountered in plants, with the selectivity in recognition shown in just *At*GSTF2 and *At*GSTU19 demonstrating how these compounds could perform multiple and species-specific roles relating to signaling, transport and storage roles in both primary (fatty acid) and secondary (phenolic, alkaloid, and glucosinolate) metabolism, as has been recently proposed (Labrou et al., 2015). Using the results of these ligand capture experiments it will now be of interest to carry out directed metabolomic experiments to see if disruption of the expression of these 'ligandin' GSTs causes subtle alterations in these respective branches of metabolism under differing conditions of stress and plant growth.

AUTHOR CONTRIBUTIONS

DD and RE conceived the experiments, interpreted the data and wrote the manuscript. DD conducted the experimental work.

FUNDING

This work was carried out as part of grants BBC51227X1 and BB/L001489/1 funded by the Biotechnology and Biological Sciences Research Council (BBSRC).

SUPPLEMENTARY MATERIAL

The Supplementary Material for this article can be found online at: https://www.frontiersin.org/articles/10.3389/fpls.2018.01659/full#supplementary-material

REFERENCES

Ahmad, L., Rylott, E. L., Bruce, N. C., Edwards, R., and Grogan, G. (2017). Structural evidence for *Arabidopsis* glutathione transferase AtGSTF2 functioning as a transporter of small organic ligands. *FEBS Open Biol.* 7, 122–132. doi: 10.1002/2211-5463.12168

Chen, I.-C., Huang, I.-C., Liu, M.-J., Wang, Z.-G., Chung, S.-S., and Hsieh, H.-L. (2007). Glutathione S-transferase interacting with far-red insensitive 219 is involved in phytochrome A-mediated signaling in Arabidopsis. *Plant Physiol.* 143, 1189–1202. doi: 10.1104/pp.106.094185

Clough, S. J., and Bent, A. F. (1998). Floral dip: a simplified method for Agrobacterium-mediated tranformation of *Arabidopsis thaliana*. *Plant J.* 16, 735–743. doi: 10.1046/j.1365-313x.1998.00343.x

Davoine, C., Douki, T., Iacazio, G., Montillet, J. L., and Triantaphylides, C. (2005). Conjugation of keto fatty acids to glutathione in plant tissues. Characterization and quantification by HPLC-tandem mass spectrometry. *Anal. Chem.* 77, 7366–7372. doi: 10.1021/ac051155y

Davoine, C., Falletti, O., Douki, T., Iacazio, G., Ennar, N., Montillet, J. L., et al. (2006). Adducts of oxylipin electrophiles to glutathione reflect a 13 specificity of the downstream lipoxygenase pathway in the tobacco hypersensitive response. *Plant Physiol.* 140, 1484–1493. doi: 10.1104/pp.105.074690

Dean, J. V., and Devarenne, T. P. (1997). Peroxidase-mediated conjugation of glutathione to unsaturated phenylpropanoids. Evidence against glutathione S-transferase involvement. *Physiol. Plant.* 99, 271–278. doi: 10.1111/j.1399-3054.1997.tb05412.x

DeRidder, B. P., Dixon, D. P., Beussman, D. J., Edwards, R., and Goldsbrough, P. B. (2002). Induction of glutathione S-transferases in Arabidopsis by herbicide safeners. *Plant Physiol.* 130, 1497–1505. doi: 10.1104/pp.010066

Dixon, D. P., and Edwards, R. (2009). Selective binding of glutathione conjugates of fatty acid derivatives by plant glutathione transferases. *J. Biol. Chem.* 284, 21249–21256. doi: 10.1074/jbc.M109.020107

Dixon, D. P., and Edwards, R. (2010). *Glutathione Transferases. In: The Arabidopsis Book*. Rockville, MD: American Society of Plant Biologists, 1–15. doi: 10.1199/tab.0131

Dixon, D. P., Hawkins, T., Hussey, P. J., and Edwards, R. (2009). Enzyme activities and subcellular localization of members of the *Arabidopsis* glutathione transferase superfamily. *J. Exp. Bot.* 60, 1207–1218. doi: 10.1093/jxb/ern365

Dixon, D. P., Lapthorn, A., Madesis, P., Mudd, E. A., Day, A., and Edwards, R. (2008). Binding and glutathione conjugation of porphyrinogens by plant glutathione transferases. *J. Biol. Chem.* 283, 20268–20276. doi: 10.1074/jbc.M802026200

Dixon, D. P., Sellars, J. D., and Edwards, R. (2011). The Arabidopsis phi class glutathione transferase AtGSTF2: binding and regulation by biologically active heterocyclic ligands. *Biochem. J.* 438, 63–70. doi: 10.1042/BJ20101884

Dixon, D. P., Sellars, J. D., Kenwright, A. M., and Steel, P. G. (2012). The maize benzoxazinone DIMBOA reacts with glutathione and other thiols to form spirocyclic adducts. *Phytochemistry* 77, 171–178. doi: 10.1016/j.phytochem.2012.01.019

Dixon, R. A., Xie, D.-Y., and Sharma, S. B. (2005). Proanthocyanidins - a final frontier in flavonoid research? *New Phytol.* 165, 9–28.

Gomez, C., Conejero, G., Torregrosa, L., Cheynier, V., Terrier, N., and Ageorges, A. (2011). *In vivo* grapevine anthocyanin transport involves vesicle-mediated trafficking and the contribution of anthoMATE transporters and GST. *Plant J.* 67, 960–970. doi: 10.1111/j.1365-313X.2011.04648.x

Himel, C. M., Lee, N., and Silverstein, R. M. (1962). *Condensed Ring Heterocyclic Disulfides and Sulfides*. Baltimore: U.S.P.

Jiang, L., Shen, X., Shoji, T., Kanda, T., Zhou, J., and Zhao, L. (2013). Characterization and activity of anthocyanins in Zijuan Tea (*Camellia sinensis* var. kitamura). *J. Agric. Food Chem.* 61, 3306–3310. doi: 10.1021/jf304860u

Kitamura, S., Matsuda, F., Tohge, T., Yonekura-Sakakibara, K., Yamazaki, M., Saito, K., et al. (2010). Metabolic profiling and cytological analysis of proanthocyanidins in immature seeds of *Arabidopsis thaliana* flavonoid accumulation mutants. *Plant J.* 62, 549–559. doi: 10.1111/j.1365-313X.2010.04174.x

Kitamura, S., Shikazono, N., and Tanaka, A. (2004). TRANSPARENT TESTA 19 is involved in the accumulation of both anthocyanins and proanthocyanidins in Arabidopsis. *Plant J.* 37, 104–114. doi: 10.1046/j.1365-313X.2003.01943.x

Labrou, N. E., Papageorgiou, A. C., Pavli, O., and Flemetakis, E. (2015). Plant GSTome: structure and functional role in xenome network and plant stress response. *Curr. Opin. Biotechnol.* 32, 186–194. doi: 10.1016/j.copbio.2014.12.024

Larsen, E., Alfenito, M., Briggs, W., and Walbot, V. (2003). A carnation anthocyanin mutant is complemented by the glutathione S-transferases encoded by maize Bz2 and petunia An9. *Plant Cell Rep.* 21, 900–904.

Marrs, K. A. (1996). The functions and regulation of glutathione S-transferases in plants. *Annu. Rev. Plant Physiol. Plant Mol. Biol.* 47, 127–158. doi: 10.1146/annurev.arplant.47.1.127

Marrs, K. A., Alfenito, M. R., Lloyd, A. M., and Walbot, V. (1995). A glutathione S-transferase involved in vacuolar tansfer encoded by the maize gene Bronze-2. *Nature* 375, 397–400. doi: 10.1038/375397a0

Moons, A. (2005). Regulatory and functional interactions of plant growth regulators and plant glutathione S-transferases (GSTs). *Vitam. Horm.* 72, 155–202. doi: 10.1016/S0083-6729(05)72005-7

Mueller, L. A., Goodman, C. D., Silady, R. A., and Walbot, V. (2000). AN9, a petunia glutathione S-transferase required for anthocyanin sequestration, is a flavonoid-binding protein. *Plant Physiol.* 123, 1561–1570. doi: 10.1104/pp.123.4.1561

Mueller, S., Hilbert, B., Dueckershoff, K., Roitsch, T., Krischke, M., Mueller, M. J., et al. (2008). General detoxification and stress responses are mediated by oxidized lipids through TGA transcription factors in Arabidopsis. *Plant Cell* 20, 768–785. doi: 10.1105/tpc.107.054809

Nianiou-Obeidat, I., Madesis, P., Kissoudis, C., Voulgari, G., Chronopoulou, E., Tsaftaris, A., et al. (2017). Plant glutathione transferase-mediated stress tolerance: functions and biotechnological applications. *Plant Cell Rep.* 36, 791–805. doi: 10.1007/s00299-017-2139-7

Sakakibara, I., Ikeya, Y., Hayashi, K., and Mitsuhashi, H. (1992). Three phenyldihydronaphthalene lignanamides from fruits of *Cannabis sativa*. *Phytochemistry* 31, 3219–3223. doi: 10.1016/0031-9422(92)83479-I

Seca, A. M. L., Silva, A. M. S., Silvestre, A. J. D., Cavaleiro, J. A. S., Domingues, F. M. J., and Pascoal-Neto, C. (2001). Lignanamides and other phenolic constituents from the bark of kenaf (*Hibiscus cannabinus*). *Phytochemistry* 58, 1219–1223. doi: 10.1016/S0031-9422(01)00311-9

Shinohara, H., and Matsubayashi, Y. (2007). Functional immobilization of plant receptor-like kinase onto microbeads towards receptor array construction and receptor-based ligand fishing. *Plant J.* 52, 175–184. doi: 10.1111/j.1365-313X.2007.03204.x

Smith, A. P., Nourizadeh, S. D., Peer, W. A., Xu, J., Bandyopadhyay, A., Murphy, A. S., et al. (2003). Arabidopsis AtGSTF2 is regulated by ethylene and auxin, and encodes a glutathione S-transferase that interacts with flavonoids. *Plant J.* 36, 433–442. doi: 10.1046/j.1365-313X.2003.01890.x

Staub, R. E., Feng, C., Onisko, B., Bailey, G. S., Firestone, G. L., and Bjeldanes, L. F. (2002). Fate of indole-3-carbinol in cultured human breast tumor cells. *Chem. Res. Toxicol.* 15, 101–109. doi: 10.1021/tx010056m

Sun, Y., Li, H., and Huang, J. R. (2012). Arabidopsis TT19 functions as a carrier to transport anthocyanin from the cytosol to tonoplasts. *Mol. Plant.* 5, 387–400. doi: 10.1093/mp/ssr110

Villegas, M., and Brodelius, P. E. (1990). Elicitor-induced hydroxycinnamoyl-CoA: tyramine hydroxycinnamoyltransferase in plant cell suspension cultures. *Physiol. Plant.* 78, 414–420. doi: 10.1111/j.1399-3054.1990.tb09057.x

Wang, W., and Ballatori, N. (1998). Endogenous glutathione conjugates: occurrence and biological functions. *Pharmacol. Rev.* 50, 335–355.

Weller, M. G. (2012). A unifying review of bioassay-guided fractionation, effect-directed analysis and related techniques. *Sensors* 12, 9181–9209. doi: 10.3390/s120709181

Wisser, R. J., Kolkman, J. M., Patzoldt, M. E., Holland, J. B., Yu, J. M., Krakowsky, M., et al. (2011). Multivariate analysis of maize disease resistances suggests a pleiotropic genetic basis and implicates a GST gene. *Proc. Natl. Acad. Sci. U.S.A.* 108, 7339–7344. doi: 10.1073/pnas.1011739108

Yoshihara, T., Yamaguchi, K., Takamatsu, S., and Sakamura, S. (1981). A new lignan amide, grossamide, from bell pepper (*Capsicum annuum* var. grossum). *Agric. Biol. Chem.* 45, 2593–2598.

Yu, M., and Facchini, P. J. (2000). Molecular cloning and characterization of a type III glutathione S-transferase from cell suspension cultures of opium poppy treated with a fungal elicitor. *Physiol. Plant.* 108, 101–109. doi: 10.1034/j.1399-3054.2000.108001101.x

Zettl, R., Schell, J., and Palme, K. (1994). Photoaffinity labeling of *Arabidopsis thaliana* plasma membrane vesicles by 5-azido-[7-3H]indole-3-acetic acid: identification of a glutathione S-transferase. *Proc. Natl. Acad. Sci. U.S.A.* 91, 689–693. doi: 10.1073/pnas.91.2.689

Conflict of Interest Statement: The authors declare that the research was conducted in the absence of any commercial or financial relationships that could be construed as a potential conflict of interest.

frontiers in Plant Science

ORIGINAL RESEARCH
published: 30 November 2018
doi: 10.3389/fpls.2018.01737

Expanding the Plant GSTome Through Directed Evolution: DNA Shuffling for the Generation of New Synthetic Enzymes With Engineered Catalytic and Binding Properties

*Evangelia G. Chronopoulou[1], Anastassios C. Papageorgiou[2], Farid Ataya[3], Irini Nianiou-Obeidat[4], Panagiotis Madesis[5] and Nikolaos E. Labrou[1]**

[1] Laboratory of Enzyme Technology, Department of Biotechnology, School of Food, Biotechnology and Development, Agricultural University of Athens, Athens, Greece, [2] Turku Centre for Biotechnology, University of Turku and Åbo Akademi University, Turku, Finland, [3] Department of Biochemistry, College of Science, King Saud University, Riyadh, Saudi Arabia, [4] Laboratory of Genetics and Plant Breeding, School of Agriculture, Forestry and Natural Environment, Aristotle University of Thessaloniki, Thessaloniki, Greece, [5] Institute of Applied Biosciences, Centre for Research and Technology Hellas (CERTH), Thessaloniki, Greece

OPEN ACCESS

Edited by:
Danièle Werck,
Centre national de la recherche scientifique (CNRS), France

Reviewed by:
Arnaud Hecker,
Université de Lorraine, France
Manosh Kumar Biswas,
University of Leicester, United Kingdom

***Correspondence:**
Nikolaos E. Labrou
lambrou@aua.gr

Specialty section:
This article was submitted to Plant Metabolism and Chemodiversity, a section of the journal Frontiers in Plant Science

Received: 28 May 2018
Accepted: 08 November 2018
Published: 30 November 2018

Citation:
Chronopoulou EG, Papageorgiou AC, Ataya F, Nianiou-Obeidat I, Madesis P and Labrou NE (2018) Expanding the Plant GSTome Through Directed Evolution: DNA Shuffling for the Generation of New Synthetic Enzymes With Engineered Catalytic and Binding Properties. Front. Plant Sci. 9:1737. doi: 10.3389/fpls.2018.01737

Glutathione transferases (GSTs, EC. 2.5.1.18) are inducible multifunctional enzymes that are essential in the detoxification and degradation of toxic compounds. GSTs have considerable biotechnological potential. In the present work, a new method for the generation of synthetic GSTs was developed. Abiotic stress treatment of *Phaseolus vulgaris* and *Glycine max* plants led to the induction of total GST activity and allowed the creation of a GST-enriched cDNA library using degenerated GST-specific primers and reverse transcription-PCR. This library was further diversified by employing directed evolution through DNA shuffling. Activity screening of the evolved library led to the identification of a novel tau class GST enzyme (*PvGm*GSTUG). The enzyme was purified by affinity chromatography, characterized by kinetic analysis, and its structure was determined by X-ray crystallography. Interestingly, *PvGm*GSTUG displayed enhanced glutathione hydroperoxidase activity, which was significantly greater than that reported so far for natural tau class GSTs. In addition, the enzyme displayed unusual cooperative kinetics toward 1-chloro-2,4-dinitrochlorobenzene (CDNB) but not toward glutathione. The present work provides an easy approach for the simultaneous shuffling of GST genes from different plants, thus allowing the directed evolution of plants GSTome. This may permit the generation of new synthetic enzymes with interesting properties that are valuable in biotechnology.

Keywords: glutathione transferase, directed evolution, DNA shuffling, protein engineering, synthetic biotechnology

INTRODUCTION

GSTs are multifunctional enzymes that have evolved from a thioredoxin-like ancestor gene (Mannervik, 2012; Labrou et al., 2015). They are involved in different functions such as the detoxification, metabolism, and transport or sequestration of a wide range of endogenous or xenobiotic compounds. GSTs catalyze the nucleophilic attack of reduced GSH (γ-Glu–Cys–Gly)

on the electrophilic center of these compounds, leading to the formation of GSH conjugates that display higher solubility and reduced toxicity (Deponte, 2013; Labrou et al., 2015; Perperopoulou et al., 2018).

The majority of cytoplasmic GSTs forms dimers of two identical or different subunits of 23–30 kDa (Labrou et al., 2015; Pégeot et al., 2017). Each subunit displays two ligand-binding sites: a G-site and an H-site. The GSH binds with high specificity to the G-site, which is conserved and is located at the N-terminal domain of the polypeptide. The H-site is the binding site for the electrophilic substrate. It is less conserved and determines the affinity and specificity of GSTs toward the electrophile substrates (Labrou et al., 2015; Pégeot et al., 2017). An induced-fit mechanism has been proposed to facilitate the binding and accommodation of the substrates (GSH and electrophile substrate) to the G- and H-sites (Neuefeind et al., 1997; Axarli et al., 2009a,b).

GSTs are expressed both constitutively and in response to biotic and abiotic stresses including herbicides, herbicide safeners, temperature, chill, drought, light, heavy metals, pathogens, and others (Skipsey et al., 2011; Kissoudis et al., 2015; Islam et al., 2017, 2018; Nianiou-Obeidat et al., 2017; Skopelitou et al., 2017). GSTs are encoded by a large and diverse gene family in plants, which is termed the GSTome. The GSTome differs in the number of GSTs, herbicide specificity, and inducibility in different plants and stress conditions (Liu et al., 2013; Csiszár et al., 2014; Pégeot et al., 2014; Han et al., 2018). Heavy metals and high temperature are also considered as inductors of GST expression and function (Gajewska and Skłodowska, 2008; Wang et al., 2017).

The GSTome consists of the functional GSTs that are encoded and expressed by a genome (Mannervik, 2012). The GSTome comprises the cytosolic, mitochondrial, and microsomal superfamilies. Each superfamily composed by several diverse classes (Nianiou-Obeidat et al., 2017). For example, the cytosolic superfamily in plants has fourteen different classes: tau (U), phi (F), theta (T), zeta (Z), lambda (L), γ-subunit of the eukaryotic translation elongation factor 1B (EF1Bγ), dehydroascorbate reductase (DHAR), metaxin, tetrachlorohydroquinone dehalogenase (TCHQD), Ure2p, and microsomal prostaglandin E synthase type 2 (mPGES-2) (Liu et al., 2013; Lallement et al., 2014a,b). Recently, three new classes were identified in plants: hemerythrin (GSTH), iota (GSTI), and glutathionyl-hydroquinone reductases (GHRs) (Yang et al., 2014). The tau and phi classes have the largest number of GSTs in plants (Liu et al., 2013; Csiszár et al., 2014; Pégeot et al., 2014; Han et al., 2018). Both classes contribute considerable and play key roles in the detoxification of several classes of herbicides (Edwards and Dixon, 2000; Chronopoulou and Labrou, 2009).

The wide catalytic capabilities of GSTs along with their ideal structural features, such as stability, efficient heterologous expression in *E. coli* and purification by a single-step affinity chromatography have encouraged their exploitation in different areas of biotechnology (Perperopoulou et al., 2018). For example, selected GST isoenzymes are being exploited for the assembly of enzyme biosensors, which can find application in the measurements of xenobiotics, such as drugs, toxins, and herbicides (Kapoli et al., 2008; Chronopoulou et al., 2012b; Oliveira et al., 2013; Materon et al., 2014). Furthermore, GSTs have been used in nanobiotechnology for the construction of biochips (Voelker and Viswanathan, 2013; Zhang et al., 2013; Zhou et al., 2014), nanowires and nanorings (Bai et al., 2013; Hou et al., 2013). In plant biotechnology, GSTs are useful tools in plant breeding programs for the development of plant varieties with multiple stresses resistant traits. Alternatively, the use of genetic engineering allows the development of transgenic plants with traits beyond the limitation of the existing genetic variability (Kissoudis et al., 2015; Nianiou-Obeidat et al., 2017). There is, therefore, an urgent need to discover new GST isoenzymes with desired properties for the development of new or novel applications. Protein engineering efforts for the design of new enzymes with improved catalytic and structural properties are required (Broo et al., 2002; Kurtovic et al., 2008; Runarsdottir and Mannervik, 2010).

In the present work, DNA shuffling was employed for the design and creation of a library of tau class GSTs (GSTUs) from abiotic stress-treated *Phaseolus vulgaris* and *Glycine max*. Screening of the library led to the selection of a new GST variant. The new enzyme was characterized by kinetic analysis and X-ray crystallography. The results demonstrated that random recombination of fragments from homologous GSTUs from different plants can give rise to new functionally synthetic GST enzyme.

RESULTS AND DISCUSSION

Analysis of the Catalytic Diversity of GSTome From *P. vulgaris* and *G. max* Under Control and Abiotic Stress Treatments

Transcriptomics and genomics projects have showed that plants have multiple genes coding for GSTs (Nianiou-Obeidat et al., 2017; Han et al., 2018). For example, in the *Glycine max* var. Williams 82 genome, 101 gene loci encode putative GSTs (Liu et al., 2015). The analysis of *P. vulgaris* trascriptomic and genomic data (available at https://phytozome.jgi.doe.gov) reveal the presence of at least 52 transcripts that encode putative GSTs (unpublished results). Plant GSTs are inducible enzymes that respond to biotic and abiotic stresses (Chronopoulou et al., 2012a; Csiszár et al., 2014; Pégeot et al., 2014; Han et al., 2018). In the present study, the induction of total GST activity in *P. vulgaris* and *G. max* tissues was evaluated in response to different chemical and physical stress agents to expand the repertoire of differently expressed GST isoenzymes with diverse catalytic and functional properties.

Abbreviations: Abbreviations: BDNB, 1-bromo-2,4-dinitrobenzene; CDNB, 1-chloro-2,4-dinitrobenzene; IDNB, 1-iodo-2,4-dinitrobenzene; FDNB, 1-fluoro-2,4-dinitrobenzene; CuOOH, cumenehydroperoxide; DHAR, dehydroascorbate; Fluorodifen, 4-nitrophenyl 2-nitro-4-trifluoromethylphenyl ether; G-site, glutathione binding site; GSH, glutathione; GST, glutathione transferase; HED, 2-hydroxyethyldisulfide; H-site, hydrophobic binding site; *PvGm*GST, GST variant created by DNA shuffling of GSTome from *Phaseolus vulgaris* and *Glycine max*.

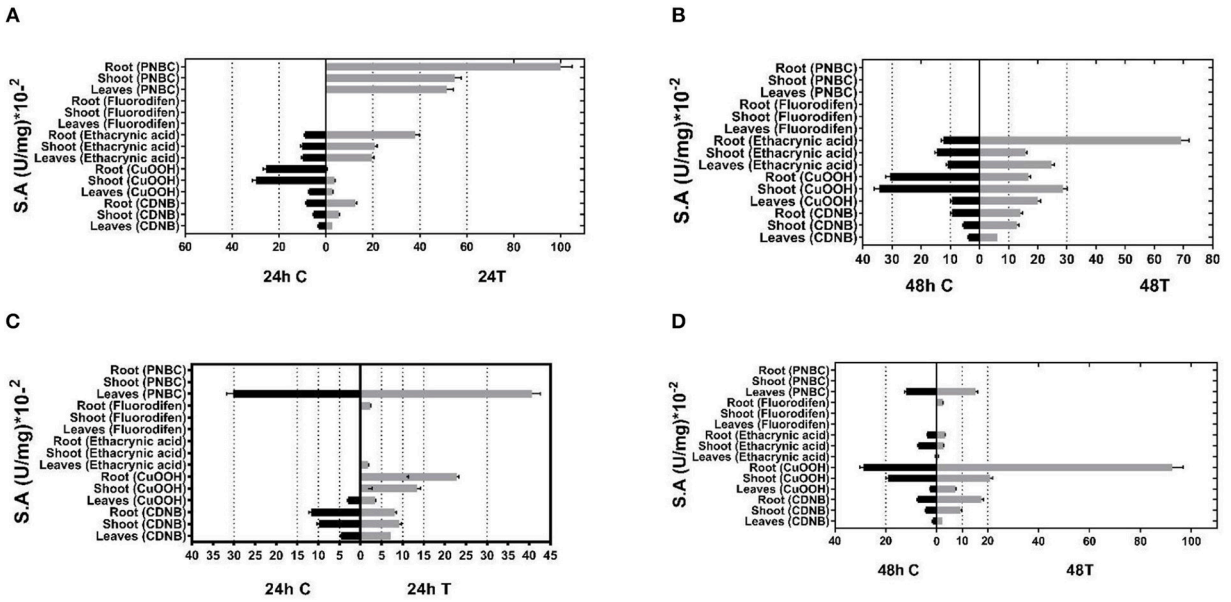

FIGURE 1 | GST-specific activities of extracts from tissues (leaves, shoots, roots) of control and stressed plants after 24 and 48 h treatment for (**A**,**B**, respectively) and Phaseolus vulgaris (**C**,**D**, respectively) total activity was measured using CDNB, CuOOH, ethacrynic acid, fluorodifen, and NBD-Cl as substrates. Results represent the means of triplicate determinations, with variation less than 5% in all cases.

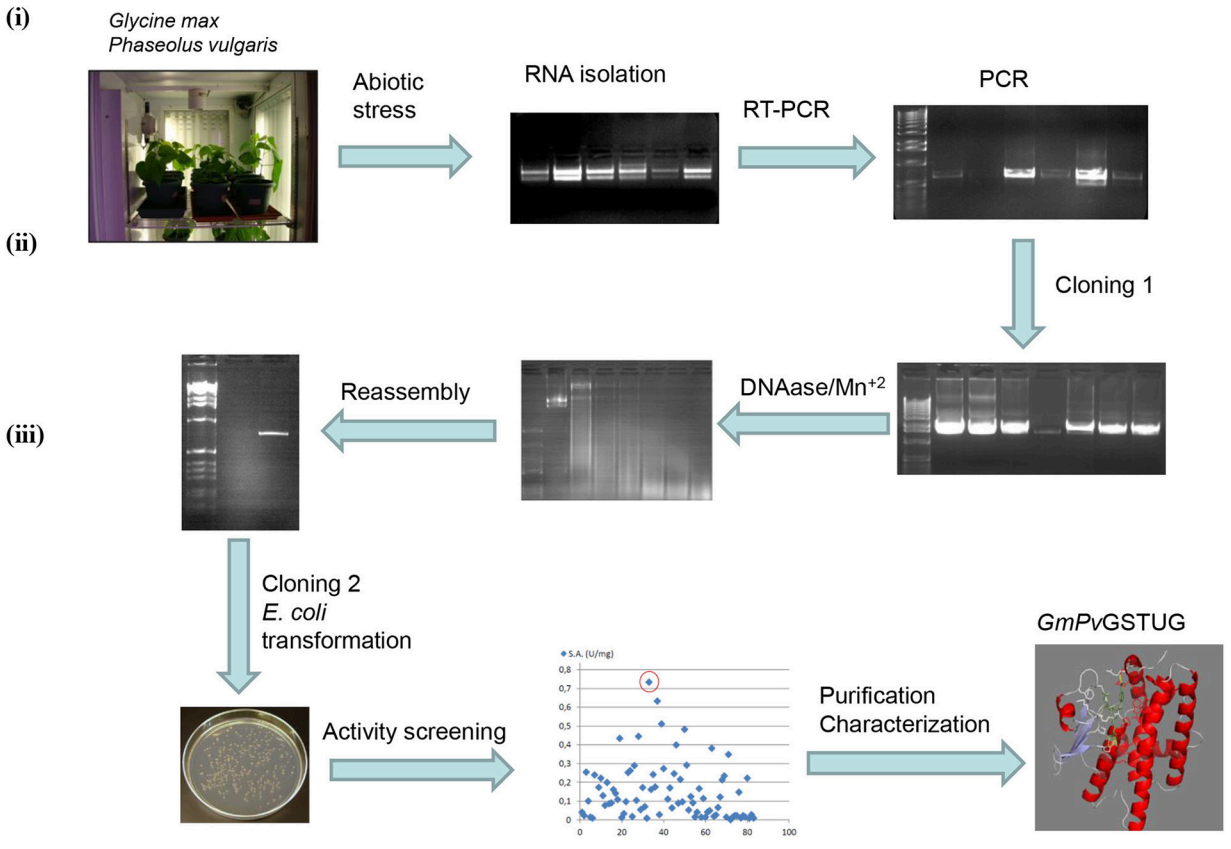

FIGURE 2 | Schematic diagram of the experimental approach used for the generation of the synthetic GST gene and its corresponding enzyme *PvGm*GSTUG (i) Abiotic stress treatments of *Phaseolus vulgaris* and *Glycine max* plants lead to induction of total GST activity and allowed the creation of a GST-enriched cDNA library using degenerated GST-specific primers and reverse transcription-PCR; (ii) The GST-enriched library was further diversified employing directed evolution through DNA shuffling; (iii) Activity screening of the evolved library led to the isolation of a novel *tau* class GST enzyme (*PvGm*GST), which was purified and characterized.

Given the inducible expression of GSTs under different abiotic stress conditions, young *P. vulgaris* and *G. max* plants were exposed to different abiotic stressors, such as a mixture of different herbicides (atrazine, alachlor, fluazifop-p-butyl), heavy metals (nickel, zinc, and chromium) as well as heat-shock (37°C). The purpose of these combined stress treatments was to invoke the expression of GST activities that are induced only following exposure to abiotic stresses (Kissoudis et al., 2015). Following the treatments, plants were harvested, homogenized, and crude extracts were assayed for GST activities using spectrophotometric assays and a range of different model substrates. Total GST activity was extracted from different plant tissues (leaf, root, and shoot) of both control plants and treated plants and measured using five different substrates: 1-chloro-2,4-dinitrobenzene (CDNB), cumene hydroperoxide (CuOOH), the herbicide fluorodifen, ethacrynic acid, and p-nitrobenzyl chloride (pNBC). The choice of these substrates was based on different chemistries involved in catalytic reactions (e.g., nucleophile substitution, addition, hydroperoxidation) to expand the possibilities of obtaining a broad range of catalytic functionalities. Prior experience has demonstrated that a high proportion of functional GSTs can be obtained by this approach (Chronopoulou et al., 2012a; Li et al., 2017a,b). The results (**Figure 1**) showed that the application of multiple stress conditions resulted in a large increase in total GST activity. For example, using CDNB as a substrate, a 1.4–2.3-fold increase was observed in different tissues, compared to the control plants in the 48 h treatment. CuOOH and ethacrynic acid produced a 1.1–3.2-fold and 1.1–5.6-fold increase in total GST activity, respectively. The results indicated that following abiotic stress treatment different GST isoenzymes were upregulated in different *P. vulgaris* and *G. max* tissues, suggesting an increased diversity in catalytic activities.

Shuffling of cDNAs Encoding GSTs From *P. vulgaris* and *G. max* and Selection of a New Variant

The method of DNA shuffling is an effective strategy for generating genetic diversity and for identifying protein variants with improved or altered functional or structural properties. The DNA shuffling protocol consists of the following steps: (i) selection and preparation of genes to be shuffled, (ii) digestion of the selected genes with DNase I for generation of a mixture of DNA fragments (size 50–100 bp), (iii) reassembly of DNA fragments with PCR without primers, and (iv) amplification of reassembled products by a conventional PCR. During the PCR reactions, point mutations may be generated. Abiotic stress treatment of *P. vulgaris* and *G. max* makes them perfect starting materials for producing a cDNA library enriched with GSTs (**Figure 2**). Thus, RNA from stressed tissues (leaf, root, and shoot treated for 48 h) was reverse transcribed and the GST genes were amplified using PCRs and degenerate primers. The PCR amplicons of putative GST genes were cloned and the resulted recombinant plasmids were isolated, mixed, and used for *in vitro* recombination by DNA shuffling (Zhao and Arnold, 1997; Axarli et al., 2016, 2017). Following *in vitro* recombination, a single PCR product was cloned into the pEXP5-CT/TOPO®TA plasmid. Different colonies (180 in total) were screened for GST activity. Approximately 46% of the picked colonies exhibited GST activity, suggesting that the recombination produced a library with high proportion of catalytically active GSTs (**Figure 3**). Interestingly, the mean specific activity was 0.17 U/mg and 52% of the active colonies displayed specific activity higher than 0.1 U/mg. The GST variant that displayed the highest activity was selected for further characterization. This clone was sequenced (**Figure 4A**) and revealed a 672 bp open reading frame encoding a protein of 224 amino acid residues with a molecular mass of 26,088.08 Da and a theoretical pI of 5.80. BLAST searches showed that both its nucleotide (BLASTN) as well as amino acid sequences (BLASTP) were novel and absent from all public databases (**Tables 1**, **2**; **Supplementary Figures 1**, **2**). The phylogenetic relationship of this new enzyme with other GSTs from all known classes was investigated by the construction of a phylogenetic tree that was generated by multiple amino acid sequence alignment (**Figure 4B**). The alignment was created using representative members of all classes of the *Glycine max* GST family (*Gm*GSTs) (McGonigle et al., 2000; Liu et al., 2015). The enzyme that resulted from DNA shuffling, which was denoted as *PvGm*GSTUG in accordance with the nomenclature proposed by Edwards et al. (2000), clustered together with the tau class GSTs. Of note, as evident from the data provided in **Tables 1**, **2**, *PvGm*GSTUG displayed the highest homology

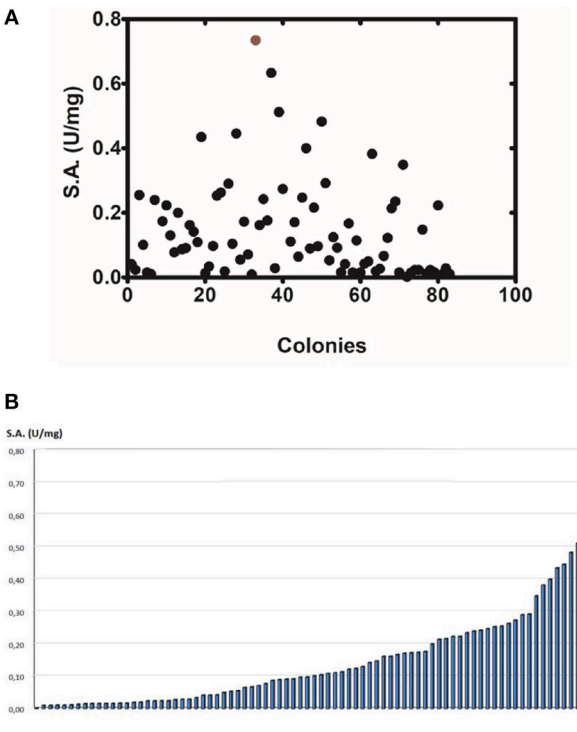

FIGURE 3 | Activity screening **(A)**. Activity screening of different colonies obtained following DNA shuffling. The graph depicts only the colonies with detectable activity toward the substrate system CDNB/GSH. **(B)** Distribution of the specific activity of different colonies.

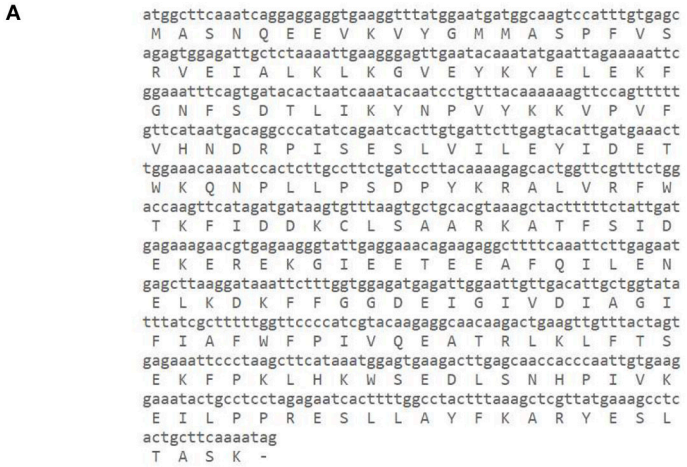

FIGURE 4 | Sequence and phylogenetic analysis **(A)**. Nucleotide and amino acid sequence of the *PvGm*GSTUG **(B)**. Phylogenetic analysis of *PvGm*GSTUG with representative members from all classes of the *Glycine max* GST family. Sequences were aligned with the CLUSTAL Omega sequence alignment program (Sievers et al., 2011) and the phylogenetic tree was constructed using Geneious 9.1.2 software (http://www.geneious.com; Kearse et al., 2012) with the UPGMA tree building method and iTOL v1.0 software (Ciccarelli et al., 2006). Various classes can be distinguished: *Phi* (GSTF), *Tau* (GSTU), *Lambda* (GSTL), *Theta* (GSTT), *Dehydroascorbate reductase* (DHAR), *Elongation factor 1Bγ* (EF1Bγ), *Zeta* (GSTZ), and *Tetrachloro-hydroquinone dehalogenase* (TCHQD). The accession numbers of Glycine max GSTs that were used for this phylogenetic tree are: *Phi* class: *Gm*GSTF1 (AJE59615.1), *Gm*GSTF2 (AJE59616.1), *Gm*GSTF3 (AJE59618.1), *Tau* class: *Gm*GSTU1 (AJE59646.1), *Gm*GSTU2 (AJE59647.1), *Gm*GSTU3 (AJE59651.1), *Lambda* class: *Gm*GSTL1 (AJE59633.1), *Gm*GSTL2 (AJE59634.1), *Gm*GSTL3 (AJE59635.1), *Theta* class: *Gm*GSTT1 (AJE59641.1), *Gm*GSTT2 (AJE59642.1), *Gm*GSTT3 (AJE59643.1), *DHAR* class: *Gm*GSTDHAR1 (AJE59631.1), *Gm*GSTDHAR2 (AJE59630.1), *Gm*GSTDHAR3 (AJE59629.1), *EF1Bgamma* class: *Gm*GSTEF1Bgamma1 (AJE59625.1),*Gm*GSTEF1Bgamma2 (AJE59626.1), *Gm*GSTEF1Bgamma3 (AJE59627.1) *Zeta* class: *Gm*GSTZ2 (AJE59689.1), *Gm*GSTZ1 (AJE59691.1) *TCHQD* class: *Gm*GSTTCHQD1 (AJE59638.1), *Gm*GSTTCHQD2 (AJE59639.1), and *Gm*GSTTCHQD3 (AJE59640.1).

(87 and 86 % homology at the nucleotide and amino acid level, respectively,) with a GST from *Medicago truncatula* (nucleotide and amino acid accession codes XM_003623148.2 and XP_003623196.1, respectively), rather than the GSTs from *Phaseolus vulgaris* and *Glycine max*, in excellent agreement with their evolution history. This important observation further supports the evolution theory of legume plants (Cronk et al., 2006). Amino acid sequence alignments and phylogenetic analysis of *PvGm*GSTUG with the *tau* class GSTs from *G. max* and *P. vulgaris* revealed that the *PvGm*GSTUG displayed higher

TABLE 1 | Percent amino acid identity matrix of *PvGm*GSTUG with the first 12 sequences identified in the BLASTP search.

	***PvGm*GSTUG**	***Mt*GS1**	***Mt*GST2**	***Mt*GST3**	***Ts*Pr1**	***Ts*Pr2**	***Ca*GST1**	***Ca*GST2**	***Mt*GST4**	***Mt*GST5**	***Ts*Pr3**	***Mt*GST6**
1:*PvGm*GSTUG	**100.00**	85.71	77.68	77.68	77.23	75.00	74.55	72.77	73.66	76.26	71.82	71.43
2:*Mt*GST1	85.71	**100.00**	79.91	78.12	77.23	75.00	78.57	74.55	75.00	78.54	72.73	74.55
3:*Mt*GST2	77.68	79.91	**100.00**	79.02	80.36	77.68	74.55	74.55	77.23	80.37	76.36	75.45
4:*Mt*GST3	77.68	78.12	79.02	**100.00**	74.55	73.66	74.11	75.45	89.29	81.28	80.00	86.61
5:*Ts*Pr1	77.23	77.23	80.36	74.55	**100.00**	87.95	75.89	73.66	74.11	79.91	76.82	70.54
6:*Ts*Pr2	75.00	75.00	77.68	73.66	87.95	**100.00**	70.54	69.64	72.32	77.17	72.73	69.20
7:*Ca*GST1	74.55	78.57	74.55	74.11	75.89	70.54	**100.00**	79.46	72.32	75.34	73.64	71.43
8:*Ca*GST2	72.77	74.55	74.55	75.45	73.66	69.64	79.46	**100.00**	74.11	75.80	72.27	72.77
9:*Mt*GST4	73.66	75.00	77.23	89.29	74.11	72.32	72.32	74.11	**100.00**	80.37	77.73	87.50
10:*Mt*GST5	76.26	78.54	80.37	81.28	79.91	77.17	75.34	75.80	80.37	**100.00**	79.07	76.26
11:*Ts*Pr3	71.82	72.73	76.36	80.00	76.82	72.73	73.64	72.27	77.73	79.07	**100.00**	74.55
12:*Mt*GST6	71.43	74.55	75.45	86.61	70.54	69.20	71.43	72.77	87.50	76.26	74.55	**100.00**

For the analysis, the amino acid sequence of PvGmGSTUG was used in the query. Percent identity matrix was calculated with the CLUSTAL Omega sequence alignment program (Sievers et al., 2011). The accession numbers of the GST sequences that resulted from the searches were: MtGST.1, (Medicago truncatula GST, XP_003623196.1); MtGST.2, (Medicago truncatula GST, XP_003623195.1); MtGST.3, (Medicago truncatula GST, XP_003623174.1); CaGST1, (Cicer arietinum GST3, ALZ41813.1); CaGST2, (Cicer arietinum GST, XP_004492376.1); MtGST4, (Medicago truncatula GST, XP_013449023.1); MtGST5, (Medicago truncatula GST, XP_003623168.1); MtGST6, (Medicago truncatula GST, XP_003623173.1); LaGST, (Lupinus angustifolius GST, XP_019459310.1); MtGST7, (Medicago truncatula GST, XP_003623171.2); GmGST1, (Glycine max GST, NP_001238439.1); CcGST, (Cajanus cajan GST, XP_020206357.1); GmGST2, (Glycine max GST, NP_001304556.1); GsGST1, (Glycine soja, KHN05112.1); and GsGST2, (Glycine soja, KHN06986.1). The GST isoenzymes and 100% identity are in bold.

TABLE 2 | Percent nucleotide identity matrix of *PvGm*GSTUG with the first 12 sequences identified in the BLASTP search.

	***PvGm*GSTUG**	***Mt*GST1**	***Ca*GST1**	***Mt*GST2**	***Mt*GST3**	***Ca*GST2**	***Ca*GST3**	***Mt*GST4**	***Mt*GST5**	***Mt*Pr1**	***Ai*GST1**	***Ai*GST2**
*1.PvGm*GSTUG	**100.00**	87.26	82.37	82.22	81.97	75.85	74.66	75.23	74.21	74.06	72.35	71.45
*2.Mt*GST1	87.26	**100.00**	82.81	83.26	85.91	74.67	75.87	75.99	73.91	73.76	73.24	72.80
*3.Ca*GST1	82.37	82.81	**100.00**	83.70	83.48	74.22	74.96	74.31	73.00	72.85	70.55	70.10
*4.Mt*GST2	82.22	83.26	83.70	**100.00**	86.52	75.85	73.76	74.01	72.55	72.40	73.09	72.65
*5.Mt*GST3	81.97	85.91	83.48	86.52	**100.00**	73.03	74.92	75.19	74.01	73.85	70.95	70.49
*6.Ca*GST2	75.85	74.67	74.22	75.85	73.03	**100.00**	76.47	75.99	74.81	74.66	74.29	73.39
*7.Ca*GST3	74.66	75.87	74.96	73.76	74.92	76.47	**100.00**	85.08	84.68	84.53	72.23	72.23
*8.Mt*GST4	75.23	75.99	74.31	74.01	75.19	75.99	85.08	**100.00**	87.98	87.82	71.43	71.27
*9.Mt*GST5	74.21	73.91	73.00	72.55	74.01	74.81	84.68	87. 98	**100.00**	99.85	71.32	71.32
*10.Mt*Pr1	74.06	73.76	72.85	72.40	73.85	74.66	84.53	87.82	99.85	**100.00**	71.17	71.17
*11.Ai*GST1	72.35	73.24	70.55	73.09	70.95	74.29	72.23	71.43	71.32	71.17	**100.00**	97.32
*12.Ai*GST2	71.45	72.80	70.10	72.65	70.49	73.39	72.23	71.27	71.32	71.17	97.32	**100.00**

For the analysis, the nucleotide sequence of PvGmGSTUG was used in the query. Percent identity matrix was calculated with the CLUSTAL omega sequence alignment program (Sievers et al. 2011). The accession numbers of the sequences are: MtGST1, (Medicago truncatula GST, XM_003623148.2); CaGST1, (Cicer arietinum GST, XM_004492319.2); MtGST2, (Medicago truncatula GST, XM_003623126.2); MtGST3, (Medicago truncatula GST, XM_003623120.2); CaGST2, (Cicer arietinum GST: KT336759.1); CaGST3, (Cicer arietinum GST, XM_012713550.1); MtGST4, (Medicago truncatula GST, XM_003623159.1); MtGST5, (Medicago truncatula GST 5, XM_003623156.2); MtPr1, (Medicago truncatula GST:BT053471.1); AiGST1 (Arachis ipaensis GST:XM_016342954.2); and AiGST2 (Arachis ipaensis GST: XM_016333558.2). The GST isoenzymes and 100% identity are in bold.

identity with the *Pv*GSTU2-2 and *Gm*GSTU8-8 isoenzymes and, from the evolutionary point of view, formed a separate clade (**Figure 5**). Although the accurate prediction of the parent sequences was impossible, we can nevertheless speculate that most of the *PvGm*GSTUG sequence was derived from *Pv*GSTU2-2 (Chronopoulou et al., 2012a) and *Gm*GSTU8-8 (Pouliou et al., 2017).

Substrate Specificity and Kinetic Analysis of *PvGm*GSTUG Enzyme

Recombinant *PvGm*GSTUG was purified to homogeneity by affinity chromatography on S-hexyl-GSH-agarose adsorbent (**Figure 6**). The substrate specificity of *PvGm*GSTUG was evaluated using a broad range of substrates. The results (**Table 3**) showed that *PvGm*GSTs could catalyze a broad range of reactions. Several halogenated aromatic compounds were acceptable substrates. They included CDNB and its analogs: 1-bromo-2,4-dinitrobenzene (BDNB), 1-iodo-2,4-dinitrobenzene (IDNB), and 4-chloro-7-nitrobenzofurazan. *PvGm*GSTUG was also examined for GST-dependent peroxidase activity (GPOX) using CuOOH, tert-butyl hydroperoxide, and benzoyl peroxide as substrates. Among all the peroxides tested, CuOOH and lauroyl peroxide were the best substrates. *PvGm*GSTUG also catalyzed the conjugation of GSH with isothiocyanates.

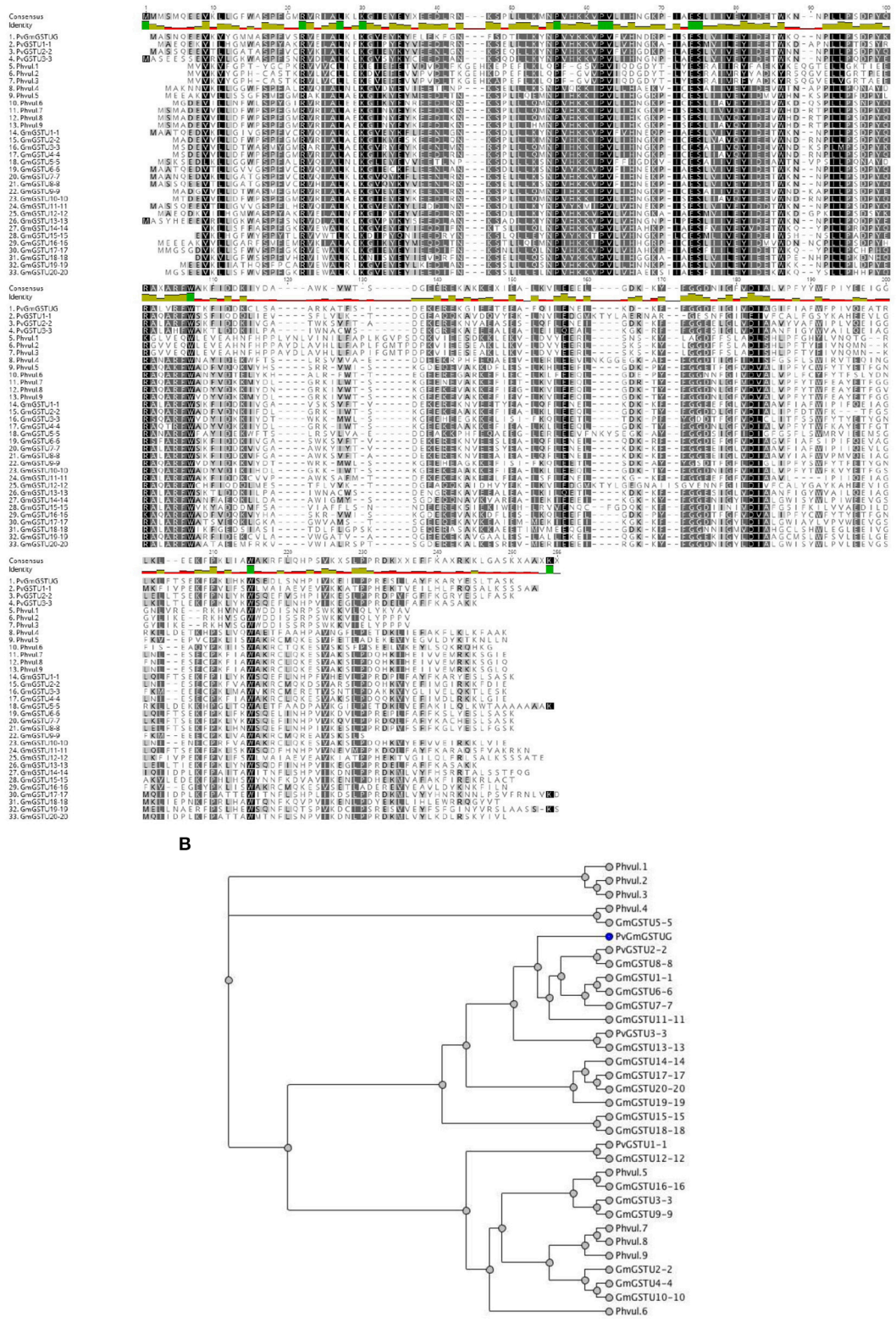

FIGURE 5 | Sequence and phylogenetic analysis **(A)**. Amino acid sequence alignments of *PvGm*GSTUG with the tau class GSTs from *Glycine max* and *Phaseolus vulgaris* **(B)**. Phylogenetic analysis of *GmPv*GSTUG with the tau class GSTs from *Glycine max* and *Phaseolus vulgaris*. Phylogenetic tree was constructed by the

(Continued)

FIGURE 5 | neighbor joining method using Geneious v9.1.2 software (Kearse et al., 2012) after alignment of the protein sequences using the Clustal Omega sequence alignment program (Sievers et al., 2011). The figures were created using Geneious v9.1.2 software (Kearse et al., 2012). Conserved areas are shown shaded: ■ 100% identity, ■ 80–100% identity, ■ 60–80% identity, <60% identity. The accession numbers and gene codes of the GST sequences that were used were: PvGSTU1-1 (AEX38000.1); PvGSTU2-2 (AEX38001.1); PvGSTU3-3 (NP_171792); Phvul.1 (006G023500.1|PACid:27165305); Phvul.2 (008G195500.1|PACid:27155547); Phvul.3 (008G195600.1|PACid:27155113); Phvul.4 (002G080200.1|PACid:27169916); Phvul.5 (005G053300.1 PACid:27149482); Phvul.6 (005G053200.1|PACid:27149239); Phvul.7 (005G054000.1|PACid:27150418); Phvul.8 (code 005G054100.1|PACid:27148744); and Phvul.9 (005G054200.1|PACid:27149131). The accession numbers of *Glycine max* GST sequences that were used were: *Gm*GSTU1-1, AAA33973; *Gm*GSTU2-2, CAA71784; *Gm*GSTU3-3, CAA48717; *Gm*GSTU4-4, AAC18566; *Gm*GSTU5-5, AAG34795; *Gm*GSTU6-6, AAG34796; *Gm*GSTU7-7, AAG34797; *Gm*GSTU8-8, AAG34798; *Gm*GSTU9-9, AAG34799; *Gm*GSTU10-10, AAG34800; *Gm*GSTU11-11, AAG34801; *Gm*GSTU12-12, AAG34802; *Gm*GSTU13-13, AAG34803; *Gm*GSTU14-14, AAG34804; *Gm*GSTU15-15, AAG34805; *Gm*GSTU16-16, AAG34806; *Gm*GSTU17-17, AAG34807; *Gm*GSTU18-18, AAG34808; *Gm*GSTU19-19, AAG34809; and *Gm*GSTU20-20, AAG34810.

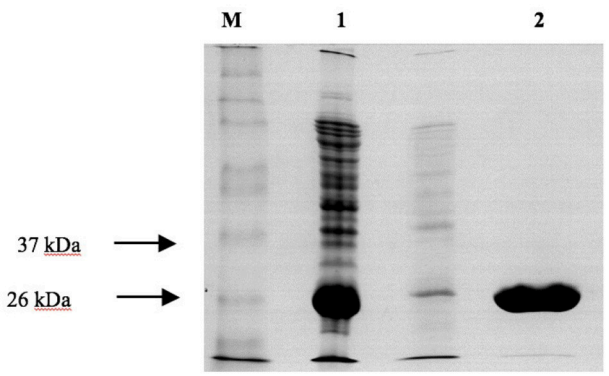

FIGURE 6 | SDS-PAGE analysis of the purification of recombinant *PvGm*GSTUG by affinity chromatography on S-hexyl-GSH-agarose M denotes the molecular mass markers. Lane 1 contains recombinant *E. coli* BL21 (DE3) crude extract after induction with 1 mM IPTG. Lane 2 contains *PvGm*GSTUG eluted fractions from the S-hexyl-GSH-Sepharose. Elution was achieved with 10 mM GSH.

*PvGm*GST, displayed high catalytic activity toward the aliphatic allyl-isothiocyanate, compared to the aromatic phenethyl-isothiocyanate.

The dependence of catalytic activity of *PvGm*GSTUG enzyme was investigated using steady-state kinetic analysis. The analysis was performed by employing two different model reaction systems: the GSH/CDNB and the GSH/CuOOH (**Figure 7**). The GSH/CDNB is a typical SN2 nucleophilic substitution reaction whereas the GSH/CuOOH reaction is an oxidative reaction (e.g., hydroperoxidase activity). The results are summarized in **Table 4**. *PvGm*GSTUG obeyed normal Michaelis-Menten kinetics when GSH was used as a variable substrate in both types of reactions. The unusual low K_m value (K_m 17 ± 1 μM) obtained for GSH in its reaction with CuOOH suggested that the enzyme is able to perform efficient catalysis under physiological conditions where the concentration of GSH is reduced, as for example under oxidative stress (Skopelitou et al., 2017).

When CDNB was used as the variable substrate, the enzyme showed cooperative allosteric kinetics. A Hill coefficient (n_H) of 1.8 ± 0.1 was measured with CDNB. Previous studies have established that in several *tau* class GSTs, although the H-site of neighboring subunits is remote, a reasonable communication between them exists. For example, in the case of a mutant form of *Gm*GST4-4 (Axarli et al., 2016) structural examination revealed that Lys104, which is located at the dimer interface, plays a key role in inter-subunit communication as well as in the cooperative allosteric kinetics observed with this enzyme.

Thermal Stability

To evaluate whether the simultaneous shuffling of GST genes from different plants allowed the generation of structurally stable GST fold, thermal inactivation and unfolding measurements were achieved as illustrated in **Figure 8A**. The half-inactivation temperature (T_m) was 45.9 ± 0.2°C, which lies within the expected range for mesophilic enzyme and is close to that determined for other native GST isoenzymes (Skopelitou et al., 2017; Perperopoulou et al., 2018). This suggests that the *PvGm*GSTUG structure displays normal stability and that no detrimental mutations or insertions were introduced during the shuffling of GST genes.

Differential scanning fluorometry (DSF) was also performed to assess the temperature-induced unfolding of the enzyme. DSF was carried out in the absence (**Figure 8B**) or presence of different concentrations of the substrate (GSH) and the reaction product [S-(p-nitrobenzyl)-GSH] (**Figures 8C,D**). The unfolding profile of the free enzyme as well as of the enzyme-GSH complex exhibited a single transition with a symmetric peak, with the maximum fluorescence intensity, corresponding to T_m, at 55 ± 0.1°C (n = 4) (**Supplementary Figures 3A-C**). On the other hand, in the presence of S-(p-nitrobenzyl)-GSH, an increase of the protein Gibbs free energy of unfolding was observed, which usually is depicted as a T_m shift at higher temperatures (**Supplementary Figure 3C**) (Lea and Simeonov, 2012). This T_m shift suggested a more stable structure with a closed, compact conformation, compared to that of the free enzyme or the enzyme-GSH complex, an indication of an induced-fit mechanism of *PvGm*GSTUG catalysis (Axarli et al., 2009a; **Figure 8B**).

Crystallographic Analysis and Structural Characterization of *PvGm*GSTUG

To better understand its properties, *PvGm*GSTUG was subjected to structural determination by X-ray crystallography (**Figure 9**). *PvGm*GSTUG was crystallized with two molecules in the crystallographic asymmetric unit that followed the typical dimer formation found in other GSTs (Axarli et al., 2009a; Pégeot

TABLE 3 | Substrate specificity for purified recombinant *PvGm*GSTUG.

Substrate	Structure	Specific activity (U/mg)
1-Chloro-2,4-dinitrobenzene	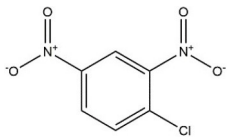	14.6
1-Bromo-2,4-dinitrobenzene	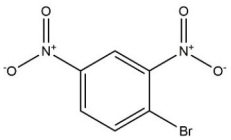	6.9
1-Fluoro-2,4-dinitrobenzene	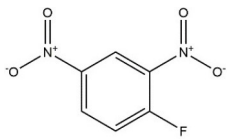	ND
1-Iodo-2,4-dinitrobenzene	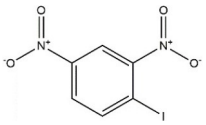	0.8
p-Nitrobenzyl chloride	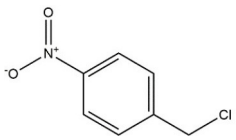	ND
4-Chloro-7-nitrobenzofurazan	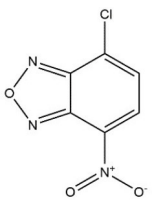	4.5
Cumene hydroperoxide	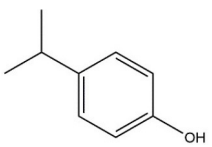	6.64
t-Butyl hydroperoxide	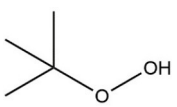	0.5
Benzoyl peroxide	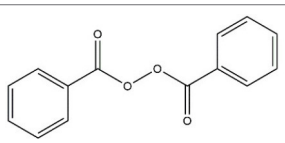	ND
Trans-2-Nonenal	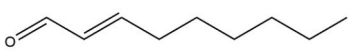	0.07
Trans-4-Phenyl-3-buten-2-one	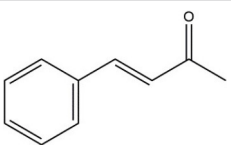	ND

(Continued)

TABLE 3 | Continued

Substrate	Structure	Specific activity (U/mg)
Ethacrynic acid	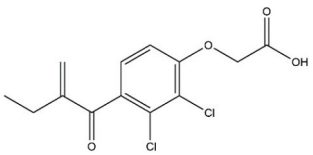	1.2
Fluorodifen	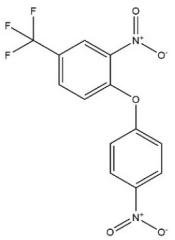	ND
Allylisothiocyanate	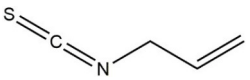	7.3
Phenethylisothiocyanate	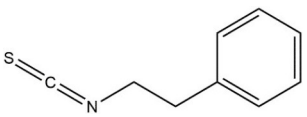	1.6
2-Hydroxyethyl disulfide (2-2-dithiodiethanol)	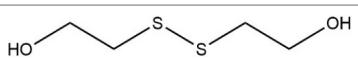	ND
Dehydroascorbate	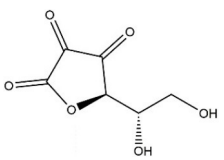	ND
Bromosulfophthalein	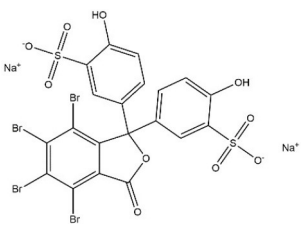	ND

ND: Non-detectable enzyme activity
Results represent the means of triplicate determinations, with variation less than 5% in all cases.

et al., 2014; Skopelitou et al., 2017). The final structure (**Table 5**) displayed good geometry with 93.7% of the residues in the preferred and accepted regions of the Ramachandran plot and 6.3% in the disallowed regions. Residues 1–5 in both chains, and the fragments 214–224 (chain B), and 216–224 (chain A) were not included in the structure owing to high disorder. The root mean square deviation in bond length and angle was 0.010 Å and 1.52°, respectively. The analysis revealed that each monomer of *PvGm*GSTUG consists of two distinct domains: at the N-terminal region a small α/β thioredoxin-like domain with βαβαββα folding topology is formed. The topology is arranged in the order β2, β1, β3, and β4. At the C-terminal region a large helical domain is formed (**Figure 8B**). At the end of helix H3 a short linker (residues 79–91) begins that joins the N- and C-terminal domains.

Coulombic surface analysis has previously shown that the G-site exhibits positive electrostatic potential, which may play a key role in -SH ionization of the bound GSH (Labrou et al., 2001). Similarly, the contribution of positively-charged residues in the adjustment of the electrostatic field has also been found in other GSTs (Patskovsky et al., 2000; Chronopoulou et al., 2012a). It is widely accepted that a Ser residue is the catalytic amino acid in GSTs of tau and phi classes (Labrou et al., 2001; Chronopoulou et al., 2012a), and that it stabilizes the

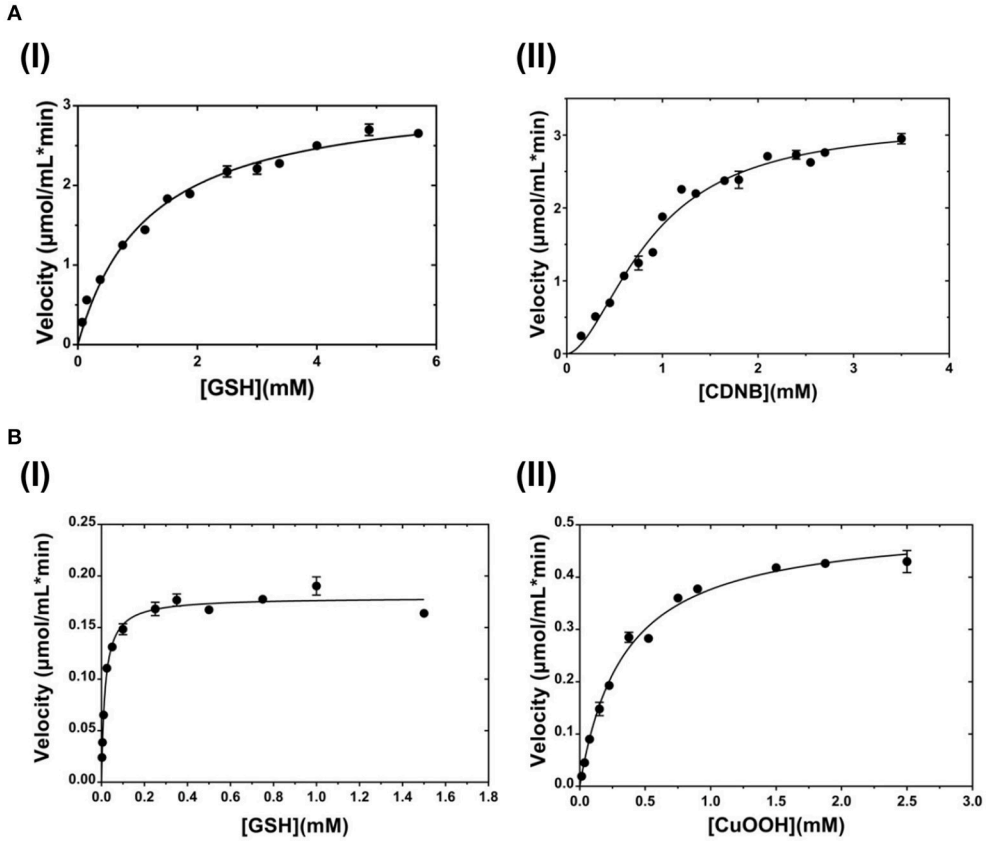

FIGURE 7 | Steady-state kinetic analysis **(A)**. Steady-state kinetic analysis of *PvGm*STUG using GSH as a variable substrate (I) and CDNB at a fixed concentration. Steady-state kinetic analysis of *PvGm*STUG using the CDNB as a variable substrate (II) and GSH at a fixed concentration **(B)**. Steady-state kinetic analysis of *PvGm*STUG using GSH as a variable substrate (I) and CuOOH at a fixed concentration. Steady-state kinetic analysis of *PvGm*STUG using the CuOOH as a variable substrate (II) and GSH at a fixed concentration. Experiments were performed in triplicate.

TABLE 4 | Steady-state kinetic parameters of *PvGm*GSTUG for the CDNB/GSH substrate system (A) and for the CuOOH/GSH substrate system (B).

Substrate system	K_m (mM) (GSH)	$S_{0.5}$ (mM) (CDNB)	k_{cat} (min^{-1}) (GSH)	n_H (CDNB)	k_{cat}/K_m (mM^{-1} min^{-1}) (GSH)	$k_{cat}/S_{0.5}$ (mM^{-1} min^{-1}) (CDNB)
A						
CDNB/GSH	1.17 ± 0.09	0.88 ± 0.05	194.1 ± 4.85	1.77 ± 0.14	165.9 ± 0.14	217.5
Substrate system	**K_m (mM) (GSH)**	**K_m (mM) (CuOOH)**	**k_{cat} (min^{-1}) (GSH)**		**k_{cat}/K_m (mM^{-1} min^{-1}) (GSH)**	**k_{cat}/K_m (m^{-1} min^{-1}) (CuOOH)**
B						
CuOOH/GSH	0.017±0.001	0.34 ± 0.02	29.61 ± 0.32		1,741.5 ± 127.9	87.1 ± 3.08

deprotonated form (GS^-) of bound GSH (Lo Piero et al., 2009). Structure superposition of *PvGm*GSTUG with *G. max* GSTU4-4 (PDB id 2vo4) revealed an rms deviation of 0.92 Å in Cα positions for 131 aligned residues and identified Ser16 as the catalytic residue. However, several changes were found in the vicinity of the active site (**Figure 9**). The conserved Glu69 and Ser70 correspond to Glu66 and Ser67 that form hydrogen bonds with the γ-Glu moiety of GSH (**Figure 10A**). The glycyl moiety of GSH interacts with Lys40 in *Gm*GSTU4-4. In *PvGm*GSTUG, a Phe residue replaces Lys, a change that could affect the orientation of GSH. Arg18, another conserved residue among tau GST sequences corresponds to Arg21in *PvGm*GSTUG. Arg18 has been suggested to stabilize the interactions between helices H1 and H4 through a strong electrostatic interaction with Asp103. A similar interaction appears also in *PvGm*GSTUG with Asp105, the structural equivalent residue of Asp103 in *Gm*GSTU4-4. Tyr107, a key residue at the H-site of *Gm*GSTU4-4, which forms aromatic interactions with the benzyl group of Nb-GSH in the *Gm*GSTU4-4–Nb-GSH complex (Axarli et al., 2009a). In *PvGm*GSTUG, it is replaced by a Cys residue, a change that

TABLE 5 | Data collection and refinement statistics.

Beamline	ESRF ID23-1
Wavelength (Å)	0.9730
Resolution range (Å)	50.0–3.5 (3.6–3.5)[#]
Space group	$P4^3$
Cell parameters	
a, b, c (Å) $\alpha = \beta = \gamma$ (°)	51, 51, 227.5 90
Total observations/unique	34,044/7132
Completeness	98.6 (99.0)
R_{meas}	0.099 (1.38)
$CC_{1/2}$	0.998 (0.656)
Reflections used in refinement (work/free)	6,380/709
R_{work}/R_{free}	0.29/0.34
Number of non-hydrogen atoms	3,431
RMS bonds (Å)	0.010
RMS angles (°)	1.52
Clashscore	14.4
B-factor (Å^2)	80.5
PDB id	6GHF

[#]*Numbers in parenthesis refer to the outermost resolution shell.*

could make the H-site more open and possibly alter its binding properties.

The subunit-subunit interactions in the folded dimeric structure of GSTs are important for both the stabilization of the tertiary structures of the folded subunits of the dimer as well as for the catalytic activity and substrate specificity. Comparison of the subunit-subunit interface revealed conservation of the interactions between the two subunits and of the hydrophobic interactions. *PvGm*GSTUG Val53 corresponds to Val50 in *Gm*GSTU4-4 and forms a lock with aromatic residues Phe99 (Phe97), Trp100 (Trp98), and Phe103 (Tyr101). A fourth hydrophobic residue, Leu134, is replaced by Ala134 in *PvGm*GSTUG, a change that may contribute to weakening of the interface. Salt bridges between Glu79 and side chains of Arg94′ and Arg98′ from the second subunit of the dimer are maintained as in *Gm*GSTU4-4 (Glu76, Arg92′ and Arg96′, respectively, in *Gm*GSTU4-4). Further analysis of the subunit-subunit interface revealed a putative mechanism that may affect the inter-subunit communication and promote the observed positive cooperativity. Structural examination revealed that the key residue bridging the dimer interface, Asp105, may play an important role in inter-subunit communication (**Figure 10B**). This residue could interact with Lys102 from the second subunit, forming a strong salt bridge. Since Lys102 is located in the α-helix H4, the signal may be transmitted via the α-helix H4 to the H-site residues (e.g., Phe117, Leu109), which are located at the end of this helix.

CONCLUSIONS

We report here the first directed-evolution study of GST genes from different plants and provide the first crystal structure of a synthetic GST. The data demonstrate the power of protein engineering and DNA shuffling in developing enzymes with engineered catalytic activities. From the evolutionary point of view, the results show that the recombination of segments from homologous GSTs from different plants can generate synthetic enzymes of practical significance that can be exploited for the creation of more sustainable and environmentally-friendly biocatalysts. The unusual low K_m value obtained for GSH with CuOOH suggests that the enzyme is able to perform efficient catalysis under conditions where the concentration of GSH is low, such as in the case of oxidative stress. This supports the potential for the future application of this enzyme as a genetic tool in agricultural biotechnology for the development of genetically engineered plants with high resistant to stress conditions.

MATERIALS AND METHODS

Materials

All enzyme substrates and antibiotics were obtained from Sigma-Aldrich (USA). The pCR T7/CT-TOPO kit, pEXP5-CT TOPO TA Cloning Kit, DNAse I, and SuperScript™ II reverse transcriptase were purchased from Invitrogen (USA). KAPA Taq and KAPA High fidelity DNA polymerase were purchased from KAPA Biosystems (USA). The miniplasmid isolation kit was purchased from Macherey–Nagel, (Germany). The QIAquick™ Gel Extraction kit was purchased from Qiagen (USA).

Methods

Plant Growth and Stress Conditions

P. vulgaris and *G. max* seeds were pre-germinated (72 h at 30°C) on distilled water-moistened Whatman 2MM filter paper. After germination, they were transferred to plastic pots containing soil. The plants were grown in a controlled environment (12-h day/12-h night cycle, at 25°C during the day and 21°C during the night at 65% humidity) and watered with deionized water every 4 days. Plants (3–4 weeks after germination with three or four pairs of leaves) were stressed using a three-step protocol. In the first step, plants were sprayed with a mixture of heavy metals consisting of nickel (150 μM), zinc (200 μM), and chromium (50 μM) and left for 24 h. In the second step, a herbicide mixture composed of fluazifop-p-butyl (diluted 1:250), atrazine (0.2 mM), and alachlor (0.2 mM) in ethanol solution (20% v/v) was used to treat plants. In the third step, plants were subjected to heat stress at 37°C for 24 h. Control plants did not receive any treatment. Tissue samples (leaves, shoots, and roots) from treated and control plants were collected after 24 and 48 h.

GST Activity Measurements in *P. vulgaris* and *G. max* Extracts in Response to Multiple Stresses

For protein and GST enzyme assays, plant tissues (roots, shoots, leaves) of treated, and control plants were ground to a fine powder using a mortar and liquid nitrogen. The ground material was extracted with potassium phosphate buffer (50 mM, pH 6) containing 0.1 mM EDTA and 1% w/v polyvinylpyrrolidone (3:1 buffer volume/fresh weight. The homogenate was subsequently centrifuged at 13,000 × *g* for

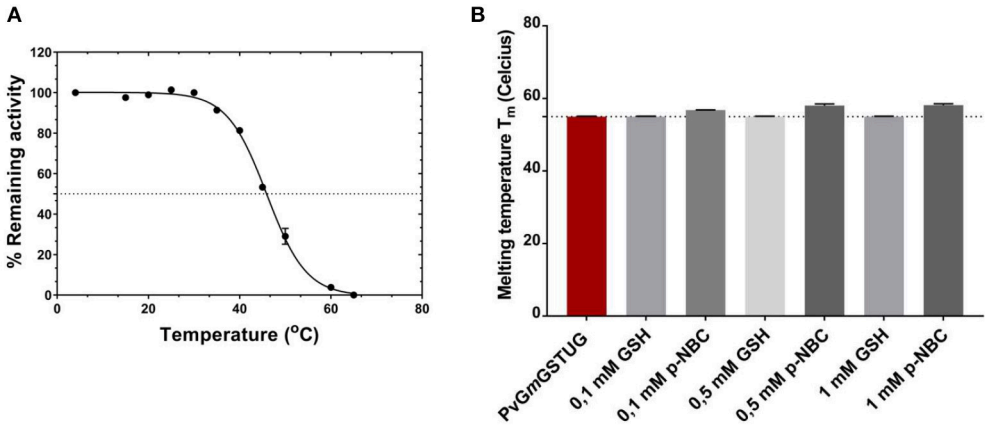

FIGURE 8 | Thermal inactivation curves for *PvGm*GSTUG **(A)**. Thermal inactivation curves for *PvGm*GSTUG. The residual activities were measured after heat treatment at various temperatures (°C) for 5 min **(B)**. Histogram depicting melting temperature of the protein in the different conditions tested.

10 min (4°C) and the supernatant was used for enzyme activity and protein determinations (Bradford, 1976), using bovine serum albumin as the standard. Enzyme activity was estimated toward CDNB, CuOOH, fluorodifen, ethacrynic acid, and p-nitrobenzyl chloride (Tappel, 1978; Satoh, 1995; Dixon et al., 2003; Axarli et al., 2009a).

Molecular Cloning

Total RNA from leaves, shoots, and roots was isolated as previously described (Brusslan and Tobin, 1992) and checked by agarose electrophoresis for its integrity. Total RNA was subjected to DNase treatment with the RNase-free DNase. cDNA synthesis was achieved in a total volume of 20 μL using 1–5 μg of total RNA, 0.5 μg oligo(dT)12–18, 10 mM of each dNTP, and sterile water to a final volume of 12 μL. After incubation at 65°C for 5 min, 5 × superscript buffer, 10 mM dithiothreitol, 40 Units RNAseOUT^{TM}, and 200 Units reverse transcriptase Superscript II (Invitrogen) were added in a thermocycler, which was operated at 42°C for 50 min and then at 70°C for 15 min.

Amplification of the GST genes by gradient PCR was performed using KapaTaq DNA polymerase and degenerate primers. Degenerated primers (**Supplementary Table 1**) were used in order to recover known and probably unknown GST sequences from *P. vulgaris* and *G. max*. The degenerated primers were designed based on nucleotide and aminoacid sequence alignments (Lang and Orgogozo, 2012) of theta class GST genes, derived from multiple related species (Axarli et al., 2009a; Han et al., 2018). The primers were designed based on similarities of the nucleotides at the 5′ and 3′ end sequences.

The following conditions were used for all sets of primers (see below) in a PCR volume of 50 μL: 1 μg cDNA, 10 pmol of forward primer, 30 pmol of reverse primer, 100 μM of each dNTP, 5 × KapaTaq buffer, and 1 Unit KAPA Taq DNA polymerase. The program used in the thermocycler was the same for all set of primers: 94°C for 60 s, T_m annealing 37°C for 90 s (the first 7–10 cycles), 44°C for 90 s (the next 7–10 cycles), 53°C for 90 s (the last 30–40 cycles), and 72°C for 50 s.

The PCR products were analyzed on a 1% (w/w) agarose gel and the corresponding bands were cut out and cleaned using the QIAquick^{TM} Gel Extraction kit (Qiagen), according to the manufacturer's instructions. The clean PCR products were A-tailed using Taq polymerase before being ligated to the pEXP5-CT vector using the TOPO®TA Kit (Invitrogen, USA). The recombinant plasmids (pEXP5-CT-GSTs) were used to transform competent *Escherichia coli* TOP10 cells.

Preparation of DNA for Shuffling and Construction of GST Gene Library

Recombinant plasmids (pEXP5-CT-GSTs) were mixed 1:1 in a final volume of 24 μL. The mixture was equilibrated at 15°C and supplemented with 5 μL of DNase buffer (400 mM Tris-HCl pH 8.0, 100 mM $MgSO_4$, and 10 mM $CaCl_2$), 21 μL of TE buffer (10 mM Tris pH 8.3 and 1 mM EDTA), and DNase (0.7 Units). At different times, aliquots of 6 μL were obtained and stop solution (20 mM EGTA, pH 8.0) was added and heated at 65°C for 10 min. Agarose gel electrophoresis 2% (w/w) of the DNase products was performed to check for digestion. Random fragments of 50–100 bp obtained after 8–15 min were selected for the shuffling procedure.

Reassembly of DNA fragments was carried out. The DNA fragments were used in PCR in the presence of 10 × Pfu buffer, 100 μM of each dNTP, and 1.25 units Pfu polymerase. The PCR cycle consisted of denaturation at 94°C for 0.5 min, annealing at 55°C for 1 min, and polymerization at 72°C for 1 65 s per cycle, with 40 repeats of the cycle to amplify the reassembled products. PCR reassembly product (1 μg) was used as template in a second PCR with the degenerate primers (**Supplementary Table 1**). This PCR contained 10 pmol of each forward primer, 30 pmol of each reverse primer, 10 × Pfu buffer, 100 μM of each dNTP, and 1.25 Units Taq/Pfu DNA polymerases. The reaction consisted of 11 cycles of denaturation at 94°C for 30 s, annealing at 55°C for 30 s, and polymerization at 72°C for 45 s, as well as of 14 cycles of denaturation at 94°C for 30 s, annealing at 55°C for 30 s, and polymerization at 72°C for 45 s and 25 s per cycle, followed by

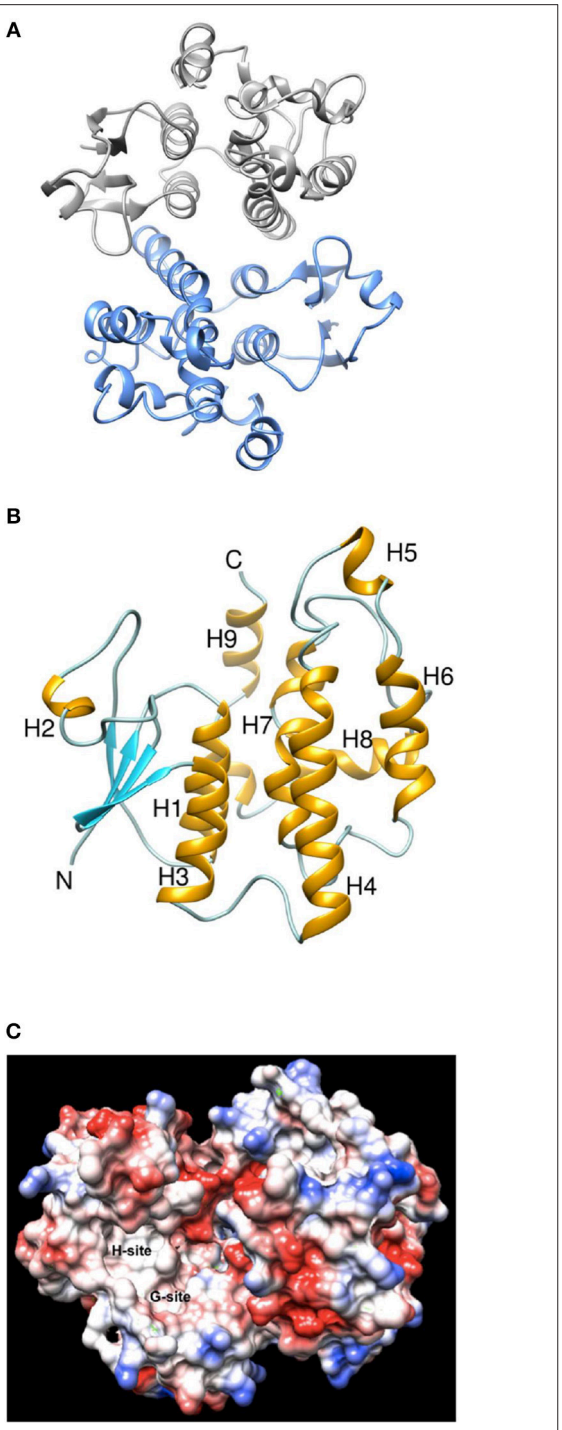

FIGURE 9 | Ribbon representation and Coulombic surface analysis of the *PvGm*GSTUG dimer. **(A)** Ribbon representation of the *PvGm*GSTUG dimer. Each subunit is shown in a different color. The two-fold axis that relates the two subunits is perpendicular to the plane of the page. **(B)** Ribbon representation of *PvGm*GSTUG subunit. Helices and strands are shown in orange and cyan, respectively. The helices are labeled. The figures were using CHIMERA (Pettersen et al., 2004). **(C)** Coulombic surface analysis of *PvGm*GSTUG dimer. The analysis was carried out using UCSF Chimera (http://www.cgl.ucsf.edu/chimera). The Coulomb electrostatic surface shows regions of neutral (white), positive (blue), and negative (red) charge.

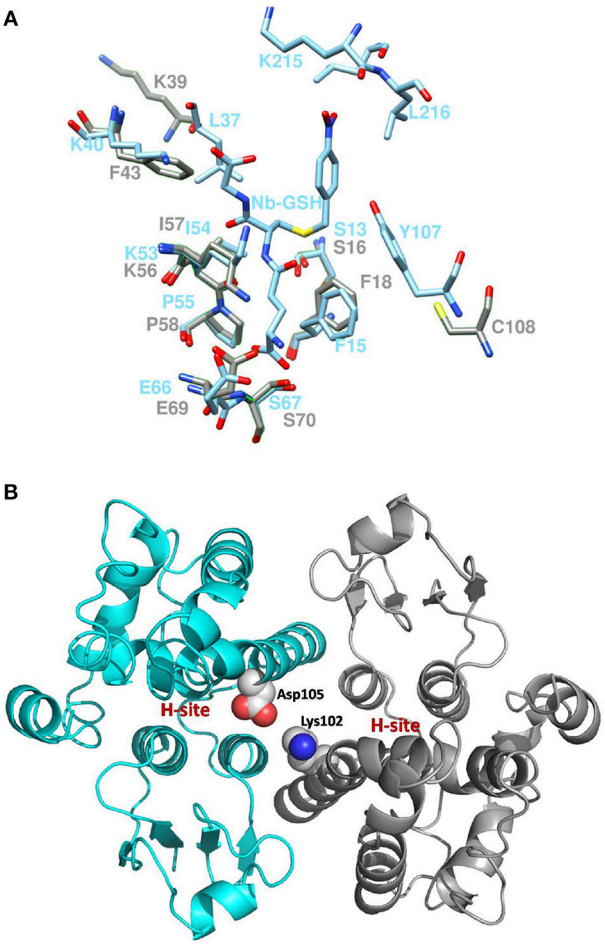

FIGURE 10 | Active site comparison and residue interaction **(A)**. Comparison of *PvGm*GSTUG and *Gm*GSTU4-4 active sites after superposition. *PvGm*GSTUG and *Gm*GSTU4-4 residues are depicted and labeled in cyan and gray, respectively. Nb-GSH bound to *Gm*GSTU4-4 is shown **(B)**. Representation of the interaction between Asp105 and Lys102 in the *PvGm*GSTUG dimer. Asp105 and Lys102 are shown as spheres and are colored according to the atom type. The picture also depicts the location of the H-site in each subunit.

final extension of 10 min at 72°C. The product of this reaction was run on a 1% (w/v) agarose gel, excised, and purified using a QIAquick™ Gel Extraction, kit (Qiagen). The extracted product was ligated to a T7 expression vector (pEXP5-CT/TOPO®TA). The resulting plasmid library was transformed into *E. coli* TOP10 and *E. coli* BL21(DE3) cells.

Screening of Library, and Expression and Purification of Recombinant Enzymes

Screening of the library and expression of the recombinant enzymes were carried out as described by Axarli et al. (2016). Enzyme purification was carried out using affinity chromatography on S-hexyl-GSH-Agarose as previously described (Axarli et al., 2009a). Protein purity was judged by SDS PAGE.

Assay of Enzyme Activity and Kinetic Analysis

Enzyme assays were carried out as previously described (Axarli et al., 2009a; Skopelitou et al., 2012). The Bradford assay was used for protein determination. Kinetic analysis was performed as described by Axarli et al. (2016).

Thermal Stability and Inactivation

Thermal inactivation of purified *PvGm*GSTUG was performed in potassium phosphate buffer (20 mM, pH 7) for 5 min at different temperatures (15–65°C). The enzyme was subsequently assayed for residual activity (enzyme activity at 4°C was considered 100%). Melting temperatures (T_m) were determined from the plot of relative inactivation (%) vs. temperature (°C). The T_m value corresponds to the temperature at which 50% of the initial enzyme activity is lost after heat treatment.

The thermal stability of *PvGm*GSTUG was also investigated using DSF on a Real-time PCR StepOne™ instrument (Applied Biosystems, USA). The thermal stability was measured in potassium phosphate buffer (20 mM, pH 7) using the Protein Thermal Shift™ Dye (Applied Biosystems, USA). Fluorescence monitoring was carried out at 10–95°C in increments of 1°C with a ramping rate of 2%. Melting temperatures (T_m) were estimated using the Protein Thermal Shift™ Analysis Software (Applied Biosystems). Ligand-binding analysis was also achieved with DSF in the presence of different concentrations (0.1, 0.5, 1.0 mM) of GSH and S-(p-nitrobenzyl)-GSH under the same heating and buffer conditions.

Crystallization and Data Analyses

The protein was crystallized with the hanging drop vapor diffusion method using 2 μL of protein mixed with 2 μL of reservoir solution containing polyethylene glycol 4000, 20% (w/v), sodium succinate 0.2 M, and HEPES-NaOH (0.1 M, pH 7.0). X-ray diffraction data (**Table 5**) were collected on the ID23-1 beamline at the European Synchotron Radiation Facility (France) under cryogenic conditions (100 K). Crystals were initially transferred to a reservoir solution containing 20% v/v glycerol for 2 s and then flash-cooled in liquid nitrogen. Diffraction data were processed with XDS (Kabsch, 2010) and scaled with AIMLESS (Evans and Murshudov, 2013).

Structure Determination, Refinement, and Analysis

Structure determination was pursued with the molecular replacement method using PHASER (McCoy et al., 2007). The structure of a *Ricinus communis* GST (PDB ID 4J2F; sequence identity 46.8% with *PvGm*GSTUG) was employed as the search model after modification with SCULPTOR (Bunkóczi and Read, 2011) that truncated side-chains from non-identical residues. Refinement was carried out initially with PHENIX (Adams et al., 2010) and subsequently with REFMAC (Murshudov et al., 2011). The low-resolution refinement options in REFMAC (Kovalevskiy et al., 2016) were utilized owing to the limited resolution of the structure. Structure-based sequence alignment was performed with Secondary Structure Matching (Krissinel and Henrick, 2004). The structure was validated using validation tools in COOT and PHENIX. Figures were created with CHIMERA (Pettersen et al., 2004). The structure has been deposited in the Protein Data Bank (PDB id 6GHF).

AUTHOR CONTRIBUTIONS

NEL, EGC, and ACP conceived and designed the experiments; EGC and ACP performed the experiments; FA, PM, and IN-O analyzed the data; NEL, EGC, ACP, PM, and IN-O wrote the paper.

ACKNOWLEDGMENTS

NEL and FA acknowledge the International Scientific Partnership Program at King Saud University, Saudi Arabia, for funding this research work through ISPP# 0071.

SUPPLEMENTARY MATERIAL

The Supplementary Material for this article can be found online at: https://www.frontiersin.org/articles/10.3389/fpls.2018.01737/full#supplementary-material

REFERENCES

Adams, P. D., Afonine, P. V., Bunkóczi, G., Chen, V. B., Davis, I. W., Echols, N., et al. (2010). PHENIX: a comprehensive Python-based system for macromolecular structure solution. *Acta Crystallogr. D Biol. Crystallogr.* 66, 213–221. doi: 10.1107/S0907444909052925

Axarli, I., Dhavala, P., Papageorgiou, A. C., and Labrou, N. E. (2009a). Crystallographic and functional characterization of the fluorodifen inducible glutathione transferase from *Glycine max* reveals an active site topography suited for diphenylether herbicides and a novel L-site. *J. Mol. Biol.* 385, 984–1002. doi: 10.1016/j.jmb.2008.10.084

Axarli, I., Labrou, N. E., Petrou, C., Rassias, N., Cordopatis, P., and Clonis, Y. D. (2009b). Sulphonamide- based bombesinprodrug analogues for glutathione transferase, useful in targeted cancer chemotherapy. *Eur. J. Med. Chem.* 44, 2009–2016. doi: 10.1016/j.ejmech.2008.10.009

Axarli, I., Muleta, A. W., Chronopoulou, E. G., Papageorgiou, A. C., and Labrou, N. E. (2017). Directed evolution of glutathione transferases towards a selective glutathione-binding site and improved oxidative stability. *Biochim. Biophys. Acta* 1861, 3416–3428. doi: 10.1016/j.bbagen.2016.09.004

Axarli, I., Muleta, A. W., Vlachakis, D., Kossida, S., Kotzia, G., Maltezos, A., et al. (2016). Directed evolution of Tau class glutathione transferases reveals a site that regulates catalytic efficiency and masks co-operativity. *Biochem. J.* 473, 559–570. doi: 10.1042/BJ20150930

Bai, Y., Luo, Q., Zhang, W., Miao, L., Xu, J., Li, H., et al. (2013). Highly ordered protein nanorings designed by accurate control of glutathione S-transferase self-assembly. *J. Am. Chem. Soc.* 135, 10966–10969. doi: 10.1021/ja405519s

Bradford, M. (1976). A rapid and sensitive method for the detection of microgram quantities of proteins. *Anal. Biochem.* 72, 248–254. doi: 10.1016/0003-2697(76)90527-3

Broo, K., Larsson, A. K., Jemth, P., and Mannervik, B. (2002). An ensemble of theta class glutathione transferases with novel catalytic properties generated by stochastic recombination of fragments of two mammalian enzymes. *J. Mol. Biol.* 318, 59–70. doi: 10.1016/S0022-2836(02)00032-3

Brusslan, J. A., and Tobin, E. M. (1992). Light-independent developmental regulation of cab gene expression in *Arabidopsis thaliana* seedlings. *Proc. Natl. Acad. Sci. U.S.A.* 89, 7791–7795. doi: 10.1073/pnas.89.16.7791

Bunkóczi, G., and Read, R. J. (2011). Improvement of molecular-replacement models with Sculptor. *ActaCrystallogr. D Biol. Crystallogr*. 67, 303–312. doi: 10.1107/S0907444910051218

Chronopoulou, E., Madesis, P., Asimakopoulou, B., Platis, D., Tsaftaris, A., and Labrou, N. E. (2012a). Catalytic and structural diversity of the fluazifop-inducible glutathione transferases from Phaseolus vulgaris. *Planta* 235, 1253–1269. doi: 10.1007/s00425-011-1572-z

Chronopoulou, E. G., and Labrou, N. E. (2009). Glutathione transferases: emerging multidisciplinary tools in red and green biotechnology. *Rec. Patents Biotech*. 3, 211–223. doi: 10.2174/187220809789389135

Chronopoulou, E. G., Papageorgiou, A. C., Markoglou, A., and Labrou, N. E. (2012b). Inhibition of human glutathione transferases by pesticides: development of a simple analytical assay for the quantification of pesticides in water. *J. Mol. Catal. B Enzym.* 81, 43–51. doi: 10.1016/j.molcatb.2012.04.022

Ciccarelli, F. D., Doerks, T., von Mering, C., Creevey, C. J., Snel, B., and Bork, P. (2006). Toward automatic reconstruction of a highly resolved tree of life. *Science* 311, 1283–1287. doi: 10.1126/science.1123061

Cronk, Q., Ojeda, I., and Pennington, R. T. (2006). Legume comparative genomics: progress in phylogenetics and phylogenomics. *Curr. Opin. Plant Biol*. 9, 99–103. doi: 10.1016/j.pbi.2006.01.011

Csiszár, J., Horváth, E., Váry, Z., Gallé, Á., Bela, K., Brunner, S., et al. (2014). Glutathione transferase supergene family in tomato: Salt stress-regulated expression of representative genes from distinct GST classes in plants primed with salicylic acid. *Plant Physiol. Biochem*. 78, 15–26. doi: 10.1016/j.plaphy.2014.02.010

Deponte, M. (2013). Glutathione catalysis and the reaction mechanisms of glutathione-dependent enzymes. *Biochim. Biophys. Acta*. 1830, 3217–3266. doi: 10.1016/j.bbagen.2012.09.018

Dixon, D. P., McEwen, A. G., Lapthorn, A. J., and Edwards, R. (2003). Forced evolution of a herbicide detoxifying glutathione transferase. *J. Biol. Chem*. 278, 23930–23935. doi: 10.1074/jbc.M303620200

Edwards, R., and Dixon, D. P. (2000). "The role of glutathione transferases in herbicide metabolism," in *Herbicides and Their Mechanisms of Action*, ed. A.H. Cobb and R.C. Kirkwood (Sheffield: Academic Press Ltd), 38–71.

Edwards, R., Dixon, D. P., and Walbot, V. (2000). Plant glutathione S-transferases: enzymes with multiple functions in sickness and in health. *Trends Plant Sci*. 5, 193–198. doi: 10.1016/S1360-1385(00)01601-0

Evans, P. R., and Murshudov, G. N. (2013). How good are my data and what is the resolution? *ActaCrystallogr. D Biol. Crystallogr*. 69, 1204–1214. doi: 10.1107/S0907444913000061

Gajewska, E., and Skłodowska, Z.M. (2008). Differential biochemical responses of wheat shoots and roots to nickel stress: antioxidative reactions and proline accumulation. *Plant Growth Regul*. 54, 179–188. doi: 10.1007/s10725-007-9240-9

Han, X. M., Yang, Z. L., Liu, Y. J., Yang, H. L., and Zeng, Q. Y. (2018). Genome-wide profiling of expression and biochemical functions of the Medicago glutathione S-transferase gene family. *Plant Physiol. Biochem*. 126, 126–133. doi: 10.1016/j.plaphy.2018.03.004

Hou, C., Li, J., Zhao, L., Zhang, W., Luo, Q., Dong, Z., et al. (2013). Construction of protein nanowires through cucurbit[8]uril-based highly specific host-guest interactions: an approach to the assembly of functional proteins. *Angew. Chem. Int. Ed. Engl*. 52, 5590–5593. doi: 10.1002/anie.201300692

Islam, M. S., Choudhury, M., Majlish, A. K., Islam, T., and Ghosh, A. (2018). Comprehensive genome-wide analysis of Glutathione S-transferase gene family in potato (*Solanum tuberosum* L.) and their expression profiling in various anatomical tissues and perturbation conditions. *Gene* 639, 149–162. doi: 10.1016/j.gene.2017.10.007

Islam, S., Rahman, I. A., Islam, T., and Ghosh,. A. (2017). Genome-wide identification and expression analysis of glutathione S-transferase gene family in tomato: Gaining an insight to their physiological and stress-specific roles. *PLoS ONE* 12:e0187504. doi: 10.1371/journal.pone.0187504

Kabsch, W. (2010). XDS. *ActaCrystallogr. D Biol. Crystallogr*. 66, 125–132. doi: 10.1107/S0907444909047337

Kapoli, P., Axarli, I. A., Platis, D., Fragoulaki, M., Paine, M., Hemingway, J., et al. (2008). Engineering sensitive glutathione transferase for the detection of xenobiotics. *Biosens. Bioelectron*. 24, 498–503. doi: 10.1016/j.bios.2008.06.037

Kearse, M., Moir, R., Wilson, A., Stones-Havas, S., Cheung, M., Sturrock, S., et al. (2012). Geneious Basic: an integrated and extendable desktop software platform for the organization and analysis of sequence data. *Bioinformatics* 28, 1647–1649. doi: 10.1093/bioinformatics/bts199

Kissoudis, C., Kalloniati, C., Flemetakis, E., Madesis, P., Labrou, N. E., Tsaftaris, A., et al. (2015). Maintenance of metabolic homeostasis and induction of cytoprotectants and secondary metabolites in alachlor treated *Gm*GSTU4 overexpressing tobacco plants, as resolved by metabolomics. *Plant Biotechnol*. 9, 287–296. doi: 10.1007/s11816-015-0364-5

Kovalevskiy, O., Nicholls, R. A., and Murshudov, G. N. (2016). Automated refinement of macromolecular structures at low resolution using prior information. *Acta Crystallogr. D Struct. Biol*. 72, 1149–1161. doi: 10.1107/S2059798316014534

Krissinel, E., and Henrick, K. (2004). Secondary-structure matching (SSM), a new tool for fast protein structure alignment in three dimensions. *Acta Crystallogr D Biol Crystallogr*. 60, 2256–2268. doi: 10.1107/S0907444904026460

Kurtovic, S., Modén, O., Shokeer, A., and Mannervik, B. (2008). Structural determinants of glutathione transferases with azathioprine activity identified by DNA shuffling of alpha class members. *J. Mol. Biol*. 375:13651379. doi: 10.1016/j.jmb.2007.11.034

Labrou, N. E., Mello, L. V., and Clonis, Y. D. (2001). Functional and structural roles of the glutathione-binding residues in maize (Zea mays) glutathione S-transferase I. *Biochem. J*. 358, 101–110. doi: 10.1042/bj3580101

Labrou, N. E., Papageorgiou, A. C., Pavli, O., and Flemetakis, E. (2015). Plant GSTome: structure and functional role in xenome network and plant stress response. *Curr. Op. Biotech*. 32, 186–194. doi: 10.1016/j.copbio.2014.12.024

Lallement, P. A., Brouwer, B., Keech, O., Hecker, A., and Rouhier, N. (2014a). The still mysterious roles of cysteine-containing glutathione transferases in plants. *Front Pharmacol*. 5:192. doi: 10.3389/fphar.2014.00192

Lallement, P. A., Meux, E., Gualberto, J. M., Prosper, P., Didierjean, C., Saul, F., et al. (2014b). Structural and enzymatic insights into Lambda glutathione transferases from *Populus trichocarpa*, monomeric enzymes constituting an early divergent class specific to terrestrial plants. *Biochem. J*. 462, 39–52. doi: 10.1042/BJ20140390

Lang, M., and Orgogozo, V. (2012). "Identification of homologous gene sequences by PCR with degenerate primers," in *The Molecular Methods for Evolutionary Genetics*, eds V. Orgogozo and M. Rockman (New York, NY: Humana Press), 245–256.

Lea, W. A., and Simeonov, A. (2012). Differential scanning fluorometry signatures as indicators of enzyme inhibitor mode of action: case study of glutathione S-transferase. *PLoS ONE* 7: e36219. doi: 10.1371/journal.pone.0036219

Li, D., Xu, L., Pang, S., Liu, Z., Wang, K., and Wang, C. (2017a). Variable levels of glutathione S-transferases are responsible for the differential tolerance to metolachlor between maize (*Zea mays*) shoots and roots. *J. Agric. Food Chem*. 65, 39–44. doi: 10.1021/acs.jafc.6b04129

Li, D., Xu, L., Pang, S., Liu, Z., Zhao, W., and Wang, C. (2017b). Multiple pesticides detoxification function of maize (*Zea mays*) GST34. *J. Agric. Food Chem*. 65, 1847–1853. doi: 10.1021/acs.jafc.7b00057

Liu, H. J., Tang, Z. X., Han, X. M., Yang, Z. L., Zhang, F. M., Yang, H. L., et al. (2015). Divergence in enzymatic activities in the soybean GST supergene family provides new insight into the evolutionary dynamics of whole-genome duplicates. *Mol. Biol. Evol*. 32, 2844–2859. doi: 10.1093/molbev/msv156

Liu, Y. J., Han, X. M., Ren, L. L., Yang, H. L., and Zeng, Q. Y. (2013). Functional divergence of the glutathione S-transferase supergene family in *Physcomitrella patens* reveals complex patterns of large gene family evolution in land plants. *Plant Physiol*. 161, 773–786. doi: 10.1104/pp.112.205815

Lo Piero, A. R., Mercurio, V., Puglisi, I., and Petrone, G. (2009). Gene isolation and expression analysis of two distinct sweet orange [*Citrus sinensis* L. (Osbeck)] tau-type glutathione transferases. *Gene* 443, 143–150. doi: 10.1016/j.gene.2009.04.025

Mannervik, B. (2012). Five decades with glutathione and the GSTome. *J. Biol. Chem*. 287, 6072–6083. doi: 10.1074/jbc.X112.342675

Materon, E. M., Huang, P. J., Wong, A., Pupim Ferreira, A. A., Sotomayor, M. d, P. T., and Liu, J. (2014). Glutathione-s-transferase modified electrodes for detecting anticancer drugs. *Biosens. Bioelectron*. 58, 232–236. doi: 10.1016/j.bios.2014.02.070

McCoy, A. J., Grosse-Kunstleve, R. W., Adams, P. D., Winn, M. D., Storoni, L. C., and Read, R. J. (2007). Phaser crystallographic software. *J. Appl. Crystallogr*. 40, 658–674. doi: 10.1107/S0021889807021206

McGonigle, B., Keeler, S. J., Lau, S. M., Koeppe, M. K., and O'Keefe, D. P. (2000). A genomics approach to the comprehensive analysis of the glutathione S-transferase gene family in soybean and maize. *Plant Physiol.* 124, 1105–1120. doi: 10.1104/pp.124.3.1105

Murshudov, G. N., Skubák, P., Lebedev, A. A., Pannu, N. S., Steiner, R. A., Nicholls, R. A., et al. (2011). REFMAC5 for the refinement of macromolecular crystal structures. *Acta Crystallogr. D Biol. Crystallogr.* 67, 355–367. doi: 10.1107/S0907444911001314

Neuefeind, T., Huber, R., Dasenbrock, H., Prade, L., and Bieseler, B. (1997). Crystal structure of herbicide-detoxifying maize glutathione S-transferase-I in complex with lactoyl glutathione: evidence for an induced-fit mechanism. *J. Mol. Biol.* 274, 446–453. doi: 10.1006/jmbi.1997.1402

Nianiou-Obeidat, I., Madesis, P., Kissoudis, C., Voulgari, G., Chronopoulou, E., Tsaftaris, A., et al. (2017). Plant glutathione transferase-mediated stress tolerance: functions and biotechnological applications. *Plant Cell Rep.* 36, 791–805. doi: 10.1007/s00299-017-2139-7

Oliveira, T. I., Oliveira, M., Viswanathan, S., FátimaBarroso, M., Barreiros, L., Nunes, O. C., et al. (2013). Molinate quantification in environmental water by a glutathione-S-transferase based biosensor. *Talanta* 106, 249–254. doi: 10.1016/j.talanta.2012.10.074

Patskovsky, Y. V., Patskovska, L. N., and Listowsky, I. (2000). The enhanced affinity for thiolate anion and activation of enzyme-bound glutathione is governed by an arginine residue of human Mu class glutathione S-transferases. *J Biol. Chem.* 275, 3296–3304. doi: 10.1074/jbc.275.5.3296

Pégeot, H., Koh, C. S., Petre, B., Mathiot, S., Duplessis, S., Hecker, A., et al. (2014). The poplar Phi class glutathione transferase: expression, activity and structure of GSTF1. *Front. Plant Sci.* 23:712. doi: 10.3389/fpls.2014.00712

Pégeot, H., Mathiot, S., Perrot, T., Gense, F., Hecker, A., Didierjean, C., et al. (2017). Structural plasticity among glutathione transferase Phi members: natural combination of catalytic residues confers dual biochemical activities. *FEBS J.* 284, 2442–2463. doi: 10.1111/febs.14138

Perperopoulou, F., Pouliou, F., and Labrou, N. E. (2018). Recent advances in protein engineering and biotechnological applications of glutathione transferases. *Crit. Rev. Biotechnol.* 38, 511–528. doi: 10.1080/07388551.2017.1375890

Pettersen, E. F., Goddard, T. D., Huang, C. C., Couch, G. S., Greenblatt, D. M., Meng, E. C., et al. (2004). UCSF Chimera–a visualization system for exploratory research and analysis. *J. Comput. Chem.* 25, 1605–1612. doi: 10.1002/jcc.20084

Pouliou, F., Perperopoulou, F., and Labrou, N. E. (2017). Comparative analysis of two stress-inducible tau class glutathione transferases from Glycine max revealed significant catalytic and structural diversification. *Protein Pept. Lett.* 24, 922–935. doi: 10.2174/0929866524666171026125300

Runarsdottir, A., and Mannervik, B. (2010). A novel quasi-species of glutathione transferase with high activity towards naturally occurring isothiocyanates evolves from promiscuous low-activity variants, J Mol *Biol.* 401, 451–464. doi: 10.1016/j.jmb.2010.06.033

Satoh, K. (1995). The high non-enzymatic conjugation rates of some glutathione S-transferase (GST) substrates at high glutathione concentrations. *Carcinogenesis* 16, 869–874. doi: 10.1093/carcin/16.4.869

Sievers, F., Wilm, A., Dineen, D., Gibson, T. J., Karplus, K., Li, W., et al. (2011). Fast, scalable generation of high-quality protein multiple sequence alignments using Clustal Omega. *Mol. Syst. Biol.* 7:539. doi: 10.1038/msb.2011.75

Skipsey, M., Knight, K. M., Brazier-Hicks, M., Dixon, D. P., Steel, P. G., and Edwards, R. (2011). Xenobiotic responsiveness of Arabidopsis thaliana to a chemical series derived from a herbicide safener. *J. Biol. Chem.* 286, 32268–32276. doi: 10.1074/jbc.M111.252726

Skopelitou, K., Muleta, A. W., Papageorgiou, A. C., Chronopoulou, E. G., Pavli, O., Flemetakis, E., et al. (2017). Characterization and functional analysis of a recombinant tau class glutathione transferase GmGSTU2-2 from *Glycine max*. *Int. J. Biol. Macromol.* 94, 802–812. doi: 10.1016/j.ijbiomac.2016.04.044

Skopelitou, K., Muleta, A. W., Pavli, O., Skaracis, G. N., Flemetakis, E., Papageorgiou, A. C., et al. (2012). Overlapping protective roles for glutathione transferase gene family members in chemical and oxidative stress response in *Agrobacterium tumefaciens*. *Funct. Integr. Genomics.* 12, 157–172. doi: 10.1007/s10142-011-0248-x

Tappel, A. L. (1978). "Glutathione peroxidase and hydroperoxides," in *The Methods in Enzymology*, ed. S. Fleischer, and L. Packer (New York, NY:Academic Press), 506–513.

Voelker, A. E., and Viswanathan, R. (2013). Synthesis of a suite of bioorthogonal glutathione S-transferase substrates and their enzymatic incorporation for protein immobilization. *J. Org. Chem.* 78, 9647–9658. doi: 10.1021/jo401278x

Wang, D., Li, L., Wu, G., Vasseur, L., Yang, G., and Huang, P. (2017). *De novo* transcriptome sequencing of *Isaria cateniannulata* and comparative analysis of gene expression in response to heat and cold stresses. *PLoS ONE* 12:e0186040. doi: 10.1371/journal.pone.0186040

Yang, Q., Liu, Y. J., and Zeng, Q. Y. (2014). Biochemical functions of the glutathione transferase supergene family of *Larix kaempferi*. *Plant Physiol. Biochem.* 77, 99–107. doi: 10.1016/j.plaphy.2014.02.003

Zhang, C., Spokoyny, A. M., Zou, Y., Simon, M. D., and Pentelute, B. L. (2013). Enzymatic "click" ligation: selective cysteine modification in polypeptides enabled by promiscuous glutathione S-transferase. *Angew. Chem. Int. Ed. Engl.* 52, 14001–14005. doi: 10.1002/anie.201306430

Zhao, H., and Arnold, F. H. (1997). Optimization of DNA shuffling for high fidelity recombination. *Nucleic Acids Res.* 25, 1307–1308. doi: 10.1093/nar/25.6.1307

Zhou, Y., Guo, T., Tang, G., Wu, H., Wong, N. K., and Pan, Z. (2014). Site-selective protein immobilization by covalent modification of GST fusion proteins. *Bioconjugate Chem.* 25, 1911–1915. doi: 10.1021/bc500347b

Conflict of Interest Statement: The authors declare that the research was conducted in the absence of any commercial or financial relationships that could be construed as a potential conflict of interest.

The reviewer AH is currently co-organizing a Research Topic with one of the authors NEL and confirms the absence of any other collaboration.

frontiers in Plant Science

ORIGINAL RESEARCH
published: 12 December 2018
doi: 10.3389/fpls.2018.01846

Structure-Guided Mechanisms Behind the Metabolism of 2,4,6-Trinitrotoluene by Glutathione Transferases U25 and U24 That Lead to Alternate Product Distribution

Kyriakos Tzafestas[1], Laziana Ahmad[1,2], M. Paulina Dani[1], Gideon Grogan[2], Elizabeth L. Rylott[1] and Neil C. Bruce[1]**

[1] Centre for Novel Agricultural Products, Department of Biology, University of York, York, United Kingdom, [2] York Structural Biology Laboratory, Department of Chemistry, University of York, York, United Kingdom

OPEN ACCESS

Edited by:
Peter Schröder,
German Research Center for Environmental Health (HZ), Germany

Reviewed by:
Uener Kolukisaoglu,
University of Tubingen, Germany
Jacqueline Vanni Shanks,
Iowa State University, United States

***Correspondence:**
Elizabeth L. Rylott
liz.rylott@york.ac.uk
Neil C. Bruce
neil.bruce@york.ac.uk

Specialty section:
This article was submitted to Plant Physiology, a section of the journal Frontiers in Plant Science

Received: 14 August 2018
Accepted: 28 November 2018
Published: 12 December 2018

Citation:
Tzafestas K, Ahmad L, Dani MP, Grogan G, Rylott EL and Bruce NC (2018) Structure-Guided Mechanisms Behind the Metabolism of 2,4,6-Trinitrotoluene by Glutathione Transferases U25 and U24 That Lead to Alternate Product Distribution. Front. Plant Sci. 9:1846. doi: 10.3389/fpls.2018.01846

The explosive xenobiotic 2,4,6-trinitrotoluene (TNT) is a major worldwide environmental pollutant and its persistence in the environment presents health and environmental concerns. The chemical structure of TNT dictates that biological detoxification pathways follow predominantly reductive transformation of the nitro groups, and as a result, TNT is notoriously recalcitrant to mineralization in the environment. Plant-based technologies to remediate this toxic pollutant rely on a solid understanding of the biochemical detoxification pathways involved. Toward this, two Arabidopsis Tau class glutathione transferases, GSTU24 and GSTU25, have been identified that catalyze the formation of three TNT-glutathionylated conjugates. These two GSTs share 79% identity yet only GSTU25 catalyzes the substitution of a nitro group for sulfur to form 2-glutathionyl-4,6-dinitrotoluene. The production of this compound is of interest because substitution of a nitro group could lead to destabilization of the aromatic ring, enabling subsequent biodegradation. To identify target amino acids within GSTU25 that might be involved in the formation of 2-glutathionyl-4,6-dinitrotoluene, the structure for GSTU25 was determined, in complex with oxidized glutathione, and used to inform site-directed mutagenesis studies. Replacement of five amino acids in GSTU24 established a conjugate profile and activity similar to that found in GSTU25. These findings contribute to the development of plant-based remediation strategies for the detoxification of TNT in the environment.

Keywords: 2,4,6-trinitrotoluene, TNT, Arabidopsis, glutathione transferase, GST, detoxification, xenobiotic

INTRODUCTION

The continual use of explosives, along with production and decommissioning is progressively contaminating military sites worldwide (Amaral et al., 2009; Zheng et al., 2009). The total area of operational ranges in the United States contaminated with munitions constituents is estimated to be more than 10 million hectares (United States General Accounting Office, 2004). Pollution in European countries, from former WWII manufacturing and disposal sites is also widespread

(Spain et al., 2000). The most broadly used explosive, 2,4,6-trinitrotoluene (TNT) is associated with extensive soil and water contamination (Lewis et al., 2004). Contaminated training ranges have hotspots of TNT that can reach concentrations of up to 87000 mg kg^{-1} soil (Talmage et al., 1999), with 100–1000 mg kg^{-1}, or lower for surface soils in artillery training ranges and 1–36 mg kg^{-1} for hand grenade ranges (Jenkins et al., 2006; Clark and Boopathy, 2007).

Nitro-substituted organic compounds, such as TNT, pose a specific challenge to plant and bacterial degradation. The electron withdrawing nitro groups on the TNT molecule provide stability to the aromatic ring through resonance, rendering the ring particularly resistant to oxidative attack and subsequent ring cleavage (Qasim et al., 2009). Thus TNT is particularly recalcitrant to biodegradation and persists in the environment (Rylott et al., 2011).

In a previous study, two *Arabidopsis thaliana* (Arabidopsis) glutathione transferases, GSTU24 and GSTU25, were shown to conjugate TNT to glutathione (GSH) producing three distinct TNT-GSH conjugates, shown in **Figure 1** (Gunning et al., 2014). For two of the compounds, GSH conjugation occurred through the methyl group of TNT; however, the third conjugate (conjugate 3) resulted from the nucleophilic substitution of a nitro group to form 2-glutathionyl-4,6-dinitrotoluene (GDNT). Replacement of the nitro group with sulfur could destabilize the aromatic ring. Fungi and bacteria with the ability to mineralize dinitrotoluenes exist (Valli et al., 1992; Nishino et al., 2000; Johnson et al., 2002) and enzymatic pathways for DNT biodegradation have been characterized (Nishino et al., 2000; Johnson et al., 2002). Thus, production of GDNT could present an opportunity for cleavage and subsequent biodegradation of this toxic environmental pollutant.

Plant GSTs are a superfamily of enzymes: In Arabidopsis, there are 54 GSTs subdivided into seven classes. While many GSTs are able to conjugate GSH to a wide range of xenobiotic substrates, they are also involved in catalyzing ascorbate recycling and various metabolic reactions, with some GSTs also exhibiting glutathione peroxidase (GPOX) activity (Dixon and Edwards, 2010), and non-enzymatic ligand binding properties (Smith et al., 2003; Dixon et al., 2011). The Tau class, to which GSTU24 and GSTU25 belong, can be subdivided into three distinct clades. Many of the GSTs within the clade GSTU19 to GSTU28 are implicated in the detoxification of xenobiotics such as herbicides and safeners (Edwards et al., 2005; Labrou et al., 2015). Expression of both GSTU24 and GSTU25 is induced by TNT, with GSTU25 also exhibiting relatively high GPOX activity (Dixon and Edwards, 2009) and activity toward the model substrate 1-chloro-2,4-dinitrobenzene (CDNB; Mezzari et al., 2005; Gandia-Herrero et al., 2008). To date, Tau class GSTs are unique in their ability to bind glutathione-conjugated fatty acid derivatives (Mezzari et al., 2005; Dixon and Edwards, 2009), with GSTU25 known to selectively bind hydroxylated fatty acids. Yet, despite the mounting knowledge on these enzymes, the endogenous roles for GSTU24 and GSTU25, and the vast majority of plant GSTs in general, remains elusive.

The structures of several Tau class plant GSTs have been solved: The wheat (*Triticum aestivum*), *Ta*GSTU4-4 structure was determined in complex with *S*-hexylglutathione (Thom et al., 2002) and rice (*Oryza sativa*) *Os*GSTU1 (Protein Data Bank code 1OYJ), while two soybean (*Glycine max*) GSTs have been determined; *Gm*GST-U4-4 in complex with *S*-(*p*-nitrobenzyl)-glutathione (Axarli et al., 2009) and *Gm*GSTU10-10 (Skopelitou et al., 2015). Although there is high protein sequence variability between these GSTs, the structures are remarkably conserved (Dixon and Edwards, 2010; Skopelitou et al., 2015). Existing as soluble homo or heterodimers, each 23–30 kDa subunit is 200–300 amino acids in length. Within each subunit is a kinetically independent active site containing G and H sites. The G site, which is relatively well conserved, is formed from the N-terminal domain which exhibits α/β topology, and binds GSH and, less commonly, other closely related peptides. The H-site exists within an α-helical structure in the C-terminal domain but is less well conserved than the G site and, as a result, GSTs have wide substrate specificity.

Only 1.3 kb apart on chromosome I, GSTU24 and GSTU25 share 79% protein identity, indicative of a relatively recent gene duplication event. In this study, we report the structure of GSTU25. We then use this structure, in combination with alignment from other Tau-class plant GSTS whose structures have previously been solved (Axarli et al., 2009, 2016), to predict the key amino acids in the active site of GSTU25 that are associated with the specificity of the conjugation reactions of TNT with GSH.

MATERIALS AND METHODS

Expression and Protein Purification for Crystallization

The GSTU24 and GSTU25 from *A. thaliana* (Arabidopsis) ecotype Col0, and mutants, were cloned from pET-YSBLIC3C (described below) into pET22a to remove the his-tag, then transformed into *Escherichia coli* Tuner (DE3) cells (Novagen) that also contained the pRARE plasmid from Rosetta (Novagen). Transformants were grown on agar plates of Luria Bertani medium containing kanamycin (100 μg mL^{-1}) and 50 μg mL^{-1} chloramphenicol (50 μg mL^{-1}) (LB+KC). A single colony of a plate grown overnight was used to inoculate a 5 mL starter culture of LB+KC medium, which was grown overnight at 37°C, 180 rpm. The starter culture was then used to inoculate 400 mL LB+KC medium which was incubated at 37°C with shaking until an OD_{600} of 0.5–0.8 was reached. At this point expression of the GST was induced by the addition of isopropyl β-D-1-thiogalactopyranoside (IPTG, final concentration of 1 mM) and culture incubated at 20°C, 180 rpm. After approximately 18 h growth, cells were harvested by centrifugation at 5000 *g* for 15 min then resuspended in 20 mM Tris/HCl buffer pH 7.5. Cells were disrupted by ultrasonication, centrifuged at 15,000 *g* for 30 min then the supernatant loaded onto a 10 mL GSH Sepharose 4B (GE healthcare). Column fractions were analyzed by SDS-PAGE and the fraction containing purified proteins were pooled and concentrated using a 10 kDa cut-off Centricon® filter membrane. Concentrated protein was loaded onto an S75 Superdex^{TM} gel filtration column and fractions containing pure

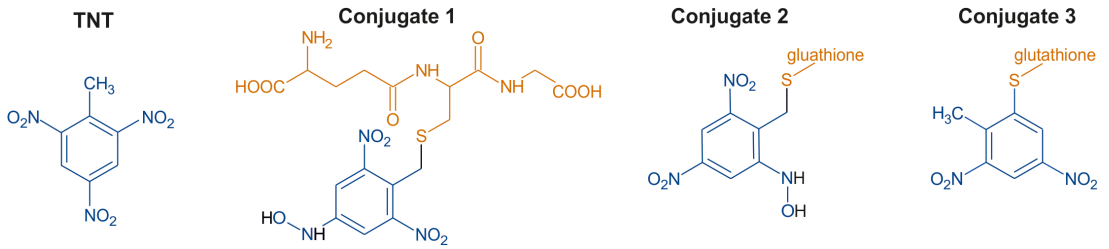

FIGURE 1 | Chemical structures of 2,4,6-trinitrotoluene (TNT) and the three glutathione-TNT conjugates, as determined by Gunning et al. (2014).

protein, as determined by SDS-PAGE, were pooled and stored at −20°C.

Protein Crystallization

Commercially available crystallization screens in 96-well plate sitting drop format were pre-incubated with 2 mM GSH and 2 mM TNT in 54 μL of reservoir solution in reservoir well. Pure *At*GSTU25 was then subjected to crystallization trials using a Mosquito® ROBOT (TTP LabTech) in which each drop contained 150 nL protein and 150 nL precipitant reservoir solution. Initial crystals observed for the complex of *At*GSTU25 mixture were obtained in solutions containing 0.2 M ammonium acetate, 0.1 M bis-tris propane pH 5.5 and 25% (w/v) PEG 3350. Larger crystals for diffraction analysis were obtained using the hanging-drop vapor diffusion method in 24-well plate Linbro dishes with 2 μL drops of a ratio of mother liquor to protein solution. The best crystals of the complex of GSTU25 with oxidized glutathione were obtained in crystal drops containing 0.2 M ammonium acetate, 0.1 M bis-tris propane pH 5.5 and 23% (w/v) PEG 3350. Prior to analysis on in-house X-ray equipment, the crystals were washed with the reservoir solution containing 20% (v/v) ethylene glycol as the cryoprotectant, followed by flash-cooling in the liquid nitrogen. Crystals were tested for diffraction using a Rigaku Micromax-007HF fitted with Osmic multilayer optics and a MARRESEARCH MAR345 imaging plate detector. Those crystals that diffracted to a resolution of equal to, or better than, 3 Å were retained for dataset collection at the synchrotron.

Data Collection, Structure Solution, Model Building, and Refinement

The complete dataset described in this report was collected at the Diamond Light Source, Didcot, United Kingdom on beamline I02. The data were processed and integrated using XDS (Kabsch, 2010) and scaled using SCALA (Evans, 2006) included in the Xia2 processing system (Winter, 2010). Data collection statistics are provided in **Table 1**. All crystals of U25 were obtained in space group $P2_12_12_1$, with four molecules in the asymmetric unit, constituting two dimers. The structure of *At*GSTU25 was solved using MOLREP (Vagin and Teplyakov, 1997), with a monomer of the structure of the Tau class glutathione transferase from *G. max* (PDB 4TOP; 65% sequence identity) as a model. The solvent content in crystals was 51%. Structures were built and refined using iterative cycles using Coot (Emsley and Cowtan, 2004) and REFMAC (Murshudov et al., 1997), employing local NCS restraints in the refinement cycles. After building and refinement of the protein and water molecules, clear residual density was observed in the omit maps at the GSH binding site. This could be clearly modeled as glutathione disulfide (GSSG). The final structure exhibited R_{cryst} and R_{free} values of 20.5 and 21.7%, respectively. All structures were validated and checked using PDB validation software upon deposition. Refinement statistics for all structures are presented in **Table 1**. The Ramachandran plot for *At*GSTU25-GSSG showed 98.4% of residues to be situated in the most favored regions, 1.1% in additional allowed and 0.5% residues in outlier regions.

Generation of the GST Mutants

A QuickChange II Site-Directed Mutagenesis Kit (Agilent Technologies) was used to generate the mutants, using the primers listed in **Table 2**. Wild-type and mutated GSTU24 and GSTU25 were cloned into pET-YSBLIC3C, used to transform *E. coli* (BL21) cells, and expressed and purified as described previously (Gunning et al., 2014).

TABLE 1 | Data collection and refinement statistics for GSTU25-GSSG complex.

Beamline	**Diamond I02**
Wavelength (Å)	0.97949
Resolution (Å)	48.54–1.95 (1.99–1.95)
Space group	$P2_12_12_1$
Unit cell (Å)	a = 87.83; b = 107.67; c = 108.75' α = β = γ = 90°
No. of molecules in the asymmetric unit	4
Unique reflections	75638 (4446)
Completeness (%)	99.8 (100.0)
R_{merge} (%)	0.07 (0.54)
$R_{p.i.m.}$	0.05 (0.36)
Multiplicity	6.4 (6.2)
$<I/\sigma(I)>$	12.7 (3.0)
Overall B factor from Wilson plot (Å^2)	25
R_{cryst}/R_{free} (%)	20.5/21.7
r.m.s.d 1–2 bonds (Å)	0.02
r.m.s.d 1–3 angles (°)	1.94
Avge main chain B (Å^2)	31
Avge side chain B (Å^2)	35
Avge water B (Å^2)	42
Avge ligand B (Å^2)	40

Numbers in brackets refer to data for highest resolution shells.

TABLE 2 | Primers used for the site-directed mutagenesis of GSTU24 and GSTU25.

GSTU24		
Mutation	**Primer set**	**Primer sequence (5′–>3′)**
Ala12Pro	U24-A12P-F	GGCAGATGAGGTGATTCTTCTGGATTTCTGGCCGAGTATGTTTGGG
	U24-A12P-R	GCCAGAGCAATTCTTGTCCTCATCCCAAACATACTCGGCCAGAAATC
Asn107Tyr	U24-N107Y-F	CTGGGCCGACTTCATCGACAAAAAGGTGTATGTTACGGCGAG
	U24-N107Y-R	GACCGCCCAAATCCTTCTCGCCGTAACATACACCTTTTTGTCG
Ala115Gly	U24-A115G-F	GGTGAATGTTACGGCGAGAAGGATTTGGGGGGTCAAAGG
	U24-A115G-R	GCTGCTTCTTGCTCCTCACCTTTGACCCCCCAAATCC
Ala115Gly*	U24-A115Gb-F	GGTGTATGTTACGGCGAGAAGGATTTGGGGGGTCAAAGG
	U24-A115Gb-R	Same as U24-A115G-R
Ile208Val	U24-I208V-F	GCCCTGCCTGAGTCAGAGAAGGTCATTACATTCGTTTCCGAACG
	U24-I208V-R	CTCCAACCCAAGTTTCTTCCTACGTTCGGAAACGAATGTAATG
Arg211Leu	U24-R211L-F	GGTCATTACATTCATTTCCGAACTTAGGAAGAAACTTGGGTTGG
	U24-R211L-R	CTCCAACCCAAGTTTCTTCCTAAGTTCGGAAATGAATGTAATGACC
Arg211Leu*	U24-R211Lb-F	GGTCATTACATTCGTTTCCGAACTTAGGAAGAAACTTGGGTTGG
	U24-R211Lb-R	CTCCAACCCAAGTTTCTTCCTAAGTTCGGAAACGAATGTAATGACC
Pro12Ala	U25-P12A-F	GGCAGACGAGGTGATTCTTCTTGATTTCTGGGCGAGCATG
	U25-P12A-R	GCAATCCTCGTCCTCATTCCAAACATGCTCGCCCAGAAATC
Tyr107Asn	U25-Y107N-F	GGCCAAATTTTGGGGAGATTTCATTGATAAGAAGGTGAATGCTTCAGC
	U25-Y107N-R	GCTCCCCAAATCAACCTCGCTGAAGCATTCACCTTCTTATC
Gly115Ala	U25-G115A-F	GGTGTATGCTTCAGCGAGGTTGATTTGGGCAGCTAAAGGC
	U25-G115A-R	CGCCTCATGCTCTTCGCCTTTAGCTGCCCAAATCAACCT
Gly115Ala*	U25-G115Ab-F	GGTGAATGCTTCAGCGAGGTTGATTTGGGCAGCTAAAGGC
	U25-G115Ab-R	Same as U25-G115A-R
Val209Ile	U25-V209I-F	GTCTCTTCCTGATTCGGAGAAGATCATTAAGTTCATTCCTGAGC
	U25-V209I-R	CCCAAGTTTTTTCCTTAGCTCAGGAATGAACTTAATGATCTTCTCCG
Leu212Arg	U25-L212R-F	CGGAGAAGATCATTAAGTTCGTTCCTGAGCGAAGGAAAAAAC
	U25-L212R-R	CTATTCGATTTCGATCCCAAGTTTTTTCCTTCGCTCAGGAACG
Leu212Arg*	U25-L212Rb-F	CGGAGAAGATCATTAAGTTCATTCCTGAGCGAAGGAAAAAAC
	U25-L212Rb-R	CTATTCGATTTCGATCCCAAGTTTTTTCCTTCGCTCAGGAATG

The asterisks (*) mark primer sets that were designed for the generation of sequential mutations and carry in their sequence the previous mutation, e.g., the Ala115Gly primer set is designed to insert the Ala115Gly mutation into a sequence that already has the Asn107Tyr mutation.*

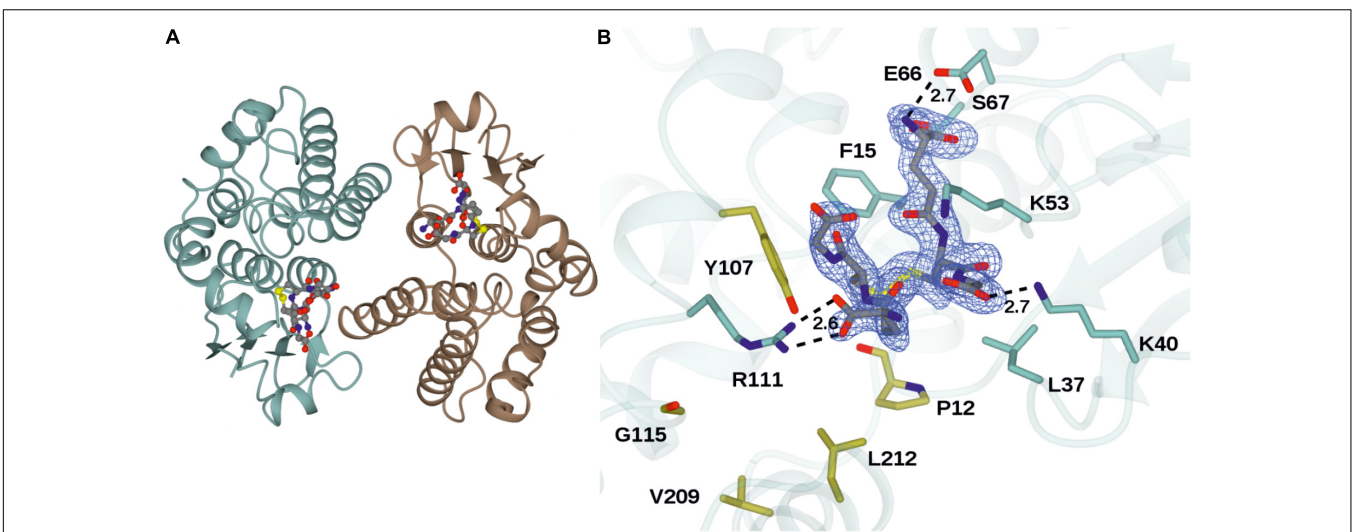

FIGURE 2 | Structures of GSTU25 and target residues. **(A)** Structure of the GSTU25 dimer, with monomers in blue and brown. Oxidized glutathione can be observed in each of the monomer active sites, in stick format. **(B)** Active site of the GSTU25 monomer showing binding of GSSG. The electron density corresponds to the F_o-F_c omit map contoured at a level of 3σ, and is that which was obtained prior to refinement of the ligand atoms, which have been added from the refined ligand complex for clarity. Side chains of residues conserved between U24 and U25 are shown with side-chain carbon atoms in Blue; Side-chains of residue positions chosen for mutation are shown with side-chain carbon atoms in gold.

GST Assays Using CDNB

Conjugating activity of the purified proteins, and crude extracts from rosette leaves, was assessed using CDNB as described previously (Colville and Smirnoff, 2008). Briefly, the reaction, at 25°C, comprised 100 mM potassium phosphate buffer pH 6.5, 5 mM GSH and a range of CDNB concentrations, and was initiated by addition of 5 µg of purified enzyme to a final volume of 1 mL. Increase in absorbance at A_{340} was measured spectrophotometrically. The Michaelis–Menten plots and kinetic calculations (K_m and V_{max}) were performed using SigmaPlot 14 software. Statistical analysis was performed using Statistical Package for Social Sciences (SPSS) software (version 25, SPSS, Inc., Chicago, IL, United States). Results were analyzed using the analysis of variance (ANOVA) for continuous variables. *P*-values <0.05 were considered to be statistically significant.

GST Assays Using TNT

Reactions, carried out at 20°C, contained 100 mM potassium phosphate buffer pH 7.0, 300 µg of purified enzyme and 5 mM GSH and was initiated by addition of TNT to a final volume of 250 µL. Reactions were stopped by the addition of trichloroacetic acid, to a final concentration of 10% (v/v), and samples analyzed by HPLC.

Measurement of TNT and Products

The TNT and conjugates were analyzed by HPLC using a Waters HPLC system (Waters 2695 separator and Waters Photodiode array detector) with Waters X-Bridge C18 column (300 mm × 4.5 mm, 5 µM). The mobile phases for the gradient conditions were: mobile phase A, acetonitrile; mobile phase B, 50 mM NaH_2PO_4, pH 2.7, with 85% (v/v) phosphoric acid. The gradient ran: 0 min 0% A 100% B, 6 min 0% A 100% B, 11 min 50% A 50% B, 25 min 100% A 0% B, 30 min 0% A 100% B, runtime 30 min. Integration was performed at 250 nm with Empower Pro Software.

Nitrite Measurement

Nitrite production was assayed according to the method of French et al. (1998) with modifications as described in Gunning et al. (2014).

Probing the Mutants With ANS

The ANS binding assay, based on the protocol by Yang et al. (2009), was used to determine conformational changes. The assay was performed in a 1 mL cuvette with 100 µl of 2 mM ANS, 50 µg of enzyme and 100 mM potassium phosphate buffer pH 6.5. The fluorescence emission was monitored using a FluoroMax®-4 Spectrofluorometer (Horiba Scientific).

Accession Numbers

*At*GSTU24; TAIR accession number At1g17180, *At*GSTU25; TAIR acc. no. At1g17170. *At*GSTU25-GSSG coordinates; Protein Databank (PDB) acc. no. 5g5a. *Gm*GSTU4-4; PDB acc. no. 2VO4, Sh14; PDB acc. no. 5AGY, *Pc*Ure2pA; PDB acc. no. 4F0B, *Ec*YghU; PDB acc. no. 3C8E, *Ec*YfcG; PDB acc. no. 3GX0, *Co*GRX2; PDB acc. no. 4TR0.

RESULTS

Structure of GSTU25

The structure of GSTU25 was solved using molecular replacement at a resolution of 1.99 Å with *Gm*GSTU4-4 as template (Axarli et al., 2009). Analysis of the protein structure using the DALI server (Holm and Rosenstrom, 2010) revealed that the monomer was more similar to the structure of a Tau class GST mutant from *G. max*, called Sh14 (Axarli et al., 2016). Both structures were 68% identical, with a RMS value of 1.2 Å over 219 residues. Each monomer of GSTU25 has four β-strands and nine α-helices adopting the canonical GST fold. The first 77 residues at the N-terminus fold into a thioredoxin-like domain followed by an α-helical domain at the C-terminus from position 89 to 216, with the two domains connected together by a short linker. Although the crystals were incubated with TNT and GSH, binding of TNT was not detected. Instead, multiple rounds of structure refinement cycles using the REFMAC5 program (Murshudov et al., 2011) revealed two GSH molecules covalently linked by a disulfide bond, showing the structure of GSTU25 in complex with glutathione disulfide (GSSG) (**Figure 2A**). At the binding site, the GSSG subunits: GSH-1 and GSH-2, were located in a binding pocket surrounded by polar, non-polar and charged amino acids (**Figure 2B**). This pocket was similar to the

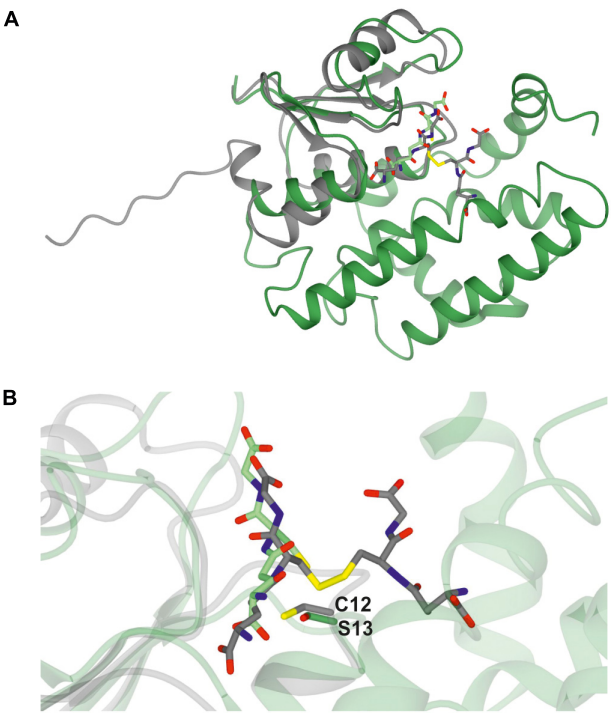

FIGURE 3 | Comparison of GSTU25 with CoGRX2. **(A)** Superimposed structures of the glutaredoxin subunit from Clostridium oremlandii (CoGRX2 in complex with GSSG (C-atoms in gray), and the GSTU25 subunit (green) in complex with GSSG (C-atoms in green). The RMS value for the superimposed structures is 2.3 Å over 73 residues. **(B)** Position of the active residue for GSH thiol stabilization: serine 13, in GSTU25 and cysteine 12 in CoGRX2.

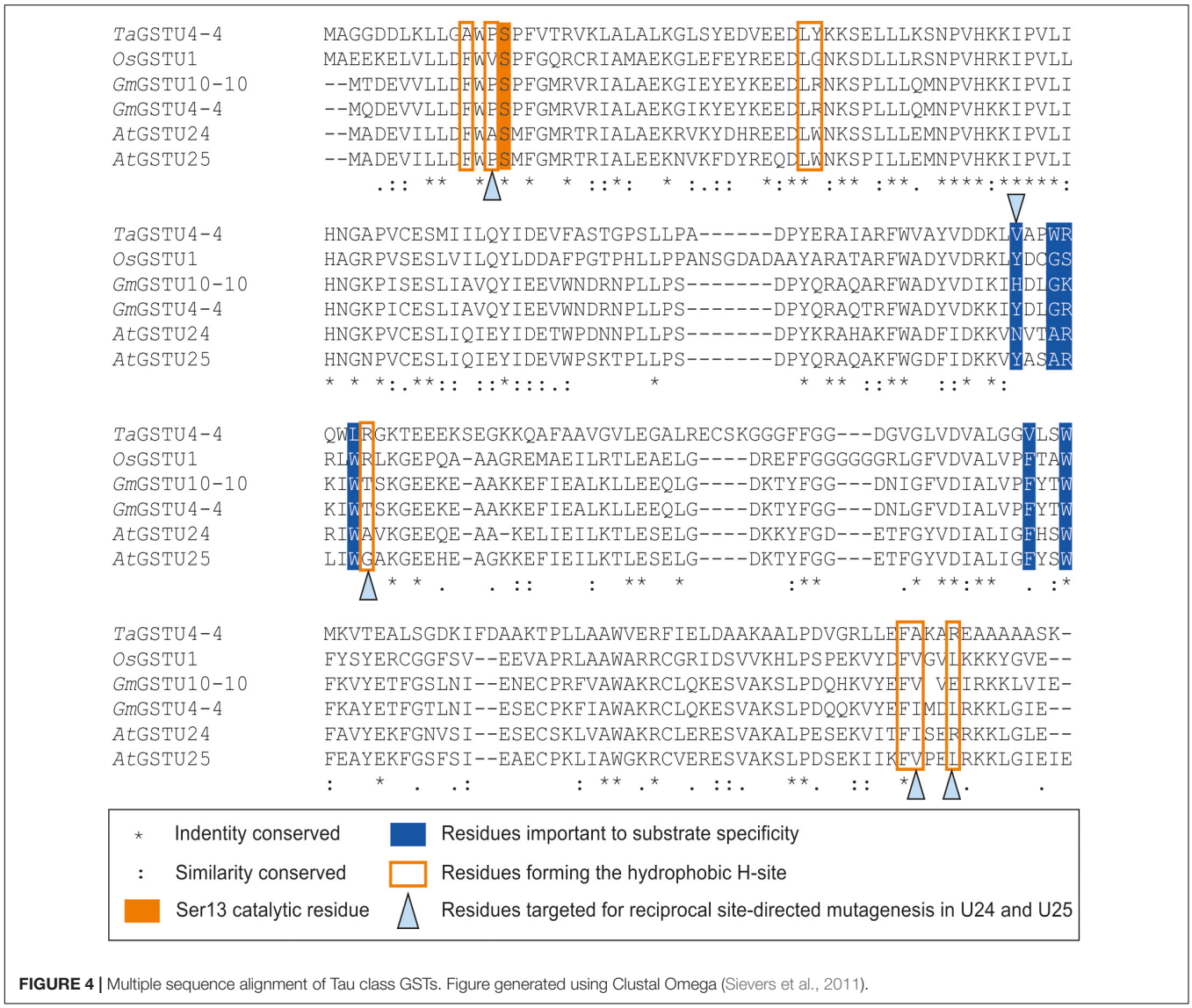

FIGURE 4 | Multiple sequence alignment of Tau class GSTs. Figure generated using Clustal Omega (Sievers et al., 2011).

active site identified for most GSTs, where the hydroxyl group of S13 and Y107 has been shown to contribute to the ionization of the GSH sulfhydryl group (Brock et al., 2013). Similar locations were observed for the same S and Y residues of *Gm*GSTU4-4 in complex with *S*-(*p*-nitrobenzyl)-glutathione (Axarli et al., 2009). The S residue was found to stabilize the thiolate anion of GSH and enhance its nucleophilicity, while the Y residue was important in regulating catalytic function. The GSTU25-GSSG structure also revealed that the terminal carboxylate group of the GSH-1 γ-glutamyl moiety formed an interaction at 2.6 Å with the nitrogen atom of the guanidinium group of R111, and that the glycine moiety of GSH-1 protruded toward the GSTU25 α4 chain. The GSH-2 molecule, at the carboxylate terminal of the glycine moiety, formed an interaction with the oxygen atom of K40 at a distance of 2.7 Å with the γ-glutamyl moiety located in between the helices α1 and α3.

A *Clostridium oremlandii* glutaredoxin (*Co*GRX2) with two GSSG molecules per dimer has been reported (Lee et al., 2014) and exhibits significant similarity with GSTU25 at the core of the thioredoxin fold where four β-strands and α-helices, can be observed (**Figure 3A**). In GSTU25, a serine interacts with the

TABLE 3 | Amino acid substitutions in the GSTU24 and GSTU25 mutants.

Enzyme	Mutation identifier	Substitution
GSTU24	A	A12P
	B	N107Y
	C	A115G
	D	I208V
	E	R211L
GSTU25	F	P12A
	G	Y107N
	H	G115A
	I	V209I
	J	L212R

GSSG molecule (**Figure 3B**), whereas in *Co*GRX2, cysteine acts as the GSH thiol stabilizer.

Identification of Target Amino Acids for Site-Directed Mutagenesis

Seven key residues (F15, L37, K40, K53, E66, S67, R111) identified in the structure of GSTU25, and shown in **Figure 2B** with side-chain carbon atoms in blue, are all conserved in GSTU24. Comparisons with the structure of *Ta*GSTU4-4 (Thom et al., 2002) and *Gm*GSTU4-4 (Axarli et al., 2009) were used to highlight further amino acid residues in GSTU24 and GSTU25 that are likely to be involved in the formation of the hydrophobic H-site and thus in the determination of substrate specificity (shown as orange-outlined boxes in **Figure 4**). Of the six residues known to be important for substrate specificity in Tau class GSTs (shown in blue boxes), the residue at position 107 (N for GSTU24, Y for GSTU25) was the only one not identical between GSTU24 and GSTU25, and was thus targeted for mutagenesis. Subsequent homology modeling using the published structure of *Gm*GSTU4-4 (Axarli et al., 2009), which shares high (>60%) protein sequence identity with GSTU24 and GSTU25, identified four, further, non-identical residues, at positions 12, 115, 208 (209 for GSTU25) and 211 (212 for GSTU25), as shown in **Figure 2B**. The five amino acid residues targeted for reciprocal mutagenesis are listed in **Table 3**, marked as blue triangles in **Figure 4**, and highlighted with side-chain carbon atoms in gold for U25 in **Figure 2B**.

Activity of GSTU24 and GSTU25 Mutants Toward TNT

To determine the effects of the target mutations on the ability of the GST proteins to produce the three different TNT-conjugates, the mutated proteins were assayed using TNT as substrate. For GSTU24, mutation BCD significantly reduced ($p = 0.003$) overall levels of conjugates produced to 52% of the wild-type GSTU24, whereas mutations AB and ABCDE displayed significantly higher (82 and 163%, respectively, $p < 0.0001$) conjugating activity than the wild type GSTU24 (**Figure 5A**). **Figure 5B** shows that all five mutants were able to produce conjugate 1, which was not detectable from wild type GSTU24 under these conditions. The mutant ABCDE was distinct from the others tested as it displayed the highest overall conjugating activity of the five U25-derived mutants. This ABCDE mutant was also able to produce significantly higher ($p < 0.0001$) amounts of conjugate 3, GDNT, than GSTU24, or the other four mutants. Moreover, ABCDE produced all three conjugates in almost equimolar concentrations.

For the GSTU25, mutations, FG and G significantly reduced ($p < 0.0001$) overall levels of conjugates produced to 31 and 24%, respectively, of the wild-type GSTU25. Compared to GSTU25,

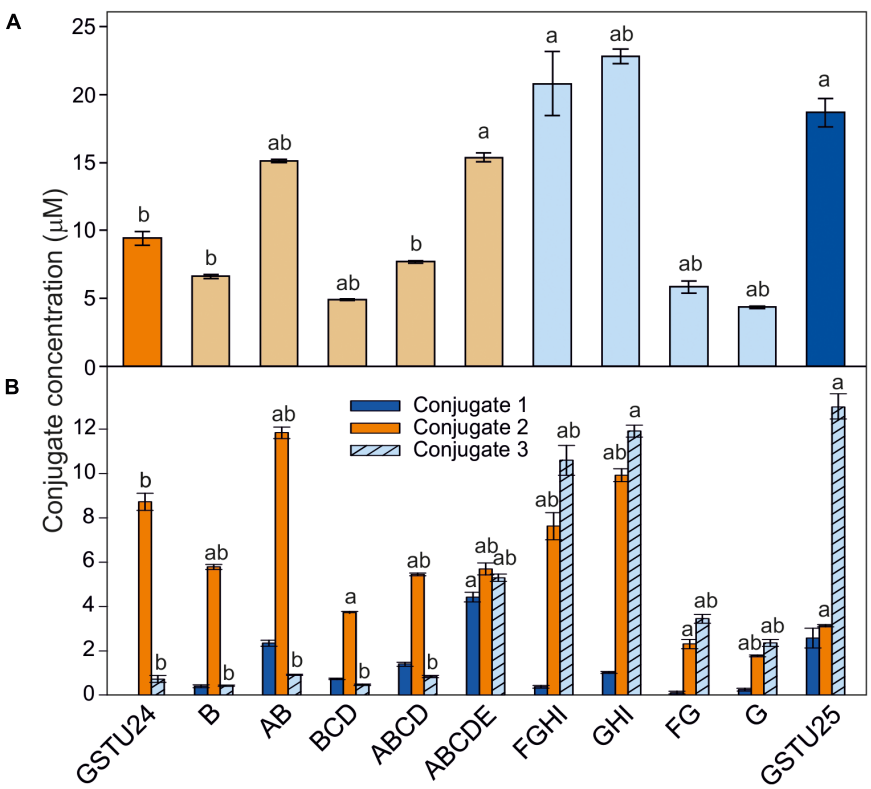

FIGURE 5 | TNT-conjugate profiles from GSTs. **(A)** Total conjugates and **(B)** conjugate profiles produced by *At*GSTU24, *At*GSTU25, and mutants. Conjugate 3 = 2-glutathionyl-4,6-dinitrotoluene (GDNT). Results are means of three replicates ± SE, a, significantly different from *At*GSTU24, b, significantly different from *At*GSTU25.

these FG and G mutants also yielded significantly reduced ($p < 0.0001$) overall levels of GDNT, while levels of conjugate 2 were not significantly affected for G (**Figure 5B**). Mutant GHI produced significantly more overall conjugates ($p = 0.007$) when compared to wild-type GSTU25, with both GHI and FGHI also producing significantly more conjugate 2 ($p < 0.0001$).

Probing the GSTU24 and GSTU25 Mutants for Conformational Changes

To identify any conformational changes in protein structure resulting from the presence of the mutated residues, the mutants were probed with 1-anilino-8-naphthalene-sulfonate (ANS) and the spectra measured. Both GSTU24 and GSTU25 shared a similar structure in the hydrophobic site (**Figure 6A**), with only the ABCDE mutant generating a significantly different fluorescence spectrum, indicative of a change in conformation

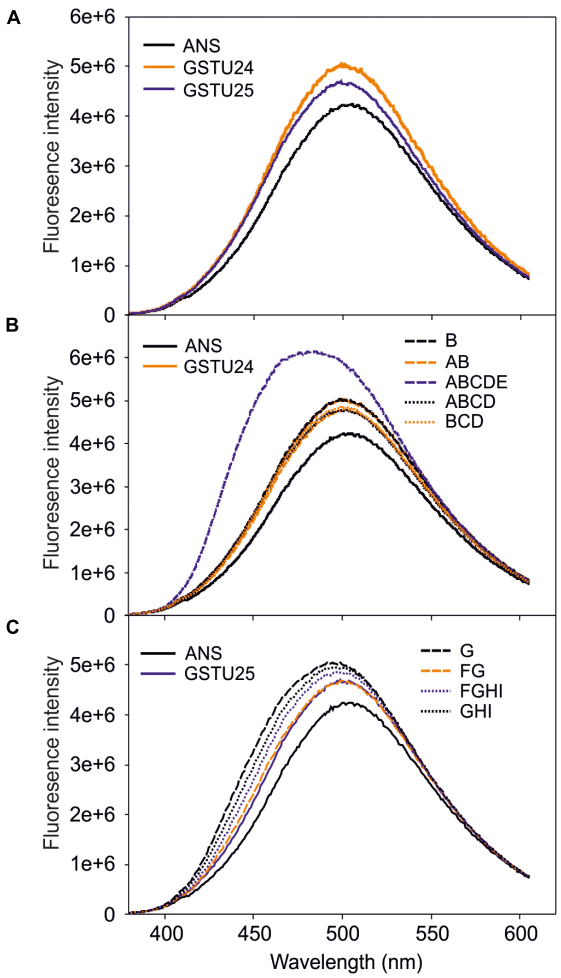

FIGURE 6 | Fluorescence-emission spectra of 1-anilino-8-naphthalene-sulfonate (ANS) binding to the active site of the GSTs. **(A)** Spectra from GSTU24 and GSTU25. **(B)** Spectra from GSTU24 and its respective mutants. **(C)** Spectra from GSTU25 and its respective mutants. ANS, blank sample without enzyme; A-I, GSTU24 and GSTU25 mutants as presented in **Table 3**. Results are means of three technical replicates.

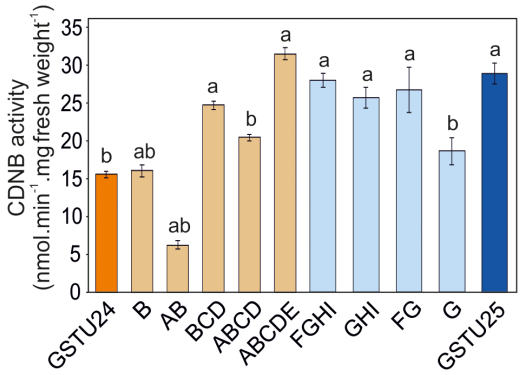

FIGURE 7 | GST activity using 1 mM 1-chloro-2,4-dinitrobenzene (CDNB) substrate for GSTU24, GSTU25 and their respective mutants. Results are means of three technical replicates ± SE, a, significantly different from *At*GSTU24; b, significantly different from *At*GSTU25.

(**Figure 6B**). The fluorescence spectra of the different GSTU25 mutants, varied slightly to one another, but none of them suggested a significant conformational change had occurred (**Figure 6C**).

Activity of GSTU24, GSTU25, and Mutants Toward CDNB

The activity of the mutants was measured using CDNB as a substrate. The results in **Figure 7** show that all the mutants exhibited changes in activity that were significantly different to either, or both of the wild type GSTs. Given that the mutant ABCDE was distinct in displaying the highest overall conjugating activity, and producing significantly higher amounts of the desired target, GDNT, kinetic analysis was performed using CDNB substrate (**Figure 8** and **Table 4**). While GSTU24 and GSTU25 exhibited similar V_{max} values, the K_m for GSTU24 was 45-fold higher than for GSTU25. In agreement with our reported conjugate profiles, the GSTU24 ABCDE mutant also displayed a reduced, GSTU25-like, K_m value.

DISCUSSION

The aim of this study was to identify the amino acids within GSTU25 involved in the formation of GDNT. To achieve this, the structure of GSTU25 was first determined. The structure, along with comparisons with the known Tau class GST structures *Ta*GSTU4-4 (Thom et al., 2002) and *Gm*GSTU4-4 (Axarli et al., 2009); and amino acid sequence of the closely related GSTU24, were used to highlight the amino acid residues in GSTU25 most likely to be involved.

Crystal Structure of GSTU25

The electron density map for GSTU25 revealed unambiguously one GSSG per subunit. Within the GSTU25-GSSG structure, the GSH-1 moiety is stabilized by an arginine side chain (R111) while the GSH-2 moiety is located at a well-documented GSH binding site (Axarli et al., 2009, 2016; Skopelitou et al., 2015). The binding

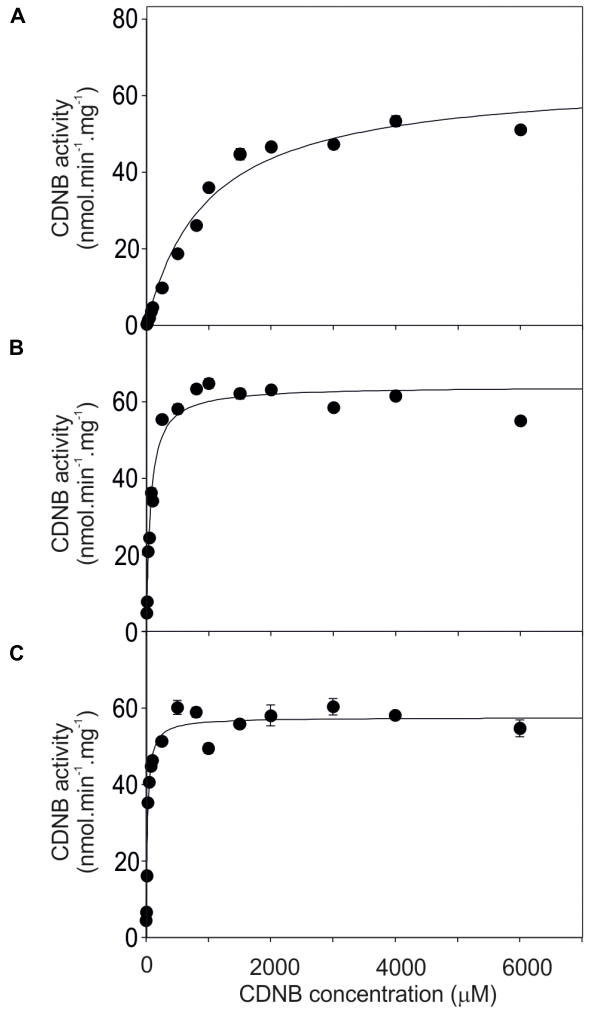

FIGURE 8 | Michaelis–Menten plots from purified GST proteins. **(A)** GSTU24, **(B)** ABDCE mutant, and **(C)** GSTU25, assayed with 1-chloro-2,4-dinitrobenzene (CDNB) substrate. Values represent the mean of at least four reactions ± SE.

of GSTs to GSSG has been reported in the wood fungus, *Phanerochaete chrysosporium Pc*Ure2pA (Roret et al., 2015), and *E. coli* homologs *Ec*YghU and *Ec*YfcG. These bacterial and fungal GSTs have GSH transferase activity and are distantly related to glutaredoxins, redox enzymes that reduce disulfide bonds using glutathione (GSH) as an electron donor (Stourman et al., 2011). As shown in **Figure 3**, U25 shares significant similarity *Co*GRX2. In yeast (*Saccharomyces cerevisiae*), glutaredoxins *Sc*GRX1 and *Sc*GRX2 display GST-like activities, catalyzing the conjugation of CDNB to GSH (Collinson and Grant, 2003). As a multifunctional enzyme, exhibiting glutaredoxin, GPOX, and GST activities, GSTU25 would be well-suited to detoxify a wide range of the xenobiotics and oxidants present in diverse stress conditions.

TABLE 4 | Enzyme kinetics for **Figure 8**, assayed using CDNB substrate.

Enzyme	K_m (μM)	V_{max} (nmole min^{-1} mg^{-1})	R^2
GSTU24	972 ± 72.9	64.7 ± 1.6	0.98
ABCDE	64.8 ± 4.3	64.0 ± 0.8	0.96
GSTU25	21.5 ± 1.9	57.6 ± 0.7	0.95

Residues Important to TNT-Conjugation Activity

Both GSTU24 and GSTU25 contain a serine residue (S13) in the active site at a position that allows it to stabilize the thiolate anion of glutathione. This is in agreement with structures of GSTs from Theta and Phi classes that are known to have GSH conjugating activity (Thom et al., 2001) and is replaced by cysteine for Lambda and DHAR GSTs (Dixon et al., 2002). The effects of the mutations on the activity toward TNT showed that Y107 in GSTU25 is important for conjugate specificity. GSTU24 does not produce conjugate 1 under the conditions tested; however, the N107Y mutation confers the ability to produce albeit small (6%) amounts of this conjugate. The data presented here also indicate that high activity of toward TNT requires both Y107 and P12. At the binding site of GSTU25, the GSSG subunits are located in a binding pocket surrounded by polar, non-polar and charged amino acids; a well-characterized active site for GSTs (Brock et al., 2013). In *Gm*GSTU4-4, the same S and Y residues of *Gm*GSTU4-4 are present in this binding pocket. When in complex with *S*-(*p*-nitrobenzyl)-glutathione, the S residue stabilizes the thiolate anion of GSH and enhances its nucleophilicity, while the Y residue is important in regulating catalytic function (Axarli et al., 2009). In GST25, L212 could also contribute to the production of GDNT; in *Gm*GSTU4-4, the close proximity of this residue to the nitro group of 4-nitrobenzyl (Axarli et al., 2009) could orientate TNT in the active site.

The five consecutive mutations present in GSTU25 ABCDE were predicted to engineer the near-complete active site of GSTU25 into GSTU24. The resulting conjugate profile and activity of ABCDE were similar to GSTU25 in that all three conjugates were produced, and at levels of overall conjugating activity similar to those of GSTU24. Furthermore, the K_m value of ABCDE was more in-line with that of GSTU25. Nonetheless, the fluorescence emission spectrum of ABCDE was significantly different from both GSTU24 and GSTU25, indicating a conformational change in the hydrophobic site, and TNT was not crystalized within the GSTU25 structure. Although TNT and reduced GSH were supplied during the crystallization process, incorporation of TNT into the active site was likely to have been hindered by the low aqueous solubility of TNT. Using synthesized, and more soluble, GDNT, in the absence of GSH, during the crystallization process could perhaps yield more information about the residues involved during the formation of this conjugate.

In summary, we have solved the structure for GSTU25, and identified key residues involved in the formation of 2-GDNT. Substitution of a nitro group for sulfur in 2-GDNT could render the aromatic ring more susceptible to subsequent degradation, and endogenous degradative pathways may already exist *in planta*. Alternatively, both bacteria and fungi are able to mineralize DNT (Serrano-González et al., 2018), and may

have activity toward 2-GDNT. These fundamental studies will contribute toward the development of plant-based remediation strategies to degrade TNT, a toxic environmental pollutant.

AUTHOR CONTRIBUTIONS

KT, LA, and MD carried out the experiments. ER took the lead in writing the manuscript. All authors conceived and planned the experiments, provided critical feedback, helped shape the research, performed the analysis, and wrote the manuscript.

ACKNOWLEDGMENTS

This work was funded by the United Kingdom Biotechnology and Biological Sciences Research Council (BB/P005713/1), and the Strategic Environmental Research and Development Program (ER-1498) and Environmental Security Technology Certification Program (ER-201436) of the United States Department of Defense. KT acknowledges funding from a Burgess studentship and LA funding for a studentship from a Majlis Amanah Rakyat (MARA), Malaysia. This study used the University of York Technology Facilities.

REFERENCES

Amaral, H. I., Fernandes, J., Berg, M., Schwarzenbach, R. P., and Kipfer, R. (2009). Assessing TNT and DNT groundwater contamination by compound-specific isotope analysis and 3H-3He groundwater dating: a case study in Portugal. *Chemosphere* 77, 805–812. doi: 10.1016/j.chemosphere.2009.08.011

Axarli, I., Dhavala, P., Papageorgiou, A. C., and Labrou, N. E. (2009). Crystallographic and functional characterization of the fluorodifen-inducible glutathione transferase from Glycine max reveals an active site topography suited for diphenylether herbicides and a novel L-site. *J. Mol. Biol.* 385, 984–1002. doi: 10.1016/j.jmb.2008.10.084

Axarli, I., Muleta, A. W., Vlachakis, D., Kossida, S., Kotzia, G., Maltezos, A., et al. (2016). Directed evolution of Tau class glutathione transferases reveals a site that regulates catalytic efficiency and masks co-operativity. *Biochem. J.* 473, 559–570. doi: 10.1042/bj20150930

Brock, J., Board, P. G., and Oakley, A. J. (2013). Structural insights into omega-class glutathione transferases: a snapshot of enzyme reduction and identification of a non-catalytic ligandin site. *PLoS One* 8:e60324. doi: 10.1371/journal.pone.0060324

Clark, B., and Boopathy, R. (2007). Evaluation of bioremediation methods for the treatment of soil contaminated with explosives in Louisiana Army Ammunition Plant, Minden, Louisiana. *J. Hazard. Mater.* 143, 643–648. doi: 10.1016/j.jhazmat.2007.01.034

Collinson, E. J., and Grant, C. M. (2003). Role of yeast glutaredoxins as glutathione S-transferases. *J. Biol. Chem.* 278, 22492–22497. doi: 10.1074/jbc.M301387200

Colville, L., and Smirnoff, N. (2008). Antioxidant status, peroxidase activity, and PR protein transcript levels in ascorbate-deficient Arabidopsis thaliana vtc mutants. *J. Exp. Bot.* 59, 3857–3868. doi: 10.1093/jxb/ern229

Dixon, D., Davis, B., and Edwards, R. (2002). Functional divergence in the glutathione transferase superfamily in plants - Identification of two classes with putative functions in redox homeostasis in Arabidopsis thaliana. *J. Biol. Chem.* 277, 30859–30869. doi: 10.1074/jbc.M202919200

Dixon, D., and Edwards, R. (2009). Selective binding of glutathione conjugates of fatty acid derivatives by plant glutathione transferases. *J. Biol. Chem.* 284, 21249–21256. doi: 10.1074/jbc.M109.020107

Dixon, D., Sellars, J., and Edwards, R. (2011). The Arabidopsis phi class glutathione transferase AtGSTF2: binding and regulation by biologically active heterocyclic ligands. *Biochem. J.* 438, 63–70. doi: 10.1042/BJ20101884

Dixon, D. P., and Edwards, R. (2010). Glutathione transferases. *Arabidopsis Book* 8:e0131. doi: 10.1199/tab.0131

Edwards, R., Dixon, D., Sies, H., and Packer, L. (2005). Plant glutathione transferases. *Gluthione Transferases Gamma Glutamyl Transpeptidases* 401, 169–186. doi: 10.1016/S0076-6879(05)01011-6

Emsley, P., and Cowtan, K. (2004). Coot: model-building tools for molecular graphics. *Acta Crystallogr. D Biol.Crystallogr.* 60, 2126–2132. doi: 10.1107/S0907444904019158

Evans, P. (2006). Scaling and assessment of data quality. *Acta Crystallogr. D Biol. Crystallogr.* 62, 72–82. doi: 10.1107/s0907444905036693

French, C. E., Nicklin, S., and Bruce, N. C. (1998). Aerobic degradation of 2,4,6-trinitrotoluene by *Enterobacter cloacae* PB2 and by pentaerythritol tetranitrate reductase. *Appl. Environ. Microbiol.* 64, 2864–2868.

Gandia-Herrero, F., Lorenz, A., Larson, T., Graham, I. A., Bowles, D. J., Rylott, E. L., et al. (2008). Detoxification of the explosive 2,4,6-trinitrotoluene in Arabidopsis: discovery of bifunctional O- and C-glucosyltransferases. *Plant J.* 56, 963–974. doi: 10.1111/j.1365-313X.2008.03653.x

Gunning, V., Tzafestas, K., Sparrow, H., Johnston, E. J., Brentnall, A. S., Potts, J. R., et al. (2014). Arabidopsis glutathione transferases U24 and U25 exhibit a range of detoxification activities with the environmental pollutant and explosive, 2,4,6-Trinitrotoluene. *Plant Physiol.* 165, 854–865. doi: 10.1104/pp.114.237180

Holm, L., and Rosenstrom, P. (2010). Dali server: conservation mapping in 3D. *Nucleic Acids Res.* 38, W545–W549. doi: 10.1093/nar/gkq366

Jenkins, T. F., Hewitt, A. D., Grant, C. L., Thiboutot, S., Ampleman, G., Walsh, M. E., et al. (2006). Identity and distribution of residues of energetic compounds at army live-fire training ranges. *Chemosphere* 63, 1280–1290. doi: 10.1016/j.chemosphere.2005.09.066

Johnson, G. R., Jain, R. K., and Spain, J. C. (2002). Origins of the 2,4-dinitrotoluene pathway. *J. Bacteriol.* 184, 4219–4232. doi: 10.1128/JB.184.15.4219-4232.2002

Kabsch, W. (2010). XDS. *Acta Crystallogr. D Biol. Crystallogr.* 66, 125–132. doi: 10.1107/s0907444909047337

Labrou, N. E., Papageorgiou, A. C., Pavli, O., and Flemetakis, E. (2015). Plant GSTome: structure and functional role in xenome network and plant stress response. *Curr. Opin. Biotechnol.* 32, 186–194. doi: 10.1016/j.copbio.2014.12.024

Lee, E. H., Kim, H. Y., and Hwang, K. Y. (2014). The GSH- and GSSG-bound structures of glutaredoxin from Clostridium oremlandii. *Arch. Biochem. Biophys.* 564, 20–25. doi: 10.1016/j.abb.2014.09.001

Lewis, T. A., Newcombe, D. A., and Crawford, R. L. (2004). Bioremediation of soils contaminated with explosives. *J.Environ.Manage.* 70, 291–307. doi: 10.1016/j.jenvman.2003.12.005

Mezzari, M. P., Walters, K., Jelinkova, M., Shih, M. C., Just, C. L., and Schnoor, J. L. (2005). Gene expression and microscopic analysis of arabidopsis exposed to chloroacetanilide herbicides and explosive compounds. A Phytoremediation Approach. *Plant Physiol.* 138, 858–869. doi: 10.1104/pp.104.056168

Murshudov, G. N., Skubák, P., Lebedev, A. A., Pannu, N. S., Steiner, R. A., Nicholls, R. A., et al. (2011). REFMAC5 for the refinement of macromolecular crystal structures. *Acta Crystallogr. D Biol. Crystallogr.* 67, 355–367. doi: 10.1107/S0907444911001314

Murshudov, G. N., Vagin, A. A., and Dodson, E. J. (1997). Refinement of macromolecular structures by the maximum-likelihood method. *Acta Crystallogr. D Biol. Crystallogr.* 53, 240–255. doi: 10.1107/S0907444996012255

Nishino, S. F., Paoli, G. C., and Spain, J. C. (2000). Aerobic degradation of dinitrotoluenes and pathway for bacterial degradation of 2,6-dinitrotoluene. *Appl. Environ. Microbiol.* 66, 2139–2147. doi: 10.1128/AEM.66.5.2139-2147.2000

Qasim, M., Gorb, L., Magers, D., Honea, P., Leszczynski, J., Moore, B., et al. (2009). Structure and reactivity of TNT and related species: application of spectroscopic approaches and quantum-chemical approximations toward understanding transformation mechanisms. *J. Hazard. Mater.* 167, 154–163. doi: 10.1016/j.jhazmat.2008.12.105

Roret, T., Thuillier, A., Favier, F., Gelhaye, E., Didierjean, C., and Morel-Rouhier, M. (2015). Evolutionary divergence of Ure2pA glutathione transferases in wood degrading fungi. *Fungal Genet. Biol.* 83, 103–112. doi: 10.1016/j.fgb.2015.09.002

Rylott, E. L., Lorenz, A., and Bruce, N. C. (2011). Biodegradation and biotransformation of explosives. *Curr. Opin. Biotechnol.* 22, 434–440. doi: 10.1016/j.copbio.2010.10.014

Serrano-González, M. Y., Chandra, R., Castillo-Zacarias, C., Robledo-Padilla, F., Rostro-Alanis, M. D. J., and Parra-Saldivar, R. (2018). Biotransformation and degradation of 2,4,6-trinitrotoluene by microbial metabolism and their interaction. *Defence Technol.* 14, 151–164. doi: 10.1016/j.dt.2018.01.004

Sievers, F., Wilm, A., Dineen, D., Gibson, T. J., Karplus, K., Li, W., et al. (2011). Fast, scalable generation of high-quality protein multiple sequence alignments using Clustal Omega. *Mol. Syst. Biol.* 7:539. doi: 10.1038/msb.2011.75

Skopelitou, K., Muleta, A. W., Papageorgiou, A. C., Chronopoulou, E., and Labrou, N. E. (2015). Catalytic features and crystal structure of a tau class glutathione transferase from Glycine max specifically upregulated in response to soybean mosaic virus infections. *Biochim. Biophys. Acta* 1854, 166–177. doi: 10.1016/j.bbapap.2014.11.008

Smith, A. P., Nourizadeh, S. D., Peer, W. A., Xu, J., Bandyopadhyay, A., Murphy, A. S., et al. (2003). Arabidopsis AtGSTF2 is regulated by ethylene and auxin, and encodes a glutathione S-transferase that interacts with flavonoids. *Plant J.* 36, 433–442. doi: 10.1046/j.1365-313X.2003.01890.x

Spain, J. C., Hughes, J. B., and Knackmuss, H. J. (2000). *Biodegradation of Nitroaromatic Compounds and Explosives*. Boca Raton, FL: Lewis.

Stourman, N. V., Branch, M. C., Schaab, M. R., Harp, J. M., Ladner, J. E., and Armstrong, R. N. (2011). Structure and function of YghU, a nu-class glutathione transferase related to YfcG from *Escherichia coli*. *Biochemistry* 50, 1274–1281. doi: 10.1021/bi101861a

Talmage, S. S., Opresko, D. M., Maxwell, C. J., Welsh, C. J., Cretella, F. M., Reno, P. H., et al. (1999). Nitroaromatic munition compounds: environmental effects and screening values. *Rev. Environ. Contam. Toxicol.* 161, 1–156. doi: 10.1007/978-1-4757-6427-7_1

Thom, R., Cummins, I., Dixon, D. P., Edwards, R., Cole, D. J., and Lapthorn, A. J. (2002). Structure of a tau class glutathione S-transferase from wheat active in herbicide detoxification. *Biochemistry* 41, 7008–7020. doi: 10.1021/bi015964x

Thom, R., Dixon, D., Edwards, R., Cole, D., and Lapthorn, A. (2001). The structure of a zeta class glutathione S-transferase from Arabidopsis thaliana: characterisation of a GST with novel active-site architecture and a putative role in tyrosine catabolism. *J. Mol. Biol.* 308, 949–962. doi: 10.1006/jmbi.2001.4638

United States General Accounting Office (2004). *Department of Defense Operational Ranges, More Reliable Cleanup Cost Estimates and a Proactive Approach to Identifying Contamination are Needed*. Available at: http://www.gao.gov/new.items/d04601.pdf

Vagin, A., and Teplyakov, A. (1997). MOLREP: an automated program for molecular replacement. *J. Appl. Crystallogr.* 30, 1022–1025. doi: 10.1107/S0021889897006766

Valli, K., Brock, B. J., Joshi, D. K., and Gold, M. H. (1992). Degradation of 2,4-dinitrotoluene by the lignin-degrading fungus *Phanerochaete chrysosporium*. *Appl. Environ. Microbiol.* 58, 221–228.

Winter, G. (2010). xia2: an expert system for macromolecular crystallography data reduction. *J. Appl. Crystallogr.* 43, 186–190. doi: 10.1107/S0021889809045701

Yang, X., Sun, W., Liu, J.-P., Liu, Y.-J., and Zeng, Q.-Y. (2009). Biochemical and physiological characterization of a tau class glutathione transferase from rice (*Oryza sativa*). *Plant Physiol. Biochem.* 47, 1061–1068. doi: 10.1016/j.plaphy.2009.07.003

Zheng, W., Lichwa, J., D'alessio, M., and Ray, C. (2009). Fate and transport of TNT, RDX, and HMX in streambed sediments: implications for riverbank filtration. *Chemosphere* 76, 1167–1177. doi: 10.1016/j.chemosphere.2009.06.043

Conflict of Interest Statement: The authors declare that the research was conducted in the absence of any commercial or financial relationships that could be construed as a potential conflict of interest.

frontiers in Plant Science

REVIEW
published: 21 December 2018
doi: 10.3389/fpls.2018.01836

Glutathione S-Transferase Enzymes in Plant-Pathogen Interactions

*Gábor Gullner[1], Tamas Komives[1], Lóránt Király[1] and Peter Schröder[2]**

[1] *Plant Protection Institute, Centre for Agricultural Research, Hungarian Academy of Sciences, Budapest, Hungary,*
[2] *Research Unit for Comparative Microbiome Analyses, Department of Environmental Sciences, Helmholtz Zentrum München, German Research Center for Environmental Health (GmbH), Neuherberg, Germany*

Plant glutathione S-transferases (GSTs) are ubiquitous and multifunctional enzymes encoded by large gene families. A characteristic feature of *GST* genes is their high inducibility by a wide range of stress conditions including biotic stress. Early studies on the role of GSTs in plant biotic stress showed that certain *GST* genes are specifically up-regulated by microbial infections. Later numerous transcriptome-wide investigations proved that distinct groups of *GST*s are markedly induced in the early phase of bacterial, fungal and viral infections. Proteomic investigations also confirmed the accumulation of multiple GST proteins in infected plants. Furthermore, functional studies revealed that overexpression or silencing of specific *GSTs* can markedly modify disease symptoms and also pathogen multiplication rates. However, very limited information is available about the exact metabolic functions of disease-induced GST isoenzymes and about their endogenous substrates. The already recognized roles of GSTs are the detoxification of toxic substances by their conjugation with glutathione, the attenuation of oxidative stress and the participation in hormone transport. Some GSTs display glutathione peroxidase activity and these GSTs can detoxify toxic lipid hydroperoxides that accumulate during infections. GSTs can also possess ligandin functions and participate in the intracellular transport of auxins. Notably, the expression of multiple *GSTs* is massively activated by salicylic acid and some GST enzymes were demonstrated to be receptor proteins of salicylic acid. Furthermore, induction of *GST* genes or elevated GST activities have often been observed in plants treated with beneficial microbes (bacteria and fungi) that induce a systemic resistance response (ISR) to subsequent pathogen infections. Further research is needed to reveal the exact metabolic functions of GST isoenzymes in infected plants and to understand their contribution to disease resistance.

Keywords: bacterium, fungus, glutathione S-transferase, oxidative stress, plant pathogen, salicylic acid, virus, WRKY

OPEN ACCESS

Edited by:
Stanislav Kopriva,
Universität zu Köln, Germany

Reviewed by:
Aziz Aziz,
Université de Reims Champagne-Ardenne, France
Mari-Anne Newman,
University of Copenhagen, Denmark

***Correspondence:**
Peter Schröder
peter.schroeder@helmholtz-muenchen.de

Specialty section:
This article was submitted to Plant Physiology, a section of the journal Frontiers in Plant Science

Received: *28 September 2018*
Accepted: *27 November 2018*
Published: *21 December 2018*

Citation:
Gullner G, Komives T, Király L and Schröder P (2018) Glutathione S-Transferase Enzymes in Plant-Pathogen Interactions. Front. Plant Sci. 9:1836. doi: 10.3389/fpls.2018.01836

INTRODUCTION

The first reports about a plant glutathione S-transferase enzyme (GST, EC 2.5.1.18) appeared in 1970, when it was revealed that a GST catalyzed the detoxification of the herbicide atrazine by its conjugation to the endogenous tripeptide glutathione (GSH, γ-L-glutamyl-L-cysteinyl-glycine) in sorghum and maize plants (Frear and Swanson, 1970; Lamoureux et al., 1970). These initial results sparked an intensive GST research, which focused on the detoxification of various herbicides

and other toxic xenobiotic compounds in plants (Lamoureux and Rusness, 1989; Timmerman, 1989; Dixon et al., 1998; Schröder et al., 2007). GSTs were shown to catalyze the conjugation between various xenobiotics with electrophilic centers (**Figure 1**) and the nucleophilic GSH, thus tagging the xenobiotic for vacuolar sequestration (Martinoia et al., 1993). The resulting GSH or homoglutathione (γ-L-glutamyl-L-cysteinyl-β-alanine) conjugates were usually much less toxic and more water-soluble than the original xenobiotics (Brown and Neighbors, 1987; Dixon et al., 1998). Importantly, it was revealed that multiple GST enzymes possess also glutathione peroxidase activities, thus these GSTs can participate in antioxidative defense (**Figure 1**) (Bartling et al., 1993; Wagner et al., 2002; Dixon et al., 2009). Plant GSTs are mostly cytosolic, and they can represent up to 2% of soluble proteins (Pascal and Scalla, 1999). Several GSTs were shown to be auxin-inducible and to bind auxins as non-substrate ligands (ligandin function) as well as to participate in auxin transport (Bilang and Sturm, 1995; Droog et al., 1995). Furthermore, it was revealed that GSTs play a role during the normal metabolism of plant secondary products like anthocyanins (Marrs, 1996). Nevertheless, in contrast to the vast knowledge collected about the detoxification function of GSTs, the understanding of their role in endogenous plant processes and about their metabolic substrates had been still far from complete (Marrs, 1996; Edwards et al., 2000; Dixon and Edwards, 2009; Dixon et al., 2010).

With the advent of "omics" technologies it was soon recognized that GST enzymes are encoded by large gene families in plants (McGonigle et al., 2000; Wagner et al., 2002). The genome of the model plant *Arabidopsis thaliana* harbors 54 *GST* genes, which were grouped into seven distinct classes in plants (Dixon et al., 2002, 2009). The well-studied large phi (GSTF) and tau (GSTU) classes are specific to plants whereas the small zeta (GSTZ) and theta (GSTT) classes exist also in animal tissues (Dixon et al., 1998, 2002). Less information is available about the three outlying minor GST classes including lambda GSTs (GSTL), dehydroascorbate reductases (DHARs), and tetrachlorohydroquinone dehalogenase (Dixon et al., 2002, 2009). In many cases *GST* genes displayed high inducibility by diverse abiotic and biotic stimuli (DeRidder et al., 2002; Wagner et al., 2002; Sappl et al., 2009; Dixon et al., 2011; Csiszár et al., 2014). Notably, multiple *GST* genes were shown to be strongly inducible by the key defense hormone salicylic acid (SA) (Fodor et al., 1997; Sappl et al., 2004, 2009). More recently GSTF2, GSTF8, GSTF10 and GSTF11 were identified as SA-binding receptor proteins in *A. thaliana*, but the biological relevance of SA binding to these GSTFs still remains to be explored (Tian et al., 2012).

Plants use a sophisticated surveillance system to recognize signals of microbial pathogens (Jones and Dangl, 2006). The investigation of the mechanisms whereby pathogens elicit defense responses in plant cells is of key importance to the understanding of plant disease resistance. Resistance is determined by the timely recognition of the pathogen and by the rapid deployment of efficient plant defense reactions (incompatible plant-pathogen interaction). Late and weak host defense reactions, however, result in susceptibility and disease (compatible interactions). Recognition of pathogens in resistant plant genotypes activates several consecutive downstream signaling cascades. Signals are transmitted to the nucleus leading to the rapid and extensive reprogramming of gene expression patterns in host plant cells (Chisholm et al., 2006; Boller and He, 2009). Resistance is often associated with the accumulation of reactive oxygen species (ROS) and programmed cell death at the sites of infection (hypersensitive response, HR) (Barna et al., 2012; O'Brien et al., 2012). In this regard, GSTs that also possess glutathione peroxidase activities may play a crucial role in plant antioxidative defense by limiting the excessive spread of HR-associated cell death (Levine et al., 1994; Wagner et al., 2002). It should be noted, however, that resistance and HR (programmed cell death) do not necessarily correlate (Bendahmane et al., 1999; Künstler et al., 2016).

Intriguingly, the marked accumulation of multiple GST transcripts and proteins as well as elevated total GST enzyme

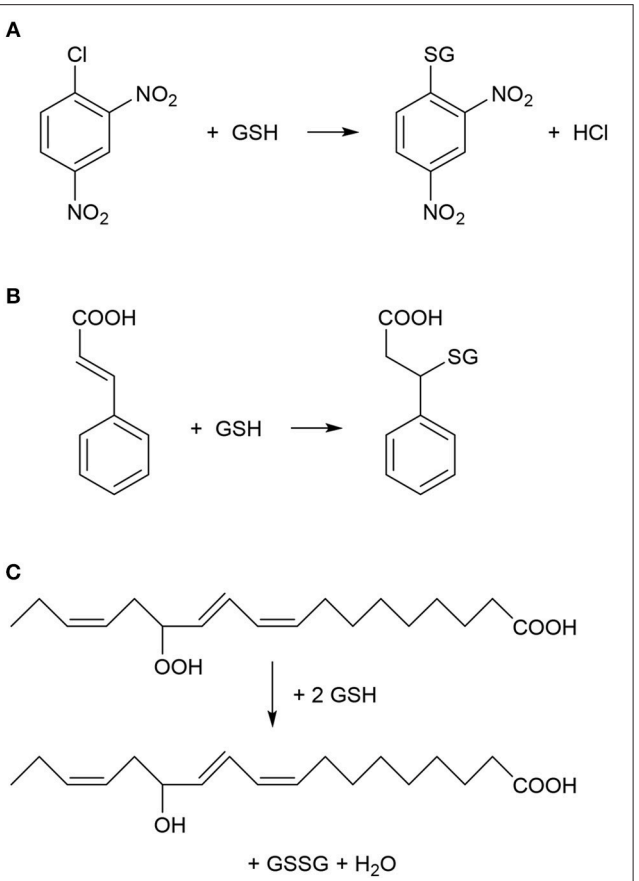

FIGURE 1 | Typical chemical reactions catalyzed by plant glutathione S-transferase (GST) enzymes. **(A)** Nucleophilic substitution reaction between 1-chloro-2,4-dinitrobenzene (CDNB) and reduced glutathione (GSH). CDNB has been extensively used as a xenobiotic model substrate for GST activity determination (Habig et al., 1974). **(B)** Nucleophilic addition reaction between cinnamic acid and GSH (Edwards and Dixon, 1991). **(C)** Reduction (detoxification) of fatty acid hydroperoxides to corresponding hydroxy derivatives by the peroxidase activity of GST as described by Bartling et al. (1993). The substrate 13(S)-hydroperoxy-9,11,15-octadecatrienoic acid was found to accumulate during membrane-damaging lipid peroxidation in infected plants (Wagner et al., 2002).

activities have often been observed in various plant-pathogen interactions. In addition, functional studies of individual GSTs proved in several cases that these enzymes can positively contribute to antimicrobial resistance in host plants by mostly unknown mechanisms (Dixon et al., 2009, 2010; Sappl et al., 2009; Liao et al., 2014; Wahibah et al., 2018). A clearly recognized function of GSTs is their participation in antioxidative reactions together with the pivotal cellular antioxidant GSH in order to eliminate ROS and lipid hydroperoxides that accumulate in infected tissues (**Figure 1**) (Wagner et al., 2002). Furthermore GSH, which is the most important non-protein thiol compound in plants, plays important roles in both signaling and defense reactions in infected plants (Datta et al., 2015; Gullner et al., 2017; Hernández et al., 2017).

Since the beginning of plant GST research a massive amount of information has been gathered on the role of GSTs in various plant-pathogen interactions (reviewed earlier by Gullner and Komives, 2001, 2006). The present review is an attempt to summarize the most important findings on GSTs in fungus-, bacterium- and virus-infected plants with a special attention to the possible functions of GSTs in disease resistance.

GSTs IN PLANT-FUNGUS INTERACTIONS

Numerous pathogenic fungi that infect plants are biotrophic, since they require live plant cells and tissues for host invasion. On the other hand, necrotrophic fungi obtain nutrients by killing infected tissues of the plant host. Hemibiotrophs are a third group of plant pathogenic fungi characterized by an early biotrophic phase of pathogenesis later converting into a necrotrophic lifestyle (Barna et al., 2012; Spanu and Panstruga, 2017). In this section, firstly the contribution of GSTs to interactions of plants with biotrophic fungi are discussed in a historical context, followed by the description of physiological roles of GSTs in infections caused by hemibiotrophic and necrotrophic fungi.

Biotrophic Fungi

A pioneering paper reported in 1991 the first evidence on the participation of a specific GST in the interaction between wheat and the biotrophic fungal pathogen powdery mildew. Winter wheat (*Triticum aestivum*) infected with the non-adapted pathogen (i.e., eliciting nonhost resistance in wheat) barley powdery mildew (*Blumeria graminis* f. sp. *hordei*, formerly *Erysiphe graminis* f. sp. *hordei*) developed local, induced resistance against a second infection with wheat powdery mildew (*B. graminis* f. sp. *tritici*). The onset of this resistance correlated with the activation of defense genes including a 20-fold increase in the transcript abundance of a *GST* gene (*GstA1*) in wheat leaves infected with *B. graminis* f. sp. *hordei* (Dudler et al., 1991). The *GstA1* gene, which encodes a 29 kD GST protein (GST29) was specifically inducible by fungal infections and exogenous GSH, but not by various xenobiotics that typically induce GST activity (paraquat, atrazine, alachlor, metolachlor) (Mauch and Dudler, 1993). The transcript abundance of *GstA1* increased dramatically within 2 h after infection with barley or wheat powdery mildew. However, in the incompatible and compatible interactions the level and time course of *GstA1*expression were similar. The accumulation of *GstA1* mRNA was also induced following inoculation with another fungal pathogen, *Puccinia recondita* f. sp. *tritici*. It was supposed that GST29 likely prevents plant cell disruption and death caused by highly toxic radicals that accumulate during infection, localizing thereby the host response during HR (Mauch and Dudler, 1993). Some years later total GST enzyme activity was measured in three barley cultivars inoculated with barley powdery mildew. A marked (3.6-fold) elevation of GST activity was found in infected leaves of a very susceptible barley cultivar, while the GST activity increased only to a much lesser extent in moderately susceptible and resistant cultivars. These results imply that GSTs are not associated with the resistance of barley against powdery mildew (El-Zahaby et al., 1995). The above findings were later confirmed by a report, in which a powdery mildew-susceptible barley line (*Hordeum vulgare* cv. Ingrid) and related near-isogenic lines expressing different resistance genes (*Mla12*, *Mlg,* or *mlo5*) were inoculated with *B. graminis* f. sp. *hordei* race A6. Activities of GST and some antioxidative enzymes were markedly induced 5–7 days after inoculation in susceptible barley leaves. Less significant pathogen-induced enzyme activity changes were detected in *Mla*-type resistant plants that showed HR-type cell death following inoculation, and, to an even lesser extent, in *Mlg* and *mlo* lines with no visible symptoms accompanying the incompatible interaction (Harrach et al., 2008). In addition, infection of *A. thaliana* plants with the biotrophic powdery mildew fungus *Erysiphe orontii* led to the up-regulation of pathogenesis-related (*PR*) genes and a *GST*. No differences were observed in the expression of this *GST* between wild-type *A. thaliana* and its mutants displaying enhanced disease susceptibility (Reuber et al., 1998).

In contrast to the above results, in some cases GSTs were shown to contribute to resistance against powdery mildew. In a gene chip study of wheat–wheat powdery mildew interactions, the up-regulation of ROS-eliminating genes was observed including those encoding DHAR, glutaredoxin, peroxidase, and GST enzymes. The comparison of resistant and susceptible wheat biotypes revealed that the *GSTF5* gene was more strongly induced in the incompatible interaction than in the compatible one (Wang et al., 2012). Furthermore, responses of tomato against the biotrophic fungal pathogen tomato powdery mildew (*Oidium neolycopersici*) were compared between incompatible and compatible interactions. A GST was more rapidly up-regulated in resistant wild tomato plants (*Solanum habrochiates*) harboring the *Ol-1* resistance gene than in susceptible plants. Virus-induced gene silencing was used to knock-down the expression of this *GST* gene in resistant plants, and the *GST*-silenced plants showed a susceptible phenotype after inoculation with *O. neolycopersici*. The resistance against *O. neolycopersici* was associated with HR. These results indicated that a *GST* was required for resistance against *O. neolycopersici* in tomato (Pei et al., 2011).

The expression of *GSTs* was functionally characterized in *A. thaliana* plants in response to treatment with herbicides, phytohormones, oxidative stress and inoculation with virulent and avirulent strains of the obligate biotrophic downy mildew oomycete *Hyaloperonospora parasitica* (formerly *Peronospora*

parasitica). The abundance of AtGSTF6 transcripts was up-regulated by all treatments while AtGSTF2, AtGSTF8, AtGSTU19, and AtGSTZ1 showed a selective individual spectrum of inducibility to the different stresses suggesting that regulation of gene expression is controlled by multiple mechanisms (Wagner et al., 2002). Transcriptome profiling using whole genome Affymetrix microarrays of soybean (*Glycine max*) plants exposed to the rust pathogen *Phakopsora pachyrhizi* identified 112 differentially expressed genes, including a markedly induced *GST* (Panthee et al., 2007). A similar transcriptome profiling was conducted in resistant and susceptible genotypes of *Glycine tomentella* following *P. pachyrhizi* infection. Genes encoding stress and defense response-related proteins including GSTs were up-regulated consistently in infected plants (Soria-Guerra et al., 2010).

A proteomics approach was used to compare compatible and incompatible interactions of wheat and the biotrophic yellow rust pathogen *Puccinia striiformis* f. sp. *tritici*. A matrix-assisted laser desorption/ionization time-of-flight mass spectrometry (MALDI-TOF MS) assay revealed several proteins with antioxidant functions including a GST that were differentially expressed between compatible and incompatible interactions, indicating the differential accumulation of ROS in infected tissues (Li et al., 2011).

Hemibiotrophic Fungi

The important role of GSTs in antifungal plant resistance was demonstrated also in hemibiotrophic plant-fungus interactions. The late blight oomycete *Phytophthora infestans* was shown to activate a *GST* gene (*prp1-1*) in potato. The levels of PRP1-1 mRNA as well as protein rapidly increased in potato leaves after fungal infection. Photoaffinity labeling of this GST with tritiated 5-azido-indole-3-acetic acid suggested that the phytohormone indole-3-acetic acid (IAA) serves as a regulator or substrate of the enzyme (Hahn and Strittmatter, 1994). In *Nicotiana benthamiana* infected by the fungi *Colletotrichum destructivum* and *C. orbiculare,* expression of two genes encoding GSTs (*NbGSTU1* and *NbGSTU3*) was markedly induced. Remarkably, the resistance toward *C. orbiculare* was highly suppressed in *N. benthamiana* when the transcription of *NbGSTU1* was blocked by gene silencing: 67% more colonization and 130% more lesions caused by *C. orbiculare* was observed as compared to control plants. These results unequivocally demonstrated that one GST gene/isoenzyme in *N. benthamiana* certainly has an important role in resistance to hemibiotrophic fungal pathogens (Dean et al., 2005).

In contrast to the above results, a *GST* gene cloned from roots of tobacco (*Nicotiana tabacum*) infected by the hemibiotrophic oomycete *Phytophthora parasitica* var. *nicotianae* was demonstrated to be required for disease susceptibility. The resistance of tobacco markedly increased against the fungus in plants that were GST-silenced. These observations show that individual GST genes/enzymes may suppress plant resistance in the initial biotrophic phase of the infection, possibly by providing a high antioxidative capacity favorable to the fungus (Hernández et al., 2009).

A cDNA library enriched for defense response mRNAs was constructed by suppression subtractive hybridization of sorghum tissues infected with *Colletotrichum sublineolum*, which causes the devastating anthracnose disease. A *GST* was induced in the resistant cultivar but its expression was hardly detectable in susceptible plants, suggesting that this GST may play a significant role in anthracnose resistance (Li et al., 2013). Furthermore, GSTs catalyzed the conjugation of cinnamic acid with GSH in suspension cultured cells of legume species (**Figure 1**). The activity of this bean GST was increased 2- to 3-fold by exposing plant cells to an elicitor prepared from cell walls of the fungal bean pathogen *Colletotrichum lindemuthianum* (Edwards and Dixon, 1991). In *A. thaliana*, GSH and indole glucosinolates were shown to exert key functions in the immune system. A tau class GST (GSTU13) was identified as an indispensable component of an immune pathway producing defensive indole glucosinolates. The lack of functional GSTU13 resulted in enhanced disease susceptibility toward several fungal pathogens including *Erysiphe pisi*, *Colletotrichum gloeosporioides*, and *Plectosphaerella cucumerina* (Pislewska-Bednarek et al., 2018).

A tau GST gene, *LrGSTU5*, isolated from *Lilium regale* was found to be markedly inducible by signaling agents like SA and ethylene as well as after inoculation with the soilborne, hemibiotrophic fungal pathogen *Fusarium oxysporum*. In order to verify *LrGSTU5* gene function, a constitutive plant expression vector of *LrGSTU5* was transferred into tobacco. Defense-related genes encoding osmotin, PR-1b, chitinase, and superoxide dismutase (SOD) enzymes were up-regulated in the transgenic lines as compared to wild-type plants. In addition, three important antioxidant enzymes, GST, SOD, and ascorbate peroxidase (APX), displayed significantly higher activities in transgenic lines after inoculation with *F. oxysporum*. Notably, the antifungal resistance of transgenic *LrGSTU5*-overexpressing tobacco lines against *F. oxysporum* infection was markedly increased (Han et al., 2016).

An important aspect of GSH metabolism in fungus-infected plants is the detoxification of fungal toxins (mycotoxins) by GSTs of host plants. Trichothecenes are an important group of mycotoxins that are produced by several phytopathogenic fungi, including the hemibiotrophic *Fusarium graminearum*. Treatment of barley spikes with the type B trichothecene deoxynivalenol (DON) led to the marked up-regulation of gene transcripts encoding e.g., GSTs. The formation of DON-GSH conjugates was also observed. These results showed that GSH-conjugation catalyzed by GSTs may reduce the impact of trichothecenes (Gardiner et al., 2010). Furthermore, a highly up-regulated *GST* gene was identified by a microarray approach in peanut in response to *Aspergillus parasiticus*, which is a saprophytic mold fungus producing carcinogenic aflatoxins (Luo et al., 2005).

Necrotrophic Fungi

Necrotrophic fungal pathogens destroy host plant tissues usually by toxins and feed on the remains of dead cells. ROS play a central role during plant–necrotrophic fungus interactions by stimulating the plant's defense responses. To overcome ROS-induced damage, both the host and pathogen developed

antioxidant systems to quench excess ROS (Barna et al., 2012). A typical necrotrophic pathogen is *Botrytis cinerea*, causing the gray mold disease of plants (Veloso and van Kan, 2018). A proteomic study showed that *B. cinerea* infection led to the accumulation of catalase 3 and multiple GSTs in *A. thaliana*, demonstrating the importance of an antioxidant system in defense against the fungus, which is known to cause oxidative stress in infected host tissues (Mulema et al., 2011). In addition, a reprogramming of carbohydrate and lipid metabolism was observed in grape (*Vitis vinifera*) berries infected with *B. cinerea* that resulted in an increased biosynthesis of secondary metabolites involved in plant defense. Genes encoding WRKY transcription factors, PR-proteins, a phenylalanine ammonia-lyase (PAL) and a GST were up-regulated in infected berries (Agudelo-Romero et al., 2015). Grapevine (*Vitis*) species may resist fungal infections by accumulating secondary metabolites like stilbenoid phytoalexins (trans-resveratrols). A tau class GST (GSTU-2) was identified in *V. vinifera* cell cultures and shown to be involved in extracellular transport of trans-resveratrols: grapevine cell cultures overexpressing GSTU-2 accumulated trans-resveratrols in the extracellular medium even without any elicitation of plant defenses or pathogen infection (Martínez-Márquez et al., 2017). However, in *Vitis flexuosa* different GTSs may play diverse roles in pathogen defense, since only one out of five characterized GST genes was induced, while expression of the other GSTs was down-regulated following infection by the necrotrophic fungi *B. cinerea* and *Elsinoe ampelina* (Ahn et al., 2016).

In leaf tissue of *A. thaliana* inoculated with the necrotrophic fungus *Alternaria brassicicola*, a microarray analysis revealed a significant increase in the abundance of 168 mRNAs. Activation of genes encoding antioxidant enzymes such as catalases and GST1 was detected in the tissue surrounding the initial infection site (Schenk et al., 2000). Changes in the proteome of *A. thaliana* were also studied following *A. brassicicola* infection by two-dimensional gel electrophoresis combined with mass spectrometry. The abundance of several proteins including two GSTs (AtGSTF7 and AtGSTU7) markedly increased (Mukherjee et al., 2010). In a different study, multiple *GSTs* belonging to various GST classes were strongly activated in the leaves of *A. thaliana* following *A. brassicicola* infection (De Vos et al., 2005). Particularly the *GSTU11*, *GSTU1* and *GSTU10* genes were robustly induced 48 h post-inoculation by *A. brassicicola*. The expression of several *GSTFs* including *GSTF7* and a *GSTL* gene were also markedly up-regulated after the fungal inoculation (**Figure 2A**).

In a proteomic study, cotyledons of two *B. napus* cultivars resistant and susceptible to the causal agent of stem rot (*Sclerotinia sclerotiorum*) were infected with *S. sclerotiorum* and proteins differentially regulated between the two cultivars identified. Certain enzymes accumulated only in the resistant oilseed rape cultivar following inoculation, such as those related to antioxidative defense including a GST, to ethylene biosynthesis, protein synthesis and protein folding (Garg et al., 2013). Multiple markedly up-regulated *GST* genes were also observed by a microarray approach in partially resistant oilseed rape cultivars following *S. sclerotiorum* infection (Zhao et al., 2007, 2009). To identify resistance genes and PR-genes, five highly resistant and susceptible *B. napus* lines were selected for transcriptome sequencing following inoculation with *S. sclerotiorum*. Twenty-four genes were identified that were differentially expressed in resistant or susceptible genotypes, including a tau class *GST* (*GSTU*) gene cluster (Wei et al., 2016; Seifbarghi et al., 2017).

The soil borne necrotrophic fungus *Verticillium dahliae* causes the very destructive Verticillium wilt disease in a wide

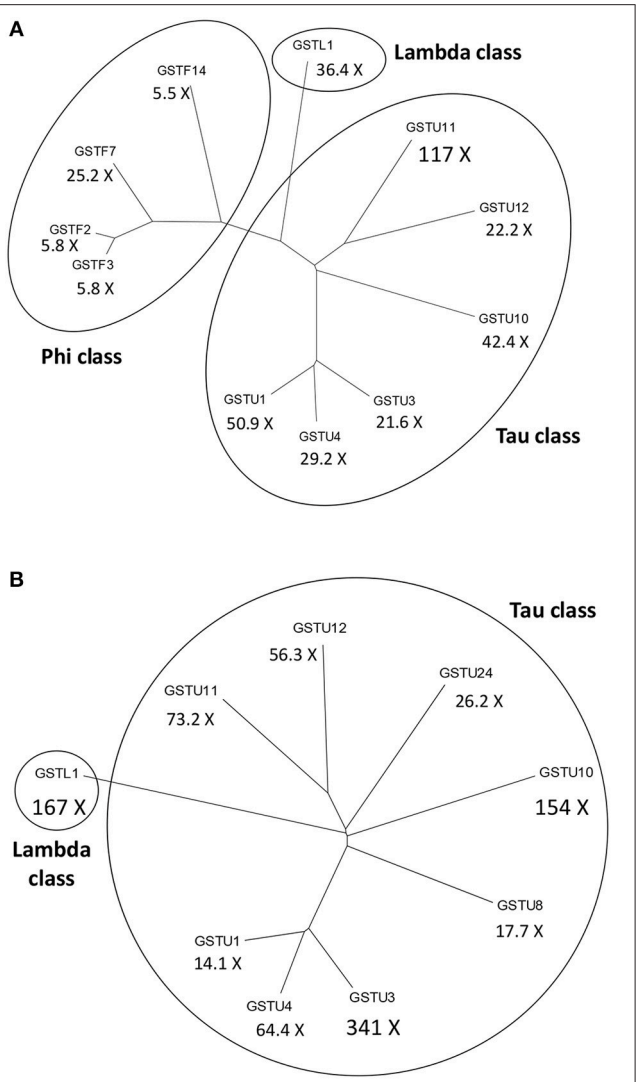

FIGURE 2 | Dendrograms of the most significantly activated *Arabidopsis thaliana* glutathione S-transferase (*GST*) genes following a fungal or a bacterial infection. Below the abbreviated gene names the magnitudes of gene inductions are shown (X = -fold). **(A)** More than 5-fold up-regulated *GSTs* at 48 h following infection of *A. thaliana* with the necrotrophic fungal pathogen *Alternaria brassicicola*. **(B)** More than 10-fold up-regulated *GSTs* at 12 h following infection of *A. thaliana* with the *Pseudomonas syringae* pv. *tomato* DC3000 strain carrying the *avrRpt2* effector gene (incompatible interaction). The expression data obtained by De Vos et al. (2005) were collected from the NCBI Gene Expression Omnibus database.

range of host plants including cotton plants. A genome-wide association study identified the *GaGSTF9* gene in *V. dahliae*-infected tree cotton (*Gossypium arboreum*) as a positive key regulator of resistance against Verticillium wilt. Silencing of *GaGSTF9* in a resistant *G. arboreum* accession resulted in significantly more fungal colonies after *V. dahliae* infection. Transgenic *A. thaliana* plants overexpressing *GaGSTF9* showed significantly lower SA and H_2O_2 levels than wild type plants. Upon *V. dahliae*-infection SA levels massively increased in transgenic plants but H_2O_2 accumulation was low as compared to wild type plants, indicating that GST may regulate the content of ROS via catalytic reduction with GSH that affects also the SA content (Gong et al., 2018).

Plant-Fungus Consortium Interactions

GSTs play an important role also in the esca disease of grapevine. The esca disease is a devastating, but still poorly understood fungal disease of grapevine trunks. Several fungi inhabiting the woody tissues were shown to be causal agents of the esca disease complex (Bertsch et al., 2013). The GSH pool decreased and PR-proteins were induced in leaves of esca-infected grapes before the appearance of visible symptoms. In addition, GST activities in leaves, expression of genes encoding GSTU1 and GSTF2 and GSTU1 and GSTF2 protein abundance were highest at early infection stages but decreased as visible symptoms later appeared. GSTF2 was found in the nucleus and in the cytoplasm, whereas GSTU1 was detected mostly in plastids. The expression of *GSTs* and the ratio of GSSG to total glutathione were suggested as early indicators of the presence of the esca disease in grapevine canes (Valtaud et al., 2009; Magnin-Robert et al., 2017).

Regulation of GST Genes During Plant-Fungus Interactions

Limited information is available about the regulation of plant *GSTs* during fungal infections. Several aspects of regulation of the *A. thaliana GSTF8* have been revealed and this gene has become a marker commonly used for early stress and defense responses (Thatcher et al., 2015). The response of the promoter of *GSTF8* from *A. thaliana* to infection by the soil-borne necrotrophic fungal pathogen *Rhizoctonia solani* was investigated using a luciferase reporter system. Although the reporter gene was induced in infected roots, the response differed markedly between *R. solani* strains and was not observed with aggressive strains that caused death of the seedlings. The induction was observed also in plants harboring a tetramer of the *ocs* element from the *GSTF8* promoter, suggesting that this element helps to mediate the response (Perl-Treves et al., 2004). Interestingly, antioxidant genes of plants and fungal pathogens including *GSTs* were distinctly regulated during disease development in different *R. solani* pathosystems (Samsatly et al., 2018). A forward genetic screen for *Arabidopsis* mutants with up-regulated *GSTF8* promoter activity was conducted by fusing a *GSTF8* promoter fragment to the luciferase reporter gene. The *esr1-1* (enhanced stress response 1) mutant was identified conferring enhanced resistance to the fungal pathogen *F. oxysporum*. It was found that the *ESR1* gene encodes a KH domain-containing RNA-binding protein. Transcriptome sequencing of *esr1-1* revealed altered expression of several genes involved in responses to biotic and abiotic stresses and hormone signaling pathways (Thatcher et al., 2015). An additional complexity in the regulation of *GSTF8* promoter results from the occurrence of multiple transcription start sites (TSS) in this gene, which gives rise to alternate *GSTF8* transcripts. The most 3′ TSS gives rise to the shorter, major message (GSTF8-S) that is much more stress-responsive than the longer transcript (GSTF8-L) originating from an upstream TSS, which encodes the larger form of the protein. Analysis of the GSTF8-L and GSTF8-S proteins demonstrated that GSTF8-L is solely targeted to plastids, whereas GSTF8-S is cytoplasmic (Thatcher et al., 2007).

WRKY transcription factor proteins have often been associated with the regulation of antimicrobial defense reactions in host plants (Eulgem and Somssich, 2007). Constitutive overexpression of a cotton gene encoding a WRKY transcription factor (*GhWRKY39*) in *N. benthamiana* conferred elevated resistance to bacterial and fungal infections. The transgenic plants exhibited enhanced tolerance against oxidative stress and increased transcription of antioxidant genes including a *GST* (Shi et al., 2014). Overexpression of *WRKY70* led to the marked up-regulation of numerous target genes of WRKY70 including *GSTF7* in *A. thaliana* (Li et al., 2004). Notably, WRKY70 was shown to determine the balance between SA-dependent and jasmonate-dependent defense pathways (Li et al., 2004, 2006). The overexpression of *WRKY70* in transgenic *A. thaliana* plants caused enhanced SA-mediated resistance to the biotrophic *Erysiphe cichoracearum*, but compromised the jasmonate-mediated resistance against the necrotrophic *A. brassicicola*. Conversely, down-regulation of *WRKY70* impaired resistance to *E. cichoracearum* (Li et al., 2006). In rice, WRKY45 is a positive regulator of resistance against the hemibiotrophic rice blast fungus *Magnaporthe grisea*. In the SA signaling pathway WRKY45 acts independently of NH1, a rice ortholog of the *A. thaliana* master regulator NPR1. Two defense-related genes, encoding a GST and a cytochrome P450, were regulated downstream of WRKY45, but were not regulated by NH1, suggesting independence of the WRKY45 and NH1 pathways (Shimono et al., 2007).

To obtain more knowledge on potential roles of WRKYs in *GST* gene regulation we identified the canonical W-box regulatory elements in 1500 bp long promoter segments of eight *A. thaliana GST* genes, which participate in defense reactions (De Vos et al., 2005). These (C/T)TGAC(C/T) motifs have been shown to be pathogen-responsive *cis*-elements that bind WRKY transcription factors (Eulgem and Somssich, 2007). In addition, we also searched for WT-boxes (core sequence GACTTTT), which are the binding sites of WRKY70 in *A. thaliana* (Machens et al., 2014). The number of W-boxes and their distribution patterns highly varied between *GST* promoters (**Figure 3**). WT-boxes occurred much less frequently in *GST* promoters (1–2 copies) than W-boxes (1–8 copies). Some promoters, like those of *GSTU11* and *GSTF7*, contained an outstandingly large number of W-boxes (8 and 7 copies, respectively) (**Figure 3**), which was already reported in the case of *GSTF7* (Li et al., 2004). These results suggest that WRKY transcription factors participate in the regulation of *GSTU11* and other *GSTs*, in concert with

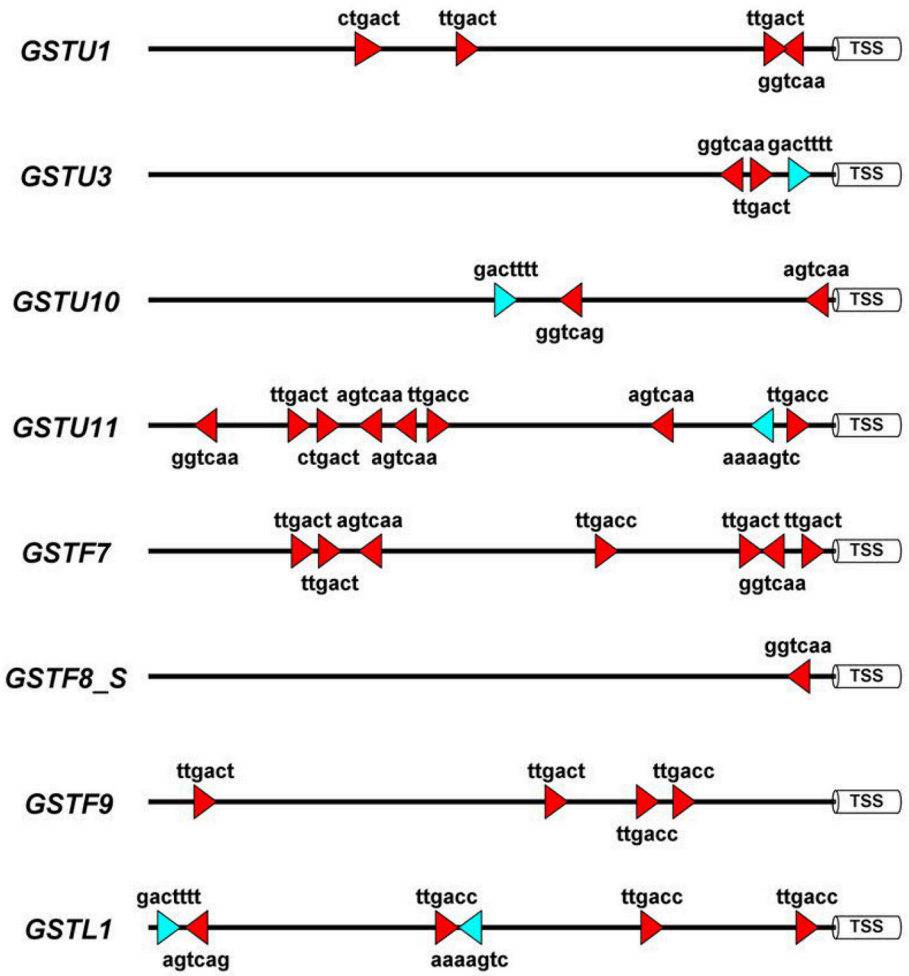

FIGURE 3 | Schematic representation of the disease-related W-box and WT-box *cis*-regulatory elements in the promoter sequences of eight *Arabidopsis thaliana* glutathione S-transferase (*GST*) genes. These sequence motifs are the binding sites of WRKY transcription factor proteins. For *in silico* analyses 1,500 bp DNA segments upstream of the transcription start sites (TSS) were selected from the NCBI GenBank database. In the case of the *GSTF8* gene the promoter of the shorter transcript variant (GSTF8_S) (Thatcher et al., 2007) was analyzed. Symbols: red triangles, W-boxes; blue triangles, WT-boxes. Promoter motifs were found on both DNA strands, which is represented by the orientation of the red and blue symbols. The diagram was prepared by the Illustrator for Biological Sequences (IBS) software (Liu et al., 2015).

a large number of other transcription factors and signaling compounds.

Fungal GSTs

Beside plants, the genomes of plant pathogenic fungi also encode *GST* genes (McGoldrick et al., 2005; Calmes et al., 2015; Sevastos et al., 2017). Fungal GSTs may have a pivotal role in protecting fungi against plant-derived toxic metabolites and ROS accumulating during infection at the host-pathogen interface. Thus, a *GST* gene (*Bcgst1*) was cloned from *B. cinerea*, which was supposed to contribute to the chemical stress tolerance of the fungus. The role of *Bcgst1* in the virulence of *B. cinerea* in tomato was evaluated by constructing gene disruption mutants. Neither of the mutants showed a decrease in virulence, indicating that the *Bcgst1* gene is not essential for virulence on tomato leaves under the conditions tested (Prins et al., 2000). The transcription of a *GST* gene of *A. brassicicola* (*AbGst1*) was significantly enhanced by isothiocyanates, heavy metals and 1-chloro-2,4-dinitrobenzene, but the superoxide-generating menadione and paraquat were inefficient. Isothiocyanates are antimicrobial volatiles produced from glucosinolates by myrosinase enzymes (Bones and Rossiter, 1996). *AbGst1* was up-regulated *in planta* during infection suggesting the potential involvement of this enzyme in isothiocyanate detoxification mechanisms during host plant infection (Sellam et al., 2006, 2007). A more detailed mining of the *A. brassicicola* genome revealed 23 *GST* sequences. Five isothiocyanate-inducible *GSTs* that belong to five different GST classes were more thoroughly investigated. Two GSTs displayed GSH transferase activity with isothiocyanates and peroxidase activity with cumene hydroperoxide substrates. On the other hand, mutants deficient for these two *GSTs* were neither more susceptible to isothiocyanate nor less aggressive than the

wild-type parental strain during infection of the host plant *Brassica oleracea*. Three among the five isothiocyanate-inducible GSTs analyzed, were essential for full aggressiveness of *A. brassicicola* on host plants suggesting that GSTs might be essential virulence factors of fungal necrotrophs (Calmes et al., 2015). In addition, multiple GST enzymes identified in the genome of *S. sclerotiorum* participate in the detoxification of isothiocyanates and toxic volatiles from *Brassica* species. This detoxification capacity may allow *S. sclerotiorum* to parasitize tissues of *Brassica* species despite the production of toxic metabolites (Rahmanpour et al., 2009). Also, a *GSTT* gene termed *PiGSTT1* has been cloned from an oomycete pathogen of potato, *P. infestans*. The enzyme PiGSTT1 was shown to be a glutathione peroxidase highly active with organic hydroperoxide substrates like 9(*S*)-hydroperoxy-(10*E*,12*Z*,15*Z*)-octadecatrienoic acid that is synthesized in potato during infection by *P. infestans* (Bryant et al., 2006).

GSTs IN PLANT-BACTERIUM INTERACTIONS

Plant-bacterium interactions can lead to three different outcomes: resistance gene (R-gene) mediated resistance, basal resistance and virulence. The *R*-gene mediated, hypersensitive-type resistance (HR, incompatible interaction) is based on a specific interaction, either directly or indirectly, of a bacterial effector gene product with the *R* gene of the host plant. This form of resistance is generally associated with the accumulation of ROS and localized cell death in infected plant tissues. Contrary to the *R*-gene mediated HR-type cell death, recognition in the case of basal resistance is unspecific, as intruders are recognized based on their common molecular patterns. Induction of basal resistance is not associated with visible symptoms, in contrast to the HR-type cell death. An insufficient plant defense results in virulence (compatible interaction) (Truman et al., 2006).

GSTs in R-gene Mediated Resistance

In HR-type resistance, bacterial infections often cause oxidative stress that leads to the accumulation of ROS including hydrogen peroxide (Baker and Orlandi, 1995; O'Brien et al., 2012). In infected plants, hydrogen peroxide generated during an oxidative stress has a dual role. It may act as a trigger for localized cell death (HR) but also as a rapid signal for induction of antioxidative defenses. An increase in expression of cellular protectant genes occurs at lower doses of H_2O_2 than required for HR, and takes place in healthy cells adjacent to necrotic, HR-type lesions in infected leaves (Levine et al., 1994; O'Brien et al., 2012). The up-regulation of plant *GST* genes as a consequence of bacterium-induced oxidative stress was early recognized. H_2O_2-accumulation in cell suspension cultures of soybean was shown to be activated by an avirulent strain of the bacterial pathogen *Pseudomonas syringae* pv. *glycinea*. Accumulation of an mRNA encoding a GST was observed as a consequence of this oxidative burst after bacterial infection. However, infection by a virulent strain of *P. syringae* pv. *glycinea* did not result in GST transcript accumulation (Levine et al., 1994). Pretreatment with a tyrosine kinase inhibitor or with a serine/threonine kinase inhibitor inhibited both the oxidative burst and the induction of *GST* in the incompatible interaction (Rajasekhar et al., 1999). The up-regulation of a *GST* gene was observed also in *A. thaliana* inoculated with an avirulent strain of *P. syringae* pv. *maculicola* (Greenberg et al., 1994). Following these early observations, the up-regulation of plant *GST* genes has often been used as an indicator of oxidative stress and HR in plant-bacterium interactions (Alvarez et al., 1998; Desikan et al., 1998; Maleck et al., 2000). However, oxidative stress can occur also in compatible plant-bacterium interactions. The role of GST was also investigated in pear and tobacco infected with the causal agent of fire blight, *Erwinia amylovora*. The bacterium caused GST induction and a sustained oxidative stress in leaves of both pear and tobacco (in compatible and incompatible interactions, respectively). The unexpected fact that *E. amylovora* generates oxidative stress even in compatible plant-pathogen interactions could be linked to its functional *hrp* gene cluster. As suggested by the authors, *E. amylovora* may utilize the production of ROS as a tool to provoke host cell death for a more successful invasion of plant tissues (Venisse et al., 2001).

Bacterial speck disease caused by *P. syringae* pv. *tomato* is one of the most devastating diseases of tomato. The antioxidative ascorbate-GSH cycle was studied in two tomato cultivars infected with *P. syringae* pv. *tomato*. GSH levels, GSH redox ratio and glutathione peroxidase activities were decreased, while the accumulation of GSSG was increased in an inoculated cultivar susceptible to the bacterium. By contrast, in a resistant cultivar the GSH pool homeostasis was maintained throughout the bacterial attack. Moreover, in the resistant interaction a significantly higher constitutive and pathogen-induced GST activity was observed. This research demonstrated the significance of GSH pool homeostasis and GST induction in resistance to *P. syringae* pv. *tomato* (Kuzniak and Sklodowska, 2004). In a more recent study, the expression of selected defense-response genes was investigated in heirloom tomatoes challenged with *P. syringae* pv. *tomato*. Transcript levels of defense genes including *PR-1a*, peroxidase and a *GST* were up-regulated in two resistant cultivars. On the other hand, transcripts from these genes were down-regulated in two susceptible cultivars (compatible interaction). The induction of defense response occurred in the early infection phase at 3 days post-inoculation and it was consistent with lower levels of disease severity in resistant cultivars (Veluchamy and Panthee, 2015). The pepper gene *CaBPR1*, which encodes basic PR1, was strongly induced by ethephon, wounding, and virus infection. Overexpressing *CaBPR1* in tobacco conferred increased tolerance to the oomycete pathogen *Phytophthora nicotianae*, and the bacterial pathogens *Ralstonia solanacearum* and *P. syringae* pv. *tabaci*. The *CaBPR1* transgene increased the expression of the *PR-Q* and *GST* genes (Sarowar et al., 2005).

Microarray expression profiling of the incompatible interaction between *A. thaliana* and *P. syringae* pv. *tomato* DC3000 (*Pst* DC3000) carrying the *avrRpt2* effector (avirulence) gene markedly contributed to the elucidation of plant defense responses in bacterium-infected plants. Thus, data of De Vos et al. (2005) deposited in the GEO database showed that infection with *Pst* DC3000 carrying *avrRpt2* very strongly induced the

expression of several *GSTs* in leaves of *A. thaliana* at 12 h post-inoculation, particularly those of *GSTU3*, *GSTL1*, *GSTU10,* and *GSTU11* (**Figure 2B**). Another microarray assay compared early gene expression responses in *A. thaliana* to exogenous SA treatment and to a *Pst* DC3000 strain harboring the effector gene *AvrRpm1*. The presence of this effector gene results in an incompatible plant-bacterium interaction (resistance). Several hundreds of early SA-inducible genes were identified including two *GSTs*. The induction of *GSTU7* and *GSTF8* by SA was independent of the master regulator *NPR1* gene. Examination of the expression patterns for selected early SA-induced genes indicated that their activation by SA required the TGA2/5/6 subclass of transcription factors. These genes were also activated by *Pst* DC3000 *AvrRpm1*, suggesting that they might also play a role in defense against bacteria (Blanco et al., 2009).

Ralstonia solanacearum is an important plant pathogenic, soil-borne bacterium, which causes the widespread bacterial wilt disease (Peeters et al., 2013). Northern blot analysis was used to compare expression of defense-related genes in two ecotypes of *A. thaliana* resistant and susceptible to *R. solanacearum* following pathogen inoculation, revealing a significant accumulation of transcripts encoding PR-1, Cu, Zn SOD, and a GST1. In the susceptible ecotype the induction of these defense-related genes was clearly delayed as compared to the resistant one (Ho and Yang, 1999). More recently, a PCR-based suppression subtractive hybridization was carried out to compare defense gene activations between ginger (*Zingiber officinale*) and mango ginger (*Curcuma amada*) leaves following *R. solanacearum* infection. *C. amada* is a potential donor for bacterial wilt resistance to the susceptible *Z. officinale*. Three transcripts were discriminative: the expression of genes encoding a leucine-rich protein, a xyloglucan transglycosylase and a GST was much higher in the resistant species (*C. amada*) than in the susceptible species (*Z. officinale*) at every time point studied (Prasath et al., 2013).

Bacterial leaf blight disease caused by *Xanthomonas oryzae* pv. *oryzae* (Xoo) gives rise to devastating crop losses in rice. The expression of a constitutively active tobacco mitogen-activated protein kinase kinase ($NtMEK2^{DD}$) in transgenic rice plants resulted in HR-like cell death preceded by the activation of endogenous rice 48-kDa MBP kinase, which was also activated by Xoo. The expression of $NtMEK2^{DD}$ induced the generation of hydrogen peroxide and up-regulated the expression of defense-related genes including *PR*-genes, peroxidases and *GSTs* including *GSTTU4* and *GSTTU12* (Jeong et al., 2008). A transgenic rice cultivar overexpressing the pattern recognition receptor-like kinase Xa21 was used for comprehensive metabolomic and transcriptomic profiling to compare incompatible and compatible rice-Xoo interactions. The rice Xa21 protein confers broad-spectrum resistance against Xoo. Many differential changes occurred in the Xa21-mediated response to Xoo strains. Acetophenone, xanthophylls, fatty acids, alkaloids, GSH, carbohydrate, and lipid biosynthetic pathways were affected. In addition, significant transcriptional induction of several *PR* genes as well as differential changes in multiple GST transcripts were observed (Sana et al., 2010). The accumulation of 16 rice proteins associated with leaf blight was studied by Western blot analysis in various rice-Xoo interactions. The comparison of their accumulation patterns in resistance, susceptible, and mock responses revealed a marked GST accumulation during resistance responses pointing to the role of GST as a positive regulator of resistance (Bai et al., 2012).

External factors, such as light have a strong influence on plant defense reactions and disease resistance. Interaction of *A. thaliana* with an avirulent strain of *P. syringae* pv. *maculicola* in the dark resulted in increased apoplastic bacterial growth and therefore reduced local resistance as compared to infection in light. The extent of oxidative burst, as estimated by induction of a *GST* gene, was not weakened by the absence of light (Zeier et al., 2004). The pathogen-induced expression of *GST1* proved to be higher and faster in younger leaves, whereas the induction of the *PR-1* gene was largely independent of leaf age. Despite these differences in inducible defense, bacterial growth as a measure of disease resistance proved to be similar in inoculated younger and older leaves (Zeier, 2005). Furthermore, diurnal changes were observed in the resistance of tomato against *Pst* DC3000, with the greatest susceptibility before midnight. Nightly red light treatment significantly enhanced the resistance and this effect correlated with increased SA accumulation, defense-related gene transcription and reduced redox homeostasis. Genes involved in redox homeostasis including those encoding GSTs as well as WRKY transcription factors were differentially induced by red light in response to pathogen challenge (Yang et al., 2015).

GSTs in Basal Resistance

To analyze the early events of basal resistance in tobacco a subtractive hybridization was carried out between leaves treated with the HR-negative mutant strain *P. syringae* pv. *syringae* 61 hrcC and non-treated control leaves. The HR-negative hrcC mutant is still capable to elicit the unspecific, symptomless basal resistance response. Several representative genes associated with basal resistance were identified including a *GST* gene *(EBR-52)* closely related to the auxin-inducible tobacco gene *par-B*. Gene activation patterns showed early peaks 3–12 h after inoculation, paralell with the development of basal resistance. Infection of tobacco with different types of bacteria revealed that incompatible pathogens, their *hrp* mutants, and non-pathogenic bacteria induce high levels of defense gene expression, including that of the above mentioned *GST* (*EBR-52)*, while virulent pathogens induce only a limited response. Furthermore, *GST* (*EBR-52)* expression seems to be specific to bacterial infections as no activation was detected following viral infections (Szatmári et al., 2006).

GSTs and Virulent Bacteria

In an early report, the accumulation of a *GST* transcript was observed in *A. thaliana* leaves inoculated with the virulent bacterium *Pst* DC3000. This bacterium produces the phytotoxin coronatine that markedly contributes to disease symptom development (lesion expansion, chlorosis formation). Interestingly, a coronatine-deficient mutant bacterium caused only mild symptoms but consistently induced 2- to 5-times higher *GST* transcript levels than

the coronatine-producing wild type strain. These results demonstrated that in early stages of infection coronatine may play a critical role by suppressing activation of defense-related genes including *GSTs* (Mittal and Davis, 1995). The expression of the *Pst* DC3000-inducible *AtGSTF2* and *AtGSTF6* genes was shown to be regulated by combined SA- and ethylene-signaling. However, the jasmonate-insensitive *A. thaliana* mutant *jar1* showed normal induction kinetics for both *GSTs* (Lieberherr et al., 2003).

Proteome alterations in leaves of *A. thaliana* during early host responses to *Pst* DC3000 inoculation were analyzed by two-dimensional gel electrophoresis. Protein changes characteristic of virulence, basal resistance and R-gene mediated resistance were assessed by comparing responses to *Pst* DC3000, a *hrp* mutant of the bacterium and a *Pst* DC3000 strain expressing the effector gene *avrRpm1*, respectively. The abundance of selected transcripts was also analyzed in gene-chip experiments. GSTs and peroxiredoxins consistently showed clear differences in abundance after various infections and time intervals. Bacterial challenges generally induced multiple GSTs, however individual members of the GST family were specifically modified depending upon the virulence of bacterial strains and the outcome of interaction. GSTF8 was the only GST to show specificity for the R-gene response. In addition, pathogen challenge elicited particularly dynamic responses of GSTF8: by 2 h after inoculation the corresponding transcript was already significantly up-regulated and the post-translational protein modifications detected were specific for incompatible interactions (Jones et al., 2004). The *GSTF8* gene was also induced by H_2O_2 through the activation of MPK3/MPK6 kinases (Kovtun et al., 2000) the promoter of which contains an *as-1* motif, which is implicated in response to oxidative stress (Garretón et al., 2002).

The *A. thaliana* mutant *cir1* (constitutively induced resistance 1) showed enhanced resistance to *Pst* DC3000. Differential gene expression in wild type and *cir1* plants without pathogen challenge were examined using a microarray biased toward defense-response and signaling genes in order to identify transcripts required for resistance. The induction of genes encoding a sodium inducible calcium binding protein, a protein phosphatase, a PAL and GSTF7 were observed (Naidoo et al., 2007).

Bacterial GSTs

Bacterial genomes also harbor *GST* genes (Vuilleumier, 1997; Kanai et al., 2006; Travensolo et al., 2008; Fang et al., 2011). Genome sequencing projects were particularly useful for the identification of large numbers of *GSTs* of unknown function in bacterial and yeast genomes (Vuilleumier and Pagni, 2002; Skopelitou et al., 2012a,b). Bacterial *GST* genes are often located within gene clusters, which suggests an important role of GST proteins in metabolic degradation and detoxification pathways (Marsh et al., 2008). Bacterial GSTs are implicated in a variety of distinct processes such as the biodegradation of xenobiotics, protection against chemical and oxidative stresses and antimicrobial drug resistance. In addition to their role in detoxification, bacterial GSTs are also involved in other metabolic processes like the degradation of lignin (Allocati et al., 2009, 2012).

GSTs IN PLANT-VIRUS INTERACTIONS

Plant viruses are obligate biotrophic pathogens that need living tissues for their multiplication. The interaction of plants with the invading virus can be either incompatible (resistance) or compatible (susceptibility) depending on the rapidity and intensity of defense reactions in host plants. In fact, during incompatible plant-virus interactions, the success of resistance at sites of virus infection may also depend on the speed of the host response. Thus, a rapid, efficient host reaction may result in early elimination of viruses and no obvious disease symptoms (extreme resistance). In contrast, a slightly delayed and less efficient host response allows limited virus replication and movement first resulting in oxidative stress and programmed cell death before conferring a final arrest of virus invasion (HR) (Bendahmane et al., 1999; Hernández et al., 2016).

GSTs and the Hypersensitive Type Resistance

It has been known for decades that treatment of leaves with antioxidants like GSH decrease the number of HR-type necrotic lesions caused by virus infections but virus levels essentially remain the same (Farkas et al., 1960). A paraquat tolerant (i.e., tolerant to oxidative stress) tobacco biotype (*N. tabacum* cv. Samsun) displayed high levels of GSH following e.g., herbicide exposure and enhanced activities of GST associated with reduced development of HR caused by *Tobacco necrosis virus* (TNV) (Gullner et al., 1991, 1995a; Barna et al., 1993). Accordingly, GSTs, in concert with GSH, may have a pivotal function in controlling HR-type necrotization during plant virus resistance, as initially proposed by Fodor et al. (1997). These authors showed that visible HR following *Tobacco mosaic virus* (TMV) inoculation was preceded by a transient drop in antioxidant enzyme activities, e.g., APX, glutathione reductase (GR) and GST. On the other hand, after HR development antioxidant activities and levels of GSH, increased significantly (Fodor et al., 1997). Furthermore, markedly elevated activities of APX, catalase and GST in a cytokinin-overproducing tobacco line were accompanied with a significantly lower number of HR-lesions and reduced levels of TNV, as compared to wild type controls (Pogány et al., 2004). Elevated expression of tau and theta class *GST* genes (*NtGSTU1* and *NtGSTT2*) is also correlated with HR induced by TMV in tobacco (Király et al., 2012; Juhász and Gullner, 2014). In addition, a further increase in *NtGSTU1* expression at 3 and 6 h after virus inoculation was associated with enhanced HR-type resistance (i.e., significantly less necrotic lesions and reduced TMV-replication) in plants with a sufficient sulfate supply (Király et al., 2012).

Enhanced expression of *GST* genes during HR-type virus resistance has been also observed in several other host-virus combinations. For example, the appearance of macroscopically visible lesions in the *A. thaliana* ecotype C-24 resistant to the yellow strain of *Cucumber mosaic virus* (CMV Y) was coupled

to elevated induction of a *GST* gene (Ishihara et al., 2004). In pepper, at least two *GST* genes were among the most highly up-regulated defense-related sequences identified in a line resistant to *Capsicum chlorosis virus* (CaCV) at the time point when lesions were fully developed (Widana Gamage et al., 2016).

Importantly, the above results imply that certain GST isoenzymes are not only antioxidants but also have a role in the establishment and/or signaling of virus resistance. This is supported by several additional studies of different plant-virus interactions. For example, purification of virus-host protein complexes from infected plants coupled to mass spectrometry identified a GST co-purifying with *Rice yellow mottle virus* (RYMV) in a partially resistant rice cultivar but not in a susceptible one (Brizard et al., 2006). In sugar beet displaying a strong, symptomless (not HR-type) resistance to *Beet necrotic yellow vein virus* (BNYVV), the causal agent of rhizomania disease, a GST was identified by tandem MALDI-TOF MS. Although this GST was also present in a near isogenic susceptible line, evaluation of corresponding transcript accumulation revealed that *GST* gene expression was significantly induced only in the BNYVV-resistant line (Larson et al., 2008). Comparing gene expression profiles of two rice cultivars showing asymptomatic resistance and susceptibility to *Rice tungro spherical virus* (RTSV) demonstrated the induction of at least twenty GST genes in both interactions. However, almost all of these *GST* genes were expressed to higher levels in the resistant rice cultivar (Satoh et al., 2013).

The importance of GST enzymatic activity in establishing virus resistance has been demonstrated by comparing three sorghum cultivars in their responses to *Sugarcane mosaic virus* (SCMV). The sorghum cultivar GKC-84 displayed a symptomless resistance response ("immunity") to the virus, which was associated with a more than 50 % increase in GST activity in the first 3 days after SCMV inoculation, while a susceptible cultivar displayed strongly decreased GST activities (Gullner et al., 1995b). Interestingly, a sorghum cultivar of intermediate susceptibility (cv. Róna-2) that develops an initial HR before systemic SCMV spread displayed GST activities intermediate between those of the susceptible and resistant ("immune") plants. These results suggested that GST activity may be tightly associated with the strength of the virus resistance response. A marked induction of GST isoenzymes could contribute to a strong and possibly early symptomless type of resistance, while a less increase or a decrease of GST activity may confer only a weak virus resistance that eventually results in susceptibility (Gullner et al., 1995b). Furthermore, in a maize cultivar with symptomless SCMV-resistance, a proteomic analysis revealed a down-regulation of two different GSTs in later phases of virus infection, pointing to a role of GSTs in establishing virus resistance at the early stages of pathogenesis (Wu et al., 2013a,b).

GSTs and Virus Susceptibility

The role of GSTs in inhibiting oxidative stress should be considered not only during HR, but also during virus susceptibility, i.e., systemic infections. Enhanced expression of defense-related genes like *GSTs* during systemic infections could be also due to the silencing suppressor activity of the infecting virus, as shown for *A. thaliana* susceptible to *Beet severe curly top virus* (BSCTV) (Yang et al., 2013). Several *GST* genes were also induced in a RTSV-susceptible rice cultivar that developed no visible systemic symptoms following virus inoculation (Satoh et al., 2013). Similar results were obtained by Casado-Vela et al. (2006) demonstrating a differential expression of antioxidant enzymes, including at least one GST in TMV-infected but asymptomatic tomato fruits. It is tempting to speculate that in cases of systemic virus infections with no or mild symptoms GSTs might significantly contribute to the absence of large scale oxidative stress. Indeed, in *A. thaliana* susceptible to *Cauliflower mosaic virus* (CaMV), compatible infection resulted in the marked systemic induction of *GST1* concomitantly with increased CaMV titers and development of mosaic symptoms (Love et al., 2005). An analysis of soybean susceptible to viruses that cause yellow mosaic disease (*Mungbean yellow mosaic India virus*, MYMIV and *Mungbean yellow mosaic virus*, MYMV) demonstrated the marked accumulation of a GST protein and its corresponding transcript in systemically infected leaves (Pavan Kumar et al., 2017). Furthermore, GSTU10-10 was identified in soybean specifically induced in response to systemic infection by *Soybean mosaic virus* (SMV). Characterization of the GSTU10-10 isoenzyme revealed that it has an antioxidant catalytic function by acting as a hydroperoxidase and has a very low K_m for GSH suggesting that GSTU10-10 is able to perform efficient catalysis under conditions where GSH concentrations are low, e.g., during oxidative stress (Skopelitou et al., 2015). A long term systemic infection of peach by *Apple chlorotic leaf spot virus* (ACLSV), the causal agent of "viruela" disease was investigated focusing on changes in host oxidative stress parameters and antioxidant capacity (García-Ibarra et al., 2011). Overall, data showed that systemic infection by ACLSV did not produce any visible symptoms or membrane damage in leaves (i.e., no changes in lipid peroxidation), while antioxidant defenses increased, including GST. Plant defense responses were analyzed in potato (cv. Desiree) leaves systemically infected with *Potato virus X* (PVX). The appearance of mild-yellowish, mosaic symptoms was associated with a dramatic, 20-fold induction of defense-related genes like *PR-1*, *chitinase* and *GST* (Niehl et al., 2006). Interestingly, no correlation occurred between virus titers and defense gene expression in systemic leaves, suggesting that these plant responses are directed primarily against oxidative stress rather than against the invading virus. Furthermore, responses of two potato cultivars (Igor and Nadine) were compared to two *Potato virus Y* (PVY) strains, the aggressive PVY^{NTN} and the mild PVY^{N} (Kogovsek et al., 2010). PVY^{NTN}-inoculated leaves displayed chlorotic and/or necrotic ringspot type lesions, while PVY^{N} caused a mild chlorotic ringspot. Potato cv. Igor plants infected by PVY^{NTN} showed a higher expression of antioxidant-encoding genes (*APX*, *GR* and *GST*) than plants infected with the mild PVY^{N} strain. Interestingly, in PVY-infected cv. Nadine the response was the opposite (Kogovsek et al., 2010), suggesting that host-dependent differential patterns of antioxidant induction could contribute to altered symptom severity in response to different PVY isolates. This is likely also the case during systemic viral infections that result in severe oxidative stress (cell/tissue necrosis), a usual indication of late and failed attempts by the

host to induce resistance (Hernández et al., 2016; Künstler et al., 2016). For example, in pea plants susceptible to *Plum pox virus* (PPV), systemic PPV infection produced chlorotic and necrotic lesions, a pronounced oxidative stress indicated by increased protein oxidation, lipid peroxidation, elevated H_2O_2 levels and electrolyte leakage in infected leaves (Díaz-Vivancos et al., 2008). Although activities of certain antioxidant enzymes (APX, peroxidase) increased, catalase and GST activities decreased. On the other hand, rice plants systemically infected by *Rice black-streaked dwarf virus* (RBSDV) displayed an induction of *GST23* and the corresponding transcripts, concomitant with oxidative stress (Xu et al., 2013).

In summary, plant GSTs may participate in the establishment of resistance to virus infections, either in the presence or absence of oxidative stress (HR-type necrosis) but could also contribute to the limitation of oxidative stress during virus susceptibility, i.e., in systemic infections. In fact, GSTs, in concert with GSH, could contribute to virus susceptibility in an even more general sense by supporting optimal subcellular conditions for virus replication. It has been shown that the expression of *NbGSTU4* was up-regulated by *Bamboo mosaic virus* (BaMV) in *N. benthamiana*. NbGSTU4 binds to the 3′ untranslated region (UTR) of BaMV positive sense (+) RNA in a GSH-dependent manner and is necessary for efficient viral RNA replication i.e., production of a viral negative sense (–) RNA and then new genomic (+) RNA (Chen et al., 2013). GSH was shown to stimulate *in vivo* BaMV replication and *in vitro* (–) RNA synthesis, while oxidative agents inhibit *in vitro* (–) RNA synthesis (Chen et al., 2013). NbGSTU4 induced by BaMV may provide an antioxidative environment for BaMV RNA replication to eliminate oxidative stress that could be induced by BaMV infection. Therefore, certain plant GSTs may bind viral RNA and deliver GSH to the replication complex thus creating reduced conditions for an efficient viral RNA synthesis.

RESISTANCE-INDUCING SYMBIOTIC MICROORGANISMS AND PLANT GSTs

Non-pathogenic, symbiotic bacteria and fungi living in the rhizosphere of plants can be highly beneficial to plants attacked by pathogenic microorganisms. These symbiotic microorganisms can produce antimicrobial toxins that are released into the soil and thus restrain pathogens. Furthermore, they are able to activate biochemical defense pathways of plants. This phenomenon is known as induced systemic resistance (ISR) (Pieterse et al., 2014).

The induction of *GST* genes or elevated GST activities has often been observed in plants treated with beneficial bacteria (Hassan et al., 2015; Agisha et al., 2017). Thus, the application of the well-known symbiotic, ISR-inducing rhizobacterium *Pseudomonas fluorescens* to the phyllosphere of an apple scab-susceptible apple (*Malus domestica*) cultivar led to the up-regulation of genes encoding proteins participating in pathogen recognition, signaling and antimicrobial defense such as PR-proteins, thioredoxin-like proteins, heat shock proteins and a GST (Kürkcüoglu et al., 2007). In rice plants, inoculation with *P. fluorescens* led to the accumulation of 23 rice proteins including a GST (Kandasamy et al., 2009). In wheat roots colonized by *P. fluorescens* an antifungal metabolite was identified that suppresses soil-borne root pathogens and activates host defense reactions. In addition, the beneficial bacterium up-regulated the expression of several defense genes encoding PR-10a, the antioxidative monodehydroascorbate reductase enzyme and two GSTs (Maketon et al., 2012). Another important beneficial bacterium, the endophytic *Pseudomonas putida* strongly increased the drought tolerance of chickpea. This beneficial effect was supposedly due to the increased expression of genes involved in biotic stress response (*PR1*), ethylene biosynthesis and ROS scavenging including a *GST* (Tiwari et al., 2016). Colonization of black pepper by *P. putida* led to the induction of several host genes that encoded defense-related proteins such as PR-1, PR-4, catalase, metallothionein, and a GST (Agisha et al., 2017). These transcriptional changes including the induction of *GSTs* may significantly increase plant disease resistance. Indeed, it was observed that the inoculation of wheat roots with *P. fluorescens* markedly suppressed the infection caused by the fungus *Gaeumannomyces graminis* var. *tritici* (Ggt) on the roots. During the early phase of this tripartite interaction, a wheat *GST* gene was induced by Ggt alone while in a later phase of infection the *GST* gene was up-regulated also by *P. fluorescens*. In contrast to *GST*, the expression of two host genes encoding an enolase and a cinnamyl alcohol dehydrogenase did not change significantly during this tripartite interaction (Daval et al., 2011).

Beneficial, symbiotic fungi can not only promote plant growth and nutrient uptake but they are also able to induce key defense reactions in plants including the activation of *GSTs*. Thus, application of the biocontrol agent *Trichoderma harzianum* to cabbage (*B. oleracea* var. *capitata*) plantlets induced resistance against the soil-borne fungal pathogen *R. solani*. The beneficial fungus markedly attenuated the host tissue damage (necrosis) elicited by *R. solani* infection. Concomitantly with the development of resistance the up-regulation of a hydrogen-peroxide inducible *GST* was observed that might contribute to the elimination of cytotoxic reactive metabolites containing an electrophilic moiety (Shibu et al., 2012). Application of *T. harzianum* markedly increased the growth of melon and activated several GSH-related enzymes such as DHAR and GST in melon leaves (Bernal-Vicente et al., 2015). Furthermore, *Trichoderma velutinum* markedly suppressed the infection caused by *R. solani* in common bean and markedly induced the expression of several defense genes including *GSTs* (Mayo et al., 2016).

The endophytic root-colonizing fungus *Piriformospora indica* can markedly promote plant growth and enhance the tolerance of host plants against abiotic and biotic stress. These beneficial effects were attributed to the elevated antioxidative capacity of *P. indica*-inoculated plants due to an activation of GSH-dependent antioxidative pathways (Waller et al., 2005; Harrach et al., 2013). Thus, the significant up-regulation of a tau-class *GST* (*BcGSTU*) was observed in *P. indica*-treated Chinese cabbage roots (Lee et al., 2011; Kao et al., 2016). The overexpression of *BcGSTU* in *A. thaliana* resulted in the stimulation of plant growth and increased resistance against *Alternaria brassicae* infection. This increased resistance against the fungal pathogen was explained

TABLE 1 | A model of diverse roles of plant GSTs in four different interaction types between plant hosts and pathogenic microbes.

Role of plant GSTs	Fungal and oomycete infections	Bacterial infections	Viral infections
SYMPTOMLESS RESISTANCE			
Maintaining resistance/preventing localized cell death (oxidative stress)	Pislewska-Bednarek et al., 2018	Szatmári et al., 2006	Gullner et al., 1995b; Larson et al., 2008; Satoh et al., 2013; Wu et al., 2013a,b
GSTs and auxin	–	Szatmári et al., 2006	–
GSTs and glucosinolate metabolism	Pislewska-Bednarek et al., 2018	–	–
HR-ASSOCIATED RESISTANCE			
Maintaining resistance/preventing spread of localized cell death (oxidative stress)	Mauch and Dudler, 1993 Pei et al., 2011; Wang et al., 2012	Levine et al., 1994; Sarowar et al., 2005 Kuzniak and Sklodowska, 2004	Gullner et al., 1995a,b; Fodor et al., 1997 Király et al., 2012; Widana Gamage et al., 2016
Differential ROS accumulation	Li et al., 2011	Levine et al., 1994; Rajasekhar et al., 1999	Pogány et al., 2004
GST regulation by WRKY TFs	Li et al., 2004, 2006	–	–
GST regulation by PR1	Sarowar et al., 2005	Sarowar et al., 2005	–
GST regulation by SA and ethylene	–	Lieberherr et al., 2003; Blanco et al., 2009	–
LIMITING SUSCEPTIBILITY			
Controlling (limiting) spread of cell death (oxidative stress) and pathogens in infected, necrotic plant tissues	Schenk et al., 2000; Dean et al., 2005; Li et al., 2013; Shi et al., 2014; Han et al., 2016; Gong et al., 2018	Mittal and Davis, 1995; Venisse et al., 2001	Kogovsek et al., 2010; Xu et al., 2013
GST regulation by WRKY TFs	Shimono et al., 2007; Shi et al., 2014	Shi et al., 2014	–
GST regulation by SA and ethylene	Shimono et al., 2007; Han et al., 2016	–	–
SA regulation by GST	Gong et al., 2018	–	–
GST catalyzing cinnamic acid-GSH conjugation	Edwards and Dixon, 1991	–	–
GST catalyzing detoxification of mycotoxins	Gardiner et al., 2010; Wahibah et al., 2018	–	–
PROMOTING SUSCEPTIBILITY			
Maintaining reduced conditions (preventing cell death) in infected, non-necrotic plant tissues	El-Zahaby et al., 1995; Harrach et al., 2008; Hernández et al., 2009	–	Love et al., 2005; Casado-Vela et al., 2006 Niehl et al., 2006; García-Ibarra et al., 2011 Skopelitou et al., 2015; Pavan Kumar et al., 2017

by elevated levels of GSH, auxin, SA and jasmonic acid in host tissues. It was supposed that this GSTU enzyme contributed to a balance between growth and defense responses (Kao et al., 2016). Furthermore, the accumulation of two GST proteins was explored by a proteomic study in *A. thaliana* roots inoculated with *P. indica* (Peskan-Berghofer et al., 2004).

In conclusion, the activation of *GSTs* together with other host genes encoding antioxidative and defense enzymes has been often observed during plant-symbiotic microbe interactions that resulted in enhanced resistance against microbial pathogens. However, the exact role of GST enzymes in the mechanism of ISR is still far from elucidated because transgenic plants overexpressing or suppressing the symbiont-inducible *GSTs* have been rarely studied (Kao et al., 2016). GSTs may participate in the detoxification of microbial toxins or in antioxidative reactions.

CONCLUSIONS AND FUTURE PERSPECTIVES

Since the beginning of plant GST research in 1970 the fundamental questions have remained largely unanswered: what are the physiological roles of GST isoenzymes and which metabolites are the natural, endogenous substrates of GSTs? In particular, what are the exact functions of distinct GSTs in conferring pathogen resistance and/or alleviating oxidative stress in the host? The marked induction of *GST* genes has been often observed in various plant-pathogen interactions, but these observations were rarely followed by functional studies. Thus, the cellular function of most plant GST enzymes in plant-pathogen interactions has remained elusive. Nevertheless, the profile of pathogen-inducible *GSTs* could provide a characteristic signature for a particular plant-pathogen interaction. Obviously, the large number of GST isoenzymes presents a challenge when studying the functions of GSTs in infected plants due to the high likelihood of functional redundancy. The presence of multiple GSTs with overlapping functions and substrate specificities might preclude the observation of phenotypic alteration in knockout mutants (Sappl et al., 2009). Furthermore, in spite of considerable research efforts (Dixon et al., 2009, 2010), only a few endogenous GST substrates have been identified.

We propose a model describing the diverse roles of plant GSTs in the interactions of plant hosts with pathogenic microbes considering four different plant-pathogen interaction types

(**Table 1**): (1) symptomless resistance (including basal resistance to bacteria and symptomless *R* gene-mediated resistance to viruses), (2) HR-associated resistance, (3) limiting susceptibility to systemic spread of pathogens and plant cell/tissue death (during infections by hemibiotrophic/necrotrophic fungi, bacteria, and viruses), (4) promoting susceptibility to biotrophic fungi and viruses (maintaining reduced conditions in infected non-necrotic plant tissues). Certain biochemical and physiological functions of plant GSTs are characteristic of a given plant-pathogen interaction type (e.g., glucosinolate metabolism, detoxification of mycotoxins), while other functions may be common for several or all interaction types, e.g., the control of plant cell death (oxidative stress) by GSTs and regulation of plant GSTs by various hormones and transcription factors. Overall, probably the most important function of GSTs in influencing the outcome of plant-pathogen interactions is the suppression of oxidative stress in infected host tissues (Edwards et al., 2000; Wagner et al., 2002; Gullner and Komives, 2006).

In the case of several plant-pathogen interactions, transgenic plants overexpressing or silenced for individual *GSTs* have been useful tools to study resistance mechanisms. In addition, the comparison of *GST* up-regulations between compatible and incompatible plant-pathogen interactions has also proved that GSTs can contribute to disease resistance, however, most of the underlying molecular mechanisms are still not completely known. For example, we need to gain more information on the regulation of *GST* expression during incompatible plant-pathogen interactions. In addition, further studies are needed to elucidate the regulatory elements in the 5′ flanking promoter regions of *GST* genes that are responsive to various infections. Once these cis-acting regulatory elements are identified, the transcription factor proteins required for transcriptional activation can be also determined. The tight metabolic links between GSTs and plant defense hormones, particularly SA, should be more deeply understood. The future characterization of the fascinating, large and diverse GST family will fill in many gaps in our knowledge on plant signaling processes, defense responses and disease resistance.

AUTHOR CONTRIBUTIONS

GG and PS conceived the idea of the manuscript, wrote the introduction and the conclusions as well as prepared the figures. GG wrote the plant-fungus section. TK discussed the plant-bacterium interactions, while LK prepared the plant-virus section.

ACKNOWLEDGMENTS

The financial support of the Hungarian National Research, Development and Innovation Office (K-111995 and K-124131) is gratefully acknowledged.

REFERENCES

Agisha, V. N., Eapen, S. J., Monica, V., Sheoran, N., Munjal, V., Suseelabhai, R., et al. (2017). Plant endophytic *Pseudomonas putida* BP25 induces expression of defense genes in black pepper roots: deciphering through suppression subtractive hybridization analysis. *Physiol. Mol. Plant Pathol.* 100, 106–116. doi: 10.1016/j.pmpp.2017.07.006

Agudelo-Romero, P., Erban, A., Rego, C., Carbonell-Bejerano, P., Nascimento, T., Sousa, L., et al. (2015). Transcriptome and metabolome reprogramming in *Vitis vinifera* cv. Trincadeira berries upon infection with *Botrytis cinerea*. *J. Exp. Bot.* 66, 1769–1785. doi: 10.1093/jxb/eru517

Ahn, S. Y., Kim, S. A., and Yun, H. K. (2016). Glutathione S-transferase genes differently expressed by pathogen-infection in *Vitis flexuosa*. *Plant Breed. Biotech.* 4, 61–70. doi: 10.9787/PBB.2016.4.1.61

Allocati, N., Federici, L., Masulli, M., and Di Ilio, C. (2009). Glutathione transferases in bacteria. *FEBS J.* 276, 58–75. doi: 10.1111/j.1742-4658.2008.06743.x

Allocati, N., Federici, L., Masulli, M., and Di Ilio, C. (2012). Distribution of glutathione transferases in Gram-positive bacteria and Archaea. *Biochimie* 94, 588–596. doi: 10.1016/j.biochi.2011.09.008

Alvarez, M. E., Pennell, R., Meijer, P. J., Ishikawa, A., Dixon, R. A., and Lamb, C. (1998). Reactive oxygen intermediates mediate a systemic signal network in the establishment of plant immunity. *Cell* 92, 773–784. doi: 10.1016/S0092-8674(00)81405-1

Bai, H., Lan, J. P., Gan, Q., Wang, X. Y., Hou, M. M., Cao, et al. (2012). Identification and expression analysis of components involved in rice *Xa21*-mediated disease resistance signalling. *Plant Biol.* 14, 914–922. doi: 10.1111/j.1438-8677.2012.00585.x

Baker, C. J., and Orlandi, E. W. (1995). Active oxygen in plant pathogenesis. *Annu. Rev. Phytopathol.* 33, 299–321. doi: 10.1146/annurev.py.33.090195.001503

Barna, B., Ádám, A., and Király, Z. (1993). Juvenility and resistance of a superoxide-tolerant plant to diseases and other stresses. *Naturwissenschaften* 80, 420–422. doi: 10.1007/bf01168338

Barna, B., Fodor, J., Harrach, B. D., Pogány, M., and Király, Z. (2012). The Janus face of reactive oxygen species in resistance and susceptibility of plants to necrotrophic and biotrophic pathogens. *Plant Physiol. Biochem.* 59, 37–43. doi: 10.1016/j.plaphy.2012.01.014

Bartling, D. B., Radzio, R., Steiner, U., and Weiler, E. W. (1993). A glutathione S-transferase with glutathione-peroxidase activity from *Arabidopsis thaliana*. Molecular cloning and functional characterization. *Eur. J. Biochem.* 216, 579–586. doi: 10.1111/j.1432-1033.1993.tb18177.x

Bendahmane, A., Kanyuka, K., and Baulcombe, D. C. (1999). The *Rx* gene from potato controls separate virus resistance and cell death responses. *Plant Cell* 11, 781–791. doi: 10.1105/tpc.11.5.781

Bernal-Vicente, A., Pascual, J. A., Tittarelli, F., Hernández, J. A., and Díaz-Vivancos, P. (2015). *Trichoderma harzianum* T-78 supplementation of compost stimulates the antioxidant defence system in melon plants. *J. Sci. Food Agric.* 95, 2208–2214. doi: 10.1002/jsfa.6936

Bertsch, C., Ramirez-Suero, M., Magnin-Robert, M., Larignon, P., Chong, J., Abou-Mansour, E., et al. (2013). Grapevine trunk diseases: complex and still poorly understood. *Plant Pathol.* 62, 243–265. doi: 10.1111/j.1365-3059.2012.02674.x

Bilang, J., and Sturm, A. (1995). Cloning and characterization of a glutathione S-transferase that can be photolabelled with 5-azido-indole-3-acetic acid. *Plant Physiol.* 109, 253–260. doi: 10.1104/pp.109.1.253

Blanco, F., Salinas, P., Cecchini, N. M., Jordana, X., Van Hummelen, P., Alvarez, M. E., et al. (2009). Early genomic responses to salicylic acid in *Arabidopsis*. *Plant Mol. Biol.* 70, 79–102. doi: 10.1007/s11103-009-9458-1

Boller, T., and He, S. Y. (2009). Innate immunity in plants: an arms race between pattern recognition receptors in plants and effectors in microbial pathogens. *Science* 324, 742–744. doi: 10.1126/science.1171647

Bones, A. M., and Rossiter, J. T. (1996). The myrosinase-glucosinolate system, its organisation and biochemistry. *Physiol. Plant*. 97, 194–208. doi: 10.1111/j.1399-3054.1996.tb00497.x

Brizard, J. P., Carapito, C., Delalande, F., Van Dorsselaer, A., and Brugidou, C. (2006). Proteome analysis of plant-virus interactome. Comprehensive data for virus multiplication inside their hosts. *Mol. Cell. Proteomics* 5, 2279–2297. doi: 10.1074/mcp.M600173-MCP200

Brown, H. M., and Neighbors, S. M. (1987). Soybean metabolism of chlorimuron ethyl: physiological basis for soybean selectivity. *Pestic. Biochem. Physiol*. 29, 112–120. doi: 10.1016/0048-3575(87)90068-X

Bryant, D., Cummins, I., Dixon, D. P., and Edwards, R. (2006). Cloning and characterization of a theta class glutathione transferase from the potato pathogen *Phytophthora infestans*. *Phytochemistry* 67, 1427–1434. doi: 10.1016/j.phytochem.2006.05.012

Calmes, B., Morel-Rouhier, M., Bataillé-Simoneau, N., Gelhaye, E., Guillemette, T., and Simoneau, P. (2015). Characterization of glutathione transferases involved in the pathogenicity of *Alternaria brassicicola*. *BMC Microbiol*. 15:123. doi: 10.1186/s12866-015-0462-0

Casado-Vela, J., Sellés, S., and Martínez, R. B. (2006). Proteomic analysis of tobacco mosaic virus-infected tomato (*Lycopersicon esculentum* M.) fruits and detection of viral coat protein. *Proteomics* 6 (Suppl. 1), S196–S206. doi: 10.1002/pmic.200500317

Chen, I. H., Chiu, M. H., Cheng, S. F., Hsu, Y. H., and Tsai, C. H. (2013). The glutathione transferase of *Nicotiana benthamiana* NbGSTU4 plays a role in regulating the early replication of *Bamboo mosaic virus*. *New Phytol.* 199, 749–757. doi: 10.1111/nph.12304

Chisholm, S. T., Coaker, G., Day, B., and Staskawicz, B. J. (2006). Host-microbe interactions: shaping the evolution of the plant immune response. *Cell* 124, 803–814. doi: 10.1016/j.cell.2006.02.008

Csiszár, J., Horváth, E., Váry, Z., Gallé, Á., Bela, K., Brunner, S., et al. (2014). Glutathione transferase supergene family in tomato: salt stress-regulated expression of representative genes from distinct GST classes in plants primed with salicylic acid. *Plant Physiol. Biochem*. 78, 15–26. doi: 10.1016/j.plaphy.2014.02.010

Datta, R., Kumar, D., Sultana, A., Hazra, S., Bhattacharyya, D., and Chattopadhyay, S. (2015). Glutathione regulates 1-aminocyclopropane-1-carboxylate synthase transcription via WRKY33 and 1-aminocyclopropane-1-carboxylate oxidase by modulating messenger RNA stability to induce ethylene synthesis during stress. *Plant Physiol*. 169, 2963–2981. doi: 10.1104/pp.15.01543

Daval, S., Lebreton, L., Gazengel, K., Boutin, M., Guillerm-Erckelboudt, A. Y., and Sarniguet, A. (2011). The biocontrol bacterium *Pseudomonas fluorescens* Pf29Arp strain affects the pathogenesis-related gene expression of the take-all fungus *Gaeumannomyces graminis* var. *tritici on wheat roots*. *Mol. Plant Pathol*. 12, 839–854. doi: 10.1111/j.1364-3703.2011.00715.x

De Vos, M., Van Oosten, V. R., Van Poecke, R. M., Van Pelt, J. A., Pozo, M. J., Mueller, M. J., et al. (2005). Signal signature and transcriptome changes of *Arabidopsis* during pathogen and insect attack. *Mol. Plant Microbe Interact*. 18, 923–937. doi: 10.1094/MPMI-18-0923

Dean, J. D., Goodwin, P. H., and Hsiang, T. (2005). Induction of glutathione S-transferase genes of *Nicotiana benthamiana* following infection by *Colletotrichum destructivum* and *C. orbiculare* and involvement of one in resistance. *J. Exp. Bot.* 56, 1525–1533. doi: 10.1093/jxb/eri145

DeRidder, B. P., Dixon, D. P., Beussman, D. J., Edwards, R., and Goldsbrough, P. B. (2002). Induction of glutathione S-transferases in *Arabidopsis* by herbicide safeners. *Plant Physiol*. 130, 1497–1505. doi: 10.1104/pp.010066

Desikan, R., Reynolds, A., Hancock, J. T., and Neill, S. J. (1998). Harpin and hydrogen peroxide both initiate programmed cell death but have differential effects on defence gene expression in *Arabidopsis* suspension cultures. *Biochem. J*. 330, 115–120. doi: 10.1042/bj3300115

Díaz-Vivancos, P., Clemente-Moreno, M. J., Rubio, M., Olmos, E., García, J. A., Martínez-Gómez, P., et al. (2008). Alteration in the chloroplastic metabolism leads to ROS accumulation in pea plants in response to plum pox virus. *J. Exp. Bot.* 5, 2147–2160. doi: 10.1093/jxb/ern082

Dixon, D. P., Cummins, I., Cole, D. J., and Edwards, R. (1998). Glutathione-mediated detoxification systems in plants. *Curr. Opin. Plant Biol.* 1, 258–266. doi: 10.1016/S1369-5266(98)80114-3

Dixon, D. P., Davis, B. G., and Edwards, R. (2002). Functional divergence in the glutathione transferase superfamily in plants. Identification of two classes with putative functions in redox homeostasis in *Arabidopsis thaliana*. *J. Biol. Chem.* 277, 30859–30869. doi: 10.1074/jbc.M202919200

Dixon, D. P., and Edwards, R. (2009). Selective binding of glutathione conjugates of fatty acid derivatives by plant glutathione transferases. *J. Biol. Chem*. 284, 21249–21256. doi: 10.1074/jbc.M109.020107

Dixon, D. P., Hawkins, T., Hussey, P. J., and Edwards, R. (2009). Enzyme activities and subcellular localization of members of the *Arabidopsis* glutathione transferase superfamily. *J Exp. Bot.* 60, 1207–1218. doi: 10.1093/jxb/ern365

Dixon, D. P., Sellars, J. D., and Edwards, R. (2011). The *Arabidopsis* phi class glutathione transferase AtGSTF2: binding and regulation by biologically active heterocyclic ligands. *Biochem. J*. 438, 63–70. doi: 10.1042/BJ20101884

Dixon, D. P., Skipsey, M., and Edwards, R. (2010). Roles for glutathione transferases in plant secondary metabolism. *Phytochemistry* 71, 338–350. doi: 10.1016/j.phytochem.2009.12.012

Droog, F. J. N., Hooykaas, P. J. J., and van der Zaal, B. J. (1995). 2,4-Dichlorophenoxyacetic acid and related chlorinated compounds inhibit two auxin-regulated type-III tobacco glutathione S-transferases. *Plant Physiol*. 107, 1139–1146. doi: 10.1104/pp.107.4.1139

Dudler, R., Hertig, C., Rebmann, G., Bull, J., and Mauch, F. (1991). A pathogen-induced wheat gene encodes a protein homologous to glutathione-S-transferases. *Mol. Plant-Microbe Interact.* 4, 14–18. doi: 10.1094/MPMI-4-014

Edwards, R., Dixon, D. P., and Walbot, V. (2000). Plant glutathione S-transferases: enzymes with multiple functions in sickness and in health. *Trends Plant Sci.* 5, 193–198. doi: 10.1016/S1360-1385(00)01601-0

Edwards, R., and Dixon, R. A. (1991). Glutathione S-cinnamoyl transferases in plants. *Phytochemistry* 30, 79–84. doi: 10.1016/0031-9422(91)84102-X

El-Zahaby, H. M., Gullner, G., and Király, Z. (1995). Effects of powdery mildew infection of barley on the ascorbate - glutathione cycle and other antioxidants in different host-pathogen interactions. *Phytopathology* 85, 1225–1230. doi: 10.1094/Phyto-85-1225

Eulgem, T., and Somssich, I. E. (2007). Networks of WRKY transcription factors in defense signaling. *Curr. Opin. Plant Biol.* 10, 366–371. doi: 10.1016/j.pbi.2007.04.020

Fang, T., Li, D. F., and Zhou, N. Y. (2011). Identification and clarification of the role of key active site residues in bacterial glutathione S-transferase zeta/maleylpyruvate isomerase. *Biochem. Biophys. Res. Commun*. 410, 452–456. doi: 10.1016/j.bbrc.2011.05.155

Farkas, G., Király, Z., and Solymosi, F. (1960). Role of oxidative metabolism in the localization of plant viruses. *Virology* 12, 408–421. doi: 10.1016/0042-6822(60)90163-x

Fodor, J., Gullner, G., Ádám, A. L., Barna, B., Komives, T., and Király, Z. (1997). Local and systemic responses of antioxidants to tobacco mosaic virus infection and to salicylic acid in tobacco. Role in systemic acquired resistance. *Plant Physiol*. 114, 1443–1451. doi: 10.1104/pp.114.4.1443

Frear, D. S., and Swanson, H. R. (1970). Biosynthesis of S-(4-ethylamino-6-isopropyl-amino-2-s-triazino) glutathione: partial purification and properties of a glutathione S-transferase from corn. *Phytochemistry* 9, 2123–2132. doi: 10.1016/S0031-9422(00)85377-7

García-Ibarra, A., Clemente-Moreno, M. J., Barba-Espín, G., Díaz-Vivancos, P., Rubio, M., Dicenta, F., et al. (2011). Changes in the antioxidative metabolism induced by Apple chlorotic leaf spot virus infection in peach [*Prunus persica* (L.) Batsch]. *Environ. Exp. Bot*. 70, 277–282. doi: 10.1016/j.envexpbot.2010.10.004

Gardiner, S. A., Boddu, J., Berthiller, F., Hametner, C., Stupar, R. M., Adam, G., et al. (2010). Transcriptome analysis of the barley-deoxynivalenol interaction: evidence for a role of glutathione in deoxynivalenol detoxification. *Mol. Plant Microbe Interact.* 23, 962–976. doi: 10.1094/MPMI-23-7-0962

Garg, H., Li, H., Sivasithamparam, K., and Barbetti, M. J. (2013). Differentially expressed proteins and associated histological and disease progression changes in cotyledon tissue of a resistant and susceptible genotype of *Brassica napus* infected with *Sclerotinia sclerotiorum*. *PLoS ONE* 8:e65205. doi: 10.1371/journal.pone.0065205

Garretón, V., Carpinelli, J., Jordana, X., and Holuigue, L. (2002). The *as-1* promoter element is an oxidative stress-responsive element and salicylic acid activates it via oxidative species. *Plant Physiol.* 130, 1516–1526. doi: 10.1104/pp.009886

Gong, Q., Yang, Z., Chen, E., Sun, G., He, S., Butt, H. I., et al. (2018). A phi-class glutathione S-transferase gene for Verticillium wilt resistance in *Gossypium*

arboreum identified in a genome-wide association study. *Plant Cell Physiol.* 59, 275–289. doi: 10.1093/pcp/pcx180.

Greenberg, J. T., Guo, A., Klessig, D. F., and Ausubel, F. M. (1994). Programmed cell death in plants: a pathogen-triggered response activated coordinately with multiple defense functions. *Cell* 77, 551–563. doi: 10.1016/0092-8674(94)90217-8

Gullner, G., Fodor, J., and Király, L. (1995a). Induction of glutathione S-transferase activity in tobacco by tobacco necrosis virus infection and by salicylic acid. *Pestic. Sci.* 45, 290–291. doi: 10.1002/ps.2780450317

Gullner, G., and Komives, T. (2001). "The role of glutathione and glutathione-related enzymes in plant-pathogen interactions," in *Significance of Glutathione in Plant Adaptation to the Environment*, eds D. Grill, M. Tausz, and L. J. De Kok (Dordrecht: Kluwer Academic Publishers), 207–239. doi: 10.1007/0-306-47644-4_9

Gullner, G., and Komives, T. (2006). Defense reactions of infected plants: roles of glutathione and glutathione S-transferase enzymes. *Acta Phytopathol. Entomol. Hung.* 41, 3–10. doi: 10.1556/APhyt.41.2006.1-2.1

Gullner, G., Komives, T., and Gáborjányi, R. (1995b). Differential alterations of glutathione S-transferase enzyme activities in three sorghum varieties following viral infection. *Z. Naturforsch. C* 50, 459–460. doi: 10.1515/znc-1995-5-619

Gullner, G., Komives, T., and Király, L. (1991). Enhanced inducibility of antioxidant systems in a *Nicotiana tabacum* L. biotype results in acifluorfen resistance. *Z. Naturforsch.* 46c, 875–881. doi: 10.1515/znc-1991-9-1025

Gullner, G., Zechmann, B., Künstler, A., and Király, L. (2017). "The signaling roles of glutathione in plant disease resistance," in *Glutathione in Plant Growth, Development, and Stress Tolerance*, eds M. A. Hossain, M. G. Mostofa, P. D. Vivancos, D. J. Burritt, M. Fujita, and L. S. P. Tran (Cham: Springer International Publishing), 331–357. doi: 10.1007/978-3-319-66682-2_15

Habig, W. H., Pabst, M. J., and Jakoby, W. B. (1974). Glutathione S-transferases. The first enzymatic step in mercapturic acid formation. *J. Biol. Chem.* 249, 7130–7139.

Hahn, K., and Strittmatter, G. (1994). Pathogen-defense gene *prp1-1* from potato encodes an auxin-responsive glutathione S-transferase. *Eur. J. Biochem.* 226, 619–626. doi: 10.1111/j.1432-1033.1994.tb20088.x

Han, Q., Chen, R., Yang, Y., Cui, X., Ge, F., Chen, C., et al. (2016). A glutathione S-transferase gene from *Lilium regale* Wilson confers transgenic tobacco resistance to *Fusarium oxysporum*. *Sci. Hortic.* 198, 370–378. doi: 10.1016/j.scienta.2015.11.047

Harrach, B. D., Baltruschat, H., Barna, B., Fodor, J., and Kogel, K. H. (2013). The mutualistic fungus *Piriformospora indica* protects barley roots from a loss of antioxidant capacity caused by the necrotrophic pathogen *Fusarium culmorum*. *Mol. Plant Microbe Interact.* 26, 599–605. doi: 10.1094/MPMI-09-12-0216-R

Harrach, B. D., Fodor, J., Pogány, M., Preuss, J., and Barna, B. (2008). Antioxidant, ethylene and membrane leakage responses to powdery mildew infection of near-isogenic barley lines with various types of resistance. *Eur. J. Plant Pathol.* 121, 21–33. doi: 10.1007/s10658-007-9236-3

Hassan, W., Hussain, M., Bashir, S., Shah, A. N., Bano, R., and David, J. (2015). ACC-deaminase and/or nitrogen fixing rhizobacteria and growth of wheat (*Triticum aestivum* L.). *J. Soil Sci. Plant Nutr.* 15, 232–248. doi: 10.4067/S0718-95162015005000019

Hernández, I., Chacón, O., Rodriguez, R., Portieles, R., López, Y., Pujol, M., et al. (2009). Black shank resistant tobacco by silencing of glutathione S-transferase. *Biochem. Biophys. Res. Commun.* 387, 300–304. doi: 10.1016/j.bbrc.2009.07.003

Hernández, J. A., Barba-Espín, G., and Díaz-Vivancos, P. (2017). "Glutathione-mediated biotic stress tolerance in plants," in *Glutathione in Plant Growth, Development, and Stress Tolerance*, eds M. A. Hossain, M. G. Mostofa, P. D. Vivancos, D. J. Burritt, M. Fujita, and L. S. P. Tran (Cham: Springer International Publishing), 309–329. doi: 10.1007/978-3-319-66682-2_14

Hernández, J. A., Gullner, G., Clemente-Moreno, M. J., Künstler, A., Juhász, C., Díaz-Vivancos, P., et al. (2016). Oxidative stress and antioxidative responses in plant-virus interactions. *Physiol. Mol. Plant Pathol.* 94, 134–148. doi: 10.1016/j.pmpp.2015.09.001

Ho, G. D., and Yang, C. H. (1999). A single locus leads to resistance of *Arabidopsis thaliana* to bacterial wilt caused by *Ralstonia solanacearum* through a hypersensitive-like response. *Phytopathology* 89, 673–678. doi: 10.1094/PHYTO.1999.89.8.673

Ishihara, T., Sakurai, N., Sekine, K. T., Hase, S., Ikegami, M., Shibata, D., et al. (2004). Comparative analysis of expressed sequence tags in resistant and susceptible ecotypes of *Arabidopsis thaliana* infected with *Cucumber mosaic virus*. *Plant Cell Physiol.* 45, 470–480. doi: 10.1093/pcp/pch057

Jeong, J. A., Yoo, S. A., Yang, D. H., Shin, S. H., Lee, M. C., Cho, B. H., et al. (2008). Transgenic rice plants expressing an active tobacco mitogen-activated protein kinase kinase induce multiple defense responses. *Plant Pathol. J.* 24, 375–383. doi: 10.5423/PPJ.2008.24.4.375

Jones, A. M., Thomas, V., Truman, B., Lilley, K., Mansfield, J., and Grant, M. (2004). Specific changes in the *Arabidopsis* proteome in response to bacterial challenge: differentiating basal and R-gene mediated resistance. *Phytochemistry* 65, 1805–1816. doi: 10.1016/j.phytochem.2004.04.005

Jones, J. D., and Dangl, J. L. (2006). The plant immune system. *Nature* 444, 323–329. doi: 10.1038/nature05286

Juhász, C. S., and Gullner, G. (2014). The monoterpenoid (S)-carvone massively up-regulates several classes of glutathione S-transferase genes in tobacco leaf discs. *Acta Phytopathol. Entomol. Hung.* 49, 163–176. doi: 10.1556/APhyt.49.2014.2.3

Kanai, T., Takahashi, K., and Inoue, H. (2006). Three distinct-type glutathione S-transferases from *Escherichia coli* important for defense against oxidative stress. *J. Biochem.* 140, 703–711. doi: 10.1093/jb/mvj199

Kandasamy, S., Loganathan, K., Muthuraj, R., Duraisamy, S., Seetharaman, S., Thiruvengadam, R., et al. (2009). Understanding the molecular basis of plant growth promotional effect of *Pseudomonas fluorescens* on rice through protein profiling. *Proteome Sci.* 7:47. doi: 10.1186/1477-5956-7-47

Kao, C. W., Bakshi, M., Sherameti, I., Dong, S. Q., Reichelt, M., Oelmuller, R., et al. (2016). A Chinese cabbage (*Brassica campetris* subsp. *Chinensis)* tau-type glutathione-S-transferase stimulates Arabidopsis development and primes against abiotic and biotic stress. *Plant Mol. Biol.* 92, 643–659. doi: 10.1007/s11103-016-0531-2

Király, L., Künstler, A., Höller, K., Fattinger, M., Juhász, C., Müller, M., et al. (2012). Sulfate supply influences compartment specific glutathione metabolism and confers enhanced resistance to *Tobacco mosaic virus* during a hypersensitive response. *Plant Physiol. Biochem.* 59, 44–54. doi: 10.1016/j.plaphy.2011.10.020

Kogovsek, P., Pompe-Novak, M., Baebler, S., Rotter, A., Gow, L., Gruden, K., et al. (2010). Aggressive and mild *Potato virus Y* isolates trigger different specific responses in susceptible potato plants. *Plant Pathol.* 59, 1121–1132. doi: 10.1111/j.1365-3059.2010.02340.x

Kovtun, Y., Chiu, W. L., Tena, G., and Sheen, J. (2000). Functional analysis of oxidative stress-activated mitogen-activated protein kinase cascade in plants. *Proc. Natl. Acad. Sci. U.S.A.* 97, 2940–2945. doi: 10.1073/pnas.97.6.2940

Künstler, A., Bacsó, R., Gullner, G., Hafez, Y. M., and Király, L. (2016). Staying alive - is cell death dispensable for plant disease resistance during the hypersensitive response? *Physiol. Mol. Plant Pathol.* 93, 75–84. doi: 10.1016/j.pmpp.2016.01.003

Kürkcüoglu, S., Degenhardt, J., Lensing, J., Al-Masri, A. N., and Gau, A. E. (2007). Identification of differentially expressed genes in *Malus domestica* after application of the non-pathogenic bacterium *Pseudomonas fluorescens* Bk3 to the phyllosphere. *J. Exp. Bot.* 58, 733–741. doi: 10.1093/jxb/erl249

Kuzniak, E., and Sklodowska, M. (2004). Differential implication of glutathione, glutathione-metabolizing enzymes and ascorbate in tomato resistance to *Pseudomonas syringae*. *J. Phytopathol.* 152, 529–536. doi: 10.1111/j.1439-0434.2004.00884.x

Lamoureux, G. L., and Rusness, D. G. (1989). "The role of glutathione-S-transferases in pesticide metabolism, selectivity, and mode of action in plants and insects," in *Glutathione: Chemical, Biochemical, and Medical Aspects*, Vol. 3, eds D. Dolphin, R. Poulson, and O. Avramovic (New York, NY: Wiley Intersci.), 153–196.

Lamoureux, G. L., Shimabukuro, R. H., Swanson, H. R., and Frear, D. S. (1970). Metabolism of 2-chloro-4-ethylamino-6-isopropylamino-s-triazine (atrazine) in excised sorghum leaf sections. *J. Agric. Food Chem.* 18, 81–86. doi: 10.1021/jf60167a029

Larson, R. L., Wintermantel, W. M., Hill, A., Fortis, L., and Nunez, A. (2008). Proteome changes in sugar beet in response to Beet necrotic yellow vein virus. *Physiol. Mol. Plant Pathol.* 72, 62–72. doi: 10.1016/j.pmpp.2008.04.003

Lee, Y. C., Johnson, J. M., Chien, C. T., Sun, C., Cai, D., Lou, B., et al. (2011). Growth promotion of Chinese cabbage and Arabidopsis by *Piriformospora indica* is not stimulated by mycelium-synthesized auxin. *Mol. Plant Microbe Interact.* 24, 421–431. doi: 10.1094/MPMI-05-10-0110

Levine, A., Tenhaken, R., Dixon, R., and Lamb, C. (1994). H_2O_2 from the oxidative burst orchestrates the plant hypersensitive disease resistance response. *Cell* 79, 583–593. doi: 10.1016/0092-8674(94)90544-4

Li, H., Wei, G., Xu, J., Huang, L., and Kang, Z. (2011). Identification of wheat proteins with altered expression levels in leaves infected by the stripe rust pathogen. *Acta Physiol. Plant*. 33, 2423–2435. doi: 10.1007/s11738-011-0783-z

Li, J., Brader, G., Kariola, T., and Palva, E. T. (2006). WRKY70 modulates the selection of signaling pathways in plant defense. *Plant J.* 46, 477–491. doi: 10.1111/j.1365-313X.2006.02712.x

Li, J., Brader, G., and Palva, E. T. (2004). The WRKY70 transcription factor: a node of convergence for jasmonate-mediated and salicylate-mediated signals in plant defense. *Plant Cell* 16, 319–331. doi: 10.1105/tpc.016980

Li, L., Zhu, F., Liu, H., Chu, A., and Lo, C. (2013). Isolation and expression analysis of defense-related genes in sorghum - *Colletotrichum sublineolum* interaction. *Physiol. Mol. Plant Pathol*. 84, 123–130. doi: 10.1016/j.pmpp.2013.08.005

Liao, W., Ji, L., Wang, J., Chen, Z., Ye, M., Ma, H., et al. (2014). Identification of glutathione S-transferase genes responding to pathogen infestation in *Populus tomentosa*. *Funct. Integr. Genomics* 14, 517–529. doi: 10.1007/s10142-014-0379-y

Lieberherr, D., Wagner, U., Dubuis, P. H., Métraux, J. P., and Mauch, F. (2003). The rapid induction of glutathione S-transferases *AtGSTF2* and *AtGSTF6* by avirulent *Pseudomonas syringae* is the result of combined salicylic acid and ethylene signaling. *Plant Cell Physiol.* 44, 750–757. doi: 10.1093/pcp/pcg093

Liu, W., Xie, Y., Ma, J., Luo, X., Nie, P., Zuo, Z., et al. (2015). IBS: an illustrator for the presentation and visualization of biological sequences. *Bioinformatics* 31, 3359–3361. doi: 10.1093/bioinformatics/btv362

Love, A. J., Yun, B. W., Laval, V., Loake, G. J., and Milner, J. J. (2005). *Cauliflower mosaic virus*, a compatible pathogen of Arabidopsis, engages three distinct defense-signaling pathways and activates rapid systemic generation of reactive oxygen species. *Plant Physiol.* 139, 935–948. doi: 10.1104/pp.105.066803

Luo, M., Liang, X. Q., Dang, P., Holbrook, C. C., Bausher, M. G., Lee, R. D., et al. (2005). Microarray-based screening of differentially expressed genes in peanut in response to *Aspergillus parasiticus* infection and drought stress. *Plant Sci.* 169, 695–703. doi: 10.1016/j.plantsci.2005.05.020

Machens, F., Becker, M., Umrath, F., and Hehl, R. (2014). Identification of a novel type of WRKY transcription factor binding site in elicitor-responsive cis-sequences from *Arabidopsis thaliana*. *Plant Mol Biol.* 84, 371–385. doi: 10.1007/s11103-013-0136-y

Magnin-Robert, M., Adrian, M., Trouvelot, S., Spagnolo, A., Jacquens, L., Letousey, P., et al. (2017). Alterations in grapevine leaf metabolism occur prior to esca apoplexy appearance. *Mol. Plant Microbe Interact.* 30, 946–959. doi: 10.1094/MPMI-02-17-0036-R

Maketon, C., Fortuna, A. M., and Okubara, P. A. (2012). Cultivar-dependent transcript accumulation in wheat roots colonized by *Pseudomonas fluorescens* Q8r1-96 wild type and mutant strains. *Biol. Control* 60, 216–224. doi: 10.1016/j.biocontrol.2011.11.002

Maleck, K., Levine, A., Eulgem, T., Morgan, A., Schmid, J., Lawton, K. A., et al. (2000). The transcriptome of *Arabidopsis thaliana* during systemic acquired resistance. *Nat. Genet.* 26, 403–410. doi: 10.1038/82521

Marrs, K. A. (1996). The functions and regulation of glutathione S-transferases in plants. *Annu. Rev. Plant Physiol. Plant Mol. Biol.* 47, 127–158. doi: 10.1146/annurev.arplant.47.1.127

Marsh, M., Shoemark, D. K., Jacob, A., Robinson, C., Cahill, B., Zhou, N. Y., et al. (2008). Structure of bacterial glutathione-S-transferase maleyl pyruvate isomerase and implications for mechanism of isomerisation. *J. Mol. Biol.* 384, 165–177. doi: 10.1016/j.jmb.2008.09.028

Martínez-Márquez, A., Martínez-Esteso, M. J., Vilella-Antón, M. T., Sellés-Marchart, S., Morante-Carriel, J. A., Hurtado, E., et al. (2017). A Tau class glutathione-S-transferase is involved in *trans*-resveratrol transport out of grapevine cells. *Front. Plant Sci.* 8:1457. doi: 10.3389/fpls.2017.01457

Martinoia, E., Grill, E., Tommasini, R., Kreuz, K., and Amrhein, N. (1993). ATP-dependent glutathione S-conjugate 'export' pump in the vacuolar membrane of plants. *Nature* 364, 247–249. doi: 10.1038/364247a0

Mauch, F., and Dudler, R. (1993). Differential induction of distinct glutathione-S-transferases of wheat by xenobiotics and by pathogen attack. *Plant Physiol.* 102, 1193–1201. doi: 10.1104/pp.102.4.1193

Mayo, S., Cominelli, E., Sparvoli, F., González-López, O., Rodríguez-González, A., Gutiérrez, S., et al. (2016). Development of a qPCR strategy to select bean genes ivolved in plant defense response and regulated by the *Trichoderma velutinum* - *Rhizoctonia solani* interaction. *Front. Plant Sci.* 7:1109. doi: 10.3389/fpls.2016.01109

McGoldrick, S., O'Sullivan, S. M., and Sheehan, D. (2005). Glutathione transferase-like proteins encoded in genomes of yeasts and fungi: insights into evolution of a multifunctional protein superfamily. *FEMS Microbiol. Lett.* 242, 1–12. doi: 10.1016/j.femsle.2004.10.033

McGonigle, B., Keeler, S. J., Lau, S.-L. C., Koeppe, M. K., and O'Keefe, D. P. (2000). A genomics approach to the comprehensive analysis of the glutathione S-transferase gene family in soybean and maize. *Plant Physiol.* 124, 1105–1120. doi: 10.1104/pp.124.3.1105

Mittal, S., and Davis, K. R. (1995). Role of the phytotoxin coronatine in the infection of *Arabidopsis thaliana* by *Pseudomonas syringae* pv. *tomato*. *Mol. Plant Microbe Interact.* 8, 165–171. doi: 10.1094/MPMI-8-0165

Mukherjee, A. K., Carp, M. J., Zuchman, R., Ziv, T., Horwitz, B. A., and Gepstein, S. (2010). Proteomics of the response of *Arabidopsis thaliana* to infection with *Alternaria brassicicola*. *J. Proteomics* 73, 709–720. doi: 10.1016/j.jprot.2009.10.005

Mulema, J. M. K., Okori, P., and Denby, K. J. (2011). Proteomic analysis of the *Arabidopsis thaliana-Botrytis cinerea* interaction using two-dimensional liquid chromatography. *Afr. J. Biotechnol.* 10, 17551–17563. doi: 10.5897/AJB10.2558

Naidoo, S., Murray, S. L., Denby, K. J., and Berger, D. K. (2007). Microarray analysis of the *Arabidopsis thaliana cir1* (constitutively induced resistance 1) mutant reveals candidate defence response genes against *Pseudomonas syringae* pv. *tomato* DC3000. *S. Afr. J. Bot.* 73, 412–421. doi: 10.1016/j.sajb.2007.03.006

Niehl, A., Lacomme, C., Erban, A., Kopka, J., Krämer, U., and Fisahn, J. (2006). Systemic *Potato virus X* infection induces defence gene expression and accumulation of ß-phenylethylamine-alkaloids in potato. *Funct. Plant Biol.* 33, 593–604. doi: 10.1071/FP06049

O'Brien, J. A., Daudi, A., Butt, V. S., and Bolwell, G. P. (2012). Reactive oxygen species and their role in plant defence and cell wall metabolism. *Planta* 236, 765–779. doi: 10.1007/s00425-012-1696-9

Panthee, D. R., Yuan, J. S., Wright, D. L., Marois, J. J., Mailhot, D., and Stewart, C. N. Jr. (2007). Gene expression analysis in soybean in response to the causal agent of Asian soybean rust (*Phakopsora pachyrhizi* Sydow) in an early growth stage. *Funct. Integr. Genomics* 7, 291–301. doi: 10.1007/s10142-007-0045-8

Pascal, S., and Scalla, R. (1999). Purification and characterization of a safener-induced glutathione S-transferase from wheat (*Triticum aestivum*). *Physiol. Plant.* 106, 17–27. doi: 10.1034/j.1399-3054.1999.106103.x

Pavan Kumar, B. K., Kanakala, S., Malathi, V. G., Gopal, P., and Usha, R. (2017). Transcriptomic and proteomic analysis of yellow mosaic diseased soybean. *J. Plant Biochem. Biotechnol.* 26, 224–234. doi: 10.1007/s13562-016-0385-3

Peeters, N., Guidot, A., Vailleau, F., and Valls, M. (2013). *Ralstonia solanacearum*, a widespread bacterial plant pathogen in the post-genomic era. *Mol. Plant Pathol.* 14, 651–662. doi: 10.1111/mpp.12038

Pei, D. L., Ma, H. Z., Zhang, Y., Ma, Y. S., Wang, W. J., Geng, H. X., et al. (2011). Virus-induced gene silencing of a putative glutathione S-transferase gene compromised *Ol-1*-mediated resistance against powdery mildew in tomato. *Plant Mol. Biol. Rep.* 29, 972–978. doi: 10.1007/s11105-011-0331-4

Perl-Treves, R., Foley, R. C., Chen, W., and Singh, K. B. (2004). Early induction of the *Arabidopsis GSTF8* promoter by specific strains of the fungal pathogen *Rhizoctonia solani*. *Mol. Plant Microbe Interact.* 17, 70–80. doi: 10.1094/MPMI.2004.17.1.70

Peskan-Berghofer, T., Shahollari, B., Giong, P. H., Hehl, S., Markert, C., Blanke, V., et al. (2004). Association of *Piriformospora indica* with *Arabidopsis thaliana* roots represents a novel system to study beneficial plant-microbe interactions and involves early plant protein modifications in the endoplasmic reticulum and at the plasma membrane. *Physiol. Plant.* 122, 465–477. doi: 10.1111/j.1399-3054.2004.00424.x

Pieterse, C. M., Zamioudis, C., Berendsen, R. L., Weller, D. M., Van Wees, S. C., and Bakker, P. A. (2014). Induced systemic resistance by beneficial microbes. *Annu. Rev. Phytopathol.* 52, 347–375. doi: 10.1146/annurev-phyto-082712-102340

Pislewska-Bednarek, M., Nakano, R. T., Hiruma, K., Pastorczyk, M., Sanchez-Vallet, A., Singkaravanit-Ogawa, S., et al. (2018). Glutathione transferase U13 functions in pathogen-triggered glucosinolate metabolism. *Plant Physiol.* 176, 538–551. doi: 10.1104/pp.17.01455

Pogány, M., Koehl, J., Heiser, I., Elstner, E. F., and Barna, B. (2004). Juvenility of tobacco induced by cytokinin gene introduction decreases susceptibility to

Tobacco necrosis virus and confers tolerance to oxidative stress. *Physiol. Mol. Plant Pathol.* 65, 39–47. doi: 10.1016/j.pmpp.2004.10.006

Prasath, D., Suraby, E. J., Karthika, R., Rosana, O. B., Prameela, T. P., and Anandaraj, M. (2013). Analysis of differentially expressed genes in *Curcuma amada* and *Zingiber officinale* upon infection with *Ralstonia solanacearum* by suppression subtractive hybridization. *Acta Physiol. Plant*. 35, 3293–3301. doi: 10.1007/s11738-013-1362-2

Prins, T. W., Wagemakers, L., Schouten, A., and van Kan, J. A. (2000). Cloning and characterization of a glutathione S-transferase homologue from the plant pathogenic fungus *Botrytis cinerea*. *Mol. Plant Pathol.* 1, 169–178. doi: 10.1046/j.1364-3703.2000.00021.x

Rahmanpour, S., Backhouse, D., and Nonhebel, H. M. (2009). Induced tolerance of *Sclerotinia sclerotiorum* to isothiocyanates and toxic volatiles from *Brassica* species. *Plant Pathol*. 58, 479–486. doi: 10.1111/j.1365-3059.2008.02015.x

Rajasekhar, V. K., Lamb, C., and Dixon, R. A. (1999). Early events in the signal pathway for the oxidative burst in soybean cells exposed to avirulent *Pseudomonas syringae* pv. *glycinea*. *Plant Physiol.* 120, 1137–1146. doi: 10.1104/pp.120.4.1137

Reuber, T. L., Plotnikova, J. M., Dewdney, J., Rogers, E. E., Wood, W., and Ausubel, F. M. (1998). Correlation of defense gene induction defects with powdery mildew susceptibility in *Arabidopsis* enhanced disease susceptibility mutants. *Plant J*. 16, 473–485. doi: 10.1046/j.1365-313x.1998.00319.x

Samsatly, J., Copley, T. R., and Jabaji, S. H. (2018). Antioxidant genes of plants and fungal pathogens are distinctly regulated during disease development in different *Rhizoctonia solani* pathosystems. *PLoS ONE* 13:e0192682. doi: 10.1371/journal.pone.0192682

Sana, T. R., Fischer, S., Wohlgemuth, G., Katrekar, A., Jung, K. H., Ronald, P. C., et al. (2010). Metabolomic and transcriptomic analysis of the rice response to the bacterial blight pathogen *Xanthomonas oryzae* pv. *oryzae*. *Metabolomics* 6, 451–465. doi: 10.1007/s11306-010-0218-7

Sappl, P. G., Carroll, A. J., Clifton, R., Lister, R., Whelan, J., Millar, A. H., et al. (2009). The Arabidopsis glutathione transferase gene family displays complex stress regulation and co-silencing multiple genes results in altered metabolic sensitivity to oxidative stress. *Plant J.* 58, 53–68. doi: 10.1111/j.1365-313X.2008.03761.x

Sappl, P. G., Onate-Sanchez, L., Singh, K. B., and Millar, A. H. (2004). Proteomic analysis of glutathione S-transferases of *Arabidopsis thaliana* reveals differential salicylic acid-induced expression of the plant-specific phi and tau classes. *Plant Mol. Biol.* 54, 205–219. doi: 10.1023/B:PLAN.0000028786.57439.b3

Sarowar, S., Kim, Y. J., Kim, E. N., Kim, K. D., Hwang, B. K., Islam, R., et al. (2005). Overexpression of a pepper basic pathogenesis-related protein 1 gene in tobacco plants enhances resistance to heavy metal and pathogen stresses. *Plant Cell Rep*. 24, 216–224. doi: 10.1007/s00299-005-0928-x

Satoh, K., Kondoh, H., De Leon, T. B., Macalalad, R. J. A., Cabunagan, R. C., Cabauatan, P. Q., et al. (2013). Gene expression responses to *Rice tungro spherical virus* in susceptible and resistant near-isogenic rice plants. *Virus Res.* 171, 111–120. doi: 10.1016/j.virusres.2012.11.003

Schenk, P. M., Kazan, K., Wilson, I., Anderson, J. P., Richmond, T., Somerville, S. C., et al. (2000). Coordinated plant defense responses in *Arabidopsis* revealed by microarray analysis. *Proc. Natl. Acad. Sci. USA* 97, 11655–11660. doi: 10.1073/pnas.97.21.11655

Schröder, P., Scheer, C. E., Diekmann, F., and Stampfl, A. (2007). How plants cope with foreign compounds. Translocation of xenobiotic glutathione conjugates in roots of barley *(Hordeum vulgare). Environ. Sci. Pollut. Res. Int*. 14, 114–122. doi: 10.1065/espr2006.10.352

Seifbarghi, S., Borhan, M. H., Wei, Y., Coutu, C., Robinson, S. J., and Hegedus, D. D. (2017). Changes in the *Sclerotinia sclerotiorum* transcriptome during infection of *Brassica napus*. *BMC Genomics* 18:266. doi: 10.1186/s12864-017-3642-5

Sellam, A., Dongo, A., Guillemette, T., Hudhomme, P., and Simoneau, P. (2007). Transcriptional responses to exposure to the brassicaceous defence metabolites camalexin and allyl-isothiocyanate in the necrotrophic fungus *Alternaria brassicicola*. *Mol. Plant Pathol.* 8, 195–208. doi: 10.1111/j.1364-3703.2007.00387.x

Sellam, A., Poupard, P., and Simoneau, P. (2006). Molecular cloning of *AbGst1* encoding a glutathione transferase differentially expressed during exposure of *Alternaria brassicicola* to isothiocyanates. *FEMS Microbiol Lett*. 258, 241–249. doi: 10.1111/j.1574-6968.2006.00223.x

Sevastos, A., Labrou, N. E., Flouri, F., and Malandrakis, A. (2017). Glutathione transferase-mediated benzimidazole-resistance in *Fusarium graminearum*. *Pestic. Biochem. Physiol.* 141, 23–28. doi: 10.1016/j.pestbp.2016.11.002

Shi, W., Liu, D., Hao, L., Wu, C., Guo, X., and Li, H. (2014). GhWRKY39, a member of the WRKY transcription factor family in cotton, has a positive role in disease resistance and salt stress tolerance. *Plant. Cell Tissue Organ Cult.* 118, 17–32. doi: 10.1007/s11240-014-0458-8

Shibu, M. A., Lin, H. S., Yang, H. H., and Peng, K. C. (2012). *Trichoderma harzianum* ETS 323-mediated resistance in *Brassica oleracea* var. *capitata* to *Rhizoctonia solani* involves the novel expression of a glutathione S-transferase and a deoxycytidine deaminase. *J. Agric. Food Chem*. 60, 10723–10732. doi: 10.1021/jf3025634

Shimono, M., Sugano, S., Nakayama, A., Jiang, C. J., Ono, K., Toki, S., et al. (2007). Rice WRKY45 plays a crucial role in benzothiadiazole-inducible blast resistance. *Plant Cell* 19, 2064–2076. doi: 10.1105/tpc.106.046250

Skopelitou, K., Dhavala, P., Papageorgiou, A. C., and Labrou, N. E. (2012a). A glutathione transferase from *Agrobacterium tumefaciens* reveals a novel class of bacterial GST superfamily. *PLoS ONE* 7:e34263. doi: 10.1371/journal.pone.0034263

Skopelitou, K., Muleta, A. W., Papageorgiou, A. C., Chronopoulou, E., and Labrou, N. E. (2015). Catalytic features and crystal structure of a tau class glutathione transferase from *Glycine max* specifically upregulated in response to soybean mosaic virus infections. *Biochim. Biophys. Acta* 1854, 166–177. doi: 10.1016/j.bbapap.2014.11.008

Skopelitou, K., Muleta, A. W., Pavli, O., Skaracis, G. N., Flemetakis, E., Papageorgiou, A. C., et al. (2012b). Overlapping protective roles for glutathione transferase gene family members in chemical and oxidative stress response in *Agrobacterium tumefaciens*. *Funct. Integr. Genomics* 12, 157–172. doi: 10.1007/s10142-011-0248-x

Soria-Guerra, R. E., Rosales-Mendoza, S., Chang, S., Haudenshield, J. S., Padmanaban, A., Rodriguez-Zas, S., et al. (2010). Transcriptome analysis of resistant and susceptible genotypes of *Glycine tomentella* during *Phakopsora pachyrhizi* infection reveals novel rust resistance genes. *Theor. Appl. Genet*. 120, 1315–1333. doi: 10.1007/s00122-009-1258-0

Spanu, P. D., and Panstruga, R. (2017). Editorial: biotrophic plant-microbe interactions. *Front. Plant Sci*. 8:192. doi: 10.3389/fpls.2017.00192

Szatmári, A., Ott, P. G., Varga, G. J., Besenyei, E., Czelleng, A., Klement, Z., et al. (2006). Characterisation of basal resistance (BR) by expression patterns of newly isolated representative genes in tobacco. *Plant Cell Rep*. 25, 728–740. doi: 10.1007/s00299-005-0110-5

Thatcher, L. F., Carrie, C., Andersson, C. R., Sivasithamparam, K., Whelan, J., and Singh, K. B. (2007). Differential gene expression and subcellular targeting of *Arabidopsis* glutathione S-transferase F8 is achieved through alternative transcription start sites. *J. Biol. Chem*. 282, 28915–28928. doi: 10.1074/jbc.M702207200

Thatcher, L. F., Kamphuis, L. G., Hane, J. K., Onate-Sánchez, L., and Singh, K. B. (2015). The Arabidopsis KH-domain RNA-binding protein ESR1 functions in components of jasmonate signalling, unlinking growth restraint and resistance to stress. *PLoS ONE* 10:e0126978. doi: 10.1371/journal.pone.0126978

Tian, M., von Dahl, C. C., Liu, P. P., Friso, G., van Wijk, K. J., and Klessig, D. F. (2012). The combined use of photoaffinity labeling and surface plasmon resonance-based technology identifies multiple salicylic acid-binding proteins. *Plant J*. 72, 1027–1038. doi: 10.1111/tpj.12016

Timmerman, K. P. (1989). Molecular characterization of corn glutathione S-transferase isozymes involved in herbicide detoxication. *Physiol. Plant*. 77, 465–471. doi: 10.1111/j.1399-3054.1989.tb05668.x

Tiwari, S., Lata, C., Chauhan, P. S., and Nautiyal, C. S. (2016). *Pseudomonas putida* attunes morphophysiological, biochemical and molecular responses in *Cicer arietinum* L. during drought stress and recovery. *Plant Physiol. Biochem*. 99, 108–117. doi: 10.1016/j.plaphy.2015.11.001

Travensolo, R. F., Garcia, W., Muniz, J. R. C., Caruso, C. S., Lemos, E. G. M., Carrilho, E., et al. (2008). Cloning, expression, purification and characterization of recombinant glutathione-S-transferase from *Xylella fastidiosa*. *Protein Expr. Purif.* 59, 153–160. doi: 10.1016/j.pep.2008.01.017

Truman, W., de Zabala, M. T., and Grant, M. (2006). Type III effectors orchestrate a complex interplay between transcriptional networks to modify basal defence responses during pathogenesis and resistance. *Plant J*. 46, 14–33. doi: 10.1111/j.1365-313X.2006.02672.x

Valtaud, C., Foyer, C. H., Fleurat-Lessard, P., and Bourbouloux, A. (2009). Systemic effects on leaf glutathione metabolism and defence protein expression caused by esca infection in grapevines. *Funct. Plant Biol.* 36, 260–279. doi: 10.1071/FP08293

Veloso, J., and van Kan, J. A. L. (2018). Many shades of grey in *Botrytis*-host plant interactions. *Trends Plant Sci.* 23, 613–622. doi: 10.1016/j.tplants.2018.03.016

Veluchamy, S., and Panthee, D. R. (2015). Differential expression analysis of a select list of genes in susceptible and resistant heirloom tomatoes with respect to *Pseudomonas syringae* pv. *tomato*. *Eur. J. Plant Pathol.* 142, 653–663. doi: 10.1007/s10658-015-0621-z

Venisse, J. S., Gullner, G., and Brisset., M. N. (2001). Evidence for the involvement of an oxidative stress in the initiation of infection of pear by *Erwinia amylovora*. *Plant Physiol.* 125, 2164–2172. doi: 10.1104/pp.125.4.2164

Vuilleumier, S. (1997). Bacterial glutathione S-transferases: what are they good for? *J. Bacteriol.* 179, 1431–1441. doi: 10.1128/jb.179.5.1431-1441.1997

Vuilleumier, S., and Pagni, M. (2002). The elusive roles of bacterial glutathione S-transferases: new lessons from genomes. *Appl. Microbiol. Biotechnol.* 58, 138–146. doi: 10.1007/s00253-001-0836-0

Wagner, U., Edwards, R., Dixon, D. P., and Mauch, F. (2002). Probing the diversity of the *Arabidopsis* glutathione S-transferase gene family. *Plant Mol. Biol.* 49, 515–532. doi: 10.1023/A:1015557300450

Wahibah, N. N., Tsutsui, T., Tamaoki, D., Sato, K., and Nishiuchi, T. (2018). Expression of barley *Glutathione S-Transferase13* gene reduces accumulation of reactive oxygen species by trichothecenes and paraquat in Arabidopsis plants. *Plant Biotechnol.* 35, 71–79. doi: 10.5511/plantbiotechnology.18.0205a

Waller, F., Achatz, B., Baltruschat, H., Fodor, J., Becker, K., Fischer, M., et al. (2005). The endophytic fungus *Piriformospora indica* reprograms barley to salt-stress tolerance, disease resistance, and higher yield. *Proc. Natl. Acad. Sci. U.S.A.* 102, 13386–13391. doi: 10.1073/pnas.0504423102

Wang, J. M., Liu, H. Y., Xu, H. M., Li, M., and Kang, Z. S. (2012). Analysis of differential transcriptional profiling in wheat infected by *Blumeria graminis* f. *sp. tritici* using GeneChip. *Mol. Biol. Rep.* 39, 381–387. doi: 10.1007/s11033-011-0749-7

Wei, L., Jian, H., Lu, K., Filardo, F., Yin, N., Liu, L., et al. (2016). Genome-wide association analysis and differential expression analysis of resistance to *Sclerotinia* stem rot in *Brassica napus*. *Plant Biotechnol. J.* 14, 1368–1380. doi: 10.1111/pbi.12501

Widana Gamage, S. M. K., McGrath, D. J., Persley, D. M., and Dietzgen, R. G. (2016). Transcriptome analysis of Capsicum chlorosis virus-induced hypersensitive resistance response in Bell capsicum. *PLoS ONE* 11:e0159085. doi: 10.1371/journal.pone.0159085

Wu, L., Han, Z., Wang, S., Wang, X., Sun, A., Zu, X., et al. (2013a). Comparative proteomic analysis of the plant-virus interaction in resistant and susceptible ecotypes of maize infected with *sugarcane mosaic virus*. *J. Proteomics* 89, 124–140. doi: 10.1016/j.jprot.2013.06.005

Wu, L., Wang, S., Chen, X., Wang, X., Wu, L., Zu, X., et al. (2013b). Proteomic and phytohormone analysis of the response of maize (*Zea mays* L.) seedlings to Sugarcane mosaic virus. *PLoS ONE* 8:e70295. doi: 10.1371/journal.pone.0070295

Xu, Q., Ni, H., Chen, Q., Sun, F., Zhou, T., Lan, Y., et al. (2013). Comparative proteomic analysis reveals the cross-talk between the responses induced by H_2O_2 and by long-term Rice black-streaked dwarf virus infection in rice. *PLoS ONE* 8:e81640. doi: 10.1371/journal.pone.0081640

Yang, L. P., Fang, Y. Y., An, C. P., Dong, L., Zhang, Z. H., Chen, H., et al. (2013). C2-mediated decrease in DNA methylation, accumulation of siRNAs, and increase in expression for genes involved in defense pathways in plants infected with beet severe curly top virus. *Plant J.* 73, 910–917. doi: 10.1111/tpj.12081

Yang, Y. X., Wang, M. M., Yin, Y. L., Onac, E., Zhou, G. F., Peng, S., et al. (2015). RNA-seq analysis reveals the role of red light in resistance against *Pseudomonas syringae* pv. *tomato* DC3000 in tomato plants. *BMC Genomics* 16:120. doi: 10.1186/s12864-015-1228-7

Zeier, J. (2005). Age-dependent variations of local and systemic defence responses in *Arabidopsis* leaves towards an avirulent strain of *Pseudomonas syringae*. *Physiol. Mol. Plant Pathol.* 66, 30–39. doi: 10.1016/j.pmpp.2005.03.007

Zeier, J., Pink, B., Mueller, M. J., and Berger, S. (2004). Light conditions influence specific defence responses in incompatible plant-pathogen interactions: uncoupling systemic resistance from salicylic acid and PR-1 accumulation. *Planta* 219, 673–683. doi: 10.1007/s00425-004-1272-z

Zhao, J., Buchwaldt, L., Rimmer, S. R., Sharpe, A., McGregor, L., Bekkaoui, D., et al. (2009). Patterns of differential gene expression in *Brassica napus* cultivars infected with *Sclerotinia sclerotiorum*. *Mol. Plant Pathol.* 10, 635–649. doi: 10.1111/j.1364-3703.2009.00558.x

Zhao, J., Wang, J., An, L., Doerge, R. W., Chen, Z. J., Grau, C. R., et al. (2007). Analysis of gene expression profiles in response to *Sclerotinia sclerotiorum* in *Brassica napus*. *Planta* 227, 13–24. doi: 10.1007/s00425-007-0586-z

Conflict of Interest Statement: The authors declare that the research was conducted in the absence of any commercial or financial relationships that could be construed as a potential conflict of interest.

frontiers in Plant Science

REVIEW
published: 09 January 2019
doi: 10.3389/fpls.2018.01944

Plant Glutathione Transferases and Light

Ágnes Gallé[1], Zalán Czékus[1], Krisztina Bela[1], Edit Horváth[2], Attila Ördög[1], Jolán Csiszár[1] and Péter Poór[1]*

[1] Department of Plant Biology, Faculty of Science and Informatics, University of Szeged, Szeged, Hungary, [2] Biological Research Centre, Institute of Plant Biology, Szeged, Hungary

The activity and expression of glutathione transferases (GSTs) depend on several less-known endogenous and well-described exogenous factors, such as the developmental stage, presence, and intensity of different stressors, as well as on the absence or presence and quality of light, which to date have received less attention. In this review, we focus on discussing the role of circadian rhythm, light quality, and intensity in the regulation of plant GSTs. Recent studies demonstrate that diurnal regulation can be recognized in GST activity and gene expression in several plant species. In addition, the content of one of their co-substrates, reduced glutathione (GSH), also shows diurnal changes. Darkness, low light or shade mostly reduces GST activity, while high or excess light significantly elevates both the activity and expression of GSTs and GSH levels. Besides the light-regulated induction and dark inactivation of GSTs, these enzymes can also participate in the signal transduction of visible and UV light. For example, red light may alleviate the harmful effects of pathogens and abiotic stressors by increasing GST activity and expression, as well as GSH content in leaves of different plant species. Based on this knowledge, further research on plants (crops and weeds) or organs and temporal regulation of GST activity and gene expression is necessary for understanding the complex regulation of plant GSTs under various light conditions in order to increase the yield and stress tolerance of plants in the changing environment.

Keywords: circadian regulation, cis-acting elements, dark, glutathione transferase, light

OPEN ACCESS

Edited by:
Francisco Javier Cejudo, Universidad de Sevilla, Spain

Reviewed by:
Peter J. Gollan, University of Turku, Finland
Hsu-Liang Hsieh, National Taiwan University, Taiwan
Paula Mulo, University of Turku, Finland

****Correspondence:***
Ágnes Gallé
gallea@bio.u-szeged.hu

Specialty section:
This article was submitted to Plant Physiology, a section of the journal Frontiers in Plant Science

Received: *28 September 2018*
Accepted: *13 December 2018*
Published: *09 January 2019*

Citation:
Gallé Á, Czékus Z, Bela K, Horváth E, Ördög A, Csiszár J and Poór P (2019) Plant Glutathione Transferases and Light. Front. Plant Sci. 9:1944. doi: 10.3389/fpls.2018.01944

INTRODUCTION

Light is required for optimal plant growth and development, as well as being the most important energy source for biomass production (Chen et al., 2004; Kangasjärvi et al., 2012). At the same time, the presence or absence, period, quality, intensity, and timing of light can alter and influence plant defense responses and induce new signaling and regulation pathways (Chandra-Shekara et al., 2006; Griebel and Zeier, 2008; Ballaré, 2014). Defense responses of plants, especially the induction of locally and systemically acquired resistance or the detoxification mechanism, are significantly regulated by light (Liu et al., 2011; Luschin-Ebengreuth and Zechmann, 2016; Poór et al., 2018). These processes strongly depend on the production and elimination of reactive oxygen species (ROS). Since ROS generation can be influenced by light-driven electron transport chains in the chloroplasts, the production and physiological role of various forms of ROS may differ in illuminated or dark environments (Asada, 2006). Herbicides and other stress factors can decrease and inhibit photosynthetic activity and promote significant ROS generation in plant leaves, thus

inducing cell death or several detoxification enzymes implicated in the metabolization of reactive compounds, such as glutathione transferases (GSTs) (Boulahia et al., 2016). However, there is little information about the effects of different stress factors on the expression and activity of many GSTs under various light conditions; furthermore, knowledge on the light-dependent regulation of *GSTs* is still lacking.

The aim of this review was to summarize the current knowledge on the regulation of GSTs in plant developmental processes and stress responses under various light conditions, because these enzymes play a crucial role in the regulation of detoxification processes and homeostasis of ROS. Furthermore, information on the light-dependent molecular regulation of plant GSTs is summarized, which can help to develop innovative procedures in plant protection and crop science depending on light conditions.

BASIC PROPERTIES OF PLANT GSTs

Plant GSTs (EC 2.5.1.18; GSTs) are a diverse group of multifunctional enzymes, which catalyze a wide range of reactions involving the conjugation of glutathione (GSH; γ-Glu–Cys–Gly) into electrophilic compounds to form more soluble derivatives, which can be transported to the vacuole and further metabolized (Labrou et al., 2015). Plant GSTs consist of three super families (cytosolic, mitochondrial, and microsomal) and can be further divided into distinct classes: tau (U), phi (F), theta (T), zeta (Z), lambda (L), γ-subunit of the eukaryotic translation elongation factor 1B (EF1Bγ), dehydroascorbate reductase (DHAR), metaxin, tetrachlorohydroquinone dehalogenase (TCHQD), Ure2p, microsomal prostaglandin E synthase type 2 (mPGES-2), hemerythrin (GSTH), iota (GSTI), and glutathionyl-hydroquinone reductases (GHRs) (Csiszár et al., 2016).

GSTs represent a relatively large ratio of the total soluble proteins in plant cells, e.g., they comprise ∼2% of the soluble protein in wheat seedlings (Pascal and Scalla, 1999). The accumulation of genome sequence data in previous decades revealed several GST homologs organized in complex supergene families in a wide range of plants (Labrou et al., 2015); for instance, in *Arabidopsis thaliana, Solanum lycopersicum, Oryza sativa, Triticum aestivum* there are 55, 81, 83, and 98 members, respectively (Gallé et al., 2009; Dixon and Edwards, 2010; Liu et al., 2013; Csiszár et al., 2014).

Tau and phi classes are the largest groups in plants and play crucial roles in the remediation of environmental pollution by organic xenobiotics, including herbicides, as well as industrial chemicals (Dixon et al., 2003; Benekos et al., 2010; Cicero et al., 2015). Forty-two of the 55 GSTs in *Arabidopsis thaliana* are classified as tau and phi (Dixon and Edwards, 2010; Chronopoulou et al., 2017). Biologically active tau and phi GSTs are dimers and these GST classes are characterized by the presence of a conserved Ser residue at their catalytic site (Nianiou-Obeidat et al., 2017). Tau and phi classes additionally possess glutathione-dependent hydroperoxidase (GPOX) activity in fatty acid hydroperoxides and glutathione conjugation activity in cytotoxic lipid peroxidation products (Nianiou-Obeidat et al., 2017). As they are involved mainly in xenobiotic metabolism, these enzymes possess high affinity for a broad spectrum of harmful compounds, including xenobiotics and endogenous stress metabolites, e.g., lipid peroxides and reactive aldehydes, and may result in high tolerance to abiotic stresses (Gallé et al., 2009; Dixon and Edwards, 2010; Liu et al., 2013; Csiszár et al., 2014). According to detailed studies on safener-induced genome activation, some tau-class GSTs (*AtGSTU19* and *AtGSTU24*) seem to be of significant importance. The induction kinetics of these genes define two classes of xenobiotic response (XR), namely, a rapid (20 min) and a slow (60 min) XR (Skipsey et al., 2011; Brazier-Hicks et al., 2018). The latest results show that a rapid XR is functionally linked to herbicide safening, while testing of oxylipid-inspired safeners differing in their electrophilic properties suggests that differing chemistries result in a distinctive rapid XR (Brazier-Hicks et al., 2018).

Other groups of GSTs have various roles, e.g., participating in hormone signaling or exhibiting peroxidase and isomerase activity (Gallé et al., 2009). The previously mentioned findings about phi- and tau-class GSTs and their ratio to the other members of the GST superfamily also underline their pivotal roles.

At the same time, the complex regulation of GST activity is dependent on the transcriptional and post-translational regulation, which is orchestrated by several promoter elements and transcription factors, and by phosphorylation and S-glutathionylation, which may be dependent on light (Dixon and Edwards, 2010).

ROLES OF THE MULTIFACETED GLUTATHIONE

Glutathione, the GST co-substrate is synthesized by two ATP-dependent enzymatic steps in the cytosol and chloroplasts (Diaz-Vivancos et al., 2015). First, γ-glutamyl-cysteine is formed by the plastidic glutamate-cysteine ligase, also known as γ-glutamyl-cysteine synthetase (γ-ECS or GSH1), which is the rate-limiting reaction. Glutathione synthetase (GSH2) catalyzes the addition of glycine to γ-glutamyl-cysteine (Noctor et al., 2011). Both *GSH1* and *GSH2* genes respond to light and some stress conditions, such as drought, heavy metals, and certain pathogens (Noctor et al., 2011); thus, GSH may accumulate rapidly under diverse stress effects. It is an essential low-molecular-weight thiol, which fulfills a broad range of functions including as an electron-donating co-factor in biochemical reactions (Noctor and Foyer, 1998; Szalai et al., 2009; Sabetta et al., 2017). GSH is able to control directly or indirectly the level of ROS; thus, it is considered to be one of the most important cellular antioxidants. ROS, such as singlet oxygen ($^1O_2$), the superoxide radical ($O_2^{\bullet -}$), hydrogen peroxide (H_2O_2) and the hydroxyl radical ($OH^{\bullet}$), are unavoidable by-products of aerobic metabolism (Foyer and Noctor, 2005). GSH takes part in the removal of the excess amount of H_2O_2 as a component of the "Foyer-Halliwell-Asada" or ascorbate-glutathione pathway (Noctor and Foyer, 1998).

When GSH reacts with oxidants, it becomes converted into an oxidized form, glutathione disulphide (GSSG).

As a result of the reversible convertibility between the reduced and the oxidized form and the relatively high concentration of the GSH in the cells, glutathione is one of the most important redox buffers. It also represents a storage form of reduced sulfur and can be a signal in the modulation of sulfate uptake and assimilation (Kopriva and Rennenberg, 2004). Being the substrate for phytochelatin synthesis, GSH is a key player in the detoxification of heavy metals (Freeman et al., 2004). As a co-substrate of GSTs, it is involved in the detoxification of different endogenous and exogenous harmful compounds (Cummins et al., 2011). Furthermore, GSH fulfills important roles in the regulation of plant growth, development, and stress tolerance. It is involved in embryo, meristem, and flower primordia development and in pollen germination (Vernoux et al., 2000; Cairns et al., 2006; Gulyás et al., 2014), as well as mediates cell cycle progression and programmed cell death (Kranner et al., 2006; Diaz-Vivancos et al., 2010a,b). In addition, sub-cellular GSH content in leaves of *Arabidopsis* shows a diurnal pattern. The highest content was found after 2–3 h of illumination caused by a strong increase in glutathione synthesis induced by daylight when glycine and cysteine production is restored. In contrast, the lowest GSH content was observed in most cell compartments (mitochondria, plastids, nuclei, peroxisomes, and cytosol) at the end of the dark period, when there was a lack of glutathione precursors, glycine, and cysteine. Thus, GSH content plays a role in the daytime/light-dependent redox balance (Zechmann, 2017).

GST EXPRESSION AND ACTIVITY ARE AFFECTED BY GSH CONCENTRATION AND GSH/GSSG RATIO

Plants use oxidants and antioxidants as flexible integrators of signals from metabolism and the environment (Foyer and Noctor, 2013). According to the latest conception, ROS-producing enzymes, antioxidants, and their reduction-oxidation states all contribute to the general redox homeostasis in the plant cell (Potters et al., 2010), but the glutathione has been considered to be the master regulator of intracellular redox homeostasis (Noctor et al., 2011; Foyer and Noctor, 2013). High GSH/GSSG ratio, maintained by increased GSH synthesis and/or GSSG reduction catalyzed by the glutathione reductases (GRs), may provide efficient protection for plants against abiotic stress-induced accumulation of ROS (Szalai et al., 2009).

Characterization of the *Arabidopsis rootmeristemless1* (*rml1*) mutant, which is severely limited in GSH synthesis capacity, revealed that, among the genes regulated by low GSH, 28 GSTs were found (Schnaubelt et al., 2015). Mining of the proteome data for GSH-associated genes showed that disruption of the pathway for the synthesis and degradation of glutathione in the *Atggt1* (γ-glutamyl transpeptidase, which has a function in the degradation of GSH S-conjugates in the vacuole) knockout leaves was associated with the induction of genes encoding four GSTs in the phi class (AtGSTF2, AtGSTF6, AtGSTF9, and AtGSTF10 Ashraf et al., 2010).

Moreover, shifts in the cellular glutathione redox state may reversibly modify redox-sensitive thiol groups in target proteins, either through glutathionylation or formation of cysteine cross bridges. Interestingly, this is even the case for the *Arabidopsis* GSH1 enzyme; thus the synthesis of GSH is under redox regulation. The active enzyme in the oxidized state works as a homodimer linked by two intermolecular disulphide bonds between specific cysteines (Hothorn et al., 2006). As the GSH level increases, in the more reduced intracellular environment, these bonds are disrupted and the enzyme takes on the less-active monomeric form. This post-translational modification provides an efficient and rapid switch mechanism for the control of GSH biosynthesis, ensuring that γ-ECS (GSH1) is activated in parallel with the increased demand for GSH (Jez et al., 2004; Hicks et al., 2007). Furthermore, as a post-translational modification, several GSTs can reversibly be modified by GSH to form disulphides. GSTs containing cysteine in the active site (DHARs, GSTLs, GSTZ1, GSTF7, and GSTU19) and one GST with the ability to form heterodimers with a previously mentioned one (GSTF10 with GSTF7) were proven to undergo S-glutathionylation (Dixon and Edwards, 2010).

DIURNAL REGULATION OF PLANT GSTs

In plants, very important steps of detoxification are catalyzed by cytochrome P450 mono-oxygenases (CYPs) and GSTs. These enzyme systems also contribute to the detoxification of several herbicides, depending on the chemical structure of the herbicide substrate (Cole, 1994; Cummins et al., 1999). Certain herbicides (e.g., triazine, triazinone, and substituted urea) have photo-inhibitory effects by competing with the plastoquinone (PQ) at the QB binding site located on the D1 protein of the PSII complex, causing a high production of ROS and leading to lipid peroxidation and proteolysis of thylakoid membrane proteins, thus inducing cell death (Hess, 2000; Rutherford and Krieger-Liszkay, 2001). Due to their effectiveness in photosynthesis inhibition, they are routinely used for weed control in agro-systems, forests, and roadsides. However, the usefulness of herbicide applications can depend on the light, the photo-inhibitory action of the used herbicide, and the circadian rhythm-regulated defense reaction of plants in the day- or night-time or under different light availability. It is known that phytotoxicity is less prevalent under low light conditions than under strong sunlight (Camargo et al., 2012; Lati et al., 2016; Frenkel et al., 2017). These results also suggest that circadian rhythm and light can be crucial components in these processes, which may determine the effective detoxification of various pollutants or herbicides in plants.

Most organisms do not simply respond to sunrise; rather, they anticipate the dawn and adjust their biology accordingly, as they have the innate ability to measure the time (McClung, 2006). The circadian clock is entrained by light perceived by phytochromes (red and far-red [FR] light receptors), cryptochromes (blue light receptors), and temperature (Greenham and McClung, 2015). Several different clock components with specific peak phases of expression have been described in *Arabidopsis thaliana*

(McClung, 2006; Hsu and Harmer, 2014). The endogenous system of the circadian clock allows for the daily adaptation and optimization of plant physiology and metabolism. A major function of the circadian clock was suggested to confer an adaptive advantage by the synchronization of metabolic and physiological processes with environmental changes (Alderete et al., 2018). Moreover, the circadian clock acts as a strategic planner to prime active defense responses, which depend on the cellular redox state (Karapetyan and Dong, 2017). Hence, the disturbance of the circadian clock leads to a number of cellular misregulations, including the downregulation of immune responses (Grundy et al., 2015). In addition, circadian rhythm could have important consequences for physiological outcomes of chemical exposures (e.g., herbicide application) at different times of the day (Hooven et al., 2009). ROS are key components in the signaling of immune response. The production, response, and transcriptional regulation of ROS scavenging genes are controlled by the circadian clock. ROS-dependent genes show time of day-specific expression patterns regulated and coordinated by the core-clock regulator, *Circadian Clock Associated 1* (*CCA1*) (Lai et al., 2012).

Based on the first observations, GSH content showed high concentrations during the midday period and low concentrations during the night in spruce (*Picea abies* L.) needles (Schupp and Rennenberg, 1988) and in Canary Island pine (*Pinus canariensis* C.Sm.) needles (Tausz et al., 2001). Other authors have also confirmed that GSH content was relatively low in the dark phase, but increased by illumination in the light phase in poplar (*Populus tremula* × *Populus alba* L.) leaves (Noctor et al., 1997). GSH slightly increased during the day in tobacco (*Nicotiana sylvestris* Speg. & Comes) leaves (Dutilleul et al., 2003). Huseby et al. (2013) also demonstrated that the first 4 h of exposure to daylight significantly elevated GSH content in the leaves of *Arabidopsis*. Thus, diurnal regulation of GSH takes part in cellular redox control (Zechmann, 2017).

In mammals, it is already well-known that key detoxification enzymes, like GSTs, show strong circadian transcriptional regulation (Abhilash et al., 2009). However, there is little information about the putative circadian regulation of these genes in plants. Alderete et al. (2018) analyzed the putative circadian regulation of genes involved in the metabolism of xenobiotic compounds, such as *NtGST* in tobacco plants. Tobacco (*Nicotiana tabacum* var. Wisconsin) seedlings and tobacco hairy root cultures were synchronized by 12 h of light/12 h of dark and treated with phenol, after which the expression of detoxification enzymes was determined in 2- and 3-weeks-old cultures. In tobacco seedlings, the selected *NtGST* gene (phi class) showed diurnal regulation with increased expression at the end of the light phase, with transcript levels decreasing in the dark period. In 2-weeks-old hairy root cultures, the relative transcript amount of *NtGST* was rather oscillating, while, in 3-weeks-old hairy root cultures, the expression pattern was similar to that in seedlings. Phenol treatment highly affected the expression of *NtGST* as it revealed a trend consisting of downregulation during the day and upregulation during the night (Alderete et al., 2018). Gallé et al. (2018) also found that both the GST activity and expression levels of selected *GSTs* reached the maximum at the end of the light period, before both decreased under darkness in leaves of tomato (*Solanum lycopersicum* L.).

GST GENE EXPRESSION AND ENZYME ACTIVITY ARE AFFECTED BY LIGHT QUALITY

Light as one of the most important environmental signals regulates plant development and defense mechanisms throughout the plant life cycle. For plants, the blue and red wavelengths of the light spectrum, which is utilized for photosynthesis, are the most important. Thus, the blue light-sensing cryptochrome (CRY) and red light-absorbing phytochrome (PHY) play important roles in the regulation of plant light responses, such as light-dependent seed germination, de-etiolation, shade avoidance, stomatal development, circadian rhythm, and photoperiodic flowering (Su et al., 2017). However, high light and particularly its integral ultraviolet (UV) part causes stress, potentially leading to serious damage to DNA, proteins and other cellular components (Müller-Xing et al., 2014).

Loyall et al. (2000) were pioneers in the research on *GSTs* transcriptional response to short wavelength light. UV-A, UV-B, and red and blue light-induced genes were identified by fluorescent differential display in parsley (*Petroselinum crispum* (Mill.) Fuss) cell cultures, and it was found that UV-B induced the expression of tau-class *GSTs* (Loyall et al., 2000). This was the first report on UV-B inducibility of *GSTs*. Other regulator signals of the identified *GST* were defined with RNA gel blot analysis. Two-hours-long UV-B and hormone (2,4-D and α-naphthylene acetic acid) treatments resulted in an outstanding induction of *PcGST1* (AF177944) expression in parsley cell culture. The UV-B caused rapid increase of PcGST1 mRNA preceded the induction of chalcone synthase (CHS), which gene product is produced in the vacuoles protecting plants from UV-B irradiation (Müller-Xing et al., 2014). The co-expression of *PcGST1*, together with a *LUC* reporter gene under the control of a *CHS* promoter, resulted in an earlier UV-dependent *CHS*:*LUC* induction. The addition of GSH to the *GST* × *CHS:LUC* cell cultures led to an UV-B-independent elevation of the LUC emission 2 h after the application. This first peak was followed by a peak at 6 h. In brief, Loyall et al. (2000) provided evidence for a novel function of GSTs involved in the UV-B mediated signal transduction to CHS, in which external GSH and *PcGST1* possibly affected the *CHS* transcription by changing the redox state. Further, in a proposed model for UV-B-mediated signal transduction, the changes in the redox state and in GST gene expression were preceded by increased intracellular calcium levels in CHS-specific gene expression (Frohnmeyer and Staiger, 2003). More recently, the induction of plant GST activity and/or gene expression by UV-B, UV-A, or UV-C stress was verified in several other higher plant species: *Brassica rapa* L. (Zhou et al., 2007), *Vitis vinifera* L. (Kobayashi et al., 2010; Pontin et al., 2010), *Brassica oleracea* L. var. italica (Mewis et al., 2012), *Miscanthus sinensis* Andersson (Seong et al., 2015), *Vaccinium*

corymbosum L. (Inostroza-Blancheteau et al., 2016), and *Azolla* sp. plants (Prasad et al., 2016).

Red and FR light-absorbing photoreceptors (PHY family) regulate multiple plant growth and developmental responses. Tepperman et al. (2001) firstly observed that the expression of one *Arabidopsis GST* belonging to the tau class (AAD32887) increased rapidly after FR light irradiation, but it was inhibited by phytochrome A (*PHYA*) mutation (Tepperman et al., 2001). Later, Chen et al. (2007) identified that AtGSTU20 interacts with FIN219 (FR-insensitive 219), meaning it is a part of the PHYA-mediated, FR-induced signaling network. Using gain-of-function and loss-of-function mutants, AtGSTU20, also called FIP1 (FIN219–interacting protein) was proven to have a complex function in the regulation of development, as it resulted in a FR-hyposensitive hypocotyl (gain of function) or in a delayed flowering phenotype (loss of function). Recently, the interaction of FIN219 and FIP1 was particularly investigated (Chen et al., 2017). To extend the understanding of the regulatory mechanism between FR light signaling and the jasmonate (JA) response, Chen et al. (2017) determined the crystal structures of the FIN219-FIP1 complex with substrates. Furthermore, they showed that the interaction with FIP1 triggers enhanced activity of FIN219. According to their results, FIP1 (AtGSTU20) may regulate FIN219 activity, which further alters the level of JA signaling. Interestingly, the expression of tau GSTs, which were upregulated by methyl-JA treatment, was obviously higher than when treated with ethylene or salicylic acid (Wagner et al., 2002). The revealed structures of FIN219-FIP1 shed light on how FR light signaling may affect JA biosynthesis in order to regulate seedling photomorphogenesis in *Arabidopsis*. To define the functional role of *Arabidopsis* GSTs in light-signaling pathways, Jiang et al. (2010) focused on several candidates affected by PHYA or FIN219. They performed dark-light transition experiments, where *AtGSTU17* expression depended strictly on PHYA. The phenotype examination of the *Atgstu17* mutant indicated that AtGSTU17 might have a function in the control of hypocotyl elongation in response to FR irradiation. Furthermore, the *AtGSTU17* overexpression line in the *phyA* mutant background revealed that this protein participates in the control of hypocotyl elongation, anthocyanin accumulation, FR blockage of greening, and flowering in a PHYA-dependent manner. Moreover, the expression pattern of *AtGSTU17* also appeared to be associated with auxin and abscisic acid (ABA) signaling and the GSH/GSSG ratio in the regulation of *Arabidopsis* development (Jiang et al., 2010). According to their results, AtGSTU17 protein is not only influenced by a PHYA-dependent pathway, but mediates the signaling and has a strong impact on the GSH/GSSG ratio, and thus on the redox status of the cells. Shohael et al. (2006) also found that light quality can influence the secondary metabolites and enzyme activities of somatic embryos grown in a bioreactor. The authors observed higher GST, but lower DHAR activity in *Eleutherococcus senticosus* somatic embryos affected by red or red and blue light. In contrast, blue light did not change significantly the activity of GST and DHAR in somatic embryos after 45 days (Shohael et al., 2006). Interestingly, it was found that, in red light, irradiated grapevine leaves, where the accumulation of resveratrol compound was enhanced (to protect grapevine from fungal pathogen, *Botrytis cinerea*), the expression of *GST* was rapidly upregulated and showed a peak after 12 h (Ahn et al., 2015). Yang et al. (2015) also revealed that red light induced resistance to *Pseudomonas syringae* pv. tomato DC3000 in tomato plants at night is associated with enhancement of GSH content and expression of *GST1*. In addition, red and blue light could effectively delay the symptom expression and replication of cucumber mosaic virus (CMV) in tobacco by increasing GSH content in the leaves (Chen et al., 2015). Interestingly, not only light quality but duration of the light application can determine the GSH content in leaves. High R/FR ratios induced accumulation of ascorbic acid and GSH content after 12 days in common bean (*Phaseolus vulgaris* L.) (Bartoli et al., 2009), but did not significantly changes the GSH levels after weeks in wheat (*Triticum aestivum* L.) leaves (Monostori et al., 2018). It can be concluded that pretreatment with artificial red light could alleviate the harmful effects of pathogens and abiotic stressors by increasing GST activity and expression, as well as GSH content in the leaves (**Figure 1**).

GST GENE EXPRESSION AND ENZYME ACTIVITY ARE AFFECTED BY LIGHT INTENSITY

Light quality, as well as light intensity, has a great impact on the regulation of GST activity and gene expression. First of all, it was shown that darkness has a significant effect on GST activity and gene expression. In 2003, Dean et al. published a study in which the expression of the *GSTs* in darkness was determined in *Malva pusilla.* The main aim of the study was to identify *MpGST* genes connected to *Colletotrichum gloeosporioides* infection. According to their results, the transcript amount of some *GSTs* (*MpGSTZ1* and *MpGSTU2*) was induced as the infection developed, while *MpGSTF1* was induced during the transition from the biotrophic to the necrotrophic phase of the infection. They utilized dark pretreatment and found that the expression of both *MpGSTZ1* and *MpGSTU2* remained unchanged following transfer to the darkness, whereas the expression of *MpGSTU1* and *MpGSTF1* decreased by ∼50 and 75%, respectively, when plants were placed in the dark for 2 h (Dean et al., 2003). However, Scalla and Roulet (2002) found that herbicide safener mefenpyr-diethyl treatment significantly increased GST activity and the expression of *HvGST6* (phi class) in dark-grown barley (*Hordeum vulgare* L. cv. Alexis) after 4 days.

Besides dark, low light and shade (reduced daylight) also influenced GST activity in plants. GST activity did not change under low light (60 μmol m^{-2} s^{-1}) compared to controlled (160 μmol m^{-2} s^{-1}) conditions in leaves and roots of micropropagated *Phalaenopsis* plantlet grown for 30 days (Ali et al., 2005). In contrast, GST activity declined under low (75 μmol m^{-2} s^{-1}) and suboptimal light (225 μmol m^{-2} s^{-1}) compared to controlled (400 μmol m^{-2} s^{-1}) conditions in *Helianthus annuus* L. var. DRSF-113 seedlings after 72 h (Yadav et al., 2014). Similar changes were found in red leaf lettuce (*Lactuca sativa* L.) after 3 days in low light (40 μmol m^{-2} s^{-1}), where the expression of *LsGST* (Unigene10814_All) significantly

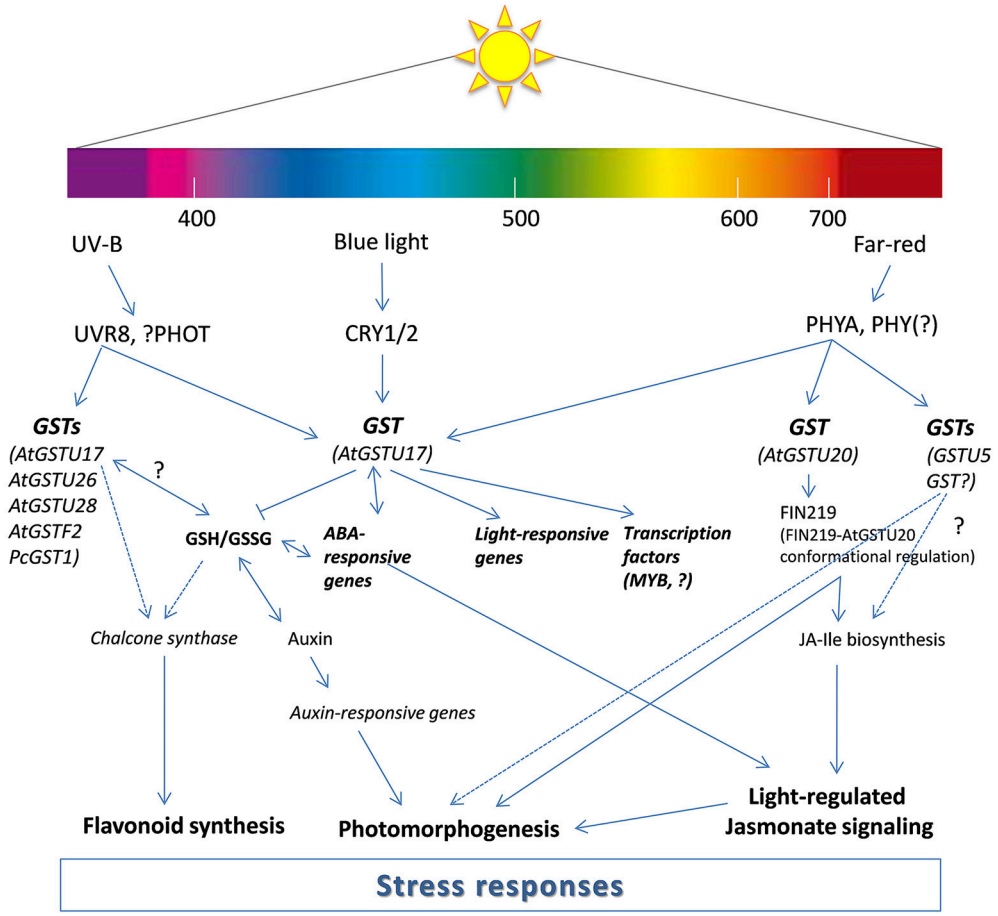

FIGURE 1 | Proposed model for the participation of glutathione transferases (GSTs) in light signal transduction. The model is modified from Frohnmeyer and Staiger (2003), Jiang et al. (2010), Loyall et al. (2000) and Chen et al. (2017). The model illustrates transcriptional and post-transcriptional regulation of GSTs by light (UV-B, blue, and far-red) and possible function of GST proteins in the light induced signaling pathways. *AtGSTU17* was reported to fine tune GSH homeostasis and GSH/GSSG ratio and regulate auxin, ABA, and light response. AtGST20 is having a role in jasmonate (JA) signaling as a conformational regulator of FIN (FR-insensitive 219). Other *GSTs* (*AtGSTU26, ATGSTU28, AtGSTF2,* and *PcGST1*) are also parts of light (UV-B)-regulated signaling which possibly affect chalcone synthase transcription. ABA, abscisic acid; CRY1/2, cryptochrome 1/2; GSH, reduced glutathione; GSSG, oxidized glutatione; JA-Ile, jasmonoyl-isoleucine; MYB, myeloblastosis transcription factors; PHOT, phototropin; PHY, phytochrome; UVR8, UV resistance locus 8.

decreased compared to the control (100 μmol m^{-2} s^{-1}) leaves (Zhang et al., 2018). GSH content also decreased upon low light in duckweed (*Lemna minor* L.) plants (Artetxe et al., 2002, 2006) and in *Arabidopsis* leaves (Oelze et al., 2011).

In contrast, high or excess light (2,500 μmol m^{-2} s^{-1}) significantly elevated GST activity in *Arabidopsis* leaves (Mullineaux et al., 2000). A similar tendency was found by Ali et al. (2005) in leaves of micropropagated *Phalaenopsis* plantlet upon high light (300 μmol m^{-2} s^{-1}). Moreover, based on gene expression data, high light (500 μmol m^{-2} s^{-1}) stress caused a rapid induction of *PgGST* within 1 h in *Panax ginseng* (Kim et al., 2012). Lv et al. (2015) also observed that high light (1,200 μmol m^{-2} s^{-1}) significantly increased the expression of *GST5* and *GST13* (tau class) and elevated GST activity in *Arabidopsis* leaves. Based on their result, β-cyclocitral (β-CC), a volatile oxidized derivative of β-carotene, can regulate NPR1 in order to promote GST transcription and subsequently increase GST activity in response to excess light. High light (1,000 μmol m^{-2} s^{-1}) stimulated the elevation on GSH content in mustard (*Sinapis alba* L.) chloroplasts after 3 h (Baena-González et al., 2001) and in cashew plants (*Anacardium occidentale* L.) after 12 h upon high light (2,000 μmol m^{-2} s^{-1}) (Lima et al., 2018). In contrast, high light (2,500 μmol m^{-2} s^{-1}) decreased GSH content in Golden Agave (*Agave Americana* L.) leaves after 2 h (Deng, 2012) and in exocarp of apple (*Malus spp.*) after 3 h (Davey et al., 2004). However, there were not significant changes in GSH content after 4 days upon high light (600 μmol m^{-2} s^{-1}) in cucumber (*Cucumis sativus* L.) leaves (Jiang et al., 2013). Interestingly, total GSH showed an initial increase during the first 30–40 min of high light (800 μmol m^{-2} s^{-1}) treatment followed by a decrease (60 min) and an increase during dark recovery in two Antarctic lichens (*Usnea antarctica* Du Rietz) (Balarinová et al., 2014). Based on these results, increase in GST activity and GSH content was an adaptive response of the plants

FIGURE 2 | Heat map showing the light conditions as identified by Genevestigator which perturb *Arabidopsis* GST expression. The studies used in the analysis were *Arabidopsis* Col-0 seedlings with UV-A, UV-AB, white, blue, red far red light treatments compared to continuous dark (experiment ID: AT-00109 and AT-00002), the effect of low light-high light shift compared to low light control on detached rosette leaves of *Arabidopsis* (experiment ID: AT-00682), treatment of *Arabidopsis* cell cultures with high light and dark compared to untreated cell cultures (experiment ID: AT-00424), *Arabidopsis* Col-0 plant samples exposed to low red/far red compared to continuous high red/far red (experiment ID: AT-002013) and *Arabidopsis* Col-0 seedlings grown in filtered UV-B light conditions exposed to UV-B with a low UV-B filter for 6 h compared to continuously high and low UV-B (345 nm and 305 mn) filtered samples (experiment ID: AT-00616). Microarray data for all GSTs was used to construct heat map. Red indicates up-regulation, black no change, and green down-regulation with the color intensity reflecting the Log2 perturbation.

to higher amounts of ROS generated at higher light intensities. However, these changes were dependent on the light intensity, duration of irradiation and plant species or organs.

MOLECULAR MECHANISM OF LIGHT REGULATION OF PLANT GSTs

Regarding the functional overlaps and variability of GSTs, their expression and regulation show high diversity. Several microarray and transcriptome sequencing data confirm the effect of quality and quantity of light on the expression pattern of *GSTs*. *Arabidopsis GST* gene transcript data originating from Genevestigator (www.genevestigator.com, Hruz et al., 2008) are shown in **Figure 2**. The highlighted *GST* genes (*AtGSTU17* and *AtGSTU5*), were induced by most of the treatments, underlining their importance in light response and signaling. For example, the above-mentioned *AtGSTU17*, which participates in the signal transduction pathway of visible light, showed induction after almost every treatment. Besides *AtGSTU17, AtGSTU5* was similarly upregulated in most cases (**Figure 2**). Furthermore, UVB in several cases (AT-00616 and At-00109 datasets) induced the tau group *GST* expression except of some gene (e.g., *AtGSTU13* and *AtGSTU14*). White light, UV-B, red, and far red decreased the expression of some phi group sequences: *AtGSTF6*, *AtGSTF3,* and *AtGSTF11*. Downregulation of several *GST* genes (for instance *AtGSTF11, AtGSTU9, AtGSTU13*, and *AtGSTU27)* was seen after exposure to elevated light intensity.

To understand the processes other than gene expression changes in *GST* transcripts, it is necessary to collect the elements that are probably participating in the regulation. The 5′ *cis*-regulating elements (CRE) of *GST*s were described and categorized in several species, e.g., carnation (Itzhaki et al., 1994), soybean (Ulmasov et al., 1994, 1995), tobacco (Droog et al., 1995), *Arabidopsis* (Chen and Singh, 1999), Tausch's goatgrass (Xu et al., 2002), tomato (Csiszár et al., 2014), and pickleweed (Tiwari et al., 2016). Among the CREs, a great number of elements participates in the mediation of light signals. In *Arabidopsis*, among the upregulated GSTs, which were induced by different wavelength and light intensities, *AtGSTU17* and *AtGSTU5* share some common light-responsive elements (ATC-motif, Box 4, G-box, and LAMP–element).

In silico analysis of the 5′ regulatory region of 11 selected tomato *GSTs* revealed the presence of a high number of putative light-responsive elements in these genes (Csiszár et al., 2014). The CREs in the promoter regions of four *GSTs* with a light-responsive expression pattern were compared (Gallé et al., 2018), revealing that there was one common element (Box 4) in all four *GSTs*. Several G-box and Box I elements also presented in the promoters. Box 4 was described in the 5′ region of oat α-amylase. As it is a hyphenated palindrome sequence, it is likely to be a binding site of the helix-turn-helix and zinc finger classes of transcription factors (Rushton et al., 1992). Four *cis*-acting elements, designated as Boxes I, II, III, and IV, have previously been identified as functionally relevant components of the light-responsive *CHS* promoter in parsley (Weisshaar et al., 1991). Among them, Box I and Box II presented among the tomato *GST* CREs. These two elements are together called Unit 1 and necessary *cis*-acting elements for light response in the context of a minimal *CHS* promoter (Schulze-Lefert et al., 1989; Weisshaar et al., 1991). However, Unit 2 (Box III and Box IV), which enlarges the light responsiveness of Unit 1 is missing. The position of the two boxes differs

from that in parsley *CHS*, as in most cases they are further than −600.

CONCLUSION AND PERSPECTIVES

Light intensity and quality are the major factors limiting photosynthesis, in turn affecting carbohydrate production and eventually plant growth and development as well as defense reaction (Chen et al., 2004). It has been suggested that red and blue light or both low- (shade) and high-light intensities can influence the fitness of plants (Su et al., 2017). Moreover, light regulates the activity and gene expression of *GSTs*, which are key elements of detoxification. Two classes of GSTs, tau and phi, play pivotal role in the detoxification of the effects of herbicides (Dixon et al., 2003). The effectiveness of some commonly used photo-inhibitor herbicide compounds, such as terbuthylazine or metribuzin, depends on the photosynthetic electron transport, meaning they are light-dependent. A majority of herbicides are detoxified through substitution reactions and, on a much rarer basis, GSH addition reactions (Cummins et al., 2011; Chronopoulou et al., 2017). In this way, GSTs are involved in desired traits of herbicide tolerance or resistance, e.g., in crops or weeds, respectively (Chronopoulou et al., 2017). Moreover, candidates of tau and phi groups of GSTs were found to play roles in altering the capacity of crops to metabolize herbicides and other xenobiotics; thus, they are important components of safener effects (Brazier-Hicks et al., 2018). Detailed information about the transcriptional inductions of these detoxifying enzymes has been a valuable addition to safener innovation in agriculture. Light regulation of these processes may interact, strengthen or weaken safener-induced enhancement in detoxification efficiency, thereby offering the possibility to reduce pesticide usage.

Circadian regulation in several plant species revealed some similarities: the activity and expression levels of GSTs reached the maximum at the end of the light period before both decreased under darkness. Thus, GSTs seem to be regulated by light, while their participation in light-dependent cellular mechanisms is complex: some of them were found to be a transducer of the UV- and red light-regulated signaling pathways. Processes behind the light-induced switch of GSTs are often altered by the intensity, duration and quality of the illumination, where the wavelength seems to be the most emphasized parameter. Especially red light, when it was applied as a pretreatment, was proven to be so effective that it could even alleviate the effect of biotic stressors by increasing GST activity. UV-B radiation in combination with herbicides may also enhance oxidative stress and decrease glutathione-mediated detoxification in weeds, causing severe damages to lipids and proteins and, in turn, decreasing membrane stability and inducing cell death. However, both light quality as well as light intensity influences GST activity and gene transcription. Darkness, low light or shade mostly reduced GST activity, while high light significantly elevated the activity and expression of GSTs and also GSH levels. Nevertheless, these changes are not only dependent on the light intensity, but also on the duration of the illumination and plant species and organs, respectively. The light-dependent regulation of plant *GST* expression was also confirmed by *in silico* promoter analysis. The presence of a high number of light-responsive elements also indicates that light plays an important role in the regulation of GST activity and gene expression. However, further research on plant species (crops and weeds) or organs and temporal regulation of GST activity and gene expression is necessary for understanding their complex regulation under various light conditions. Moreover, the crosstalk among other detoxifying enzymes and other signaling compounds under different light conditions is also worthy of further investigation.

As a summary, light responsiveness seems to be a constant and permanent feature of GSTs, which determines the detoxification, adaptation, stress responses, and even their reaction to dark. Understanding the mechanism that can regulate plant GSTs activity and gene expression at molecular and physiological levels is a major problem in current plant biology as well as in agriculture. Based on this knowledge, integrating the application time of spraying herbicides or safeners (in the light or dark period) with the knowledge of plant detoxification processes by GSTs into weed and pest management programs can reduce agricultural costs and increase the effectiveness of crop protection.

AUTHOR CONTRIBUTIONS

ÁG and PP conceived of the presented idea. ÁG and PP were involved in planning and drafted the manuscript. JC supervised the work. KB designed the table. EH performed the promoter test. AÖ and ZC aided in interpreting the results. ÁG, PP, and JC worked on the manuscript. All authors discussed the results and commented on the manuscript.

FUNDING

This work was supported by the Hungarian National Scientific Research Foundation [grant number NKFI K 125265 and NKFI FK 124871].

REFERENCES

Abhilash, P. C., Jamil, S., and Singh, N. (2009). Transgenic plants for enhanced biodegradation and phytoremediation of organic xenobiotics. *Biotechnol. Adv.* 27, 474–488. doi: 10.1016/j.biotechadv.2009.04.002

Ahn, S. Y., Kim, S. A., and Yun, H. K. (2015). Inhibition of *Botrytis cinerea* and accumulation of stilbene compounds by light-emitting diodes of grapevine leaves and differential expression of defense-related genes. *Eur. J. Plant Pathol.* 143, 753–765. doi: 10.1007/s10658-015-0725-5

Alderete, L. G. S., Guido, M. E., Agostini, E., and Mas, P. (2018). Identification and characterization of key circadian clock genes of tobacco hairy roots: putative regulatory role in xenobiotic metabolism. *Environ. Sci. Pollut. Res. Int.* 25, 1597–1608. doi: 10.1007/s11356-017-0579-9

Ali, M. B., Hahn, E. J., and Paek, K. Y. (2005). Effects of light intensities on antioxidant enzymes and malondialdehyde content during short-term

acclimatization on micropropagated *Phalaenopsis* plantlet. *Environ. Exp. Bot.* 54, 109–120. doi: 10.1016/j.envexpbot.2004.06.005

Artetxe, U., García-Plazaola, J. I., Hernández, A., and Becerril, J. M. (2002). Low light grown duckweed plants are more protected against the toxicity induced by Zn and Cd. *Plant Physiol. Biochem.* 40, 859–863. doi: 10.1016/S0981-9428(02)01446-8

Artetxe, U., Hernández, A., García-Plazaola, J. I., and Becerril, J. M. (2006). Do light acclimation mechanisms reduce the effects of light-dependent herbicides in duckweed (*Lemna minor*)?. *Weed Sci.* 54, 230–236. doi: 10.1614/WS-05-54.2.230

Asada, K. (2006). Production and scavenging of reactive oxygen species in chloroplasts and their functions. *Plant Physiol.* 141, 391–396. doi: 10.1104/pp.106.082040

Ashraf, M. A., Ashraf, M., and Ali, Q. (2010). Response of two genetically diverse wheat cultivars to salt stress at different growth stages: leaf lipid peroxidation and phenolic contents. *Pak. J. Bot.* 42, 559–565.

Baena-González, E., Baginsky, S., Mulo, P., Summer, H., Aro, E. M., and Link, G. (2001). Chloroplast transcription at different light intensities. Glutathione-mediated phosphorylation of the major RNA polymerase involved in redox-regulated organellar gene expression. *Plant Physiol.* 127, 1044–1052. doi: 10.1104/pp.010168

Balarinová, K., Barták, M., Hazdrová, J., Hájek, J., and Jílková, J. (2014). Changes in photosynthesis, pigment composition and glutathione contents in two Antarctic lichens during a light stress and recovery. *Photosynthetica* 52, 538–547. doi: 10.1007/s11099-014-0060-7

Ballaré, C. L. (2014). Light regulation of plant defense. *Annu. Rev. Plant. Biol.* 65, 335–363. doi: 10.1146/annurev-arplant-050213-040145

Bartoli, C. G., Tambussi, E. A., Diego, F., and Foyer, C. H. (2009). Control of ascorbic acid synthesis and accumulation and glutathione by the incident light red/far red ratio in *Phaseolus vulgaris* leaves. *FEBS Lett.* 583, 118–112. doi: 10.1016/j.febslet.2008.11.034

Benekos, K., Kissoudis, C., Nianiou-Obeidat, I., Labrou, N., Madesis, P., Kalamaki, M., et al. (2010). Overexpression of a specific soybean GmGSTU4 isoenzyme improves diphenyl ether and chloroacetanilide herbicide tolerance of transgenic tobacco plants. *J. Biotechnol.* 150, 195–201. doi: 10.1016/j.jbiotec.2010.07.011

Boulahia, K., Carol, P., Planchais, S., and Abrous-Belbachir, O. (2016). *Phaseolus vulgaris* L. seedlings exposed to prometryn herbicide contaminated soil trigger an oxidative stress response. *J. Agric. Food Chem.* 64, 3150–3160. doi: 10.1021/acs.jafc.6b00328

Brazier-Hicks, M., Knight, K. M., Sellars, J. D., Steel, P. G., and Edwards, R. (2018). Testing a chemical series inspired by plant stress oxylipin signalling agents for herbicide safening activity. *Pest Manag. Sci.* 74, 828–836. doi: 10.1002/ps.4859

Cairns, N. G., Pasternak, M., Wachter, A., Cobbett, C. S., and Meyer, A. J. (2006). Maturation of *Arabidopsis* seeds is dependent on glutathione biosynthesis within the embryo. *Plant Phys.* 141, 446–455. doi: 10.1104/pp.106.077982

Camargo, E. R., Senseman, S. A., McCauley, G. N., Bowe, S., Harden, J., and Guice, J. B. (2012). Interaction between saflufenacil and imazethapyr in red rice (*Oryza* ssp.) and hemp sesbania (*Sesbania exaltata*) as affected by light intensity. *Pest Manag. Sci.* 68, 1010–1018. doi: 10.1002/ps.3260

Chandra-Shekara, A. C., Gupte, M., Navarre, D., Raina, S., Raina, R., Klessig, D., et al. (2006). Light-dependent hypersensitive response and resistance signaling against Turnip Crinkle Virus in *Arabidopsis*. *Plant J.* 45, 320–334. doi: 10.1111/j.1365-313X.2005.02618.x

Chen, C., Huang, I. C., Liu, M. J., Wang, Z. G., Chung, S. S., and Hsieh, H. L. (2007). Glutathione S-transferase interacting with far-red insensitive 219 is involved in phytochrome A-mediated signaling in *Arabidopsis*. *Plant Physiol.* 143, 1189–1202. doi: 10.1104/pp.106.094185

Chen, C. Y., Ho, S. S., Kuo, T. Y., Hsieh, H. L., and Cheng, Y. S. (2017). Structural basis of jasmonate-amidosynthetase FIN219 in complex with glutathione S-transferase FIP1 during the JA signal regulation. *Proc. Natl. Acad. Sci. U.S.A.* 114, E1815–E1824. doi: 10.1073/pnas.1609980114

Chen, L. J., Zhao, F. F., Zhang, M., Lin, H. H., and Xi, D. H. (2015). Effects of light quality on the interaction between Cucumber Mosaic Virus and *Nicotiana tabacum*. *J. Phytopathol.* 163, 1002–1013. doi: 10.1111/jph.12408

Chen, M., Chory, J., and Fankhauser, C. (2004). Light signal transduction in higher plants. *Annu. Rev. Genet.* 38, 87–117. doi: 10.1146/annurev.genet.38.072902.092259

Chen, W., and Singh, K. B. (1999). The auxin, hydrogen peroxide and salicylic acid induced expression of the *Arabidopsis* GST6 promoter is mediated in part by an ocs element. *Plant J.* 19, 667–677. doi: 10.1046/j.1365-313x.1999.00560.x

Chronopoulou, E., Georgakis, N., Nianiou-Obeidat, I., Madesis, P., Perperopoulou, F., Vasilopoulou, E., et al. (2017). "Plant glutathione transferases in abiotic stress response and herbicide resistance," in *Glutathione in Plant Growth, Development, and Stress Tolerance*. eds M. A. Hossain, M. G. Mostofa, P. Diaz-Vivancos, D. J. Burritt, M. Fujita, and L. S. P. Tran (Berlin: Springer International Publishing), 215–233.

Cicero, L. L., Madesis, P., Tsaftaris, A., and Piero, A. R. L. (2015). Tobacco plants over-expressing the sweet orange tau glutathione transferases (CsGSTUs) acquire tolerance to the diphenyl ether herbicide fluorodifen and to salt and drought stresses. *Phytochemistry* 116, 69–77. doi: 10.1016/j.phytochem.2015.03.004

Cole, D. J. (1994). Detoxification and activation of agrochemicals in plants. *Pest Manag. Sci.* 42, 209–222. doi: 10.1002/ps.2780420309

Csiszár, J., Horváth, E., Bela, K., and Gallé, Á. (2016). "Glutathione-related enzyme system: glutathione reductase (GR), glutathione transferases (GSTs) and glutathione peroxidases (GPXs)," in *Redox State as a Central Regulator of Plant-Cell Stress Responses*. eds D. K. Gupta, J. M. Palma, and F. J. Corpas (Cham: Springer International Publishing), 137–158. doi: 10.1007/978-3-319-44081-1_7

Csiszár, J., Horváth, E., Váry, Z., Gallé, Á., Bela, K., Brunner, S., et al. (2014). Glutathione transferase supergene family in tomato: salt stress-regulated expression of representative genes from distinct GST classes in plants primed with salicylic acid. *Plant Physiol. Biochem.* 78, 15–26. doi: 10.1016/j.plaphy.2014.02.010

Cummins, I., Cole, D. J., and Edwards, R. (1999). A role for glutathione transferases functioning as glutathione peroxidases in resistance to multiple herbicides in black-grass. *Plant J.* 18, 285–292. doi: 10.1046/j.1365-313X.1999.00452.x

Cummins, I., Dixon, D. P., Freitag-Pohl, S., Skipsey, M., and Edwards, R. (2011). Multiple roles for plant glutathione transferases in xenobiotic detoxification. *Drug Metab. Rev.* 43, 266–280. doi: 10.3109/03602532.2011.552910

Davey, M. W., Franck, C., and Keulemans, J. (2004). Distribution, developmental and stress responses of antioxidant metabolism in *Malus*. *Plant Cell Environ.* 27, 1309–1320. doi: 10.1111/j.1365-3040.2004.01238.x

Dean, J. D., Goodwin, P. H., and Hsiang, T. (2003). *Colletotrichum gloeosporioides* infection induces differential expression of glutathione S-transferase genes in *Malva pusilla*. *Funct. Plant Biol.* 30, 821–828. doi: 10.1071/FP03080

Deng, B. (2012). Antioxidative response of Golden Agave leaves with different degrees of variegation under high light exposure. *Acta Physiol. Plant.* 34, 1925–1933. doi: 10.1007/s11738-012-0993-z

Diaz-Vivancos, P., de Simone, A., Kiddle, G., and Foyer, C. H. (2015). Glutathione—linking cell proliferation to oxidative stress. *Free Radical Bio. Med.* 89, 1154–1164. doi: 10.1016/j.freeradbiomed.2015.09.023

Diaz-Vivancos, P., Dong, Y., Ziegler, K., Markovic, J., Pallardo, F. V., Pellny, T. K., et al. (2010a). Recruitment of glutathione into the nucleus during cell proliferation adjusts whole-cell redox homeostasis in *Arabidopsis thaliana* and lowers the oxidative defence shield. *Plant J.* 64, 825–838. doi: 10.1111/j.1365-313X.2010.04371.x

Diaz-Vivancos, P., Wolff, T., Markovic, J., Pallardo, F. V., and Foyer, C. H. (2010b). A nuclear glutathione cycle within the cell cycle. *Biochem. J.* 431, 169–178. doi: 10.1042/BJ20100409

Dixon, D. P., and Edwards, R. (2010). Glutathione Transferases. *Arabidopsis Book* 8:e0131. doi: 10.1199/tab.0131

Dixon, D. P., McEwen, A. G., Lapthorn, A. J., and Edwards, R. (2003). Forced evolution of a herbicide detoxifying glutathione transferase. *J. Biol. Chem.* 278, 23930–23935. doi: 10.1074/jbc.M303620200

Droog, F., Spek, A., van der Kooy, A., de Ruyter, A., Hoge, H., Libbenga, K., et al. (1995). Promoter analysis of the auxin-regulated tobacco glutathione S-transferase genes *Nt103-1* and *Nt103-35*. *Plant Mol. Biol.* 29, 413–429. doi: 10.1007/BF00020974

Dutilleul, C., Garmier, M., Noctor, G., Mathieu, C., Chétrit, P., Foyer, C. H., et al. (2003). Leaf mitochondria modulate whole cell redox homeostasis, set antioxidant capacity, and determine stress resistance through altered

signaling and diurnal regulation. *Plant Cell* 15, 1212–1226. doi: 10.1105/tpc.009464

Foyer, C. H., and Noctor, G. (2005). Redox homeostasis and antioxidant signaling: a metabolic interface between stress perception and physiological responses. *Plant Cell* 17,1866–1875. doi: 10.1105/tpc.105.033589

Foyer, C. H., and Noctor, G. (2013). Redox signaling in plants. *Antioxid. Redox Signal.* 18, 2087–2090. doi: 10.1089/ars.2013.5278

Freeman, J. L., Persans, M. W., Nieman, K., Albrecht, C., Peer, W., Pickering, I. J., et al. (2004). Increased Glutathione biosynthesis plays a role in nickel tolerance in thlaspi nickel hyperaccumulators. *Plant Cell* 16, 2176–2191. doi: 10.1105/tpc.104.023036

Frenkel, E., Matzrafi, M., Rubin, B., , and Peleg, Z. (2017). Effects of environmental conditions on the fitness penalty in herbicide resistant *Brachypodium hybridum*. *Front. Plant Sci.* 8:94. doi: 10.3389/fpls.2017.00094

Frohnmeyer, H., and Staiger, D. (2003). Ultraviolet-B radiation-mediated responses in plants. Balancing damage and protection. *Plant Physiol.* 133, 1420–1428. doi: 10.1104/pp.103.030049

Gallé, Á., Csiszár, J., Secenji, M., Guóth, A., Cseuz, L., Tari, I., et al. (2009). Glutathione transferase activity and expression patterns during grain filling in flag leaves of wheat genotypes differing in drought tolerance: response to water deficit. *J. Plant Physiol.* 166, 1878–1891. doi: 10.1016/j.jplph.2009.05.016

Gallé, Á., Czékus, Z., Bela, K., Horváth, E., Csiszár, J., and Poór, P. (2018). Diurnal changes in tomato glutathione transferase activity and expression. *Acta Biol. Hun.* 69, 505–509. doi: 10.1556/018.69.2018.4.11

Greenham, K., and McClung, C. R. (2015). Integrating circadian dynamics with physiological processes in plants. *Nat. Rev. Genet.* 16, 598–610. doi: 10.1038/nrg3976

Griebel, T., and Zeier, J. (2008). Light regulation and daytime dependency of inducible plant defenses in *Arabidopsis*: phytochrome signaling controls systemic acquired resistance rather than local defense. *Plant Physiol.* 147, 790–801. doi: 10.1104/pp.108.119503

Grundy, J., Stoker, C., and Carré, I. A. (2015). Circadian regulation of abiotic stress tolerance in plants. *Front. Plant Sci.* 6:648. doi: 10.3389/fpls.2015.00648

Gulyás, Z., Boldizsár, Á., Novák, A., Szalai, G., Pál, M., Galiba, G., et al. (2014). Central role of the flowering repressor ZCCT2 in the redox control of freezing tolerance and the initial development of flower primordia in wheat. *BMC Plant Biol.* 14:91. doi: 10.1186/1471-2229-14-91

Hess, F. D. (2000). Light-dependent herbicides: an overview. *Weed Sci.* 48, 160–170. doi: 10.1614/0043-1745(2000)048[0160:LDHAO]2.0.CO;2

Hicks, L. M., Cahoon, R. E., Bonner, E. R., Rivard, R. S., Sheffield, J., and Jez, J. M. (2007). Thiol-based regulation of redox-active glutamate-cysteine ligase from *Arabidopsis thaliana*. *Plant Cell* 19, 2653–2661. doi: 10.1105/tpc.107.052597

Hooven, L. A., Sherman, K. A., Butcher, S., and Giebultowicz, J. M. (2009). Does the clock make the poison? Circadian variation in response to pesticides. *PLoS ONE.* 4:e6469. doi: 10.1371/journal.pone.0006469

Hothorn, M., Wachter, A., Gromes, R., Stuwe, T., Rausch, T., and Scheffzek, K. (2006). Structural basis for the redox control of plant glutamate cysteine ligase. *J. Biol. Chem.* 281 27557–27565. doi: 10.1074/jbc.M602770200

Hruz, T., Laule, O., Szabo, G., Wessendorp, F., Bleuler, S., Oertle, L., et al. (2008). Genevestigator V3: a reference expression database for the meta-analysis of transcriptomes. *Adv. Bioinformatics.* 2008:420747. doi: 10.1155/2008/420747

Hsu, P. Y., and Harmer, S. L. (2014). Wheels within wheels: the plant circadian system. *Trends Plant Sci.* 19, 240–249. doi: 10.1016/j.tplants.2013.11.007

Huseby, S., Koprivova, A., Lee, B. R., Saha, S., Mithen, R., Wold, A. B., et al. (2013). Diurnal and light regulation of sulphur assimilation and glucosinolate biosynthesis in *Arabidopsis*. *J. Exp. Bot.* 64, 1039–1048. doi: 10.1093/jxb/ers378

Inostroza-Blancheteau, C., Acevedo, P., Loyola, R., Arce-Johnson, P., Alberdi, M., and Reyes-Díaz, M. (2016). Short-term UV-B radiation affects photosynthetic performance and antioxidant gene expression in highbush blueberry leaves. *Plant Physiol. Biochem.* 107, 301–309. doi: 10.1016/j.plaphy.2016.06.019

Itzhaki, H., Maxson, J. M., and Woodson, W. R. (1994). An ethylene-responsive enhancer element is involved in the senescence-related expression of the carnation glutathione-S-transferase (GST1) gene. *Proc. Natl. Acad. Sci. U.S.A.* 91, 8925–8929. doi: 10.1073/pnas.91.19.8925

Jez, J. M., Cahoon, R. E., and Chen, S. (2004). *Arabidopsis thaliana* glutamate-cysteine ligase: functional properties, kinetic mechanism, and regulation of activity. *J. Biol. Chem.* 279, 33463–33470. doi: 10.1074/jbc.M405127200

Jiang, H. W., Liu, M. J., Chen, C., Huang, C. H., Chao, L. Y., , and Hsieh, H. L. (2010). A glutathione S-transferase regulated by light and hormones participates in the modulation of *Arabidopsis* seedling development. *Plant Physiol.* 154, 1646–1658. doi: 10.1104/pp.110.159152

Jiang, Y. P., Huang, L. F., Cheng, F., Zhou, Y. H., Xia, X. J., Mao, W. H., et al. (2013). Brassinosteroids accelerate recovery of photosynthetic apparatus from cold stress by balancing the electron partitioning, carboxylation and redox homeostasis in cucumber. *Physiol. Plant.* 148, 133–145. doi: 10.1111/j.1399-3054.2012.01696.x

Kangasjärvi, S., Neukermans, J., Li, S., Aro, E. M., and Noctor, G. (2012). Photosynthesis, photorespiration, and light signalling in defence responses. *J. Exp. Bot.* 63, 1619–1636. doi: 10.1093/jxb/err402

Karapetyan, S., and Dong, X. (2017). Redox and the circadian clock in plant immunity: a balancing act. *Free Radic. Biol. Med.* 119, 56–61. doi: 10.1016/j.freeradbiomed.2017.12.024

Kim, Y. J., Lee, O. R., Lee, S., Kim, K. T., and Yang, D. C. (2012). Isolation and characterization of a theta glutathione S-transferase gene from *Panax ginseng* Meyer. *J. Ginseng Res.* 36:449. doi: 10.5142/jgr.2012.36.4.449

Kobayashi, H., Takase, H., Suzuki, Y., Tanzawa, F., Takata, R., Fujita, K., et al. (2010). Environmental stress enhances biosynthesis of flavor precursors, S-3-(hexan-1-ol)-glutathione and S-3-(hexan-1-ol)-L-cysteine, in grapevine through glutathione S-transferase activation. *J. Exp. Bot.* 62, 1325–1336. doi: 10.1093/jxb/erq376

Kopriva, S., and Rennenberg, H. (2004). Control of sulphate assimilation and glutathione synthesis: interaction with N and C metabolism. *J. Exp. Bot.* 55, 1831–1842. doi: 10.1093/jxb/erh203

Kranner, I., Birtić, S., Anderson, K. M., and Pritchard, H. W. (2006). Glutathione half-cell reduction potential: a universal stress marker and modulator of programmed cell death? *Free Radic. Biol. Med.* 40, 2155–2165. doi: 10.1016/j.freeradbiomed.2006.02.013

Labrou, N. E., Papageorgiou, A. C., Pavli, O., and Flemetakis, E. (2015). Plant GSTome: structure and functional role in xenome network and plant stress response. *Curr. Opin. Biotechnol.* 32, 186–194. doi: 10.1016/j.copbio.2014.12.024

Lai, A. G., Doherty, C. J., Mueller-Roeber, B., Kay, S. A., Schippers, J. H., and Dijkwel, P. P. (2012). CIRCADIAN CLOCK-ASSOCIATED 1 regulates ROS homeostasis and oxidative stress responses. *Proc. Natl. Acad. Sci. U.S.A.* 109, 17129–17134. doi: 10.1073/pnas.1209148109

Lati, R. N., Mou, B., Rachuy, J. S., and Fennimore, S. A. (2016). Evaluation of cycloate followed by evening two-leaf–stage phenmedipham application in fresh market spinach. *Weed Technol.* 30, 464–471. doi: 10.1614/WT-D-15-00102.1

Lima, C. S., Ferreira-Silva, S. L., Carvalho, F. E. L., Neto, M. C. L., Aragão, R. M., Silva, E. N., et al. (2018). Antioxidant protection and PSII regulation mitigate photo-oxidative stress induced by drought followed by high light in cashew plants. *Environ. Exp. Bot.* 149, 59–69. doi: 10.1016/j.envexpbot.2018.02.001

Liu, P. P., von Dahl, C. C., and Klessig, D. F. (2011). The extent to which methyl salicylate is required for signaling systemic acquired resistance is dependent on exposure to light after infection. *Plant Physiol.* 157, 2216–2226. doi: 10.1104/pp.111.187773

Liu, Y. J., Han, X. M., Ren, L. L., Yang, H. L., and Zeng, Q. Y. (2013). Functional divergence of the glutathione S-transferase supergene family in Physcomitrella patens reveals complex patterns of large gene family evolution in land plants. *Plant Physiol.* 161, 773–786. doi: 10.1104/pp.112.205815

Loyall, L., Uchida, K., Braun, S., Furuya, M., and Frohnmeyer, H. (2000). Glutathione and a UV light–induced glutathione S-transferase are involved in signaling to chalcone synthase in cell cultures. *Plant Cell* 12, 1939–1950. doi: 10.1105/tpc.12.10.1939

Luschin-Ebengreuth, N., and Zechmann, B. (2016). Compartment-specific investigations of antioxidants and hydrogen peroxide in leaves of *Arabidopsis thaliana* during dark-induced senescence. *Acta Physiol. Plant.* 38:133. doi: 10.1007/s11738-016-2150-6

Lv, F., Zhou, J., Zeng, L., and Xing, D. (2015). β-cyclocitral upregulates salicylic acid signalling to enhance excess light acclimation in *Arabidopsis*. *J. Exp. Bot.* 66, 4719–4732. doi: 10.1093/jxb/erv231

McClung, C. R. (2006). Plant circadian rhythms. *Plant Cell.* 18, 792–803. doi: 10.1105/tpc.106.040980

Mewis, I., Schreiner, M., Nguyen, C. N., Krumbein, A., Ulrichs, C., Lohse, M., et al. (2012). UV-B irradiation changes specifically the secondary metabolite profile in broccoli sprouts: induced signaling overlaps with defense response to biotic stressors. *Plant Cell Physiol.* 53, 1546–1560. doi: 10.1093/pcp/pcs096

Monostori, I., Heilmann, M., Kocsy, G., Rakszegi, M., Ahres, M., Altenbach, S. B., et al. (2018). LED lighting–modification of growth, metabolism, yield and flour composition in wheat by spectral quality and intensity. *Front. Plant Sci.* 9:605. doi: 10.3389/fpls.2018.00605

Müller-Xing, R., Xing, Q., and Goodrich, J. (2014). Footprints of the sun: memory of UV and light stress in plants. *Front. Plant Sci.* 5:474. doi: 10.3389/fpls.2014.00474

Mullineaux, P., Ball, L., Escobar, C., Karpinska, B., Creissen, G., and Karpinski, S. (2000). Are diverse signalling pathways integrated in the regulation of *Arabidopsis* antioxidant defence gene expression in response to excess excitation energy?. *Philos. Trans. R. Soc. Lond. B, Biol. Sci.* 355, 1531–1540. doi: 10.1098/rstb.2000.0713

Nianiou-Obeidat, I., Madesis, P., Kissoudis, C., Voulgari, G., Chronopoulou, E., Tsaftaris, A., et al. (2017). Plant glutathione transferase-mediated stress tolerance: functions and biotechnological applications. *Plant Cell Rep.* 36, 791–805. doi: 10.1007/s00299-017-2139-7

Noctor, G., Arisi, A. C. M., Jouanin, L., Valadier, M. H., Roux, Y., and Foyer, C. H. (1997). Light-dependent modulation of foliar glutathione synthesis and associated amino acid metabolism in poplar overexpressing γ-glutamylcysteine synthetase. *Planta* 202, 357–369. doi: 10.1007/s004250050138

Noctor, G., and Foyer, C. H. (1998). Ascorbate and glutathione: keeping active oxygen under control. *Annu. Rev. Plant Physiol. Plant Mol. Biol.* 49, 249–279. doi: 10.1146/annurev.arplant.49.1.249

Noctor, G., Mhamdi, A., Chaouch, S., Han, Y. I., Neukermans, J., Marquez-Garcia, B., et al. (2011). Glutathione in plants: an integrated overview. *Plant, Cell Environ.* 35, 454–484. doi: 10.1111/j.1365-3040.2011.02400.x

Oelze, M. L., Vogel, M. O., Alsharafa, K., Kahmann, U., Viehhauser, A., Maurino, V. G., et al. (2011). Efficient acclimation of the chloroplast antioxidant defence of *Arabidopsis thaliana* leaves in response to a 10- or 100-fold light increment and the possible involvement of retrograde signals. *J. Exp. Bot.* 63, 1297–1313. doi: 10.1093/jxb/err356

Pascal, S., and Scalla, R. (1999). Purification and characterization of a safener-induced glutathione S-transferase from wheat (*Triticum aestivum*). *Physiol Plant.* 106, 17–27. doi: 10.1034/j.1399-3054.1999.106103.x

Pontin, M. A., Piccoli, P. N., Francisco, R., Bottini, R., Martinez-Zapater, J. M., and Lijavetzky, D. (2010). Transcriptome changes in grapevine (*Vitis vinifera* L.) cv. Malbec leaves induced by ultraviolet-B radiation. *BMC Plant Biol.* 10:224. doi: 10.1186/1471-2229-10-224

Poór, P., Ördög, A., Czékus, Z., Borbély, P., Takács, Z., Kovács, J., et al. (2018). Regulation of the key antioxidant enzymes by developmental processes and environmental stresses in the dark. *Biol. Plant.* 62, 201–210. doi: 10.1007/s10535-018-0782-7

Potters, G., Horemans, N., and Jansen, M. A. K. (2010). The cellular redox state in plant stress biology—A charging concept. *Plant Physiol. Bioch.* 48, 292–300. doi: 10.1016/j.plaphy.2009.12.007

Prasad, S. M., Kumar, S., Parihar, P., and Singh, R. (2016). Interactive effects of herbicide and enhanced UV-B on growth, oxidative damage and the ascorbate-glutathione cycle in two *Azolla* species. *Ecotoxicol. Environ. Saf.* 133, 341–349. doi: 10.1016/j.ecoenv.2016.07.036

Rushton, P. J., Hooley, R., and Lazarus, C. M. (1992). Aleurone nuclear proteins bind to similar elements in the promoter regions of two gibberellin-regulated α-amylase genes. *Plant Mol. Biol.* 19, 891–901. doi: 10.1007/BF00040522

Rutherford, A. W., and Krieger-Liszkay, A. (2001). Herbicide-induced oxidative stress in photosystem II. *Trends Biochem. Sci.* 26, 648–653. doi: 10.1016/S0968-0004(01)01953-3

Sabetta, W., Paradiso, A., Costantino, P., and Concetta de Pinto, M. (2017). "Chemistry, Biosynthesis, and Antioxidative Function of Glutathione in Plants." in *Glutathione in Plant Growth, Development, and Stress Tolerance*. eds M. Hossain, M. Mostofa, P. Diaz-Vivancos, D. Burritt, M. Fujita, L. S.Tran (Cham: Springer), 1–27

Scalla, R., and Roulet, A. (2002). Cloning and characterization of a glutathione S-transferase induced by a herbicide safener in barley (*Hordeum vulgare*). *Physiol. Plant.* 116, 336–344. doi: 10.1034/j.1399-3054.2002.1160308.x

Schnaubelt, D., Queval, G., Dong, Y., Diaz-Vivancos, P., Makgopa, M. E., Howell, G., et al. (2015). Low glutathione regulates gene expression and the redox potentials of the nucleus and cytosol in *Arabidopsis thaliana*. *Plant Cell Environ.* 38, 266–279. doi: 10.1111/pce.12252

Schulze-Lefert, P., Becker-Andre, M., Schulz, W., Hahlbrock, K., and Dangl, J. L. (1989). Functional architecture of the light-responsive chalcone synthase promoter from parsley. *Plant Cell.* 1, 707–714. doi: 10.1105/tpc.1.7.707

Schupp, R., and Rennenberg, H. (1988). Diurnal changes in the glutathione content of spruce needles (*Picea abies* L.). *Plant Sci.* 57, 113–117. doi: 10.1016/0168-9452(88)90076-3

Seong, E. S., Yoo, J. H., Choi, J. H., Kim, N. J., Kim, H. Y., Heo, K., et al. (2015). Construction and classification of a cDNA library from '*Miscanthus sinensis*' (*Eulalia*) treated with UV-B. *Plant Omics.* 8, 264–269.

Shohael, A. M., Ali, M. B., Yu, K. W., Hahn, E. J., Islam, R., and Paek, K. Y. (2006). Effect of light on oxidative stress, secondary metabolites and induction of antioxidant enzymes in *Eleutherococcus senticosus* somatic embryos in bioreactor. *Process Biochem.* 41, 1179–1185. doi: 10.1016/j.procbio.2005.12.015

Skipsey, M., Knight, K. M., Brazier-Hicks, M., Dixon, D. P., Steel, P. G., and Edwards, R. (2011). Xenobiotic responsiveness of *Arabidopsis thaliana* to a chemical series derived from a herbicide safener. *J. Biol. Chem.* 286, 32268–32276. doi: 10.1074/jbc.M111.252726

Su, J., Liu, B., Liao, J., Yang, Z., Lin, C., and Oka, Y. (2017). Coordination of cryptochrome and phytochrome signals in the regulation of plant light responses. *Agronomy* 7:25. doi: 10.3390/agronomy7010025

Szalai, G., Kellos, T., Galiba, G., and Kocsy, G. (2009). Glutathione as an antioxidant and regulatory molecule in plants under abiotic stress conditions. *J. Plant Growth Regul.* 28, 66–80. doi: 10.1007/s00344-008-9075-2

Tausz, M., Wonisch, A., Peters, J., Jiménez, M. S., Morales, D., and Grill, D. (2001). Short-term changes in free radical scavengers and chloroplast pigments in *Pinus canariensis* needles as affected by mild drought stress. *J. Plant Physiol.* 158, 213–219. doi: 10.1078/0176-1617-00178

Tepperman, J. M., Zhu, T., Chang, H. S., Wang, X., and Quail, P. H. (2001). Multiple transcription-factor genes are early targets of phytochrome A signaling. *Proc. Natl. Acad. Sci.U.S.A.* 98, 9437–9442. doi: 10.1073/pnas.161300998

Tiwari, V., Patel, M. K., Chaturvedi, A. K., Mishra, A., and Jha, B. (2016). Functional characterization of the tau class glutathione-S-transferases gene (SbGSTU) promoter of *Salicornia brachiata* under salinity and osmotic stress. *PLoS ONE* 11:e0148494. doi: 10.1371/journal.pone.0148494

Ulmasov, T., Hagen, G., and Guilfoyle, T. (1994). The ocs element in the soybean GH2/4 promoter is activated by both active and inactive auxin and salicylic acid analogues. *Plant Mol. Biol.* 26, 1055–1064. doi: 10.1007/BF00040688

Ulmasov, T., Ohmiya, A., Hagen, G., and Guilfoyle, T. (1995). The soybean GH2/4 gene that encodes a glutathione S-transferase has a promoter that is activated by a wide range of chemical agents. *Plant Physiol.* 108, 919–927. doi: 10.1104/pp.108.3.919

Vernoux, T., Wilson, R. C., Seeley, K. A., Reichheld, J. P., Muroy, S., Brown, S., et al. (2000). The root meristemless1/cadmium sensitive 2 gene defines a glutathione dependent pathway involved in initiation and maintenance of cell division during postembryonic root development. *Plant Cell* 12, 97–110. doi: 10.1105/tpc.12.1.97

Wagner, U., Edwards, R., Dixon, D. P., and Mauch, F. (2002). Probing the diversity of the *Arabidopsis* glutathione S-transferase gene family. *Plant Mol. Biol.* 49, 515–532. doi: 10.1023/A:1015557300450

Weisshaar, B., Block, A., Armstrong, G. A., Herrmann, A., Schulze-Lefert, P., and Hahlbrock, K. (1991). Regulatory elements required for light-mediated expression of the *Petroselinum crispum* chalcone synthase gene. *Proc. Soc. Exp. Biol. Med.* 45, 191–210.

Xu, F., Lagudah, E. S., Moose, S. P., and Riechers, D. E. (2002). Tandemly duplicated safener-induced glutathione S-transferase genes from *Triticum tauschii* contribute to genome-and organ-specific expression in hexaploid wheat. *Plant Physiol.* 130, 362–373. doi: 10.1104/pp.004796

Yadav, G., Srivastava, P. K., Singh, V. P., and Prasad, S. M. (2014). Light intensity alters the extent of arsenic toxicity in *Helianthus annuus* L. *seedlings. Biol. Trace Elem. Res.* 158, 410–421. doi: 10.1007/s12011-014-9950-6

Yang, Y. X., Wang, M. M., Yin, Y. L., Onac, E., Zhou, G. F., Peng, S., et al. (2015). RNA-seq analysis reveals the role of red light in resistance against *Pseudomonas syringae* pv. tomato DC3000 in tomato plants. *BMC Genom.* 16:120 doi: 10.1186/s12864-015-1228-7

Zechmann, B. (2017). Diurnal changes of subcellular glutathione content in *Arabidopsis thaliana*. *Biol. Plant.* 61, 791–796. doi: 10.1007/s10535-017-0729-4

Zhang, Y., Xu, S., Cheng, Y., Peng, Z., and Han, J. (2018). Transcriptome profiling of anthocyanin-related genes reveals effects of light intensity on anthocyanin biosynthesis in red leaf lettuce. *PeerJ*. 6:e4607. doi: 10.7717/peerj.4607

Zhou, B., Li, Y., Xu, Z., Yan, H., Homma, S., and Kawabata, S. (2007). Ultraviolet A-specific induction of anthocyanin biosynthesis in the swollen hypocotyls of turnip (*Brassica rapa*). *J. Exp. Bot.* 58, 1771–1781. doi: 10.1093/jxb/erm036

Conflict of Interest Statement: The authors declare that the research was conducted in the absence of any commercial or financial relationships that could be construed as a potential conflict of interest.

frontiers in Plant Science

ORIGINAL RESEARCH
published: 11 January 2019
doi: 10.3389/fpls.2018.01861

Tolerance of Transplastomic Tobacco Plants Overexpressing a Theta Class Glutathione Transferase to Abiotic and Oxidative Stresses

*Evangelia Stavridou[1], Michail Michailidis[2], Stella Gedeon[3], Antri Ioakeim[3], Stefanos Kostas[4], Evangelia Chronopoulou[5], Nikolaos E. Labrou[5], Robert Edwards[6], Anil Day[7], Irini Nianiou-Obeidat[8] and Panagiotis Madesis[1]**

[1] Institute of Applied Biosciences, Centre for Research & Technology Hellas, Thessaloniki, Greece, [2] Laboratory of Pomology, Department of Horticulture, School of Agriculture, Aristotle University of Thessaloniki, Thessaloniki, Greece, [3] Department of Botany, School of Biology, Aristotle University of Thessaloniki, Thessaloniki, Greece, [4] Laboratory of Ornamental Plants, School of Agriculture, Forestry and Natural Environment, Aristotle University of Thessaloniki, Thessaloniki, Greece, [5] Laboratory of Enzyme Technology, Department of Biotechnology, School of Food, Biotechnology and Development, Agricultural University of Athens, Athens, Greece, [6] School of Natural and Environmental Sciences, Faculty of Science, Agriculture and Engineering, Newcastle University, Newcastle upon Tyne, United Kingdom, [7] School of Biological Sciences, The University of Manchester, Manchester, United Kingdom, [8] Laboratory of Genetics and Plant Breeding, School of Agriculture, Forestry and Natural Environment, Aristotle University of Thessaloniki, Thessaloniki, Greece

OPEN ACCESS

Edited by:
Veronica Graciela Maurino, Heinrich Heine Universität Düsseldorf, Germany

Reviewed by:
José Manuel Ugalde, Universität Bonn, Germany
Baris Uzilday, Ege University, Turkey

***Correspondence:**
Panagiotis Madesis
pmadesis@certh.gr

Specialty section:
This article was submitted to Plant Physiology, a section of the journal Frontiers in Plant Science

Received: *04 September 2018*
Accepted: *03 December 2018*
Published: *11 January 2019*

Citation:
Stavridou E, Michailidis M, Gedeon S, Ioakeim A, Kostas S, Chronopoulou E, Labrou NE, Edwards R, Day A, Nianiou-Obeidat I and Madesis P (2019) Tolerance of Transplastomic Tobacco Plants Overexpressing a Theta Class Glutathione Transferase to Abiotic and Oxidative Stresses. Front. Plant Sci. 9:1861. doi: 10.3389/fpls.2018.01861

Chloroplasts are organelles subjected to extreme oxidative stress conditions. Biomolecules produced in the chloroplasts act as signals guiding plant metabolism toward stress tolerance and play a major role in regulating gene expression in the nucleus. Herein, we used transplastomic plants as an alternative approach to expression of transgenes in the nucleus for conferring stress tolerance to abiotic stresses and herbicides. To investigate the morphophysiological and molecular mechanisms and the role of plastid expressed GSTs in tobacco stress detoxification and stress tolerance, we used transplastomic tobacco lines overexpressing a theta class *glutathione transferase* (GST) in chloroplasts. The transplastomic plants were tested under drought (0, 100, and 200 mM mannitol) and salinity (0, 150, and 300 mM NaCl) *in vitro,* and under herbicide stress (Diquat). Our results suggest that pt$^{At\text{GSTT}}$ lines were tolerant to herbicide-induced oxidative and salinity stresses and showed enhanced response tolerance to mannitol-induced osmotic stress compared to WT plants. Overexpression of the *Arabidopsis thaliana At*GSTT in the chloroplasts resulted in enhanced photo-tolerance and turgor maintenance under stress. Whole-genome transcriptome analysis revealed that genes related to stress tolerance, were upregulated in pt$^{At\text{GSTT}}$2a line under both control and high mannitol stress conditions. Transplastomic plants overexpressing the pt$^{At\text{GSTT}}$2a in the chloroplast showed a state of acclimation to stress, as only limited number of genes were upregulated in the pt$^{At\text{GSTT}}$2a transplastomic line compared to WT under stress conditions while at the same time genes related to stress tolerance were upregulated in pt$^{At\text{GSTT}}$2a plants compared to WT in stress-free conditions. In parallel, the metabolic profile indicated limited perturbations of the metabolic homeostasis in the transplastomic lines and greater accumulation of mannitol, and soluble sugars under high mannitol stress. Therefore, transplastomic lines seem to be in a state of acclimation to stress

under stress-free conditions, which was maintained even under high mannitol stress. The results help to elucidate the role of GSTs in plant abiotic stress tolerance and the underlying mechanisms of the GSTs expressed in the chloroplast, toward environmental resilience of cultivated crops.

Keywords: chloroplasts, glutathione-S-transferases, tobacco, transplastomics, abiotic stresses, herbicide, transcriptomics, metabolomics

INTRODUCTION

Developing crop plants, able to yield better under abiotic stresses or plants with multiple herbicide resistance, is a prerequisite for improved crop production. The chloroplast, abundant in plant cells and eukaryotic algae, is the site of photosynthesis, providing the primary source of the world's food productivity (Verma and Daniell, 2007). As chloroplasts are the organelles responsible for photosynthesis they are also a source of reactive oxygen species (ROS) in plants (Foyer and Shigeoka, 2011). Furthermore, environmental stresses have been found to produce an excess of excitation energy in chloroplasts, resulting in the production of ROS, thus they are also considered to be implicated in the regulation of stress responses or even act as a sensor of cellular stress (Mullineaux and Karpinski, 2002). Genetic transformation of chloroplasts has been used as an alternative approach to the expression of transgenes in the nucleus (Wang et al., 2009). The transplastomic system has three main advantages: (i) prevents gene flow via pollen through transgene containment due to maternal inheritance, (ii) has highly active chloroplast transcription and translation machineries, and (iii) a lack of epigenetic interference allows stable transgene expression (Bock, 2014). Chloroplast engineering has been applied for the development of resistant crops to various abiotic and biotic stresses (Clarke and Daniell, 2011), production of biopharmaceuticals, metabolic pathway engineering and advances on RNA editing (reviewed in Wang et al., 2009) and phytoremediation (reviewed in Verma and Daniell, 2007).

Understanding the adaptation of plants to different climatic conditions, such as high temperatures, water logging, and drought is essential for addressing climate change challenges. Improving the resilience of chloroplasts through plastid engineering may provide a solution toward the improvement of crop productivity (Clarke and Daniell, 2011). To date, there are a limited number of studies regarding the development of transplastomic plants and their response to abiotic stress. Transplastomic tobacco plants expressing a choline monooxygenase (*BvCMO*) from *Beta vulgaris* demonstrated increased tolerance to salt (100 and 150 mM NaCl) and drought (300 mM mannitol) stresses (Zhang et al., 2008). Genetic engineering of carrot chloroplast genome expressing the *Betaine-aldehyde dehydrogenase* (*badh)* gene also improved tolerance to high salinity (400 mM L^{-1} NaCl) (Kumar et al., 2004). Similarly, transplastomic *Nicotiana benthamiana* plants expressing multiple defense genes encoding protease inhibitors and chitinase were more tolerant to 200 mM NaCl and 3% PEG compared to the wild type plants and were able to maintain greater root growth activity due to transgene expression in the leucoplasts of roots (Chen et al., 2014). Transplastomic tobacco lines overexpressing an *A. thaliana γ-tocopherol methyltransferase* (*Atγ-tmt)* gene accumulated higher levels of α-tocopherol when grown in 400 mM NaCl, compared to wild-type plants, which accumulated higher starch and total soluble sugars, but transplastomic plants better regulated sugar transport (Jin and Daniell, 2014). Genetically engineered plastomes have provided a generation of herbicide-tolerant plants demonstrated in tobacco for tolerance to glyphosate (Ye et al., 2001; Chin et al., 2003), phosphinothricin (Iamtham and Day, 2000; Lutz et al., 2001) sulcotrione (Falk et al., 2005), isoxaflutole (IFT) (Dufourmantel et al., 2007) and paraquat (methyl-viologen) (Poage et al., 2011; Chen et al., 2014).

Plant glutathione S-transferases (GSTs) have been shown to modulate redox homeostasis by alterations in GSH content and redox state (Sappl et al., 2009), conferring tolerance to a wide range of abiotic stresses (Kumar et al., 2013; Csiszár et al., 2014; Kissoudis et al., 2015b; Kayum et al., 2018) including herbicides (Kissoudis et al., 2015a; Lo Cicero et al., 2015, 2017). Glutathione transferases (GSTs; EC 2.5.1.18) are a superfamily of multifunctional proteins that in plants, have evolved into six discreet groups classified as the zeta (Z), theta (T), phi (F), tau (U), lambda (L), and dehydroascorbate reductase (DHAR) classes, respectively, (Dixon and Edwards, 2010). Functions ascribed to date include the detoxification of herbicides (phi and tau), tyrosine degradation (zeta), the reduction of intermediates involved in redox cycling (DHAR and lambda), and acting as glutathione peroxidases toward organic hydroperoxides (theta). In the case of the theta enzymes (GSTTs), this ability to use glutathione to reduce organic hydroperoxides is conserved between plants and animals and is thought to be important in oxidative metabolism, most notably through the processing of phytotoxic oxidized lipids in the peroxisomes (Dixon et al., 2009; Dixon and Edwards, 2010).

GSTs have been used before in chloroplast transformation; The *Sj*GST26 (EC:2.5.1.18), from *Schistomosoma japonicum* (Smith and Johnson, 1988) and His-tagged derivative of the maltose- binding protein (His_6-MBP) were expressed in tobacco chloroplasts to be used as affinity tags for the rapid purification of chloroplast-expressed proteins (Ahmad et al., 2012). Transplastomic tobacco lines overexpressing glutathione reductase (GR) alone or combined with GST were more tolerant under 10°C, whereas lines overexpressing dehydroascorbate reductase (DHAR) alone or in combination with GR were more sensitive compared to wild type plants (Grant et al.,

2014). When these lines were chilled at 4°C and under relatively high photosynthetically active radiation (PAR), all lines were more sensitive compared to wild type plants, indicating that overexpression of the ROS-scavenging enzymes may be dependent on the interaction of light and cold stress (Grant et al., 2014). Transplastomic seedlings expressing either DHAR or an *Escherichia coli* GST B1-1, which has been shown to exhibit a GSH-dependent peroxidase activity against cumene hydroperoxide (Nishida et al., 1994) and proved to be important for bacterial resistance to hydrogen peroxide- induced oxidative stress (Kanai et al., 2006), or a combination of DHAR:GR and GST:GR in chloroplasts were less sensitive to salt (200 mM NaCl) and cold (4°C) compared to wild type seedlings (Le Martret et al., 2011). However, only the simultaneous expression of DHAR:GR and GST:GR conferred tolerance to methyl viologen (MV) (Le Martret et al., 2011). Transplastomic tobacco lines expressing GR in combination with either DHAR or GST (from *E. coli*) exhibited better tolerance to supplemental UV-B than wild type plants (Czégény et al., 2016). The expression of GSTs in compartments where they are not normally found in, can reveal new insights into their functions. For example, the expression of GSTs in cellular compartments (recombinant bacteria, plant chloroplasts) producing porphyrins has revealed their ability to bind to porphyrinogen intermediates (Dixon et al., 2008). In the case of the *Zm*GSTU1-*Zm*GSTU2, the transplastomics ability to protect plants against herbicides that inhibit porphyrin synthesis in the chloroplast shed light into the functional role of the engineered chimeric enzyme (Dixon et al., 2008).

The GSTs are predominantly not targeted for expression in the chloroplast, however, if they are expressed in this organelle, they could deliver some of their key antioxidant and detoxification functions, such as metabolizing photosystem herbicides, and reducing lipid hydroperoxides generated by ROS formed during photosynthesis. In addition to the efficiency of transplastomic expression, we were also interested in how the protective functions of GSTs could be manifested in an organelle where they are not normally targeted for expression. GSTs are important enzymes of the antioxidant pathway and when expressed in the plastome we hypothesized that the leaf physiology and performance would be enhanced under stress compared to the non-transformed wild type plants. None of the above-mentioned examples were performed with plant derived GSTs from the Theta or Tau classes. Therefore, to investigate whether the overexpression of these GSTs in the chloroplast enhances tolerance to salinity, drought, and herbicide induced oxidative stress we used T1 transplastomic tobacco lines overexpressing a theta class GST from *Arabidopsis thaliana* *At*GSTT1 *(At5g41210),* an enzyme normally only expressed in the peroxisomes which is highly active as a glutathione peroxidase toward organic hydroperoxide substrates or a *Zea mays* tau class chimeric *Zm*GSTU1/ZmGSTU2 enzyme (EFD6-115A), which has been previously shown to protect the transformed plants from herbicide injury through its ability to detoxify fluorodifen (Dixon et al., 2003) and in subsequent studies it was confirmed that the chimera had the additional ability to bind porphyrinogen intermediates formed during chlorophyll biosynthesis, a trait shared with its *Zm*GSTU parent proteins (Dixon et al., 2008). To assess plant tolerance to abiotic stresses, we investigated the morphophysiological parameters, and the metabolic and transcriptomic reactions involved in the response of transplastomic tobacco lines. Herein, we approach plant stress tolerance from an alternative perspective via chloroplast engineering to (i) mitigate the oxidative stress imposed under various abiotic and anthropogenic stress conditions and (ii) unravel the complex networks of molecular interactions controlling plant acclimation to field conditions.

MATERIALS AND METHODS

Plant Material and Experimental Design

For the experiments we used homoplastomic, transplastomic tobacco lines pt^{AtGSTT} and $pt^{EFD6-115A}$ overexpressing the *At*GSTT (lines 2a and 6-1) or a *ZmGSTU1-ZmGSTU2* chimera in chloroplasts, respectively (Dixon et al., 2008). The seeds of the pt^{AtGSTT} and $pt^{EFD6-115A}$ T1 lines were initially grown on MS selection medium supplemented with Streptomycin Sulfate (500 mg L^{-1}) and Spectinomycin Dihydrochloride (250 mg L^{-1}) (Duchefa Biochemie, The Netherlands), whereas the wild-type (WT) tobacco seeds were placed on plain MS medium. After selection, the plantlets were transferred to MS media for further growth and when they reached four true leaves were tested *in vitro* under drought (0, 100, and 200 mM mannitol; AppliChem-PanReac, Germany) and salinity (0, 150, and 300 mM NaCl; Centralchem, Slovakia) conditions ($n = 6$). The experiments lasted for 35 and 20 days, respectively.

The *in vivo* herbicide experiment was performed in a controlled glasshouse environment with a photoperiod of 14/10 h light/dark. The temperature was between 20 and 27°C, with a mean temperature of 23°C. Plantlets undergone acclimatization for 3 weeks and Diquat a non-selective contact herbicide, was applied as Reglone 20 SL formulation (Syngenta Hellas) at 1 and 2 L of Reglone/ha (200-low dose; Diq_L and 400 -high dose; Diq_H, g ai of diquat per hectare, respectively). Herbicide treatments were performed with a portable field plot sprayer (AZO-SPRAYERS, P.O. Box 350-6710 BJ EDE, The Netherlands) using flat-fan nozzles (Teejet Spray System Co., P.O. Box 7900, Wheaton, IL 60188) and calibrated to deliver 300 L/ha of water at 280 kPa pressure.Diquat (REGLONE® Desiccant, Syngenta Canada Inc), Control plants were sprayed with the same volume of water only (no herbicide). All pots were placed in a randomized complete block design (transgenic lines: $n = 15$ and WT: $n = 9$). The experiment lasted for 2 days after herbicide application.

Morphophysiological Measurements

Dark-adapted chlorophyll *a* fluorescence measurements were performed on the youngest fully developed leaf on the adaxial leaf surface using the OS30p+ chlorophyll fluorometer (Opti-Sciences Inc., Hudson, USA) following dark adaptation of 30 min. Relative chlorophyll content was measured according to Stavridou et al. (2016) on one leaf per plant with three averaged measurements using a CCM-200 plus chlorophyll content meter (Opti-Sciences Inc., Hudson, USA). Harvested

plants were separated into leaves, stems, and roots and the final morphological parameters, such as stem length, root length, number of leaves, and plant fresh matter (M_F) were measured. The plant dry matter (M_D) was obtained after drying at 60°C until constant weight.

Transcriptomic Analysis

Total RNA from whole plant tissue of pt^{AtGSTT}2a line and WT plants under control and high mannitol stress conditions *in vitro* was isolated using the Monarch Total RNA Miniprep kit (BioLabs Inc., UK) and their concentration was determined spectrophotometrically. The RNA sequencing was performed by the BGI (Denmark). The RNA results were compared as follows: pt^{AtGSTT}2a and WT in control conditions (groups 1 and 3) and pt^{AtGSTT}2a and WT in high mannitol (200 mM) stress (groups 2 and 4) (**Table 1**).

Agilent 2100 Bioanalyzer (Agilent RNA 6000 Nano Kit) was used for the total RNA sample QC: RNA concentration, RIN value, 28S/18S and the fragment length distribution. We use NanoDrop^{TM} to identify the purity of the RNA samples. The first step in the workflow involves purifying the poly-A containing mRNA molecules using poly-T oligo-attached magnetic beads. Following purification, the mRNA is fragmented into small pieces using divalent cations under elevated temperature. The cleaved RNA fragments are copied into first strand cDNA using reverse transcriptase (Takara Bio Inc.) and random primers. This is followed by second strand cDNA synthesis using DNA Polymerase I and RNase H (Takara Bio Inc.). These cDNA fragments then have the addition of a single "A" base and subsequent ligation of the adapter. The products are then purified and enriched with PCR amplification. The PCR yield was quantified by Qubit and the samples were pooled together to make a single strand DNA circle (ssDNA circle), which gave the final library. DNA nanoballs (DNBs) were generated with the ssDNA circle by rolling circle replication (RCR) to enlarge the fluorescent signals at the sequencing process. The DNBs were loaded into the patterned nanoarrays and pair-end reads of 100 bp were read through on the BGISEQ-500 platform for the following data analysis study. For this step, the BGISEQ-500 platform combines the DNA nanoball-based nano arrays and stepwise sequencing using Combinational Probe-Anchor Synthesis Sequencing Method.

TABLE 1 | Plants used for RNA extraction and transcriptomics analysis.

Analysis group	Plant	Conditions
Group 1	pt^{AtGSTT}2a	Control
	pt^{AtGSTT}2a	Control
Group 2	pt^{AtGSTT}2a	Mannitol High
	pt^{AtGSTT}2a	Mannitol High
Group 3	WT	Control
	WT	Control
Group 4	WT	Mannitol High
	WT	Mannitol High

Bioinformatics Workflow

The reads were filtered for low-quality reads (>20% of the bases qualities are lower than 10), reads with adaptors and reads with unknown bases (N bases more than 5%) to get the clean reads using SOAPnuke software. Then we mapped the clean reads onto reference genome, followed by novel gene prediction, SNP & INDEL calling and gene splicing detection. Finally, we identified DEGs (differentially expressed genes) between samples and performed clustering analysis and functional annotations. After filtering, the remaining reads are called "Clean Reads" and stored in FASTQ format.

Regarding Genome Mapping, HISAT (Hierarchical Indexing for Spliced Alignment of Transcripts) was used to do the mapping step (Kim et al., 2015). The StringTie (Pertea et al., 2015) was used to reconstruct transcripts and Cuffcompare [Cufflinks tools- Trapnell et al. (2012)] to compare reconstructed transcripts to reference annotation. After that, the "u," "I," "o," "j" class code types were used as novel transcripts followed by a support vector machine-based classifier, named Coding Potential Calculator (CPC) (Kong et al., 2007) to predict coding potential of novel transcripts, then the coding novel transcripts were merged with reference transcripts to get a complete reference, and downstream analysis was based on this reference. The clean reads were mapped to reference using Bowtie2 (Langmead and Salzberg, 2012), and then gene expression level was calculated with RSEM (Li and Dewey, 2011), a software package for estimating gene and isoform expression levels from RNA-Seq data. After calculating Pearson's correlation between all samples using cor, hierarchical clustering was performed between all samples using hclust, and PCA analysis with all samples using princomp, and the diagrams were drawn with ggplot2 in R (R Core Team, 2016). The detection of DEGs was performed with NOIseq, which is based on noisy distribution model, as described in Tarazona et al. (2011). The Hierarchical Clustering Analysis of DEGs was performed using heat map function in R. With the GO annotation result, DEGs were classified according to official classification, and GO functional enrichment was also performed using p hyper in R. The *p*-value calculating formula in hypergeometric test is Equation 1:

$$P = 1 - \sum_{i=0}^{m-1} \frac{\binom{M}{i}\binom{N-M}{n-i}}{\binom{N}{n}}$$

Then the false discovery rate (FDR) for each *p*-value was calculated and in general, the terms which FDR was not larger than 0.01 were defined as significantly enriched. With the KEGG annotation result, we classified DEGs according to official classification, and we also performed pathway functional enrichment using phyper in R with the same *p*-value calculating formula in Equation 1 and the FDR was calculated as described above.

To find the ORF of each DEG the getorf function was used. For plants, ORF were aligned to TF domains (from PlntfDB) using hmmsearch (Mistry et al., 2013). DIAMOND (Buchfink

et al., 2014) was used to map the DEGs to the STRING database (von Mering et al., 2005) to obtain the interaction between DEG-encoded proteins using homology with known proteins. The top 100 interaction networks were selected to unfold the pathways involved and for the entire interaction result we provide an input file that can be imported directly into Cytoscape for complex network analysis and visualization.

Metabolite Extraction, Derivatization, and GC–MS Analysis

Determination of primary polar metabolites was performed as described by Lisec et al. (2006) and Michailidis et al. (2017) with slight modifications. Whole plant lyophilized material (∼0.040 gr) from pt^{AtGSTT}2a and WT plants under *in vitro* high mannitol stress and control conditions (three biological replicates) were transferred in 2 mL screw cap tubes with 1400 μL of precooled (−20°C) pure methanol. Adonitol (100 μL of 0.2 mg mL^{-1}) was added as internal quantitative standard, and incubated for 10 min at 70°C. The supernatant was collected after centrifugation (11000 g, 4°C, 10 min) and 750 μL chloroform (−20°C) plus 1500 μL dH_2O (4°C) were added. Following centrifugation (2200 g, 4°C, 10 min), 150 μL of the upper polar phase were transferred into a 1.5 mL glass vial and placed under vacuum until drying. Dried residues were re-dissolved by gentle shaking in 40 μL of 20 mg mL^{-1} methoxyamine hydrochloride for 120 min at 37°C, thereafter they were treated with 70 μL of N-methyl-N-(trimethylsilyl) trifluoroacetamide reagent (MSTFA), and incubated for 30 min at 37°C. GC-MS analysis was carried out in Thermo Trace Ultra GC equipped with ISQ MS and TriPlus RSH^{TM} auto-sampler (Thermo Fisher Scientific^{TM}, Switzerland). One μL was injected with a split ratio of 70:1. GC separation was held on a TR-5MS capillary column 30 m x 0.25 mm x 0.25 mm (Thermo Fisher Scientific^{TM}, Switzerland). Injector temperature was 220°C, ion source 230°C, and the interface 250°C. A constant flow of 1 mL min^{-1} was used for carrier gas. The GC temperature program was held at 70°C for 2 min, then increased to 260°C (rate 8°C min^{-1}), where it remained for 18 min. Mass range of m/z 550 was recorded, after 5 min of solvent delay. The mass spectra were acquired in electron impact ionization mode. The peak area integration and chromatogram visualization was performed using the X-calibur processing program. Standards were used for peak identification or NIST11 database (Michailidis et al., 2017) in case of unknown peaks. The detected metabolites were assessed based on the relative response compared to adonitol and expressed as relative abundance.

Statistical Analysis

All the statistical analyses were performed using the computing environment R. The effects of stress treatments and the genotypes on the morpho-physiological parameters of the *in vitro* experiments and harvesting parameters of the *in vivo* experiments and treatments genotypes and time (days-where applicable) on the physiological parameters were assessed using two-way or three-way ANOVA, respectively, with the *ez* and *afex* packages (Lawrence, 2016; Singmann et al., 2018). All data were tested for normality (Shapiro test) and if normality failed and transformations were attempted. Data were also tested with Mauchly's test for sphericity, and if the assumption of sphericity was violated, the corresponding Greenhouse–Geisser corrections were performed. If significant differences were found among treatments, then the Tukey's HSD *post hoc* test was performed to determine specific treatment differences using the *agricolae* package (de Mendiburu, 2017). For metabolic data, two-way ANOVA was conducted using SPSS (SPSS v21.0., Chicago, USA) and statistically significant differences were based on Duncan's multiple range test (raw data) and Student's *t*-test for comparisons between genotypes or treatments at $P < 0.05$ (**Table S1**). The raw data are presented in **Table S2** and the reported data are relative to the M_F of the pt^{AtGSTT}2a line and WT plants.

RESULTS

Effect of GST Overexpression on Oxidative Stress Tolerance

Both low and high Diquat concentrations were severe enough to cause chlorotic lesions from day one (**Figure S1**) and senescence by day 2 on both WT plants and transplastomic lines (**Figure S2**). Transplastomic lines pt^{AtGSTT}2a and 6.1 showed chlorophyll content with increasing Diquat dose, compared to the WT control, except line pt$^{EFD6-115A}$, which showed reduced chlorophyll content following Diquat exposure (**Table 2** and **Table S3**). Both Diquat doses negatively affected the maximum quantum efficiency of photosystem II (PSII) photochemistry in both WT and transplastomic lines, indicating that the oxidative stress was too severe possibly as a result of extensive free radical formation. The high diquat dose had a more severe effect on the M_F of transplastomic line pt^{AtGSTT} 6.1 (not statistically significant to the control) and WT plants ($p < 0.05$), and a less severe reduction was induced in pt^{AtGSTT} 2a (not statistically significant to the control) and pt$^{EFD6-115A}$ ($p < 0.05$) (**Table 2** and **Table S3**). M_D was not affected by any Diquat dose, indicating that any reduction in M_F was a result of turgor loss potentially, inhibiting the respiratory processes due to the function of Diquat as a rapid-acting translocated desiccant (Cronshey, 1961; McNaughton et al., 2015). An increase in M_D of pt^{AtGSTT} 2a was observed under both Diquat doses, however, the M_D of WT plants and transplastomic lines pt^{AtGSTT} 6.1 and pt$^{EFD6-115A}$ was decreased with increasing Diquat concentration (**Table 2**).

Tolerance of Transplastomic Lines Under *in vitro* NaCl Stress

Transplastomic pt^{AtGSTT} line 6-1 and 2a, when grown in 150 mM NaCl, exhibited increased tolerance compared to WT plants (**Figure S3**, **Table 3** and **Table S4**), with shoot length and M_F not showing statistically significant differences with the stress-free plants. Transplastomic line pt^{AtGSTT}6-1 also showed a non-statistically significant decrease in the shoot length even under the double salt concentration, 300 mM NaCl. Transplastomic line pt$^{EFD6-115A}$ showed reduced M_F

TABLE 2 | Percent of change difference in growth (fresh-M_F and dry-M_D matter; g) and photophysiological parameters (relative chlorophyll content- Chl and Maximum quantum yield of PSII-*Fv*/*Fm*) of *GST transplastomic* lines and WT tobacco plants grown for 2 days in low (Diq_L) and high (Diq_H) Diquat dose compared to control conditions.

Genotype	Treatment	$M_{F\%}$	HSD	$M_{D\%}$	HSD	$Chl_{\%}$	HSD	$Fv/Fm_{\%}$	HSD
pt$^{At\text{GSTT}}$6.1	Diq_L	−44.86	a	−7.41	a	24.67	a	−41.25	b
pt$^{At\text{GSTT}}$6.1	Diq_H	−51.4	a	−23.46	a	35.16	a	−45	b
pt$^{At\text{GSTT}}$2a	Diq_L	−49.84	b	23.73	a	−0.28	a	−43.04	b
pt$^{At\text{GSTT}}$2a	Diq_H	−30.11	a	62.71	a	8.52	a	−49.37	b
pt$^{\text{EFD6}-115\text{A}}$	Diq_L	−71.95	b	−28.23	a	−18.87	ab	−48.75	b
pt$^{\text{EFD6}-115\text{A}}$	Diq_H	−67.53	b	−29.41	a	−24.49	b	−51.25	b
WT	Diq_L	−46.99	b	−7.55	a	−15.65	b	−44.44	b
WT	Diq_H	−53.72	b	−21.69	a	−9.34	ab	−41.97	b

Data are the % change of the mean. Different letters indicate significant differences between treatments with the control for each genotype at $p < 0.05$.

in both salinity concentrations compared to the stress-free plants, however showed statistically significant increase in root length at low NaCl concentration (**Table S3** and **Table S4**). Root length and maximum quantum efficiency of PSII were only reduced under the 300 mM NaCl concentration in all transplastomic lines and WT plants (**Table 3**). Wild-type plants showed the lowest chlorophyll content in both low and high NaCl concentrations compared to the transplastomic lines, although not significantly different. Relative chlorophyll content was maintained in 300 mM NaCl concentration in the transplastomic line pt$^{\text{EFD6}-115\text{A}}$, and it was reduced in all other genotypes including the WT compared to 150 mM NaCl concentration (**Figure 1**). Overall, the transplastomic line pt$^{At\text{GSTT}}$2a demonstrated tolerance to both salt concentrations and especially at 150 mM NaCl as indicated by non-significant decrease in shoot length.

Tolerance of Transplastomic Lines Under *in vitro* Mannitol Stress

Overexpression of the theta class *At*GSTT in chloroplasts increased PS II functionality in both mannitol concentrations (100 and 200 mM) compared to the stress-free plants and relative to pt$^{\text{EFD6}-115\text{A}}$ and WT plants, which only increased the *Fv*/*Fm* at low mannitol stress and reduced their quantum yield under high osmotic stress (**Table 4** and **Table S5**). Additionally, the pt$^{At\text{GSTT}}$ lines showed increased chlorophyll content in 200 mM mannitol compared to pt$^{\text{EFD6}-115\text{A}}$ and WT plants, which maintained their relative chlorophyll content in similar levels to the control plants (**Figure 2**). With respect to the effect of mannitol on growth, only pt$^{At\text{GSTT}}$2a increased the shoot and root length in 200 mM mannitol, yet not significantly, in comparison to the stress-free plants, whilst the other transplastomic lines and the WT plants reduced the shoot length in high mannitol treatment. All transcriptomic lines reduced their M_F in the high mannitol stress, yet this reduction was less severe compared to the WT plants. Interestingly, in low mannitol stress only line pt$^{At\text{GSTT}}$6.1 showed a non-significant reduction in the M_F and increased the shoot length and *Fv*/*Fm*, compared to the stress-free plants and the other transplastomic lines and WT plants (**Table 4** and **Table S5**).

Effect of GST Overexpression to the Transcriptome in Control and High Mannitol Stress

Based on the results the overexpression of the *At*GSTT in the transplastomic 2a line resulted in enhanced tolerance to both salinity concentrations and osmotic stress (200 mM mannitol), along with tolerance to herbicide induced oxidative stress based on the increase in M_D and relative chlorophyll content. Taking into consideration the osmotic component of salinity, we have selected this line for further investigation of the changes occurred in transcriptome and metabolome level under osmotic stress as it looked to be the most promising one for acquired stress tolerance to investigate the whole transcriptome and metabolome response of this line in order to understand in a systemic way the response of the transplastomic line.

The transcriptome data were analyzed with RNA-Seq technology based on which, we performed the analysis of variance. The differential expression gene was selected according to the standard of $P < 0.05$ and the false discovery rate (FDR) was set to 0.001 to determine the threshold of the *P*-value for multiple tests. The absolute value of $|\log_2 \text{Ratio}| \geq 1$ was used to determine the difference between the gene expression transcription group and the database. Gene function, annotation, and classification were researched by GO analysis (**Figures 3A,B**). The RNA analysis through next generation sequencing of the entire transcriptome of the pt$^{At\text{GSTT}}$2a and WT plants under control conditions and under high mannitol (osmotic stress) was studied (each sample in duplicate). The comparison between the two samples in each group showed that the expression profile was similar, thus allowing their combination and their analysis. The analysis generated 47.105 million clean reads in total with a Q20 (%) 98.38%. The reads generated a total of 80.623 transcripts of which 51.879 are known genes and 28.744 are unknown genes. On average 93.55% reads are mapped, and the uniformity of the mapping result for each sample suggests that the samples are comparable. Analysis of differentially expressed genes (DEGs) (**Table S6**) between the transplastomic plants under control conditions (group 1) and WT under control conditions (group 3) showed that there are 80858 commonly expressed DEGs while there 4869 unique DEGs expressed in pt$^{At\text{GSTT}}$2a and 3864 in

TABLE 3 | Morphological parameters and maximum quantum yield of PSII (*Fv*/*Fm*) of GST transplastomic lines and WT tobacco plants grown for 20 days in salinity stress (150 and 300 mM NaCl) *in vitro*.

Genotype	Treatment	Shoot length (cm)	HSD	Root length (cm)	HSD	$M_{F\ (g)}$	HSD	*Fv*/*Fm*	HSD
pt^{AtGSTT}6-1	Control	2.13 ± 0.14	a	6.9 ± 0.45	a	2.23 ± 0.38	a	0.82 ± 0.004	a
pt^{AtGSTT}6-1	NaCl_L	1.68 ± 0.30	a	6.71 ± 0.67	a	1.47 ± 0.29	ab	0.83 ± 0.001	a
pt^{AtGSTT}6-1	NaCl_H	0.82 ± 0.10	b	2.41 ± 0.13	b	0.63 ± 0.1	b	0.78 ± 0.008	b
pt^{AtGSTT}2a	Control	3.23 ± 0.97	a	8.2 ± 0.97	a	2.6 ± 0.81	a	0.82 ± 0.003	a
pt^{AtGSTT}2a	NaCl_L	2.72 ± 0.44	a	6.9 ± 0.42	a	1.57 ± 0.22	ab	0.81 ± 0.002	a
pt^{AtGSTT}2a	NaCl_H	1.85 ± 0.28	a	2.26 ± 0.34	b	0.7 ± 0.12	b	0.78 ± 0.007	b
pt$^{EFD6-115A}$	Control	3.4 ± 1.12	a	6.83 ± 0.59	a	2.51 ± 0.16	a	0.82 ± 0.012	ab
pt$^{EFD6-115A}$	NaCl_L	1.5 ± 0.126	b	7.38 ± 0.62	a	1.6 ± 0.15	b	0.83 ± 0.001	a
pt$^{EFD6-115A}$	NaCl_H	1.12 ± 0.19	b	2.78 ± 0.39	b	0.82 ± 0.21	c	0.78 ± 0.012	b
WT	Control	2.93 ± 0.29	a	7.26 ± 0.27	a	1.72 ± 0.12	a	0.82 ± 0.002	a
WT	NaCl_L	2.05 ± 0.22	b	6.78 ± 0.2	a	1.36 ± 0.1	a	0.83 ± 0.003	a
WT	NaCl_H	1.38 ± 0.15	b	1.86 ± 0.18	b	0.47 ± 0.05	b	0.76 ± 0.02	b

Data (cm and g) are the mean ± SE (morphological data- control: n = 3 and treatments: n = 4; Fv/Fm: n = 6). Different letters indicate significant differences between treatments with the control for each genotype at p < 0.05.

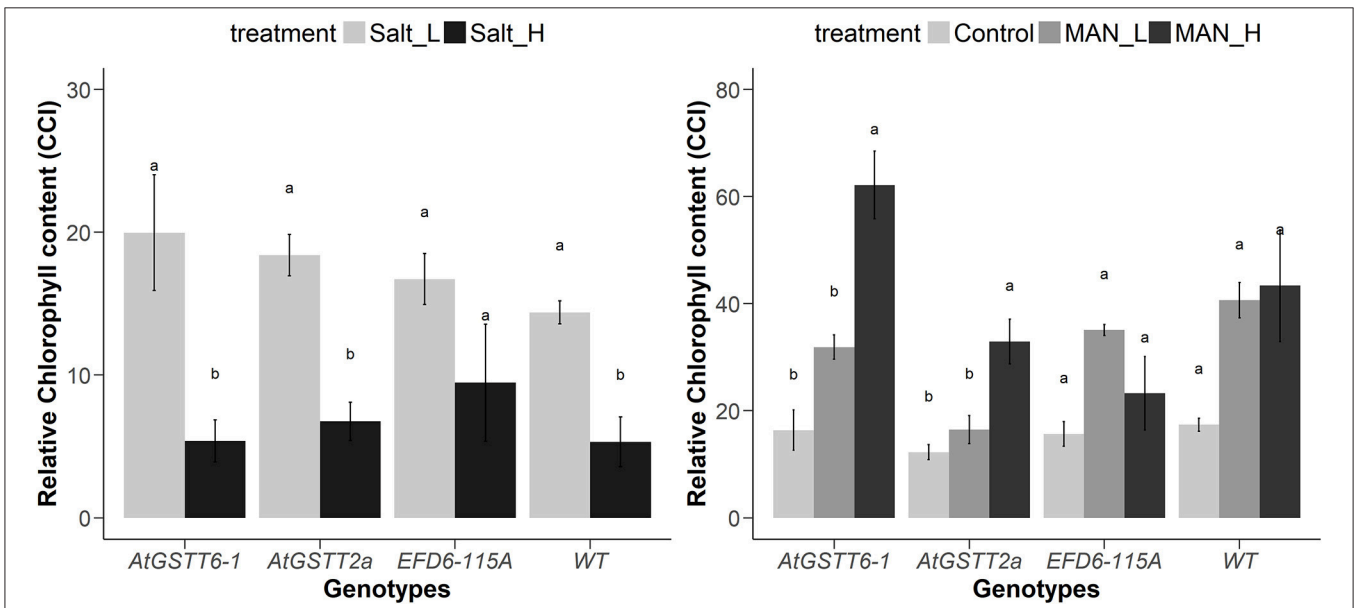

FIGURE 1 | Changes in the relative chlorophyll content in pt^{AtGSTT} (6-1 and 2a) and pt$^{EFD6-115A}$ transplastomic lines, and WT plants growing under salinity (**left panel**) and drought (**right panel**) for 20 and 35 days, respectively. Different letters indicate significant differences between treatments for each genotype at $P < 0.05$ ($n = 3$ for control treatment and $n = 6$ for stress treatments).

WT (**Figure 4A**). Furthermore, when we applied the mannitol (osmotic stress simulating drought) we found 82765 commonly expressed DEGs, 4181 in pt^{AtGSTT}2a plants, and 3337 in WT plants, thus there is a difference of 1907 more common DEGs, 688 fewer DEGs in pt^{AtGSTT}2a plants, and 527 fewer DEGs in WT plants under stress showing a reduction in differentially expressed genes both in WT and pt^{AtGSTT}2a plants (**Figure 4B**).

Regarding the differentially expressed genes, between pt^{AtGSTT}2a and WT in control conditions (groups 1 and 3), we depicted 431 DEGs that were upregulated and 1500 downregulated (**Figure 5A**). Moreover, it is important to mention that between pt^{AtGSTT}2a and WT in high mannitol (200 mM) stress (groups 2 and 4), which are the samples under high mannitol stress only 264 were upregulated and 80 were downregulated (**Figure 5B**; **Table S6**).

Analysis of pt^{AtGSTT}2a overexpressing line and WT plants before the application of the high mannitol (osmotic stress) showed that genes like alanine transaminase and glutamate decarboxylase both implicated in alanine metabolism and biosynthesis were upregulated in pt^{AtGSTT}2a under control conditions. Additionally, 2,3-bisphosphoglycerate-dependent, phosphoglycerate mutase, glycine hydroxymethyl transferase

TABLE 4 | Morphological traits and maximum quantum yield of PSII (*Fv/Fm*) of transplastomic lines and WT tobacco plants grown for 35 days in osmotic stress (100 and 200 mM mannitol stress).

Genotype	Treatment	Shoot length (cm)	HSD	Root length (cm)	HSD	$M_{F\ (g)}$	HSD	*Fv/Fm*	HSD
pt$^{At\text{GSTT}}$6-1	Control	2.33 ± 0.03	ab	7.96 ± 0.56	a	2.7 ± 0.73	a	0.77 ± 0.01	b
pt$^{At\text{GSTT}}$6-1	Man_L	2.73 ± 0.19	a	7.18 ± 0.36	a	2.15 ± 0.08	a	0.83 ± 0.001	a
pt$^{At\text{GSTT}}$6-1	Man_H	2 ± 0.12	b	6.68 ± 0.31	a	0.96 ± 0.12	b	0.81 ± 0.005	a
pt$^{At\text{GSTT}}$2a	Control	2.9 ± 0.36	a	7.2 ± 0.47	a	4.06 ± 0.57	a	0.79 ± 0.002	a
pt$^{At\text{GSTT}}$2a	Man_L	0.52 ± 0.12	b	1.8 ± 0.55	b	0.56 ± 0.11	b	0.79 ± 0.005	a
pt$^{At\text{GSTT}}$2a	Man_H	3.38 ± 0.46	a	8.85 ± 1.27	a	1.18 ± 0.14	b	0.75 ± 0.05	a
pt$^{\text{EFD6}-115\text{A}}$	Control	6.1 ± 0.17	a	7.03 ± 0.37	a	4.63 ± 0.74	a	0.793 ± 0.001	b
pt$^{\text{EFD6}-115\text{A}}$	Man_L	2.9 ± 0.29	b	6.63 ± 1.19	a	1.68 ± 0.11	b	0.823 ± 0.002	a
pt$^{\text{EFD6}-115\text{A}}$	Man_H	2.23 ± 0.09	b	6.95 ± 0.39	a	1.11 ± 0.09	b	0.805 ± 0.008	b
WT	Control	5 ± 0.35	a	6.96 ± 0.43	a	5.11 ± 0.66	a	0.81 ± 0.002	ab
WT	Man_L	2.33 ± 0.18	b	7.13 ± 0.42	a	2.5 ± 0.22	b	0.82 ± 0.001	a
WT	Man_H	2.32 ± 0.1	b	7.51 ± 0.3	a	1.44 ± 0.13	c	0.79 ± 0.01	b

Data are the mean ± SE (morphological data- control: n = 3 and treatments: n = 4; Fv/Fm: n = 6). Different letters indicate significant differences between treatments with the control for each genotype at p < 0.05.

were also upregulated whilst phosphoserine phosphatase was downregulated in the pathway of Glycine, serine, and threonine metabolism. Thus, high glycine content should be expected in pt$^{At\text{GSTT}}$2a plants under control conditions.

Histone-lysine N-methyltransferase ASH1L, was down regulated in pt$^{At\text{GSTT}}$2a plants whereas in histidine metabolism genes responsible for phosphoribosyl-ATP pyrophosphohydrolase, phosphoribosyl-AMP cyclohydrolase, histidinol dehydrogenase, and histidine decarboxylase were upregulated, suggesting that histidine should be accumulated in the pt$^{At\text{GSTT}}$2a plants. Glutamate decarboxylase implicated in the Alanine, aspartate and glutamate metabolism and taurine and hypotaurine metabolism was upregulated in the transplastomic lines. Furthermore, glutathione S-transferases were found to be overexpressed (BGI_novel_G036737 K00799: BGI_novel_G036737 (-2.6), BGI_novel_G008526 (-2.3), BGI_novel_G023189 (-2.3).

An important metabolic pathway related to stress tolerance is starch and sucrose metabolism where trehalose 6-phosphate synthase was downregulated in pt$^{At\text{GSTT}}$2a line under control conditions suggesting that plants were in a state of stress-priming. Transplastomic line pt$^{At\text{GSTT}}$2a upregulated inositol polyphosphate 5-phosphatase and inositol-pentakis phosphate 2-kinase in the Inositol phosphate metabolism and Phosphatidylinositol signaling system. Alanine transaminase involved in Alanine, aspartate, and glutamate metabolism was upregulated, whilst glycine hydroxyl methyltransferase and phosphoserine phosphatase were found to be downregulated in the biosynthesis of amino acids pathway.

In the comparison of pt$^{At\text{GSTT}}$2a vs. WT plants under the high mannitol stress the number of transcripts for pt$^{At\text{GSTT}}$2a and WT plants was similar to those in control conditions; however, there were only 264 DEGs upregulated and 80 downregulated compared with 431 and 1500, respectively, in control conditions (**Table S6**). Important genes found with altered expression are glycerate dehydrogenase and hydroxypyruvate reductase upregulated in Glycine, serine and threonine metabolism as well as in DNA repair pathway, which is expected as stress produces ROS, to also affect nucleic acids. Additionally, the gene responsible for spermidine synthase implicated in glutathione metabolism, cysteine, and methionine metabolism and in arginine and proline metabolism was downregulated along with pectinesterase, an important gene implicated in Pentose and glucuronate interconversions as well as in cell wall degradation, in pt$^{At\text{GSTT}}$2a compared to WT plants under stress. In the Phenylalanine, tyrosine and tryptophan biosynthesis pathway, the genes encoding bifunctional anthranilate synthase/indole-3-glycerol-phosphate synthase (G005943) related to tryptophane biosynthesis were upregulated as was the 5-methyltetrahydrofolate-homocysteine methyltransferase (G005943), leading to methionine.

Effect of GST Overexpression in the Chloroplast to the Metabolome in High Mannitol Stress

The response of transplastomic line pt$^{At\text{GSTT}}$2a and the WT plants was investigated further through the induced metabolic alterations. A total of 51 polar metabolites were identified (**Figure 6**; **Table S1**), of which 11 were soluble sugars, 5 soluble alcohols, 9 organic acids, 21 amino acids, and 5 other compounds (**Figure 6**; **Tables S1, S2**). The differences between the transplastomic line and WT plants under stress-free and high mannitol stress, revealed that ∼78, 66.6, and 90% of the metabolic changes occurred due to treatment, genotypic, and treatment x genotype interaction effects, respectively.

In stress-free conditions, the overexpression of the *At*GSTT had a significant effect to the metabolic profile of transplastomic plants as indicated by the 27 out of 51 metabolites being significantly altered from the WT plants, 26 of which were down-regulated and only the benzoic acid was up-regulated (27.6-fold) (**Table 5**). The downregulated metabolites were mostly amino acids (13), such as proline, oxoproline, and valine, organic acids (5), such as citric, quinic, and threonic acids, soluble sugars (5),

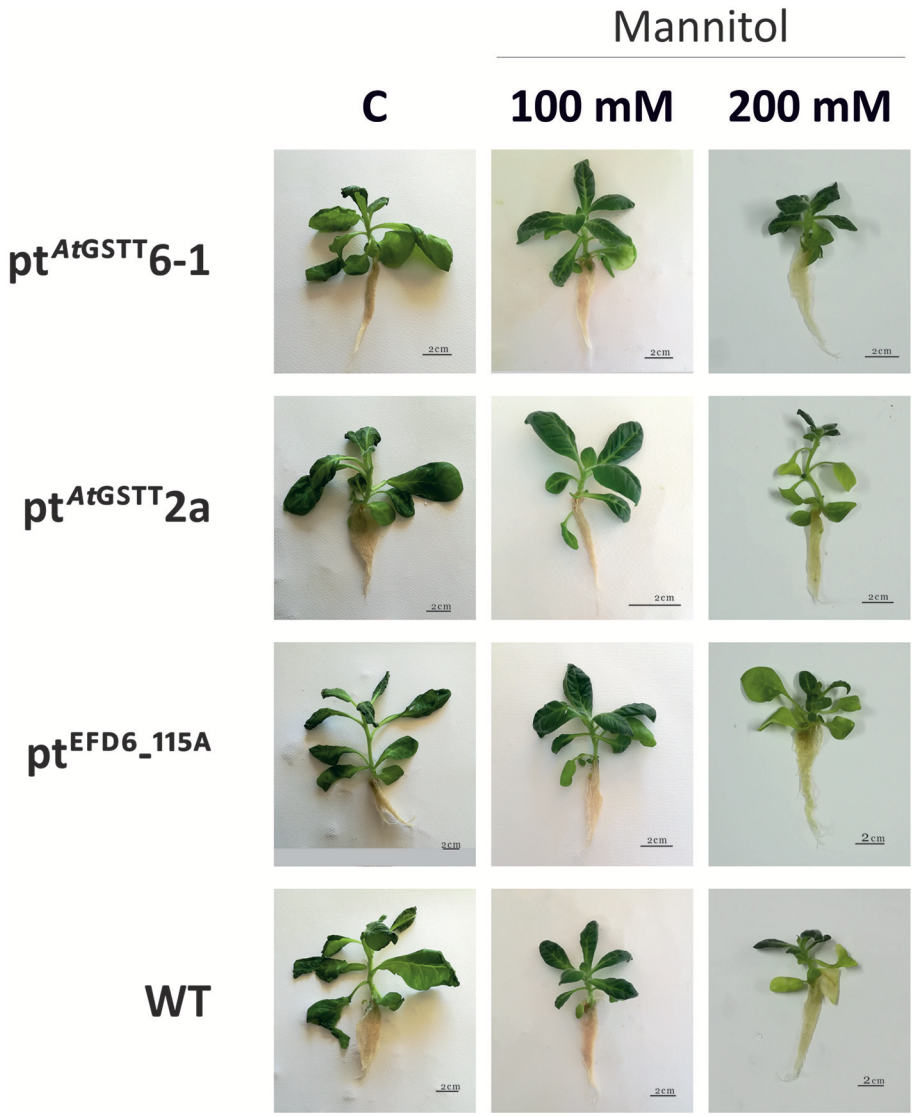

FIGURE 2 | Effect of mannitol (100 and 200 mM) stress on growth of transplastomic lines and WT tobacco plants after 35 days in mannitol and stress-free (C) conditions.

such as sucrose, fructose, and glucose and the soluble alcohols, erythritol, myo-inositol and glycerol. In contrast, the effect of high mannitol stress on plants overexpressing the GST chimera was moderate as only 16 metabolites were significantly changed. More specifically, plants overexpressing the GST chimera up-regulated only the soluble sugars threose (9.5-fold) and arabinose (0.82-fold), whilst, 14 metabolites were downregulated compared to the WT plants (**Table 5**). These results indicate that pt$^{At\text{GSTT}}$2a transplastomic line was osmotolerant and able to maintain cellular homeostasis in comparison to the WT plants that required more energy to tolerate high mannitol stress.

The pt$^{At\text{GSTT}}$2a line under high mannitol stress significantly altered more metabolites (38) compared to the 34 metabolites of the WT plants (**Figures 7**, **8**; **Table S7**). The pt$^{At\text{GSTT}}$2a line upregulated six metabolites of which four were common. In the increased metabolites two were soluble sugars, such as arabinose, which was unique for the transplastomic line, two were soluble alcohols, such as mannitol, and quinic acid (**Figure 7**). Erythrose and sorbitol were accumulated in greater concentrations in the WT plants than in the transplastomic line under high mannitol compared to control conditions (**Table S7**). Interestingly, the compatible solute mannitol was accumulated in greater concentration in the pt$^{At\text{GSTT}}$2a by 6.84-fold compared to the 4.73-fold increase in the WT plants.

The WT plants down-regulated 31 metabolites compared to the 28 of the pt$^{At\text{GSTT}}$2a plants. Among the metabolites that were decreased, 24 were common (6 soluble sugars, 12 amino acids, and 2 organic acids), such as the TCA cycle intermediate citric acid and the precursor of various amino acids aspartic acid (**Figure 8**; **Table S7**). Additionally, the WT plants had more

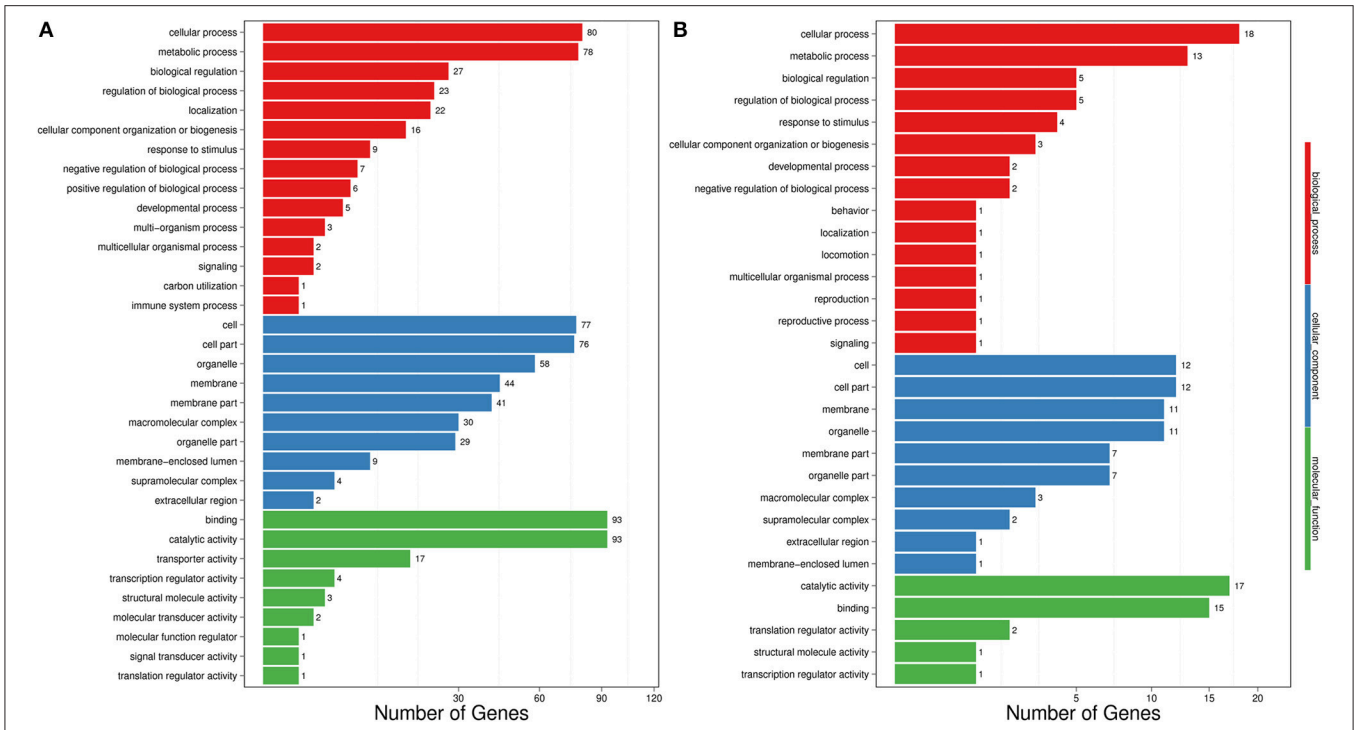

FIGURE 3 | Histogram representation of Gene Ontology classification. **(A)** control conditions **(B)** under high mannitol stress (200 mM).

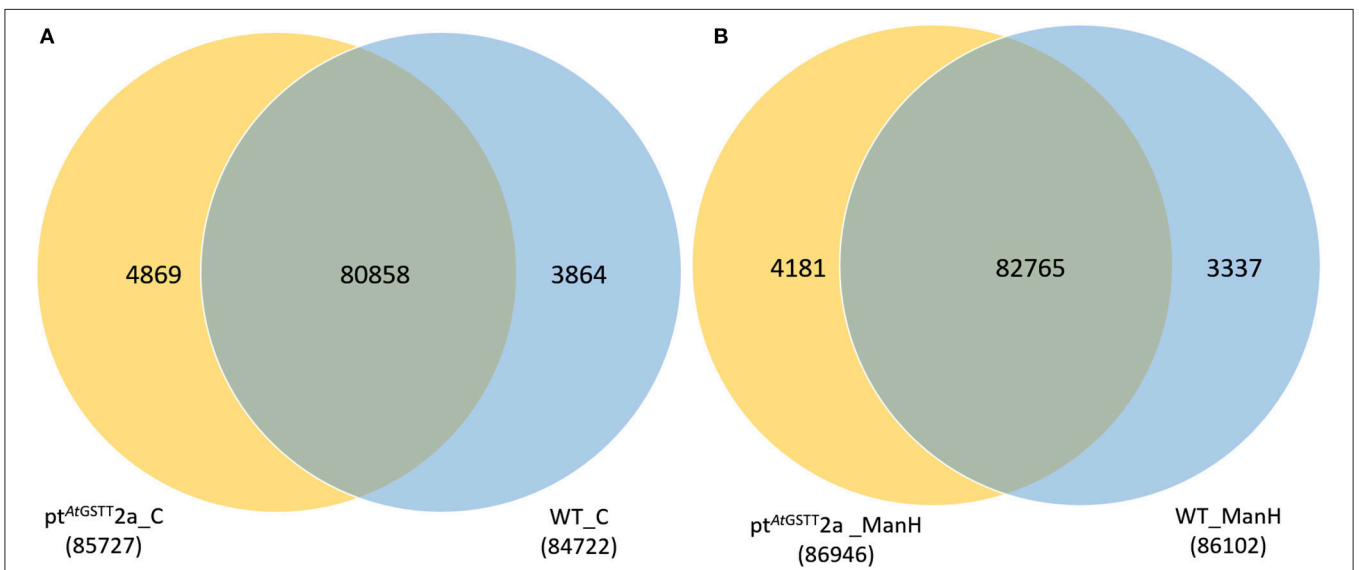

FIGURE 4 | Venn diagram of differentially expressed genes. Comparison among **(A)** pt^{AtGSTT}2a and WT in control conditions (groups 1 and 3) and **(B)** pt^{AtGSTT}2a and WT in high mannitol (200 mM) stress (groups 2 and 4).

differentially decreased metabolites compared to the pt^{AtGSTT}2a plants (**Figure 8**).

DISCUSSION

The adaptation response mechanisms of plants to adverse abiotic stresses result in the up-regulation of the reactive oxygen species (ROS) detoxification network, to mitigate the negative effects of oxidative stress, commonly induced under such conditions (Gill and Tuteja, 2010; Nianiou-Obeidat et al., 2017). Enhancing the ROS scavenging capacity in plants by direct gene expression in the chloroplast, an active cell compartment could in theory increase the photosynthetic rate and thus increase in yield, yet this is only a speculation that needs thorough investigation,

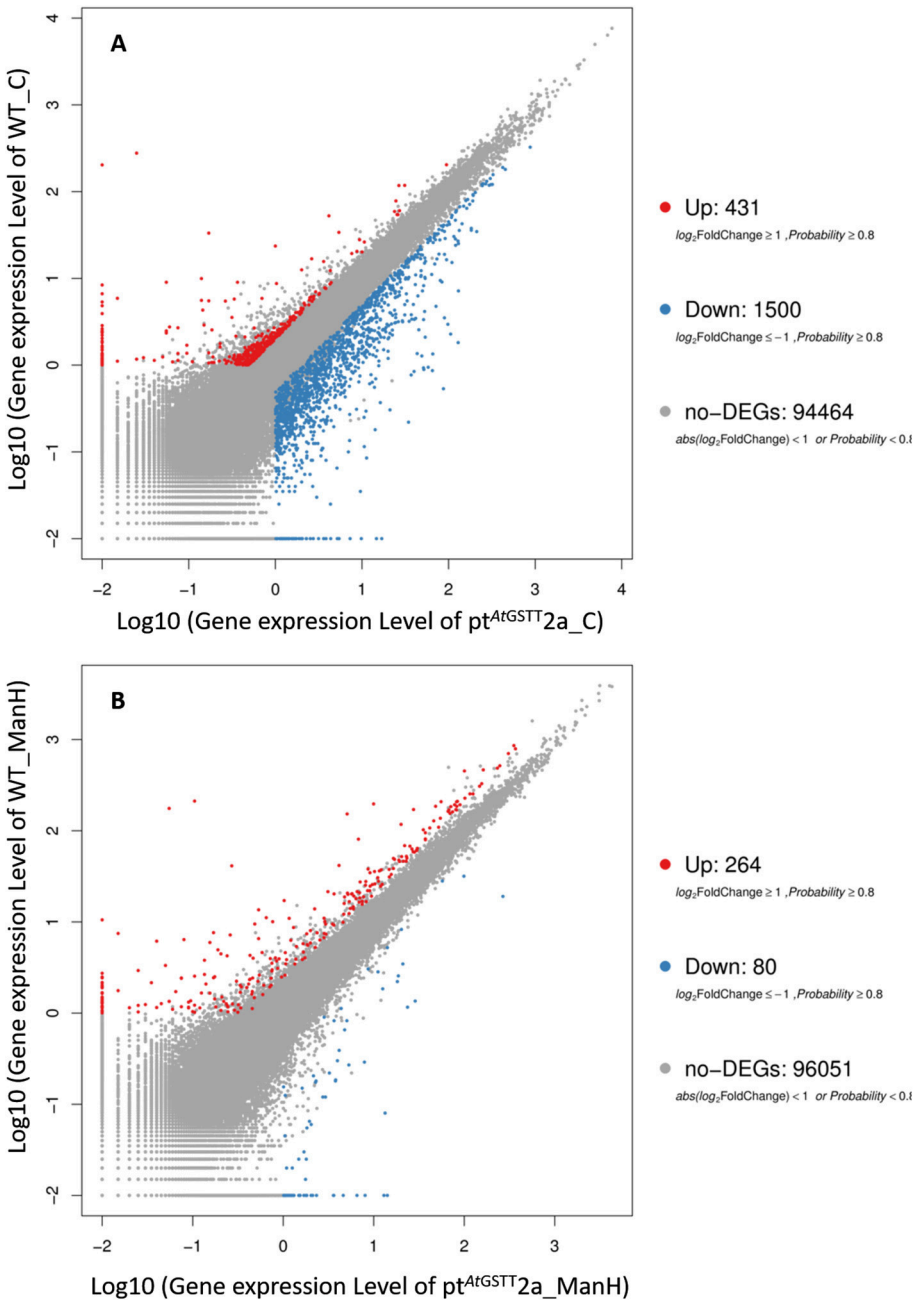

FIGURE 5 | Scatter plot of differentially expressed genes in **(A)** pt^{AtGSTT}2a and WT in control conditions (groups 1 and 3), and **(B)** pt^{AtGSTT}2a and WT in high mannitol (200 mM) stress (groups 2 and 4).

which is beyond the scope of this research. The functional role of tobacco lines overexpressing the *At*GSTT in chloroplasts has been previously characterized (Dixon et al., 2008), yet, the roles of this *At*GSTT in plant homeostasis and response mechanisms both under abiotic and herbicide-induced oxidative stresses, and non-stress conditions are still required to be unraveled. Targeting the chloroplasts, we have assessed the osmotic, ionic, and oxidative potential of the pt^{AtGSTT} lines and the *Zm*GSTU1-*Zm*GSTU2 chimera overexpressing line in comparison to WT plants. Our work shows that pt^{AtGSTT} lines were tolerant to herbicide-induced oxidative and salinity stresses and showed enhanced response tolerance to mannitol-induced osmotic stress compared to WT plants.

The mode of bipyridiniums action is within the chloroplast by diverting electrons from photosystem I (PSI) of photosynthesis to form the Diquat radical, which in turn generates a highly destructive superoxide radical (Devine et al., 1992; Hawkes, 2014). Despite the observed reduction in maximum

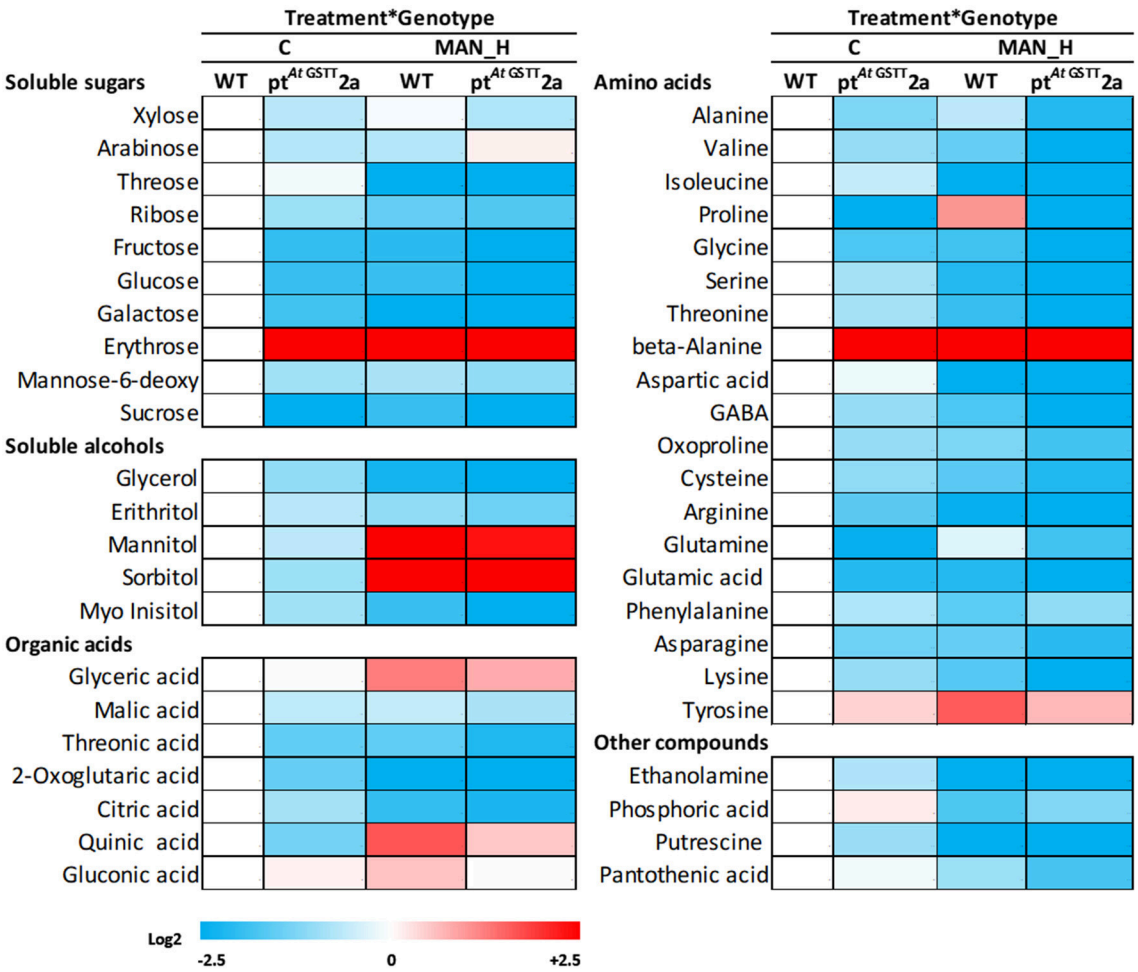

FIGURE 6 | Heat map of primary metabolites of pt$^{At\text{GSTT}}$2a and WT plants under high mannitol (200 mM) stress compared to WT control plants. Increase is indicated as red and decrease as blue (see color scale). Mean values of 3 independent determinations for each treatment were expressed as relative abundance compared to internal standard adonitol and are reported relative to the respective M_F. Actual data are provided in **Table S1**.

quantum yield of PSII, the transplastomic lines pt$^{At\text{GSTT}}$ showed differential response mechanism in the accumulation of relative chlorophyll content in both half- and recommended field dose of Diquat, possibly to alleviate the negative effect of oxidative damage on PSII, which was apparent under all levels of Diquat in WT plants. It has been observed that transplastomic tobacco plants expressing simultaneously DHAR:GR and GST:GR showed enhanced tolerance to paraquat induced oxidative stresses while expression of either single transgene did not (Le Martret et al., 2011). Transplastomic overexpression of glutathione peroxidase (GP) in tobacco plants has shown to confer moderate tolerance to paraquat (Yoshimura et al., 2004), whereas, transplastomic tobacco lines overexpressing an *Escherichia coli* glutathione reductase (*gor*) gene have not enhanced protection from paraquat induced photooxidative stress (Poage et al., 2011). In the present study pt$^{At\text{GSTT}}$ lines also had enhanced turgor maintenance in contrast to WT plants, which showed extensive dehydration, since Diquat is a rapid desiccant (Cronshey, 1961; Hawkes, 2014).

At 150 mM of NaCl concentration, both pt$^{At\text{GSTT}}$ transplastomic lines showed enhanced growth (shoot length and M_F) and pt$^{At\text{GSTT}}$2a moderate tolerance to high salinity stress (300 mM NaCl) by maintaining the shoot length compared to WT plants. Additionally, under both NaCl concentrations, all transplastomic lines demonstrated a higher relative chlorophyll content compared to the WT plants. Similar results were observed in transplastomic tobacco plants overexpressing a choline monooxygenase (*Bv*CMO) from beetroot which increased photosynthetic rate and apparent quantum yield of photosynthesis in the presence of 150 mM NaCl when compared to WT, and the maximal efficiency of PSII photochemistry in both wild type and transplastomic plants was not affected (Zhang et al., 2008). This is also consistent with our results indicating that the overexpression of the *At*GSTT and the *ZmGSTU1-ZmGSTU2* chimera can protect PSII reaction centers

TABLE 5 | Metabolites that were significantly ($p < 0.05$) altered in pt^{AtGSTT}2a and WT plants under high mannitol (200 mM) and control conditions.

pt^{AtGSTT}2a C/ WT C		pt^{AtGSTT}2a MAN_H/ WT MAN_H	
Metabolites	**Fold-change**	**Metabolites**	**Fold-change**
Benzoic acid	27.6	Threose	9.5
Erithritol	−0.37	Arabinose	0.82
Xylose	−0.37	Serine	−0.31
Citric acid	−0.45	Putrescine	−0.46
Threonine	−0.45	Quinic acid	−0.54
Serine	−0.45	Glucose	−0.56
Myo-inositol	−0.46	Valine	−0.56
Putrescine	−0.49	Fructose	−0.57
Oxoproline	−0.5	Glycine	−0.65
Lysine	−0.5	Glutamine	−0.66
Valine	−0.51	Galactose	−0.68
Glycerol	−0.51	Sorbitol	−0.69
Cysteine	−0.53	Sucrose	−0.75
Alanine	−0.57	Proline	−0.94
Quinic acid	−0.61	Glycerol	−0.99
Asparagine	−0.62	Lysine	−1
Citruline	−0.64		
2-Isopropylmalic acid	−0.64		
2-Oxoglutaric acid	−0.64		
Threonic acid	−0.65		
Arginine	−0.67		
Glycine	−0.69		
Galactose	−0.72		
Glucose	−0.74		
Fructose	−0.75		
Sucrose	−0.82		
Proline	−0.85		

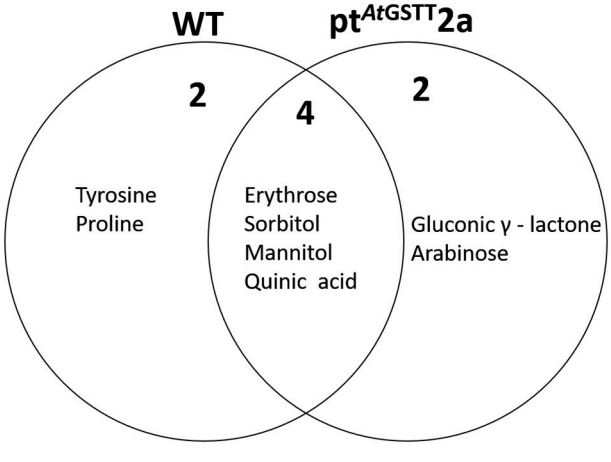

FIGURE 7 | Venn diagram representation of metabolites commonly or differentially increased in the leaves of WT and pt^{AtGSTT}2a tobacco plants under high mannitol (200 mM) compared to non-stressed plants.

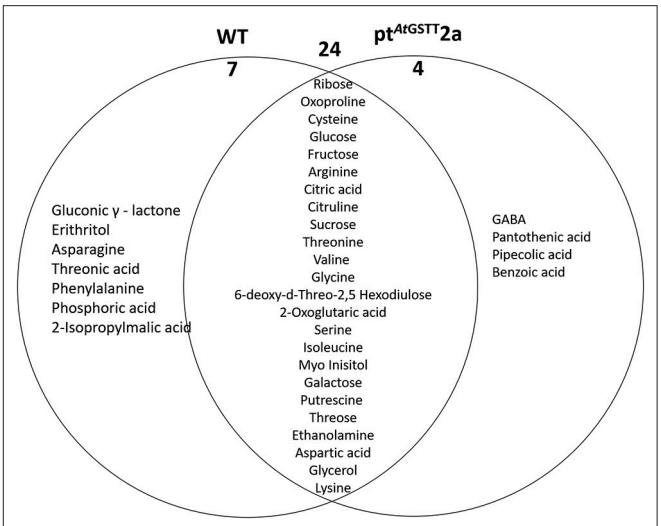

FIGURE 8 | Venn diagram representation of metabolites commonly or differentially decreased in the leaves of WT and pt^{AtGSTT}2a tobacco plants under high mannitol (200 mM) compared to non-stressed plants.

from damage. Transplastomic carrot plants expressing the *badh* gene demonstrated enhanced tolerance up to up to 400 mM NaCl compared to untransformed plants exhibiting severe growth inhibition at 200 mM NaCl (Kumar et al., 2004).

Herein, the pt^{AtGSTT} transplastomic lines pt^{AtGSTT}2a and especially pt^{AtGSTT}6-1 demonstrated enhanced photo-tolerance when exposed to 200 mM mannitol stress demonstrating increased relative chlorophyll content and maximum yield of PSII compared to WT plants. Increasing or maintaining the chlorophyll content in transgenic chloroplasts suggests the integrity of thylakoid membranes, even in the presence of high concentrations of NaCl and mannitol, demonstrating the advantage of overexpressing the *At*GSTT in the chloroplasts. Similar results were observed by Lee et al. (2003).

The transcriptomics analysis of pt^{AtGSTT}2a line and WT plants under control and high mannitol stress suggests that plants of the pt^{AtGSTT}2a overexpressing line, before the application of the high mannitol (osmotic stress) upregulated genes related to stress tolerance such as genes encoding for alanine transaminase and glutamate decarboxylase both implicated in alanine metabolism and biosynthesis. Alanine was found to be the main amino acid accumulated in *Medicago truncatula* seedlings under hypoxic stress (Limami et al., 2008). Furthermore, genes encoding for 2,3-bisphosphoglycerate-dependent phosphoglycerate mutase and glycine hydroxymethyl transferase were also upregulated, while phosphoserine phosphatase was downregulated in glycine, serine and threonine metabolism, which may lead to increased glycine. Therefore, high glycine content should be expected in pt^{AtGSTT}2a plants under control conditions but considering that high glycine content is correlated with stress tolerance and especially drought resistance (Thankur and Rai, 1982), the pt^{AtGSTT}2a line is probably in a stress primed state before the application of the stress. . Also, glutamate decarboxylase is upregulated which is implicated in Alanine, aspartate and glutamate metabolism and in taurine and hypotaurine metabolism and was also confirmed in metabolomics analysis. Interestingly, in the resurrection plant *Sporobolus stapfianus* Martinelli et al. (2007) reported that the accumulation of asparagine and glutamate might have

led to its conversion to arginine and asparagine, as all of the above are considered to play important role in plant protection against drought stress (Martinelli et al., 2007). Moreover, we found that the histone-lysine N-methyltransferase ASH1L, was down regulated in pt$^{At\text{GSTT}}$2a plants in histidine metabolism whereas, genes responsible for histidine metabolism like phosphoribosyl-ATP pyrophosphohydrolase phosphoribosyl-AMP cyclohydrolase, histidinol dehydrogenase and histidine decarboxylase were upregulated, suggesting that histidine should be accumulated in the pt$^{At\text{GSTT}}$2a plants prior to the application of stress, which reinforces the notion that the transplastomic plants are in a primed condition as before (Tran et al., 2007; Witt et al., 2012). Similarly, trehalose 6-phosphate synthase was found to be downregulated in pt$^{At\text{GSTT}}$2a line under control conditions highlighting the stress primed condition of the transplastomic line (Lee et al., 2003; Ilhan et al., 2015).

When the transplastomic line pt$^{At\text{GSTT}}$2a and WT plants were exposed to osmotic stress (high mannitol), the number of transcripts for pt$^{At\text{GSTT}}$2a and WT plants did not change compared to those in control conditions. However, important genes found with an altered expression such as those encoding for glycerate dehydrogenase and hydroxypyruvate reductase which were found to be upregulated in glycine, serine and threonine metabolism as well as in DNA repair pathway, which, as stress produces ROS is expected to affect nucleic acids. In contrast, the gene responsible for spermidine synthase implicated in glutathione metabolism, cysteine and methionine metabolism and in arginine, and proline metabolism was down regulated. Proline is important in stress tolerance and has been found to increase during different environmental stresses like salinity, drought, UV, and extreme temperatures (Ashraf and Foolad, 2007). In addition, polyamines like spermidine have been reported to play a role in inducing stress response under various stresses that produce ROS as they might serve as ROS scavengers, and as positive regulators for expression of stress response genes. Thus, polyamines like spermidine could perform as primal stress molecules in plants (Rhee et al., 2007). Additionally, pectinesterase was found to be downregulated in pt$^{At\text{GSTT}}$2a compared to WT plants under stress. This is an important gene implicated in pentose and glucuronate interconversions as well as in cell wall degradation as it was found to be upregulated in plants exposed to permissive high temperature conditions (37°C). This parallels to acclimation in order to acquire thermotolerance as a result of the cell wall modification (Yang et al., 2006). However, the downregulation of such enzymes in the pt$^{At\text{GSTT}}$2a line under mannitol stress suggests that these plants might be in a state of acclimation prior to the application of the stress. In the Phenylalanine, tyrosine and tryptophan biosynthesis pathway the genes encoding bifunctional anthranilate synthase/indole-3-glycerol-phosphate synthase (G005943) related to tryptophane biosynthesis were upregulated as was the 5-methyltetrahydrofolate-homocysteine methyltransferase (G005943), leading to methionine. In a rat model, actin oxidative damage by ROS was found to occur through the oxidation of cysteine, tryptophan and methionine (Fedorova et al., 2010). If this is also the case in plants, then increased amounts of these amino acids might be needed and thus, leading to the upregulation of the genes responsible for their production, as it was found herein; however, this hypothesis needs further investigation.

The metabolomics analysis was performed on transplastomic and WT plants grown under high mannitol stress and controlled conditions *in vitro* for 35 days. The overexpression of the *At*GSTT had a significant effect to the metabolic profile of transplastomic plants, since many metabolites were downregulated under both control and drought conditions indicating limited perturbation of metabolic homeostasis in the transplastomic lines. Especially under high mannitol stress the pt$^{At\text{GSTT}}$2a line had higher concentrations of the soluble sugars, threose and arabinose, which demonstrates the protective role against osmotic stress (Keunen et al., 2013). The soluble alcohol mannitol was accumulated in greater concentration in pt$^{At\text{GSTT}}$2a line despite the common increase in WT plants under high mannitol stress. In contrast to our results mannitol accumulation was decreased in transgenic tobacco plants overexpressing a *Gmgstu4* gene under salinity stress (Kissoudis et al., 2015b). Mannitol accumulation plays an important role in osmotic adjustment and signaling molecule enhance tolerance to water stress in various plant species (Slama et al., 2015). Additionally, the greater M_F and shoot length of pt$^{At\text{GSTT}}$2a compared to the WT plants under mannitol stress indicates a possible relation between increase in mannitol and improved growth. Similar results were observed in peanut (Bhauso et al., 2014) and *Zea mays* (Nguyen et al., 2013) plants overexpressing *mtlD* genes, which conferred water-deficit stress tolerance by inducing the accumulation of mannitol and increase in biomass and relative water content under drought conditions.

The results above suggest that overexpression of the *At*GSTT in the chloroplasts resulted in enhanced photo-tolerance and turgor maintenance under herbicide-induced oxidative (increased M_D and Relative chlorophyll content) and salinity stresses (higher chlorophyll, non-significant decrease in shoot length and M_F compared to the control plants) and enhanced response tolerance to high mannitol-induced osmotic stress (increased shoot and root length). Whole-genome transcriptome analysis revealed that genes related to stress tolerance, such as GSTs, were upregulated in pt$^{At\text{GSTT}}$2a line under both control and high mannitol stress conditions indicating an acclimation state to stress. In parallel, the metabolic profile indicated limited perturbations of the metabolic homeostasis in the transplastomic lines and greater accumulation of mannitol and soluble sugars under high mannitol stress. We have therefore established that the transplastomic plants overexpressing the pt$^{At\text{GSTT}}$2a in the chloroplast are probably in a state of acclimation to stress, thus, when the actual stress is applied there is limited need for overexpression of the whole array of stress tolerance mechanisms, which is imprinted in the levels of relative gene expression. As mentioned before, we found only limited genes to be upregulated in the pt$^{At\text{GSTT}}$2a transplastomic line compared to WT under stress conditions while at the same time we have found genes related to stress tolerance upregulated in pt$^{At\text{GSTT}}$2a plants compared to WT in stress-free conditions, strengthening the hypothesis that the *AtGSTT* overexpressed in plastids might have conferred plant stress tolerance.

Challenges caused by climate change will demand for quick action of the scientific community in order to develop stress tolerant varieties to secure enough food for the increasing world population. GSTs, for have proven to be enzymes involved in stress tolerance (Dixon et al., 1998, 2008, 2011; Axarli et al., 2009, 2017; Chronopoulou and Labrou, 2009; Benekos et al., 2010; Chronopoulou et al., 2011, 2012, 2014; Madesis et al., 2013; Kissoudis et al., 2015a,b; Labrou et al., 2015; Lo Cicero et al., 2015, 2017; Nianiou-Obeidat et al., 2017) might help toward the development of plant acclimation to environmental stresses. In some cases, the overexpression of a single antioxidant enzyme might not provide protection against oxidative stress whilst, simultaneous expression of multiple antioxidant enzymes is more effective than a single expression for enhancing tolerance to environmental stresses (Le Martret et al., 2011). Herein, the *Zm*GSTU1-*Zm*GSTU2 chimera was able to induce photoprotection of the photosystem II under sever salinity stress, yet it was not as tolerant as the single AtGSTTs overexpressed in the chloroplasts. Potentially, the expression of multiple defense genes encoding enzymes belonging to different classes could generate plants with enhanced stress tolerance (Zhao and Zhang, 2006) able to withstand multiple stresses, which needs to be further investigated. This study provides evidence that overexpression of both the theta class *At*GSTT and the unique chimera GSTU1-GSTU2 from *Zea mays* in the chloroplast resulted in enhanced tolerance of the transplastomic plants to abiotic stresses. Furthermore, transcriptomics and metabolomics analysis showed that the GST overexpressing plants were in a stress tolerance priming state even before the application of the severe osmotic stress (high mannitol concentration) thus, enhancing the plant's ability to tolerate abiotic stresses.

AUTHOR CONTRIBUTIONS

ES designed and performed part of the experiments, and the statistical analysis, and wrote the manuscript. SG and AI performed part of the experiments. SK performed part of the experiments. MM performed part of the metabolomics and wrote part of the metabolomics section. EC performed part of the experiments and read the manuscript. RE wrote and edited part of the manuscript. AD wrote and edited the manuscript. NL, IN-O and PM designed the research, wrote and edited the manuscript.

ACKNOWLEDGMENTS

We acknowledge the General Secretariat for Research and Development that financed the work described here under the project Intelligent και Automated systems for enabling the design, simulation and development of integrated processes and products –ODYSSEAS, (MIS) 5002462.

SUPPLEMENTARY MATERIAL

The Supplementary Material for this article can be found online at: https://www.frontiersin.org/articles/10.3389/fpls.2018.01861/full#supplementary-material

REFERENCES

Ahmad, N., Michoux, F., McCarthy, J., and Nixon, P. J. (2012). Expression of the affinity tags, glutathione-S-transferase and maltose-binding protein, in tobacco chloroplasts. *Planta* 235, 863–871. doi: 10.1007/s00425-011-1584-8

Ashraf, M., and Foolad, M. R. (2007). Roles of glycine betaine and proline in improving plant abiotic stress resistance. *Environ. Exp. Bot.* 59, 206–216. doi: 10.1016/j.envexpbot.2005.12.006

Axarli, I., Dhavala, P., Papageorgiou, A. C., and Labrou, N. E. (2009). Crystallographic and functional characterization of the fluorodifen-inducible glutathione transferase from *Glycine max* reveals an active site topography suited for diphenylether herbicides and a novel L-site. *J. Mol. Biol.* 385, 984–1002. doi: 10.1016/j.jmb.2008.10.084

Axarli, I., Muleta, A. W., Chronopoulou, E. G., Papageorgiou, A. C., and Labrou, N. E. (2017). Directed evolution of glutathione transferases towards a selective glutathione-binding site and improved oxidative stability. *Biochim. Biophys. Acta Gen. Subj.* 1861, 3416–3428. doi: 10.1016/j.bbagen.2016.09.004

Benekos, K., Kissoudis, C., Nianiou-Obeidat, I., Labrou, N., Madesis, P., Kalamaki, M., et al. (2010). Overexpression of a specific soybean GmGSTU4 isoenzyme improves diphenyl ether and chloroacetanilide herbicide tolerance of transgenic tobacco plants. *J. Biotechnol.* 150, 195–201. doi: 10.1016/j.jbiotec.2010.07.011

Bhauso, T. D., Radhakrishnan, T., Kumar, A., Mishra, G. P., Dobaria, J. R., Patel, K., et al. (2014). Overexpression of bacterial mtlD gene in peanut improves drought tolerance through accumulation of mannitol. *Sci. World J.* 2014:125967. doi: 10.1155/2014/125967

Bock, R. (2014). Genetic engineering of the chloroplast: novel tools and new applications. *Curr. Opin. Biotechnol.* 26, 7–13. doi: 10.1016/j.copbio.2013.06.004

Buchfink, B., Xie, C., and Huson, D. H. (2014). Fast and sensitive protein alignment using diamond. *Nat. Methods* 12, 59–60. doi: 10.1038/nmeth.3176

Chen, P. J., Senthilkumar, R., Jane, W. N., He, Y., Tian, Z., and Yeh, K. W. (2014). Transplastomic *Nicotiana benthamiana* plants expressing multiple defence genes encoding protease inhibitors and chitinase display broad-spectrum resistance against insects, pathogens and abiotic stresses. *Plant Biotechnol. J.* 12, 503–515. doi: 10.1111/pbi.12157

Chin, H. G., Kim, G.-D., Marin, I., Mersha, F., Evans, T. C., Chen, L., et al. (2003). Protein trans-splicing in transgenic plant chloroplast: reconstruction of herbicide resistance from split genes. *Proc. Natl. Acad. Sci. U.S.A.* 100, 4510–4515. doi: 10.1073/pnas.0736538100

Chronopoulou, E., Axarli, I., Nianiou-obeidat, I., Madesis, P., and Labrou, N. E. (2011). Structure and antioxidant catalytic function of plant glutathione transferases. *Curr. Chem. Biol.* 5, 64–74. doi: 10.2174/187231311793564306

Chronopoulou, E., Madesis, P., Asimakopoulou, B., Platis, D., Tsaftaris, A., and Labrou, N. E. (2012). Catalytic and structural diversity of the fluazifop-inducible glutathione transferases from *Phaseolus vulgaris*. *Planta* 235, 1253–1269. doi: 10.1007/s00425-011-1572-z

Chronopoulou, E., Madesis, P., Tsaftaris, A., and Labrou, N. E. (2014). Cloning and characterization of a biotic-stress-inducible glutathione transferase from *Phaseolus vulgaris*. *Appl. Biochem. Biotechnol.* 172, 595–609. doi: 10.1007/s12010-013-0509-3

Chronopoulou, E. G., and Labrou, N. E. (2009). Glutathione transferases : emerging multidisciplinary tools in red and green biotechnology. *Recent Pat. Biotechnol.* 3, 211–223. doi: 10.2174/187220809789389135

Clarke, J. L., and Daniell, H. (2011). Plastid biotechnology for crop production: present status and future perspectives. *Plant Mol. Biol.* 76, 211–220. doi: 10.1007/s11103-011-9767-z

Cronshey, J. F. H. (1961). A review of experimental work with diquat and related compounds. *Weed Res.* 1, 68–77. doi: 10.1111/j.1365-3180.1961.tb00007.x

Csiszár, J., Horváth, E., Váry, Z., Gallé, Á., Bela, K., Brunner, S., et al. (2014). Glutathione transferase supergene family in tomato: salt stress-regulated expression of representative genes from distinct GST classes in plants primed with salicylic acid. *Plant Physiol. Biochem.* 78, 15–26. doi: 10.1016/j.plaphy.2014.02.010

Czégény, G., Le Martret, B., Pávkovics, D., Dix, P. J., and Hideg, É. (2016). Elevated ROS-scavenging enzymes contribute to acclimation to UV-B exposure in transplastomic tobacco plants, reducing the role of plastid peroxidases. *J. Plant Physiol.* 201, 95–100. doi: 10.1016/j.jplph.2016.05.026

de Mendiburu, F. (2017). *agricolae: Statistical Procedures for Agricultural Research*. R package version 1.2-8. Available online at: https://CRAN.R-project.org/package=agricola

Devine, M., Duke, S. O., and Fedtke, C. (1992). Physiology of herbicide action. *Exp. Agric.* 29:441. doi: 10.1017/S0014479700021281

Dixon, D. P., Cummins, L., Cole, D. J., and Edwards, R. (1998). Glutathione-mediated detoxification systems in plants. *Curr. Opin. Cell Biol.* 1, 258–266.

Dixon, D. P., and Edwards, R. (2010). "Gutathione transferases," in *The Arabidopsis Book American Society of Plant Physiologist*. doi: 10.1199/tab.0131

Dixon, D. P., Hawkins, T., Hussey, P. J., and Edwards, R. (2009). Enzyme activities and subcellular localization of members of the arabidopsis glutathione transferase superfamily. *J. Exp. Bot.* 60, 1207–1218. doi: 10.1093/jxb/ern365

Dixon, D. P., Lapthorn, A., Madesis, P., Mudd, E. A., Day, A., and Edwards, R. (2008). Binding and glutathione conjugation of porphyrinogens by plant glutathione transferases. *J. Biol. Chem.* 283, 20268–20276. doi: 10.1074/jbc.M802026200

Dixon, D. P., McEwen, A. G., Lapthorn, A. J., and Edwards, R. (2003). Forced evolution of a herbicide detoxifying glutathione transferase. *J. Biol. Chem.* 278, 23930–23935. doi: 10.1074/jbc.M303620200

Dixon, D. P., Sellars, J. D., and Edwards, R. (2011). The Arabidopsis phi class glutathione transferase *AtGSTF2*: binding and regulation by biologically active heterocyclic ligands. *Biochem. J.* 438, 63–70. doi: 10.1042/BJ20101884

Dufourmantel, N., Dubald, M., Matringe, M., Canard, H., Garcon, F., Job, C., et al. (2007). Generation and characterization of soybean and marker-free tobacco plastid transformants over-expressing a bacterial 4-hydroxyphenylpyruvate dioxygenase which provides strong herbicide tolerance. *Plant Biotechnol. J.* 5, 118–133. doi: 10.1111/j.1467-7652.2006.00226.x

Falk, J., Brosch, M., Schäfer, A., Braun, S., and Krupinska, K. (2005). Characterization of transplastomic tobacco plants with a plastid localized barley 4-hydroxyphenyl-pyruvate dioxygenase. *J. Plant Physiol.* 162, 738–742. doi: 10.1016/j.jplph.2005.04.005

Fedorova, M., Kuleva, N., and Hoffmann, R. (2010). Identification of cysteine, methionine and tryptophan residues of actin oxidized *in vivo* during oxidative stress. *J. Proteome Res.* 9, 1598–1609. doi: 10.1021/pr901099e

Foyer, C. H., and Shigeoka, S. (2011). Understanding oxidative stress and antioxidant functions to enhance photosynthesis. *Plant Physiol.* 155, 93–100. doi: 10.1104/pp.110.166181

Gill, S. S., and Tuteja, N. (2010). Reactive oxygen species and antioxidant machinery in abiotic stress tolerance in crop plants. *Plant Physiol. Biochem.* 48, 909–930. doi: 10.1016/j.plaphy.2010.08.016

Grant, O. M., Brennan, D. P., Mellisho Salas, C. D., and Dix, P. J. (2014). Impact of enhanced capacity to scavenge reactive oxygen species on cold tolerance of tobacco. *Int. J. Plant Sci.* 175, 544–554. doi: 10.1086/675976

Hawkes, T. R. (2014). Mechanisms of resistance to paraquat in plants. *Pest Manag. Sci.* 70, 1316–1323. doi: 10.1002/ps.3699

Iamtham, S., and Day, A. (2000). Removal of antibiotic resistance genes from transgenic tobacco plastids. *Nat. Biotechnol.* 18, 1172–1176. doi: 10.1038/81161

Ilhan, S., Ozdemir, F., and Bor, M. (2015). Contribution of trehalose biosynthetic pathway to drought stress tolerance of *Capparis ovata* Desf. *Plant Biol.* 17, 402–407. doi: 10.1111/plb.12227

Jin, S., and Daniell, H. (2014). Expression of γ-tocopherol methyltransferase in chloroplasts results in massive proliferation of the inner envelope membrane and decreases susceptibility to salt and metal-induced oxidative stresses by reducing reactive oxygen species. *Plant Biotechnol. J.* 12, 1274–1285. doi: 10.1111/pbi.12224

Kanai, T., Takahashi, K., and Inoue, H. (2006). Three distinct-type glutathione S-transferases from Escherichia coli important for defense against oxidative stress. *J. Biochem.* 140, 703–711. doi: 10.1093/jb/mvj199

Kayum, M. , Nath, U. K., Park, J. I., Biswas, M. K., Choi, E. K., Song, J. Y., et al. (2018). Genome-wide identification, characterization, and expression profiling of glutathione S-transferase (GST) family in pumpkin reveals likely role in cold-stress tolerance. *Genes* 9, 1–21. doi: 10.3390/genes9020084

Keunen, E., Peshev, D., Vangronsveld, J., Van Den Ende, W., and Cuypers, A. (2013). Plant sugars are crucial players in the oxidative challenge during abiotic stress: extending the traditional concept. *Plant Cell Environ.* 36, 1242–1255. doi: 10.1111/pce.12061

Kim, D., Langmead, B., and Salzberg, S. L. (2015). HISAT: a fast spliced aligner with low memory requirements. *Nat. Methods* 12, 357–360. doi: 10.1038/nmeth.3317

Kissoudis, C., Kalloniati, C., Flemetakis, E., Madesis, P., Labrou, N. E., Tsaftaris, A., et al. (2015a). Maintenance of metabolic homeostasis and induction of cytoprotectants and secondary metabolites in alachlor-treated *GmGSTU4*-overexpressing tobacco plants, as resolved by metabolomics. *Plant Biotechnol. Rep.* 9, 287–296. doi: 10.1007/s11816-015-0364-5

Kissoudis, C., Kalloniati, C., Flemetakis, E., Madesis, P., Labrou, N. E., Tsaftaris, A., et al. (2015b). Stress-inducible *GmGSTU4* shapes transgenic tobacco plants metabolome towards increased salinity tolerance. *Acta Physiol. Plant.* 37, 1–11. doi: 10.1007/s11738-015-1852-5

Kong, L., Zhang, Y., Ye, Z. Q., Liu, X. Q., Zhao, S. Q., Wei, L., et al. (2007). CPC: assess the protein-coding potential of transcripts using sequence features and support vector machine. *Nucleic Acids Res.* 35, 345–349. doi: 10.1093/nar/gkm391

Kumar, S., Asif, M. H., Chakrabarty, D., Tripathi, R. D., Dubey, R. S., and Trivedi, P. K. (2013). Expression of a rice Lambda class of glutathione S-transferase, OsGSTL2, in Arabidopsis provides tolerance to heavy metal and other abiotic stresses. *J. Hazard. Mater.* 248–249, 228–237. doi: 10.1016/j.jhazmat.2013.01.004

Kumar, S., Dhingra, A., and Daniell, H. (2004). Plastid-expressed *betaine aldehyde dehydrogenase* gene in carrot cultured cells, roots, and leaves confers enhanced salt tolerance. *Plant Physiol.* 136, 2843–2854. doi: 10.1104/pp.104.045187.and

Labrou, N. E., Papageorgiou, A. C., Pavli, O., and Flemetakis, E. (2015). Plant GSTome: structure and functional role in xenome network and plant stress response. *Curr. Opin. Biotechnol.* 32, 186–194. doi: 10.1016/j.copbio.2014.12.024

Langmead, B., and Salzberg, S. L. (2012). Fast gapped-read alignment with Bowtie 2. *Nat. Methods* 9, 357–359. doi: 10.1038/nmeth.1923

Lawrence, M. A. (2016). *ez: Easy Analysis and Visualization of Factorial Experiments*. R package version 4.4-0. Available online at: https://CRAN.R-project.org/package=ez

Le Martret, B., Poage, M., Shiel, K., Nugent, G. D., and Dix, P. J. (2011). Tobacco chloroplast transformants expressing genes encoding dehydroascorbate reductase, glutathione reductase, and glutathione-S-transferase exhibit altered anti-oxidant metabolism and improved abiotic stress tolerance. *Plant Biotechnol. J.* 9, 661–673. doi: 10.1111/j.1467-7652.2011.00611.x

Lee, S. B., Kwon, H.-B., Kwon, S.-J., Park, S.-C., Jeong, M.-J., Han, S.-E., et al. (2003). Accumulation of trehalose within transgenic chloroplasts confers drought tolerance. *Mol. Breed.* 11, 1–13. doi: 10.1023/A:1022100404542

Li, B., and Dewey, C. N. (2011). RSEM : accurate transcript quantification from RNA - Seq data with or without a reference genome. *BMC Bioinformatics* 12, 1–16. doi: 10.1186/1471-2105-12-323

Limami, A. M., Glévarec, G., Ricoult, C., Cliquet, J. B., and Planchet, E. (2008). Concerted modulation of alanine and glutamate metabolism in young Medicago truncatula seedlings under hypoxic stress. *J. Exp. Bot.* 59, 2325–2335. doi: 10.1093/jxb/ern102

Lisec, J., Schauer, N., Kopka, J., Willmitzer, L., and Fernie, A. R. (2006). Gas chromatography mass spectrometry-based metabolite profiling in plants. *Nat. Protoc.* 1, 387–396. doi: 10.1038/nprot.2006.59

Lo Cicero, L., Catara, V., Strano, C. P., Bella, P., Madesis, P., and Lo Piero, A. R. (2017). Over-expression of *CsGSTU* promotes tolerance to the herbicide alachlor and resistance to *Pseudomonas syringae* pv. tabaci in transgenic tobacco. *Biol. Plant.* 61, 169–177. doi: 10.1007/s10535-016-0659-6

Lo Cicero, L., Madesis, P., Tsaftaris, A., and Lo Piero, A. R. (2015). Tobacco plants over-expressing the sweet orange tau glutathione transferases (*CsGSTU*s) acquire tolerance to the diphenyl ether herbicide fluorodifen and to salt and drought stresses. *Phytochemistry* 116, 69–77. doi: 10.1016/j.phytochem.2015.03.004

Lutz, K. A., Knapp, J. E., and Maliga, P. (2001). Expression of bar in the plastid genome confers herbicide resistance. *Plant Physiol.* 125, 1585–1590. doi: 10.1104/pp.125.4.1585

Madesis, P., Nianiou-Obeidat, I., Labrou, N. E., and Tsaftaris, A. (2013). "The Use of highly specific GSTs towards the development of stress tolerant transgenic plants," in *Glutathione: Biochemistry, Mechanisms of Action and Biotechnological Implications*, eds N. E. Labrou, and E. Flemetakis (New York, NY: Nova Science Pub Inc.) 263–274. doi: 10.1146/annurev.soc.30.012703.110603

Martinelli, T., Whittaker, A., Bochicchio, A., Vazzana, C., Suzuki, A., and Masclaux-Daubresse, C. (2007). Amino acid pattern and glutamate metabolism during dehydration stress in the "resurrection" plant *Sporobolus stapfianus*: a comparison between desiccation-sensitive and desiccation-tolerant leaves. *J. Exp. Bot.* 58, 3037–3046. doi: 10.1093/jxb/erm161

McNaughton, K. E., Blackshaw, R. E., Waddell, K. A., Gulden, R. H., Sikkema, P. H., and Gillard, C. L. (2015). Effect of five desiccants applied alone and in combination with glyphosate in dry edible bean (*Phaseolus vulgaris* L.). *Can. J. Plant Sci.* 95, 1235–1242. doi: 10.4141/cjps-2015-098

Michailidis, M., Karagiannis, E., Tanou, G., Karamanoli, K., Lazaridou, A., Matsi, T., et al. (2017). Metabolomic and physico-chemical approach unravel dynamic regulation of calcium in sweet cherry fruit physiology. *Plant Physiol. Biochem.* 116, 68–79. doi: 10.1016/j.plaphy.2017.05.005

Mistry, J., Finn, R. D., Eddy, S. R., Bateman, A., and Punta, M. (2013). Challenges in homology search: HMMER3 and convergent evolution of coiled-coil regions. *Nucleic Acids Res.* 41:e121. doi: 10.1093/nar/gkt263

Mullineaux, P., and Karpinski, S. (2002). Signal transduction in response to excess light: getting out of the chloroplast. *Curr. Opin. Plant Biol.* 5, 43–48. doi: 10.1016/S1369-5266(01)00226-6

Nguyen, T. X., Nguyen, T., Alameldin, H., Goheen, B., Loescher, W., and Sticklen, M. (2013). Transgene pyramiding of the HVA1 and mtlD in T3 Maize (*Zea mays* L.) plants confers drought and salt tolerance, along with an increase in crop biomass. *Int. J. Agron.* 2013, 1–10. doi: 10.1155/2013/598163

Nianiou-Obeidat, I., Madesis, P., Kissoudis, C., Voulgari, G., Chronopoulou, E., Tsaftaris, A., et al. (2017). Plant glutathione transferase-mediated stress tolerance: functions and biotechnological applications. *Plant Cell Rep.* 36, 791–805. doi: 10.1007/s00299-017-2139-7

Nishida, M., Kong, K.-H., Inoue, H., and Takahashi, K. (1994). Molecular cloning and site-directed mutagenesis of glutathione s-transferase from *Escherichia coli*. *J. Biol. Chem.* 269, 32536–32541.

Pertea, M., Pertea, G. M., Antonescu, C. M., Chang, T. C., Mendell, J. T., and Salzberg, S. L. (2015). Stringtie enables improved reconstruction of a transcriptome from RNA-seq reads. *Nat. Biotechnol.* 33, 290–295. doi: 10.1038/nbt.3122

Poage, M., Le Martret, B., Jansen, M. A., Nugent, G. D., and Dix, P. J. (2011). Modification of reactive oxygen species scavenging capacity of chloroplasts through plastid transformation. *Plant Mol. Biol.* 76, 371–384. doi: 10.1007/s11103-011-9784-y,

R Core Team (2016). *R: A Language and Environment for Statistical Computing*. Available online at: https://cran.r-project.org/doc/manuals/r-release/fullrefman.pdf

Rhee, H. J., Kim, E. J., and Lee, J. K. (2007). Physiological polyamines: simple primordial stress molecules. *J. Cell. Mol. Med.* 11, 685–703. doi: 10.1111/j.1582-4934.2007.00077.x

Sappl, P. G., Carroll, A. J., Clifton, R., Lister, R., Whelan, J., Harvey Millar, A., et al. (2009). The Arabidopsis glutathione transferase gene family displays complex stress regulation and co-silencing multiple genes results in altered metabolic sensitivity to oxidative stress. *Plant J.* 58, 53–68. doi: 10.1111/j.1365-313X.2008.03761.x

Singmann, H., Bolker, B., Westfall, J., and Aust, F. (2018). *afex: Analysis of Factorial Experiments*. R package version 0.19-1. Available online at: https://CRAN.R-project.org/package=afex

Slama, I., Abdelly, C., Bouchereau, A., Flowers, T., and Savouré, A. (2015). Diversity, distribution and roles of osmoprotective compounds accumulated in halophytes under abiotic stress. *Ann. Bot.* 115, 433–447. doi: 10.1093/aob/mcu239

Smith, D. B., and Johnson, K. S. (1988). Single-step purification of polypeptides expressed in *Escherichia coli* as fusions with glutathione S-transferase. *Gene* 67, 31–40. doi: 10.1016/0378-1119(88)90005-4

Stavridou, E., Hastings, A., Webster, R. J., and Robson, P. R. H. (2016). The impact of soil salinity on the yield, composition and physiology of the bioenergy grass *Miscanthus x giganteus*. *GCB Bioenergy* 9, 92–104. doi: 10.1111/gcbb.12351

Tarazona, S., García-Alcalde, F., Dopazo, J., Ferrer, A., and Conesa, A. (2011). Differential expression in RNA-seq: a matter of depth. *Genome Res.* 21, 2213–2223. doi: 10.1101/gr.124321.111

Thankur, P. S., and Rai, V. K. (1982). Dynamics of amino acid accumulation of two differentially drought resistant *Zea Mays* cultivars in response to osmotic stress. *Environ. Exp. Bot.* 22, 221–225. doi: 10.1016/0098-8472(82)90042-9

Tran, L. P., Urao, T., Qin, F., Maruyama, K., Kakimoto, T., Shinozaki, K., et al. (2007). Functional analysis of AHK1/ATHK1 and cytokinin receptor histidine kinases in response to abscisic acid, drought, and salt stress in *Arabidopsis*. *PNAS* 104, 20623–20628. doi: 10.1073/pnas.0706547105

Trapnell, C., Roberts, A., Goff, L., Pertea, G., Kim, D., Kelley, D. R., et al. (2012). Differential gene and transcript expression analysis of RNA-seq experiments with tophat and cufflinks. *Nat. Protoc.* 7, 562–578. doi: 10.1038/nprot.2012.016

Verma, D., and Daniell, H. (2007). Chloroplast vector systems for biotechnology applications. *Plant Physiol.* 145, 1129–1143. doi: 10.1104/pp.107.106690

von Mering, C., Jensen, L. J., Snel, B., Hooper, S. D., Krupp, M., Foglierini, M., et al. (2005). STRING: known and predicted protein-protein associations, integrated and transferred across organisms. *Nucleic Acids Res.* 33, 433–437. doi: 10.1093/nar/gki005

Wang, H. H., Yin, W. B., and Hu, Z. M. (2009). Advances in chloroplast engineering. *J. Genet. Genomics* 36, 387–398. doi: 10.1016/S1673-8527(08)60128-9

Witt, S., Galicia, L., Lisec, J., Cairns, J., Tiessen, A., Araus, J. L., et al. (2012). Metabolic and phenotypic responses of greenhouse-grown maize hybrids to experimentally controlled drought stress. *Mol. Plant* 5, 401–417. doi: 10.1093/mp/ssr102

Yang, K. A., Lim, C. J., Hong, J. K., Park, C. Y., Cheong, Y. H., Chung, W. S., et al. (2006). Identification of cell wall genes modified by a permissive high temperature in Chinese cabbage. *Plant Sci.* 171, 175–182. doi: 10.1016/j.plantsci.2006.03.013

Ye, G. N., Hajdukiewicz, P. T. , Broyles, D., Rodriguez, D., Xu, C. W., Nehra, N., et al. (2001). Plastid-expressed 5-enolpyruvylshikimate-3-phosphate synthase genes provide high level glyphosate tolerance in tobacco. *Plant J.* 25, 261–270. doi: 10.1046/j.1365-313X.2001.00958.x

Yoshimura, K., Miyao, K., Gaber, A., Takeda, T., Kanaboshi, H., Miyasaka, H., et al. (2004). Enhancement of stress tolerance in transgenic tobacco plants overexpressing *Chlamydomonas glutathione* peroxidase in chloroplasts or cytosol. *Plant J.* 37, 21–33. doi: 10.1046/j.1365-313X.2003.01930.x

Zhang, J., Tan, W., Yang, X. H., and Zhang, H. X. (2008). Plastid-expressed choline monooxygenase gene improves salt and drought tolerance through accumulation of glycine betaine in tobacco. *Plant Cell Rep.* 27, 1113–1124. doi: 10.1007/s00299-008-0549-2

Zhao, F., and Zhang, H. (2006). Salt and paraquat stress tolerance results from co-expression of the *Suaeda salsa* glutathione S-transferase and catalase in transgenic rice. *Plant Cell. Tissue Organ Cult.* 86, 349–358. doi: 10.1007/s11240-006-9133-z

Conflict of Interest Statement: The authors declare that the research was conducted in the absence of any commercial or financial relationships that could be construed as a potential conflict of interest.

frontiers in Plant Science

ORIGINAL RESEARCH
published: 08 March 2019
doi: 10.3389/fpls.2019.00192

Transcriptome Profiling and Genome-Wide Association Studies Reveal *GSTs* and Other Defense Genes Involved in Multiple Signaling Pathways Induced by Herbicide Safener in Grain Sorghum

You Soon Baek[1†], *Loren V. Goodrich*[1,2†], *Patrick J. Brown*[1,3], *Brandon T. James*[1,4], *Stephen P. Moose*[1], *Kris N. Lambert*[1] *and Dean E. Riechers*[1*]

[1] *Department of Crop Sciences, University of Illinois at Urbana-Champaign, Urbana, IL, United States,* [2] *Jerseyville Research Center, Monsanto Company, Jerseyville, IL, United States,* [3] *Department of Plant Sciences, University of California, Davis, Davis, CA, United States,* [4] *HudsonAlpha Institute for Biotechnology, Huntsville, AL, United States*

OPEN ACCESS

Edited by:
Stanislav Kopriva, Universität zu Köln, Germany

Reviewed by:
Wusirika Ramakrishna, Central University of Punjab, India
Kanwarpal Singh Dhugga, Consultative Group on International Agricultural Research (CGIAR), United States

***Correspondence:**
Dean E. Riechers
riechers@illinois.edu

[†] *These authors have contributed equally to this work*

Specialty section:
This article was submitted to Plant Physiology, a section of the journal Frontiers in Plant Science

Received: *07 September 2018*
Accepted: *05 February 2019*
Published: *08 March 2019*

Citation:
Baek YS, Goodrich LV, Brown PJ, James BT, Moose SP, Lambert KN and Riechers DE (2019) Transcriptome Profiling and Genome-Wide Association Studies Reveal GSTs and Other Defense Genes Involved in Multiple Signaling Pathways Induced by Herbicide Safener in Grain Sorghum. Front. Plant Sci. 10:192. doi: 10.3389/fpls.2019.00192

Herbicide safeners protect cereal crops from herbicide injury by inducing genes and proteins involved in detoxification reactions, such as glutathione *S*-transferases (GSTs) and cytochrome P450s (P450s). Only a few studies have characterized gene or protein expression profiles for investigating plant responses to safener treatment in cereal crops, and most transcriptome analyses in response to safener treatments have been conducted in dicot model species that are not protected by safener from herbicide injury. In this study, three different approaches were utilized in grain sorghum (*Sorghum bicolor* (L.) Moench) to investigate mechanisms involved in safener-regulated signaling pathways. An initial transcriptome analysis was performed to examine global gene expression in etiolated shoot tissues of hybrid grain sorghum following treatment with the sorghum safener, fluxofenim. Most upregulated transcripts encoded detoxification enzymes, including P450s, GSTs, and UDP-dependent glucosyltransferases (UGTs). Interestingly, several of these upregulated transcripts are similar to genes involved with the biosynthesis and recycling/catabolism of dhurrin, an important chemical defense compound, in these seedling tissues. Secondly, 761 diverse sorghum inbred lines were evaluated in a genome-wide association study (GWAS) to determine key molecular-genetic factors governing safener-mediated signaling mechanisms and/or herbicide detoxification. GWAS revealed a significant single nucleotide polymorphism (SNP) associated with safener-induced response on chromosome 9, located within a phi-class *SbGST* gene and about 15-kb from a different phi-class *SbGST*. Lastly, the expression of these two candidate *SbGSTs* was quantified in etiolated shoot tissues of sorghum inbred BTx623 in response to fluxofenim treatment. *SbGSTF1* and *SbGSTF2* transcripts increased within 12-hr after fluxofenim treatment but the level of safener-induced expression differed between the two genes. In addition to identifying specific

GSTs potentially involved in the safener-mediated detoxification pathway, this research elucidates a new direction for studying both constitutive and inducible mechanisms for chemical defense in cereal crop seedlings.

Keywords: herbicide safeners, transcriptome analysis-RNAseq, glutathione *S*-transferases, plant defense, defense signaling network, dhurrin metabolism, detoxification

INTRODUCTION

Plants have the unique capability of stimulating selective signaling pathways in response to diverse stimuli, including natural and synthetic compounds as well as abiotic and biotic stresses. Subsequently, plants activate specific defense, and detoxification mechanisms for survival and/or adaptation (Cole and Edwards, 2000; Goda et al., 2004; Riechers et al., 2010; Züst and Agrawal, 2017). Plant defense mechanisms elicited under biotic and abiotic stress are typically activated through plant hormone-mediated signaling (Bari and Jones, 2009), which may include the upregulation of detoxification enzymes that recognize and metabolize a diverse range of natural and synthetic compounds (*xenobiotics*; Edwards et al., 2000; Cummins et al., 2011). In addition to direct metabolism of xenobiotic substrates, other important detoxification mechanisms also include transport and compartmentalization of non-phytotoxic, polar metabolites (Coleman et al., 1997; Riechers et al., 2010; Ramel et al., 2012).

One of the most well-studied xenobiotic responses is the herbicide detoxification pathway, consisting of a complex, multistep process that metabolizes different herbicide substrates. These detoxification processes occur in three sequential phases: Phase I involves hydrolysis or oxidation and Phase II involves conjugation with endogenous sugars or reduced glutathione (GSH). During Phase III, the conjugates are exported from the cytosol and sequestrated within the vacuole. Interestingly, herbicide detoxification reactions can also be induced by certain synthetic compounds called herbicide safeners. Safeners are non-phytotoxic chemical compounds that selectively increase tolerance to herbicides in certain monocotyledonous crop species, such as maize, wheat, rice, and grain sorghum, without reducing herbicide susceptibility in target weeds (Hatzios and Hoagland, 1989; Riechers et al., 2010). The predominant mechanisms for safener-induced plant detoxification include an enhanced rate of herbicide metabolic detoxification and/or sequestration (Davies and Caseley, 1999; Hatzios and Burgos, 2004; Riechers et al., 2010; Edwards et al., 2011).

Key proteins/enzymes in these detoxification pathways include esterases, amidases, oxidases, and cytochrome P450 monooxygenases (P450s) in Phase I, glutathione *S*-transferases (GSTs) and UDP-dependent glucosyltransferases (UGTs) in Phase II, and ATP-binding cassette (ABC)-transporters in Phase III (Kreuz et al., 1996). Several studies have shown that safeners induce the expression of genes encoding these key enzymes (reviewed by Riechers et al., 2010). Grain sorghum (*Sorghum bicolor*) has previously demonstrated a massive induction of herbicide-metabolizing GSTs in response to several herbicide safeners (Fuerst and Gronwald, 1986; Gronwald et al., 1987; Gronwald and Plaisance, 1998). This biochemical reaction of GST-mediated detoxification through conjugation with GSH is well characterized (Dixon et al., 2002), but the precise molecular mechanism for the induction of GSTs and other defense enzymes is poorly understood (Riechers et al., 2010). Previously, proteomic approaches identified proteins involved in safener responses in the model grass *Aegilops tauschii,* a diploid wheat species (Zhang and Riechers, 2004; Zhang et al., 2007). These studies detected large increases of GST expression in coleoptile tissues and identified several new safener-inducible proteins, including 12-oxophytodienoate reductases (OPRs). The coleoptile is a transient organ and the outermost structure of emerging grass shoots exposed to environmental factors and stressors, analogous to the leaf epidermis (Javelle et al., 2011). The coleoptile protects inner leaf tissues through both structural and chemical defense mechanisms. Taken together, these results suggest that safeners may coordinately induce the expression of detoxification enzymes in a tissue-specific manner in cereal crop seedlings (Riechers et al., 2010; Riechers and Green, 2017).

Several hypotheses for potential signaling mechanism(s) underlying safener-regulated detoxification reactions have been proposed, based mainly on research performed with model dicots (Rishi et al., 2004; Behringer et al., 2011; Skipsey et al., 2011). Expression of several safener-induced genes related to detoxification were dependent on TGA transcription factors and/or NON-Expressor of PR-1 (NPR1) (Behringer et al., 2011), the key regulators of salicylic acid (SA) synthesis (Zhang et al., 1999; Uquillas et al., 2004; Mueller et al., 2008). Additionally, linkages have been hypothesized between safener-mediated detoxification and signaling pathways utilizing oxylipins, which are oxidation products of membrane-derived polyunsaturated fatty acids (Mueller et al., 2008; Mosblech et al., 2009). A dramatic decrease in safener-induced *GST* expression levels was measured in root cultures of *Arabidopsis fad* mutants unable to synthesize oxylipins, implying a direct link between safener-regulated responses and the oxylipin signaling pathway (Skipsey et al., 2011). Recent research to functionally test this hypothesis showed that oxylipin treatment induced *GST* expression in rice plants but did not confer a safening phenotype from herbicide injury (Brazier-Hicks et al., 2018), suggesting that the pathway(s) mediating safener responses contain signaling components in addition to oxylipins.

Safeners hold great promise for discovering and commercializing novel agrochemicals for crop protection (Riechers and Green, 2017) as well as understanding the regulation of plant defense mechanisms and signaling pathways. However, detailed molecular mechanisms are limited in the literature pertaining to regulation of gene expression by safeners

in cereal crops where a clear phenotypic response is observed (Riechers et al., 2010). To test the hypothesis that safeners induce expression of numerous genes involved in detoxification and signaling pathways, which may involve oxylipins and/or phytohormones, our objectives were to: (1) investigate global transcriptome expression of the safener response in etiolated grain sorghum shoots by RNAseq, (2) identify genes responsible for natural or safener-induced herbicide tolerance via a genome-wide association study (GWAS), and (3) investigate the expression of candidate safener upregulated genes (identified by GWAS) at different time points, using validated reference genes in etiolated shoot tissues. This study provides novel insights pertaining to how safeners reprogram the plant transcriptome and elucidates mechanisms involved in detoxification reactions in grain sorghum seedlings.

MATERIALS AND METHODS

Plant Materials, Growth Conditions, and Treatments

Sorghum seeds (commercial sorghum hybrid 7431; Advanta Seeds, USA) were surface sterilized with 5% (v/v) sodium hypochlorite for 5 min and rinsed with deionized water 3 times for 5 min each. Twenty-five sterilized seeds were planted at the depth of 3.8 cm in each 4 × 4 cm pot containing vermiculite, and three pots were prepared for each of the following treatments. Each pot was watered with 150 mL deionized water applied via soil drench, covered with aluminum foil, then incubated in a growth chamber at 27°C in the dark for 42 h. A non-treated control (0.4% DMSO only) or safener (20 μM fluxofenim) treatment was then applied to each pot in 50 mL deionized water. After 12 h, etiolated shoot tissues were harvested (1–2 cm above the seed) and frozen in liquid nitrogen, then stored at −80 °C until RNA extraction. Whole-plant responses to fluxofenim, *S*-metolachlor (herbicide), and the combination treatment 14 d after application are shown in **Supplementary Figure 1**.

RNA Extraction, Library Construction, and Transcriptomic Analysis

To test the whole sorghum transcriptome response to safener, frozen shoot samples were ground in liquid nitrogen and total RNA was isolated from 500 mg of shoot material using previously described methods (Xu et al., 2002) with Trizol reagent (Invitrogen). The concentration and purity of extracted RNA were determined with NanoDrop 1,000 spectrophotometer (Thermo Scientific, Waltham, MA, USA) and a Qubit 2.0 fluorometer (Invitrogen, USA). Samples with concentrations ranging between 50 and 100 ng/μL and an A_{260}/A_{280} >1.95 were utilized for library preparation. To visually evaluate rRNA integrity, total RNA (1 μg) was denatured at 55 °C in the presence of formamide and formaldehyde and visualized on 1% EtBr-stained agarose gels containing 0.4 M formaldehyde as previously described (Riechers et al., 2003).

Three individual pots for each of the two treatments were treated as biological replicates, resulting in a total of six libraries. RNA samples were obtained and libraries were constructed from two independent experiments, in which the first experiment consisted of two libraries (one replicate per treatment) and the second experiment consisted of four libraries (two replicates per treatment) for a total of three biological replicates per treatment (i.e., with or without safener). RNA quality control and library preparation analyses were performed by the High-Throughput Sequencing and genotyping unit at the University of Illinois Biotechnology center (http://www.biotech.illinois.edu). Briefly, stranded, single-read libraries of total RNA were generated for each sample using the Illumina Truseq Stranded RNAseq sample preparation kits. The libraries were quantitated by qPCR and sequenced on one lane for 101 cycles from one end of the fragments on a HiSeq2000 for the first experiment and Hiseq2500 for the second experiment, using a TrueSeq SBS sequencing kit (version 3 or 4, respectively). Fastq files were generated and demultiplexed with the bcl2fasq v2.17.1.14 conversion software (and the Illumina software Casava 1.8.2) for the first experiment). Two RNAseq libraries from the first experiment were sequenced on a single lane that produced 100-bp single-end reads, and four RNAseq libraries from the second experiment were sequenced separately on a single lane.

The published sorghum reference genome (*S. bicolor v3.1.1*) and genome annotations for analyzing differentially expressed transcripts were downloaded from Phytozome (phytozome.jgi.doe.gov). Prior to mapping and assembly, total reads were filtered to remove reads with adapters, low-quality reads (mean Q < 10), incomplete reads (< 50-bp), or repetitive reads with mutual information score >0.5 using Trimmomatic/0.36-Java-1.8.0_121. Both reads in a pair were removed if either one of them failed the filters. On average, <1% of all reads failed to pass the filter. Clean reads were then mapped to the reference genome using the STAR/2.5.3a-aligner with default parameters. On average across libraries, 89% of reads mapped uniquely to the reference genome. Read numbers that mapped to each gene were counted by featureCounts v.1.4.5-pl under the subread/1.5.0 package. The Illumina RNAseq datasets analyzed for this study have been deposited in SRA database with the accession number of PRJNA490688 (https://www.ncbi.nlm.nih.gov/bioproject/PRJNA490688).

All tests of significance for differential expression were analyzed with a linear model implemented by the limma package (Smyth, 2005; Law et al., 2014) and modules from the edgeR package (Robinson et al., 2010) in R (R Development Core Team, 2011), in which the TMM normalization method was used to adjust expression values to a common scale. Gene expression levels were calculated using counts-per-million (CPM) and transformed to $\log_2$-counts per million (log-CPM). Global changes in differentially expressed genes (DEGs) were identified if transcripts showed differences in expression >2 log ($\log_2$)-fold, with false-discovery rate (FDR)-corrected *p*-values (q-values) <0.05. The genome-wide patterns of expression were visualized through a principal component analysis (PCA) of the normalized mean read counts per gene (CPM in the library) to estimate the possible variances among libraries, since libraries from two independent experiments were combined. Major biological and molecular functions of DEGs were determined by Gene Othology (GO) enrichment analysis. GO was determined using annotations from agriGO (Du et al., 2010) and as described in Fracasso et al. (2016). Each unique gene within

a GO annotation was allowed to contribute to the enrichment of that category. Enrichment analysis of Kyoto Encyclopedia of Genes and Genomes (KEGG; http://www.genome.ad.jp/kegg/; Kanehisa and Goto, 2000) were performed using KEGG Orthology IDs provided by Phytozome.

Genome Wide Association Study, Phenotyping, and Genotyping Sorghum Inbred Lines

Sorghum inbred lines were from the Sorghum Conversion Program (Thurber et al., 2013). Three independent trials replicated in time (i.e., biological replicates) were conducted using a different randomization scheme in each trial. Flats for trials one and two were planted in a soil, peat, sand mix at a ratio of 1:1:1, whereas flats in trial three were planted in Metro Mix 900 (BFG Supply Co., USA) series soil. Flats contained 24 cells of randomized sorghum genotypes in unsafened/safened pairs plus inbred BTx623 as a control-check in each flat. Safened seeds were treated with fluxofenim (Sigma-Aldrich, St. Louis, MO, USA) at the rate of 0.4 g kg^{-1} seed. Unsafened seeds were not subjected to treatment. Sorghum seeds were planted 3.5 cm deep and 1 cm apart in the flats, bottom watered, and allowed to sit under greenhouse conditions for 24 h before the herbicide treatment was applied. Flats were planted in pairs; one to receive a herbicide treatment and the other to serve as the control (sprayed with water only). For trials one and two, the herbicide *S*-metolachlor was applied at a rate of 2.5 kg ha^{-1} to the soil of the herbicide flats. Herbicide treatments were applied using a Generation III Research Sprayer (DeVries Manufacturing, USA) with a moving-nozzle, compressed air research spray chamber with an adjustable platform and equipped with a TeeJet 80015EVS even flat-spray nozzle. The nozzle was maintained at ∼35 cm above the flat and the sprayer was calibrated to deliver 185 L ha^{-1} at 275 kPa. For trial three, *S*-metolachlor was applied at a concentration of 37 μM in a 40 mL solution as a soil drench treatment to each individual flat cell using a 50 mL syringe to ensure that an optimal herbicide response was achieved. Greenhouse conditions for trials one and three were set at 28/22°C day/night with a 16/8-hr photoperiod. Greenhouse conditions for trial two were set at 24/22°C day/night with a 16/8-hr photoperiod. Sorghum seedlings were overhead watered daily. After two weeks, seedlings were harvested at the soil level, then total seedling fresh weights and numbers of emerged seedlings were recorded to quantitatively evaluate herbicide injury. Germination rate in the herbicide-untreated tray was monitored for quality control, and data from one week in the first trial were discarded due to low germination. Data for individual genotypes with very poor seed quality, defined as <25% germination in the herbicide-untreated tray, were also discarded.

The four treatment conditions (+/– herbicide; +/– safener) enabled the analysis of four different contrasts. However, only results from the contrast of greatest interest, the "safener-induced response" (safener-treated vs. safener-untreated in the presence of herbicide), are presented. Using data from all three trials, a single predicted value for each sorghum inbred line was estimated via regression using ASREML-R, where the model included trial, week within trial, tray-pair within week within trial, and inbred line as random effects. Additionally, the inbred sorghum line BTx623, the genotype used to create the sorghum reference genome (Paterson et al., 2009), was included as a control in each tray throughout the experiment, and the mean phenotypic value of BTx623 in the planting for each week was tested as a fixed effect covariate to improve model fit as measured by Bayesian Information Criterion (BIC).

Genotyping-by-sequencing was used to generate genome-wide SNP data for the 761 inbred sorghum genotypes evaluated in this study (Thurber et al., 2013). There were 100,610 SNPs overall, but SNPs with a minor allele frequency below 0.026 and identical SNPs within 64-bp of each other were excluded, leaving 60,167 SNPs for GWAS. A GWAS was performed using the genomic association and prediction-integrated tool (GAPIT) in R (Lipka et al., 2012) using a (non-compressed) mixed linear model (MLM) with the population parameters previously determined (P3D) method. SNPs with FDR-corrected *p*-values (q-values) <0.05 were then compared to the sorghum reference genome and paired with closely-associated genes. Unadjusted *p*-values were displayed as a Manhattan plot, and candidate genes identified through GWAS were selected for further quantitative expression analysis by RT-qPCR.

Primer Specificity, Determining Suitable Reference Genes, and *SbGST* Expression Analysis in Sorghum Inbred BTx623

Semi-quantitative RT-PCR was performed to determine target *SbGST* gene and candidate reference gene primer specificity and amplicon size. Sequences of two *SbGST* candidate genes identified through GWAS were analyzed for gene-specific primer (GSP) design using Primer3 software and BLAST. Primer sequences for eight candidate reference genes, which had previously displayed stable expression in various sorghum tissues and organs (Zhang et al., 2013; Reddy et al., 2016), were redesigned to meet specific criteria for RT-qPCR analysis in etiolated sorghum shoot tissue. The candidate *SbGST* GSPs and reference gene primers were required to meet the following stringent parameters: melting temperature (T_m) of 60–63°C, primer lengths of 20–25 bp, guanine-cytosine content 45–55%, amplicon length of 100–250 bp, and the absence of stable hairpins and dimers, determined using the OligoAnalyzer 3.1 tool (Integrated DNA Technologies, USA).

Plant growth conditions and RNA extractions were performed as described previously under "Transcriptomic Analysis," except the safener treatment was 10 μM fluxofenim and only sorghum inbred BTx623 was used. First-strand cDNA synthesis was performed with 500 ng total RNA using the Maxima H-minus cDNA synthesis kit (Thermo Scientific, Waltham, MA, USA) following the manufacturer's protocol. The following amplification program was used with 1 μL first-strand cDNA reaction for semi-quantitative RT-PCR with a PTC-200 Pellier Thermal Cycler (MJ Research Inc., USA): initial denaturation at 95°C for 4.5 min, then 30 amplification cycles of 95°C for 30 s and 62°C for 1 min, followed by a final extension at 72°C for 5 min. RT-PCR products were separated and visualized on 1.8% agarose gels stained with EtBr. To test primer specificity of two candidate *SbGST* genes, synthetic gene plasmids were synthesized using

GeneArt Gene Synthesis (Invitrogen, USA). Each plasmid was synthesized using the entire coding region of the corresponding candidate gene. Semi-quantitative RT-PCR was conducted as above using 1 μL of a 10 ng/μL plasmid solution with both sets of primers to test for specificity of amplification at varying annealing temperatures.

For each candidate reference gene, standard curves were determined by qPCR using 10-fold dilution series over five dilution points of pooled cDNA as a template using the linear regression model (Pfaffl et al., 2004). Primer efficacy for the standard curves was calculated in the SDS 2.3 software (Applied Biosystems, USA). Gene expression stability of the seven candidate reference genes (**Supplementary Table 1**) was estimated using four statistical algorithms: geNorm (Vandesompele et al., 2002), NormFinder (Andersen et al., 2004), BestKeeper (Pfaffl et al., 2004), and the comparative ΔCt method (Silver et al., 2006). RefFinder was used to compare and integrate the ranking of the tested candidate reference genes (Xie et al., 2012). GeNorm was used to determine the gene expression stability value (M) with a cutoff value for M of 1.5 (Vandesompele et al., 2002). The *CYP* gene was omitted from further RT-PCR analysis due to the inability to design GSPs and form a product.

RT-qPCR was conducted to analyze expression of two *SbGSTs* using a 7900 HT Sequence Detection System (Applied Biosystems, USA) and reactions performed in 20 μL volumes following the manufacturer's protocol (Power Syber® Green RNA-to-C_T™ 1-Step Kit; Applied Biosystems, USA). The following program was used for qRT-PCR: 48°C for 30 min, 95°C for 10 min, then 40 cycles at 95°C for 15 s, 62°C for 1 min, and a melting curve at 95°C for 15 s and 62°C for 15 s. Each sample was analyzed in three technical replicates and mean Cq values were calculated. Reverse-transcription negative controls were included to ensure the absence of genomic DNA in the template. Dissociation curves for each reaction were analyzed to ensure only one replicon was amplified. Safener-induced gene expression for each *SbGST* gene was calculated relative to transcript levels in the unsafened control samples (per genotype and time after treatment) and normalized using three reference genes (*GTPB*, *SAND*, and *EIF4a*; described below) using the $2^{-\Delta\Delta Ct}$ method. For quantitative analysis of *SbGSTF1* and *SbGSTF2* expression in inbred BTx623, expression data represent the combined results from three independent experiments (i.e., biological replicates), with three technical replicates per sample. ANOVA followed by Tukey's multiple comparison test and LSD ($\alpha = 0.05$) using PROC GLM in SAS (Release 9.2) was conducted to determine significant differences in gene expression among sorghum genotypes at each harvest time point.

RESULTS

Transcriptome Profiling of Responses to Safener Treatment in Commercial Sorghum Hybrid 7431 Shoots

To identify gene expression changes following safener treatment in etiolated grain sorghum shoots, a total of 390 million clean reads (each 100 nucleotides long) from a total of six libraries were generated with ∼70 million clean reads from each library (**Table 1**). Of the total reads, 99% passed quality filtering standards with 584.2 million (90.4% on average) of those reads being uniquely mapped to the sorghum genome. Approximately 5% were not mapped on a gene and 4% were multi-mapped. The raw sequences were aligned to the sorghum reference genome v. 3.1 (∼90% on average) among the six libraries (**Table 1**). Since libraries were combined from two independent experiments to obtain replicates, PCA was performed on all six libraries to confirm the variation among libraries. Most of the variation among samples represented in PCA could be explained by the safener treatment (PC1), and the two independent sample collections (PC2) (**Supplementary Figure 2**). Before the analysis of DEGs between treatments, transcript reads were adjusted to remove the variance that occurred due to independent sample collections (**Supplementary Figure 3**). After normalization and a single pairwise comparison between control and safener-treated shoots (q-value = 0.05), 419 genes were significantly upregulated

TABLE 1 | RNA-sequencing libraries prepared from sorghum hybrid 7431 etiolated shoots.

Libraries	NumReads	QCfiltered	Unmapped	Mapped	Multimapped	Not.in.gene	In.a.gene
WT.C.1	57671251	3264	1738123 (3.0%)	55929864 (96.9%)	1750141 (3.1%)	2822493 (5.1%)	51310389 (91.7%)
WT.C.2	62852240	4411	6025099 (9.6%)	56822730 (90.4%)	2430627 (4.3%)	3048958 (5.4%)	51294803 (90.3%)
WT.C.3	86054181	349559	2472284 (2.9%)	83232338 (96.7%)	2635497 (3.2%)	3789743 (4.6%)	76739154 (92.2%)
SA.S.1	65945347	4940	6071142 (9.2%)	59869265 (90.8%)	2459105 (4.1%)	3400576 (5.7%)	53956371 (90.1%)
SA.S.2	61534915	5320	15168564 (24.7%)	46361031 (75.3%)	3519136 (7.6%)	2718756 (5.9%)	40086035 (86.5%)
SA.S.3	88750015	384906	4265564 (4.8%)	84099545 (94.8%)	2916656 (3.5%)	4000866 (4.8%)	77111315 (91.7%)

Three individual pots for each treatment (control or safener) were treated as biological replicates, resulting in a total of 6 libraries. Libraries were constructed from two independent experiments, where the first experiment consisted of two libraries (one replicate per treatment) and the second experiment consisted of four libraries (two replicates per treatment) for a total of three biological replicates. Two libraries from the first experiment were sequenced on a single lane that produced 100-bp single-end reads, and four libraries from the second experiment were sequenced separately on a single lane.

in safener-treated shoots compared to the control treatment and 73 were significantly down-regulated. The comparison between treatments identified 103 DEGs in response to safener treatment (**Figure 1**), whereas significantly downregulated DEGs were not detected using a threshold of $\log_2$ 2-fold change in expression in our studies.

Among the 103 differentially safener-upregulated genes, 70 transcripts are annotated as xenobiotic detoxification processes, based on *Arabidopsis* gene annotations. Those transcripts involved in detoxification processes include oxidative enzymes including P450s (11), NAD(P)-linked oxidoreductases (6), OPRs (3), short-chain dehydrogenase/reductase protein (SDR; 4) in Phase I reactions; transferases such as GSTs (11) and UGTs (17) in Phase II reactions; and transporters including ATP-binding cassette (ABC) proteins (3), multidrug resistance-associated protein (MRP; 1), and multidrug and toxic compound extrusion (MATE) efflux family protein (1) in Phase III transport processes (**Supplementary Table 2** and **Figure 2**). The most strongly upregulated transcript ($\log_2$FC = 10.6) was a P450, CYP709B (Sobic.003G156200), whereas the most significantly up-regulated transcript (FDR = 1.69E−11) was an NADP-dependent oxidoreductase (Sobic.005G082600). Several upregulated genes, which were not categorized by general xenobiotic detoxification based on previous research (Baerson et al., 2005; Riechers et al., 2010; Behringer et al., 2011; Skipsey et al., 2011), may be related to phytohormone-mediated defense signaling pathways. Two transcripts encoding kinase proteins were identified including calcium-dependent protein kinases (Sobic.008G015600) and leucine-rich repeat transmembrane protein kinases (Sobic.003G402100), and one transcript encoding pathogen-related thaumatin superfamily protein (Sobic.005G226500) was identified.

The most abundant safener-upregulated transcripts (17 out of 130 genes) encode UGTs, an enzyme family that transfers glucose to diverse endogenous and xenobiotic substrates (Bowles et al., 2006; Osmani et al., 2008). Of these 17 upregulated UGTs, 10 belong to the D or L classes (five each) and 4 belong to E class. In previous research, UGTs were also the most highly represented family of upregulated genes in *Arabidopsis* following treatment with the allelochemical benzoxazolin-2(3H)-one (BOA, 11 different members; Baerson et al., 2005). In addition, the majority of safener-inducible genes encoding UGTs in rice and *Arabidopsis* in prior studies belonged to the D and L classes (Gandia-Herrero et al., 2008; Brazier-Hicks et al., 2018), and 44 *Arabidopsis* UGTs in the D, E, and L groups were responsive to 2,4,5-trichlorophenol (Brazier-Hicks et al., 2007a,b). Several of the most upregulated UGTs by the safener fenclorim in rice were also inducible by different chemical treatments such as SA, methyl jasmonate, phytoprostane-A_1, sulfometuron-methyl, and/or pacloburtrazole (Brazier-Hicks et al., 2018).

Compartmentalization of xenobiotic conjugates in vacuoles requires transporter proteins, which are inducible by safener and xenobiotics in maize, wheat, *Arabidopsis*, and *Populus* (Gaillard et al., 1994; Rishi et al., 2004; Zhang et al., 2007; Behringer et al., 2011). Consistent with previous studies, transcripts encoding transporter-like proteins were induced by

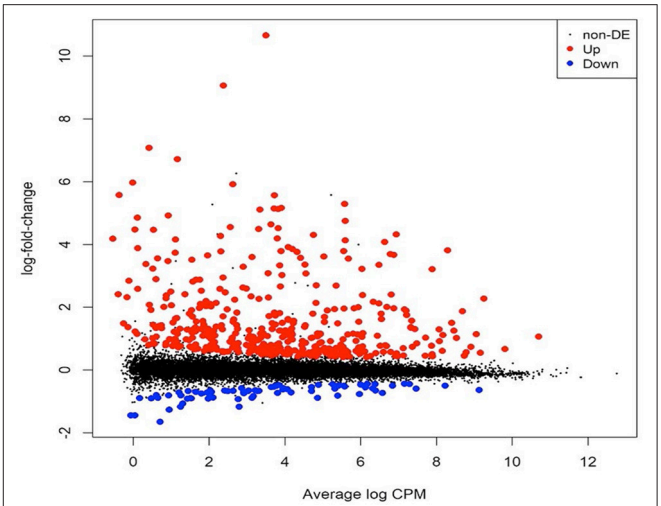

FIGURE 1 | Mean-difference plot showing the $\log_2$ fold change (FC) and average abundance of each transcript. Significantly up- and down-regulated, differentially expressed genes based on $\log_2$ FC are highlighted in red and blue, respectively. RNA samples were obtained and libraries constructed from two independent experiments. The first experiment consisted of two libraries (one replicate per treatment) and the second experiment consisted of four libraries (two replicates per treatment), for a total of three biological replicates per treatment (i.e., with or without safener).

fluxofenim in our research, including four ABC transporter family proteins (Sobic.003G215800, Sobic.003G216232, Sobic.003G216166, Sobic.003G216166, and Sobic.003G267700), a MRP (Sobic.010G169000), and a MATE-type transporter (Sobic.001G185400) (**Supplementary Table 2**). Interestingly, the *Arabidopsis* homolog of the ABC transporter (Sobic.003G215800; AT1G15520) was also induced by BOA (Baerson et al., 2005) and by numerous other biotic and abiotic stresses (van den Brule and Smart, 2002; Campbell et al., 2003).

Transcripts possibly related to defense mechanisms other than genes encoding kinases are transcription factors (TFs) or gene-regulator proteins:ethylene-responsive element binding factor (Sobic.003G297600) and VQ motif-containing protein (Sobic.004G058000). VQ motif-containing protein is a TF known to interact with WRKY TFs, which are involved in jasmonate-dependent defense pathways (Schaller and Stintzi, 2009; Phukan et al., 2016). Interestingly, three transcripts encoding cellulose synthase-like proteins (Sobic.002G237900, Sobic.003G442500, and Sobic.006G080800) from different genetic loci were upregulated by fluxofenim, which implies the safener-mediated signaling pathway may be associated with cell development or defense processes through strengthening the cell wall and apoplast (**Supplementary Table 2**).

GO and KEGG Enrichment Analysis of Sorghum DEGs Upregulated by Safener

DEGs were further compared with annotated genes in the sorghum genome. A singular enrichment analysis (SEA) was carried out with AgriGO software on the 103 upregulated

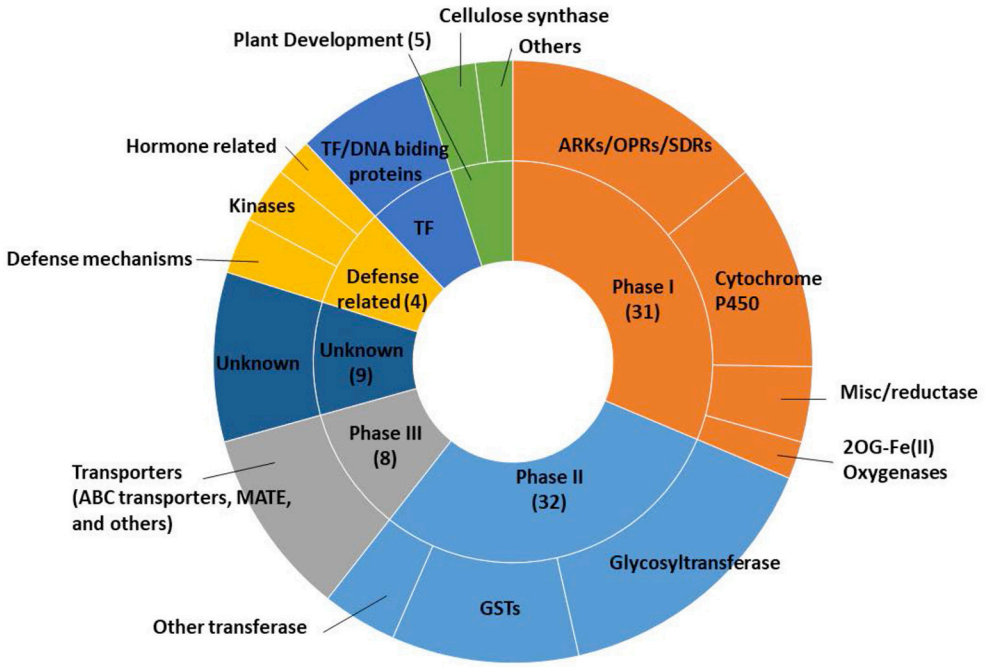

FIGURE 2 | Functional categorizations related to xenobiotic detoxification of upregulated genes in etiolated sorghum shoot tissues 12 h after safener (fluxofenim) treatment.

genes. DEGs were assigned to different GO domains and ∼26% of expressed transcripts were not assigned to any of the categories. To streamline the analysis, upregulated transcripts were categorized by cellular, metabolic processes and molecular function (**Supplementary Figure 4**). The significantly enriched GO categories included "oxidoreductase activity" ($P = 0.02$), and "transferase activity" (transferring hexosyl groups, $P = 1.8e^{-10}$) among safener-induced genes compared with the reference genome (**Supplementary Figure 4**). Genes categorized by transferase and oxidoreductase activities include UGTs and NADP-dependent oxidoreductases, SDRs, and OPRs, respectively. With respect to cellular processes, genes involved in oxidation/reduction were significantly enriched (**Supplementary Figure 4**) while in molecular function analysis the most highly enriched genes are involved with detoxification processes.

A KEGG enrichment analysis of DEGs in a pairwise comparison of nontreated with safener- treated tissue was also conducted, although only 49 transcripts were annotated in this analysis. As shown in **Figure 3**, "glutathione *S*-transferase" was the most significantly enriched in upregulated transcripts by fluxofenim treatment. While transcripts related to detoxification mechanisms are enriched in the KEGG analysis as GO annotations, the analysis leads to other possible defense-signal transduction or biosynthetic secondary metabolite pathways induced by safeners (**Figure 3**). For example, the most enriched and upregulated glycosyltransferases (17 transcripts) were also annotated in different KEGG orthologies: "UGT73C (K13496)," "pathogen-inducible SA glucosyltransferase (K13691)," "hydroquinone glucosyltransferase (K08237)," and "UDP-glucose:(indol-3-yl) acetate beta-D-glucosyltransferase (K13692)". This suggests that some glycosyltransferases induced by phytohormones (such as auxin and SA) may also participate in safener-regulated signaling pathways for induction of plant defense mechanisms.

Genome-Wide Association Mapping Identifies Potential Candidate Genes Involved in Seedling Safener Response

GWAS analysis was performed on the growth parameter "safener-induced response" (safener-treated *vs.* safener-untreated in the presence of herbicide) of seedling fresh weights from 761 diverse sorghum inbreds. One cluster of four SNPs was located on chromosome 9, each with q-values of < 0.13. Three SNPs fell within a putative sulfite oxidase gene (Hänsch and Mendel, 2005; Brychkova et al., 2013), but the only significant SNP (q-value = 0.016) was located at 4128074-bp on chromosome 9 within the 5′ untranslated region of a phi-class *SbGST* gene (Sobic.009G043600) and about 15-kb from a second phi-class *SbGST* gene (Sobic.009G043700) (**Figures 4**, **5**). The two *SbGSTs* were renamed *SbGSTF1* and *SbGSTF2*, respectively, according to the proposed nomenclature system for plant GSTs (Edwards et al., 2000; Pearson, 2005). These three genes are located within a linkage disequilibrium block in the sorghum genome, which on average spans 10–30 kb (Wang et al., 2013). The minor allele of the SNP at 4128074-bp, present

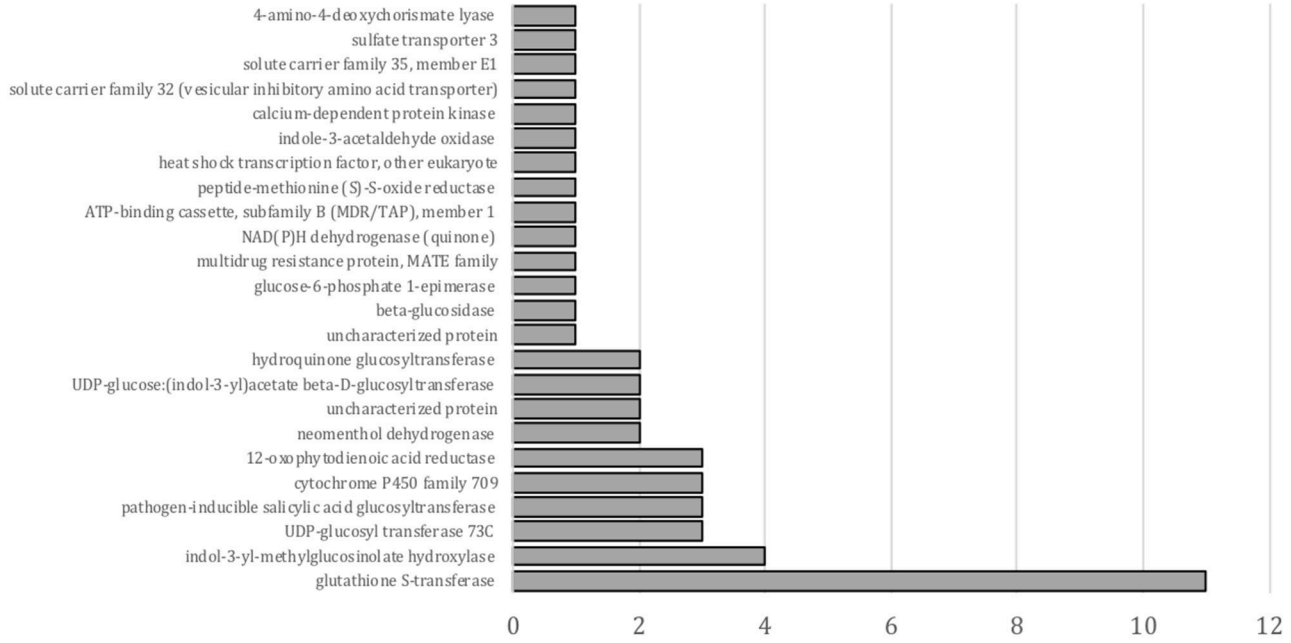

FIGURE 3 | KEGG enrichment test for genes upregulated by fluxofenim treatment. The X-axis represents gene numbers.

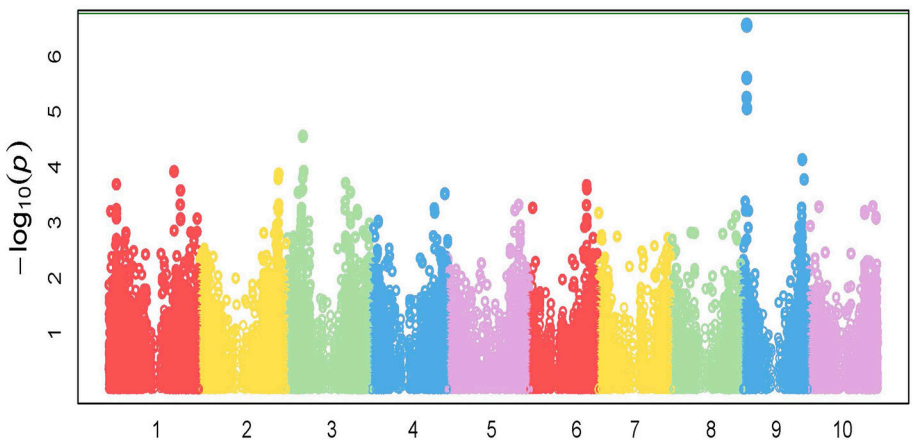

FIGURE 4 | Manhattan plot of the marker-trait associations for plant fresh weight (g pot^{-1}) for the safener-induced response phenotype (safener-treated vs. safener-untreated in the presence of herbicide) of grain sorghum across the sorghum reference genome (BTx623). The green horizontal line at the top of the figure represents a Bonferroni correction with $\alpha = 0.01$.

in 11% of inbreds tested, was associated with a reduction in safener-induced response.

In order to validate the significant GWAS-predicted SNP and associated *SbGST* genes, expression analyses were conducted using RT-qPCR and reference genes verified from among several tested previously in various sorghum tissues and organs in inbred BTx623, which contains the major allele. Inbred BTx623 has a sequenced genome (Paterson et al., 2009) and is commonly used for molecular-genetic sorghum research (Jiao et al., 2016), and was therefore utilized instead of commercial hybrid 7431 since gene-specific primers could be designed by directly analyzing genes within the publicly available genome (phytozome.jgi.doe.gov).

Expression Analysis of Candidate *SbGSTs* Identified Through GWAS

Prior to examining the expression of the two *SbGST* genes, expression profiles of eight candidate reference genes (listed in **Supplementary Table 1**) were tested for stable expression in etiolated shoot tissues because their expression had only been examined previously in sorghum leaves in response to abiotic or biotic stresses (Zhang et al., 2013; Reddy

et al., 2016). The primers tested amplified each candidate reference gene except *CYP* (**Supplementary Figure 5A**) in etiolated shoot tissues, so this transcript was omitted from further analysis. Amplicons from successful primer pairs ranged from 117- to 172-bp. Quantification cycle (Cq) values obtained from each reaction with the seven primer pairs varied in their transcript abundance. The mean Cq value for the seven candidate reference genes ranged from 17.2 to 21.0 cycles, with most falling between 19 and 21. *GTPB* had the lowest mean Cq value of 17.2, indicating the most abundant transcript level followed by *UK* at 18.8. Overall, the majority of candidate reference genes were expressed at intermediate levels with a mean Cq value of about 20 (**Supplementary Figure 5B**).

Three different evaluations were performed to analyze expression stability among the seven reference genes tested. Each evaluation determined a similar ranking order for gene stability but showed subtle differences; however, *GTPB, SAND*, and *PP2A.4/EIF4a* were typically the most stable genes while *ACT1* and *UK* were the least stable. Based on the consensus among the reference gene evaluations utilized (determined with the RefFinder analysis tool) and also considering PCR amplification efficiencies and regression coefficients (**Supplementary Table 1**), three reference genes (*SAND*, *GTPB*, and *EIF4a*) were selected as the most suitable, stably expressed candidate reference genes for etiolated sorghum seedling shoot tissues (**Supplementary Figure 6**). Furthermore, consistent and stable expression of the three references genes was also confirmed in RNA-seq reads from hybrid sorghum 7431 shoots, with and without safener treatment (**Supplementary Figure 7**; reads are reported as raw CPM).

Due to the high nucleotide sequence identity (81%) in the coding region between the two *SbGSTs* identified by GWAS, primer specificity was tested prior to examining their expression. Each GSP set designed for *SbGSTF1* and *SbGSTF2* only amplified products of 245-bp and 159-bp, respectively, from their specific, synthetic DNA templates (**Supplementary Figure 8**). Expression of the two *SbGST* genes was also tested at three different time points following fluxofenim treatment. Fold-induction levels of both *SbGSTF1* and *SbGSTF2* (relative to the controls) increased as time increased, ranging from 1-fold at 4 h after treatment (HAT) to 3-fold at 12 HAT (**Figure 6**). A difference in the magnitude of fold induction in response to fluxofenim was noted between the two *SbGST* genes, where *SbGSTF1* was induced at higher levels during the time course (1.1–2.6 fold) compared to *SbGSTF2* (1–1.6-fold), indicating that *SbGSTF1* is initially more responsive to fluxofenim treatment than *SbGSTF2* in this tissue. In accord with this finding, safener-induced expression of these two *SbGSTs* in hybrid 7431 in the RNAseq experiment (12 HAT; **Supplementary Figure 9**) is consistent with their expression in inbred BTx623 using RT-qPCR described above (**Figure 6**). These results imply that induction of *SbGSTF1 and SbGSTF2* expression may play a role in determining phenotypic responses to herbicide plus safener applications and is in accord with the GWAS results (**Figures 4**, **5**). However, additional functional analyses are needed to further explore this hypothesis.

DISCUSSION

Transcriptional Reprogramming by Safener in Etiolated Grain Sorghum Shoots

Although mechanisms of safener action have been investigated at the transcriptome level in several prior studies with model dicots (Rishi et al., 2004; Behringer et al., 2011), the precise underlying molecular basis of how safeners regulate defense and detoxification mechanisms is not fully understood. In the current study, RNAseq and GWAS approaches allowed for identification of new candidate genes involved with the safener response in sorghum and yielded new insights about possible safener-mediated signaling mechanisms. For example, all DEGs consisted of upregulated transcripts (**Figure 1**), indicating that the safener response at 12 HAT appears to involve transcriptional activation and not repression. Importantly, among the 103 differentially upregulated genes, 70 genes homologous to *Arabidopsis* gene annotations potentially encode important detoxification enzymes including oxidative enzymes, transferases and vacuolar transporter proteins (**Figure 2** and **Supplementary Table 2**). This finding is consistent with previous studies showing induction of individual components of the cellular detoxification machinery by safeners in dicots, including *Arabidopsis* and *Populus* (Rishi et al., 2004; Smith et al., 2004; DeRidder and Goldsbrough, 2006; Behringer et al., 2011). Similar findings were also reported for the diploid wheat *Aegilops tauschii* in response to the safener cloquintocet-mexyl (Zhang et al., 2007). Some of these enzymes are not only upregulated by safeners but are also inducible by various xenobiotics, including the allelochemical BOA (Baerson et al., 2005) and environmental pollutant 3,4-dichloroaniline (Loutre et al., 2003).

The majority of safener-inducible plant GSTs identified in previous research (Riechers et al., 1997; Zhang et al., 2007; Dixon et al., 2009; Brazier-Hicks et al., 2018) belong to the tau class. Similarly, eight of the 11 transcripts encoding GSTs identified in this study belong to the tau class (**Supplementary Table 2**). In addition to eight tau-class GSTs, one lambda-class and two phi-class GSTs were upregulated by fluxofenim. Interestingly, it is still not understood why safeners upregulate *GSTs* and other defense/detoxification genes in dicot plants without eliciting a phenotypic response; i.e., confer protection from herbicide injury (DeRidder et al., 2002; Riechers and Green, 2017). For example, *AtGSTU19* expression was most abundant in the roots of *Arabidopsis* seedlings rather than shoots (DeRidder and Goldsbrough, 2006). Differential gene expression among seedling tissues may result from differing anatomy between monocot and dicot seedlings during seedling development, which might partially explain why dicots are not protected from soil-applied herbicide injury by safener treatment. Taken together, these findings suggest that detoxification mechanisms regulated by safeners require not only certain subclasses of GSTs with the appropriate substrate specificities, but also require the proper subcellular location and tissue distribution of GST expression (Riechers et al., 2003, 2010).

Detoxification enzymes are often upregulated by oxylipins derived from fatty acid oxidation (Loeffler et al., 2005; Mueller et al., 2008; Mueller and Berger, 2009), thus leading to the

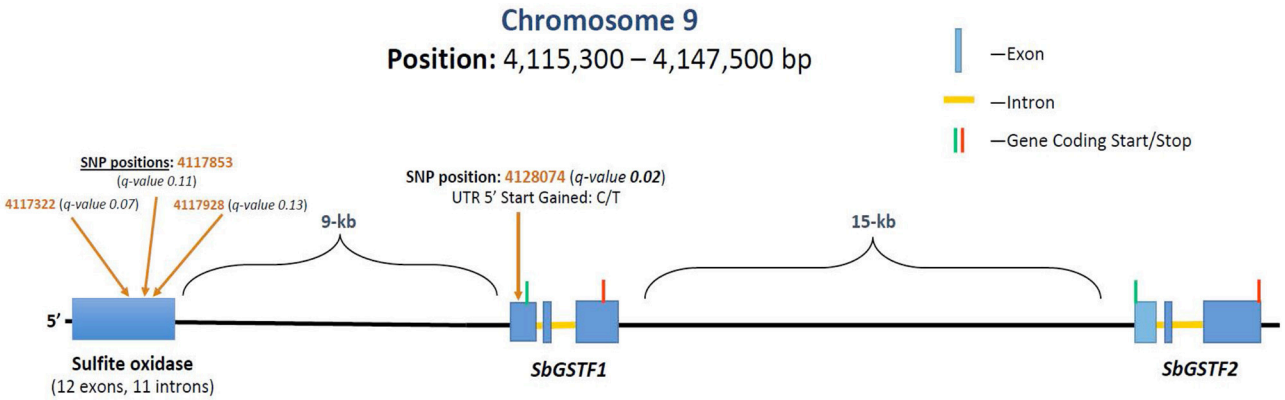

FIGURE 5 | Grain sorghum safener-response associated SNPs in a 32-kb region of chromosome 9, including two tandemly duplicated *SbGSTs* and a sulfite oxidase gene. Three independent trials replicated in time (i.e., biological replicates) were conducted using a different randomization scheme in each trial. Linkage disequilibrium decays, on average, within 10–30 kb in the sorghum genome (Wang et al., 2013).

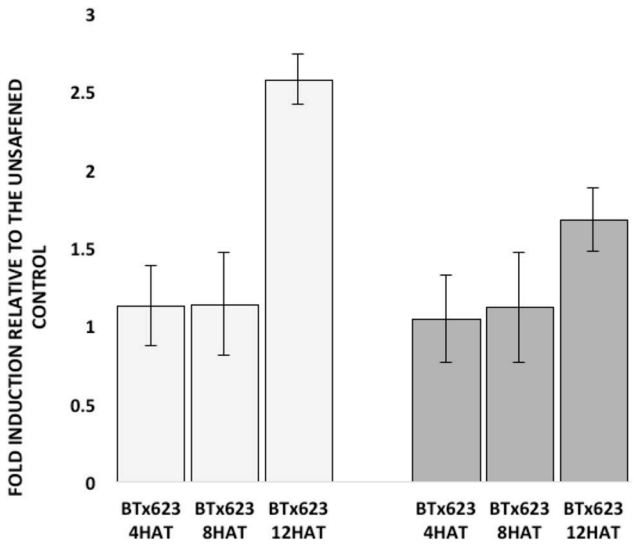

FIGURE 6 | Fold induction of sorghum glutathione *S*-transferase (*GST*) genes, previously identified by GWAS, at three different hours after treatment (HAT) (**Left**, open bars). Fold induction of the *SbGSTF1* gene relative to the unsafened control for each sample at each time point. (**Right**, solid bars) Fold induction of the *SbGSTF2* gene relative to the unsafened control for each sample at each time point. Fold induction for each gene at each time point was calculated by the $2^{-\Delta\Delta Ct}$ method. Data represent the combined results from three independent experiments (i.e., biological replicates) with three technical replicates per sample.

hypothesis that safeners may in part utilize an oxylipin-mediated signaling pathway to induce detoxification enzymes in cereal crops (Riechers et al., 2010; Skipsey et al., 2011). Common genes, such as *GSTs, P450s, UGTs*, and *OPRs*, are induced by both safeners and oxylipins in *Arabidopsis* (Taki et al., 2005; Mueller et al., 2008; Riechers et al., 2010; Behringer et al., 2011). Consistent with previous findings, 24 safener-upregulated transcripts in this study (*P450s, GSTs, UGTs, OPR2*, and an ABC transporter; **Supplementary Table 2**) were also reported as inducible by oxylipin treatment in prior studies. However, a recent study examining possible phenotypic effects provided by oxylipin treatments (OPDA and phytoprostane-A_1) toward herbicide safening did not show complete protection in rice, despite the induction of *GST* expression (Brazier-Hicks et al., 2018). Collectively, these results imply that oxylipin-signaling pathways may be a secondary pathway safeners utilize to enhance seedling protection from herbicide injury, or that additional, essential signaling pathways might operate in parallel.

Biosynthesis, Metabolism, and Cellular Sequestration of Chemical Defense Compounds

The vast majority of safener-upregulated transcripts identified in our study are involved in detoxification, but several transcripts also fell within categories related to plant secondary metabolism (**Figure 3**). The most well-studied example of a biosynthetic pathway for secondary metabolites in grain sorghum is the chemical defense compound dhurrin, a toxic cyanogenic glycoside (Halkier and Møller, 1989; Tako and Rook, 2012; Darbani et al., 2016; Nielsen et al., 2016; Bjarnholt et al., 2018; Yeats, 2018). Interestingly, strong similarities exist between the safener-upregulated transcripts identified in our research and the genes/proteins that participate in synthesis and catabolism of dhurrin (Halkier and Møller, 1989; Darbani et al., 2016). For example, dhurrin synthesis is catalyzed by two P450s and UGT85B1 that form a gene cluster on chromosome 1, which co-localize and are co-expressed with genes encoding *SbMATE* and an *SbGST* (Sobic.001G412700) (Tako and Rook, 2012; Blomstedt et al., 2016; Hayes et al., 2015; Darbani et al., 2016). Although several safener-upregulated transcripts identified in our study encode P450s (6), GSTs (6), UGTs (2), and a MATE protein (Sobic.001G185400) located on chromosome 1, they are not identical to those transcripts encoding dhurrin biosynthetic genes in sorghum grain (Darbani et al., 2016).

In contrast to the genes described above, fluxofenim induced the transcript encoding a specific β-glucosidase [dhurrinase, (Sobic.002G261600)] in our study that degrades dhurrin and releases hydrogen cyanide (HCN) upon tissue disruption by pathogen or insect attack (Halkier and Møller, 1989; Cicek and Esen, 1998; Morant et al., 2008; Nielsen et al., 2008; Gleadow and Møller, 2014). The rate of dhurrin metabolism as compared to HCN concentration exceeds synthesis in the later stages of seedling growth. However, dhurrin concentration decreased (with a concomitant lack of HCN production) during later stages of grain development, suggesting that dhurrin is turned over and recycled to avoid auto-toxicity (Busk and Møller, 2002; Gleadow and Møller, 2014; Nielsen et al., 2016). In relation to a previous profiling study of dhurrin concentrations and transcriptomes during sorghum grain development (Nielsen et al., 2016), the majority (10 out of 17) of safener-upregulated transcripts encoding UGTs in our research are similar to those induced after dhurrin dissipates (Nielsen et al., 2016). Moreover, eight of 11 safener-induced *GSTs* in our study are also expressed in sorghum grain during later developmental stages when dhurrin concentrations decline. A more recent study revealed that two specific lambda-class GSTs (SbGSTL1 and SbGSTL1; transcripts Sobic.002G421200 and Sobic.009G033200) participate in the dhurrin recycling pathway via reductive cleavage of a dhurrin-derived glutathione conjugate, *p*-hydroxyphenyl(*S*-glutathione)acetonitrile (Bjarnholt et al., 2018), thereby preventing HCN accumulation. Fluxofenim predominantly induced several tau-class GSTs, but additionally a similar but distinct lambda-class GSTL (Sobic.001G412700) was induced by safener treatment. This transcript encodes SbGSTL3, which does not convert *p*-hydroxyphenyl(*S*-glutathione)acetonitrile to *p*-hydroxyphenyl acetonitrile (Bjarnholt et al., 2018), but shares high sequence identity with the maize safener-inducible In2-1 protein (Hershey and Stoner, 1991). While the majority of dhurrin accumulates in young sorghum seedlings (mainly in coleoptiles) at 48 h after germination (Halkier and Møller, 1989; Bjarnholt et al., 2018), the shoot RNAseq libraries in our transcriptome analysis were prepared from sorghum shoots collected at a total of 54 h after germination (42 h after germination then 12 h after fluxofenim). This suggests that the safener-mediated signaling pathway and the dhurrin biosynthetic pathway may share a common regulator, such as a TF and/or signaling molecules, to promote similar gene and protein expression profiles during early seedling development in sorghum. It is also possible that dhurrin and fluxofenim share common detoxification enzymes involved in their own metabolism in sorghum shoots, based on similarities between their chemical structures (**Supplementary Figure 10**). In support of this theory, previous reports indicated that GSTs can metabolize both safeners and the herbicides from which they protect in cereal crops (reviewed by Riechers et al., 2010).

It has not been determined if the safener-upregulated transcripts on chromosome 1 are transcriptionally co-regulated. However, four upregulated transcripts encoding P450s on chromosome 1 (Sobic.001G082200, Sobic.001G082300, Sobic.001G082400, and Sobic.001G082500) are clustered, possibly within the physical range for gene co-regulation along with a *MATE* and several *GSTs* (e.g., Sobic.001G185400, Sobic.001G065900, and Sobic.001G318700) (Reimegård et al., 2017; Soler-Oliva et al., 2017). Clustering of non-homologous genes involved in the same biological process, such as dhurrin biosynthetic genes, may be an adaptive trait that enables coordinated regulation and inheritance while maintaining a functional metabolic pathway (Tako and Rook, 2012; Darbani et al., 2016) and suggests a common system in plants to efficiently avoid auto-toxicity following chemical defense synthesis (Busk and Møller, 2002). For example, P450s determine the specificity of xenobiotic detoxification by recognizing distinct substrates (Siminszky, 2006; Mizutani and Ohta, 2010) while UGTs and MATEs coordinately function in the conjugation and transport of secondary compounds from the cytosol to the vacuole. These coordinated cellular processes likely minimize the risk of auto-toxicity, as is the case with many constitutive and inducible plant defense compounds (Mithöfer and Boland, 2012; Gleadow and Møller, 2014) and secondary metabolites (Gierl and Frey, 2001; Frey et al., 2009; Winzer et al., 2012).

Genome-Wide Association Studies

A 32-kb interval on chromosome 9, which comprises *ca.* one linkage disequilibrium block within the sorghum genome (Wang et al., 2013), contains a sulfite oxidase gene and two sorghum phi-class *GST* genes (*SbGSTF1* and *SbGSTF2*), of which *SbGSTF1* is strongly associated with variation in safener-induced response phenotypes. Five main GST subclasses exist in plants, of which tau- and phi-class GSTs are the most abundant (Labrou et al., 2015). A total of 99 *GSTs* have been identified in the sorghum genome with a distribution of 64% tau-class and 22% phi-class genes (Chi et al., 2011), which is typical of cultivated cereal crops, and frequently occur as tandem gene duplications. Both GST classes are closely associated with plant stress responses and their expression is highly responsive to external stimuli such as herbicides (Cummins et al., 2011). GSH is required as a co-substrate for GST-catalyzed conjugation of xenobiotics in plants (Farago and Brunold, 1990; Farago et al., 1994). Plant sulfite oxidases are peroxisomal enzymes involved with maintaining leaf sulfite homeostasis (Brychkova et al., 2013), protecting cells from sulfitolysis (Hänsch and Mendel, 2005), and detoxifying sulfur dioxide (Brychkova et al., 2007) but are not involved with primary sulfate assimilation in plants (Hänsch and Mendel, 2005), so their possible role in alleviating herbicide-induced phytotoxicity is unclear. The presence of safener-upregulated *SbGSTF1* and *SbGSTF2* and lack of sulfite oxidase transcripts in the RNAseq experiment (**Supplementary Table 2**), however, strongly implicate the tandem *SbGSTs* as part of a major QTL associated with the safener-induced phenotype in grain sorghum.

Using the sorghum reference genome, the deduced amino acid sequences of SbGSTF1 and SbGSTF2 were compared to the N-terminal amino acid sequences of several safener-upregulated phi-class GST isozymes purified and biochemically characterized previously and before the sorghum genome was publicly available (Gronwald and Plaisance, 1998). However, based on alignments with these partial N-terminal sequences,

SbGSTF1 and SbGSTF2 are different safener-responsive phi-class SbGSTs. However, the coding region of the deduced *SbGSTF2* cDNA is 81% identical with the coding region of the *SbGSTF1* cDNA (data not shown). As a result, we hypothesize that *SbGSTF2* is most likely a paralog of *SbGST1* (Lynch, 2013) resulting from a relatively old tandem duplication event (Chi et al., 2011). Fluxofenim-induced *SbGSTF1* and *SbGSTF2* expression levels in inbred BTx623 shoots increased with time (**Figure 6**), consistent with the theory that inducible detoxification mechanisms are preferred over constitutively expressed mechanisms in response to variable, unpredictable stress exposure (Züst and Agrawal, 2017). The difference in the scale of gene expression in response to fluxofenim between *SbGSTF1* and *SbGSTF2* may reflect functional divergence of these paralogous genes (Lynch, 2013). For example, as a result of this duplication event one of the *SbGSTs* may have acquired additional function(s) that the other lacks, or could have lost by accumulating degenerative mutations (Innan and Kondrashov, 2010). Although our GWAS study identified two specific phi-class *SbGSTs* associated with safener-induced responses, further studies such as analyzing substrate specificity and protein localization in sorghum shoot tissues and cells, before and after safener treatment, are required to fully understand the function of these phi-class GSTs in detoxification and/or inducible defense processes.

By understanding which genes to target via cis-genic manipulation (i.e., CRISPR-Cas9) or conventional plant breeding, an increase of certain enzyme activities encoded by these genes could result in the development of grain sorghum lines that are tolerant to a wide range of xenobiotics, as well as abiotic and biotic stresses. Since increasing weed pressure and development of herbicide- resistant weed populations are two of the biggest problems facing agriculture today (Yu and Powles, 2014), it is imperative to develop more effective, herbicide-resistant and stress-tolerant crop varieties. Chemical manipulation of mechanisms that regulate metabolic detoxification of natural and synthetic toxic compounds is of great agricultural interest, such as safener-regulated enhancement of herbicide tolerance and the greater herbicide selectivity margin between cereal crops and target weeds (Riechers and Green, 2017). This is a particularly important trait in cultivated grain sorghum where wild, weedy relatives preclude the development of genetically modified varieties due to high risk of gene flow (Ohadi et al., 2017).

Overall, our integrated approach for identification of safener-responsive genes and transcripts has provided new information about the safener-regulated signaling pathway in sorghum shoots, as well as assist in defining the precise mechanism by which safeners upregulate xenobiotic detoxification pathways in cereal crops. Based on our global transcriptome analysis, we now hypothesize that safeners utilize the same or similar biosynthetic and recycling pathways typically used for chemical defense compounds to also enhance herbicide tolerance, in addition to phytohormone- or oxylipin-mediated signaling pathways. Future studies by our research group will further investigate safener-mediated signaling pathways and detoxification mechanisms in dissected coleoptiles from safener-treated, etiolated sorghum shoots to comprehensively understand cell- and tissue-specific gene expression patterns.

AUTHOR CONTRIBUTIONS

DR and PB conceptualized and designed the work. YB, BJ, and SM acquired and analyzed the RNA-seq transcriptome data. LG and PB conducted and analyzed the genome-wide association studies. LG and KL performed RT-qPCR, validated candidate reference genes, and analyzed *SbGST* expression. YB, LG, PB, and DR wrote the manuscript. All authors revised and approved the final version to be published and agree to be accountable for all aspects of the work in ensuring that questions related to the accuracy or integrity of any part of the work are appropriately investigated and resolved.

FUNDING

This work was supported by the Agriculture and Food Research Initiative, Competitive Grant No. 2015-67013-22818 of the USDA-National Institute of Food and Agriculture, to DR and PB.

ACKNOWLEDGMENTS

The authors thank Dr. Rong Ma, Jeshurun Asher Marayag, Edward H. Ross, and the HPCBio group at University of Illinois at Urbana-Champaign for assistance with analyzing RNAseq data and preparing graphs, Derek Lewis and Chris Kaiser for greenhouse assistance, and Olivia Obenland for help in editing earlier versions of the manuscript.

SUPPLEMENTARY MATERIAL

The Supplementary Material for this article can be found online at: https://www.frontiersin.org/articles/10.3389/fpls.2019.00192/full#supplementary-material

Supplementary Table 1 | Primer sequences used for quantitative RT-PCR analysis.

Supplementary Table 2 | Classification of safener-induced transcripts based on detoxification pathways.

Supplementary Figure 1 | Safener and herbicide responses in grain sorghum hybrid 7431 seedlings two weeks after treatment.

Supplementary Figure 2 | Genome-wide variation in gene expression across six libraries.

Supplementary Figure 3 | Plots of the quarter-root QL dispersion against the average abundance of each gene before **(A)** and after **(B)** adjusting sequencing batches.

Supplementary Figure 4 | Gene ontology analysis of safener-upregulated genes for molecular **(A)** and cellular processes **(B)**.

Supplementary Figure 5 | Confirmation of amplicon size and primer specificity for eight candidate reference genes **(A)** and expression levels of the final seven candidate reference genes **(B)**.

Supplementary Figure 6 | Expression stability and ranking of the seven candidate reference genes calculated by three different evaluation methods.

Supplementary Figure 7 | Raw CPM reads of three selected references genes *(GTPB, EIF4a, and SAND)* by RNAseq analysis at 12 h after treatment with 20 μM fluxofenim in sorghum hybrid 7431 shoots.

Supplementary Figure 8 | Specificity of glutathione *S*-transferase *(SbGSTF1 and SbGSTF2)* gene primers.

Supplementary Figure 9 | Raw CPM reads from the two tandem *SbGSTs* via RNA-seq analysis at 12 h after treatment with 20 μM fluxofenim in sorghum hybrid 7431 shoots.

Supplementary Figure 10 | Chemical structures of the sorghum safener fluxofenim (**A**; an oxime ether) and the cyanogenic glycoside dhurrin **(B)**.

REFERENCES

Andersen, C. L., Jensen, J. L., and Ørntoft, T.F. (2004). Normalization of real-time quantitative reverse transcription-PCR data: a model-based variance estimation approach to identify genes suited for normalization, applied to bladder and colon cancer data sets. *Cancer Res.* 64, 5245–5250. doi: 10.1158/0008-5472.CAN-04-0496

Baerson, S. R., Sanchez-Moreiras, A., Pedrol-Bonjoch, N., Schulz, M., Kagan, I. A., Agarwal, A. K., et al. (2005). Detoxification and transcriptome response in *Arabidopsis* seedlings exposed to the allelochemical benzoxazolin-2(3H)-one. *J. Biol. Chem.* 280, 21867–21881. doi: 10.1074/jbc.M500694200

Bari, R., and Jones, J. D. G. (2009). Role of plant hormones in plant defense responses. *Plant Mol. Biol.* 69, 473–488. doi: 10.1007/s11103-008-9435-0

Behringer, C., Bartsch, K., and Schaller, A. (2011). Safeners recruit multiple signaling pathways for the orchestrated induction of the cellular xenobiotic detoxification machinery in *Arabidopsis*. *Plant Cell Environ.* 34, 1970–1985. doi: 10.1111/j.1365-3040.2011.02392

Bjarnholt, N., Neilson, E. H., Crocoll, C., Jørgensen, K., Motawia, M. S., Olse, C. E., et al. (2018). Glutathione transferases catalyze recycling of auto-toxic cyanogenic glucosides in sorghum. *Plant J.* 94, 1109–1125. doi: 10.1111/tpj.13923

Blomstedt, C. K., O'Donnell, N. H., Bjarnholt, N., Neale, A. D., Hamill, J. D., Møller, B. L., et al. (2016). Metabolic consequences of knocking out UGT85B1, the gene encoding the glucosyltransferase required for synthesis of dhurrin in *Sorghum bicolor* (L. *Moench). Plant Cell Physiol.* 57, 373–386. doi: 10.1093/pcp/pcv153

Bowles, D., Lim, E. K., Poppenberger, B., and Vaistij, F. E. (2006). Glycosyltransferases of lipophilic small molecules. *Annu. Rev. Plant Biol.* 57, 567–597. doi: 10.1146/annurev.arplant.57.032905.105429

Brazier-Hicks, M., Edwards, L. A., and Edwards, R. (2007a). Selection of plants for roles in phytoremediation: the importance of glucosylation. *Plant Biotechnol. J.* 5, 627–635. doi: 10.1111/j.1467-7652.2007.00266.x

Brazier-Hicks, M., Knight, K. M., Sellars, J. D., Steel, P. G., and Edwards, R. (2018). Testing a chemical series inspired by plant stress oxylipin signaling agents for herbicide safening activity. *Pest Manag. Sci.* 74, 828–836. doi: 10.1002/ps.4859

Brazier-Hicks, M., Offen, W. A., Gershater, M. C., Revett, T. J., and Lim, E. -K., Bowles, D. J., et al. (2007b). Characterization and engineering of the bifunctional *N*- and *O*- glucosyltransferase involved in xenobiotic metabolism in plants. *Proc. Natl. Acad. Sci. U.S.A.* 104, 20238–20243. doi: 10.1073/pnas.0706421104

Brychkova, G., Grishkevich, V., Fluhr, R., and Sagi, M. (2013). An essential role for tomato sulfite oxidase and enzymes of the sulfite network in maintaining leaf sulfite homeostasis. *Plant Physiol.* 161, 148–164. doi: 10.1104/pp.112.208660

Brychkova, G., Xia, Z., Yang, G., Yesbergenova, Z., Zhang, Z., Davydov, O., et al. (2007). Sulfite oxidase protects plants against sulfur dioxide toxicity. *Plant J.* 50, 696–709. doi: 10.1111/j.1365-313X.2007.03080.x

Busk, P. K., and Møller, B. L. (2002). Dhurrin synthesis in sorghum is regulated at the transcriptional level and induced by nitrogen fertilization in older plants. *Plant Physiol.* 129, 1221–1231. doi: 10.1104/pp.00068

Campbell, E. J., Schenk, P. M., Kazan, K., Penninckx, I. A., Anderson, J. P., Maclean, D. J., et al. (2003). Pathogen-responsive expression of a putative ATP-binding cassette transporter gene conferring resistance to the diterpenoid sclareol is regulated by multiple defense signaling pathways in *Arabidopsis*. *Plant Physiol.* 133, 1272–1284. doi: 10.1104/pp.103.024182

Chi, Y., Cheng, Y., Vanitha, J., Kumar, N., Ramamoorthy, R., Ramachandran, S., et al. (2011). Expansion mechanisms and functional divergence of the glutathione *S*-transferase family in sorghum and other higher plants. *DNA Res.* 18, 1–16. doi: 10.1093/dnares/dsq031

Cicek, M., and Esen, A. (1998). Structure and expression of a dhurrinase (β-glucosidase) from sorghum. *Plant Physiol.* 166, 1469–1478. doi: 10.1104/pp.116.4.1469

Cole, D. J., and Edwards, R. (2000). "Secondary metabolism of agrochemicals in plants," in *Metabolism of Agrochemicals in Plants*, ed T. R. Roberts *(Chichester: Wiley)*, 107–154.

Coleman, J. O. D., Blake-Kalff, M. M. A., and Davies, T. G. E. (1997). Detoxification of xenobiotics by plants: chemical modification and vacuolar compartmentation. *Trends Plant Sci.* 2, 144–151. doi: 10.1016/S1360-1385(97)01019-4

Cummins, I., Dixon, D. P., Freitag-Pohl, S., Skipsey, M., and Edwards, R. (2011). Multiple roles for plant glutathione transferases in xenobiotic detoxification. *Drug Metab. Rev.* 43, 266–280. doi: 10.3109/03602532.2011.552910

Darbani, B., Motawia, M. S., Olsen, C. E., Nour-Eldin, H., Møller, B. L., and Rook, F. (2016). The biosynthetic gene cluster for the cyanogenic glucoside dhurrin in *Sorghum bicolor* contains its co-expressed vacuolar MATE transporter. *Sci. Rep.* 14:37079. doi: 10.1038/srep37079

Davies, J., and Caseley, J. C. (1999). Herbicide safeners: a review. *Pestic Sci.* 55, 1043–1058. doi: 10.1002/(SICI)1096-9063(199911)55:11<1043::AID-PS60>3.0.CO;2-L

DeRidder, B. P., Dixon, D. P., Beussman, D. J., Edwards, R., and Goldsbrough, P. B. (2002). Induction of glutathione *S*-transferases in *Arabidopsis* by herbicide safeners. *Plant Physiol.* 130, 1497–1505. doi: 10.1104/pp.010066

DeRidder, B. P., and Goldsbrough, P. B. (2006). Organ-specific expression of glutathione *S*-transferases and the efficacy of herbicide safeners in *Arabidopsis*. *Plant Physiol.* 140, 167–175. doi: 10.1104/pp.105.067199

Dixon, D. P., Lapthorn, A., and Edwards, R. (2002). Plant glutathione transferases. *Genome Biol.* 3, 3004.1–3004.10. doi: 10.1186/gb-2002-3-3-reviews3004

Dixon, D. P., Skipsey, M., and Edwards, R. (2009). Roles for glutathione transferases in plant secondary metabolism. *Phytochemistry* 71, 338–350. doi: 10.1016/j.phytochem.2009.12.012

Du, Z., Zhou, X., Ling, Y., Zhang, Z., and Su, Z. (2010). agriGO: a GO analysis toolkit for the agricultural community. *Nucl. Acids Res.* 38, W64–W70. doi: 10.1093/nar/gkq310

Edwards, R., Dixon, D. P., Cummins, I., Brazier-Hicks, M., and Skipsey, M. (2011). "New perspective on the metabolism and detoxification of synthetic compounds in plants," in *Organic Xenobiotics and Plants: From Mode of Action to Ecophysiology*, eds P. *Schröder and C. D. Collins (Dordrecht: Springer)*, 125–148. doi: 10.1007/978-90-481-9852-8_7

Edwards, R., Dixon, D. P., and Walbot, V. (2000). Plant glutathione *S*-transferases: enzymes with multiple functions in sickness and in health. *Trends Plant Sci.* 5, 193–198. doi: 10.1016/S1360-1385(00)01601-0

Farago, S., and Brunold, C. (1990). Regulation of assimilatory sulfate reduction by herbicide safeners in *Zea mays* L. *Plant Physiol.* 94, 1808–1812. doi: 10.1104/pp.94.4.1808

Farago, S., Brunold, C., and Kreuz, K. (1994). Herbicide safeners and glutathione metabolism. *Physiol. Plant.* 91, 537–542. doi: 10.1111/j.1399-3054.1994.tb02985.x

Fracasso, A., Trindade, L., and Amaducci, S. (2016). Drought stress tolerance strategies revealed by RNA-seq in two sorghum genotypes with contrasting WUE. *BMC Plant Biol.* 16:115. doi: 10.1186/s12870-016-0800-x

Frerigmann, H., Berger, B., and Gigolashvili, T. (2014). bHLH05 is an interaction partner of MYB51 and a novel regulator of glucosinolate biosynthesis in *Arabidopsis*. *Plant Physiol.* 166, 349–369. doi: 10.1104/pp.114.240887

Frey, M., Schullehner, K., Dick, R., Fiesselmann, A., and Gierl, A. (2009). Benzoxazinoid biosynthesis, a model for evolution of secondary metabolic pathways in plants. *Phytochemistry* 70, 1646–1651. doi: 10.1016/j.phytochem.2009.05.012

Fuerst, E. P., and Gronwald, J. W. (1986). Induction of rapid metabolism of metolachlor in sorghum (*Sorghum bicolor*) shoots by CGA-92194 and other antidotes. *Weed Sci.* 34, 354–361. doi: 10.1017/S0043174500066972

Gaillard, C., Dufaud, A., Tommasini, R., Kreuz, K., Amrhein, N., and Martinoia, E. (1994). A herbicide antidote (safener) induces the activity of both the herbicide detoxifying enzyme and of a vacuolar transporter for the detoxified herbicide. *FEBS Lett.* 352, 219–221. doi: 10.1016/0014-5793(94)00961-9

Gandia-Herrero, F., Lorenz, A., Larson, T., Graham, I. A., Bowles, D. J., Rylott, E. L., et al. (2008). Detoxification of the explosive 2,4,6-trinitrotoluence in *Arabidopsis*: discovery of bifunctional *O*- and *C*- glucosyltransferases. *Plant J.* 56, 963–974. doi: 10.1111/j.1365-313X.2008.03653.x

Gierl, A., and Frey, M. (2001). Evolution of benzoxazinone biosynthesis and indole production in maize. *Planta* 213, 493–498. doi: 10.1007/s004250100594

Gleadow, R. M., and Møller, B. L. (2014). Cyanogenic glycosides: synthesis, physiology, and phenotypic plasticity. *Annu. Rev. Plant Biol.* 65, 155–185. doi: 10.1146/annurev-arplant-050213-040027

Goda, H., Sawa, S., Asami, T., Fujioka, S., Shmada, Y., and Yoshida, S. (2004). Comprehensive comparison of auxin-regulated and brassinosteroid-regulated genes in *Arabidopsis*. *Plant Physiol.* 134, 1555–1573. doi: 10.1104/pp.103.034736

Gronwald, J. W., Fuerst, E. P., Eberlein, C. V., and Egli, M. A. (1987). Effect of herbicide antidotes on glutathione content and glutathione *S*-transferase activity of sorghum shoots. *Pestic. Biochem. Physiol.* 29, 66–76. doi: 10.1016/0048-3575(87)90085-X

Gronwald, J. W., and Plaisance, K. L. (1998). Isolation and characterization of glutathione *S*-transferase isozymes from sorghum. *Plant Physiol.* 117, 877–892. doi: 10.1104/pp.117.3.877

Halkier, B. A., and Møller, B. L. (1989). Biosynthesis of the cyanogenic glucoside dhurrin in seedlings of *Sorghum bicolor* (L.) Moench and partial purification of the enzyme system involved. *Plant Physiol.* 90, 1552–1559. doi: 10.1104/pp.90.4.1552

Hänsch, R., and Mendel, R. R. (2005). Sulfite oxidation in plant peroxisomes. *Photosyn. Res.* 86, 337–343. doi: 10.1007/s11120-005-5221-x

Hatzios, K. K., and Burgos, N. (2004). Metabolism-based herbicide resistance: regulation by safeners. *Weed Sci.* 52, 454–467. doi: 10.1614/P2002-168C

Hatzios, K. K., and Hoagland, R. E. (1989). "Mechanisms of action of herbicide safeners: an overview," in *Crop Safeners for Herbicides*, eds K. K. Hatzios and R. E. *Hoagland (San Diego, CA: Academic Press)*, 65–101.

Hayes, C. M., Burow, G. B., Brown, P. J., Thurber, C., Xin, Z., and Burke, J. J. (2015). Natural variation in synthesis and catabolism genes influences dhurrin content in sorghum. *Plant Genome* 8, 1–9. doi: 10.3835/plantgenome2014.09.0048

Hershey, H. P., and Stoner, T. D. (1991). Isolation and characterization of cDNA clones for RNA species induced by substituted benzenesulfonamides in corn. *Plant Mol. Biol.* 17, 679–690. doi: 10.1007/BF00037053

Innan, H., and Kondrashov, F. (2010). The evolution of gene duplications: classifying and distinguishing between models. *Nat. Rev. Genet.* 11, 97–108. doi: 10.1038/nrg2689

Javelle, M., Vernoud, V., Rogowsky, P. M., and Ingram, G. C. (2011). Epidermis: the formation and functions of a fundamental plant tissue. *New Phytol.* 189, 17–39. doi: 10.1111/j.1469-8137.2010.03514.x

Jiao, Y., Burke, J., Chopra, R., Burow, G., Chen, J., Wang, B., et al. (2016). A sorghum mutant resource as an efficient platform for gene discovery in grasses. *Plant Cell* 28, 1551–1562. doi: 10.1105/tpc.16.00373

Kanehisa, M., and Goto, S. (2000). KEGG: Kyoto encyclopedia of genes and genomes. *Nucleic Acids Res.* 28, 27–30. doi: 10.1093/nar/28.1.27

Kreuz, K., Tommasini, R., and Martinoia, E. (1996). Old enzymes for a new job. *Herbicide detoxification in plants. Plant Physiol.* 111, 349–353. doi: 10.1104/pp.111.2.349

Labrou, N. E., Papageorgiou, A. C., Pavil, O., and Flemetakis, E. (2015). Plant GSTome: structure and functional role in xenome network and plant stress response. *Curr. Opin. Biotechnol.* 32, 186–194. doi: 10.1016/j.copbio.2014.12.024

Law, C. W., Chen, Y., Shi, W., and Smyth, G. K. (2014). Voom: precision weights unlock linear model analysis tools for RNA-seq read counts. *Genome Biol.* 15:R29. doi: 10.1186/gb-2014-15-2-r29

Libault, M., Wan, J., Czechowski, T., Udvardi, M., and Stacey, G. (2007). Identification of 118 *Arabidopsis* transcription factor and 30 ubiquitin-ligase genes responding to chitin, a plant-defense elicitor. *Mol. Plant Microbe Interact.* 20, 900–911. doi: 10.1094/MPMI-20-8-0900

Lipka, A. E., Tian, F., Wang, Q., Peiffer, J., Li, M., Bradbury, P. J., et al. (2012). GAPIT: genome association and prediction integrated tool. *Bioinformatics* 28, 2397–2399. doi: 10.1093/bioinformatics/bts444

Loeffler, C., Berger, S., Guy, A., Durand, T., Bringmann, G., Dreyer, M., et al. (2005). B_1-phytoprostanes trigger plant defense and detoxification responses. *Plant Physiol.* 137, 328–340. doi: 10.1104/pp.104.051714

Loutre, C., Dixon, D., Brazier, M., Slater, M., Cole, D., and Edwards, R. (2003). Isolation of glucosyltransferase from *Arabidopsis thaliana* active in the metabolism of the persistent pollutant 3,4-dichloroaniline. *Plant J.* 34, 485–493. doi: 10.1046/j.1365-313X.2003.01742.x

Lynch, M. (2013). Evolutionary diversification of the multimeric states of proteins. *Proc. Natl. Acad. Sci. U.S.A.* 110, E2821–E2828. doi: 10.1073/pnas.1310980110

Mithöfer, A., and Boland, W. (2012). Plant defense against herbivores: chemical aspects. *Annu. Rev. Plant Biol.* 63, 431–450. doi: 10.1146/annurev-arplant-042110-103854

Mizutani, M., and Ohta, D. (2010). Diversification of P450 genes during land plant evolution. *Annu. Rev. Plant Biol.* 61, 291–315. doi: 10.1146/annurev-arplant-042809-112305

Morant, A. V., Jørgensen, K., Jørgensen, C., Paquette, S. M., Sánchez-Péreza, R., Møller, B. L., et al. (2008). β-Glucosidases as detonators of plant chemical defense. *Phytochemistry* 69, 1759–1813. doi: 10.1016/j.phytochem.2008.03.006

Mosblech, A., Feussner, I., and Heilmann, I. (2009). Oxylpins: structurally diverse metabolites from fatty acid oxidation. *Plant Physiol. Biochem.* 47, 511–517. doi: 10.1016/j.plaphy.2008.12.011

Mueller, M. J., and Berger, S. (2009). Reactive electrophilic oxylipins: pattern recognition and signaling. *Phytochemistry* 70, 1511–1521. doi: 10.1016/j.phytochem.2009.05.018

Mueller, S., Hilbert, B., Dueckershoff, K., Roitsch, T., Krischke, M., Mueller, M. J., et al. (2008). General detoxification and stress responses are mediated by oxidized lipids through TGA transcription factors in *Arabidopsis*. *Plant Cell* 20, 768–785. doi: 10.1105/tpc.107.054809

Nielsen, K. A., Tattersall, D. B., Jones, P. R., and Møller, B. L. (2008). Metabolon formation in dhurrin biosynthesis. *Phytochemistry* 69, 88–98. doi: 10.1016/j.phytochem.2007.06.033

Nielsen, L. J., Stuart, P., Picmanova, M., Rasmussen, S., Olsen, C. E., Harholt, J., et al. (2016). Dhurrin metabolism in the developing grain of *Sorghum bicolor* (L.) Moench investigated by metabolite profiling and novel clustering analyses of time-resolved transcriptomic data. *BMC Genom.* 17:1021. doi: 10.1186/s12864-016-3360-4

Ohadi, S., Hodnett, G., Rooney, W., and Bagavathiannan, M. (2017). Gene flow and its consequences in *Sorghum* spp. *Crit. Rev. Plant Sci.* 36, 367–385. doi: 10.1080/07352689.2018.1446813

Osmani, S. A., Bak, S., Imberty, A., Olsen, C. E., and Møller, B. L. (2008). Catalytic key amino acids and UDP-sugar donor specificity of a plant glucuronosyltransferase, UGT94B1: molecular modeling substantiated by site-specific mutagenesis and biochemical analyses. *Plant Physiol.* 148, 1295–1308. doi: 10.1104/pp.108.128256

Paterson, A. H., Bowers, J. E., Bruggmann, R., Dubchak, I., Grimwood, J., Gundlach, H., et al. (2009). The *Sorghum bicolor* genome and the diversification of grasses. *Nature* 457, 551–556. doi: 10.1038/nature07723

Pearson, W. R. (2005). Phylogenies of glutathione transferase families. *Methods Enzymol.* 401, 186–204. doi: 10.1016/S0076-6879(05)01012-8

Pfaffl, M. W., Tichopad, A., Prgomet, C., and Neuvians, T. P. (2004). Determination of stable housekeeping genes, differentially regulated target genes and sample integrity: bestkeeper–excel-based tool using pair-wise correlations. *Biotechnol. Lett.* 26, 509–515. doi: 10.1023/B:BILE.0000019559.84305.47

Phukan, U. J., Jeena, G. S., and Shukla, R. K. (2016). WRKY transcription factors: molecular regulation and stress responses in plants. *Front. Plant Sci.* 7:760. doi: 10.3389/fpls.2016.00760

R Development Core Team (2011). *R: A Language and Environment for Statistical Computing*. (Vienna: R Foundation for Statistical Computing). Available online at http://www.R-project.org/

Ramel, F., Sulmon, C., Serra, A. A., Gouesbet, G., and Couée, I. (2012). Xenobiotic sensing and signaling in higher plants. *J. Exp. Bot.* 63, 3999–4014. doi: 10.1093/jxb/ers102

Reddy, P. S., Reddy, D. S., Sivasakthi, K., Bhatnagar-Mathur, P., Vadez, V., and Sharma, K. K. (2016). Evaluation of sorghum [*Sorghum bicolor* (L.)] reference genes in various tissues and under abiotic stress conditions for quantitative real-time PCR data normalization. *Front. Plant Sci.* 7:529. doi: 10.3389/fpls.2016.00529

Reimegård, J., Kundu, S., Pendle, A., Irish, V. F., Shaw, P., Nakayama, N., et al. (2017). Genome-wide identification of physically clustered genes suggests chromatin-level co-regulation in male reproductive development in *Arabidopsis thaliana*. *Nucl. Acids Res.* 45, 3253–3265. doi: 10.1093/nar/gkx087

Riechers, D. E., and Green, J. M. (2017). "Crop selectivity and herbicide safeners: Historical perspectives and development, safener-regulated gene expression, signaling, and new research directions," in *Biology, Physiology and Molecular Biology of Weeds*, ed. M. Jugulam (Boca Raton, FL: CRC Press, Taylor & Francis Group), 123–143.

Riechers, D. E., Irzyk, G. P., Jones, S. S., and Fuerst, E. P. (1997). Partial characterization of glutathione *S*-transferases from wheat (*Triticum spp*.) and purification of a safener-induced glutathione *S* transferase from *Triticum tauschii*. *Plant Physiol.* 114, 1461–1470. doi: 10.1104/pp.114.4.1461

Riechers, D. E., Kreuz, K., and Zhang, Q. (2010). Detoxification without intoxication: herbicide safeners activate plant defense gene expression. *Plant Physiol*. 153, 3–13. doi: 10.1104/pp.110.153601

Riechers, D. E., Zhang, Q., Xu, F. -X., and Vaughn, K. C. (2003). Tissue-specific expression and localization of safener-induced glutathione *S*-transferase proteins in *Triticum tauschii*. *Planta* 217, 831–840. doi: 10.1007/s00425-003-1063-y

Rishi, A. S., Munir, S., Kapur, V., Nelson, N. D., and Goyal, A. (2004). Identification and analysis of safener-inducible expressed sequence tags in *Populus* using a cDNA microarray. *Planta* 220, 296–606. doi: 10.1007/s00425-004-1356-9

Robinson, M. D., McCarthy, D. J., and Smyth, G. K. (2010). edgeR: a Bioconductor package for differential expression analysis of digital gene expression data. *Bioinformatics* 26, 139–140. doi: 10.1093/bioinformatics/btp616

Schaller, A., and Stintzi, A. (2009). Enzymes in jasmonate biosynthesis – structure, function, regulation. *Phytochemistry* 70, 1532–1538. doi: 10.1016/j.phytochem.2009.07.032

Sham, A., Al-Azzawi, A., Al-Ameri, S., Al-Mahmound, B., Awwad, F., Al-Rawashdeh, A., et al. (2014). Transcriptome analysis reveals genes commonly induced by *Botrytis cinerea* infection, cold, drought and oxidative stress in *Arabidopsis*. *PLoS ONE* 9:e113718. doi: 10.1371/journal.pone.0113718

Silver, N., Best, S., Jiang, J., and Thein, S. L. (2006). Selection of housekeeping genes for gene expression studies in human reticulocytes using real-time PCR. *BMC Mol. Biol.* 7:33. doi: 10.1186/1471-2199-7-33

Siminszky, B. (2006). Plant cytochrome P450-mediated herbicide metabolism. *Phytochem. Rev.* 5, 445–458. doi: 10.1007/s11101-006-9011-7

Skipsey, M., Knight, K. M., Brazier-Hicks, M., Dixon, D. P., Steel, P. G., and Edwards, R. (2011). Xenobiotic responsiveness of *Arabidopsis thaliana* to a chemical series derived from a herbicide safener. *J. Biol. Chem.* 286, 32268–32276. doi: 10.1074/jbc.M111.252726

Smith, A. P., DeRidder, B. P., Guo, W. J., Seeley, E. H., Regnier, F. E., and Goldsbrough, P. B. (2004). Proteomic analysis of *Arabidopsis* glutathione *S*-transferases from benoxacor- and copper-treated seedlings. *J. Biol. Chem.* 279, 26098–26104. doi: 10.1074/jbc.M402807200

Smyth, G. K. (2005). "limma: linear models for microarray data," in *Bioinformatics and Computational Biology Solutions using R and Bioconductor*. Statistics for Biology and Health, eds. R. Gentleman, V. J. Carey, W. Huber, R. A. Irizarry, and S. Dudoit (New York, NY: Springer), 397–420. doi: 10.1007/0-387-29362-0_23

Soler-Oliva, M. E., Guerrero-Martínez, J. A., Bachetti, V., and Reyes, J. C. (2017). Analysis of the relationship between coexpression domains and chromatin 3D organization. *PLoS Comput. Biol.* 13:e1005708. doi: 10.1371/journal.pcbi.1005708

Taki, N., Sasaki-Sekimoto, Y., Obayashi, T., Kikuta, A., Kobayashi, K., Ainai, T., et al. (2005). 12-Oxophytodienoic acid triggers expression of a distinct set of genes and plays a role in wound induced gene expression in *Arabidopsis*. *Plant Physiol.* 139, 1268–1283. doi: 10.1104/pp.105.067058

Tako, A. M., and Rook, F. (2012). Why biosynthetic genes for chemical defense compounds cluster. *Cell Press* 17, 383–388. doi: 10.1016/j.tplants.2012.04.004

Thurber, C. S., Ma, J. M., Higgins, R. H., and Brown, P. J. (2013). Retrospective genomic analysis of sorghum adaption to temperate-zone grain production. *Genome Biol.* 14:R68. doi: 10.1186/gb-2013-14-6-r68

Uquillas, E., Letelier, I., Blanco, F., Jordana, X., and Holuigue, L. (2004). NPR1-independent activation of immediate early salicylic acid-responsive genes in *Arabidopsis*. *Mol. Plant Microbe Interact.* 17, 34–42. doi: 10.1094/MPMI.2004.17.1.34

van den Brule, S., and Smart, C. C. (2002). The plant PDR family of ABC transporters. *Planta* 216, 95–106. doi: 10.1007/s00425-002-0889-z

Vandesompele, J., De Preter, K., Pattyn, F., Poppe, B., Van Roy, N., De Paepe, A., et al. (2002). Accurate normalization of real-time quantitative RT-PCR data by geometric averaging of multiple internal control genes. *Genome Biol.* 3, 0034–0034.11. doi: 10.1186/gb-2002-3-7-research0034

Wang, Y. H., Upadhyaya, H. D., Burrell, A. M., Sahraeian, S. M. E., Klein, R. R., and Klein, P. E. (2013). Genetic structure and linkage disequilibrium in a diverse, representative collection of the C4 model plant, *Sorghum bicolor*. *Genes Genom. Genet.* 3, 783–793. doi: 10.1534/g3.112.004861

Winzer, T., Gazda, V., He, Z., Kaminski, F., Kern, M., Larson, T. R., et al. (2012). A *Papaver somniferum* 10-gene cluster for synthesis of the anticancer alkaloid noscapine. *Science* 336, 1704–1708. doi: 10.1126/science.1220757

Xie, F., Xiao, P., Chen, D., Xu, L., and Zhang, B. (2012). miRDeepFinder: a miRNA analysis tool for deep sequencing of plant small RNAs. *Plant Mol. Biol.* 80, 75–84. doi: 10.1007/s11103-012-98852

Xu, F. X., Lagudah, E. S., Moose, S. P., and Riechers, D. E. (2002). Tandemly duplicated safener-induced glutathione *S*-transferase genes from *Triticum tauschii* contribute to genome- and organ-specific expression in hexaploid wheat. *Plant Physiol.* 130, 362–373. doi: 10.1104/pp.004796

Yeats, T. H. (2018). Setting and diffusing the cyanide bomb in plant defense. *Plant Physiol.* 178, 956–957. doi: 10.1104/pp.18.01214

Yu, Q., and Powles, S. (2014). Metabolism-based herbicide resistance and cross-resistance in crop weeds: a threat to herbicide sustainability and global crop production. *Plant Physiol.* 166, 1106–1118. doi: 10.1104/pp.114.242750

Zhang, K., Niu, S., Di, D., Shi, L., Liu, D., Cao, X., et al. (2013). Selection of reference genes for gene expression studies in virus-infected monocots using quantitative real-time PCR. *J. Biotech.* 168, 7–14. doi: 10.1016/j.jbiotec.2013.08.008

Zhang, Q., and Riechers, D. E. (2004). Proteomic characterization of herbicide safener-induced proteins in the coleoptile of *Triticum tauschii* seedlings. *Proteomics* 4, 2058–2071. doi: 10.1002/pmic.200300733

Zhang, Q., Xu, F. X., Lambert, K. N., and Riechers, D. E. (2007). Safeners coordinately induce the expression of multiple proteins and MRP transcripts involved in herbicide metabolism and detoxification in *Triticum tauschii* seedling tissues. *Proteomics* 7, 1261–1278. doi: 10.1002/pmic.200600423

Zhang, Y., Fan, W., Kinkema, M., Li, X., and Dong, X. (1999). Interaction of NPR1 with basic leucine zipper protein transcription factors that bind sequences required for salicylic acid induction of the PR-1 gene. *Proc. Natl. Acad. Sci.U.S.A.* 96, 6523–6528. doi: 10.1073/pnas.96.11.6523

Zhao, J., Wang, J., An, L., Doerge, R. W., Chen, Z. J., Grau, C. R., et al. (2007). Analysis of gene expression profiles in response to *Sclerotinia sclerotiorum* in *Brassica napus*. *Planta* 227, 13–24. doi: 10.1007/s00425-007-0586-z

Züst, T., and Agrawal, A. A. (2017). Trade-offs between plant growth and defense against insect herbivory: an emerging mechanistic synthesis. *Annu. Rev. Plant Biol.* 68, 513–534. doi: 10.1146/annurev-arplant-042916-04085

Conflict of Interest Statement: The authors declare that the research was conducted in the absence of any commercial or financial relationships that could be construed as a potential conflict of interest.

frontiers in Plant Science

PERSPECTIVE
published: 24 April 2019
doi: 10.3389/fpls.2019.00487

Detoxification of Reactive Carbonyl Species by Glutathione Transferase Tau Isozymes

Jun'ichi Mano[1], Sayaka Kanameda[2], Rika Kuramitsu[2], Nagisa Matsuura[3] and Yasuo Yamauchi[3]**

[1] Science Research Center, Organization for Research Initiatives, Yamaguchi University, Yamaguchi, Japan, [2] Faculty of Agriculture, Yamaguchi University, Yamaguchi, Japan, [3] Graduate School of Agricultural Science, Kobe University, Kobe, Japan

OPEN ACCESS

Edited by:
Peter Schröder,
Helmholtz Center Munich German Research Center for Environmental Health, Germany

Reviewed by:
Karl-Josef Dietz,
Bielefeld University, Germany
Alessandra Francini,
Sant'Anna School of Advanced Studies, Italy

***Correspondence:**
Jun'ichi Mano
mano@yamaguchi-u.ac.jp
Yasuo Yamauchi
yamauchi@kobe-u.ac.jp

Specialty section:
This article was submitted to Plant Physiology, a section of the journal Frontiers in Plant Science

Received: 09 July 2018
Accepted: 29 March 2019
Published: 24 April 2019

Citation:
Mano J, Kanameda S, Kuramitsu R, Matsuura N and Yamauchi Y (2019) Detoxification of Reactive Carbonyl Species by Glutathione Transferase Tau Isozymes. Front. Plant Sci. 10:487. doi: 10.3389/fpls.2019.00487

Oxidative stimuli to living cells results in the formation of lipid peroxides, from which various aldehydes and ketones (oxylipin carbonyls) are inevitably produced. Among the oxylipin carbonyls, those with an α,β-unsaturated bond are designated as reactive carbonyl species (RCS) because they have high electrophilicity and biological activity. Plants have arrays of dehydrogenases and reductases to metabolize a variety of RCS that occur in the cells, but these enzymes are not efficient to scavenge the most toxic RCS (i.e., acrolein) because they have only low affinity. Two glutathione transferase (GST) isozymes belonging to the plant-specific Tau class were recently observed to scavenge acrolein with K_M values at a submillimolar level. This suggests that GST could also be involved in the defense system against RCS. We tested the activities of 23 Tau isozymes of *Arabidopsis thaliana* for five types of RCS, and the results revealed that 11 isozymes recognized either acrolein or 4-hydroxy-(*E*)-2-nonenal or both as a substrate(s). Such RCS-scavenging activities indicate the potential contribution of GST to RCS scavenging in plants, and they may account for the stress tolerance conferred by several Tau isozymes. RCS are therefore a strong candidate for endogenous substrates of plant GSTs.

Keywords: acrolein, lipid peroxide, oxidative stress, oxylipin, reactive electrophile species, redox signal

MAIN TEXT

Reactive Carbonyl Species (RCS) Are Signaling/Damaging Agents That Act Downstream of ROS

The production of reactive oxygen species (ROS) such as superoxide radical, hydrogen peroxide (H_2O_2), and singlet oxygen ($^1O_2$) intrinsically accompanies aerobic life. One important aspect of ROS *in vivo*, although not always noticed, is that ROS are often produced in the close vicinity of membranes, in association with chloroplastic and mitochondrial electron transport chains and the

plasma membrane-bound respiratory burst NADPH oxidase homologs (RBOHs). Membrane lipids are therefore constitutively oxidized due to the basal generation of ROS (Mène-Saffrané et al., 2007). The resulting lipid peroxides are relatively unstable and decompose or are metabolized to a variety of compounds called oxylipins, in which many types of aldehydes and ketones (oxylipin carbonyls) with different carbon chain lengths and extents of unsaturation are present. Carbonyl compounds are more reactive than corresponding alcohols and carboxylic acids, and the α,β-unsaturated carbonyls [reactive carbonyl species (RCS)] in particular have high electrophilicity and play critical biological roles in a range of functions from gene regulation to cytotoxicity (Esterbauer et al., 1991; Farmer and Mueller, 2013). Typical and well-studied RCS are acrolein, 4-hydroxy-(*E*)-2-nonenal (HNE), 4-oxo-(*E*)-2-nonenal, and malondialdehyde (MDA). The participation of RCS in oxidative injury and oxidative signaling in cells has been established for animals (Schopfer et al., 2011).

Reactive carbonyl species, e.g., acrolein and HNE, exhibit toxicity to plant cells and organelles when they are added exogenously (Millar and Leaver, 2000; Alméras et al., 2003; Mano et al., 2005, 2009). The occurrence of RCS in plant tissues was verified by extensive carbonyl analyses as follows. Yin et al. (2010) showed that tobacco roots contain dozens of carbonyls including several RCS, and they reported that the levels of some carbonyls were increased by the toxic level of aluminum ion. In leaves also, various carbonyls have been detected in tobacco (Mano et al., 2010), *Arabidopsis thaliana* (Yamauchi et al., 2012), and cyclamen (Kai et al., 2012), and their levels were increased by a high intensity of light (Mano et al., 2010), methyl viologen (Yamauchi et al., 2012), high salinity (Mano et al., 2014), injury (Matsui et al., 2012), and heat stress (Kai et al., 2012). **Table 1** summarizes the stress-related RCS and carbonyls identified in plants. The observed increases of RCS are ascribed to the increased levels of ROS by the stressors. These endogenously produced RCS were concluded to be responsible for the tissue damage because the extent of damage and the RCS levels correlated positively in transgenic plants that overexpress or lack an RCS-detoxifying enzyme (Mano et al., 2010; Yin et al., 2010; Yamauchi et al., 2012).

Reactive carbonyl species in plants also play signaling roles. Bate and Rothstein (1998) demonstrated that the exogenous addition of (*E*)-2-hexenal to *A. thaliana* plants induced a group of genes involved in defense against pathogens. The induced gene members vary by the RCS type (Alméras et al., 2003; Weber et al., 2004). Yamauchi et al. (2015) found that 2-alkenals of carbon chain length 4–8, when added as volatiles, induced heat-shock response genes in *A. thaliana*. Endogenous RCS produced upon an oxidative stimulus act as initiators of programmed cell death (PCD) in tobacco cultured cells (Biswas and Mano, 2015) by activating caspase-3-like protease (Biswas and Mano, 2016). In the stomata closure signaling of abscisic acid (ABA), the ROS production in guard cells is followed by increases in RCS, and the genetic suppression of RCS inhibited the stomata response to ABA (Islam et al., 2016). Together these observations, compiled over the past decade, indicate that RCS are endogenous agents that mediate ROS stimuli to downstream responses.

Enzymatic Regulation of RCS

Dozens of oxylipin carbonyls in plants (**Table 1**) have a broad range of reactivity and thus different toxicity and signaling effects (Mano et al., 2009; Biswas and Mano, 2015). Plants have three types of oxidoreductases for metabolizing carbonyls: (i) aldehyde dehydrogenase (ALDH) to oxidize an aldehyde to a carboxylic acid with NAD^+, (ii) aldehyde reductase to reduce an aldehyde or a ketone to a corresponding alcohol with NAD(P)H; two types of proteins, one belonging to aldo-keto reductase (AKR) family and the other to short-chain dehydrogenase/reductase family, can catalyze this reaction (Yamauchi et al., 2011), and (iii) 2-alkenal reductase (AER) and alkenal/one oxidoreductase (AOR) to reduce an RCS at the carbonyl-conjugated C-C double bond with NAD(P)H (Mano et al., 2002, 2005; Yamauchi et al., 2011). These enzyme classes, respectively, have multiple isozymes, and each isozyme shows distinct substrate specificity. **Table 1** summarizes the plant isozymes of these enzyme classes and reported substrates. Some of these isozymes have been shown to detoxify carbonyls *in planta*; their overexpression in transgenic plants reduced the carbonyl levels and conferred tolerance against several types of environmental stressors (reviewed by Mano, 2012).

Acrolein Is Scavenged by Glutathione Transferase

Among the RCS, acrolein (or 2-propenal), the C3 alkenal, is the most highly reactive and toxic compound (Esterbauer et al., 1991). It can inactivate photosynthetic machinery (Mano et al., 2009; Shimakawa et al., 2013) and induce PCD (Biswas and Mano, 2016). As seen in **Table 1**, many reductases recognize acrolein as a substrate, but they have higher affinity to longer-chain aldehydes and show only low affinity to acrolein, i.e., K_M values > 2 mM (Mano et al., 2017).

Acrolein reacts with the reduced form of glutathione (GSH) very rapidly (Esterbauer et al., 1975), and certain isozymes of glutathione transferase (GST) can catalyze the conjugation of acrolein with GSH. Human GST isozymes Alpha1, Mu1, and Pi1 recognize acrolein as a substrate (Berhane et al., 1994). Several plant GSTs have been known to react with RCS; for example, GST B1/B2 from sorghum recognizes HNE as a substrate (Gronwald and Plaisance, 1998). BI-GST and four Tau class isozymes from tomato reacted with (*E*,*E*)-2,4-nonadienal, and so did two isozymes from grapevine with (*E*)-2-hexenal (Kobayashi et al., 2011). We have investigated acrolein-scavenging GST activity and detected it in *A. thaliana*, spinach, rice, and Chinese cabbage. We then isolated a Tau isozyme from spinach for scavenging acrolein with the K_M value 93 μM for acrolein. A homologous GST isozyme Tau19 from *A. thaliana* (AtGSTU19) also scavenged acrolein with the K_M value 30 μM (Mano et al., 2017). The enzymatic scavenging of acrolein in plants had previously been attributed only to AER and AKR reactions (**Table 1**), but these GST Tau (GSTU) isozymes appear to be physiologically more

TABLE 1 | RCS and related carbonyls that are present in plants, and the plant enzymes that metabolize the carbonyls.

Compound name	Structure	Stimulus/ stressor	Compatible enzyme			
			ALDH	AKR	AER	GST
Acrolein (propenal)		H_2O_2, MV, HL, heat, NaCl, Al, ABA		AtChlAKR, AKR4C9 AKR4C10, CHR Slr0942, Slr1192	AER CsAOR AtAOR	GST-Acr AtGSTUs*
Malondialdehyde		H_2O_2, NaCl, Al		AKR4C9, MsALR		
Crotonaldehyde (*E*)-2-butenal)		MV, NaCl, Al		AtChlAKR, CsAOR AtAOR, Slr0942 Slr1192	AER	AtGSTUs*
Methylvinylketone (3-butene-2-one)		heat			AER AtAOR CsAOR	
Methacrolein						AtGSTU19
(*E*)-2-Pentenal		HL, ABA		AtChlADR AtCytADR AtChlAKR, CHR	AER	
3-Penten-2-one		MV			AER CsAOR AtAOR	
(*E*)-2-Hexenal		HL, NaCl, heat, injury	ALDH3H1 ALDH3I1	AtChlADR AtCytADR AtChlAKR, AKR4C9 CHR	AER	GST (grapevine) AtGSTU25*
HHE		H_2O_2, NaCl, Al, ABA			AER	
4-Oxo-(*E*)-2-Hexenal		injury				
(*E*)-2-Heptenal		Al		CHR		
(*E*)-2-Octenal		MV		CHR		
(*E*)-2-Nonenal		HL		AtChlADR AtCytADR AtChlAKR, CHR	AER	
HNE		H_2O_2, Al, ABA		AKR4C9	AER	GSTB1/B2 (sorghum) AtGSTUs*
(*E*,*E*)-2,4-Nonadienal	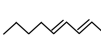					BI-GST (tomato)
Formaldehyde	HCHO	Al, ABA	ALDH			
Acetaldehyde		H_2O_2, Al, ABA	ALDH			
Propionaldehyde		H_2O_2, ABA		AtChlADR AtCytADR AtChlAKR, CHR Slr0942, Slr1192		
Butyraldehyde			ALDH	AtChlADR AtCytADR AtChlAKR, CHR		
n-Pentanal			ALDH	CHR		
n-Hexanal		H_2O_2, Al	ALDH	CHR		
(*Z*)-3-Hexenal		Al, ABA, injury		AtChlADR, AtCytADR, AtChlAKR, CHR		
n-Heptanal		H_2O_2, Al	ALDH	CHR		
n-Octanal	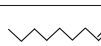	Al		CHR		

(Continued)

TABLE 1 | Continued

Compound name	Structure	Stimulus/ stressor	Compatible enzyme			
			ALDH	AKR	AER	GST
n-Nonanal	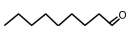			CHR		
Methylglyoxal		NaCl		AKR4C9, AKR4C10 AtChlADR AtCytADR AtChlAKR, Slr0315 Slr0942, Slr1192		

**This study. Compound names in boldface are an RCS. 'Stimulus/stressor' indicates the exogenous stressors and endogenous stimuli reported to increase the level of each carbonyl in plants (see the main text). Compatible enzymes represent isozymes for which a catalytic activity for the corresponding carbonyl has been reported. References for enzyme activity: AER (Mano et al., 2002, 2005), AKR4C9 (Simpson et al., 2009; Saito et al., 2013), AKR4C10 (Saito et al., 2013), ALDH (Asker and Davies, 1985), ALDH3H1 and ALDH3I1 (Stiti et al., 2011), AtAOR, AtChlAKR, AtChlADR, and AtCytADR (Yamauchi et al., 2011), AtGSTU19 (Mano et al., 2017), BI-GST (Kobayashi et al., 2011), CHR (Tanaka et al., 2018), MsALR (Oberschall et al., 2000), CsAOR (Yamauchi et al., 2011), GST-Acr (Mano et al., 2017), GST B1/B2 (Gronwald and Plaisance, 1998), GST from grapevine (Kobayashi et al., 2011), and Slr0545, Slr0942, Slr1192 and Slr1503 (Shimakawa et al., 2013). Slashed boxes, No data is available.*

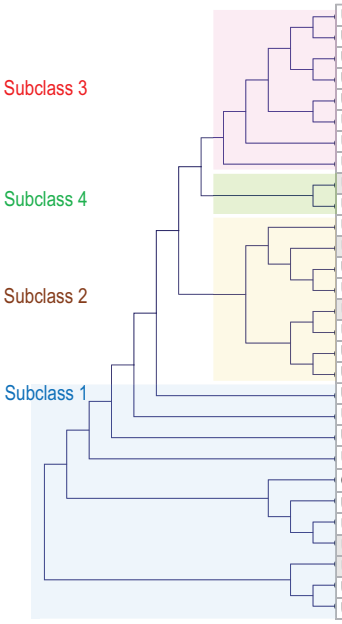

	Specific activity (nkat/mg)					
	acrolein	croton-aldehyde	methacrolein	(*E*)-2-hexenal	HNE	CDNB
U1	<0.01	<0.01	<0.01	<0.01	<0.01	8.8
U2	0.24	<0.01	<0.01	<0.01	<0.01	12.1
U3	0.72	<0.01	<0.01	<0.01	0.94	2.4
U4	15.0	<0.01	<0.01	<0.01	<0.01	275
U5	2.4	0.83	<0.01	<0.01	8.2	17.9
U6	<0.01	<0.01	<0.01	<0.01	<0.01	9.5
U8	<0.01	<0.01	<0.01	<0.01	<0.01	12.2
U7	<0.01	<0.01	<0.01	<0.01	<0.01	10.8
U9	-	-	-	-	-	-
U10	<0.01	<0.01	<0.01	<0.01	<0.01	4.6
U11	<0.01	<0.01	<0.01	<0.01	<0.01	<0.01
U12	-	-				-
U13	0.81	<0.01	<0.01	<0.01	<0.01	3.8
U14	<0.01	<0.01	<0.01	<0.01	<0.01	0.24
U15	-	-				-
U16	<0.01	<0.01	<0.01	<0.01	<0.01	84.0
U17	5.2	<0.01	<0.01	<0.01	39.0	101.7
U18	0.62	<0.01	<0.01	<0.01	21.2	36.5
U28	8.8	<0.01	<0.01	<0.01	1.0	286
U27	<0.01	<0.01	<0.01	<0.01	<0.01	414
U26	<0.01	<0.01	<0.01	<0.01	9.5	1.3
U23	<0.01	<0.01	<0.01	<0.01	<0.01	<0.01
GST-Acr	28.3	<0.01	<0.01	-	1.2	86.7
U19	50.7	1.20	9.0	<0.01	<0.01	151.7
U20	<0.01	<0.01	<0.01	<0.01	<0.01	30.2
U22	-	-	-	-	-	-
U21	-	-	-	-	-	-
U24	34.2	<0.01	<0.01	<0.01	<0.01	158
U25	<0.01	0.47	<0.01	1.41	<0.01	58.7

FIGURE 1 | Substrate specificity of AtGSTU isozymes and spinach GST-Acr. Gray rows represent the isozymes that were not recovered as soluble protein. The assay conditions are described in the "Materials and Methods" section. The GST-Acr and AtGSTU19 data are from our earlier study (Mano et al., 2017). The isozymes are arranged in the order of the phylogenetic tree, which was constructed on the amino acid sequence similarity by the neighbor-joining method using the multiple sequence alignment software Clustal W 2.0 (Larkin et al., 2007). The amino acid sequence of the spinach GST-Acr was deduced from the assembled RNA sequence (Mano et al., 2017).

relevant because their K_M values are close to the physiological range of acrolein.

Eleven AtGSTU Isozymes Recognize RCS as Substrates

GST Tau is a plant-specific class and is the largest group of GST isozymes in angiosperms, gymnosperms, and ferns (Flova, 2003; Monticolo et al., 2017). GSTU isozymes have important roles in plants' defense against environmental stress. The overexpression of a GSTU gene from the extreme halophyte *Salicornia brachiata* (Jha et al., 2011) in tobacco conferred salt tolerance. *A. thaliana* plants overexpressing rice *OsGSTU4* gene (Sharma et al., 2014), *AtGSTU17* gene (Chen et al., 2012), and *AtGSTU19* gene (Xu et al., 2016) showed more tolerance to salinity and oxidative stress than the wild type. GSTU isozymes therefore constitute part of the anti-oxidative defense, but the underlying biochemical mechanism remains unclear because the physiologically relevant

substrates of GSTU have not been elucidated. The efficient acrolein-scavenging activity observed in the two GSTU isozymes described above suggested to us the possibility that GSTU isozymes can be counted as RCS-scavenging enzymes. To test this possibility, we determined the RCS-scavenging activity of AtGSTU isozymes (**Figure 1**).

Complementary DNA of 28 AtGSTU isogenes was cloned and expressed in *Escherichia coli*, and pure recombinant proteins were obtained (see Materials and Methods). Recombinant AtGSTU9, AtGSTU12, AtGSTU15, AtGSTU21, and AtGSTU22 proteins were not recovered as the soluble form. The isozymes obtained as soluble proteins (23 in total) were first tested for activity for a universal GST substrate 1-chloro-2,4-dinitrobenzene (CDNB). Recombinant AtGSTU11 and AtGSTU23 proteins were incompetent, and the other 21 showed the CDNB-conjugating activity.

We then examined the 23 isozymes for the activity to scavenge five types of RCS, i.e., acrolein, crotonaldehyde, methacrolein, (*E*)-2-hexenal, and HNE (**Figure 1**). Acrolein-scavenging activity was detected (higher than 0.01 nkat mg^{-1}) in the following ten isozymes: AtGSTU2, AtGSTU3, AtGSTU4, AtGSTU5, AtGSTU13, AtGSTU17, AtGSTU18, AtGSTU19, AtGSTU24, and AtGSTU28. The specific activity of these isozymes ranged from 0.24 nkat mg^{-1} (AtGSTU2) to 50.7 nkat mg^{-1} (AtGSTU19). These results show that acrolein is a common endogenous substrate of GSTU.

For crotonaldehyde, three isozymes (AtGSTU5, AtGSTU19, and AtGSTU25) showed significant activity. For methacrolein, only AtGSU19 and for (*E*)-2-hexenal only AtGSTU25 showed the activity. For HNE, six isozymes (AtGSTU3, AtGSTU5, AtGST17, AtGSTU18, AtGSTU26, and ATGSTU28) exhibited significant activity. In total, at least 11 of the 28 isozymes showed RCS-scavenging activity.

GST Tau isozymes are grouped into four subclasses based on their amino acid sequence similarity (Monticolo et al., 2017) as indicated in **Figure 1**. RCS-scavenging activity was identified in the isozymes in subclasses 1, 2, and 3, and these three subclasses also have RCS-incompatible isozymes (**Figure 1**). This suggests that the acquisition of the RCS-recognizing ability during the molecular evolution of AtGSTUs occurred multiple times independently. An alternative possibility is that the common ancestor of AtGSTU had the RCS-scavenging activity and it was lost during the molecular evolution.

The Physiological Relevance of the RCS-Scavenging Activity of GST

Among these 11 RCS-compatible isozymes, AtGSTU13 and AtGSTU19 are expressed in almost all tissues except the male organ (**Supplementary Table S2**, data extracted from Dixon et al., 2010). In shoot tissues, AtGSTU1, AtGSTU17, and AtGSTU18 are strongly expressed, and in root tissues, AtGSTU2, AtGSTU4, AtGSTU24, and AtGSTU28 are expressed. AtGSTU18 and AtGSTU19 are constitutively expressed. In particular, AtGSTU19 is the most abundant GSTU isozyme in *A. thaliana* (Dixon and Edwards, 2009) and appears to be a key isozyme to protect the whole plant body from the toxicity of RCS, especially acrolein. Other isozymes, in contrast, are induced by various stressors such as salt, high osmolarity, and UV-B [**Supplementary Table S2**, from AtGenExpress database (Kilian et al., 2007)], which commonly increase the intracellular levels of ROS. Notably, two isozymes (AtGSTU17 and AtGSTU19) show relatively high RCS-scavenging activities, and they conferred stress tolerance to transgenic plants (Chen et al., 2012; Xu et al., 2016). The physiological function of GSTUs as RCS scavengers can be verified by analyses of the RCS levels in these samples.

We reported the acrolein-scavenging GST activity in leaf extracts of *A. thaliana*, *Brassica rapa* var. *pekinensis* (both are Brassicales), *Oryza sativa* (Poales), and *Spinacia oleracea* (Caryophyllales), ranging from 120 to 255 nmol/min/mg protein, as determined by the HPLC analysis of the acrolein decrease rate (Mano et al., 2017). We here detected the activity in four more species (values indicate the activity in nmol/min/mg protein): extracts from leaves of *Allium cepa* (Liliales), 185; *Apium graveolens* var. *dulce* (Apiales), 148; *Glebionis coronaria* (Asterales), 208, and green bell fruits of *Capsicum annuum* var. *grossum* (Solanales), 155. The occurrence of the activity in all tested species (seven orders of angiosperms) supports the importance of acrolein-scavenging GST activity in plants.

Conclusion

It was revealed that at least 11 of the 28 GSTU isozymes in *A. thaliana* can recognize RCS as substrates, indicating that RCS are important endogenous substrates of GSTU. Some members of the RCS-compatible GSTU isozymes are expressed in various tissues constitutively, and others are induced by a variety of environmental stressors. Acrolein-scavenging GST activity was observed in a broad range of angiosperms at similar levels of specific activity. These findings demonstrate that RCS-scavenging GST activity is a significant element constituting the anti-oxidative defense in plants.

MATERIALS AND METHODS

The cDNA Cloning of AtGSTUs, Expression, and Purification of Recombinant Proteins

Recombinant AtGSTU19 with an *N*-terminal poly(His) tag was obtained as described (Mano et al., 2017). For other isogenes, the cDNA of the corresponding open reading frame (ORF) was obtained by polymerase chain reaction (PCR)-based cloning. Briefly, total RNA was prepared from 3-week-old *A. thaliana* using an RNeasy Plant Mini Kit (Qiagen, Hilden, Germany), and then cDNA was synthesized by a ReverTra Ace Kit (Toyobo, Osaka, Japan). The ORF of the GSTU was amplified by PCR using proof-reading KOD DNA polymerase (Toyobo) and the primers listed in **Supplementary Table S1**. Amplified PCR products were subcloned into pMD19 (Takara Bio, Shiga, Japan), and the identity of subcloned cDNA was verified by DNA sequencing. The confirmed ORF of

the GSTU was ligated into the multicloning site in pASK15-plus expression vector (IBA, Göttingen, Germany), which produces the recombinant GSTU comprising an *N*-terminal streptavidin tag.

Escherichia coli BL21 cells transformed with the expression plasmid were grown at 37°C in LB broth containing 100 μg ml^{-1} ampicillin. Expression of the transgene was induced with anhydrotetracycline, and the recombinant protein was purified via affinity chromatography using Strep-Tactin Sepharose (IBA) according to the manufacturer's instruction. The purity of the GSTU was verified by sodium dodecyl sulfate-polyacrylamide gel electrophoresis (SDS–PAGE). The purified GSTU fraction was dialyzed against 10 mM Tris–HCl, pH 7.5, and finally mixed with an equal volume of 80%(v/v) glycerol and stored at −20°C until use.

The Assay Conditions for Each Substrate

CDNB: 100 mM potassium phosphate buffer, pH 6.5, 1.0 mM GSH, and 1.0 mM CDNB. The activity was monitored as the rate of absorbance increase at 340 nm (extinction coefficient 9.6 mM^{-1} cm^{-1}). Acrolein, methacrolein, and (*E*)-2-hexenal: 10 mM MES-NaOH, pH 6.0, 0.1 mM GSH and 0.1 mM aldehyde [for (*E*)-2-hexenal, 0.05 mM]. Absorbance decreases at 215 nm (15.0 mM^{-1} cm^{-1}) for acrolein, 220 nm (10.96 mM^{-1} cm^{-1}) for methacrolein, and 224 nm (19.5 mM^{-1} cm^{-1}) for (*E*)-2-hexenal. Crotonaldehyde and HNE: 100 mM Na-phosphate buffer, pH 7.5, 0.1 mM GSH, and 0.1 mM aldehyde. Absorbance decreases at 240 nm (10.7 mM^{-1} s^{-1}) for crotonaldehyde and 221 nm (13.1 mM^{-1} cm^{-1}) for HNE. The rate of non-enzymatic conjugation was subtracted as a background.

AUTHOR CONTRIBUTIONS

JM and YY conceived the project and wrote the manuscript with contributions from all of the authors. NM performed the overexpression and purification of proteins. SK and RK analyzed the GST activity.

FUNDING

This work was supported by the Japan Society for the Promotion of Science (JSPS) KAKENHI, grant no. 17H03700.

SUPPLEMENTARY MATERIAL

The Supplementary Material for this article can be found online at: https://www.frontiersin.org/articles/10.3389/fpls.2019.00487/full#supplementary-material

REFERENCES

Alméras, E., Stolz, S., Vollenweider, S., Reymond, P., Mène-Saffrané, L., and Farmer, E. E. (2003). Reactive electrophile species activate defense gene expression in *Arabidopsis*. *Plant J.* 34, 205–216. doi: 10.1046/j.1365-313x.2003.01718.x

Asker, H., and Davies, D. D. (1985). Mitochondrial aldehyde dehydrogenase from higher plants. *Phytochemistry* 24, 689–693. doi: 10.1016/s0031-9422(00)84877-3

Bate, N. J., and Rothstein, S. J. (1998). C6-volatiles derived from the lipoxygenase pathway induce a subset of defence-related genes. *Plant J.* 16, 561–569. doi: 10.1046/j.1365-313x.1998.00324.x

Berhane, K., Widersten, M., Engström, Å, Kozarich, J. W., and Mannervik, B. (1994). Detoxication of base propenals and other alpha,beta-unsaturated aldehyde products of radical reactions and lipid peroxidation by human glutathione transferases. *Proc. Natl. Acad. Sci. U.S.A.* 91, 1480–1484. doi: 10.1073/pnas.91.4.1480

Biswas, M. S., and Mano, J. (2015). Lipid peroxide-derived short-chain carbonyls mediate hydrogen peroxide-induced and salt-induced programmed cell death in plants. *Plant Physiol.* 168, 885–898. doi: 10.1104/pp.115.256834

Biswas, M. S., and Mano, J. (2016). Reactive carbonyl species activate caspase-3-like protease to initiate programmed cell death in plants. *Plant Cell Physiol.* 57, 1432–1442.

Chen, J.-H., Jiang, H.-W., Hsieh, E.-J., Chen, H.-Y., Chien, C.-T., Hsieh, H.-L., et al. (2012). Drought and salt stress tolerance of an *Arabidopsis* gluatathione S-transferase U17 knockout mutant are attributed to the combine effect of glutathione and abscisic acid. *Plant Physiol.* 158, 340–351. doi: 10.1104/pp.111.181875

Dixon, D. P., and Edwards, R. (2009). Selective binding of glutathione conjugates of fatty acid derivatives by plant glutathione transferases. *J. Biol. Chem.* 284, 21249–21256. doi: 10.1074/jbc.M109.020107

Dixon, D. P., Skipsey, M., and Edwards, R. (2010). Roles for glutathione transferases in plant secondary metabolism. *Phytochemistry* 71, 338–350. doi: 10.1016/j.phytochem.2009.12.012

Esterbauer, H., Schaur, R., and Zollner, J. H. (1991). Chemistry and biochemistry of 4-hydroxynonenal, malonaldehyde and related aldehydes. *Free Radic. Biol. Med.* 11, 81–128. doi: 10.1016/0891-5849(91)90192-6

Esterbauer, H., Zollner, J., and Scholz, N. (1975). Reaction of glutathione with conjugated carbonyls. *Z. Naturforsch.* 30, 466–473. doi: 10.1515/znc-1975-7-808

Farmer, E. E., and Mueller, M. J. (2013). ROS-mediated lipid peroxidation and RES-activated signaling. *Annu. Rev. Plant Biol.* 64, 429–450. doi: 10.1146/annurev-arplant-050312-120132

Flova, C. (2003). The plant glutathione transferase gene family: genomic structure, functions, expression and evolution. *Physiol. Plant* 119, 469–479. doi: 10.1046/j.1399-3054.2003.00183.x

Gronwald, J. W., and Plaisance, K. L. (1998). Isolation and characterization of glutathione S-transferase isozymes from sorghum. *Plant Physiol.* 117, 877–892. doi: 10.1104/pp.117.3.877

Islam, M. M., Ye, W., Matsushima, D., Munemasa, S., Okuma, E., Nakamura, Y., et al. (2016). Reactive carbonyl species mediate abscisic acid signaling in guard cells. *Plant Cell Physiol.* 57, 2552–2563. doi: 10.1093/pcp/pcw166

Jha, B., Sharma, A., and Misra, A. (2011). Expression of SbGSTU (tau class glutathione S-transferase) gene isolated from *Salicornia brachiata* in tobacco for salt tolerance. *Mol. Biol. Rep.* 38, 4823–4832. doi: 10.1007/s11033-010-0625-x

Kai, H., Hirashima, K., Matsuda, O., Ikegami, H., Winkelmann, T., Nakahara, T., et al. (2012). Thermotolerant cyclamen with reduced acrolein and methyl vinyl ketone. *J. Exp. Bot.* 63, 4143–4150. doi: 10.1093/jxb/ers110

Kilian, J., Whitehead, D., Horak, J., Wanke, D., Weinl, S., Batistic, O., et al. (2007). The AtGenExpress global stress expression data set: protocols, evaluation and model data analysis of UV-B light, drought and cold stress responses. *Plant J.* 50, 347–363. doi: 10.1111/j.1365-313x.2007.03052.x

Kobayashi, H., Takase, H., Suzuki, Y., Tanzawa, F., Tanaka, R., Fujita, K., et al. (2011). Environment stress enhances biosynthesis of flavor precursors, S-3-(hexan-1-ol)-glutathione and S-3-(hexan-1-ol) L-cysteine, in grapevine through glutathione S-transferase activation. *J. Exp. Bot.* 62, 1325–1336. doi: 10.1093/jxb/erq376

Larkin, M. A., Blackshields, G., Brown, N. P., Chenna, R., McGettingan, P. A., McWilliam, H., et al. (2007). Clustal W and Clustal X version 2.0. *Bioinformatics* 23, 2947–2948. doi: 10.1093/bioinformatics/btm404

Mano, J. (2012). Reactive carbonyl species: Their production from lipid peroxides, action in environmental stress, and the detoxification mechanism. *Plant Physiol. Biochem.* 59, 90–97. doi: 10.1016/j.plaphy.2012.03.010

Mano, J., Belles-Boix, E., Babiychuk, E., Inzé, D., Hiraoka, E., Takimoto, K., et al. (2005). Protection against photooxidative injury of tobacco leaves by 2-alkenal reductase. detoxication of lipid peroxide-derived reactive carbonyls. *Plant Physiol.* 139, 1773–1783. doi: 10.1104/pp.105.070391

Mano, J., Ishibashi, A., Muneuchi, H., Morita, C., Sakai, H., Biswas, S., et al. (2017). Acrolein-detoxifying isozymes of glutathione transferase in plants. *Planta* 245, 255–264. doi: 10.1007/s00425-016-2604-5

Mano, J., Khorobrykh, S., Matsui, K., Iijima, Y., Sakurai, N., Suzuki, H., et al. (2014). Acrolein is formed from trienoic fatty acids in chloroplasts: A targeted metabolomics approach. *Plant Biotechnol.* 31, 535–544.

Mano, J., Miyatake, F., Hiraoka, E., and Tamoi, M. (2009). Evaluation of the toxicity of stress-related aldehydes to photosynthesis in chloroplasts. *Planta* 230, 639–648. doi: 10.1007/s00425-009-0964-9

Mano, J., Tokushige, K., Mizoguchi, H., and Khorobrykh, S. A. (2010). Accumulation of lipid peroxide-derived, toxic α,β-unsaturated aldehydes (E)-2-pentenal, acrolein and (E)-2-hexenal in leaves under photoinhibitory illumination. *Plant Biotechnol.* 27, 193–197. doi: 10.5511/plantbiotechnology.27.193

Mano, J., Torii, Y., Hayashi, S., Takimoto, K., Matsui, K., Nakamura, K., et al. (2002). The NADPH:quinone oxidoreductase P1-(-crystallin in *Arabidopsis* catalyzes the α,β-hydrogenation of 2-alkenals: detoxication of the lipid peroxide-derived reactive aldehydes. *Plant Cell Physiol.* 43, 1445–1455. doi: 10.1093/pcp/pcf187

Matsui, K., Sugimoto, K., Mano, J., Ozawa, R., and Takabayashi, J. (2012). Differential metabolism of green leaf volatiles in injured and intact parts of a wounded leaf meet distinct ecophysiological requirements. *PLoS One* 7:e36433. doi: 10.1371/journal.pone.0036433

Mène-Saffrané, L., Davoine, C., Stolz, S., Majcherczyk, P., and Farmer, E. E. (2007). Genetic removal of tri-unsaturated fatty acids suppresses developmental and molecular phenotypes of an *Arabidopsis* tocopherol-deficient mutant. *J. Biol. Chem.* 282, 35749–35756. doi: 10.1074/jbc.m706838200

Millar, A. H., and Leaver, C. J. (2000). The cytotoxic lipid peroxidation product, 4-hydroxy-2-nonenal, specifically inhibits decarboxylating dehydrogenases in the matrix of plant mitochondria. *FEBS Lett.* 481, 117–121. doi: 10.1016/s0014-5793(00)01976-1

Monticolo, F., Colantuono, C., and Chusano, M. L. (2017). Shaping the evolutionary tree of green plants: Evidence from the GST family. *Sci. Rep.* 7:14363. doi: 10.1038/s41598-017-14316-w

Oberschall, A., Deák, M., Török, K., Sass, L., Vass, I., Kovács, I., et al. (2000). A novel aldose/aldehyde reductase protects transgenic plants against lipid peroxidation under chemical and drought stresses. *Plant J.* 24, 437–446. doi: 10.1111/j.1365-313x.2000.00885.x

Saito, R., Shimakawa, G., Nishi, A., Iwamoto, T., Sakamoto, K., Yamamoto, H., et al. (2013). Functional analysis of the AKR4C subfamily of *Arabidopsis thaliana*: model structures, substrate specificity, acrolein toxicity, and responses to light and [CO2]. *Biosci. Biotechnol. Biochem.* 77, 2038–2045. doi: 10.1271/bbb.130353

Schopfer, F. J., Cipollina, C., and Freeman, B. A. (2011). Formation and signaling actions of electrophilic lipids. *Chem. Rev.* 111, 5997–6021. doi: 10.1021/cr200131e

Sharma, R., Sahoo, A., Devendran, R., and Jain, M. (2014). Over-expression of a rice Tau class glutathione S-transferase gene improves tolerance to salinity and oxidative stresses in *Arabidopsis*. *PLoS One* 9:e92900. doi: 10.1371/journal.pone.0092900

Shimakawa, G., Iwamoto, T., Mabuchi, T., Saito, R., Yamamoto, H., Amako, K., et al. (2013). Acrolein, an α,β-unsaturated carbonyl, inhibits both growth and PSII activity in the cyanobacterium *Synechocystis* sp. PCC 6803. *Biosci. Biotechnol. Biochem.* 77, 1655–1660. doi: 10.1271/bbb.130186

Simpson, P. J., Tantiadapitak, C., Reed, A. M., Mather, O. C., Bunce, C. M., White, S. A., et al. (2009). Characterization of two novel aldo-keto reductases from *Arabidopsis*: Expression patterns, broad substrate specificity, and an open active-site structure suggest a role in toxicant metabolism following stress. *J. Mol. Biol.* 392, 465–480. doi: 10.1016/j.jmb.2009.07.023

Stiti, N., Adewale, I. O., Petersen, J., Bartels, D., and Kirch, H.-H. (2011). Engineering the nucleotide coenzyme specificity and sulfhydryl redox sensitivity of two stress-responsive aldehyde dehydrogenase isoenzymes of *Arabidopsis thaliana*. *Biochem. J.* 434, 459–471. doi: 10.1042/BJ20101337

Tanaka, T., Ikeda, A., Shiojiri, K., Ozawa, R., Shiki, K., Nagai-Kunihiro, N., et al. (2018). Identification of a hexenal reductase that modulates the composition of green leaf volatiles. *Plant Physiol.* 178, 552–564. doi: 10.1104/pp.18.00632

Weber, H., Chételat, A., Reymond, P., and Farmer, E. E. (2004). Selective and powerful stress gene expression in *Arabidopsis* in response to malondialdehyde. *Plant J.* 37, 877–888. doi: 10.1111/j.1365-313x.2003.02013.x

Xu, J., Tian, Y.-S., Xing, X.-J., Peng, R.-H., Zhu, B., Gao, J.-J., et al. (2016). Over-expression of AtGSTU19 provides tolerance to salt, drought and methyl viologen stresses in *Arabidopsis*. *Physiol. Plant.* 156, 164–175. doi: 10.1111/ppl.12347

Yamauchi, Y., Hasegawa, A., Mizutani, M., and Sugimoto, Y. (2012). Chloroplastic NADPH dependent alkenal/one oxidoreductase contributes to the detoxification of reactive carbonyls produced under oxidative stress. *FEBS Lett.* 586, 1208–1213. doi: 10.1016/j.febslet.2012.03.013

Yamauchi, Y., Hasegawa, A., Taninaka, A., Mizutani, M., and Sugimoto, Y. (2011). NADPH-dependent reductases involved in the detoxification of reactive carbonyls in plants. *J. Biol. Chem.* 286, 6999–7009. doi: 10.1074/jbc.M110.202226

Yamauchi, Y., Kunishima, M., Mizutani, M., and Sugimoto, Y. (2015). Reactive short-chain leaf volatiles act as powerful inducers of abiotic stress-related gene expression. *Sci. Rep.* 5:8030. doi: 10.1038/srep08030

Yin, L., Mano, J., Wang, S., Tsuji, W., and Tanaka, K. (2010). The involvement of lipid peroxide-derived aldehydes in aluminum toxicity of tobacco roots. *Plant Physiol.* 152, 1406–1417. doi: 10.1104/pp.109.151449

Conflict of Interest Statement: The authors declare that the research was conducted in the absence of any commercial or financial relationships that could be construed as a potential conflict of interest.

frontiers in Plant Science

REVIEW
published: 22 May 2019
doi: 10.3389/fpls.2019.00608

Functional, Structural and Biochemical Features of Plant Serinyl-Glutathione Transferases

Elodie Sylvestre-Gonon[1], Simon R. Law[2], Mathieu Schwartz[3], Kevin Robe[4], Olivier Keech[2], Claude Didierjean[3], Christian Dubos[4], Nicolas Rouhier[1] and Arnaud Hecker[1]**

[1] Interactions Arbres-Microorganismes, Institut National de la Recherche Agronomique, Université de Lorraine, Nancy, France, [2] Department of Plant Physiology, Umeå Plant Science Centre, Umeå University, Umeå, Sweden, [3] Centre National de la Recherche Scientifique, Cristallographie, Résonance Magnétique et Modélisations, Université de Lorraine, Nancy, France, [4] Biochimie et Physiologie Moléculaire des Plantes (BPMP), INRA, CNRS, SupAgro-M, Université de Montpellier, Montpellier, France

Glutathione transferases (GSTs) belong to a ubiquitous multigenic family of enzymes involved in diverse biological processes including xenobiotic detoxification and secondary metabolism. A canonical GST is formed by two domains, the N-terminal one adopting a thioredoxin (TRX) fold and the C-terminal one an all-helical structure. The most recent genomic and phylogenetic analysis based on this domain organization allowed the classification of the GST family into 14 classes in terrestrial plants. These GSTs are further distinguished based on the presence of the ancestral cysteine (Cys-GSTs) present in TRX family proteins or on its substitution by a serine (Ser-GSTs). Cys-GSTs catalyze the reduction of dehydroascorbate and deglutathionylation reactions whereas Ser-GSTs catalyze glutathione conjugation reactions and eventually have peroxidase activity, both activities being important for stress tolerance or herbicide detoxification. Through non-catalytic, so-called ligandin properties, numerous plant GSTs also participate in the binding and transport of small heterocyclic ligands such as flavonoids including anthocyanins, and polyphenols. So far, this function has likely been underestimated compared to the other documented roles of GSTs. In this review, we compiled data concerning the known enzymatic and structural properties as well as the biochemical and physiological functions associated to plant GSTs having a conserved serine in their active site.

Keywords: photosynthetic organisms, phylogeny, structure, glutathione transferases, ligandin property, secondary metabolism, xenobiotic detoxification

OPEN ACCESS

Edited by:
Els Jm Van Damme,
Ghent University, Belgium

Reviewed by:
Yonghai Luo,
Fujian Agriculture and Forestry University, China
Hsu-Liang Hsieh,
National Taiwan University, Taiwan

****Correspondence:***
Nicolas Rouhier
nicolas.rouhier@univ-lorraine.fr
Arnaud Hecker
arnaud.hecker@univ-lorraine.fr

Specialty section:
This article was submitted to Plant Physiology, a section of the journal Frontiers in Plant Science

Received: *04 February 2019*
Accepted: *25 April 2019*
Published: *22 May 2019*

Citation:
Sylvestre-Gonon E, Law SR, Schwartz M, Robe K, Keech O, Didierjean C, Dubos C, Rouhier N and Hecker A (2019) Functional, Structural and Biochemical Features of Plant Serinyl-Glutathione Transferases. Front. Plant Sci. 10:608. doi: 10.3389/fpls.2019.00608

INTRODUCTION

Glutathione transferases (GSTs), formerly glutathione S-transferases, constitute a ubiquitous multigenic superfamily of enzymes that conjugate the tripeptide glutathione (γ-Glu-Cys-Gly) on a broad range of molecules. They catalyze the nucleophilic attack of reduced glutathione (GSH) on the electrophilic centers of these molecules. The omnipresence of these enzymes in all types of organisms highlights an ancient origin as well as fundamental functions preserved during evolution. GSTs were discovered in the early 1960s through their GSH-conjugating activity in cellular extracts from rat liver incubated with sulfobromophthalein, chloronitrobenzenes or

halogenated aromatic molecules (Booth et al., 1961; Combes and Stakelum, 1961). Later on, this conjugating activity was identified from plant extracts (sorghum and corn) using herbicides like atrazine or triazine derivatives (Frear and Swanson, 1970; Lamoureux et al., 1970). The interest for these GSH-conjugation reactions in plants was high in the 1980s, particularly concerning the enzymatic properties of cereal GSTs in connection with the detoxification of herbicides (Shah et al., 1986; Wiegand et al., 1986). Accordingly, GSTs are generally strongly induced in response to biotic and abiotic stresses, which coincides with cellular roles in primary and secondary metabolisms, in stress tolerance or cell signaling, and in xenobiotic detoxification by acting as phase II enzymes (Jakoby, 1978; Wiegand et al., 1986; Gonzalez et al., 2018). During the detoxification process, GSTs, which represent the most important classes of conjugating enzymes, conjugate phase I-activated molecules (or toxic molecules that are already activated) with GSH. Conjugation reactions are only performed by specific GST members, i.e., those having usually a conserved serine or a tyrosine (in mammals) in their active site. Those having notably a cysteine residue lack this property. The conjugation step has several benefits in the detoxification process, including a decrease of the reactivity and toxicity of the molecules, as well as an increase of their solubility. Likewise, the addition of large anionic groups such as GSH detoxifies reactive electrophiles and produces polar molecules that cannot diffuse across membranes. These molecules are then recognized and actively transported by ATP-binding cassette transporters (ABC-transporters), also known as phase III proteins (Keppler, 1999). ABC transporters carry out the ATP-dependent transport of a large variety of hydrophobic molecules and thus participate in exocytosis (animals) or sequestration in the vacuole and/or in the cell wall (plants and fungi) of phase II products (Coleman et al., 1997).

Even though most of the studies published over the past years focused on GSTs catalyzing the addition of glutathione, other catalytic activities have been described. For instance, numerous GSTs act as GSH-dependent peroxidases by reducing organic hydroperoxides (Tang and Tu, 1994; Marrs, 1996; Hurst et al., 1998) whereas others perform isomerisation reactions. The zeta GSTs catalyze the *cis-trans* isomerisation of maleylacetoacetate into fumarylacetoacetate, as part of the tyrosine degradation pathway (Thom et al., 2001; Fernandez-Canon et al., 2002). In addition to their involvement in GSH-conjugation, several GSTs also catalyze the opposite reaction, i.e., the removal of glutathione from small molecules. This reaction will be referred to as deglutathionylation. Note that this term is also used for the reduction of glutathione adducts on protein cysteine residues, as catalyzed by another family of GSH-dependent proteins called glutaredoxins (GRXs) (Rouhier et al., 2008). Although human GSTO1-1 was shown to catalyze the deglutathionylation of peptides/proteins such as glutathionylated β-actin (Menon and Board, 2013), this has been rarely observed among GSTs. The capacity of catalyzing deglutathionylation reactions is linked to the existence of a catalytic cysteinyl residue instead of the active site serine or tyrosine residues. This residue is notably present in the bacterial-specific Beta GSTs (GSTBs); in Omega GSTs (GSTOs) found in mammals, insects, and fungi (Board et al., 2000; Kim et al., 2006; Yamamoto et al., 2009; Meux et al., 2013); in the plant-specific Lambda GSTs (GSTLs); and in glutathionyl-hydroquinone reductases (GHRs), also known as Xi GSTs (GSTX), which are found in bacteria, fungi, archaea, and plants (Xun et al., 2010; Meux et al., 2011; Lallement et al., 2015; Schwartz et al., 2016). However, with a few exceptions, the physiological role of these enzymes is poorly documented. In addition to being involved in deglutathionylation, as mentioned above, human GSTOs may be involved in arsenic biotransformation, reducing methyl and dimethyl arsenate forms (Zakharyan et al., 2001; Burmeister et al., 2008). Plant GSTLs may be involved in the metabolism or trafficking of flavonoids (Dixon and Edwards, 2010b). GHRs are involved in the catabolism of chlorinated quinones and in lignin degradation through the deglutathionylation of metabolic intermediates (Reddy and Gold, 2001; Masai et al., 2003; Huang et al., 2008; Meux et al., 2011).

In addition to these catalytic properties, some GSTs possess the property to bind ligands also referred to as ligandin properties. It consists of the binding of small hydrophobic molecules either at the catalytic site or in a specific ligandin site (L-site) for their transport or storage. This non-catalytic property has been documented in plants for the transport/binding of hydrophobic xenobiotic molecules, of endogenous compounds such as oxylipins and flavonoids (anthocyanins, proanthocyanidins) as well as of phytohormones such as auxin and cytokinin (Zettl et al., 1994; Gonneau et al., 1998), suggesting a possible role of GSTs in cell signaling and/or in plant growth and development (Smith et al., 2003; Kitamura et al., 2004; Gong et al., 2005; Moons, 2005; Ahmad et al., 2017).

Overall, although the biochemical (catalytic and ligandin) properties of representative members from almost all GST classes have been studied, sometimes extensively, the physiological role of most of them remains to be identified, essentially because the existence of several close isoforms in given classes may have hampered their characterization by reverse-genetic approaches. Therefore, having focused recently on the biochemical and structural properties of Cys-GSTs (Lallement et al., 2014), the objective of this review is to inventory the known properties and functions of Ser-GSTs in photosynthetic organisms.

History and Classification of the GSTs

Over the past years, the GST classification has constantly evolved concomitantly to the increase of the genomic resources available, and to the identification and characterization of new isoforms and classes. First discovered in rat, GSTs were characterized initially in mammals and subsequently in insects, plants, fungi, and bacteria. In mammals, GSTs were originally classified as cytosolic, mitochondrial and membrane-associated GSTs, the latter being subdivided into microsomal GSTs and leukotriene C_4 synthetases (Kraus, 1980; Hayes and Pulford, 1995). The same three subfamilies were renamed later as soluble GSTs, kappa GSTs and membrane-associated proteins in eicosanoids and glutathione metabolism (MAPEG), respectively (Jakobsson et al., 1999). However, on the basis of their immunological cross-reactivity and sequence relatedness, mammalian GSTs were also classified into the alpha, mu, pi, sigma, theta, and

zeta classes (Mannervik et al., 1985; Dixon et al., 1998; Hayes and McLellan, 1999). At the time, most non-mammalian GSTs were placed in the heterogeneous theta class (Buetler and Eaton, 1992). For plant GSTs, the first classification introduced was based on sequence analogy and on the intron-exon structure of the genes. Subsequently, three and then four distinct types of plant GSTs were recognized including type I (GSTs with herbicide-detoxifying activity), type II (GSTs close to the mammalian zeta GSTs), type III (consisted mainly of auxin-induced GSTs), and type IV (GSTs similar to classical mammalian theta enzymes) isoforms (Droog et al., 1995; Droog, 1997). In fact, with the accumulation of biochemically characterized plant GSTs in the late 1990s, it appeared that some plant GSTs clearly grouped with specific mammalian GSTs, whereas others seemed plant-specific. Together with the release of the genome of *Arabidopsis thaliana*, this contributed to the establishment of a refined phylogenetic classification in plants using the principle of Greek-letter designations, which was widely used for non-plant GSTs (Dixon et al., 1998). GSTs are designated by using a 2 letter-code corresponding to the species (At for *A. thaliana*) followed by the 3 letters "GST," a Greek or Latin letter designating the class, and a number distinguishing members of the same class. Thus, in *A. thaliana*, isoform 1 of the Phi (F) class is designated by "AtGSTF1". This classification introduced in plants the Phi (replacing former Type I), Zeta (replacing former Type II), Tau (replacing former Type III), and Theta (replacing former Type IV) classes as well as two groups more distantly related to other known plant GSTs forming the Lambda (L) and dehydroascorbate reductase (DHAR) classes (Dixon et al., 2002). The last phylogenetic study performed a few years ago using well-annotated genomes of terrestrial plants (*A. thaliana*, *Hordeum vulgare*, *Oryza sativa*, *Physcomitrella patens*, *Pinus tabulaeformis*, *Populus trichocarpa*, and *Solanum lycopersicum*) and selecting only proteins possessing the two regular N- and C-terminal domains (see below), led to the identification of 14 GST classes: phi (F), tau (U), theta (T), zeta (Z), lambda (L), hemerythrin (H), iota (I), ure2p, glutathionyl-hydroquinone reductase (GHR), elongation factor 1B gamma (EF1Bγ), DHAR, tetrachlorohydroquinone dehalogenase (TCHQD), metaxin, and microsomal prostaglandin E synthase type-2 (mPGES-2) (Lallement et al., 2014). Some of these classes are found among different kingdoms, such as Zeta or Theta classes whereas Lambda, Tau and DHAR classes are specific to plants. The Phi class is sometimes presented in the literature as specific to the plant kingdom but similar sequences have been identified in some fungi, bacteria, and protists (Morel et al., 2013; Munyampundu et al., 2016). Although it has some limitations, the primary sequence remains to date the most convenient criterion for classifying these proteins.

The evolutionary history of GSTs seems relatively complex and several scenarios have been proposed. Because Theta class GSTs were present in bacteria, the first model of evolution, dating from the early 1990s, proposed that canonical (soluble) GSTs of plants, animals, and fungi have evolved from this ancestral gene as a result of duplications followed by divergent evolution (Pemble and Taylor, 1992). In subsequent years, this model was discarded by taking into account the biochemical properties including the nature of the catalytic residue, but also the oligomeric state of the proteins, and their tridimensional structure when solved (Frova, 2006; Mashiyama et al., 2014). The structural data notably showed that the N-terminal domain of soluble GSTs adopted a TRX fold, suggesting that the evolutionary history of soluble GSTs is linked to one of the TRX superfamily members. In this model, soluble GSTs were proposed to have evolved from a TRX/GRX ancestor to which a C-terminal helical domain has been added. Subsequent major transitions are the result of the dimerization of some GSTs, the replacement of the ancestral catalytic cysteine by a serine, and finally the change of this residue by a tyrosine in many mammalian GST classes. Although these major steps likely remain true, the current model is still incomplete, as it does not include the most recently identified classes such as mPGES2, GHR, Metaxin, Hemerythrin, Iota, and Ure2p, just to cite classes present in plants.

Gene Organization and Distribution of Ser-GSTs in Eukaryote Photosynthetic Organisms

Among the 14 classes previously identified in terrestrial plants (Lallement et al., 2014), only five classes (Tau, Phi, Zeta, Theta, and TCHQD) clearly contain members possessing a conserved serine in their active site, even though this serine is absent in some isoforms. The DHAR, Hemerythrin, Iota, Lambda, GHR, mPGES2, and metaxin classes belong to the Cys-GSTs, as they primarily contain members possessing a conserved cysteine in their active site. For the EF1Bγ and Ure2p classes, the nature of the residue promoting GSH activation remains uncertain. Although this classification is based on the primary sequences, the recent release of several plant genomes allowed for its correlation with the intron-exon structure of GST-encoding genes as analyzed in *P. trichocarpa* (Lan et al., 2009), *P. patens* (Liu et al., 2013), *Capsella rubella* (He et al., 2016), *S. lycopersicum* (Islam et al., 2017), *Ipomoea batatas* (Ding et al., 2017), and *Brassica rapa* (Khan et al., 2018). Indeed, the number of exons is generally conserved for genes belonging to the same class, e.g., 1 or 2 for genes encoding GSTUs, 3 for GSTFs, 9 or 10 for GSTZs, 7 for GSTTs, and 2 for TCHQDs.

Hence, combining the gene structure analysis with protein motifs specific to GST classes, sequence alignments and phylogenetic trees provide a robust view of the Ser-GST gene copy number present in a given organism. A comparative genomic analysis was carried out using 39 sequenced photosynthetic organisms available in Phytozome database [version 12 (Goodstein et al., 2012)] including 3 chlorophytes, 1 bryophyte, 1 lycophyte, and 34 angiosperms; clearly extending previous genomic surveys (**Table 1**; Ding et al., 2017; Monticolo et al., 2017; Plomion et al., 2018). 1859 sequences were retrieved by BLASTp (Basic Local Alignment Search Tool) using *A. thaliana* GST sequences as queries and standard parameters. It is worth noting that chlorophytes but not terrestrial plants contain Tyr-GST isoforms (respectively, 6, 4, and 7 in *Chlamydomonas reinhardtii*, *Micromonas pusilla*, and *Volvox carteri*) also shared by animals. The presence of such isoforms likely compensates the absence or low number of

TABLE 1 | Ser-GST gene content in sequenced chlorophytes and embryophytes.

	GSTU	GSTF	GSTT	GSTZ	TCHQD
Chlorophyte					
Chlamydomonas reinhardtii v5.5	0	0	1	0	0
Volvox carteri v2.1	0	0	1	0	0
Micromonas pusilla CCMP1545 v3.0	0	0	0 (*)	0	0
Embryophyte					
Physcomitrella patens v3.3	0 (*)	9	2	1	5 (*)
Tracheophyte					
Selaginella moellendorffii v1.0	38	1	3	2	1
Angiosperm					
Amborella trichopoda v1.0	22	4	1	2	1
Grass					
Brachypodium distachyon v3.1	40	21	1	3	1
Oryza sativa v7_JGI	45	16	1	4	1
Panicoideae					
Setaria italica v2.2	48	16	1	5	1
Sorghum bicolor v3.1.1	53	17	2	4	1
Zea mays Ensembl-18	34	10	2	2	1
Eudicot					
Aquilegia coerulea v3.1	24	29	3	2	1
Pentapetalae					
Asterid					
Mimulus guttatus v2.0	17	5	2	0 (*)	1
Solanum lycopersicum iTAG2.4	45	4	3	2	1
Solanum tuberosum v4.03	50	4	1	2	1
Rosid					
Eucalyptus grandis v2.0	62	19	1	2	7 (*)
Vitis vinifera Genoscope.12X	36	8	1	3	1
Quercus robur	62	12	1	2	1
Poplar-Malvidae					
Malpighiales					
Linum usitatissimum v1.0	30	11	4	3	2
Manihot esculenta v6.1	44	8	4	2	1
Populus trichocarpa v3.0	54	8	2	2	1
Ricinus communis v0.1	31	4	3	2	1
SBM					
Citrus					
Citrus sinensis v1.1	25	6	1	2	1
Citrus clementina v1.0	42	8	2	3	1
Brassicales-Malvales					
Theobroma cacao v1.1	36	9	1	2	1
Brassicaceae					
Arabidopsis lyrata v2.1	29	13	1	2	1
Arabidopsis thaliana TAIR10	28	13	3	2	1
Boechera stricta v1.2	27	12	1	1	1
Brassica rapa FPsc v1.3	38	20	2	2	1
Capsella grandiflora v1.1	21	10	1	2	1
Capsella rubella v1.0	26	12	1	1	1
Eutrema salsugineum v1.0	24	11	1	2	1
Fabidae					
Nitrogen-fixing					
Cucumis sativus v1.0	24	3	1	2	1
Fragaria vesca v1.1	28	5	1	2	1
Glycine max Wm82.a2.v1	50	10	3	3	2
Malus domestica v1.0	34	10	1	4	1
Medicago truncatula Mt4.0v1	47	10	2	2	1
Phaseolus vulgaris v2.1	24	12	2	2	2
Prunus persica v2.1	47	9	1	2	1

Sequences have been retrieved from Phytozome v12.1, a Joint Genome Institute database. (*) *Unusually high/divergent gene copy number or absence of a given gene for a few specific organisms must be regarded with cautious as this may originate from bad genome assemblies or annotation problems or from remaining pseudogenes or gene alleles.*

Ser-GSTs in these organisms (1 isoform for both *C. reinhardtii* and *V. carteri,* 0 for *M. pusilla*). In the following paragraphs, we emphasize the major features of the different Ser-GST classes, i.e., gene content and protein sequence characteristics.

GSTs Theta (GSTTs)

In addition to plants, GSTTs are also found in animals, insects, fungi, and bacteria; suggesting that this class appeared early during evolution (Coggan et al., 2002; Bryant et al., 2006; Skopelitou et al., 2012; Han et al., 2016; Shao et al., 2017). In photosynthetic organisms, the number of GSTT genes ranges from 1 to 4 (**Table 1**). According to its early appearance, this is the only Ser-GST class present in the chlorophytes (green algae) analyzed. Its absence in *M. pusilla* might be due to a gene loss event during evolution, unless there are annotation problems. In organisms having 2 or more *GSTT* genes, the genes are often organized in cluster such as in *A. thaliana* (Dixon et al., 2002), *Linum usitatissimum*, *Manihot esculenta* or *Ricinus communis* suggesting that tandem duplication(s) occurred during evolution from an ancestral gene. Whether the resulting proteins have diverged in function remains to be explored. The GSTT proteins are generally about 250 amino acids long. The conserved serine is found around position 10 in a conserved SQPS active site signature, which (with a few exceptions) is conserved among mammals (SQPC) and insects (S[Q/A]PC). At the subcellular level, these proteins have a peroxisomal localization, which is consistent with the presence of C-terminal SK[I/M] targeting motif (Dixon et al., 2009). Peroxisomes are multifunctional organelles involved notably in the β-oxidation of fatty acids in plants, a catabolic pathway contributing in particular to

the production of acetyl-CoA, NADH, and $FADH_2$, but also many lipid peroxides from polyunsaturated fatty acids that are the likely physiological substrates of GSTTs. *In vitro*, these enzymes exhibit a weak GSH-conjugation activity against conventional model substrates but they have a high GSH-dependent peroxidase activity toward linoleic acid peroxides (Dixon and Edwards, 2009).

GSTs Zeta (GSTZs)

In addition to plants, GSTZs are also present in bacteria, fungi, and animals, even though this is often as a reduced number of isoforms. A possible reason is their specific involvement in a general process, the tyrosine catabolism (Edwards et al., 2011). In photosynthetic organisms used for the present analysis (**Table 1**), the number of GSTZ genes ranges from 1 to 5 but we could not find them in chlorophytes. They are often found as tandem duplicates in genomes such as in *A. thaliana*, *C. rubella*, or *O. sativa*.

At the protein level, GSTZs are about 225 amino acids long. The serine is located around position 20 and is included in a conserved SSC(S/A) active site signature, the first serine being the residue necessary for the GSH-conjugation reaction. The catalytic mechanism of GSTZs differs from other GSTs in that GSH is initially conjugated to the *cis* double bond of maleylacetoacetate allowing the isomerisation reaction, before being eliminated in a second step allowing the formation of fumarylacetoacetate (Thom et al., 2001). Thus, it is assumed that the conserved cysteine performs the deglutathionylation of the intermediate product at the manner of Cys-GSTs or as proposed also for TCHQDs (see below). However, bacterial GSTZs lacking this cysteine catalyze the same reaction.

Tetrachlorohydroquinone Dehalogenases (TCHQDs)

TCHQDs have been identified in animals, fungi and plants. Plant genomes usually contain a single gene but 2, 5, and 7 TCHQD-encoding genes were identified in *Glycine max*, *P. patens*, and *Eucalyptus grandis*, respectively (**Table 1**). At the protein level, TCHQDs are on average 265 amino acids long. These proteins were first discovered in the soil bacterium *Sphingobium chlorophenolicum*, that is able to use pentachlorophenol, a fungicide used in wood preservation, as a carbon source. During the enzymatic degradation of pentachlorophenol, this bacterial TCHQD (PcpC) catalyzes the reductive dehalogenation of tetrachlorohydroquinone to trichlorohydroquinone and then to dichlorohydroquinone (Xun et al., 1992). PcpC possesses a peculiar SCIS signature containing both a serine and a cysteine. Accordingly, it reduces chloroquinones in two steps. The first step requires the serine in the GSH-conjugation of the quinone causing the departure of a chloride ion. The second step is the removal of the glutathione moiety from the quinone, a reaction performed by a nucleophilic attack of the cysteine (Willett and Copley, 1996; Kiefer and Copley, 2002). In plant proteins, there is no cysteine in the signature (often SLDS) (Lallement et al., 2014). They should therefore not be able to carry out deglutathionylation steps and may have different substrates or reaction mechanisms. Another possibility is that other GST isoforms such as GHRs substitute to TCHQDs as they are able to catalyze quinone deglutathionylation (Lallement et al., 2015).

GSTs Phi (GSTFs)

The *GSTF* genes are found in all terrestrial non-vascular or vascular plants that have been analyzed, but are absent in green algae/chlorophytes, suggesting important functions for terrestrial life. The gene content is very variable between species as it ranges from 1 in *Selaginella moellendorffii* to 29 in *Aquilegia coerulea* (**Table 1**). In almost all genomes, a large part of these genes is organized as clusters indicating repetitive, species-specific duplications.

At the protein level, GSTFs are about 215 amino acids long and the serine is located around position 12. Given the higher number of isoforms compared to the above-described classes, the four residue signature (reminiscent of the TRX/GRX family) is more variable. Most isoforms have the conserved serine but a few, exemplified by PtGSTF8 (AVCP), AtGSTF11 (AANP), or AtGSTF12/TT19 (AACP) are lacking it. In fact, the presence of the serine is not mandatory for the GSH-conjugation reaction as shown *in vitro* using poplar GSTFs (Pégeot et al., 2017). Several subgroups have been distinguished previously, according notably to this signature but also depending on the presence of N- or C-terminal extensions (Pégeot et al., 2014). Also, it was observed that some isoforms containing a cysteine exhibit a more diversified activity profile, as they possess deglutathionylation activity in addition to the peroxidase and GSH-conjugation activities (Pégeot et al., 2017).

GSTs Tau (GSTUs)

In light of current genomic resources, GSTUs form a plant specific class as is also the case for DHARs and GSTLs; two Cys-GST classes. Except in rare instances, such as in *Triticum aestivum* and *A. coerulea*, which contains respectively 38 and 29 GSTFs vs 26 and 24 GSTUs (Gallé et al., 2009), the GSTU class represents the largest GST class. From the absence of GSTU in green algae and in the mosses *P. patens* and *Sphagnum fallax*, the presence of only 2 GSTUs in another moss: *Marchantia polymorpha*, but the presence of 38 GSTUs in the bryophyte *S. moellendorffii*, we conclude that these genes have rapidly and dramatically expanded between bryophytes and lycophytes. They became predominant in vascular plants, being supposedly required for novel functions associated to the lifestyle of these plants. In angiosperms, the GSTU gene content is variable and range from 21 (*C. grandiflora*) to 62 (*Quercus robur* and *E. grandis*) (**Table 1**). The phylogenetic analysis of this family indicates that large clades are formed by proteins from the same species pointing to the fact that species-specific expansions occurred (Plomion et al., 2018). They normally correspond to genomic clusters produced by several successive tandem duplication events as exemplified in poplar, *A. thaliana* or *O. sativa* (Wagner et al., 2002; Soranzo et al., 2004; Lan et al., 2009). Accordingly, it is difficult to define strict orthologs for a given isoform among the different species and to determine what is the set of GSTU ancestors shared by angiosperms.

Overall, the GSTU and GSTF classes represent around 75% of all GST genes as in *Q. robur* (62 out of 88 genes)

(Plomion et al., 2018) or *A. thaliana* (41 out of 55 genes) (Dixon and Edwards, 2010a). For both classes, the expansion, specific genomic organization and high sequence similarity among duplicated members have important implications. One consequence may be the existence of functional redundancy between isoforms making it difficult to study the biological functions of a particular gene using reverse-genetic approaches. However, another consequence may be that upon duplication, some of the new gene copies, which have been less subject to evolutionary pressure and have accumulated mutations, have likely acquired structural and functional diversity. The truth is certainly in between and this remains to be experimentally addressed in a more exhaustive manner.

Biochemical Properties and Catalytic Activities of Ser-GSTs

GSTs are versatile enzymes, accommodating diverse substrates/ligands in the active site or L-sites (**Table 2**), and catalyzing diverse enzymatic reactions as a function of the active site signature (Chronopoulou et al., 2017a). Besides the so-called ligandin function, Ser-GSTs catalyze GSH-conjugation reactions on numerous types of substrates, the reduction of organic hydroperoxides or substrate isomerisation whereas Cys-GSTs rather catalyze opposite reactions including the reduction of glutathione conjugates. For the latter aspect, we invite the reader to refer to the recent review describing Cys-GST properties (Lallement et al., 2014). For all the catalytic activities, the high reactivity of a cysteine residue (either from GSH or from the polypeptide) plays a central role in the biochemical properties carried out by GSTs. Noteworthy, some Ser-GSTs belonging to the GSTZ, TCHQD, or GSTF classes possess a cysteine residue in the catalytic center, which confers them dual activity profile.

GSH-Conjugating Activity

Most Ser-GSTs catalyze the conjugation of GSH onto electrophilic compounds including aromatic, aliphatic or heterocyclic compounds (Deponte, 2013). This conjugation requires the binding of a GSH molecule in the glutathione binding site (G-site). In most cases, the presence of a specific residue, most often a cysteine, serine, or tyrosine at the vicinity of the cysteine of the bound GSH, induces a decrease in the thiol pKa (Board and Menon, 2013; Deponte, 2013). This pKa, usually around 9, is lowered to approximately 6.5 or even less, promoting the formation of a nucleophilic (reactive) thiolate group *in vivo*, which is able to perform a nucleophilic attack on a nearby electrophilic substrate. In other words, the conserved serine in the active site of Ser-GSTs does not play the role of the catalytic residue; rather, this is carried out by the thiolate group of GSH. The nucleophilic attack initiated by GSH occurs either by a substitution (e.g., on a chlorine atom) or by the reduction of an electron acceptor via a Michael's addition (Deponte, 2013). Several model substrates are used to measure GSH-conjugation activity, the most common being the 1-chloro-2,4-dinitrobenzene (CDNB). The detoxification of herbicides (e.g., atrazine and fluorodifen) and pesticides (e.g., alachlor and metolachlor) through GSH-conjugation has been extensively studied over the years, notably using GSTs from crops (Gronwald and Plaisance, 1998; Cummins et al., 2003; Cho et al., 2007).

Peroxidase Activity

In the cells, hydroperoxides are reduced by several families of enzymes, in particular thiol peroxidases including the peroxiredoxin (PRX) and glutathione peroxidase-like protein (GPXL) families (Rouhier and Jacquot, 2005). Some GSTs also exhibit peroxidase activity, as they are able to reduce (hydro)peroxides into alcohols concomitant to the oxidation of GSH into GSSG. In this reaction, deprotonated GSH bound to the G-site of the enzyme induces a nucleophilic substitution of the bond between the two oxygen atoms of the hydroperoxyl group (R-OOH), leading to the release of GSOR and an OH group that is protonated into H_2O. GSOR is then cleaved into GSSG and ROH by a second nucleophilic substitution by the GSH molecule according to a mechanism that is not yet fully elucidated (Deponte, 2013). The GSTs performing this reaction have catalytic efficiencies (10^2 to 10^4 $M^{-1}{\cdot}s^{-1}$) measured in steady-state conditions in the range of those of TRX- and GRX-dependent thiol peroxidases (Pégeot et al., 2017). A major difference is, however, the rate of the first step (i.e., peroxide reduction) that occurs at turnover numbers up to 10^7 s^{-1} for some thiol peroxidases. The contribution of GSTs in the reduction of cellular hydroperoxides remains poorly described but it might be important because these are almost the only GSH-dependent peroxidases, most thiol peroxidases being dependent on GRXs or TRXs, including GPXLs (Rouhier and Jacquot, 2005; Navrot et al., 2006). Also, their contribution appears to be different depending on the organisms and the subcellular compartments considered. Among Ser-GSTs, only those belonging to the Phi, Tau, and Theta classes are able to catalyze such reactions, peroxisomal GSTTs being likely specialized in the reduction of fatty acid peroxides (Dixon et al., 2009).

Isomerase Activity

Some GSTs, in particular from the Zeta class, catalyze the GSH-dependent isomerisation of specific metabolites, such as the *cis-trans* isomerisation of maleylacetoacetate into fumarylacetoacetate occurring during the penultimate step of tyrosine catabolism in eukaryotes (Fernández-Cañón and Peñalva, 1998; Thom et al., 2001; Fernandez-Canon et al., 2002; Edwards et al., 2011). In some bacteria, GSTZs function as maleylpyruvate isomerases (Marsh et al., 2008) and catalyze the isomerisation of maleylpyruvate into fumarylpyruvate through the third committed step in the degradation of salicylate to the metabolites pyruvate and fumarate via gentisate. Contrary to other activities described above, GSH is not considered as a substrate but as a cofactor because it is not consumed during the reaction (Litwack et al., 1971; Marsh et al., 2008).

Non-enzymatic Binding and Intracellular Transport

In addition to their catalytic function, GSTs also serve as non-enzymatic carrier proteins or ligandins (Habig et al., 1974; Mannervik and Danielson, 1988). The term "ligandin" was historically associated to proteins characterized in animals,

which were able to bind a wide range of hydrophobic ligands, such as steroids, heme and its degradation product bilirubin, carcinogens, and bile salts. These proteins turned out to be GSTs from the Alpha and Mu classes (Levi and Arias, 1969; Ketley et al., 1975). Since then, plant GSTUs and GSTFs were found to bind several tetrapyrroles, e.g., protoporphyrin IX (Proto IX), Mg-protoporphyrin but also bacterial porphyrin derivatives identified upon expression of recombinant maize GSTUs (Lederer and Böger, 2005; Dixon et al., 2008). However, it is not clear whether this is strictly a ligandin function as *Zea mays* GSTU1 is able to catalyze the conjugation of GSH on protoporphyrinogen IX and harderoporphyrinogen (Dixon et al., 2008). Another example, likely the best described, concerns anthocyanins, which are phenolic antioxidant compounds conferring the colors we commonly associate with fruits and flowers. These molecules are transiently bound/transported by GSTs before their release to ABC-type transporters for vacuolar sequestration. This is documented for both Tau and Phi class members, i.e., Bz2 (GSTU) from maize, AN9, TT19, and VvGST4 (GSTFs) from *Petunia hybrida*, *A. thaliana* and *Vitis vinifera*, respectively (Marrs, 1996; Alfenito, 1998; Mueller et al., 2000; Kitamura et al., 2004; Conn et al., 2008; Gomez et al., 2011; Momose et al., 2013; Zhao, 2015). Other molecules were isolated using ligand fishing approaches (**Table 2**). GSTU2 from *V. vinifera* binds *trans*-resveratrol, a polyphenol transported from the cells into extracellular medium and conferring antimicrobial properties (Martínez-Márquez et al., 2017). GSTF2 and GSTF3 from *A. thaliana* were described *in vitro* to bind various ligands

TABLE 2 | Ligands of plant Ser-GSTs identified.

Isoform	Organism	Ligands	References
Bronze-2 or Bz2 (GSTU)	*Zea mays*	Cyanidin-3-glucoside	Marrs et al., 1995
ZmGSTI-I, ZmGSTI-II, ZmGST II-II, ZmGST III-III (GSTU et GSTF)	*Zea mays*	Protoporphyrin IX, mesoporphyrin, coproporphyrin, uroporphyrin, Mg-protoporphyrin	Lederer and Böger, 2003
ZmGSTU1	*Zea mays*	Uroporphyrin, pentacarboxyl porphyrin, harderoporphyrin-SG, coproporphyrin, heme B	Dixon et al., 2008
ZmGSTF1	*Zea mays*	Gibberellic acid, indole-3-butyric acid, 2-naphtoxyacetic acid, 2,4-dichlorophenoxyacetic acid, kinetin, quercetin, luteolin	Axarli et al., 2004
AtGSTU7	*Arabidopsis thaliana*	Protoporphyrin-SG, myristoyl-glutathione	Dixon and Edwards, 2009, 2018
AtGSTU19	*Arabidopsis thaliana*	Harderoporphyrin-SG, chlorogenic acid, 10-S-glutathionyl-12-oxo-phytodienoic acid, oxylipin-SG, 3-methylindolyl glutathionyl disulfide, 12-oxo-phytodienoic acid (OPDA)	Dixon and Edwards, 2009, 2018
Transparent testa 19 or TT19 (GSTF)	*Arabidopsis thaliana*	Anthocyanin	Kitamura et al., 2004
AtGSTF2, AtGSTF3	*Arabidopsis thaliana*	Norharmane, harmane, lumichrome, indole-3-aldehyde, quercetin-3-O-rhamnoside	Dixon et al., 2011a
AtGSTF2	*Arabidopsis thaliana*	Indole-3-aldehyde, camalexin, quercetrin, quercetin	Ahmad et al., 2017
AtGSTF2	*Arabidopsis thaliana*	Grossamide K-SG, cannabisin, 10-S-glutathionyl-12-oxo-phytodienoic acid, kaempferol-3,7,4′-trimethylether, quercetin-3,7,3′,4′-tetramethylether	Dixon and Edwards, 2018
Anthocyanin9 or An9 (GSTF)	*Petunia hybrida*	Anthocyanin	Alfenito, 1998
Anthocyanin9 or An9 (GSTF)	*Petunia hybrida*	Isoquercitrin, quercetin, cyanidin, luteolin	Mueller et al., 2000
GST	*Hyoscyamus muticus*	Indole-3-acetic acid	Bilang et al., 1993
CkmGST3 (GSTF)	*Cyclamen persicum* × *Cyclamen purpurascens*	Anthocyanin	Kitamura et al., 2012
VvGST1 (GSTU), VvGST4 (GSTF)	*Vitis vinifera*	Anthocyanin	Conn et al., 2008
VvGSTU2	*Vitis vinifera*	*Trans*-resveratrol	Martínez-Márquez et al., 2017
Flavonoid3 or Fl3	*Dianthus caryophyllus*	Anthocyanin	Larsen et al., 2003
PfGST1 (GSTF)	*Perilla frutescens*	Anthocyanin	Yamazaki et al., 2008
AtGSTU9, AtGSTU10	*Arabidopsis thaliana*	fatty acyl (C14,C16,C17, C18)	Dixon and Edwards, 2009
AtGSTU25, AtGSTU28	*Arabidopsis thaliana*	fatty acyl (C6,C8,C10,C12,C14)	Dixon and Edwards, 2009
AtGSTF6	*Arabidopsis thaliana*	Indole-3-acetonitrile	Su et al., 2011
AtGSTU13	*Arabidopsis thaliana*	Indole-3-ylmethyl-ITC (indole glucosinolate)	Piślewska-Bednarek et al., 2018

such as lumichrome, harmane, norharmane, indole-3-aldehyde, camalexin, and quercetin-3-O-rhamnoside (Dixon et al., 2011a) but the physiological significance remains unknown. In addition to a carrier function, it may be that the non-enzymatic binding of molecules prevents their oxidative damage, thus ensuring a protective effect (Mueller et al., 2000).

Structural Characteristics of Plant Ser-GSTs

Considering the high number of Ser-GSTs in plants, only a few structures have been solved so far: 27 for GSTUs, 15 for GSTFs, 1 for GSTZ, and none for TCHQD and GSTT (**Table 3**). All these plant Ser-GSTs are homodimeric enzymes in which each protomer of approximately 23–30 kDa contains two domains with a catalytic center at the interface. The N-terminal domain adopts the typical TRX-fold (with β1α1β2α2β3β4α3 topology) and the C-terminal domain is a bundle of at least five helices (α4 to α8) (**Figure 1**). GSTUs have an additional α9 helix that is oriented toward the active site without occluding it (Thom et al., 2002). In GSTFs, the α6-α7 connection systematically includes a small helix (α6′) (Reinemer et al., 1996; Pégeot et al., 2014, 2017). The atomic model of the only GSTZ crystal structure, that of *A. thaliana* GSTZ1, is incomplete between helices α4 and α5, which hinders the accurate determination of the active site (Thom et al., 2001). Within a class, the variable regions are often close to the active site and involved in the binding of the electrophilic substrate. In GSTUs, these regions include helix α9 and the segment from roughly the C-terminal end of α4 to the N-terminal end of α5 (Valenzuela-Chavira et al., 2017). In GSTFs, they include this segment and the connection β2-β3, which, in maize GSTF3, was supposed to move upon binding of the substrate in the active site (Neuefeind et al., 1997a). This connection is also involved in the dimer stabilization (see below).

Concerning dimerization, the GSTU dimer has an open V-shaped configuration with 2200 Å^2 of the accessible surface that is buried at the interface, comparable with that of GSTOs (2000 Å^2), but smaller than that of GSTFs (2700 Å^2) and

TABLE 3 | Crystal structures of Ser-GSTs from plants.

Class	Organism	Name	Ligand	PDB Entry	References
	Arabidopsis thaliana	AtGSTF2	GTX[a] (1GNW)[b], FOE[a] (1BX9)[b], 7WB[a] (5A5K)[b], QUE[a] (5A4V)[b], I3A[a] (5A4U)[b], QCT[a] (5A4W)[b]	1GNW, 1BX9, 5A5K, 5A4V, 5A4U, 5A4W	Reinemer et al., 1996; Prade et al., 1998; Ahmad et al., 2017
Phi	*Populus trichocarpa*	PtGSTF1	GSH[a] (4RI6)[b], GSH[a] (4RI7)[b]	4RI6, 4RI7[c]	Pégeot et al., 2014
		PtGSTF2		5EY6	Pégeot et al., 2017
		PtGSTF5	GSH[a]	5F05	
		PtGSTF7	GSH[a]	5F06	
		PtGSTF8	GSH[a]	5F07	
	Zea mays	ZmGSTF1	CYW[a] (1AXD)[b], ATA[a] (1BYE)[b]	1AXD, 1BYE	Neuefeind et al., 1997a; Prade et al., 1998
		ZmGSTF3		1AW9	Neuefeind et al., 1997b
	Triticum aestivum	TaGSTU4-4	GTX[a]	1GWC	Thom et al., 2002
	Arabidopsis thaliana	AtGSTU20/ FIP1	GSH[a]	5ECS, 5ECR, 5ECQ, 5ECP, 5ECO, 5ECN, 5ECM, 5ECL, 5ECK, 5ECI, 5ECH	Chen et al., 2017
		AtGSTU23	GSH[a] (6EP7)[b]	6EP6, 6EP7, 5O84	Tossounian et al., 2018
		AtGSTU25	GSSG	5G5A	[d]
Tau	*Glycine max*	GmGSTU4	GTB[a] (2VO4, 5AGY)[b], GSH[a] (4TOP)[b]	2VO4, 4TOP, 5AGY[e]	Axarli et al., 2009a,b; Burmeister et al., 2008
		GmGSTU10-10	GS8[a]	4CHS	Skopelitou et al., 2015
	Mangifera indica	MiGSTU	GSH[a] (5G5F), GTX[a] (5KEJ)	5G5E, 5G5F, 5KEJ	Valenzuela-Chavira et al., 2017
	Oryza sativa subsp. japonica	OsGSTU1	GSH[a]	1OYJ	Dixon et al., 2003
	Populus trichocarpa	PtGSTU30	GSH[a]	5J4U, 5J5N[f]	Yang et al., 2019
	Ricinus communis	EFI-501866		4J2F	[d]
Zeta	*Arabidopsis thaliana*	GSTZ1		1E6B	Thom et al., 2001

[a]PDB ligand codes: GSH, Glutathione; GTX, S-hexylglutathione; FOE, FOE-4053-glutathione conjugate; 7WB, Camalexin; QUE, Quercetin; I3A, Indole-3-aldehyde; QCT, Quercetrin; CYW, Lactoylglutathione; ATA, Atrazine glutathione conjugate; GTB, S-(P-Nitrobenzyl)glutathione; GS8, S-Hydroxy-glutathione. [b]PDB, entry where the ligand is present. [c]4RI7: crystal structure of an isoform of PtGSTF1, which contains mutation of S13 to C. [d]crystal structures only available in the PDB. [e]5AGY: crystal structure of an isoform of GmGSTU4, which contains mutations of I183 to V, Q46 to K, R38 to Q, and W114 to C. [f]5J5N: crystal structure of an isoform of PtGSTU30, which contains mutation of R39 to W.

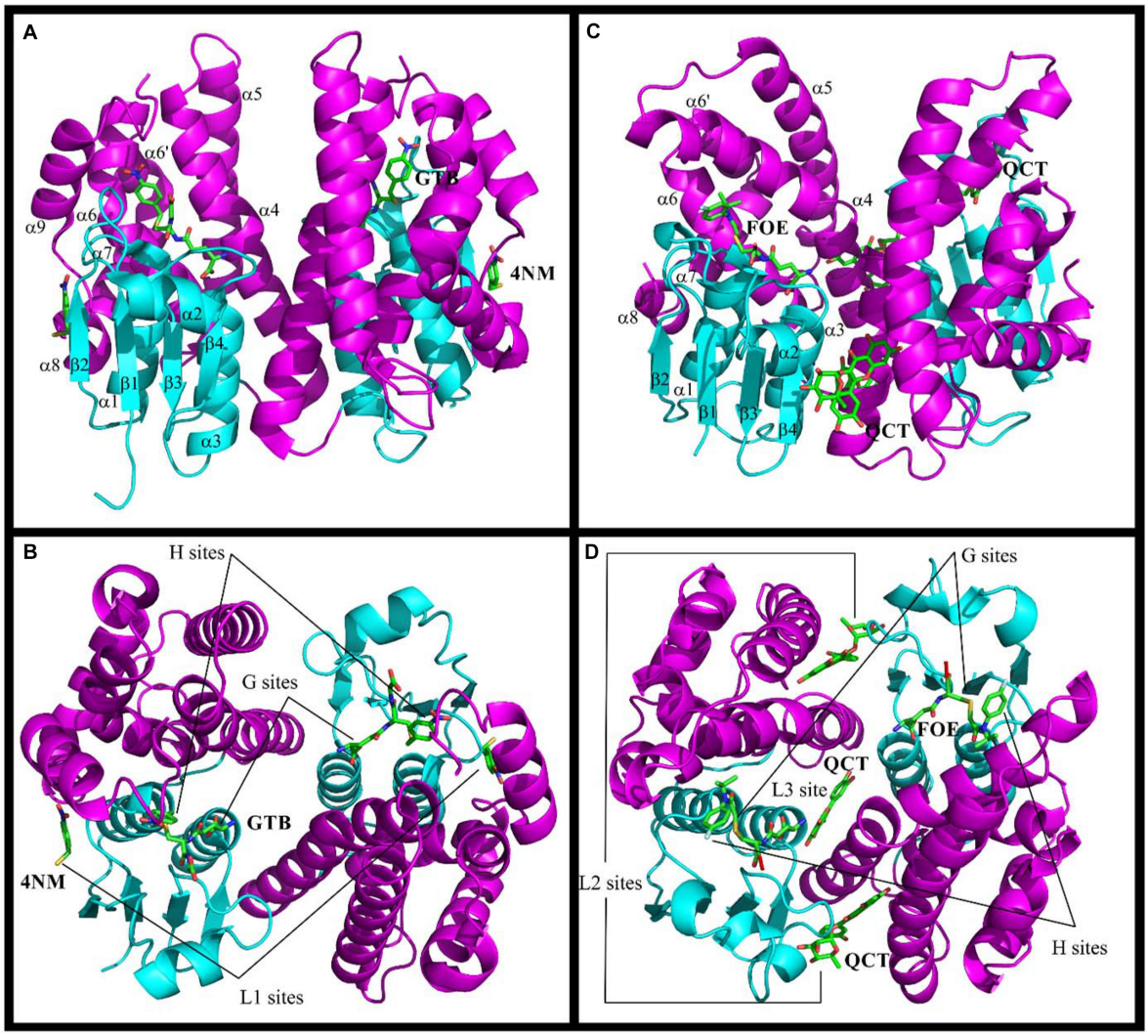

FIGURE 1 | Structures of Ser-GSTs from plants highlighting the location of ligand-binding sites. **(A–D)** schematic structure of the GmGSTU4 and AtGSTF2 dimers, respectively. **(C,D)** illustrate the complexes formed between AtGSTF2 and FOE (1BX9) or QCT (5A4W). The secondary structures and the location of the ligand-binding sites are labeled. The TRX domain is in cyan and the C-terminal domain is in magenta. The labeled ligands are: GTB, S-(P-Nitrobenzyl)glutathione; 4NM, 4-Nitrophenyl methanethiol; FOE, FOE-4053-glutathione conjugate; QCT, Quercetrin.

most other classes of GSTs (2800–3400 Å^2) (Axarli et al., 2010). The monomers are related by a two-fold symmetry where the N-terminal domain of one subunit cross-interacts with the C-terminal domain of the second one, and vice versa. The contact regions are the loop α2-β2, the strand β3 and the helix α3 of one monomer and the helices α4 and α5 of the other. The dimerization interface involves hydrophobic surface patches and a particular lock-and-key motif in which the side-chain of an aliphatic or aromatic residue extends across the dimer interface (Val52 in TaGSTU4 and Phe53 in PtGSTF1, **Table 3**). In GSTUs, conserved salt bridges close to the dyad axis bind both subunits. In GSTFs, the number and the nature of the polar interactions vary significantly from one isoform to another. Indeed, a single hydrogen bond connects the two subunits of AtGSTF2 (Reinemer et al., 1996) whereas nine are found in PtGSTF1 (Pégeot et al., 2014).

The GST catalytic center is usually divided in two distinct functional regions, a hydrophilic G-site for binding glutathione, and an adjacent hydrophobic H-site for accommodating electrophilic substrates. The anchoring residues of the G-site are well conserved among all GSTs probably because of their high specificity for glutathione. These residues are highlighted in the structural alignments (**Figure 2**). In Ser-GSTs, the GSH thiol group is normally hydrogen bonded to the hydroxyl group of the catalytic serine (Ser13 in PtGSTF1) (Pégeot et al., 2014). However, this serine is important but not mandatory for GSH-conjugating reactions as concluded from mutagenesis studies or its absence in some GSTFs (Pégeot et al., 2014). In poplar GSTFs, nearby hydroxylated residues present in the active site

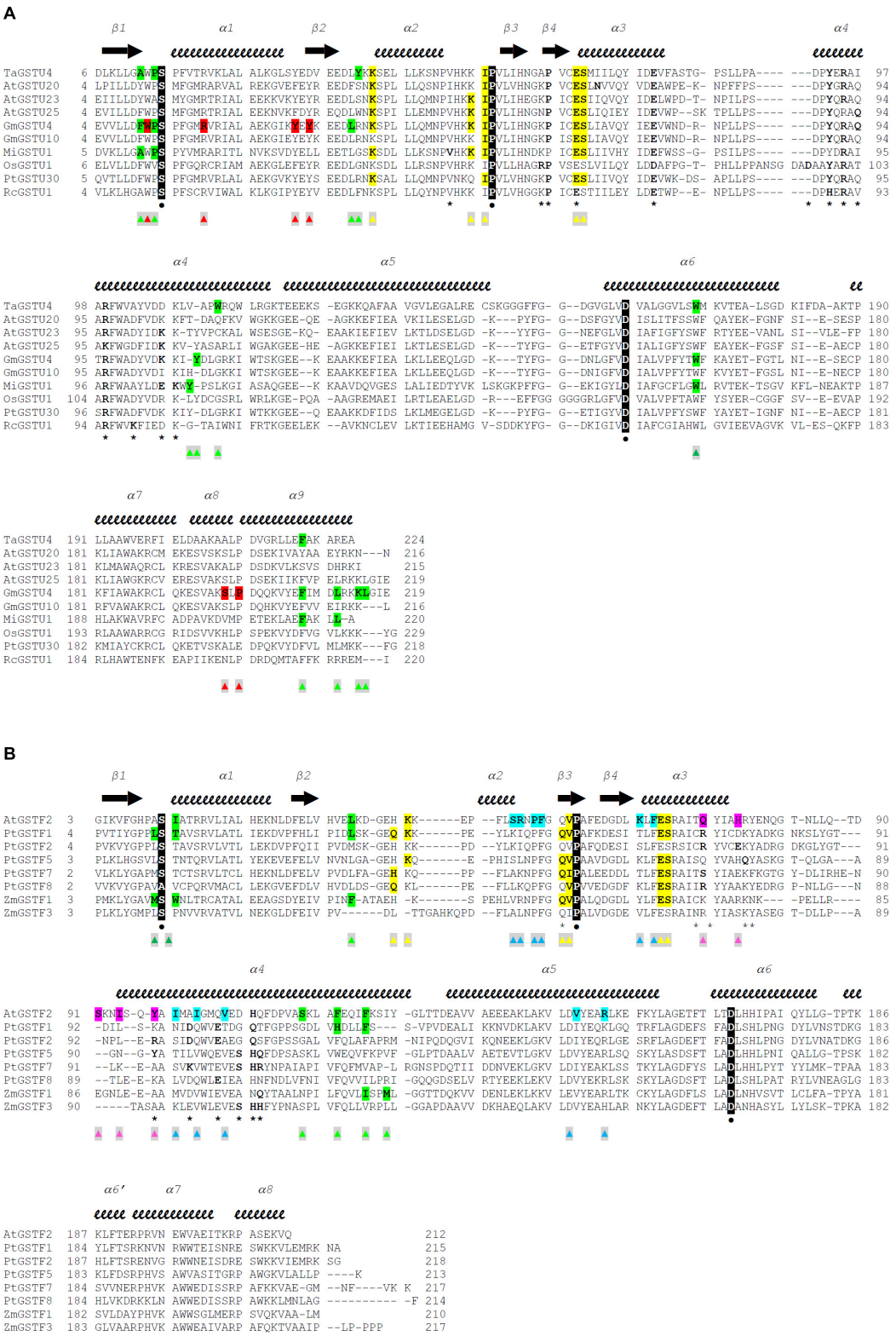

FIGURE 2 | Structure-based sequence alignments of Tau class **(A)** and Phi class **(B)** GSTs from plants. The sequence alignment was generated with Chimera (Pettersen et al., 2004) and manually adjusted. Crystal structures and sequences are available at the Protein Data Bank (http://www.rcsb.org): 1GWC for TaGSTU4, 5ECS for AtGSTU20, 6E6P for AtGSTU23, 5G5A for AtGSTU25, 2VO4 for GmGSTU4, 4CHS for GmGSTU10, 5G5E for MiGSTU1, 1OYJ for OsGSTU1, 5J4U for

(Continued)

FIGURE 2 | Continued
PtGSTU30, 4J2F for RcGSTU1, 1GNW for AtGSTF2, 4RI6 for PtGSTF1, 5EY6 for PtGSTF2, 5F05 for PtGSTF5, 5F06 for PtGSTF7, 5F07 for PtGSTF8, 1AXD for ZmGSTF1, and 1AW9 for ZmGSTF3. Secondary structures are labeled and shown using arrows (β-strands) and squiggles (helices). The active site serine, the invariant proline and the quasi-invariant aspartic acid are in bold type, colored white, highlighted black, and marked with ●. Residues that participate in dimer stabilization via strong polar interactions are in bold and marked with *. Residues involved in binding glutathione (G-site) are in bold type, highlighted yellow, and marked with ▲. Residues of the characterized H-sites are in bold type, highlighted green, and marked with ▲. Residues of the L1-site (GmGSTU4, 2VO4) are in bold type, highlighted red, and marked with ▲. Residues of the L2-site (AtGSTF2, 5A4U, 5A4V, and 5A4W) are in bold type, highlighted blue, and marked with ▲. Residues of the L3-site (AtGSTF2, 5A4K, 5A4U, and 5A4W) are in bold type, highlighted pink, and marked with ▲.

signature (often STxT) could be involved in GSH activation (Pégeot et al., 2017). Generally speaking, the H-site is built from elements from both the N- and C-terminal domains. The observed variations reflect the broad electrophilic-substrate specificities of the different GST isoforms/classes. Only AtGSTF2 and ZmGSTF1 crystal structures were obtained in the presence of herbicidal-glutathione conjugates (**Figure 1**; Prade et al., 1998). In other cases, the H-sites have been defined from the presence of inhibitors such as S-hexylglutathione or molecules from the crystallization medium. In the large majority of cases, the putative H-site residues are hydrophobic in nature. In GSTFs, the H-site involves residues located around the catalytic serine (N-terminal end of helix α1), in the loop β2-α2 and in the C-terminal end of helix α4. In GSTUs, residues from two additional regions are concerned, namely the helix α6 and the additional helix α9. A conserved tryptophan is present in the helix α6 of GSTUs (Trp171 in TaGSTU4) (Thom et al., 2002). In GSTFs, aromatic residues identified by mutagenesis studies have been clearly demonstrated as participating in the affinity toward electrophilic substrates (Axarli et al., 2004; Dixon et al., 2011a).

The structures of GSTs include other important regions that are associated with non-catalytic functions. AtGSTU20, also named FIP1 (FIN219-interacting protein 1) because it interacts with the jasmonate-amido synthetase FIN219, participates in the jasmonate signaling response under far-red light conditions (Chen et al., 2007, 2017). In a crystallographic study, it was shown that the formation of the FIP1-FIN219 complex results in the reorientation of the FIN219 C-terminal domain, which appears crucial for improving jasmonoyl-isoleucine biosynthesis. However, the overall conformation of AtGSTU20 is not altered and the FIN219-binding region includes the C-terminal α6 to α8 helices. Interestingly, the authors noted that some of the contact residues are well conserved in GSTUs and GSTs of other species (**Figure 2**; Chen et al., 2017). For their ligandin function, GSTs bind a wide range of compounds in a non-catalytic manner at so-called L-sites, which are often distinct from the active site. Three different L-sites were described in GSTs from plants (**Figure 1**). The structural analysis of GmGSTU4-4 revealed the presence of one molecule of (4-nitrophenyl)methanethiol in each subunit in a hydrophobic surface pocket (L1-site) (Axarli et al., 2016). The bottom and walls of the L1-site are lined with residues from α1, β2, and α8. The main binding residues are conserved in GSTUs. The crystal structures of AtGSTF2 in complex with two indole derivatives and two flavonoids revealed two other ligand-binding sites (L2 and L3) (Ahmad et al., 2017) extending the observation of tight protein-ligand interactions ($K_d < 1$ μM) by isothermal titration calorimetry (Dixon et al., 2011a). The L2 site is situated between helices α4 and α7 in each monomer whereas the L3 site is located at the base of the dimer interface involving helices α3 of one subunit and α4 of its neighbor (**Figure 1**). All ligands are stabilized mainly through hydrophobic interactions (Ahmad et al., 2017). Coupled to biochemical evidence, the presence of these non-catalytic L-sites in GSTUs and GSTFs suggest that at least some of them should function in the transport of endogenous metabolites (Dixon et al., 2011a). However, the residues forming these L-sites are difficult to identify because they are not well-conserved among plant GSTs (Ahmad et al., 2017).

Gene Expression of Ser-GSTs in *A. thaliana*

Analyzing the transcript abundance of these GSTs could be helpful to understand the possible redundancy between close/duplicated isoforms as well as to give clues about their functions in the absence of molecular and genetic information. In fact, it is quite well documented in many species that the expression of *GSTF* and *GSTU* genes is often induced in response to environmental constraints. This includes heavy-metal exposure (Moons, 2003; Ahsan et al., 2008; Reid et al., 2013; Tripathi et al., 2014), salinity, heat, cold, drought (Jha et al., 2011; Tiwari et al., 2016; Yang et al., 2016; Xu et al., 2018; Srivastava et al., 2019), or biotic interactions such as pathogenic interaction (Rinaldi et al., 2007; Skopelitou et al., 2015; Kao et al., 2016). The expression of several *GSTF* and *GSTU* genes is also enhanced in response to phytohormones including abscisic acid, auxin, ethylene, methyl jasmonate and salicylic acid, to herbicides and to herbicide safeners, and more generally to treatments leading to an oxidative stress (DeRidder, 2002; Wagner et al., 2002; Lieberherr et al., 2003; Smith et al., 2003, 2004; Sappl et al., 2004, 2009; Chen et al., 2012; Chronopoulou et al., 2017b). Thus, using *A. thaliana* as a representative organism, the transcript abundance of 44 out of the 47 Ser-GST genes was retrieved from the AtGenExpress datasets. The expression profiles of GSTF2 (At4g02520), GSTF7 (At1g02920), and TCHQD (At1g77290) were not available and are therefore not present in this gene expression analysis.

First, we examined the expression profiles of Ser-GST genes in the context of a developmental time-course in Arabidopsis (**Figure 3**), using the AtGenExpress Developmental Set (Schmid et al., 2005). In this case, the transcript abundance of each gene was standardized using z-score transformation (a form of normalization that is particularly useful when comparing samples from diverse treatments/tissue backgrounds), and arranged by classes. One can clearly see that most GSTFs and GSTUs, as well as the two GSTZs, have their highest expression in roots. However, for the three GSTTs, the highest expression is found in samples spanning seed development (siliques/seeds), particularly

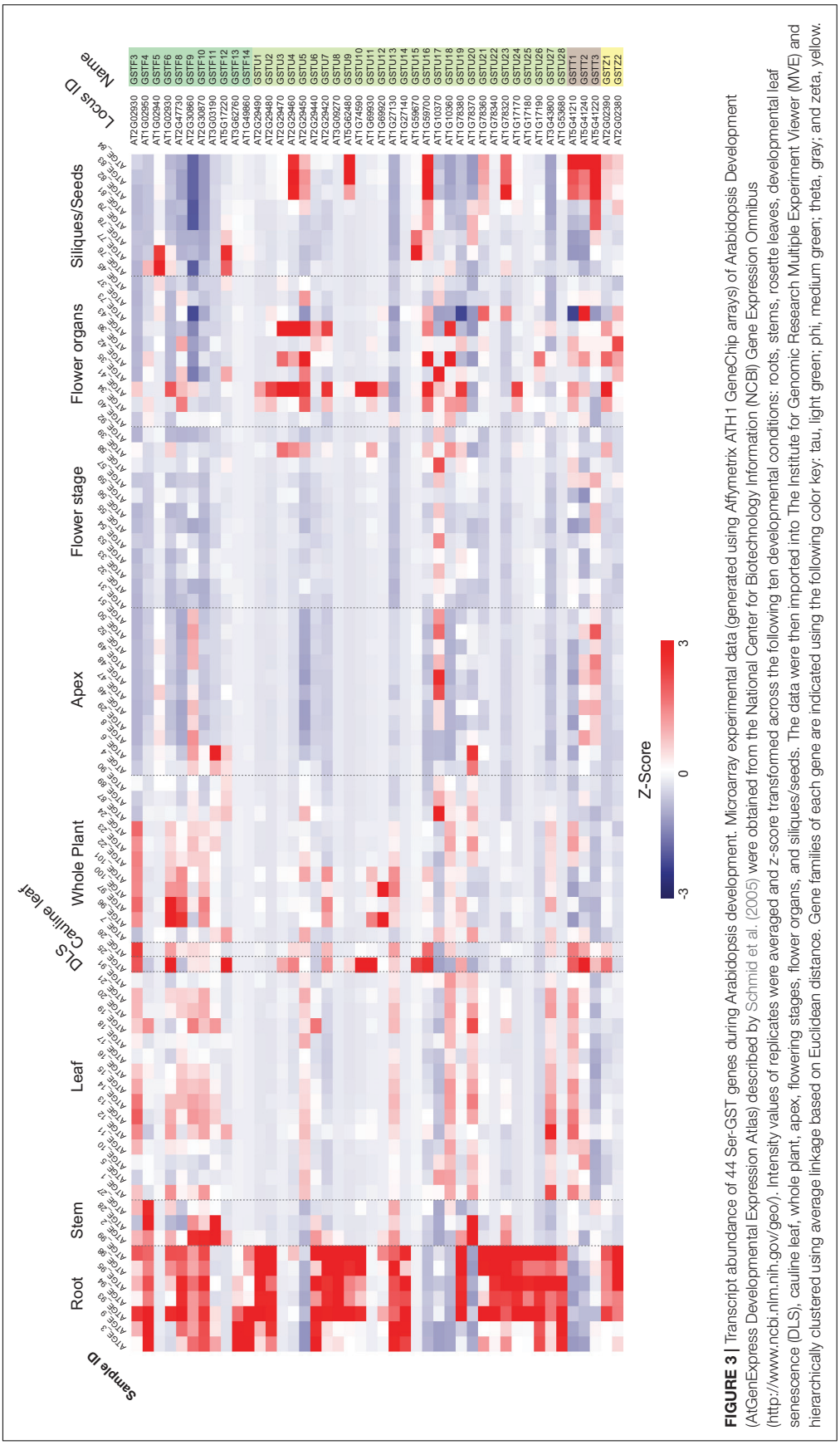

FIGURE 3 | Transcript abundance of 44 Ser-GST genes during Arabidopsis development. Microarray experimental data (generated using Affymetrix ATH1 GeneChip arrays) of Arabidopsis Development (AtGenExpress Developmental Expression Atlas) described by Schmid et al. (2005) were obtained from the National Center for Biotechnology Information (NCBI) Gene Expression Omnibus (http://www.ncbi.nlm.nih.gov/geo/). Intensity values of replicates were averaged and z-score transformed across the following ten developmental conditions: roots, stems, rosette leaves, developmental leaf senescence (DLS), cauline leaf, whole plant, apex, flowering stages, flower organs, and siliques/seeds. The data were then imported into The Institute for Genomic Research Multiple Experiment Viewer (MVE) and hierarchically clustered using average linkage based on Euclidean distance. Gene families of each gene are indicated using the following color key: tau, light green; phi, medium green; theta, gray; and zeta, yellow.

in those containing isolated maturing seeds. In addition, these GSTTs also exhibited increased transcript abundance during developmental leaf senescence (DLS), however, this cannot be relied upon too strongly as only one time point is included in this dataset. Interestingly, within the GSTF family, *GSTF5* is only highly expressed at the two first stages of siliques/seeds (siliques bearing developing seeds), a specificity that is also found for *GSTF12*, albeit the transcript abundance also peaks during DLS. The *GSTF3*, *6*, *8*, *9*, *10*, and *11* genes are also expressed in leaves and in whole plant stages, but to a much lower level than in roots. As already said, most of the *GSTUs* display their highest expression levels in roots, however, *GSTU4*, *9*, *15*, and *16* are exclusively and strongly expressed at the siliques/seeds stages. An exception is *GSTU23*, which exhibits its highest transcript abundance in both roots and siliques/seeds stages. Finally, many Ser-GSTs appear to have transient expression during whole plant, leaf, flower, and stem development, which could suggest very specific functions in response to developmental cues.

In a second stage of analysis, we examined the expression profile of these same 44 Ser-GSTs in response to a number of abiotic stresses [AtGenExpress Stress Set; (Kilian et al., 2007)]. Data are presented as a log2 fold-change of the stress treatment (at a given time point) versus its respective control sample, and the entire dataset is hierarchically clustered using Euclidean distance (**Figure 4**). This analysis clearly demonstrates that most Ser-GSTs strongly respond to stresses applied to the roots and thus, substantiates the high expression profiles observed in roots from the developmental stage analysis (**Figure 3**). Interestingly, GSTs present in clusters 3, 4, 5, 6, and 7 exhibit high transcript abundance in response to temperature changes in roots (cold and heat). That said, the five GSTs comprising clusters 3, 4, and 5 additionally exhibit high transcript abundance in response to almost all stresses, in both aerial and subterranean tissues. Also of note here, whereas the 2 GSTs of cluster 1, (*GSTF11* and *GSTU20*) have an overall low fold-change of their transcript abundance in response to all stresses as compared to most of the other GSTs, the 6 GSTs included in cluster 2 seem to consistently respond to osmotic changes, salt and drought stresses in both root and aerial parts. Altogether, this clearly indicates that Ser-GSTs are involved in the molecular responses to several environmental cues, both biotic and abiotic, a fact that is discussed further in the next chapter.

Physiological Roles of Ser-GSTs in *A. thaliana*

As highlighted above, Ser-GSTs constitute the largest group of GSTs in plants. Although several molecular and biochemical studies have shed light on their tridimensional structures, biochemical properties, and enzymatic activities, very little is known about the actual roles that these proteins play *in planta*. This lack of knowledge might reflect the functional redundancy that most probably exists between these GSTs (Sappl et al., 2009; Rahantaniaina et al., 2017). Nevertheless, the use of the model plant *A. thaliana* has aided in deciphering the role played by some of the 47 Ser-GSTs (13 GSTFs, 28 GSTUs, 1 TCHQD, 2 GSTZs, and 3 GSTTs) (**Table 4**; Wagner et al., 2002; Dixon and Edwards, 2010a).

GSTUs were first associated with plant xenobiotic detoxification, in particular the detoxification of herbicides. It was proposed that high GSTU activity, due to a high endogenous level of expression, was at the center of the observed differential sensitivity to herbicides between cereals (e.g., maize, wheat, and rice) and weeds (Cummins et al., 2011). In *A. thaliana*, it was proposed that *AtGSTU26*, whose expression is induced in response to chloroacetanilide herbicide treatments, could participate in the detoxification of these harmful chemicals by catalyzing their glutathionylation (Nutricati et al., 2006). The xenobiotic detoxification activity of GSTU extends to other chemicals. For instance, a recent study focusing on a major worldwide military pollutant, namely the 2,4,6-trinitrotoluene (TNT), highlighted the role played by GSTUs in detoxifying this harmful and highly persistent pollutant by catalyzing its GSH-conjugation (Gunning et al., 2014). In this study, the authors showed that overexpressing *AtGSTU24* and *AtGSTU25*, two genes whose expression is induced by TNT, was sufficient to enhance the ability of *A. thaliana* plants to withstand and detoxify TNT.

In addition to their role in detoxifying xenobiotic compounds, *A. thaliana* GSTUs were associated with the response to environmental cues. One of the best examples is the response to light signals. This was first demonstrated with *GSTU20*, a gene whose expression is induced under far-red irradiation and inhibited by *phytochrome A* (*phyA*) mutation (Chen et al., 2007). The characterization of gain- and loss-of-function mutant lines suggested the key role that GSTU20 plays in regulating cell elongation and flowering time in response to light (Chen et al., 2007). Similarly, *GSTU17*, whose expression is regulated by different photoreceptors (especially phyA), participates in the modulation of several aspects of seedling development (e.g., hypocotyl elongation, root development, anthocyanin accumulation) (Jiang et al., 2010). Two other GSTUs were also associated with the *A. thaliana* response to light stress, namely *GSTU5* and *GSTU14* (Liu and Li, 2002; Lv et al., 2015).

GSTU17 also plays a role in the response to drought and salt stresses (Chen et al., 2012). The *gstu17* mutation confers a higher tolerance to drought and salt stresses when compared to wild-type plants that could be attributed to an increased accumulation of GSH and ABA within the plant tissues. In this process, GSTU17 acts as a negative component of the stress-mediated signal transduction pathways. Conversely, the overexpression of GSTU19 in *A. thaliana* plants confers tolerance to drought and salt stresses (Xu et al., 2016). The fact that the overexpression of *GSTU19* also confers an increased tolerance to methyl viologen (a pro-oxidant compound) together with increased activity of antioxidant enzymes indicates that GSTU19 may be involved in counteracting the oxidative damages associated with drought or salt stresses. Additionally, the *A. thaliana* response to drought and salt stresses, mediated by the AtRGGA RNA-binding protein, involves *GSTU9* (Ambrosone et al., 2015).

GSTUs are also involved in plant response to biotic stresses. A recent example is the observation that *gstu13* mutants display an enhanced susceptibility, when compared

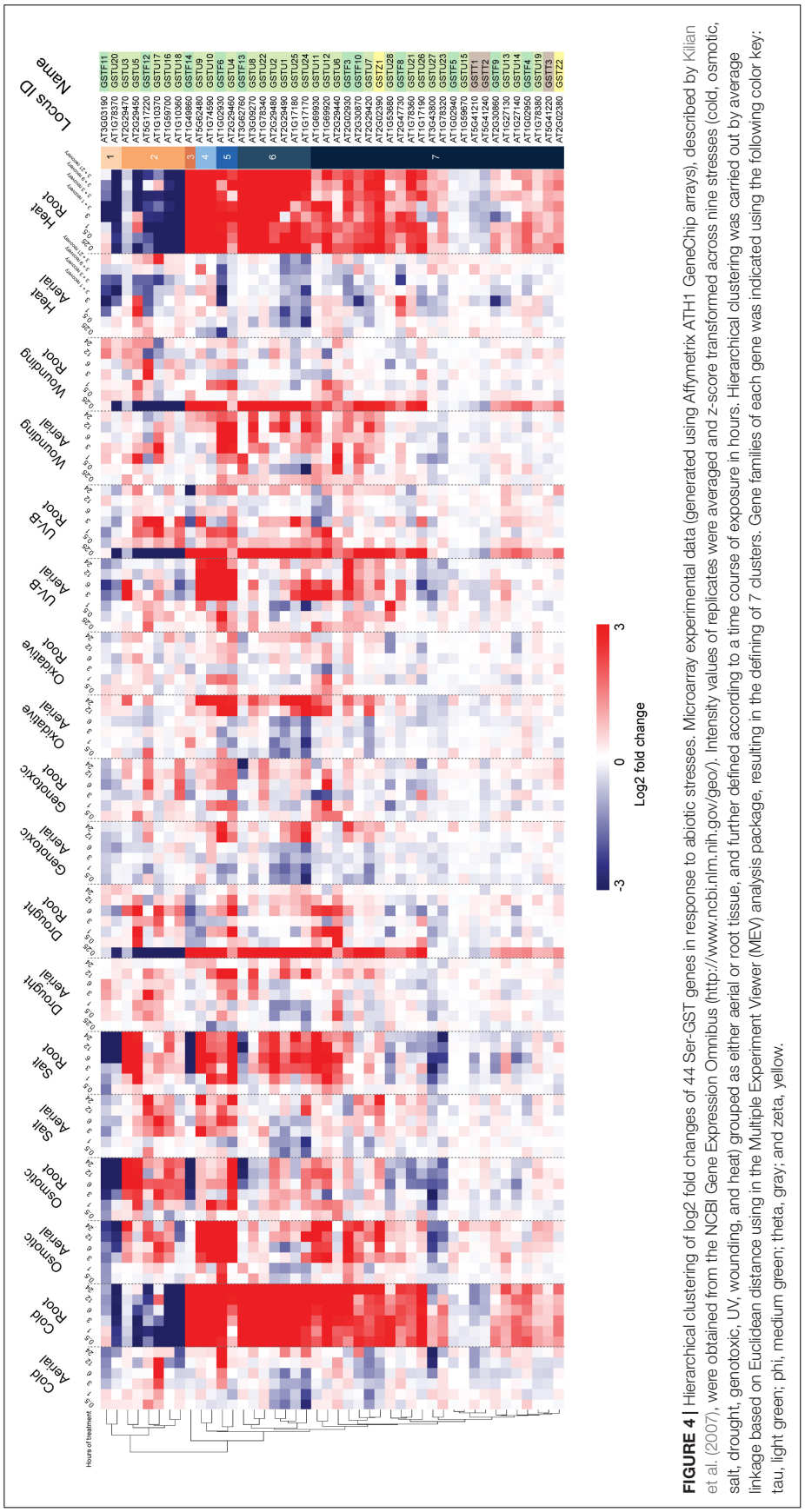

FIGURE 4 | Hierarchical clustering of log2 fold changes of 44 Ser-GST genes in response to abiotic stresses. Microarray experimental data (generated using Affymetrix ATH1 GeneChip arrays), described by Kilian et al. (2007), were obtained from the NCBI Gene Expression Omnibus (http://www.ncbi.nlm.nih.gov/geo/). Intensity values of replicates were averaged and z-score transformed across nine stresses (cold, osmotic, salt, drought, genotoxic, UV, wounding, and heat) grouped as either aerial or root tissue, and further defined according to a time course of exposure in hours. Hierarchical clustering was carried out by average linkage based on Euclidean distance using in the Multiple Experiment Viewer (MEV) analysis package, resulting in the defining of 7 clusters. Gene families of each gene was indicated using the following color key: tau, light green; phi, medium green; theta, gray; and zeta, yellow.

TABLE 4 | Diversity of Ser-GST functions.

GST	Gene ID	Acronym	Known role	Mutant characterized	References
GSTU1	At2g29490	GST19		None	
GSTU2	At2g29480	GST20		None	
GSTU3	At2g29470	GST21		None	
GSTU4	At2g29460	GST22		None	
GSTU5	At2g29450	GSTU1, AT103-1A	UV radiation acclimation	GSTU5-OE	Liu and Li, 2002
			Excess light acclimation response	None	Lv et al., 2015
GSTU6	At2g29440	GST24		None	
GSTU7	At2g29420	GST25	Part of the lipid stress response	None	Stotz et al., 2013
GSTU8	At3g09270			None	
GSTU9	At5g62480	GST14, GST14B	Salt and drought stress response	None	Ambrosone et al., 2015
GSTU10	At1g74590			None	
GSTU11	At1g69930			None	
GSTU12	At1g69920			None	
GSTU13	At1g27130	GST12	Indole glucosinolate biosynthesis / Response to fungal pathogens (*E. pisi*, *C. gloeosporioides* and *P. cucumerin*)	*gstu13*	Piślewska-Bednarek et al., 2018
GSTU14	At1g27140	GST13	Part of the excess light acclimation response	None	Lv et al., 2015
GSTU15	At1g59670			None	
GSTU16	At1g59700		Part of the plant response to fungal pathogens (*V. dahliae*)	None	Pantelides et al., 2010
GSTU17	At1g10370	ERD9, GST30, GST30B	Drought and salt stress response	GSTU17-OE and *gstu17*	Chen et al., 2012
			Light response / Seedling development / Root elongation	GSTU17-OE and *gstu17*	Jiang et al., 2010
GSTU18	At1g10360	GST29	Part of the lipid stress response	None	Mueller et al., 2008
GSTU19	At1g78380	GST8	Drought, salt and methyl viologen stress response	GSTU19-OE	Xu et al., 2016
GSTU20	At1g78370	FIP1	Light response / Seedling development / Flowering time	GSTU20-OE and *gstu20*	Chen et al., 2007
GSTU21	At1g78360			None	
GSTU22	At1g78340			None	
GSTU23	At1g78320			None	
GSTU24	At1g17170	GST	Lipid stress response	None	Mueller et al., 2008
			Xenobiotic detoxification (TNT, 2,4,6-trinitrotoluene)	GSTU24-OE	Gunning et al., 2014
GSTU25	At1g17180		Xenobiotic detoxification (TNT, 2,4,6-trinitrotoluene)	GSTU25-OE	Gunning et al., 2014
GSTU26	At1g17190		Xenobiotic detoxification (herbicides)	None	Nutricati et al., 2006
GSTU27	At3g43800			None	
GSTU28	At1g53680			None	
GSTF2	At4g02520	ATPM24, GST2	Response to bacterial inoculation (*P. syringae*)	None	Lieberherr et al., 2003
			Response to bacterial volatiles (*B. subtilis*)	None	Kwon et al., 2010
GSTF3	At2g02930	GST16		None	
GSTF4	At1g02950	GST31		None	
GSTF5	At1g02940			None	
GSTF6	At1g02930	ERD11, GST1, GSTF3	Response to bacterial inoculation (*P. syringae*)	None	Lieberherr et al., 2003
			Modulation of plant metabolism in response to oxidative stress	*gstf6 gstf7 gstf9 gstf10* RNAi lines	Sappl et al., 2009
			Camalexin biosynthesis (conjugation of GSH with IAN)	GSTF6-OE and *gstf6*	Su et al., 2011
GSTF7	At1g02920	GST11, GSTF8	Modulation of plant metabolism in response to oxidative stress	*gstf6 gstf7 gstf9 gstf10* RNAi lines	Sappl et al., 2009

(Continued)

TABLE 4 | Continued

GST*	Gene ID	Acronym	Known role	Mutant characterized	References
GSTF8	At2g47730	GST6, GSTF5, GSTF6	Part of the lipid stress response	None	Mueller et al., 2008
			Response to fungal (R. solani) and bacterial (P. syringae) pathogens	None	Gleason et al., 2011
			Response to fungal pathogens (*F. oxysporum*)	None	Thatcher et al., 2015
GSTF9	At2g30860	GLUTTR, GSTF7	Xenobiotic detoxification (CDNB, 1-chloro-2,4-dinitrobenzene)	None	Nutricati et al., 2006
			Indole glucosinolate biosynthesis	None	Wentzell et al., 2007
			Modulation of plant metabolism in response to oxidative stress	*gstf6 gstf7 gstf9 gstf10* RNAi lines	Sappl et al., 2009
			Salt stress response	*gstf9*	Horváth et al., 2015
GSTF10	At2g30870		Indole glucosinolate biosynthesis	None	Wentzell et al., 2007
			Drought and salt stress response	GSTF10-OE and *gstf10* RNA lines	Ryu et al., 2009
			Modulation of plant metabolism in response to oxidative stress	*gstf6 gstf7 gstf9 gstf10* RNAi lines	Sappl et al., 2009
GSTF11	At3g03190	GSTF6	Aliphatic glucosinolate biosynthesis	None	Wentzell et al., 2007
GSTF12	At5g17220	TT19	Flavonoid storage (anthocyanins and proanthocyanidins)	*gstfl12/tt19*	Kitamura et al., 2004; Sun et al., 2012
			Response to fungal pathogens (*V. dahliae*)	None	Pantelides et al., 2010
GSTF13	At3g62760			None	
GSTF14	At1g49860		Response to virus infection (BSCTV, beet severe curly top virus)	None	Yang et al., 2013
GSTT1	At5g41210	GST10		None	
GSTT2	At5g41240	GST10B	Systemic acquired resistance	*gstt2*	Banday and Nandi, 2018
GSTT3	At5g41220	GST10C		None	
GSTZ1	At2g02390	GST18, GSTZ1, MAAI	Tyrosine catabolism	None	Edwards and Dixon, 2000
GSTZ2	At2g02380			None	
TCHQD	At1g77290			None	

to wild-type plants, toward the fungal pathogens *Erysiphe pisi*, *Colletotrichum gloeosporioides*, and *Plectosphaerella cucumerina* (Piślewska-Bednarek et al., 2018). It was demonstrated that this phenotype is essentially due to a decrease in the biosynthesis of indole glucosinolates (IG; defense-related compounds found in Brassicaceae), where GSTU13 plays a catalytic role in conjugating GSH to IG precursors, affecting the innate immune system of *A. thaliana* plants. *GSTU16* is another member that was proposed to be part of the plant response to fungal pathogens (e.g., *Verticillium dahliae*) (Pantelides et al., 2010). However, the mechanism by which GSTU16 participates in this response still needs to be addressed.

Both biotic and abiotic stresses lead to the formation of non-enzymatically formed oxylipins, such as phytoprostanes, resulting from the oxidation of several types of lipids (most probably in response to the accumulation of stress-mediated free radicals and reactive oxygen species). These compounds serve as signaling molecules to adapt the plant response to environmental constraints, but may also enhance oxidative stress damages. Thus, their homeostasis should be tightly regulated. Interestingly, it has been shown that GSH-conjugation participates in this process, in particular in response to a *Pseudomonas syringae* infection (Mueller et al., 2008). In addition, the expression of several *GSTU* genes was shown to be responsive to phytoprostanes (i.e., *GSTU7*, *GSTU18*, and *GSTU24*) indicating that they may regulate phytoprostane homeostasis or be involved in the general detoxification pathways (Mueller et al., 2008; Stotz et al., 2013).

GSTFs constitute the second largest class of Ser-GSTs in plants, with 13 members in *A. thaliana* (Wagner et al., 2002). The GSTF1 sequence that was initially described (Bartling et al., 1993) is no longer present in the final reference genome of this plant.

As GSTUs, GSTFs are associated with the plant response to various abiotic and biotic stresses. For instance, *A. thaliana gstf9* and *gstf10* mutants are more sensitive to a salt stress than wild-type plants (Ryu et al., 2009; Horváth et al., 2015). In contrast, overexpression of *GSTF10* confers higher tolerance to salt. Together these data indicate that the *A. thaliana* GSTF9 and GSTF10 play a positive role in the plant response to a salt stress. However, several reports indicate that the role of *GSTF9* and *GSTF10* extends beyond. *GSTF10* was proposed to play a role in modulating developmental processes, such as the brassinosteroid-independent spontaneous cell death, a mechanism that is mediated by the production of reactive oxygen species (Ryu et al., 2009). *GSTF9* and *GSTF10*, as well as *GSTF11*, are also involved in the biosynthesis of glucosinolates (Wentzell et al., 2007). Whether GSTF9, GSTF10 and GSTF11 act in concert with GSTU13 in this process (Piślewska-Bednarek et al., 2018) remains to be investigated. GSTF9 and GSTF10, together with

GSTF6 and GSTF7, also play a role in limiting the metabolic changes that arise during oxidative stress (Sappl et al., 2009).

Additionally, GSTF6 activity is required for the biosynthesis of camalexin, the main phytoalexin (i.e., secondary metabolite with antimicrobial activity) present in *A. thaliana* (Su et al., 2011). The proposed role of GSTF6 in this process is to catalyze the conjugation of GSH on indole-3-acetonitrile (IAN), leading to the formation of GSH-IAN, the main precursor of camalexin biosynthesis. The above-mentioned functional roles of GSTF6 are in agreement with its first proposed biological function, which was to participate in defense mechanisms against pathogens (e.g., *P. syringae*), together with GSTF2 (Lieberherr et al., 2003; Kwon et al., 2010). GSTF8, GSTF12, and GSTF14 activities are associated with the *A. thaliana* response to various pathogens, including viruses (Pantelides et al., 2010; Gleason et al., 2011; Yang et al., 2013; Thatcher et al., 2015). GSTF8 and GSTF9 have been identified as potential actors of the lipid stress response and xenobiotic detoxification machinery, respectively (Nutricati et al., 2006; Mueller et al., 2008).

GSTF12 is another member of the phi class whose function has been extensively studies. GSTF12 is also known as TRANSPARENT TESTA 19 (TT19) and plays a key role in the control of anthocyanin and proanthocyanidin vacuolar accumulation in *A. thaliana* vegetative tissues and seed testa, respectively (Kitamura et al., 2004). In this process, TT19 acts as a carrier to convey these cytosolic flavonoids to the tonoplasts (Sun et al., 2012).

No more physiological information is available for other Ser-GST classes, namely GSTT, GSTZ, and TCHQD (3, 2, and 1 members in *A. thaliana*, respectively). *A. thaliana* GSTT2 seems involved in the modulation of systemic acquired resistance by altering the expression of key genes involved in this process through epigenetic modifications (Banday and Nandi, 2018). According to its capacity to catalyze the isomerisation of maleylacetoacetate into fumarylacetoacetate *in vitro*, AtGSTZ1 is likely involved in tyrosine catabolism, as demonstrated in animals (Edwards and Dixon, 2000). However, there is no mutant described so far and there is a second gene in *A. thaliana*, the biochemical properties of the protein having not yet been explored. Moreover, AtGSTZ1 was also able to catalyze the GSH-dependent dehalogenation of dichloroacetic acid to glyoxylic acid, suggesting other possible functions *in planta*. Finally, there is to date no clear function attributed to the sole member of the TCHQD class, either in *A. thaliana* or in another photosynthetic organisms.

CONCLUSION

The GST gene family was subject to a huge genetic expansion in terrestrial plants, with an average number of GSTs around 58 but also in some particular fungi (up to 45 isoforms) (Morel et al., 2013) compared to the 6–17 genes found in bacteria, yeast or mammals. This is linked to expansion within one or several classes as GSTU in plants. Genomic organization and phylogenetic analyses indicate that most duplication events responsible for the expansion of the GSTF and GSTU classes are species-specific. Among Ser-GSTs in plants, the GSTFs and GSTUs are highly represented, and have more diversified primary sequences and catalytic signatures compared to GSTs from the theta, zeta and TCHQD classes. This is likely at the origin of their broader range of activities and set of accommodated substrates/ligands.

According to their stress-inducible expression, it is documented that many GSTFs and GSTUs have functions connected to secondary metabolism, as exemplified by their implication in the vacuolar sequestration of anthocyanin, in the biosynthesis of camalexin, and/or in the binding of biosynthesis intermediates (porphyrin derivatives) or cellular by-products (oxylipins). Their implication in xenobiotic detoxification, such as herbicides, has likely little to do with their ancestral functions, that still remain to be delineated in many cases. However, this has led to the development of biotechnological applications in agriculture and environmental sciences [see the review in this research topic by Perperopoulou et al. (2018)]. The GSTs being targeted for the development of transgenic plants are linked to conferring tolerances against biotic and abiotic stresses or expressing engineered xenobiotic metabolizing enzymes for the bioremediation and detoxification of agrochemicals and pollutants.

To reveal the functions of Ser-GSTs, future studies will have to take into account the redundancy that most probably exists within and between the different classes of Ser-GSTs, which has limited the otherwise powerful reverse-genetic strategy. In order to inventory molecules able to bind GSTs, *in vivo* and *in vitro* ligand-fishing approaches have been used successfully in several cases (Dixon et al., 2011b; Dixon and Edwards, 2018). However, determining the nature of the identified molecules and whether, when and how they are conjugated with GSH or just bound to GSTs is a technically challenging and time-consuming task. For instance, out of the 43 structures of Ser-GSTs available to date in the Protein Data Bank, only 6 are solved with bound ligands. Hence, the validation of the physiological relevance of the detected interactions remains a major challenge.

AUTHOR CONTRIBUTIONS

ES-G, AH, and NR carried out the *in silico* genome analyses. SL and OK performed the transcriptomic analyses. ClD and MS performed structural data analyses. KR and ChD compiled data presented in **Table 4**. All authors participated to the writing of the manuscript.

FUNDING

The UMR1136 is supported by a grant overseen by the French National Research Agency (ANR) as part of the "Investissements d'Avenir" program (ANR-11-LABX-0002-01, Lab of Excellence ARBRE). OK is supported by the Swedish Research Council "VetenskapsRådet" (grant: 621-2014-4688) and the Kempe Foundations (Gunnar Öquist Fellowship). AH, ChD, NR, and KR are supported by the French National Research Agency (ANR-17-CE20-0008-01).

REFERENCES

Ahmad, L., Rylott, E. L., Bruce, N. C., Edwards, R., and Grogan, G. (2017). Structural evidence for *Arabidopsis* glutathione transferase At GSTF2 functioning as a transporter of small organic ligands. *FEBS Open Bio* 7, 122–132. doi: 10.1002/2211-5463.12168

Ahsan, N., Lee, D.-G., Alam, I., Kim, P. J., Lee, J. J., Ahn, Y.-O., et al. (2008). Comparative proteomic study of arsenic-induced differentially expressed proteins in rice roots reveals glutathione plays a central role during As stress. *Proteomics* 8, 3561–3576. doi: 10.1002/pmic.200701189

Alfenito, M. R. (1998). Functional complementation of anthocyanin sequestration in the vacuole by widely divergent glutathione S-transferases. *Plant Cell Online* 10, 1135–1150. doi: 10.1105/tpc.10.7.1135

Ambrosone, A., Batelli, G., Nurcato, R., Aurilia, V., Punzo, P., Bangarusamy, D. K., et al. (2015). The *Arabidopsis* RNA-binding protein AtRGGA regulates tolerance to salt and drought stress. *Plant Physiol.* 168, 292–306. doi: 10.1104/pp.114.255802

Axarli, I., Dhavala, P., Papageorgiou, A. C., and Labrou, N. E. (2009a). Crystallographic and functional characterization of the fluorodifen-inducible glutathione transferase from *Glycine max* reveals an active site topography suited for diphenylether herbicides and a novel L-site. *J. Mol. Biol.* 385, 984–1002. doi: 10.1016/j.jmb.2008.10.084

Axarli, I., Dhavala, P., Papageorgiou, A. C., and Labrou, N. E. (2009b). Crystal structure of *Glycine max* glutathione transferase in complex with glutathione: investigation of the mechanism operating by the Tau class glutathione transferases. *Biochem. J.* 422, 247–256. doi: 10.1042/BJ20090224

Axarli, I., Georgiadou, C., Dhavala, P., Papageorgiou, A. C., and Labrou, N. E. (2010). Investigation of the role of conserved residues Ser13, Asn48 and Pro49 in the catalytic mechanism of the tau class glutathione transferase from *Glycine max*. *Biochim. Biophys. Acta (BBA) – Proteins Proteom.* 1804, 662–667. doi: 10.1016/j.bbapap.2009.10.016

Axarli, I., Muleta, A. W., Vlachakis, D., Kossida, S., Kotzia, G., Maltezos, A., et al. (2016). Directed evolution of Tau class glutathione transferases reveals a site that regulates catalytic efficiency and masks co-operativity. *Biochem. J.* 473, 559–570. doi: 10.1042/BJ20150930

Axarli, I. A., Rigden, D. J., and Labrou, N. E. (2004). Characterization of the ligandin site of maize glutathione S-transferase I. *Biochem. J.* 382, 885–893. doi: 10.1042/BJ20040298

Banday, Z. Z., and Nandi, A. K. (2018). *Arabidopsis thaliana* GLUTATHIONE-S -TRANSFERASE THETA 2 interacts with RSI1/FLD to activate systemic acquired resistance: GSTT2 interacts with FLD and regulates SAR. *Mol. Plant Pathol.* 19, 464–475. doi: 10.1111/mpp.12538

Bartling, D., Radzio, R., Steiner, U., and Weiler, E. W. (1993). A glutathione S-transferase with glutathione-peroxidase activity from *Arabidopsis thaliana*. Molecular cloning and functional characterization. *Eur. J. Biochem.* 216, 579–586. doi: 10.1111/j.1432-1033.1993.tb18177.x

Bilang, J., Macdonald, H., King, P. J., and Sturm, A. (1993). A soluble auxin-binding protein from *Hyoscyamus muticus* is a glutathione S-transferase. *Plant Physiol.* 102, 29–34. doi: 10.1104/pp.102.1.29

Board, P. G., Coggan, M., Chelvanayagam, G., Easteal, S., Jermiin, L. S., Schulte, G. K., et al. (2000). Identification, characterization, and crystal structure of the omega class glutathione transferases. *J. Biol. Chem.* 275, 24798–24806. doi: 10.1074/jbc.M001706200

Board, P. G., and Menon, D. (2013). Glutathione transferases, regulators of cellular metabolism and physiology. *Biochim. Biophys. Acta (BBA) – Gen. Subjects* 1830, 3267–3288. doi: 10.1016/j.bbagen.2012.11.019

Booth, J., Boyland, E., and Sims, P. (1961). An enzyme from rat liver catalysing conjugations with glutathione. *Biochem. J.* 79, 516–524. doi: 10.1042/bj0790516

Bryant, D., Cummins, I., Dixon, D. P., and Edwards, R. (2006). Cloning and characterization of a theta class glutathione transferase from the potato pathogen *Phytophthora infestans*. *Phytochemistry* 67, 1427–1434. doi: 10.1016/j.phytochem.2006.05.012

Buetler, T. M., and Eaton, D. L. (1992). Complementary DNA cloning, messenger RNA expression, and induction of alpha-class glutathione S-transferases in mouse tissues. *Cancer Res.* 52, 314–318.

Burmeister, C., Lüersen, K., Heinick, A., Hussein, A., Domagalski, M., Walter, R. D., et al. (2008). Oxidative stress in *Caenorhabditis elegans*?: protective effects of the Omega class glutathione transferase (GSTO-1). *FASEB J.* 22, 343–354. doi: 10.1096/fj.06-7426com

Chen, C.-Y., Ho, S.-S., Kuo, T.-Y., Hsieh, H.-L., and Cheng, Y.-S. (2017). Structural basis of jasmonate-amido synthetase FIN219 in complex with glutathione S-transferase FIP1 during the JA signal regulation. *Proc. Natl. Acad. Sci. U.S.A.* 114, E1815–E1824. doi: 10.1073/pnas.1609980114

Chen, I.-C., Huang, I.-C., Liu, M.-J., Wang, Z.-G., Chung, S.-S., and Hsieh, H.-L. (2007). Glutathione S-transferase interacting with far-red insensitive 219 is involved in phytochrome A-mediated signaling in *Arabidopsis*. *Plant Physiol.* 143, 1189–1202. doi: 10.1104/pp.106.094185

Chen, J.-H., Jiang, H.-W., Hsieh, E.-J., Chen, H.-Y., Chien, C.-T., Hsieh, H.-L., et al. (2012). Drought and salt stress tolerance of an arabidopsis glutathione S-transferase U17 knockout mutant are attributed to the combined effect of glutathione and abscisic acid. *Plant Physiol.* 158, 340–351. doi: 10.1104/pp.111.181875

Cho, H.-Y., Lee, H. J., and Kong, K.-H. (2007). A phi class glutathione S-transferase from *Oryza sativa* (OsGSTF5): molecular cloning, expression and biochemical characteristics. *J. Biochem. Mol. Biol.* 40, 511–516. doi: 10.5483/bmbrep.2007.40.4.511

Chronopoulou, E., Ataya, F. S., Pouliou, F., Perperopoulou, F., Georgakis, N., Nianiou-Obeidat, I., et al. (2017a). "Structure, evolution and functional roles of plant glutathione transferases," in *Glutathione in Plant Growth, Development, and Stress Tolerance*, eds M. A. Hossain, M. G. Mostofa, P. Diaz-Vivancos, D. J. Burritt, M. Fujita, and L.-S. P. Tran (Cham: Springer International Publishing), 195–213. doi: 10.1007/978-3-319-66682-2_9

Chronopoulou, E., Georgakis, N., Nianiou-Obeidat, I., Madesis, P., Perperopoulou, F., Pouliou, F., et al. (2017b). "Plant glutathione transferases in abiotic stress response and herbicide resistance," in *Glutathione in Plant Growth, Development, and Stress Tolerance*, eds M. A. Hossain, M. G. Mostofa, P. Diaz-Vivancos, D. J. Burritt, M. Fujita, and L.-S. P. Tran (Cham: Springer International Publishing), 215–233. doi: 10.1007/978-3-319-66682-2_10

Coggan, M., Flanagan, J. U., Parker, M. W., Vichai, V., Pearson, W. R., and Board, P. G. (2002). Identification and characterization of GSTT3, a third murine theta class glutathione transferase. *Biochem. J.* 366, 323–332. doi: 10.1042/bj20011878

Coleman, J., Blake-Kalff, M., and Davies, E. (1997). Detoxification of xenobiotics by plants: chemical modification and vacuolar compartmentation. *Trends Plant Sci.* 2, 144–151. doi: 10.1016/S1360-1385(97)01019-4

Combes, B., and Stakelum, G. S. (1961). A liver enzyme that conjugates sulfobromophtalein sodium with glutathione. *J. Clin. Investig.* 40, 981–988. doi: 10.1172/JCI104337

Conn, S., Curtin, C., Bézier, A., Franco, C., and Zhang, W. (2008). Purification, molecular cloning, and characterization of glutathione S-transferases (GSTs) from pigmented *Vitis vinifera* L. cell suspension cultures as putative anthocyanin transport proteins. *J. Exp. Bot.* 59, 3621–3634. doi: 10.1093/jxb/ern217

Cummins, I., Dixon, D. P., Freitag-Pohl, S., Skipsey, M., and Edwards, R. (2011). Multiple roles for plant glutathione transferases in xenobiotic detoxification. *Drug Metabol. Rev.* 43, 266–280. doi: 10.3109/03602532.2011.552910

Cummins, I., O'Hagan, D., Jablonkai, I., Cole, D. J., Hehn, A., Werck-Reichhart, D., et al. (2003). Cloning, characterization and regulation of a family of phi class glutathione transferases from wheat. *Plant Mol. Biol.* 52, 591–603.

Deponte, M. (2013). Glutathione catalysis and the reaction mechanisms of glutathione-dependent enzymes. *Biochim. Biophys. Acta (BBA) – Gen. Subjects* 1830, 3217–3266. doi: 10.1016/j.bbagen.2012.09.018

DeRidder, B. P. (2002). Induction of glutathione S-transferases in *Arabidopsis* by herbicide safeners. *Plant Physiol.* 130, 1497–1505. doi: 10.1104/pp.010066

Ding, N., Wang, A., Zhang, X., Wu, Y., Wang, R., Cui, H., et al. (2017). Identification and analysis of glutathione S-transferase gene family in sweet potato reveal divergent GST-mediated networks in aboveground and underground tissues in response to abiotic stresses. *BMC Plant Biol.* 17:225. doi: 10.1186/s12870-017-1179-z

Dixon, D. P., Cummins, I., Cole, D. J., and Edwards, R. (1998). Glutathione-mediated detoxification systems in plants. *Curr. Opin. Plant Biol.* 1, 258–266. doi: 10.1016/S1369-5266(98)80114-3

Dixon, D. P., and Edwards, R. (2009). Selective binding of glutathione conjugates of fatty acid derivatives by plant glutathione transferases. *J. Biol. Chem.* 284, 21249–21256. doi: 10.1074/jbc.M109.020107

Dixon, D. P., and Edwards, R. (2010a). Glutathione transferases. *Arabidopsis Book* 8:e0131. doi: 10.1199/tab.0131

Dixon, D. P., and Edwards, R. (2010b). Roles for stress-inducible lambda glutathione transferases in flavonoid metabolism in plants as identified by ligand fishing. *J. Biol. Chem.* 285, 36322–36329. doi: 10.1074/jbc.M110.164806

Dixon, D. P., and Edwards, R. (2018). Protein-ligand fishing in planta for biologically active natural products using glutathione transferases. *Front. Plant Sci.* 9:1659. doi: 10.3389/fpls.2018.01659

Dixon, D. P., Hawkins, T., Hussey, P. J., and Edwards, R. (2009). Enzyme activities and subcellular localization of members of the *Arabidopsis* glutathione transferase superfamily. *J. Exp. Bot.* 60, 1207–1218. doi: 10.1093/jxb/ern365

Dixon, D. P., Lapthorn, A., and Edwards, R. (2002). Plant glutathione transferases. *Genome Biol.* 3:REVIEWS3004.

Dixon, D. P., Lapthorn, A., Madesis, P., Mudd, E. A., Day, A., and Edwards, R. (2008). Binding and glutathione conjugation of porphyrinogens by plant glutathione transferases. *J. Biol. Chem.* 283, 20268–20276. doi: 10.1074/jbc.M802026200

Dixon, D. P., McEwen, A. G., Lapthorn, A. J., and Edwards, R. (2003). Forced evolution of a herbicide detoxifying glutathione transferase. *J. Biol. Chem.* 278, 23930–23935. doi: 10.1074/jbc.M303620200

Dixon, D. P., Sellars, J. D., and Edwards, R. (2011a). The *Arabidopsis* phi class glutathione transferase At GSTF2: binding and regulation by biologically active heterocyclic ligands. *Biochem. J.* 438, 63–70. doi: 10.1042/BJ20101884

Dixon, D. P., Steel, P. G., and Edwards, R. (2011b). Roles for glutathione transferases in antioxidant recycling. *Plant Signal. Behav.* 6, 1223–1227. doi: 10.4161/psb.6.8.16253

Droog, F. (1997). Plant glutathione S-transferases, a tale of theta and tau. *J. Plant Growth Regul.* 16, 95–107. doi: 10.1007/PL00006984

Droog, F. N. J., Hooykaas, P. J. J., and Van Der Zaal, B. J. (1995). 2,4-Dichlorophenoxyacetic acid and related chlorinated compounds inhibit two auxin-regulated type-III tobacco glutathione S-transferases. *Plant Physiol.* 107, 1139–1146. doi: 10.1104/pp.107.4.1139

Edwards, R., and Dixon, D. P. (2000). The role of glutathione transferases in herbicide metabolism. *Environ. Fate Saf. Manage. Agrochem.* 19, 216–222.

Edwards, T. E., Bryan, C. M., Leibly, D. J., Dieterich, S. H., Abendroth, J., Sankaran, B., et al. (2011). Structures of a putative ζ-class glutathione-S-transferase from the pathogenic fungus *Coccidioides immitis*. *Acta Crystallogr. Sect. F Struct. Biol. Cryst. Commun.* 67, 1038–1043. doi: 10.1107/S1744309111009493

Fernandez-Canon, J. M., Baetscher, M. W., Finegold, M., Burlingame, T., Gibson, K. M., and Grompe, M. (2002). Maleylacetoacetate isomerase (MAAI/GSTZ)-deficient mice reveal a glutathione-dependent nonenzymatic bypass in tyrosine catabolism. *Mol. Cell. Biol.* 22, 4943–4951. doi: 10.1128/MCB.22.13.4943-4951.2002

Fernández-Cañón, J. M., and Peñalva, M. A. (1998). Characterization of a fungal maleylacetoacetate isomerase gene and identification of its human homologue. *J. Biol. Chem.* 273, 329–337. doi: 10.1074/jbc.273.1.329

Frear, D. S., and Swanson, H. R. (1970). Biosynthesis of S-(4-ethylamino-6-isopropylamino- 2-s-triazino) glutathione: partial purification and properties of a glutathione S-transferase from corn. *Phytochemistry* 9, 2123–2132. doi: 10.1016/S0031-9422(00)85377-7

Frova, C. (2006). Glutathione transferases in the genomics era: new insights and perspectives. *Biomol. Eng.* 23, 149–169. doi: 10.1016/j.bioeng.2006.05.020

Gallé, Á, Csiszár, J., Secenji, M., Guóth, A., Cseuz, L., Tari, I., et al. (2009). Glutathione transferase activity and expression patterns during grain filling in flag leaves of wheat genotypes differing in drought tolerance: response to water deficit. *J. Plant Physiol.* 166, 1878–1891. doi: 10.1016/j.jplph.2009.05.016

Gleason, C., Huang, S., Thatcher, L. F., Foley, R. C., Anderson, C. R., Carroll, A. J., et al. (2011). Mitochondrial complex II has a key role in mitochondrial-derived reactive oxygen species influence on plant stress gene regulation and defense. *Proc. Natl. Acad. Sci. U.S.A.* 108, 10768–10773. doi: 10.1073/pnas.1016060108

Gomez, C., Conejero, G., Torregrosa, L., Cheynier, V., Terrier, N., and Ageorges, A. (2011). In vivo grapevine anthocyanin transport involves vesicle-mediated trafficking and the contribution of anthoMATE transporters and GST: anthocyanin trafficking in grapevine. *Plant J.* 67, 960–970. doi: 10.1111/j.1365-313X.2011.04648.x

Gong, H., Jiao, Y., Hu, W., and Pua, E. (2005). Expression of glutathione-S-transferase and its role in plant growth and development in vivo and shoot morphogenesis in vitro. *Plant Mol. Biol.* 57, 53–66. doi: 10.1007/s11103-004-4516-1

Gonneau, M., Mornet, R., and Laloue, M. (1998). A Nicotiana plumbaginifolia protein labeled with an azido cytokinin agonist is a glutathione S-transferase. *Physiol. Plant.* 103, 114–124. doi: 10.1034/j.1399-3054.1998.1030114.x

Gonzalez, D., Fraichard, S., Grassein, P., Delarue, P., Senet, P., Nicolaï, A., et al. (2018). Characterization of a *Drosophila* glutathione transferase involved in isothiocyanate detoxification. *Insect Biochem. Mol. Biol.* 95, 33–43. doi: 10.1016/j.ibmb.2018.03.004

Goodstein, D. M., Shu, S., Howson, R., Neupane, R., Hayes, R. D., Fazo, J., et al. (2012). Phytozome: a comparative platform for green plant genomics. *Nucleic Acids Res.* 40, D1178–D1186. doi: 10.1093/nar/gkr944

Gronwald, J. W., and Plaisance, K. L. (1998). Isolation and characterization of glutathione S-transferase isozymes from sorghum. *Plant Physiol.* 117, 877–892. doi: 10.1104/pp.117.3.877

Gunning, V., Tzafestas, K., Sparrow, H., Johnston, E. J., Brentnall, A. S., Potts, J. R., et al. (2014). *Arabidopsis* glutathione transferases U24 and U25 exhibit a range of detoxification activities with the environmental pollutant and explosive, 2,4,6-trinitrotoluene. *Plant Physiol.* 165, 854–865. doi: 10.1104/pp.114.237180

Habig, W. H., Pabst, M. J., Fleischner, G., Gatmaitan, Z., Arias, I. M., and Jakoby, W. B. (1974). The identity of glutathione S-transferase B with ligandin, a major binding protein of liver. *Proc. Natl. Acad. Sci. U.S.A.* 71, 3879–3882. doi: 10.1073/pnas.71.10.3879

Han, J.-B., Li, G.-Q., Wan, P.-J., Zhu, T.-T., and Meng, Q.-W. (2016). Identification of glutathione S-transferase genes in Leptinotarsa decemlineata and their expression patterns under stress of three insecticides. *Pesticide Biochem. Physiol.* 133, 26–34. doi: 10.1016/j.pestbp.2016.03.008

Hayes, J. D., and McLellan, L. I. (1999). Glutathione and glutathione-dependent enzymes represent a co-ordinately regulated defence against oxidative stress. *Free Radic. Res.* 31, 273–300. doi: 10.1080/10715769900300851

Hayes, J. D., and Pulford, D. J. (1995). The glut athione S-transferase supergene family: regulation of GST and the contribution of the lsoenzymes to cancer chemoprotection and drug resistance part I. *Crit. Rev. Biochem. Mol. Biol.* 30, 445–520. doi: 10.3109/10409239509083491

He, G., Guan, C.-N., Chen, Q.-X., Gou, X.-J., Liu, W., Zeng, Q.-Y., et al. (2016). Genome-wide analysis of the glutathione S-transferase gene family in capsella rubella: identification, expression, and biochemical functions. *Front. Plant Sci.* 7:1325. doi: 10.3389/fpls.2016.01325

Horváth, E., Bela, K., Papdi, C., Gallé, Á, Szabados, L., Tari, I., et al. (2015). The role of *Arabidopsis* glutathione transferase F9 gene under oxidative stress in seedlings. *Acta Biol. Hungarica* 66, 406–418. doi: 10.1556/018.66.2015.4.5

Huang, Y., Xun, R., Chen, G., and Xun, L. (2008). Maintenance role of a glutathionyl-hydroquinone lyase (PcpF) in pentachlorophenol degradation by *Sphingobium chlorophenolicum* ATCC 39723. *J. Bacteriol.* 190, 7595–7600. doi: 10.1128/JB.00489-08

Hurst, R., Bao, Y., Jemth, P., Mannervik, B., and Williamson, G. (1998). Phospholipid hydroperoxide glutathione peroxidase activity of human glutathione transferases. *Biochem. J.* 332(Pt 1), 97–100. doi: 10.1042/bj3320097

Islam, S., Rahman, I. A., Islam, T., and Ghosh, A. (2017). Genome-wide identification and expression analysis of glutathione S-transferase gene family in tomato: gaining an insight to their physiological and stress-specific roles. *PLoS One* 12:e0187504. doi: 10.1371/journal.pone.01875004

Jakobsson, P. J., Morgenstern, R., Mancini, J., Ford-Hutchinson, A., and Persson, B. (1999). Common structural features of MAPEG – a widespread superfamily of membrane associated proteins with highly divergent functions in eicosanoid and glutathione metabolism. *Protein Sci.* 8, 689–692. doi: 10.1110/ps.8.3.689

Jakoby, W. B. (1978). The glutathione S-transferases: a group of multifunctional detoxification proteins. *Adv. Enzymol. Relat. Areas Mol. Biol.* 46, 383–414. doi: 10.1002/9780470122914.ch6

Jha, B., Sharma, A., and Mishra, A. (2011). Expression of SbGSTU (tau class glutathione S-transferase) gene isolated from *Salicornia brachiata* in tobacco for salt tolerance. *Mol. Biol. Rep.* 38, 4823–4832. doi: 10.1007/s11033-010-0625-x

Jiang, H.-W., Liu, M.-J., Chen, I.-C., Huang, C.-H., Chao, L.-Y., and Hsieh, H.-L. (2010). A glutathione S-transferase regulated by light and hormones participates in the modulation of *Arabidopsis* seedling development. *Plant Physiol.* 154, 1646–1658. doi: 10.1104/pp.110.159152

Kao, C. W., Bakshi, M., Sherameti, I., Dong, S., Reichelt, M., Oelmüller, R., et al. (2016). A Chinese cabbage (Brassica campetris subsp. Chinensis) τ-type

glutathione-S-transferase stimulates Arabidopsis development and primes against abiotic and biotic stress. *Plant Mol. Biol.* 92, 643–659. doi: 10.1007/s11103-016-0531-2

Keppler, D. (1999). Export pumps for glutathione S-conjugates. *Free Radic. Biol. Med.* 27, 985–991. doi: 10.1016/s0891-5849(99)00171-9

Ketley, J. N., Habig, W. H., and Jakoby, W. B. (1975). Binding of nonsubstrate ligands to the glutathione S-transferases. *J. Biol. Chem.* 250, 8670–8673.

Khan, N., Hu, C., Amjad Khan, W., and Hou, X. (2018). Genome-wide identification, classification, and expression divergence of glutathione-transferase family in *Brassica rapa* under multiple hormone treatments. *BioMed. Res. Int.* 2018, 1–19. doi: 10.1155/2018/6023457

Kiefer, P. M., and Copley, S. D. (2002). Characterization of the initial steps in the reductive dehalogenation catalyzed by tetrachlorohydroquinone dehalogenase †. *Biochemistry* 41, 1315–1322. doi: 10.1021/bi0117504

Kilian, J., Whitehead, D., Horak, J., Wanke, D., Weinl, S., Batistic, O., et al. (2007). The AtGenExpress global stress expression data set: protocols, evaluation and model data analysis of UV-B light, drought and cold stress responses: AtGenExpress global abiotic stress data set. *Plant J.* 50, 347–363. doi: 10.1111/j.1365-313X.2007.03052.x

Kim, J., Suh, H., Kim, S., Kim, K., Ahn, C., and Yim, J. (2006). Identification and characteristics of the structural gene for the *Drosophila* eye colour mutant sepia, encoding PDA synthase, a member of the Omega class glutathione S-transferases. *Biochem. J.* 398, 451–460. doi: 10.1042/BJ20060424

Kitamura, S., Akita, Y., Ishizaka, H., Narumi, I., and Tanaka, A. (2012). Molecular characterization of an anthocyanin-related glutathione S-transferase gene in cyclamen. *J. Plant Physiol.* 169, 636–642. doi: 10.1016/j.jplph.2011.12.011

Kitamura, S., Shikazono, N., and Tanaka, A. (2004). TRANSPARENT TESTA 19 is involved in the accumulation of both anthocyanins and proanthocyanidins in *Arabidopsis*. *Plant J.* 37, 104–114. doi: 10.1046/j.1365-313x.2003.01943.x

Kraus, P. (1980). Resolution, purification and some properties of three glutathione transferases from rat liver mitochondria. *Hoppe-Seyler's Z. Physiol. Chem.* 361, 9–15.

Kwon, Y. S., Ryu, C.-M., Lee, S., Park, H. B., Han, K. S., Lee, J. H., et al. (2010). Proteome analysis of *Arabidopsis* seedlings exposed to bacterial volatiles. *Planta* 232, 1355–1370. doi: 10.1007/s00425-010-1259-x

Lallement, P.-A., Brouwer, B., Keech, O., Hecker, A., and Rouhier, N. (2014). The still mysterious roles of cysteine-containing glutathione transferases in plants. *Front. Pharmacol.* 5:192. doi: 10.3389/fphar.2014.00192

Lallement, P.-A., Meux, E., Gualberto, J. M., Dumarcay, S., Favier, F., Didierjean, C., et al. (2015). Glutathionyl-hydroquinone reductases from poplar are plastidial proteins that deglutathionylate both reduced and oxidized glutathionylated quinones. *FEBS Lett.* 589, 37–44. doi: 10.1016/j.febslet.2014.11.021

Lamoureux, G. L., Shimabukuro, R. H., Swanson, H. R., and Frear, D. S. (1970). Metabolism of 2-chloro-4-ethylamino-6-isopropylamino-s-triazine (atrazine) in excised sorghum leaf sections. *J. Agric. Food Chem.* 18, 81–86. doi: 10.1021/jf60167a029

Lan, T., Yang, Z.-L., Yang, X., Liu, Y.-J., Wang, X.-R., and Zeng, Q.-Y. (2009). Extensive functional diversification of the populus glutathione S-transferase supergene family. *Plant Cell* 21, 3749–3766. doi: 10.1105/tpc.109.070219

Larsen, E. S., Alfenito, M. R., Briggs, W. R., and Walbot, V. (2003). A carnation anthocyanin mutant is complemented by the glutathione S-transferases encoded by maize Bz2 and petunia An9. *Plant Cell Rep.* 21, 900–904. doi: 10.1007/s00299-002-0545-x

Lederer, B., and Böger, P. (2003). Binding and protection of porphyrins by glutathione S-transferases of *Zea mays* L. *Biochim. Biophys. Acta (BBA) – Gen. Subjects* 1621, 226–233. doi: 10.1016/S0304-4165(03)00073-4

Lederer, B., and Böger, P. (2005). A ligand function of glutathione S-transferase, *Z. Naturforsch. C.* 60, 166–171. doi: 10.1515/znc-2005-3-403

Levi, A. J., and Arias, I. M. (1969). Two hepatic cytoplasmic protein fractions, Y and Z, and their possible role in the hepatic uptake of bilirubin, sulfobromophthalein, and other anions. *J. Clin. Invest.* 48, 2156–2167. doi: 10.1172/JCI106182

Lieberherr, D., Wagner, U., Dubuis, P.-H., Métraux, J.-P., and Mauch, F. (2003). The rapid induction of glutathione S-transferases AtGSTF2 and AtGSTF6 by avirulent *Pseudomonas* syringae is the result of combined salicylic acid and ethylene signaling. *Plant Cell Physiol.* 44, 750–757. doi: 10.1093/pcp/pcg093

Litwack, G., Ketterer, B., and Arias, I. M. (1971). Ligandin: a hepatic protein which binds steroids, bilirubin, carcinogens and a number of exogenous organic anions. *Nature* 234, 466–467. doi: 10.1038/234466a0

Liu, X.-F., and Li, J.-Y. (2002). [Characterization of an ultra-violet inducible gene that encodes glutathione S-transferase in *Arabidopsis thaliana*]. *Yi Chuan Xue Bao* 29, 458–460.

Liu, Y.-J., Han, X.-M., Ren, L.-L., Yang, H.-L., and Zeng, Q.-Y. (2013). Functional divergence of the glutathione S-transferase supergene family in physcomitrella patens reveals complex patterns of large gene family evolution in land plants. *Plant Physiol.* 161, 773–786. doi: 10.1104/pp.112.205815

Lv, F., Zhou, J., Zeng, L., and Xing, D. (2015). β-cyclocitral upregulates salicylic acid signalling to enhance excess light acclimation in *Arabidopsis*. *J. Exp. Bot.* 66, 4719–4732. doi: 10.1093/jxb/erv231

Mannervik, B., Alin, P., Guthenberg, C., Jensson, H., Tahir, M. K., Warholm, M., et al. (1985). Identification of three classes of cytosolic glutathione transferase common to several mammalian species: correlation between structural data and enzymatic properties. *Proc. Natl. Acad. Sci. U.S.A.* 82, 7202–7206. doi: 10.1073/pnas.82.21.7202

Mannervik, B., and Danielson, U. H. (1988). Glutathione transferases–structure and catalytic activity. *CRC Crit. Rev. Biochem.* 23, 283–337.

Marrs, K. A. (1996). The functions and regulation of glutathionE S-transferases in plants. *Ann. Rev. Plant Physiol. Plant Mol. Biol.* 47, 127–158. doi: 10.1146/annurev.arplant.47.1.127

Marrs, K. A., Alfenito, M. R., Lloyd, A. M., and Walbot, V. (1995). A glutathione S-transferase involved in vacuolar transfer encoded by the maize gene Bronze-2. *Nature* 375, 397–400. doi: 10.1038/375397a0

Marsh, M., Shoemark, D. K., Jacob, A., Robinson, C., Cahill, B., Zhou, N.-Y., et al. (2008). Structure of bacterial glutathione-S-transferase maleyl pyruvate isomerase and implications for mechanism of isomerisation. *J. Mol. Biol.* 384, 165–177. doi: 10.1016/j.jmb.2008.09.028

Martínez-Márquez, A., Martínez-Esteso, M. J., Vilella-Antón, M. T., Sellés-Marchart, S., Morante-Carriel, J. A., Hurtado, E., et al. (2017). A tau class glutathione-S-transferase is involved in trans-resveratrol transport out of grapevine cells. *Front. Plant Sci.* 8:1457. doi: 10.3389/fpls.2017.01457

Masai, E., Ichimura, A., Sato, Y., Miyauchi, K., Katayama, Y., and Fukuda, M. (2003). Roles of the enantioselective glutathione S-transferases in cleavage of beta-aryl ether. *J. Bacteriol.* 185, 1768–1775. doi: 10.1128/jb.185.6.1768-1775.2003

Mashiyama, S. T., Malabanan, M. M., Akiva, E., Bhosle, R., Branch, M. C., Hillerich, B., et al. (2014). Large-scale determination of sequence, structure, and function relationships in cytosolic glutathione transferases across the biosphere. *PLoS Biol.* 12:e1001843. doi: 10.1371/journal.pbio.1001843

Menon, D., and Board, P. G. (2013). A role for glutathione transferase omega 1 (GSTO1-1) in the glutathionylation cycle. *J. Biol. Chem.* 288, 25769–25779. doi: 10.1074/jbc.M113.487785

Meux, E., Morel, M., Lamant, T., Gérardin, P., Jacquot, J.-P., Dumarçay, S., et al. (2013). New substrates and activity of Phanerochaete chrysosporium Omega glutathione transferases. *Biochimie* 95, 336–346. doi: 10.1016/j.biochi.2012.10.003

Meux, E., Prosper, P., Ngadin, A., Didierjean, C., Morel, M., Dumarçay, S., et al. (2011). Glutathione transferases of *Phanerochaete chrysosporium*: S-glutathionyl-p-hydroquinone reductase belongs to a new structural class. *J. Biol. Chem.* 286, 9162–9173. doi: 10.1074/jbc.M110.194548

Momose, M., Itoh, Y., Umemoto, N., Nakayama, M., and Ozeki, Y. (2013). Reverted glutathione S-transferase-like genes that influence flower color intensity of carnation (*Dianthus caryophyllus* L.) originated from excision of a transposable element. *Breed. Sci.* 63, 435–440. doi: 10.1270/jsbbs.63.435

Monticolo, F., Colantuono, C., and Chiusano, M. L. (2017). Shaping the evolutionary tree of green plants: evidence from the GST family. *Sci. Rep.* 7:14363. doi: 10.1038/s41598-017-14316-w

Moons, A. (2003). Osgstu3 and osgtu4, encoding tau class glutathione S-transferases, are heavy metal- and hypoxic stress-induced and differentially salt stress-responsive in rice roots 1. *FEBS Lett.* 553, 427–432. doi: 10.1016/S0014-5793(03)01077-9

Moons, A. (2005). "Regulatory and functional interactions of plant growth regulators and plant glutathione s-transferases (GSTs)," in *Vitamins &*

Hormones, (Amsterdam: Elsevier), 155–202. doi: 10.1016/S0083-6729(05)72005-7

Morel, M., Meux, E., Mathieu, Y., Thuillier, A., Chibani, K., Harvengt, L., et al. (2013). Xenomic networks variability and adaptation traits in wood decaying fungi: fungal xenomic networks. *Microb. Biotechnol.* 6, 248–263. doi: 10.1111/1751-7915.12015

Mueller, L. A., Goodman, C. D., Silady, R. A., and Walbot, V. (2000). AN9, a petunia glutathione S-transferase required for anthocyanin sequestration, is a flavonoid-binding protein. *Plant Physiol.* 123, 1561–1570. doi: 10.1104/pp.123.4.1561

Mueller, S., Hilbert, B., Dueckershoff, K., Roitsch, T., Krischke, M., Mueller, M. J., et al. (2008). General detoxification and stress responses are mediated by oxidized lipids through TGA transcription factors in *Arabidopsis*. *Plant Cell Online* 20, 768–785. doi: 10.1105/tpc.107.054809

Munyampundu, J.-P., Xu, Y.-P., and Cai, X.-Z. (2016). Phi class of glutathione S-transferase gene superfamily widely exists in nonplant taxonomic groups. *Evol. Bioinform.* 12:EBO.S35909. doi: 10.4137/EBO.S35909

Navrot, N., Collin, V., Gualberto, J., Gelhaye, E., Hirasawa, M., Rey, P., et al. (2006). Plant glutathione peroxidases are functional peroxiredoxins distributed in several subcellular compartments and regulated during biotic and abiotic stresses. *Plant Physiol.* 142, 1364–1379. doi: 10.1104/pp.106.089458

Neuefeind, T., Huber, R., Dasenbrock, H., Prade, L., and Bieseler, B. (1997a). Crystal structure of herbicide-detoxifying maize glutathione S-transferase-I in complex with lactoylglutathione: evidence for an induced-fit mechanism. *J. Mol. Biol.* 274, 446–453. doi: 10.1006/jmbi.1997.1402

Neuefeind, T., Huber, R., Reinemer, P., Knäblein, J., Prade, L., Mann, K., et al. (1997b). Cloning, sequencing, crystallization and X-ray structure of glutathione S-transferase-III from *Zea mays* var. mutin: a leading enzyme in detoxification of maize herbicides. *J. Mol. Biol.* 274, 577–587. doi: 10.1006/jmbi.1997.1401

Nutricati, E., Miceli, A., Blando, F., and De Bellis, L. (2006). Characterization of two *Arabidopsis* thaliana glutathione S-transferases. *Plant Cell Rep.* 25, 997–1005. doi: 10.1007/s00299-006-0146-1

Pantelides, I. S., Tjamos, S. E., and Paplomatas, E. J. (2010). Ethylene perception via ETR1 is required in *Arabidopsis* infection by *Verticillium dahliae*. *Mol. Plant Pathol.* 11, 191–202. doi: 10.1111/j.1364-3703.2009.00592.x

Pégeot, H., Koh, C. S., Petre, B., Mathiot, S., Duplessis, S., Hecker, A., et al. (2014). The poplar Phi class glutathione transferase: expression, activity and structure of GSTF1. *Front. Plant Sci.* 5:712. doi: 10.3389/fpls.2014.00712

Pégeot, H., Mathiot, S., Perrot, T., Gense, F., Hecker, A., Didierjean, C., et al. (2017). Structural plasticity among glutathione transferase Phi members: natural combination of catalytic residues confers dual biochemical activities. *FEBS J.* 284, 2442–2463. doi: 10.1111/febs.14138

Pemble, S. E., and Taylor, J. B. (1992). An evolutionary perspective on glutathione transferases inferred from class-theta glutathione transferase cDNA sequences. *Biochem. J.* 287(Pt 3), 957–963. doi: 10.1042/bj2870957

Perperopoulou, F., Pouliou, F., and Labrou, N. E. (2018). Recent advances in protein engineering and biotechnological applications of glutathione transferases. *Crit. Rev. Biotechnol.* 38, 511–528. doi: 10.1080/07388551.2017.1375890

Pettersen, E. F., Goddard, T. D., Huang, C. C., Couch, G. S., Greenblatt, D. M., Meng, E. C., et al. (2004). UCSF chimera–a visualization system for exploratory research and analysis. *J. Comput. Chem.* 25, 1605–1612. doi: 10.1002/jcc.20084

Piślewska-Bednarek, M., Nakano, R. T., Hiruma, K., Pastorczyk, M., Sanchez-Vallet, A., Singkaravanit-Ogawa, S., et al. (2018). Glutathione transferase U13 functions in pathogen-triggered glucosinolate metabolism. *Plant Physiol.* 176, 538–551. doi: 10.1104/pp.17.01455

Plomion, C., Aury, J.-M., Amselem, J., Leroy, T., Murat, F., Duplessis, S., et al. (2018). Oak genome reveals facets of long lifespan. *Nat. Plants* 4, 440–452. doi: 10.1038/s41477-018-0172-3

Prade, L., Huber, R., and Bieseler, B. (1998). Structures of herbicides in complex with their detoxifying enzyme glutathione S-transferase – explanations for the selectivity of the enzyme in plants. *Structure* 6, 1445–1452. doi: 10.1016/S0969-2126(98)00143-9

Rahantaniaina, M.-S., Li, S., Chatel-Innocenti, G., Tuzet, A., Mhamdi, A., Vanacker, H., et al. (2017). Glutathione oxidation in response to intracellular H_2O_2: key but overlapping roles for dehydroascorbate reductases. *Plant Signal Behav.* 12:e1356531. doi: 10.1080/15592324.2017.1356531

Reddy, G. V. B., and Gold, M. H. (2001). Purification and characterization of glutathione conjugate reductase: a component of the tetrachlorohydroquinone reductive dehalogenase system from phanerochaete chrysosporium. *Arch. Biochem. Biophys.* 391, 271–277. doi: 10.1006/abbi.2001.2417

Reid, R., Gridley, K., Kawamata, Y., and Zhu, Y. (2013). Arsenite elicits anomalous sulfur starvation responses in barley. *Plant Physiol.* 162, 401–409. doi: 10.1104/pp.113.216937

Reinemer, P., Prade, L., Hof, P., Neuefeind, T., Huber, R., Zettl, R., et al. (1996). Three-dimensional structure of glutathione S-transferase from *Arabidopsis thaliana* at 2.2 Å resolution: structural characterization of herbicide-conjugating plant glutathione S-transferases and a novel active site architecture. *J. Mol. Biol.* 255, 289–309. doi: 10.1006/jmbi.1996.0024

Rinaldi, C., Kohler, A., Frey, P., Duchaussoy, F., Ningre, N., Couloux, A., et al. (2007). Transcript profiling of poplar leaves upon infection with compatible and incompatible strains of the foliar rust *Melampsora larici*-populina. *Plant Physiol.* 144, 347–366. doi: 10.1104/pp.106.094987

Rouhier, N., and Jacquot, J.-P. (2005). The plant multigenic family of thiol peroxidases. *Free Radic. Biol. Med.* 38, 1413–1421. doi: 10.1016/j.freeradbiomed.2004.07.037

Rouhier, N., Lemaire, S. D., and Jacquot, J.-P. (2008). The role of glutathione in photosynthetic organisms: emerging functions for glutaredoxins and glutathionylation. *Ann. Rev. Plant Biol.* 59, 143–166. doi: 10.1146/annurev.arplant.59.032607.092811

Ryu, H. Y., Kim, S. Y., Park, H. M., You, J. Y., Kim, B. H., Lee, J. S., et al. (2009). Modulations of AtGSTF10 expression induce stress tolerance and BAK1-mediated cell death. *Biochem. Biophys. Res. Commun.* 379, 417–422. doi: 10.1016/j.bbrc.2008.11.156

Sappl, P. G., Carroll, A. J., Clifton, R., Lister, R., Whelan, J., Harvey Millar, A., et al. (2009). The *Arabidopsis* glutathione transferase gene family displays complex stress regulation and co-silencing multiple genes results in altered metabolic sensitivity to oxidative stress: genomic and reverse genetic analysis of plant GSTs. *Plant J.* 58, 53–68. doi: 10.1111/j.1365-313X.2008.03761.x

Sappl, P. G., Oñate-Sánchez, L., Singh, K. B., and Millar, A. H. (2004). Proteomic analysis of glutathione S -transferases of *Arabidopsis thaliana* reveals differential salicylic acid-induced expression of the plant-specific phi and tau classes. *Plant Mol. Biol.* 54, 205–219. doi: 10.1023/B:PLAN.0000028786.57439.b3

Schmid, M., Davison, T. S., Henz, S. R., Pape, U. J., Demar, M., Vingron, M., et al. (2005). A gene expression map of *Arabidopsis thaliana* development. *Nat. Genet.* 37, 501–506. doi: 10.1038/ng1543

Schwartz, M., Didierjean, C., Hecker, A., Girardet, J.-M., Morel-Rouhier, M., Gelhaye, E., et al. (2016). Crystal structure of *Saccharomyces cerevisiae* ECM4, a Xi-class glutathione transferase that reacts with glutathionyl-(hydro)quinones. *PLoS One* 11:e0164678. doi: 10.1371/journal.pone.0164678

Shah, D. M., Hironaka, C. M., Wiegand, R. C., Harding, E. I., Krivi, G. G., and Tiemeier, D. C. (1986). Structural analysis of a maize gene coding for glutathione-S-transferase involved in herbicide detoxification. *Plant Mol. Biol.* 6, 203–211. doi: 10.1007/BF00015226

Shao, Y., Lv, Z., Li, C., Zhang, W., Duan, X., Qiu, Q., et al. (2017). Molecular cloning and functional characterization of theta class glutathione S-transferase from *Apostichopus japonicus*. *Fish Shellf. Immunol.* 63, 31–39. doi: 10.1016/j.fsi.2017.02.004

Skopelitou, K., Muleta, A. W., Papageorgiou, A. C., Chronopoulou, E., and Labrou, N. E. (2015). Catalytic features and crystal structure of a tau class glutathione transferase from *Glycine max* specifically upregulated in response to soybean mosaic virus infections. *Biochim. Biophys. Acta (BBA) – Proteins Proteom.* 1854, 166–177. doi: 10.1016/j.bbapap.2014.11.008

Skopelitou, K., Muleta, A. W., Pavli, O., Skaracis, G. N., Flemetakis, E., Papageorgiou, A. C., et al. (2012). Overlapping protective roles for glutathione transferase gene family members in chemical and oxidative stress response in *Agrobacterium tumefaciens*. *Funct. Integr. Genomics* 12, 157–172. doi: 10.1007/s10142-011-0248-x

Smith, A. P., DeRidder, B. P., Guo, W.-J., Seeley, E. H., Regnier, F. E., and Goldsbrough, P. B. (2004). Proteomic analysis of *Arabidopsis* glutathione S-transferases from benoxacor- and copper-treated seedlings. *J. Biol. Chem.* 279, 26098–26104. doi: 10.1074/jbc.M402807200

Smith, A. P., Nourizadeh, S. D., Peer, W. A., Xu, J., Bandyopadhyay, A., Murphy, A. S., et al. (2003). *Arabidopsis* AtGSTF2 is regulated by ethylene and auxin, and

encodes a glutathione S-transferase that interacts with flavonoids. *Plant J.* 36, 433–442. doi: 10.1046/j.1365-313x.2003.01890.x

Soranzo, N., Sari Gorla, M., Mizzi, L., De Toma, G., and Frova, C. (2004). Organisation and structural evolution of the rice glutathione S-transferase gene family. *Mol. Genet. Genomics* 271, 511–521. doi: 10.1007/s00438-004-1006-8

Srivastava, D., Verma, G., Chauhan, A. S., Pande, V., and Chakrabarty, D. (2019). Rice (*Oryza sativa* L.) tau class glutathione S -transferase (OsGSTU30) overexpression in *Arabidopsis thaliana* modulates a regulatory network leading to heavy metal and drought stress tolerance. *Metallomics* 11, 375–389. doi: 10.1039/c8mt00204e

Stotz, H. U., Mueller, S., Zoeller, M., Mueller, M. J., and Berger, S. (2013). TGA transcription factors and jasmonate-independent COI1 signalling regulate specific plant responses to reactive oxylipins. *J. Exp. Bot.* 64, 963–975. doi: 10.1093/jxb/ers389

Su, T., Xu, J., Li, Y., Lei, L., Zhao, L., Yang, H., et al. (2011). Glutathione-indole-3-acetonitrile is required for camalexin biosynthesis in *Arabidopsis thaliana*. *Plant Cell* 23, 364–380. doi: 10.1105/tpc.110.079145

Sun, Y., Li, H., and Huang, J.-R. (2012). Arabidopsis TT19 functions as a carrier to transport anthocyanin from the cytosol to tonoplasts. *Mol. Plant* 5, 387–400. doi: 10.1093/mp/ssr110

Tang, A. H., and Tu, C. P. (1994). Biochemical characterization of *Drosophila* glutathione S-transferases D1 and D21. *J. Biol. Chem.* 269, 27876–27884.

Thatcher, L. F., Kamphuis, L. G., Hane, J. K., Oñate-Sánchez, L., and Singh, K. B. (2015). The *Arabidopsis* KH-domain RNA-binding protein ESR1 functions in components of jasmonate signalling, unlinking growth restraint and resistance to stress. *PLoS One* 10:e0126978. doi: 10.1371/journal.pone.0126978

Thom, R., Cummins, I., Dixon, D. P., Edwards, R., Cole, D. J., and Lapthorn, A. J. (2002). Structure of a tau class glutathione S-transferase from wheat active in herbicide detoxification. *Biochemistry* 41, 7008–7020. doi: 10.1021/bi015964x

Thom, R., Dixon, D. P., Edwards, R., Cole, D. J., and Lapthorn, A. J. (2001). The structure of a zeta class glutathione S-transferase from *Arabidopsis thaliana*: characterisation of a GST with novel active-site architecture and a putative role in tyrosine catabolism. *J. Mol. Biol.* 308, 949–962. doi: 10.1006/jmbi.2001.4638

Tiwari, V., Patel, M. K., Chaturvedi, A. K., Mishra, A., and Jha, B. (2016). Functional characterization of the tau class glutathione-S-transferases gene (SbGSTU) promoter of salicornia brachiata under salinity and osmotic stress. *PLoS One* 11:e0148494. doi: 10.1371/journal.pone.0148494

Tossounian, M.-A., Van Molle, I., Wahni, K., Jacques, S., Gevaert, K., Van Breusegem, F., et al. (2018). Disulfide bond formation protects *Arabidopsis thaliana* glutathione transferase tau 23 from oxidative damage. *Biochim. Biophys. Acta (BBA) – Gen. Subjects* 1862, 775–789. doi: 10.1016/j.bbagen.2017.10.007

Tripathi, A., Indoliya, Y., Tiwari, M., Tiwari, P., Srivastava, D., Kumar Verma, P., et al. (2014). Transformed yeast (*Schizosaccharomyces pombe*) overexpressing rice Tau class glutathione S-transferase (OsGSTU30 and OsGSTU41) shows enhanced resistance to hexavalent chromium. *Metallomics* 6, 1549–1557. doi: 10.1039/C4MT00083H

Valenzuela-Chavira, I., Contreras-Vergara, C. A., Arvizu-Flores, A. A., Serrano-Posada, H., Lopez-Zavala, A. A., García-Orozco, K. D., et al. (2017). Insights into ligand binding to a glutathione S-transferase from mango: structure, thermodynamics and kinetics. *Biochimie* 135, 35–45. doi: 10.1016/j.biochi.2017.01.005

Wagner, U., Edwards, R., Dixon, D. P., and Mauch, F. (2002). Probing the diversity of the *Arabidopsis* glutathione S-transferase gene family. *Plant Mol. Biol.* 49, 515–532.

Wentzell, A. M., Rowe, H. C., Hansen, B. G., Ticconi, C., Halkier, B. A., and Kliebenstein, D. J. (2007). Linking metabolic QTLs with network and cis-eQTLs controlling biosynthetic pathways. *PLoS Genet.* 3:e162. doi: 10.1371/journal.pgen.0030162

Wiegand, R. C., Shah, D. M., Mozer, T. J., Harding, E. I., Diaz-Collier, J., Saunders, C., et al. (1986). Messenger RNA encoding a glutathione-S-transferase responsible for herbicide tolerance in maize is induced in response to safener treatment. *Plant Mol. Biol.* 7, 235–243. doi: 10.1007/BF00752897

Willett, S. W., and Copley, S. D. (1996). Identification and localization of a stable sulfenic acid in peroxide-treated tetrachlorohydroquinone dehalogenase using electrospray mass spectrometry. *Chem. Biol.* 3, 851–857. doi: 10.1016/S1074-5521(96)90071-X

Xu, J., Tian, Y.-S., Xing, X.-J., Peng, R.-H., Zhu, B., Gao, J.-J., et al. (2016). Over-expression of AtGSTU19 provides tolerance to salt, drought and methyl viologen stresses in *Arabidopsis*. *Physiol. Plant.* 156, 164–175. doi: 10.1111/ppl.12347

Xu, J., Zheng, A.-Q., Xing, X.-J., Chen, L., Fu, X.-Y., Peng, R.-H., et al. (2018). Transgenic *Arabidopsis* plants expressing grape glutathione S-Transferase gene (VvGSTF13) show enhanced tolerance to abiotic stress. *Biochemistry* 83, 755–765. doi: 10.1134/S0006297918060135

Xun, L., Belchik, S. M., Xun, R., Huang, Y., Zhou, H., Sanchez, E., et al. (2010). S-Glutathionyl-(chloro)hydroquinone reductases: a novel class of glutathione transferases. *Biochem. J.* 428, 419–427. doi: 10.1042/BJ20091863

Xun, L., Topp, E., and Orser, C. S. (1992). Purification and characterization of a tetrachloro-p-hydroquinone reductive dehalogenase from a *Flavobacterium* sp. *J. Bacteriol.* 174, 8003–8007. doi: 10.1128/jb.174.24.8003-8007.1992

Yamamoto, K., Nagaoka, S., Banno, Y., and Aso, Y. (2009). Biochemical properties of an omega-class glutathione S-transferase of the silkmoth, *Bombyx mori*. *Compar. Biochem. Physiol. Part C Toxicol. Pharmacol.* 149, 461–467. doi: 10.1016/j.cbpc.2008.10.108

Yamazaki, M., Shibata, M., Nishiyama, Y., Springob, K., Kitayama, M., Shimada, N., et al. (2008). Differential gene expression profiles of red and green forms of *Perilla frutescens* leading to comprehensive identification of anthocyanin biosynthetic genes: anthocyanin biosynthetic genes from *Perilla*. *FEBS J.* 275, 3494–3502. doi: 10.1111/j.1742-4658.2008.06496.x

Yang, G., Xu, Z., Peng, S., Sun, Y., Jia, C., and Zhai, M. (2016). In planta characterization of a tau class glutathione S-transferase gene from Juglans regia (JrGSTTau1) involved in chilling tolerance. *Plant Cell Rep.* 35, 681–692. doi: 10.1007/s00299-015-1912-8

Yang, L.-P., Fang, Y.-Y., An, C.-P., Dong, L., Zhang, Z.-H., Chen, H., et al. (2013). C2-mediated decrease in DNA methylation, accumulation of siRNAs, and increase in expression for genes involved in defense pathways in plants infected with beet severe curly top virus. *Plant J.* 73, 910–917. doi: 10.1111/tpj.12081

Yang, Q., Han, X.-M., Gu, J.-K., Liu, Y.-J., Yang, M.-J., and Zeng, Q.-Y. (2019). Functional and structural profiles of GST gene family from three *Populus* species reveal the sequence-function decoupling of orthologous genes. *New Phytol.* 221, 1060–1073. doi: 10.1111/nph.15430

Zakharyan, R. A., Sampayo-Reyes, A., Healy, S. M., Tsaprailis, G., Board, P. G., Liebler, D. C., et al. (2001). Human monomethylarsonic acid (MMA(V)) reductase is a member of the glutathione-S-transferase superfamily. *Chem. Res. Toxicol.* 14, 1051–1057. doi: 10.1021/tx010052h

Zettl, R., Schell, J., and Palme, K. (1994). Photoaffinity labeling of *Arabidopsis thaliana* plasma membrane vesicles by 5-azido-[7-3H]indole-3-acetic acid: identification of a glutathione S-transferase. *Proc. Natl. Acad. Sci. U.S.A.* 91, 689–693. doi: 10.1073/pnas.91.2.689

Zhao, J. (2015). Flavonoid transport mechanisms: how to go, and with whom. *Trends Plant Sci.* 20, 576–585. doi: 10.1016/j.tplants.2015.06.007

Conflict of Interest Statement: The authors declare that the research was conducted in the absence of any commercial or financial relationships that could be construed as a potential conflict of interest.

Advantages of publishing in Frontiers

OPEN ACCESS
Articles are free to read for greatest visibility and readership

FAST PUBLICATION
Around 90 days from submission to decision

HIGH QUALITY PEER-REVIEW
Rigorous, collaborative, and constructive peer-review

TRANSPARENT PEER-REVIEW
Editors and reviewers acknowledged by name on published articles

Frontiers
Avenue du Tribunal-Fédéral 34
1005 Lausanne | Switzerland

Visit us: www.frontiersin.org
Contact us: info@frontiersin.org | +41 21 510 17 00

REPRODUCIBILITY OF RESEARCH
Support open data and methods to enhance research reproducibility

DIGITAL PUBLISHING
Articles designed for optimal readership across devices

FOLLOW US
@frontiersin

IMPACT METRICS
Advanced article metrics track visibility across digital media

EXTENSIVE PROMOTION
Marketing and promotion of impactful research

LOOP RESEARCH NETWORK
Our network increases your article's readership